SECOND EDITION

INDUSTRIAL AND PROCESS FURNACES

PRINCIPLES, DESIGN AND OPERATION

PETER MULLINGER
BARRIE JENKINS

B
H

To the Late Frank David Moles who showed us a better way of thinking about furnaces, especially those where the product is directly heated by the flame.

Industrial and Process Furnaces

Principles, Design and Operation

Second Edition

Peter Mullinger
Visiting Research Fellow, School of Chemical Engineering, University of Adelaide, South Australia

Barrie Jenkins
Consulting Engineer, High Wycombe, Buckinghamshire, UK



ELSEVIER

AMSTERDAM • BOSTON • HEIDELBERG • LONDON
NEW YORK • OXFORD • PARIS • SAN DIEGO
SAN FRANCISCO • SINGAPORE • SYDNEY • TOKYO
Butterworth-Heinemann is an imprint of Elsevier



Butterworth-Heinemann is an imprint of Elsevier
The Boulevard, Langford Lane, Kidlington, Oxford OX5 1GB, UK
225 Wyman Street, Waltham, MA 02451, USA

First edition 2008
Second edition 2014

Copyright © 2014, 2008 Elsevier Ltd. All rights reserved.

No part of this publication may be reproduced, stored in a retrieval system or transmitted in any form or by any means electronic, mechanical, photocopying, recording or otherwise without the prior written permission of the publisher

Permissions may be sought directly from Elsevier's Science & Technology Rights Department in Oxford, UK: phone (+44) (0) 1865 843830; fax (+44) (0) 1865 853333; email: permissions@elsevier.com. Alternatively you can submit your request online by visiting the Elsevier web site at http://elsevier.com/locate/permissions, and selecting *Obtaining permission to use Elsevier material*

Notice
No responsibility is assumed by the publisher for any injury and/or damage to persons or property as a matter of products liability, negligence or otherwise, or from any use or operation of any methods, products, instructions or ideas contained in the material herein. Because of rapid advances in the medical sciences, in particular, independent verification of diagnoses and drug dosages should be made

British Library Cataloguing in Publication Data
A catalogue record for this book is available from the British Library

Library of Congress Cataloging-in-Publication Data
A catalog record for this book is availabe from the Library of Congress

ISBN-13: 978-0-08-099377-5

For information on all Butterworth-Heinemann publications visit our web site at books.elsevier.com

Printed and bound in the US

13 14 15 16 17 10 9 8 7 6 5 4 3 2 1



Foreword to Second Edition

Additional chapters in this second edition focus attention on a range of actual combustion related projects and the economic issues related to furnaces. In doing so, it also highlights that industrial problems can be quite complex and multi-faceted. In the past, and even today, many of these issues would almost certainly be addressed by trial and error, simply due to the lack of adequate technical knowledge, which can now be found in this book.

Combustion related projects generally require a wide range of ancillary equipment ranging from valve trains and pumping systems, blowers/fans and ducting, refractory lining, electric motors, boilers and heat exchangers, exhaust gas cleaning etc. As this book addresses all of these aspects it also provides useful information, which can be applied outside the field of combustion. I have successfully used a section in chapter 5 to assess the design of a twin fluid atomiser installed in a water spray system used for gas cooling.

To me the most important thing highlighted in the second edition through the practical examples, is that the solutions to complex combustion and heat transfer problems do exist and all we have to do is correctly apply the science but better still, use this science to get the design right in the first place!

Greg Mills
Engineering Consultant
Perth, Western Australia

Foreword to First Edition

Furnaces have been used by humans for thousands of years and yet, beyond the basic chemical reactions and heat release calculations, engineers rarely have any formal training in relation to furnace design, combustion and their integration into industrial processes. It is therefore not surprising that the solution to issues of emissions, throughput and performance related problems have relied heavily on trial and error and experience. Within industry in general, equipment would be more successful designed using the principles outlined in this book rather than relying on correlations and scale up factors that have little or no scientific basis to support them.

In the early 1970s the authors set themselves the goal of applying more scientific methods to burner design than were currently used. This led to the realisation that heat release from flames needed to be closely matched to the process requirements and that this was intimately related to the design of the furnace itself. Now, more than ever before, the need to reduce ongoing energy costs and greenhouse gas emissions requires decisions to be made on the basis of knowledge rather than guesswork and past experience. This book, being one of only a few ever published on the subject, highlights the applicable science which can be used to take much the guesswork out of furnace design. This book also emphasises the importance of ensuring that individual pieces of equipment are appropriate for the whole process and not simply selected on the basis of capacity or lowest capital cost.

Alcoa's alumina refineries operate a range of processes and equipment including boilers, rotary kilns, gas suspension alumina calciners and regenerative thermal oxidisers and, like many other industries, have needed to address emissions, throughput, performance and safety issues without a clear understanding of the science and underlying design basis. This makes it difficult to undertake reliable root cause analysis when problems occur.

In the early 1980s I was a mechanical engineer in Alcoa's Equipment Development Group. I had insufficient knowledge of, and certainly no experience with, combustion processes and was faced with having to address throughput and emissions related issues with alumina calciners. Fortunately I met the authors of this book, Peter Mullinger and Barrie Jenkins, and was delighted to discover that a scientific approach to furnace design is possible and methods are available to investigate and optimise many aspects of the combustion and associated processes.

It was highlighted through physical modelling of the flow patterns and acid alkali modelling of the combustion process mixing that both the throughput and emissions could be significantly improved by simply relocating fuel injection points. These modifications proved to be effective and have now been employed on all applicable alumina calciners at Alcoa's refineries around the world saving otherwise significant capital expenditure with potentially ineffective outcomes.

Since those early days the science as described in this book has been employed over a wide range of process issues, from the design of new equipment and in the solution of problems with existing equipment, positively impacting on performance and reliability. More recently there has been a major application in relation to the design of safety systems.

In particular the application of CFD modelling has highlighted to me that CFD doesn't replace the need for a deep understanding of the science of combustion and furnace heat transfer processes as there are many traps for the unwary and the uninformed.

Whether you are engaged in modelling, design of original equipment, or equipment or equipment upgrades or operation of combustion and heat transfer processes, this book provides much of the essential understanding required for success.

Greg Mills
Senior Consultant – Calcination,
Technology Delivery Group,
Alcoa World Alumina

Preface to the Second Edition

In the five years since the original publication of this book, feedback from readers of the original book suggested that more information on CFD modelling would be helpful, particularly examples of its application, together with case studies and worked examples to demonstrate more application of the theory. Other areas where additional information was requested was in connection with flames and burners for furnace, costing, efficiencies, optimisation, future trends and the properties of slag.

We have attended to these requests by providing a couple of examples of CFD modelling in Chapter 6. However, because we rarely used one modelling technique in isolation, we have included a new chapter of selected real furnace applications, which also includes CFD modelling, together with new chapters on furnace economics and future trends. Unfortunately, we could not find sufficient data on slag properties to include anything worthwhile.

The chapter on furnace economics includes a case study where seven options for rebuilding or upgrading a furnace are considered. The cost of each option is derived, the potential fuel savings are determined and a cost-benefit analysis prepared.

The chapter on selected real furnace applications provides detailed descriptions of six real projects, which have been chosen to demonstrate the application of the techniques to completely different industrial processes. Three of these projects also included site data collection, which is described in some detail. Most of these projects involved the application of more than one modelling technique.

Finally in the chapter on future trends, we look at trends in furnace design, construction, and control, furnace applications and emission limits. We expect the latter to drive most future developments. However, as in the 1960's and 70's, major disruptions to fuel supply could also have a significant disruptive influence. Forecasting is by its definition an uncertain exercise, and unlike the timescale used by Nostradamus, we are likely to be around to witness our failures.

Peter Mullinger, Adelaide
Barrie Jenkins, High Wycombe
2013

Preface to First Edition

This book has been more than twenty years in gestation; its lineage can be traced back to Barrie's lecturing at the University of Surry in the late 1970s and early 1980s and Peter's first combustion course, provided internally to the Rugby Cement's engineers in 1981.

We are not attempting to explain how to design any particular furnace but are advocating a more scientific approach to furnace design than the traditional methods of scaling from the last design. New approaches are essential if we are to make the advances needed to develop new processes for the twenty first century and to significantly reduce industrial energy consumption and emissions.

We have worked together to improve the efficiency of furnaces since 1977, starting with rotary kilns in the cement industry when Roger Gates, Technical Director of Rugby Cement, allowed Peter Mullinger to try the techniques developed by Fuels and Energy Research Group at the University of Surrey (FERGUS) on Rugby's South Ferriby No 3 Kiln. This work was strongly encouraged by the Plant Manager, the late Jim Bowman. The project was an immediate success and let to significantly increased production and reduced fuel consumption. The success of that projected encouraged Rugby to sign a research agreement with the late Frank Moles, founder of FERGUS which committed Barrie Jenkins and the rest of the FERGUS team to support Rugby Cement's efforts to improve the production capacity, product quality and fuel economy of their twenty one kilns.

Following time in senior technical management roles with a company supplying combustion equipment into the petrochemical industry, we founded our own business to apply more scientific methods to combustion and heat transfer problems in all industries but principally those where the product was directly heated by the flame.

We commercialised techniques that had been successfully developed and used in-house by organisations such as by British Gas, CEGB, British Steel's Swinden Laboratories, Rotherham. We added acid/alkali modelling as a means of determining fuel/air mixing and flame shape, a technique that had seen little application outside of research institutions at that time.

We built a successful business on this philosophy that continues today, managed by our successors. During the time we managed it we applied these techniques to over 250 projects in a wide range of furnace types in the alumina, cement, ceramic, chrome, copper, lead, lime, steel, mineral sands, nickel, petrochemical, pulp and paper and even the nuclear industry.

The idea for this book arose from the short course we provided on behalf of the International Kiln Association to industry and to the Portland Cement Association where we were regularly asked to recommend a book. We would have suggested Professor Thring's book "The science of flames and furnaces" but it was long out

of print so all that we could offer were the course notes. We hope that this book goes some way to filling the gap. It is the culmination of thirty years of working together, albeit for the last few years from across the globe.

Peter Mullinger, Adelaide
Barrie Jenkins, High Wycombe
2007

Acknowledgements

Over the years it has been our privilege to work with many engineers, process operators and other people who have encouraged and cooperated with us. Those who are mentioned below are but a small selection, whose influence has strongly encouraged the preparation of this book or who have directly contributed to it. Of special influence was the late Frank Moles, founder of the Fuels and Energy Research Group at the University of Surrey (FERGUS), who changed our thinking about industrial combustion, and Roger Gates, Technical Director of Rugby Cement, who allowed us to implement Frank's and our ideas on the company's plants.

We would like to thank many of the engineers at the former Midlands Research Station of British Gas, especially Neil Fricker, Malcolm Hogarth, Mike Page, Rachel Palmer, Jeff Rhine and Bob Tucker all of whom encouraged us to found Fuel and Combustion Technology Ltd. (FCT), in 1984 and to apply modelling techniques to industrial combustion and heat transfer problems. We believe that we were the first to use these techniques commercially on a large scale.

We owe a special debt of gratitude to those who were brave enough to give us our early work at FCT, including Len May, Terry Henshaw and John Salisbury of ARC Ltd., Erik Morgensen and Lars Christiansen of Haldor Topsoe A/S, Greg Mills of Alcoa Australia, Ian Flower and Con Manias of Adelaide Brighton Cement, Philip Alsop of PT Semen Cibinong, Terry Adams and Peter Gorog of the Weyerhaeuser Company, all of whom were very influential in providing FCT with its early projects. We should also like to thank Alcoa World Alumina and Hador Topose A/S for permission to publish descriptions of their projects.

Peter Mullinger would also particularly like to thank the late Emeritus Professor Sam Luxton who strongly supported his change of direction to an academic career in 1999. Without that change, it is unlikely that time would have ever been available to complete this task. Peter would also like to thank his colleagues at the University of Adelaide who, either contributed directly to the book, or who covered his teaching duties during the first half of 2005 and first half of 2007, when the majority of this book was written, particularly Prof Keith King, Dr Peter Ashman, Prof. Gus Nathan and Dr Yung Ngothai, A.Prof Dzuy Nguyen and A.Prof Brian O'Neill.

We should also like to thank those commercial companies who provided data, photographs and drawings (who are acknowledged in the captions) but special thanks are due to Adam Langman, who tuned our woeful sketches into artistic masterpieces and Dave Crawley of DCDesign Services, who produced the process and instrument drawings and flow diagrams. Grateful thanks are also due to Dr. Christine Bertrand, Mr Dennis Butcher and Dr John Smart for their invaluable contribution to the sections on 'CFD modelling', 'Furnace control and safety' and 'NO_x formation and control' respectively.

We hope that the errors are minimal, but there would be many more but for the excellent proofreading of Victoria Jenkins and Sheila Kelly, to whom very special thanks are due. We could not have managed without you. Sheila, in particular, has read every word but maintains that it is not as much fun as Harry Potter!

Finally to all those who attended our industrial combustion short courses and asked, "What book is available?" It is available at last; we hope that you won't be disappointed.

List of Figures

Figure 1.1	The iron bridge at Coalbrookdale showing the detail adjacent to an abutment and "Coalbrookdale by Night"	2
Figure 1.2	The Basic Elements of a Furnace	4
Figure 1.3	Classification of Furnaces	6
Figure 1.4	Cross section through a traditional downdraught pottery batch kiln	8
Figure 1.5	Schematic of a mixed feed vertical shaft lime kiln and a battery of six oil fired vertical shaft lime kilns	9
Figure 1.6	Twin shaft regenerative lime kiln	10
Figure 1.7	Modern cement kiln technology showing the cyclone preheater tower on the left and the satellite cooler on the right	11
Figure 1.8	Schematic of a Regenerative Glass Tank	12
Figure 1.9	Schematic of a Modern Blast Furnace with Abraham Darby's pioneering furnace on the right	14
Figure 1.10	A Reverbatory Furnace for Smelting Copper Sulphide Ores	15
Figure 1.11	A Pierce-Smith converter	15
Figure 1.12	Outokumpu flash smelter for copper smelting	16
Figure 1.13	Cross section through a copper anode furnace showing the blowing, slag skimming and casting operations	17
Figure 1.14	A hydrogen atmosphere furnace for de-sulphurisation of nickel briquettes	17
Figure 1.15	Fluid bed furnace for roasting copper ore	18
Figure 1.16	Flash furnace for alumina, lime or cement raw material calcination	19
Figure 1.17	A large billet re-heating furnace	21
Figure 1.18	Continuous rapid heating furnace for small billets	22
Figure 1.19	Schematic of Slab Re-heating Furnace	22
Figure 1.20	Two large gearbox cases entering a large annealing furnace	23
Figure 1.21	A small incinerator designed by the authors to recover energy from methanol contaminated water	24
Figure 1.22	Reducing kiln used in the mineral sands industry	25
Figure 1.23	Herreschoff multiple hearth roaster	26
Figure 1.24	Two types of petrochemical heater showing a cylindrical heater and a cabin heater	27
Figure 1.25	Heat transfer coils for petrochemical heaters showing a coil for a cabin heater and cylindrical heater	28
Figure 2.1	Effect of temperature on reaction rate in the extended Arrheneus Equation	40

Figure 2.2	Consequence of extended Arrhenius equation on temporal consumption of species A	40
Figure 2.3	Extracted reactions from the 'chemical soup' of fossil fuel combustion	41
Figure 2.4	Relationship between reactedness and mass consumption of fuel and oxidant	42
Figure 2.5	Dependence of fuel reaction rate on the reactedness of a flame	43
Figure 2.6	Equilibrium rate values for combustion reactions	44
Figure 2.7	Stages in the combustion of a fuel particle	45
Figure 2.8	Entrainment of secondary fluid into a free jet	48
Figure 2.9	Entrainment of fluid into a high momentum confined jet with external recirculation	50
Figure 2.10	Entrainment of fluid into a swirling free jet with internal recirculation	51
Figure 2.11	Typical aerodynamics in a rotary kiln associated with a grate cooler, obtained by water-bead and air modelling	60
Figure 2.12	Typical aerodynamics in a flash calciner – obtained using water-bead modelling	61
Figure 2.13	The effect of excess air on heat consumption (i.e. fuel efficiency) for a cement kiln	62
Figure 2.14	The effect of excess air on flue gas heat losses	62
Figure 3.1	Combustion characteristics of methane	74
Figure 3.2	Viscosity temperature relationship for petroleum based fuels	76
Figure 3.3	Effect of Carbon/Hydrogen ratio on flame emissivity	82
Figure 3.4	Effect of fuel type on heat transfer in a rotary kiln	82
Figure 4.1	Representation of section through compound refractory furnace wall	91
Figure 4.2	Representation of ingot shape and reheating furnace firing pattern	93
Figure 4.3	Gurnie-Lurie chart for long cylinder	94
Figure 4.4	Ingot heating predictions using Gurnie-Lurie chart	95
Figure 4.5	Representation of slab showing slice details	96
Figure 4.6	Graphical solution of slab heating problem	97
Figure 4.7	Representation of slab showing slice details with surface heat transfer	98
Figure 4.8	Development of boundary layer over a flat plate	99
Figure 4.9	Temperature profile through a tube wall	104
Figure 4.10	The electromagnetic spectrum	112
Figure 4.11	Diagrammatic representation variation of E with λ for various types of emitter	114
Figure 4.12	Evaluation chart for approximate flame gas emissivity calculations	119
Figure 4.13	Radiative exchange between large, closely spaced parallel Lambert surfaces	120
Figure 4.14	Radiative exchange between two finite surfaces	121

Figure 4.15	Example of crossed string evaluation of exchange area between curved surfaces	123
Figure 4.16	Rectilinear surface relationship	123
Figure 4.17	Complete geometry system	124
Figure 4.18	Sub division of radiating planes	124
Figure 4.19	A refractory backed row of tubes	125
Figure 4.20	Mean beam length values for two geometric systems	125
Figure 4.21	Regions of an arc	129
Figure 4.22	Induction heating of plasma	129
Figure 5.1	Premixed and diffusion flames produced by a Bunsen burner	141
Figure 5.2	Schematic diagram of the stability limits of a premixed flame	142
Figure 5.3	Carbon monoxide concentrations in an 8 MW rotary kiln flame	143
Figure 5.4	Effect of final droplet size on the additional surface area created by atomising a 10 mm sphere	145
Figure 5.5	Mechanism of spray formation from a typical atomiser	146
Figure 5.6	Rosin Rammler distribution for four different oil atomisers	148
Figure 5.7	Optimum combustion intensities for selected rotary kiln processes	150
Figure 5.8	Predicted temperatures and heat flux profiles in a cabin heater	150
Figure 5.9	Examples of stable and unstable flames on the same burner which is to the extreme left in each photograph	152
Figure 5.10	Schematic diagrams illustrating the presence of "external" and "internal" flow recirculation	153
Figure 5.11	Flame stabilisation using flow deviation caused by bluff body	154
Figure 5.12	Typical nozzle premix as applied to a tunnel burner and venturi mixer	156
Figure 5.13	Effect of excess air on adiabatic flame temperature for natural gas (37.25 MJ/m^3)	158
Figure 5.14	Partial premix radiant wall Walrad™ burner	159
Figure 5.15	Principle of flame arrestor fuel gas nozzle	160
Figure 5.16	Principle of turbulent jet diffusion flame	163
Figure 5.17	Recirculation in confined flames	164
Figure 5.18	Precessing jet gas burner nozzle	168
Figure 5.19	Typical industrial turbulent jet burner gas nozzle arrangements with gas pokers and central gas gun	169
Figure 5.20	The main components of a typical furnace oil burner – Water cooled version shown	170
Figure 5.21	General mechanism of spray combustion	171
Figure 5.22	Solid and hollow cone sprays	172
Figure 5.23	Illustration of flame stabilisation by internal recirculation zone caused by air entrainment into a hollow cone spray	172
Figure 5.24	Classification of oil burners by atomiser type	174
Figure 5.25	Schematic of simple and spill return pressure jet atomisers	174
Figure 5.26	Calibration curve for wide turndown spill return pressure jet atomiser	176

Figure 5.27	Schematic and "exploded view" of duplex wide turndown pressure jet atomiser	177
Figure 5.28	A low pressure air atomising burner	178
Figure 5.29	Examples of medium and twin fluid atomisers	178
Figure 5.30	Typical calibration curve for a high pressure twin fluid atomiser	180
Figure 5.31	Typical open ended pipe kiln burner arrangement.	182
Figure 5.32	Typical pulverised coal burner with auxiliary oil firing for rotary kilns	183
Figure 5.33	Schematic of the principle combustion air supply systems	183
Figure 5.34	Examples of how poor secondary airflow adversely affects kiln flames	187
Figure 5.35	Typical combustion air duct supplying multiple burners	188
Figure 5.36	Poor combustion air distribution caused by inadequate duct design	189
Figure 5.37	Example of constant velocity combustion air ducting	190
Figure 5.38	Example of constant velocity combustion air ducting with weirs	190
Figure 5.39	Effect of single blade damper/air door on airflow	191
Figure 5.40	Combustion air distribution following modelling and installation of flow correction devices.	192
Figure 5.41	Typical Register oil burner - note the radial airflow distribution required for optimum performance	192
Figure 5.42	Schematic and graphical representation of a sound wave	197
Figure 5.43	The Clyde Refinery flares in normal mode and oscillation mode	202
Figure 5.44	Schematic of gas supply pipework for Clyde Refinery flares	203
Figure 6.1	Physical modelling facility set up for water modelling	211
Figure 6.2	Flow visualisation in an arched furnace roof using water bead modelling	212
Figure 6.3	Simulation of fuel/air mixing in rotary kiln using acid-alkali modelling	213
Figure 6.4	Effect of furnace shape on thermal efficiency	218
Figure 6.5	Thermal performance of well-stirred furnace chambers	221
Figure 6.6	Effect of wall loss factor on well-stirrred efficiency equation	222
Figure 6.7	The effect of flame emissivity and excess air on furnace efficiency in a rotary kiln	226
Figure 6.8	Construction of a one-dimensional cylindrical furnace model with jet mixing	227
Figure 6.9	Cement kiln flame temperature calculation using 3-D zone model	230
Figure 6.10	Cement kiln measured flame temperatures	231
Figure 6.11	Comparison of measured and predicted flame temperatures	231
Figure 6.12	3-D, 1-D and well stirred furnace model predictions of wall heat flux	232
Figure 6.13	Co-ordinate grid systems used in CFD modelling	235
Figure 6.14.	Effect of burner spacing in a high alumina cement shaft kiln	236

Figure 6.15.	Effect of poor windbox design on flames in a four burner water tube boiler	237
Figure 6.16	Modelling inter-relationship for engineering design	239
Figure 7.1	Typical Gas valve safety shutoff system - double block and bleed type	247
Figure 7.2	Oil system typical ring main with multiple furnace off-takes and steam heating	250
Figure 7.3	Typical pumping and heating unit with shell and tube oil heaters and standby electric heating	251
Figure 7.4	Typical oil valve train arrangement	253
Figure 7.5	Rat hole and mass flow	255
Figure 7.6	Raw coal bunker and feeder	255
Figure 7.7	Coal drying curves	257
Figure 7.8	Ball mill for grinding coal with integral drying chamber	259
Figure 7.9	Two types of vertical spindle mill for grinding coal	260
Figure 7.10	Sardon Saxifrage Mill showing a sectional view	262
Figure 7.11	Coal mill thoughput vs fineness	264
Figure 7.12	Schematic of typical direct firing system applied to a cement kiln	266
Figure 7.13	Schematic of typical indirect firing system	267
Figure 7.14	Coal mill heat balance	272
Figure 7.15	Coal mill inlet temperatures required to dry coal from various raw coal moistures to a fine coal moisture of 2% for various mill airflows showing the effect of false air	273
Figure 7.16	Coal mill thoughput vs coal moisture	273
Figure 7.17	Schematic of a typical fine coal storage bin showing the principle instrumentation	276
Figure 7.18	Examples of volumetric fine coal feeders showing screw feeder and rotary valve	278
Figure 7.19	Schematic of an impact weigher	280
Figure 7.20	Schematic of a loss in weight fine coal feeder system	281
Figure 7.21	Pfister rotor fine coal weighfeeder	282
Figure 7.22	CERL Riffle box for Pulverised coal Distribution	283
Figure 8.1	Sources of error in temperature measurement using thermocouples and resistance thermometers	295
Figure 8.2	Suction pyrometer	296
Figure 8.3	Venturi-pneumatic pyrometer	297
Figure 8.4	Principle of remote temperature measurement using infrared radiation	298
Figure 8.5	Principle of ultrasonic temperature and flow measurement	299
Figure 8.6	Schematic of a Schenck type belt weigher	300
Figure 8.7	Schematic of a conventional flue gas sampling system	307
Figure 8.8	Typical flue gas sampling probe installation	308
Figure 8.9	Water-cooled hot gas portable sampling probe designed by the authors	309
Figure 8.10	A water-cooled probe employing automatic pneumatic cleaning	309
Figure 8.11	the principle of the dilution extractive gas sampling probe	310

Figure 8.12	Schematic of cross-duct optical obscuration dust monitor and backscatter device	311
Figure 8.13	A high temperature (700–1700°C) zirconia analyser for flue gas oxygen measurement showing a cross section of the cell	313
Figure 8.14	Procal folded beam in-situ flue gas analyser	315
Figure 8.15	An Opsis cross-duct multi-component optical gas analyser	316
Figure 8.16	The fire triangle	318
Figure 8.17	Typical furnace start sequence – actual configuration will vary with furnace application and compliance requirements	320
Figure 8.18	Principle of fail safe relay logic employed in BMS systems	325
Figure 8.19	Example of fault tree analysis	330
Figure 8.20	Example of two flow transmitters (4-20 mA) are used to prove combustion air flow using redundancy	331
Figure 8.21	Logic associated with three flow transmitters (4-20 mA) used to prove combustion air flow and reduce spurious trips	332
Figure 8.22	Ultra-violet and infra red wavelength compared with visible light	333
Figure 8.23	Principle of flame ionisation showing half wave rectification of the current	335
Figure 9.1	Schematic diagram of a generic furnace process showing flows through the system	340
Figure 9.2	Plot of typical furnace performance	344
Figure 9.3	Distribution of thermal quantities data	344
Figure 9.4	Plant trials using a suction pyrometer to measure combustion air temperature and an optical pyrometer to measure product discharge temperature	347
Figure 9.5	Process flowsheet with envelopes	352
Figure 9.6	Energy conversion trianges	363
Figure 9.7	Temerature–enthalpy data for cement, lime and alumina production	365
Figure 9.8	Composite curves for hot and cold streams for pinch analysis	366
Figure 9.9	Types of flow path configurations through recuperative heat exchangers	369
Figure 9.10	Relationship between heat transfer rate and surface area for different recuperative heat exchanger flow regimes	369
Figure 9.11	Types of flow path configurations through regenerative heat exchangers	373
Figure 9.12	Process flowsheet with air preheat option	374
Figure 9.13	Process flowsheet with air preheat and convection section options	375
Figure 10.1	The structures in which nitrogen is commonly bound in heavy oil and coal fuels	385
Figure 10.2	A simplified schematic representation of the paths of NO_x formation	386
Figure 10.3	A schematic representation of the role of HCN in the NO_x formation process	386

Figure 10.4	The temperature dependence of the NO_x formation process	387
Figure 10.5	The structure of Dioxins	391
Figure 10.6	Soot burning times for 500 Å particle at an oxygen partial pressure of 0.05 bar	395
Figure 10.7	Tendency of fuels to smoke in relation to their composition	396
Figure 10.8	Schematic mechanism for soot formation, showing the influence of reaction time and temperature	397
Figure 10.9	Typical ash structures	398
Figure 10.10	Mechanisms for ash formation	399
Figure 10.11	An example of the trade-off between NO and CO emissions, here from an internal combustion engine, which operates as pre-mixed flame	404
Figure 10.12	Effect of stoichiometry on NO_x emissions for diffusion and premixed flames	405
Figure 10.13	The effect of FGR on NO_x emissions in an oil fired boiler	406
Figure 10.14	An aerodynamically air staged burner	407
Figure 10.15	The principal of "reburn" illustrated schematically	407
Figure 10.16	The principal of reburn applied to an entire boiler	408
Figure 10.17	The principal of CO_2 sequestration using oxy-fuel combustion	411
Figure 10.18	Post-combustion gas composition from coal burned in a mixture of oxygen and recycled flue gas	412
Figure 11.1	Basic types of furnace showing direct fired and indirect fired	419
Figure 11.2	Typical brick lining construction showing alternative layers of bricks and expansion joints with casing reinforcing	420
Figure 11.3	Typical monolithic lining held to the shell by anchors	420
Figure 11.4	Typical ceramic fibre lining showing fixing details on the right	421
Figure 11.5	Brick failure caused by inadequate allowance for expansion	422
Figure 11.6	Tapered brick being installed in a rotary kiln; note the purpose built support frame to facilitate quick and accurate installation	423
Figure 11.7	Typical anchors for installation of castable refractory as manufactured by Refractory Anchors Inc	425
Figure 11.8	Use of split mould formwork to cast refractory on a burner pipe	426
Figure 11.9	Gunning refractory into place in a rotary kiln	427
Figure 11.10	Strength development during curing of castable refractory	428
Figure 11.11	Failure of an A 316 spun cast burner tube	430
Figure 11.12	Typical furnace arch construction	431
Figure 11.13	An example of an internally tiled furnace flat roof	432
Figure 11.14	Simplified schematic of closed cooling system and open circuit cooling system	434
Figure 11.15	Effect of raw materials on refractory properties	436
Figure 11.16	Example of alloying element providing strength to a metal by distortions of the crystal structure	443
Figure 11.17	Schematic illustration of how a passive oxide layer protects the metal	444
Figure 11.18	Example of intergranular decay in austenitic stainless steel	447

Figure 12.1	Design Constraints	463
Figure 12.2	Evolutionary development of the rotary kiln cement making process	465
Figure 12.3	The design process	466
Figure 12.4	Furnace process functions within the overall manufacturing process	467
Figure 12.5	Schematics of cross flow and counter flow recuperators and regenerative heat wheel for preheating combustion air	481
Figure 12.6	Time-temperature-enthalpy diagram for metal slab heating	485
Figure 12.7	Time-temperature-enthalpy diagram for multi-component oil heating	485
Figure 12.8	Time-temperature-enthalpy diagram for mineral aggregate processing	486
Figure 12.9	Temperature-enthalpy relationships for metal slab. Oil and aggregate heating processes	486
Figure 12.10	Schematic diagram of a typical single zone re-heating furnace	491
Figure 12.11	Effect of slab length on principal parameters in the design of a heating furnace	492
Figure 12.12	Schematic diagram of a typical rectangular tube-still heater	494
Figure 12.13	Effect of furnace height on principal parameters in the design of a rectangular oil heating furnace	497
Figure 12.14	Effect of furnace height on principal parameters in the design of a cylindrical oil heating furnace	498
Figure 12.15	Effect of kiln diameter on principal parameters in the design of a shaft kiln	499
Figure 12.16	Schematic of shaft kiln with integral product cooling and air preheating	500
Figure 12.17	Surface heat flux profile for slab heating	502
Figure 12.18	Surface heat flux to outside of tube for oil heating	502
Figure 12.19	Surface heat flux to lump for aggregate processing	503
Figure 12.20	Effect of adjacent burners on measured flame temperature of the centre burner of a set of three	503
Figure 13.1	General arrangement of 3 zone slab reheating furnace	521
Figure 14.1	The Everett lime sludge kiln with a schematic of the internal fittings	542
Figure 14.2	Typical temperature profiles in a lime sludge kiln	542
Figure 14.3	The multi-fuel burner nozzle with a cross section of a gas port	545
Figure 14.4	Isometric sketch of the multi-fuel burner	547
Figure 14.5	Everett kiln flames for all fuels	547
Figure 14.6	Simplified process flow diagram of the Alcoa calciner system showing the sampling points	550
Figure 14.7	The double valve lock and seal system allowing safe probe insertion and withdrawal	552

Figure 14.8 Acid Alkali Model of main furnace combustion showing normal operation on the left and intermittent unstable conditions in the centre and to the right 554
Figure 14.9 The 3-dimensional grid used for the CFD modelling 556
Figure 14.10 Photograph of the computer screen showing two CFD Modelling results 556
Figure 14.11 Example of the air and particle velocity profiles in the flash furnace showing a slice model and 3-D model 557
Figure 14.12 Example of the particle concentration profiles in the flash furnace 558
Figure 14.13 Schematic of typical tubular steam reforming plant 559
Figure 14.14 Schematic of a phosphoric acid fuel cell 561
Figure 14.15 The Haldor Topsoe convective heat exchange reformer 562
Figure 14.16 Multi-fuel burner for convective heat exchange reformer 563
Figure 14.17 The acid alkali model set up 565
Figure 14.18 Typical flames simulated using acid alkali modelling 568
Figure 14.19 Typical plot of flame length versus excess oxygen predicted by acid alkali modelling 568
Figure 14.20 Predicted heat flux profile for normal operation with anode off-gas 569
Figure 14.21 Likely failure mechanism of silicon carbide burner nozzle 570
Figure 14.22 The temporary test facility for the tri-fuel burner 571
Figure 14.23 Simplified process flow diagram for a typical fuel cell stationary PAFC system 572
Figure 14.24 Residual oil cabin heater supplying delayed coker plant 574
Figure 14.25 Predicted heat flux profiles for current operation and for proposed low excess air operation 576
Figure 14.26 The physical model set up for airflow measurement following the installation of windbox entry splitters 577
Figure 14.27 Existing air distribution determined using physical modelling 578
Figure 14.28 The improved air distribution achieved by physical modelling 579
Figure 14.29 Schematic of the existing swirl burners 580
Figure 14.30 Schematic of the modified burners 581
Figure 14.31 Simplified process flow diagram for dry process cement manufacture 583
Figure 14.32 View of the cooler offset elbows showing the resulting airflow pattern 586
Figure 14.33 Model of coolers and burner shown with kiln tube removed 591
Figure 14.34 Model of existing firing conditions, note the dark region of unmixed alkali in the vortex core 591
Figure 14.35 Predicted heat flux profile for exiting gas-firing conditions 592
Figure 14.36 Acid alkali model simulation for high momentum swirled primary air 594
Figure 14.37 Predicted heat flux profile for the proposed gas-firing conditions 595
Figure 14.38 Comparison of existing and scaled up cement kiln dimensions 596

Figure 14.39 Schematic of the submerged combustion direct reduction smelter 598
Figure 14.40 Simplified process flow diagram of rotary drum coal drying system 599
Figure 14.41 A coal dust explosion in a grinding mill – test undertaken at the HSE Buxton Research Laboratory 601
Figure 14.42 The original coal firing system installed on the plant 602
Figure 14.43 Location of sample points used to measure operational data with portable instrumentation 603
Figure 14.44 The overall mass and energy balance for the preheater kiln
Figure 14.45 Cooler mass and energy balance 604
Figure 14.46 Process and instrument diagram of revised coal grinding and firing system 605
Figure 14.47 Performance of the preheater kiln prior to and following the upgrade 606
Figure 15.1. CO_2 capture processes 613
Figure 15.2. Costs for Transportation of CO_2 617
Figure 15.3. Geological Storage Options 620
Figure 15.4. Ocean Storage Options for CO_2 621

List of Tables

Table 1.1	Examples of furnaces meeting the classifications specified in figure 1.3	6
Table 2.1	The characteristics of furnace flames with and without external recirculation	52
Table 2.2	The comparative characteristics of simple enclosed jet theories	54
Table 3.1	Typical natural gas compositions as supplied to customers	70
Table 3.2	Raw compositions of a few manufactured gases	70
Table 3.3	Flammable limits for gases at room temperature	73
Table 3.4	Typical properties of selected petroleum based furnace fuels	76
Table 3.5	Characteristic properties of selected solid fuels	78
Table 4.1	Convective heat transfer correlations for a number of common geometries	105
Table 4.2	Total emissivity of some common materials at room temperature	117
Table 4.3	Materials used for resistance heating elements	127
Table 5.1	Comparison between original and new scaled-up kilns	195
Table 6.1	Hierarchy of turbulence models	233
Table 6.2	Typical diffusion coefficients and source terms	234
Table 6.3	Comparative merits of modelling methods	237
Table 7.1	General comparison between ball, vertical spindle and high speed mills	258
Table 7.2	Comparison between direct and indirect firing systems	270
Table 8.1	Typical flue gas analysis for heavy fuel oil showing the difference between wet and dry oxygen proportions	303
Table 8.2	Summary of flue gas species analysis techniques	305
Table 8.3	Comparison between basic extractive gas sampling and in-situ gas analysis systems	306
Table 8.4	Safety integrity level defined by IEC standard 61508	328
Table 9.1	Energy flows relating to Figure 9.1	341
Table 9.2	Process measurements	351
Table 9.3	Selected fuel data	352
Table 9.4	Mass balance for the process	354
Table 9.5	Energy balance for the process	356
Table 9.6	Mass Balance for the furnace	359
Table 9.7	Energy balance for the furnace	361
Table 9.8	Energy balance for the process with reduced in-leakage and balanced burner flows	362

Table 9.9	Maximum energy conversion for various processes based on Figure 9.12	369
Table 9.10	Common types of recuperative heat exchangers used in furnace operations	371
Table 9.11	Common types of regenerative heat exchangers used in furnace operations	374
Table 9.12	Energy balance for the process with combustion air preheating	375
Table 9.13	Energy balance for the process with combustion air preheating	376
Table 10.1	Rate constants for thermal NO_x equations	385
Table 10.2	Occurrence of prompt NO_x for some combustion processes	388
Table 10.3	Chemical pathways to the formation of acid mist	389
Table 10.4	World Health Organisation total equivalence factors for human risk assessment of PBCs, dioxins and furans	392
Table 10.5	Estimated Dioxin and Furan Emissions in the UK	393
Table 11.1	Characteristics of the main classifications of stainless steels	445
Table A11.1	General properties of Silica and Siliceous refractory materials	451
Table A11.2	General properties of Alumina and Aluminous refractory materials	452
Table A11.3	General properties of Chromite/Magnesite refractory materials	453
Table A11.4	General properties of Magnesite/Alumina refractory materials	454
Table A11.5	General properties of Dolomite, Zirconia, and Carbon refractory materials	455
Table A11.6	General properties of insulating refractory bricks	456
Table A11.7	General properties of insulating refractory board, blanket and loose fill	457
Table 12.1	Ash analysis for several South Australian lignites	475
Table 12.2	Furnace design data derived from figures 12.6, 12.7 and 12.8	487
Table 12.3	Calculation of heat transfer areas and average furnace heat flux for design examples	488
Table 12.4	Input data for well-stirred furnace model analysis	490
Table 12.5	Well-stirred furnace analysis of slab heating furnace designs	492
Table 12.6	Well-stirred furnace analysis of rectangular oil heating furnace designs	495
Table 12.7	Well-stirred furnace analysis of cylindrical oil heating furnace designs	496
Table 12.8	Well-stirred furnace analysis of aggregate processing shaft furnace designs	499
Table 12.9	Analyses of the effect of kiln diameter on pressure drop through packed bed of aggregate	500
Table 12.10	Well-stirred furnace analysis of aggregate processing shaft furnace designs including integral product cooling by combustion air	501
Table 12.11	Manufacturer's technical data on nozzle mixing gas burner for slab heating furnace	503
Table 13.1	Methodology of categorising detailed cost analysis	511
Table 13.2	Financial performance ratios	515
Table 13.3	Levels of cost estimation	517

Table 13.4	Typical scaling factors for costs of standard equipment	518
Table 13.5	Determination of Lang factor for a heat exchanger	519
Table 13.6	Summary of WSF modelling of reheating furnace – oil fired base case	523
Table 13.7	Summary of modelling for case 1 – re-brick with no insulation	524
Table 13.8	Summary of modelling for case 2 – conversion to natural gas	524
Table 13.9	Summary of modelling for case 3 – conversion to natural gas with new calcium silicate lining	525
Table 13.10	Summary of modelling for case 4 – reinstate stack recuperators	525
Table 13.11	Summary of modelling for case 5 – conversion to blast furnace gas with stack recuperators	526
Table 13.12	Summary of modelling for case 6 – install self-recuperative burners	526
Table 13.13	Summary of modelling for case 7 – Oxygen enrichment	527
Table 13.14	Summary of process modelling data required for economic study	528
Table 13.15	Summary of process operating cost data required for economic study	528
Table 13.16	Base case costing sheet	529
Table 13.17	Re-brick with no insulation costing sheet	529
Table 13.18	Conversion to natural gas costing sheet	530
Table 13.19	Conversion to natural gas with new lining costing sheet	530
Table 13.20	Reinstate stack recuperators costing sheet	531
Table 13.21	Conversion to blast furnace gas with stack recuperators costing sheet	532
Table 13.22	Install self-recuperative burners costing sheet	533
Table 13.23	Oxygen enrichment costing sheet	534
Table 13.24	Variable cost analysis for case options	535
Table 13.25	Analysis of investment potential for projects	536
Table 13.26	Relationship between capital cost and project payback	537
Table 14.1	Typical dewatered catalytic steam reformer gas properties	560
Table 14.2	Acid and alkali concentrations used to represent the different fuels	567
Table 14.3	Typical cement kiln raw mix feed	583
Table 14.4	Comparison between existing wet kilns and the new large dry process kilns	585
Table 14.5	Operational data collected from temporary and plant instrumentation	588
Table 14.6	Comparison of existing and scaled up cement kiln operating parameters	588
Table 15.1	Absorption options for CO_2 capture	614
Table 15.2	Variation of CO_2 control cost predictions for a large scale project	617
Table 15.3	Existing Carbon Dioxide Pipelines	619

Chapter 1

Introduction

Chapter contents

1.1 What is a Furnace? 3
1.2 Where are Furnaces Used? Brief Review of Current Furnace Applications and Technology 7
1.3 Drivers for Improved Efficiency 28
1.4 Concluding Remarks 29
References 30

Combustion and furnaces are the very heart of our society. Furnaces and kilns are used to produce virtually everything we use and many of our food and drink items, either directly such as the metal products used in everyday life, the packaging for our food and drink or indirectly such as the tools that are used to grow that food. Even a natural product, such as timber, requires drying to make it suitable for most uses, and that drying occurs in a kiln.

From the earliest days of human existence food was cooked over open fires and sticks were charred to harden them. However, open fires provided little control over the heating process, and the birth of the Bronze Age some 5000-6000 years ago would have required the construction of a forced draft furnace to achieve the temperature required to smelt the ore and produce liquid metal for casting. Metal production remained small scale for centuries owing to the scarcity of suitable fuel (charcoal) and the high cost of its production. The breakthrough came as a result of the determination and tenacity of Abraham Darby who worked much of his life to reduce the cost of cast iron by using coke in place of charcoal. He finally succeeded and a lasting testament to his work is the world's first iron bridge, completed in 1779 crossing the River Seven at Coalbrookdale in North West England, Figure 1.1.

Darby's pioneering work laid the foundations for the industrial revolution because iron production was no longer constrained by fuel supply and blast furnaces proliferated in the Severn Valley and even changed the way artists perceived the landscape, as exemplified in Philip James de Loutherbourg's famous landscape *"Coalbrookdale by Night"* now exhibited in the Science Museum, London. In addition to pioneering the use of coke, Darby also utilised steam engines for powering his furnace bellows and hence make the operation far less dependent on water power and less reliant on local rainfall, which



Figure 1.1 The iron bridge at Coalbrookdale showing the detail adjacent to an abutment and "Coalbrookdale by Night" - Philip James de Loutherbourg

was problematic and on many occasions drought had interrupted production for long periods. By establishing his furnaces independence of the vagaries of the charcoal burners and the weather, Darby triggered an industrial revolution that is continuing to this day.

The vast majority of the materials we use, and the food and drink we consume, have been heated at some stage during the production process. Combustion processes are conveniently divided into high and low temperature process. Although there is no strict dividing line between the two, processes with wall temperatures below 400-500°C are often considered low temperature, while those above 500-800°C are generally considered high temperature. High temperature processes include, cement and lime manufacture, brick and ceramic manufacture, most metal processing, glass making, etc., while low temperature processes include drying processes, food processing and sterilisation, steam raising, oil refining, etc..

It is much more difficult to ensure efficient use of the fuel's energy in high temperature processes than their low temperature counterparts. For low temperature processes, such as steam raising, efficiencies of over 80% are commonly obtained, whereas for high temperature processes, efficiencies exceeding 50% are rare. Furnace design engineers of the future will be required to maximise overall process efficiency in a carbon constrained world. This requirement will be driven both, by the community need to achieve greenhouse gas reduction, as well as the process economics owing to high fossil fuel costs, especially for processes requiring premium fuels, such as oil and gas. The aim of this book is to assist engineers to achieve higher performance both from existing, and from new furnace designs, by providing the readers access to the tools that assist with gaining an in depth understanding of the fundamentals of the individual processes. The book does not attempt to provide an in-depth understanding of any individual process because that would require a book in itself, for each industry, as can be seen from the wide variety of furnaces outlined in this introduction. In any case, we consider that the weakness of that approach is that the knowledge remains confined to that particular industry. For example, the excellent kiln efficiencies achieved by the lime industry were almost unknown in the pulp and paper industry in the early 1980s hence their lime kilns used some 30–50% more fuel than those in the mainstream industry at that time.

1.1 What is a Furnace?

The Oxford English Dictionary defines a furnace as "*an enclosed structure for intense heating by fire, esp. of metals, or water*", whereas a kiln is described as "*as furnace or oven for burning, baking or drying, esp. for calcining lime or firing pottery*". In reality, there is little

difference between the two, kilns and furnaces both operating within a similar temperature range. The two names owe more to tradition than to functional differences.

Furnaces are the basic building block of our industrial society, indeed they are the foundation of our entire civilisation, as shown above. The principle objective of a furnace is to attain a higher processing temperature than can be achieved in the open air. Although some processes could be carried out in the open air, to do so would be far less efficient, the fuel consumption would be much higher and control of the process would be much more difficult.

Furnaces can be used to facilitate a wide range of chemical reactions, or in some cases to simply undertake physical processes, such as annealing or drying. Design of the former is normally more complex than the latter but not exclusively so. One of the challenges of furnace design is to determine the critical rate determining step(s) and to ensure that these are effectively addressed in the design. By achieving this, smaller more efficient furnaces and more cost effective designs can often be developed.

In this book we shall be dealing with furnaces for processing materials at high temperatures, that is, above 400°C, especially those where the product is directly exposed to the flame. We shall not discuss steam boilers, the design and manufacture of which is a highly specialised subject. In any case steam boilers have reached such high efficiencies that only marginal gains are possible. Future gains in the efficiency of electricity generation, for example, depend on improving the cycle efficiency; while this will impact on boiler design that is not where the gains will originate. Readers should consult Babcock and Wilcox (2005) for further information on boiler design.

1.1.1 Furnace Outline

The basic concept of a furnace is shown in Figure 1.2, below.

Heat is liberated by burning fuel with air (or oxygen), or from electrical energy, and some of this heat is transferred to the product. The

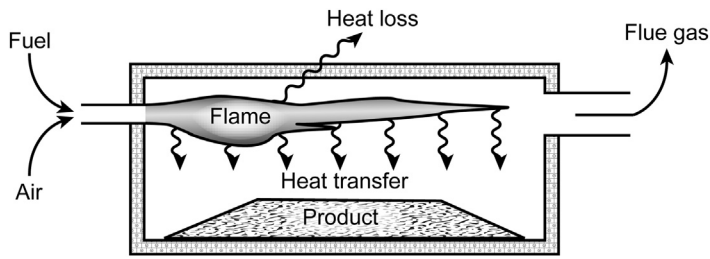


Figure 1.2 The Basic Elements of a Furnace

remaining heat leaves in the flue gas and through openings such as charging doors, or is lost from the external surface. The efficiency of the furnace can be defined as:

$$\dot{\eta} = Q_p / Q_s \tag{1.1}$$

where

$\dot{\eta}$ = furnace efficiency,
Q_p = heat embedded in the final product,
Q_s = heat supplied by combustion.

The heat embedded in the product is often quite small compared with the overall heat supplied, much heat being lost in the flue gases and by-products or waste materials such as slag. While equation 1 is a general expression for efficiency and is equally applicable to boilers etc, it has many limitations with respect to determining the effectiveness of a furnace. Later we shall examine other, more useful, measures of furnace performance.

1.1.2 Furnace Classification

There are an almost infinite number of ways of classifying furnaces, e.g. by shape, industry, product, etc., but a very simple classification based on the heat transfer concepts of the type heat source and the type of heat sink is shown in Figure 1.3. This classification system is highly simplified but it is useful because the nature of the product, the type of fuel, and the heat transfer mechanism all have a major influence on the physical arrangement of the furnace. It should be noted that many furnaces have multiple heat sinks and use several fuels, either concurrently of alternatively, which also affects the furnace design. Examples of furnaces falling in the classifications shown in Figure 1.3 are provided in Table 1.1. Descriptions and illustrations of a wide range of furnaces meeting the classification shown in Figure 1.3 follow later in this chapter. We will also refer to Figure 1.3 when considering the design of furnaces in chapter 12.

1.1.3 Principle Objectives of Furnace Designers and Operators

1. Obtain a satisfactory product
2. Use minimum fuel and energy to achieve that product
3. Construct the furnace for the lowest capital cost
4. Operate with the lowest possible manning levels
5. Achieve a satisfactorily long life with low maintenance costs

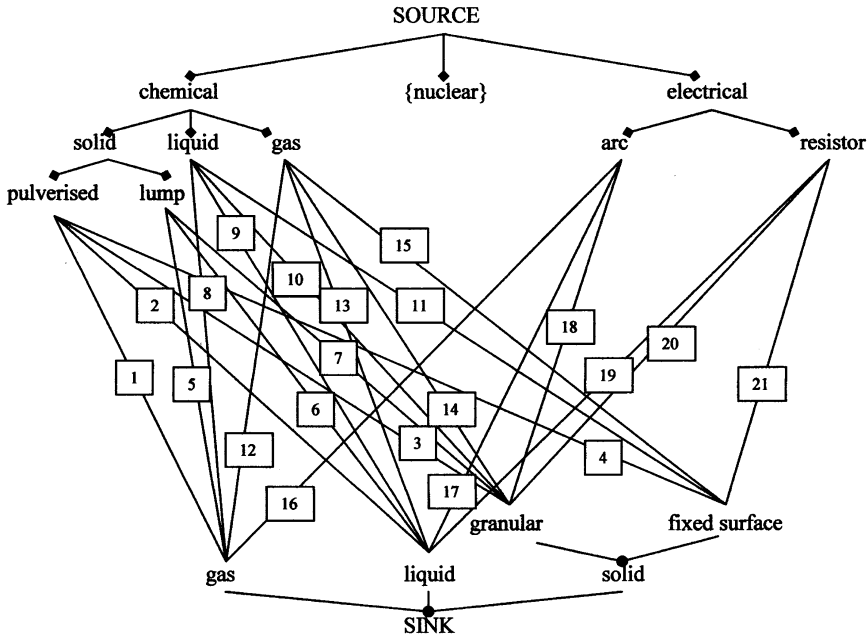


Figure 1.3 Classification of Furnaces

Table 1.1 Examples of Furnaces Meeting the Classifications Specified in Figure 1.3

Classification number	*Example of Type of Furnace*
1	watertube boiler
2	water or thermal fluid heater
3	rotary kiln, moving or rotary hearth
4	open hearth furnace
5	Fixed or moving grate with steam tubes
6	tubestill cabin heater
7	fluidised bed, multi-hearth furnace
8	refinery cracking furnace
9	tubestill heater, firetube boiler
10	rotary kiln, fluidised bed, flash heating furnace, shaft kiln, moving or rotary hearth
11	open hearth furnace, glass tank, metal reheating furnace
12	refinery cracking furnace, reformer furnace, air heater
13	firetube boiler, tubestill heater metal reheating furnace
14	rotary kiln, fluidised bed, flash heating furnace, shaft kiln, moving or rotary hearth
15	open hearth furnace, glass tank, metal reheating furnace
16	Plasma furnace
17	molten metal arc furnace
18	metal melting arc and induction furnaces
19	molten metal immersion heaters, glass tank bed heating
20	muffle furnace
21	Batch heater, annealing furnace

Objective 1 overrides all others because, if the product is unsatisfactory, then it cannot be sold or must be sold for an inferior price. While safety has not been mentioned in the above objectives, it can be taken as "a given" in today's environment and is covered extensively in chapter 8.

The art of furnace design involves achieving the best combination of these five objectives over the entire life of the furnace, in other words to produce a high quality product at the lowest achievable cost. Although these five objectives may seem self evident, in our experience they are not always achieved. Furnace users have generally purchased on the basis of capital cost, understandably so, given that the other objectives are much more difficult to assess at the tendering stage. This approach has led to relatively little engineering effort being expended on improving existing designs because engineering time is expensive and the costs are difficult to recoup for the furnace builder. However, an era of higher fuel and energy costs will put new demands on designers and operators of furnaces, forcing a new approach for many applications.

This book aims to provide designers and operators with the tools to achieve the best combination of the above five objectives for their particular process and hence meet the future challenges. Our approach is to consider the basic issues that affect furnace performance from first principals then to build a design methodology on these considerations. We hope that this approach will eventually supersede traditional techniques and achieve significant gains in practical furnace efficiency.

1.2 Where are Furnaces Used? Brief Review of Current Furnace Applications and Technology

Before examining the principles behind furnace design, we have reviewed a few of the furnaces in common use, largely for the benefit of those new to the field but also for those who have worked in one specific industry and have not been exposed to the wide variety of furnace employed in other industries.

1.2.1 Ceramics, Brick Making and Pottery

Ancient pottery and brick kilns are the precursors of modern furnaces. Pottery kilns arose to satisfy the need for durable containers for food and drink. Pottery from as early as 6000 BC was found during excavation of a Neolithic site near Catal Huyuk in central Anatolia (Raymond 1984). On this basis, high temperature furnace technology (pottery furnaces typically operate around 1000°C) is some 8000 years

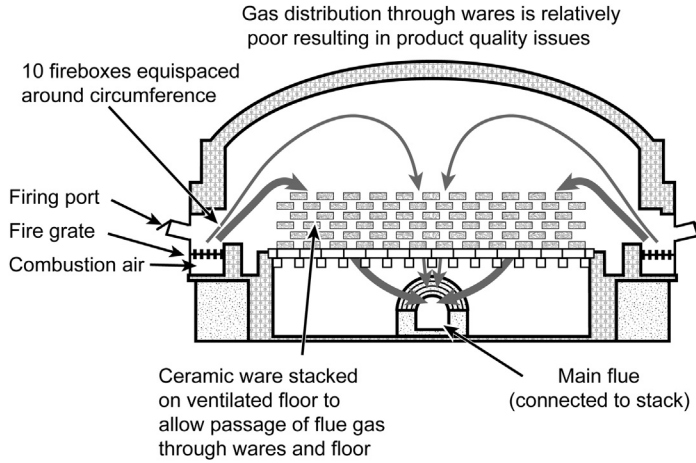


Figure 1.4 Cross section through a traditional downdraught pottery batch kiln

old. These early furnaces were very inefficient because the energy required for the chemical changes is quite small but the energy consumed in heating up the pottery and the furnace structure was large and was lost when the furnace and products were allowed to cool prior to being recovered for use. An example is the beehive kiln shown in Figure 1.4. This kiln is first stacked with ware and the entrances are then bricked up and fires lit around the periphery. The flue gases are extracted via a porous floor with flues underneath (downdraft). Some designs have a flue in the centre roof and are known as updraft kilns. At the end of the firing period the structure is allowed to cool and the entrances unbricked and the fired pottery removed. All the residual heat in the pottery and kiln structure is lost. This design is obsolete and considerable advances have been made in efficiency in the ceramics industry, with high efficiency tunnel kilns with heat recovery from the product as well as batch kilns using low thermal mass structures and high-efficiency self recuperative burners.

1.2.2 Cement and Lime

Portland cement is a relatively recent invention, dating from 1824 when Joseph Aspdin was granted British Patent 5022 for "Portland Cement" (Francis 1977), but lime has been manufactured since prehistoric times (Boynton 1980). The first recorded large scale use of lime was in mortar and plaster by the ancient Egyptians between 4000 and 2000 BC.

Even the most modern lime kilns (except rotary kilns) can trace their linage back to the early pot or flare kilns. These were intermittent and had low energy efficiency owing to the sensible heat lost in heating and cooling the stone (Oates 1998).

The earliest continuous kiln was the mixed feed vertical shaft kiln where the charge and fuel were blended together prior to feeding to the top of the kiln or fed as separate streams with mixing occurring on entry, Figure 1.5. These improved efficiency because the incoming stone was preheated by the flue gas and the combustion air was preheated by cooling the lime. However they are very difficult to operate, since once the mixture has been fed to the kiln, there is no way of adjusting the heat input and this led to the development of the side fired shaft kiln, also shown in Figure 1.5. These are fired around the kiln circumference approximately one third of the way up where the shelter is located. The stone is calcined in this region with, as with the mixed feed kiln, the top of the kiln acting to recover heat from the combustion products by preheating the stone feed, while that below the burners recovers heat from the lime to preheat the combustion air.

While these mixed feed and side-fired shaft kilns are relatively efficient, the heat recovery is limited by the size of the packed bed of stone and has been improved by the twin shaft design, Figure 1.6. In this kiln, one shaft is fired while the other recovers

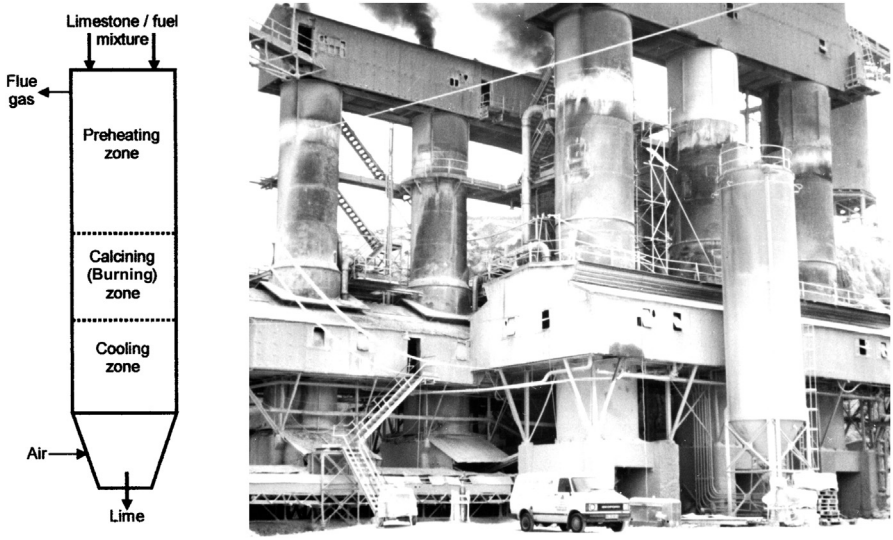


Figure 1.5 Schematic of a mixed feed vertical shaft lime kiln (left) and a battery of six oil fired vertical shaft lime kilns (right)

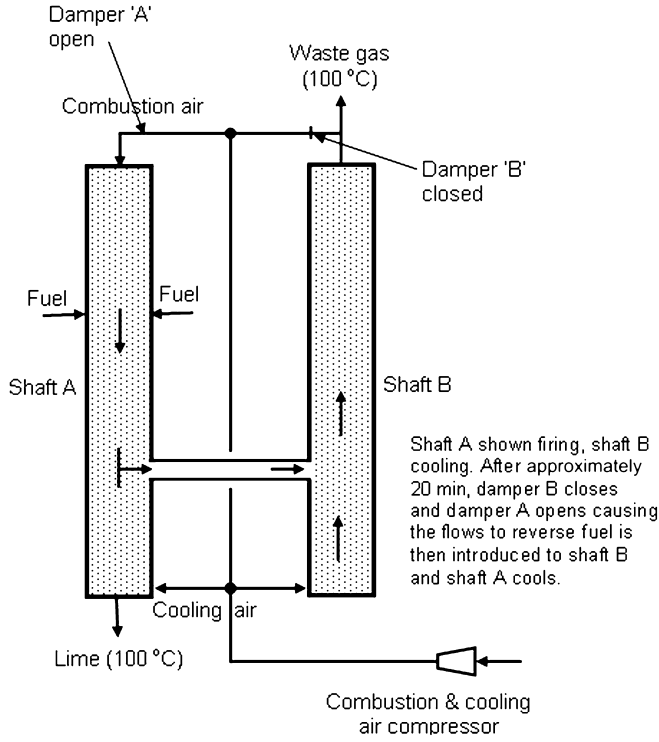


Figure 1.6 Twin shaft regenerative lime kiln

heat from the flue gas. Owing to the much larger packed bed available, the heat recovery is excellent and this kiln's fuel consumption is only slightly greater than the theoretical energy required for the endothermic calcining reaction. In operation, practical efficiencies exceed 80%, something the designers of all process furnaces can aspire to achieve.

Portland cement was first made in packed bed kilns, similar to lime and pottery kilns but indifferent quality and increasing demand drove the search for something better and led to the patenting of the rotary kiln by Ransome in 1885. Ransome's kiln was not a success, the cause being lack of effective control over the combustion and heat transfer processes. His early trials were brought to a dramatic end by an explosion of the gas producer plant. Further trials failed also owing to combustion and heat transfer related issues (Francis 1977 (2)). Success was finally achieved in 1885 at the Atlas and Alpha Cement Works in Allentown and Philadelphia, Pennsylvania, USA. By 1898 the process had been perfected by E.H. Hurry and H.J. Seaman and their design included pulverised coal firing, heat recovery from the product in

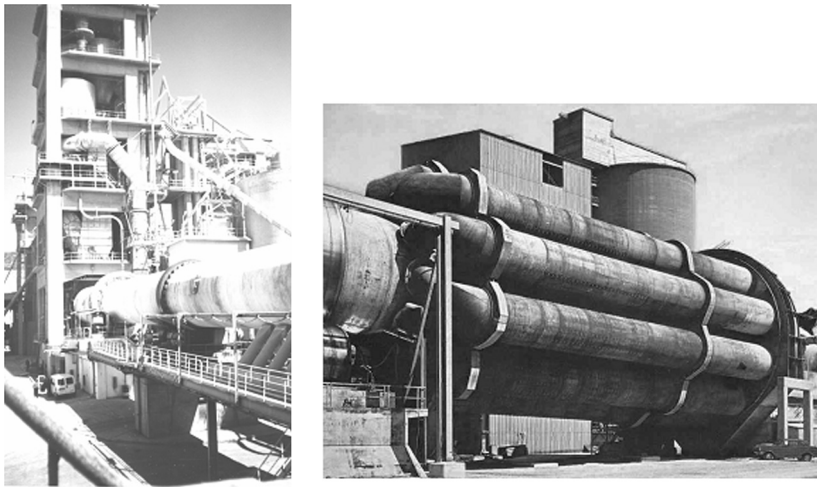


Figure 1.7 Modern cement kiln technology showing the cyclone preheater tower on the left and the satellite cooler on the right

the form of preheated combustion air and protection of the refractory lining by a layer of clinker product, all essential features of today's kilns (Francis 1977 (3)). Since its inception rotary kiln sizes have consistently increased to feed the world's hunger for cement to make concrete for the construction industry.

Modern cyclone preheater rotary kilns, Figure 1.7, produce up to 4000 tonne/day of cement clinker. Some cement kilns employ a separate calciner to undertake the de-carbonation reaction and these can produce up to 10,000 tonne/day of clinker. The high efficiency of these kilns is achieved by recovering heat from the combustion products by preheating the feed by direct contact in the cyclone preheater and also by recovering heat from the product by preheating the combustion air to 850-1000°C in the clinker cooler. Two types of cooler are in common use, the grate moving bed type and the satellite type, shown in Figure 1.7. These coolers rotate with the kiln and the hot clinker drops into the cooler through the elbows. During the clinker's passage through the cooler it is continually tumbled through the incoming combustion air and preheats it by direct contact heat exchange and very high combustion air temperatures are achieved. It will be shown later, that air preheating to high temperatures and flue gas heat recovery are important ways of achieving high efficiencies.

1.2.3 Glass Making

Like metal smelting, the early development of glass making is largely unknown. Glass making furnaces, known as "glass tanks" because

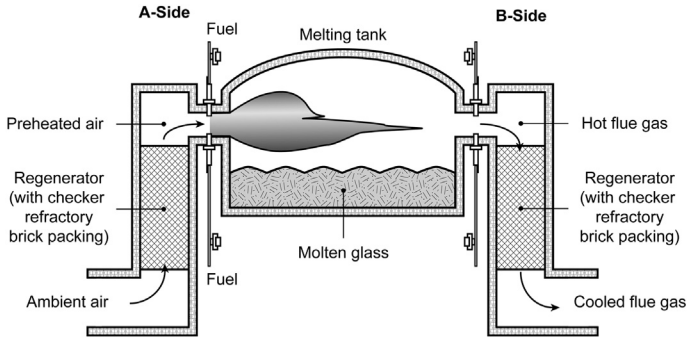


Figure 1.8 Schematic of a Regenerative Glass Tank

they house a bath of liquid glass, operate at temperatures around 1400–1600°C. Glass was originally made in small pot furnaces and expensive "craft" glasses are still made that way, but large scale production is mainly in regenerative open hearth furnaces similar to that developed by Sir William Siemens in the 1860s and, in the past, extensively used in the steel industry, Figure 1.8.

These furnaces are economical in fuel consumption owing to good heat recovery via the checker work regenerators. A few words describing how these operate is appropriate here. Firstly, the furnace is fired by the burners on the left hand side which draw their combustion air through the hot checker brickwork in the left hand regenerator. The incoming combustion air is preheated to ~1000°C by the hot brickwork. The hot combustion products exhaust via the regenerator on the right hand side and heat the checker brickwork in that regenerator. After approximately 20 minutes, the firing is reversed. The right hand burners commence firing, drawing their combustion air through the recently reheated checker brickwork in the right hand regenerator. The hot combustion products now exhaust via the left hand side regenerator and reheat that regenerator's checker brickwork. By regularly alternating the firing, combustion air preheat temperatures exceeding 1000 °C are achieved. These high air preheat temperatures give very high flame temperatures and result in high NO_x emissions. More recently, recuperative furnaces operating at low excess air and the substitution of air by oxygen have both been introduced, in an attempt to reduce NO_x emissions from glass production.

1.2.4 Metal Ore Smelting

The metals industry uses a wide range of furnaces for many applications, such as smelting (extracting metal from ore), refining, finishing and recycling. Metal smelting is still one of the major applications for high temperature furnaces. A few examples are outlined below.

While the advantages of metals were undoubtedly clear to early men given the naturally occurring native metals, such as gold or copper, extracting them from their ore was another matter. The earliest known copper smelting furnaces date from around 3500 BC and were found in the Sinai Desert, Israel in 1965 (Raymond (2) 1984). How metal smelting from ore was first achieved remains a mystery, the idea that it happened accidentally in a campfire can be discounted owing to the inability of open fires to reach the temperature required. Furthermore, the complexity of the process and the need for a reducing atmosphere make accidental smelting of metal in an open fire extremely unlikely. However, a pottery kiln has both the necessary temperature and, in parts of the kiln at least, a reducing atmosphere owing to the presence of carbon monoxide as consequence of incomplete combustion. However confirmation of this development awaits further archaeological discoveries.

As mentioned previously, Abraham Darby's pioneering work to smelt iron using coke in place of charcoal succeeded and led to the widespread use of the blast furnace. The production rate of modern blast furnaces, Figure 1.9, is orders of magnitude greater than that of Darby's furnace which, amazingly, still exits and can be visited by the public.

Blast furnaces require a nodular, or lump, feed to allow the passage of combustion air and gases so they are not suitable for smelting ores such as copper concentrate which is a finely divided powder. This is traditionally smelted in two stages:

- Chalcopyrite ore ($CuFeS_2$) is smelted in a reverbatory furnace, Figure 1.10, to produce copper matte ($Cu_2S.FeS$).
- The matte is converted to blister copper in a two-stage oxidation process to combine the iron into a silica slag and then oxidise the remaining sulphur to SO_2. This takes place in a Pierce-Smith converter, Figure 1.11.

Two stage processes are inherently expensive and usually less thermally efficient than single stage processes, owing to the cooling that occurs between stages and the higher heat losses associated with the large surface area of two furnaces. Consequentially, considerable effort was expended to produce blister copper directly from ore. The most successful is the Outokumpu process, which is a flash

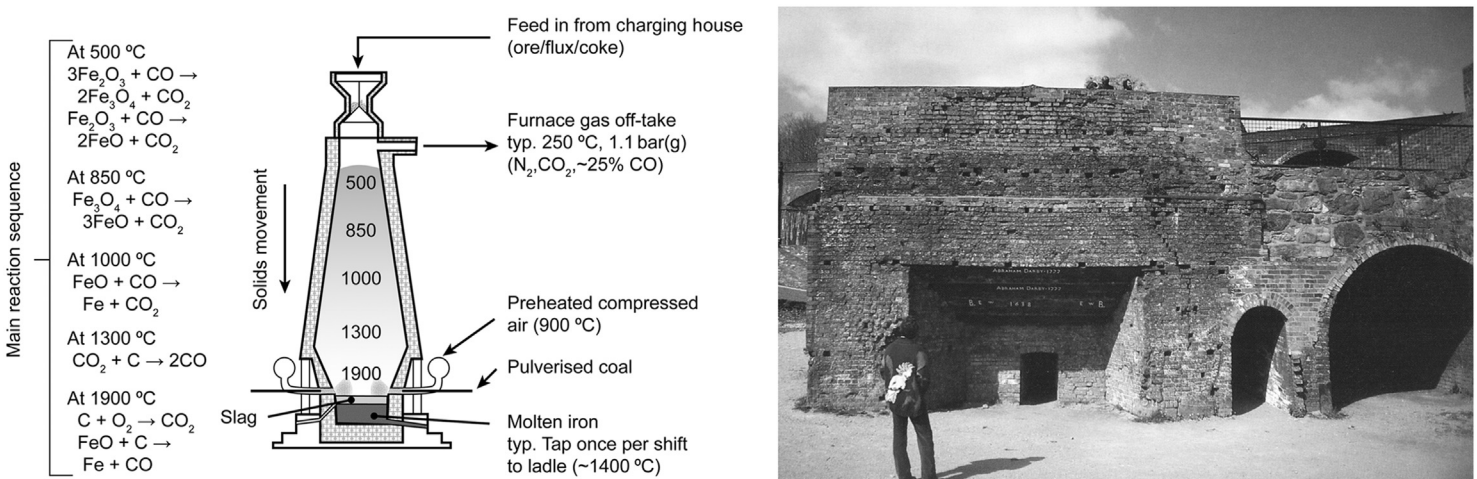


Figure 1.9 Schematic of a Modern Blast Furnace with Abraham Darby's pioneering furnace on the right

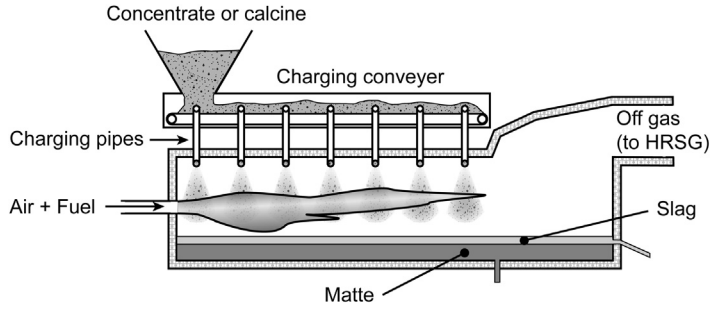


Figure 1.10 A Reverbatory Furnace for Smelting Copper Sulphide Ores

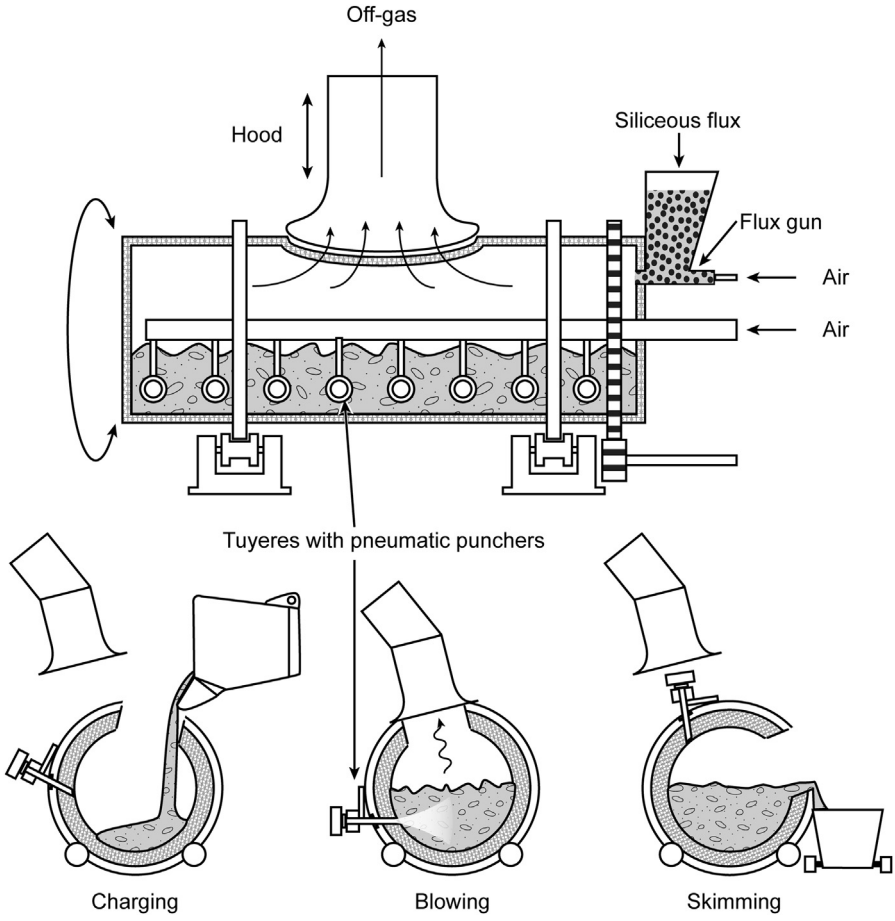


Figure 1.11 A Pierce-Smith converter

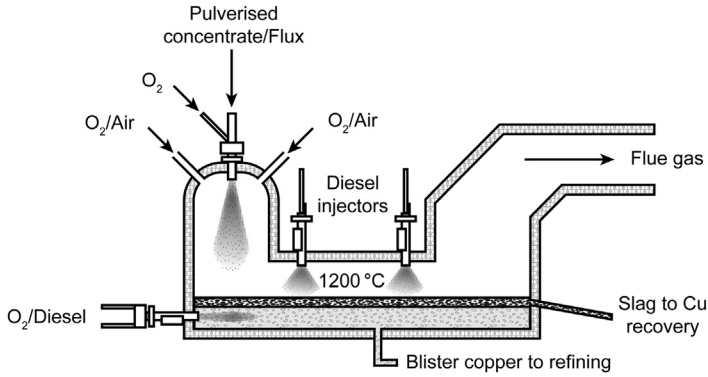


Figure 1.12 Outokumpu flash smelter for copper smelting

smelter combined with a heated bath to separate the slag and reduce the sulphur content of the melt, Figure 1.12. This process does not even require significant fuel input when oxygen enriched air is used, owing to the exothermic oxidation of the iron sulphide in the ore, so the smelting process is auto-thermal. The only fuel required is for preheating the flash furnace and maintaining the bath temperature to enable slag separation. This system is an excellent example of how a completely new approach to a traditional industry process can simultaneously gain a significantly higher thermal efficiency and reduce capital cost, compared with the traditional method.

1.2.5 Metal Refining

The copper produced by both the two stage process and the flash smelter is too high in sulphur for practical applications. Further reduction in sulphur takes place in another furnace that produces the molten copper that is cast into anodes for electro-refining. Firstly the sulphur is oxidised to SO_2 by blowing air through the molten blister copper, which also oxidises some of the copper. Then air blowing is replaced by gas blowing to reduce the oxidised copper back to metallic copper. The copper is cast into anodes on a continuous casting table, Figure 1.13. This thermal refining is a batch process whereas the flash smelter and anode casting is continuous, so two anode furnaces are installed to allow continuous operation.

Nickel sulphide ores are smelted by a similar process to the copper sulphide ores but the subsequent refining operation is largely a solvent extraction process until the final desulphurisation of the nickel briquettes. This operation is undertaken at 1000 °C in an atmosphere of hydrogen. All reducing atmosphere furnaces present special hazards owing to the flammable nature of the atmosphere which creates

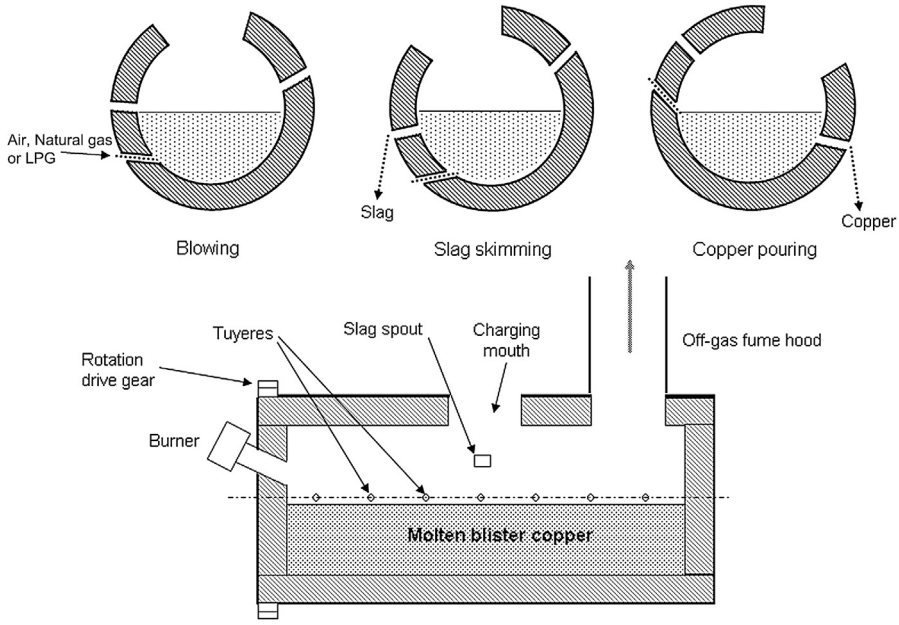


Figure 1.13 Cross section through a copper anode furnace showing the blowing, slag skimming and casting operations

an explosion risk but hydrogen at high temperature presents a special risk and great care has to be taken to prevent air ingress.

The hydrogen reacts with the residual sulphur to form H_2S, which along with the used hydrogen, is incinerated. A schematic of this furnace is shown in Figure 1.14. Two other reducing atmosphere furnaces are considered in section 1.2.9 later in this chapter.

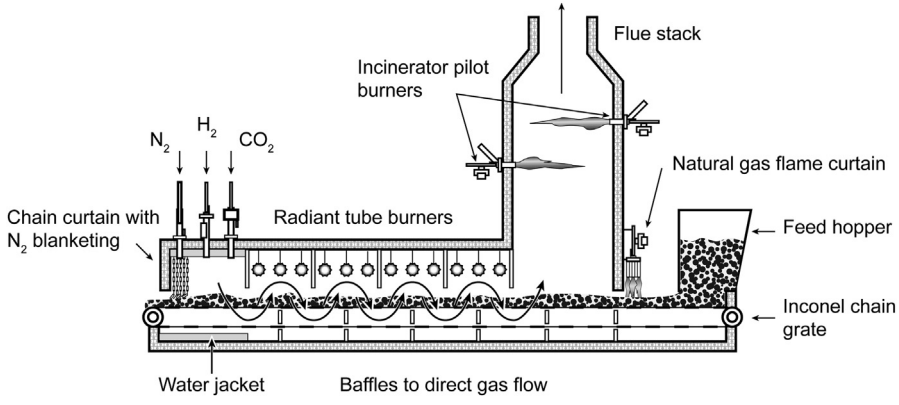


Figure 1.14 A hydrogen atmosphere furnace for de-sulphurisation of nickel briquettes

1.2.6 Flash and Fluid Bed Furnaces

Flash and fluid bed furnaces operate with the feed in suspension. The difference between them is based on concentration and residence time. In fluid bed furnaces the product must also remain in suspension, otherwise the bed agglomerates and de-fluidises. However, in some flash furnaces the product melts and is collected as a liquid.

Fluid bed furnaces utilise a high concentration of solids in air or process gas and a relatively long residence time. An example is the fluid bed furnace for roasting copper ore, prior to smelting in a reverbatory furnace, Figure 1.15. In the fluid bed roaster, the sulphides are partially oxidised to sulphates which reduces the SO_2 emissions from the smelting furnace (Biwas and Davenport 1980). This process is obsolescent, since the oxidation energy liberated in roasting is more efficiently used in a flash smelter, such as the Outokumpu unit described above. Fluid bed furnaces have seen limited use owing to difficulties in maintaining good air distribution through the bed, especially when scaled up, but are used in the alumina industry for calcining alumina tri-hydrate. They have also been used in the lime industry but with mixed success.

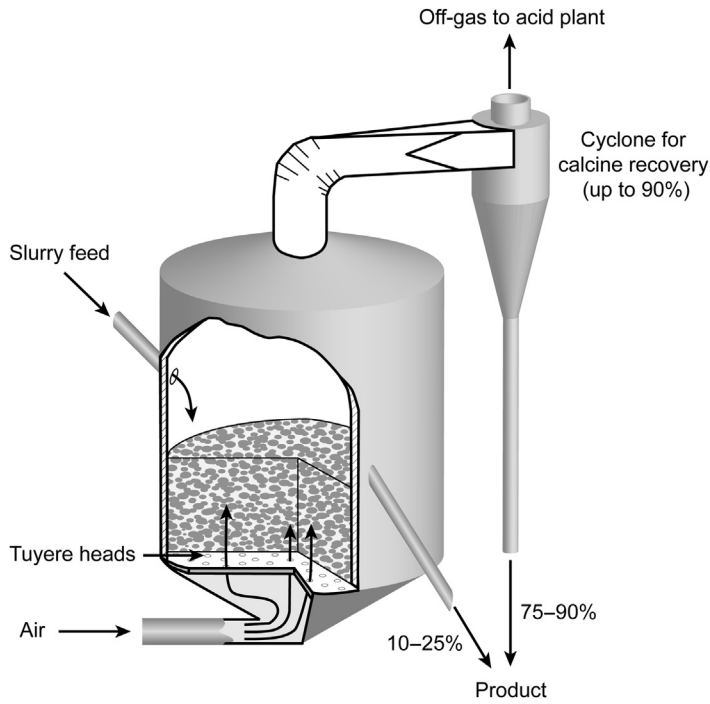


Figure 1.15 Fluid bed furnace for roasting copper ore

The flash furnace was conceived in the cement industry but, like the rotary kiln, could not initially be made to work (Martin 1932). They are so-called because of the short residence time of the product within the furnace. They should probably be called entrained flow furnaces and Martin called them suspension furnaces but flash furnace is the popular term in industry. These furnaces can only be used for pulverised material up to a few hundred micron particle size, whereas fluid bed furnaces need a particle size in the range 2–5 mm approximately, since smaller particles tend to be elutriated from the bed and lost. Flash furnaces can be upward flow or downward flow, both with or without swirl flow. The Outokumpu flash smelter is downward flow owing to the molten product, whereas most of those used in the alumina, cement and lime industries are upward flow, Figure 1.16. Hot air is introduced at the bottom with or without a swirl component and fuel is added part way up. The feed enters further up and, as it mixes with the combustion products, the reactions occur, with the heat provided by the fuel approximately equalling the endothermic energy demand giving a net temperature difference across the furnace typically 5–10% of the inlet temperature (°C). These furnaces are all

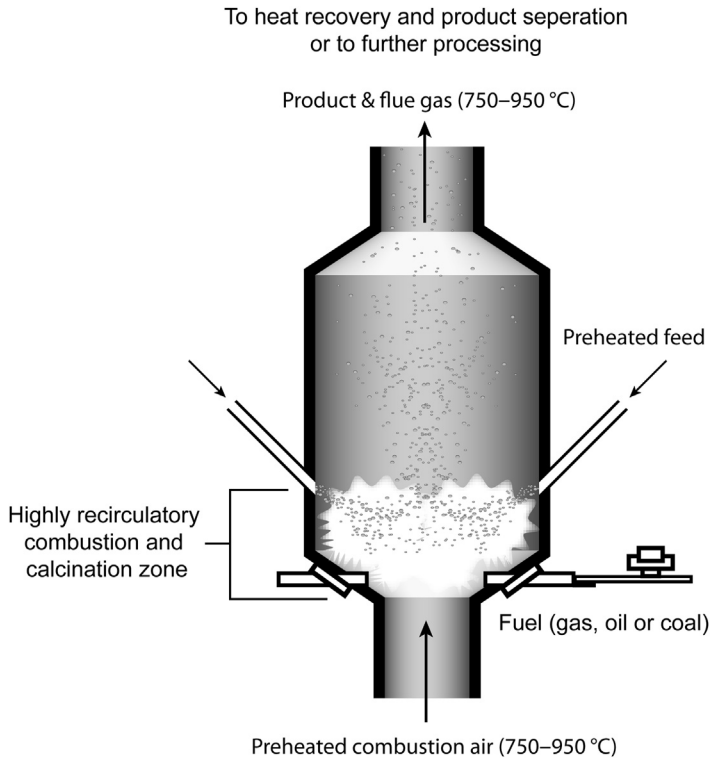


Figure 1.16 Flash furnace for alumina, lime or cement raw material calcination

used to undertake highly endothermic chemical reactions driving off CO_2 or water of crystallisation and operate under pseudo isothermal conditions. These reactions involve particle weight loss so upward flow is ideal since the heavier particles tend to remain in the furnace until the volatile component has been evolved.

These furnaces lend themselves well to the design and modelling techniques described later in this book and work undertaken by the authors working with colleagues in the alumina industry led to large increases in output from existing furnaces for relatively modest capital expenditure. These changes involved repositioning burners and feed inlets together with eliminating poor air distribution at the inlet and reducing the pressure loss across the outlet. Despite the apparent simplicity of the process, a wide range of more complex geometries exist compared with that shown in Figure 1.16. In the authors' experience, these more complex designs offer no advantage compared with the simple shape shown in Figure 1.16, indeed many exhibit a far poorer performance and the only logical explanation for these alternate designs is that they are an attempt at supplier "product differentiation" or simply the result of the designer's whim. Some designs are even fundamentally flawed, for example those based on cyclones with the claim that they promote good mixing between the feed and the hot gas, the designers obviously forgetting that cyclones are solids/gas separators!

1.2.7 Metal Physical Processing

All of the processes discussed above involve chemical reactions and the role of the furnace is to provide the energy required to drive the endothermic reactions to produce the desired products or to provide the activation energy to trigger an exothermic reaction. However in the metals industry, many furnaces are used to promote physical changes such as heating to soften the metal for further shaping, remelting for casting, and annealing to promote changes within the crystalline structure or the relieve stresses introduced during the manufacturing process. With the exception of melting, which involves significant energy input to provide the latent heat required, the energy change involved in these physical processes is small compared with the chemical processes above. Despite the low theoretical energy requirement, many of these processes are relatively inefficient because the losses are high relative to the theoretical requirements.

A good example of such a furnace is a billet reheating furnace, see Figure 1.17 which shows a large steel billet about to be discharged to be forged into a blank for a large steam turbine shaft. The efficiency of this operation is low for a number of reasons, including the fact that it is impractical to recover heat from the product following forging and the heat embedded in the furnace structure is lost on cooling owing to

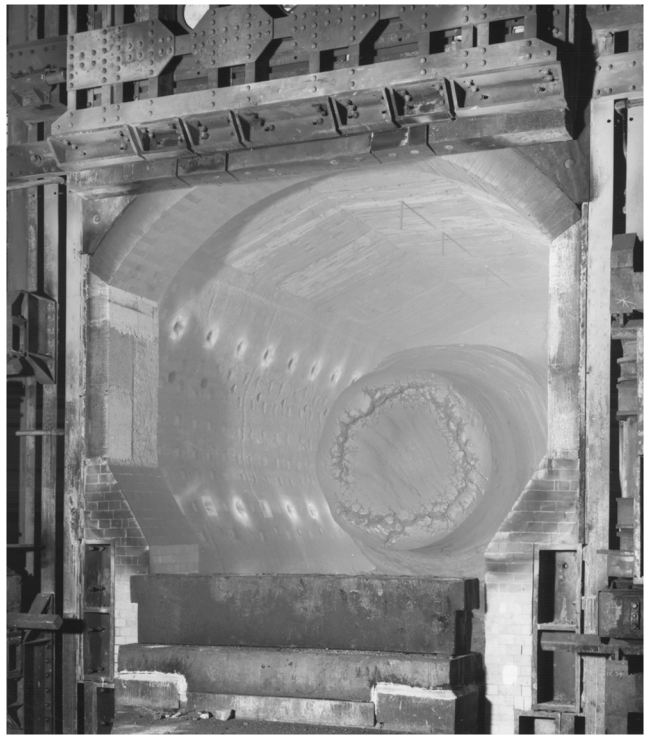


Figure 1.17 A large billet re-heating furnace (photo courtesy of John Mottershaw)

the cyclic nature of the operation. A worked example on how to calculate the heat transfer in this type of furnace is provided in chapter 4.

Continuous furnaces offer greater opportunities for energy recovery and minimise the heat lost on furnace shutdown. The forging of small billets offers the opportunity for semi-continuous process and improved heat recovery from the flue gases. A continuous furnace for heating small billets is shown in Figure 1.18.

This furnace achieves high efficiency by using high velocity burners that provide very high rates of heat transfer to the load. Combustion is complete at the burner exit nozzle and uniform gas flows ensure high rates of convective heat transfer without forming "hot spots" on the surface that would result in steel degradation. The heated billets drop onto a chain conveyor for transport to the forging machine. The flue gases pass over the load and preheat the incoming billets by counter-current heat transfer with the outgoing combustion products. According to Rhine and Tucker (1991) these furnaces achieve efficiencies of over 60%, a remarkable value considering that there is no external heat recovery system. The disadvantage is that they have limited flexibility since to maintain these high efficiencies, the gas

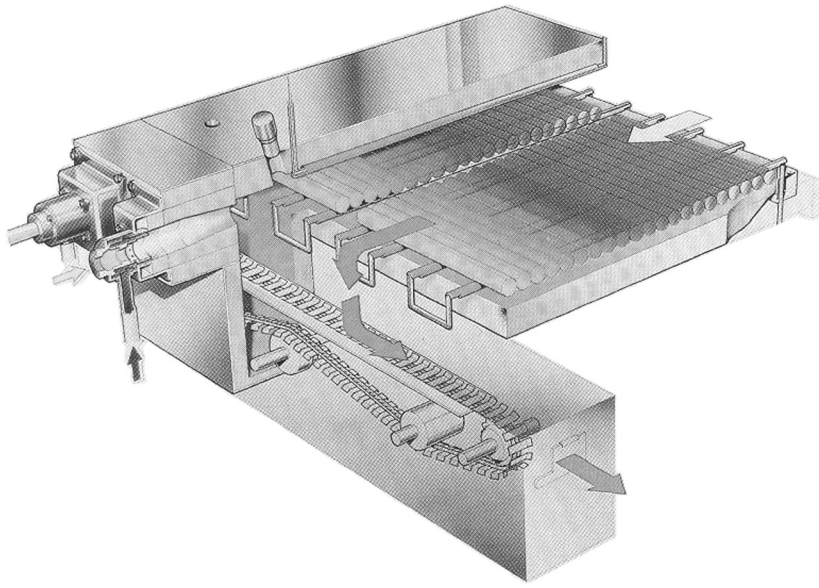


Figure 1.18 Continuous rapid heating furnace for small billets (After Rhine and Tucker)

velocity across the billets must be high to achieve the heat transfer required for effective heat recovery to the load so the furnace is only suitable for a limited range of billet sizes.

Continuous furnaces are also used for reheating steel slabs and bars prior to rolling into intermediate or finished products. A typical slab reheating furnace is shown in Figure 1.19. It consists of three zones, a preheating zone, a heating zone and a soak zone. The slabs lie horizontally and are heated by burners above and below. The slabs are transported though the furnace by water cooled "walking beams", or by a "pusher" installed at the cold end that pushes the slabs on

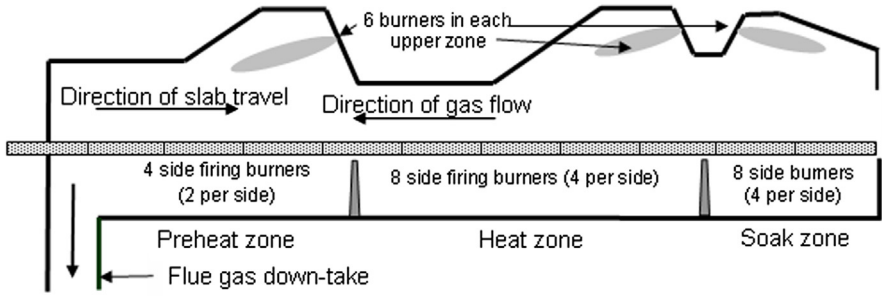


Figure 1.19 Schematic of Slab Re-heating Furnace

water-cooled skids. The slab enters the preheating zone, where it is heated to approximately 500°C. The heating rate in this zone must be sufficiently slow to prevent the outside from over heating and forming a reflective slag which, if formed, reduces the radiant heat transfer in subsequent zones (Trinks, et al 2005). In some furnaces load recuperation from the flue gases similar to that in the rapid billet heating furnace above is employed prior to the preheat zone. This improves inherent furnace efficiency and reduces the flue gas temperature prior to the recuperator, thus reducing recuperator inlet metal temperature and potentially prolonging its life.

Preheating is followed by the main heat zone, where the majority of the heat transfer takes place, and the soak zone where temperature equalisation through the slab occurs.

The slab reheating furnace shown above is effectively a continuous process with slabs being fed and discharged approximately every ten minutes or so.

Another example of a furnace used for physical processing of metal is the annealing furnace, used to stress relieve large fabrications. Fabrication processes involving welding introduce stresses into the final article which can cause premature failure by cracking or localised corrosion. During stress relieving or annealing, the completed fabrication is heated at a controlled rate and held for an extended period at one or more "soaking temperatures" for the stresses to equalise or certain crystal changes to occur. These processes are normally batch processes. Figure 1.20 shows two large gearbox cases entering an



Figure 1.20 Two large gearbox cases entering a large annealing furnace (photo courtesy of John Mottershaw)

annealing furnace on a bogie hearth. This furnace has a conventional refractory lining and, as a consequence, the energy lost during cooling will be significant. These losses could be considerably reduced if the furnace had a ceramic fibre lining, since the energy used in heating this type of lining is much less than for brick and hence less energy lost during cooling is also reduced.

1.2.8 Incinerators and Resource Recovery Furnaces

A significant number of furnaces are used to destroy toxic waste, to recover metals and to recover energy from combustible wastes. This is not new; furnaces have long been used to recover metal from scrap, for example copper, lead and steel, while there were over fifty installations in Britain recovering heat from domestic garbage in the early 20th century (Babcock and Wilcox 1913). In the future, furnaces may also be used to recover valuable metals, for example, from scrap electrical equipment. These latter furnaces are likely to offer a real challenge to the designer because there is little experience to draw on and challenging environmental constraints need to be met.

Several years ago the authors were given the challenge of destroying an aqueous waste that contained 30% methanol. Under the right conditions this waste is auto-thermal, so we designed a small incinerator that burnt the waste and recovered the energy for process use via thermal fluid heat recovery system, hence turning a toxic waste into an asset, Figure 1.21. In the absence of any previous experience of dealing

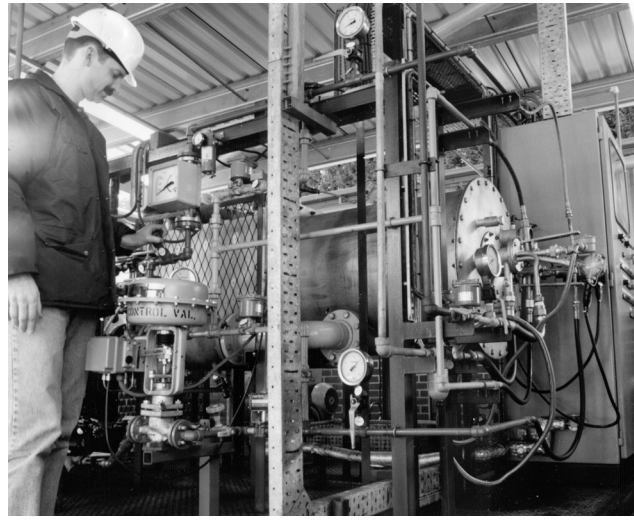


Figure 1.21 A small incinerator designed by the authors to recover energy from methanol contaminated water

with this waste, this was achieved by the application of the tools described in this book.

1.2.9 Furnaces with Reducing Atmospheres

Many furnaces use special reducing atmospheres to reduce metals from ore, minimise scale formation or to reduce sulphur content of metals. These atmospheres can be formed by either supplying insufficient combustion air and creating carbon monoxide as a product of incomplete combustion, see chapter 2, or supplying a special atmosphere such as hydrogen as described in section 1.2.5 above. Reducing atmosphere furnaces present special hazards owing to the flammable nature of the atmosphere which creates an explosion risk. Additionally where sub-stoichiometric combustion is used, the CO atmosphere is highly toxic. Examples of furnaces employing reducing atmospheres include, blast furnaces, rotary kilns used in the minerals sands industry for reducing iron oxide to metallic iron prior to leaching with acid, Figure 1.22 and the Herreschoff multiple hearth roaster, Figure 1.23. This roaster is used for reducing nickel compounds found in laterite ore to soluble nickel and cobalt in the form of ferro-nickel-cobalt alloys and the iron to insoluble iron oxides. Multiple hearth roasters are very inefficient, employing no heat recovery from the product and minimal heat recovery from the combustion products. They are also high capital cost and the rabble arm mechanism and refractory hearths are very expensive to maintain. The nickel roasting process undertaken in these furnaces would benefit from a new approach applying the fundamental principles of the process chemistry and thermodynamics to redesign the furnace based on these needs, rather than following the traditional approach.

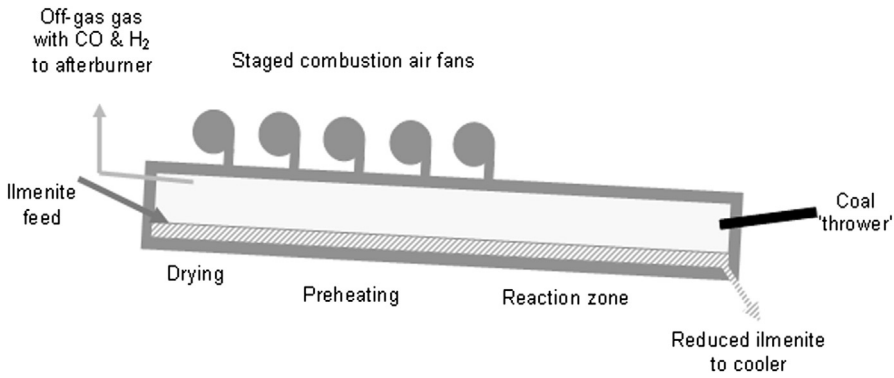


Figure 1.22 Reducing kiln used in the mineral sands industry

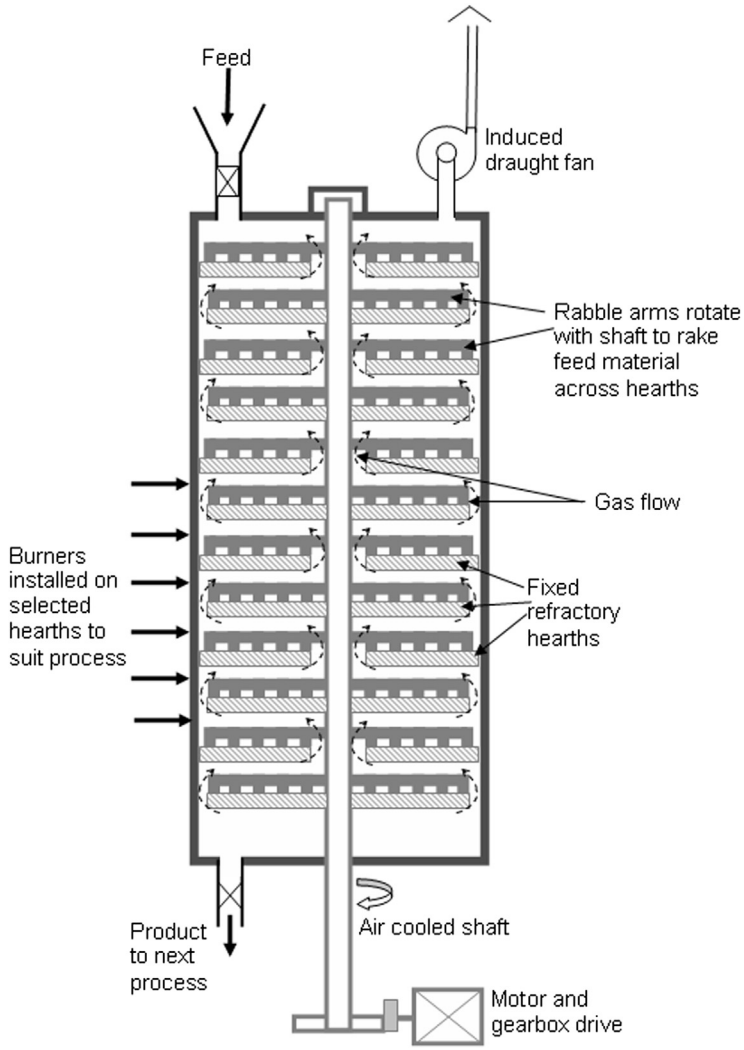


Figure 1.23 Herreschoff multiple hearth roaster

1.2.10 Oil Refining and Petrochemical Furnaces

Oil refining and petrochemical manufacture involves extensive heating of hydrocarbon and other fluids. Depending on the temperature required, this heating is achieved either by steam or direct heating. In the latter case, the fluid under pressure is contained in tubes which are heated from the outside by direct exposure to flames. These heaters commonly take two forms, cylindrical heaters with one central



Figure 1.24 Two types of petrochemical heater showing a cylindrical heater (left) and a cabin heater (Photos courtesy of Born Heaters Canada)

burner, or a ring of burners in the base and the long rectangular type with many burners in a row along the floor, Figure 1.24. The latter are generally known as cabin heaters.

Petrochemical heaters are significantly different from boilers, with fewer larger tubes, Figure 1.25. With petrochemical heaters, it is very important that the heat transfer to the tubes is carefully controlled. If the heat transfer is too low, output is lost but if too high, local "hot spots" are created. This is especially dangerous with hydrocarbon fluids because hot spots lead to carbon formation on the inside of the tube reducing the heat transfer to the fluid. However, the heat is still being transferred to the outer surface of the tube which overheats and will eventually fail, leaking hydrocarbon into the firebox. This is highly dangerous and will, at best, lead to destruction of the heater but at worst, explosion and fire that may cause multiple casualties and destroy the entire plant.

In the past petrochemical heaters have been notoriously inefficient, using natural draft burners with high excess air, high flue gas temperatures and no heat recovery. The significance of these issues is considered later in the book. Such heaters rarely transferred more than 50% of the energy in the fuel to the fluid. Modern heaters utilise convective preheating of the liquid and heat recovery from the flue gas to preheat the combustion air, together with forced draft burners operating at controlled excess air and achieve much higher efficiencies.



Figure 1.25 Heat transfer coils for petrochemical heaters showing a coil for a cabin heater (foreground) and cylindrical heater in the background (Photo courtesy of Born Heaters Canada)

1.3 Drivers for Improved Efficiency

The primary role of any furnace is to make a product that can be sold at a competitive price, so the overall cost of furnace operation is the major driver for any furnace owner. The cost of owning a furnace is based on:

- Capital cost, depreciation and interest charges
- Fuel and electricity costs
- Maintenance costs
- Environmental costs and charges (where relevant)

A furnace owner therefore needs to achieve the minimum operating cost by carefully balancing the individual contribution of each of these factors. In times of high interest rates the capital costs and depreciation charges dominate, while high labour costs drive up maintenance

charges and both of these have tended to be dominant in the 1990s. The early part of the current decade has seen low interest rates and steadily rising energy costs, a trend that seems likely to continue, or even accelerate, driven by the demand for oil exceeding the available supply, especially of low cost oil. The growing demand for easily transported liquid fuels will probably be satisfied by mining oil shale and tar sand, synthesis from natural gas and coal hence increasing the demand for, and cost of, these fuels. To operate a furnace in these circumstances will require that excellent fuel consumption is achieved.

Concerns about climate change and its relationship with carbon dioxide concentrations in the atmosphere is likely to see increasing emphasis on reducing CO_2 emissions, implemented in the form of either regulatory constraint, or environmental taxes and charges. Since CO_2 emissions are directly related to the type of fuel and the quantity used, these regulations and taxes will have a similar effect to further increases in fuel cost.

This lesson has already been assimilated by the cement and lime industries, where energy is the major production cost and well exceeds the interest charges over the life of the plant. This has led these industries to seek the highest possible thermal efficiency and considerable effort has been expended in this quest, with marked success. Further economies are currently being achieved by the use of waste derived fuels, such as spent oil, scrap plastic, worn tyres, damaged timber from building demolition, etc. In addition to cost, this drive is the result of the industry's attempts to reduce its greenhouse gas emissions and to gain sustainability credentials.

Unless there is a major discovery of easily won oil or the link between CO_2 emissions and climate change is disproved, both unlikely scenarios in our opinion, fuel, electricity and environmental charges will be the major furnace operating costs of the future, hence requiring designers to achieve much higher efficiencies than in the past. Those who succeed will have a huge competitive edge.

1.4 Concluding Remarks

In this introduction we have considered only a very small proportion of the many types of furnaces used in the process and metallurgical industries. Hopefully the forgoing provides a flavour of the huge variety of designs in use. This book does not attempt to cover in detail each and every application, to do so would require a lifetime, but concentrates on the principles that apply to the design of all types of furnaces and combustion systems.

Additionally, it should be noted that many existing designs have developed through tradition and are not necessarily ideal for the application they are applied to and would benefit from a serious critical

review to determine whether they are the best solution for current needs. Such a review should include all stages of multi-stage processes since some stages may be eliminated, for example, adoption of the flash smelter for copper smelting. By eliminating the converter, capital cost was reduced and thermal efficiency improved.

Furnace and combustion engineers of the future will be required to design flames and furnaces to suit both new processes and to maximise overall process efficiency of existing processes in a carbon constrained world. This will require a fundamental approach based on the best available knowledge and techniques.

References

Babcock, & Wilcox. (1913). Steam – its generation and use. (8th British ed, p. 113). London: Babcock and Wilcox ltd.

Babcock, & Wilcox. (2005). *Steam – its generation and use* (41st ed). Ohio: Babcock and Wilcox.

Biwas, A. K., & Davenport, W. G. (1980). *Extractive metallurgy of copper* (p. 63). Oxford: Pergamon Press.

Boynton, R. S. (1980). *Chemistry and technology of lime and limestone* (p. 3). New Jersey: John Wiley and Sons.

Francis, A. J. (1977). *The cement industry 1796-1914: a history* (p. 79). Newton Abbot: David & Charles.

Francis (2), Ibid, (pp. 233–234)

Francis (3), Ibid, (pp. 254–255)

Martin, G. B. (1932). *Chemical engineering and thermodynamics applied to the cement rotary kiln*. London: Crosby Lockwood.

Oates, J. A. H., Lime, & Limestone –. (1998). *Chemistry and technology, production and uses* (p. 158). Weinheim, Germany: Wiley-VCH.

Raymond, R. (1984). *Out of the fiery furnace p 6-7*. Melbourne: Macmillan Australia.

Raymond (2), Ibid, (p. 17)

Rhine, J. M., & Tucker, R. J. (1991). *Modelling of gas-fired furnaces and boilers*. Maidenhead: McGraw-Hill.

Trinks, W., Mawhinney, M. H., Shannon, R. A., Reed, R. J., & Garvey, J. R. (2005). *Industrial furnaces* (6th ed, P. 119). New Jersey: John Wiley and Sons.

Chapter 2

The Combustion Process

Chapter contents

2.1	Simple Combustion Chemistry	32
2.2	Combustion Calculations	33
2.3	Chemical Reaction Kinetics	37
2.4	The Physics of Combustion	47
Nomenclature for Chapter 2		63
References for Chapter 2		64

Combustion is a specific group of chemical reactions where a fuel and oxygen burn together at sufficiently high temperature to evolve heat and combustion products. The fuel can be a gas (e.g. hydrogen, natural gas), a liquid (e.g. oil, alcohol, sulphur), or a solid (e.g. coal, wood, peat). The rate at which these combustion reactions occur can vary from a very slow decay to an instantaneous explosion. Both the chemical kinetics and physical diffusion processes involved control this rate. The objective of the combustion engineer and plant operator is to obtain a steady heat release at the rate required to suit the process objectives.

2.1 Simple Combustion Chemistry

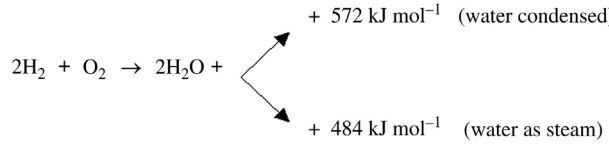
Most industrial fuels are hydrocarbons, so called because their primary elemental constituents are carbon and hydrogen. These are oxidized to release heat during combustion. The chemistry of this oxidation process involves very complex chain reactions. However, for most engineering design purposes we can reasonably simplify the chemistry to four basic reactions. The following equations define the Simple Chemically Reacting System (SCRS).

2.1.1 The Complete Oxidation of Carbon

$$C + O_2 \rightarrow CO_2 + 394\ \text{kJ mol}^{-1}$$

Providing there is sufficient oxygen present in the mixture, the above reaction describes the overall result of the oxidation of carbon. However this reaction rarely occurs in practical combustion systems but is the result of a chain of reactions involving carbon monoxide as an intermediate product, as discussed later in this section.

2.1.2 The Complete Oxidation of Hydrogen



The difference in the physical states of the water produced as a result of the oxidation of hydrogen is the reason for the complexity of the net and gross calorific values for hydrocarbon fuels. The gross heat release is that which is released when the hydrogen is oxidized and the water condensed, whilst the net calorific value is the heat

which is released while the water remains as steam. The former is also referred to as the higher heating value (HHV) and the latter as the lower heating-value (LHV).

The rate at which hydrogen oxidizes is significantly faster than that of carbon, thus hydrogen preferentially reacts with the available oxygen in the mixture.

2.1.3 The Incomplete Oxidation of Carbon

In the event of imperfect combustion, not all of the carbon in the fuel will be oxidized to carbon dioxide but some will be partially oxidized to carbon monoxide. The main effect of carbon monoxide production on the combustion process is to reduce the heat release from the fuel.

$$2C + O_2 \rightarrow 2CO + 221 \text{ kJ mol}^{-1}$$

It can be seen that only just over half of the heat is released in the production of carbon monoxide, compared with the complete combustion of carbon. Thus any burner producing carbon monoxide as a result of a stoichiometric imbalance, or poor fuel/air mixing will cause a significant drop in combustion efficiency. Carbon monoxide is also an important air pollutant and is a health hazard as a poisonous gas in high concentrations if released into the atmosphere. It is therefore absolutely essential to prevent the production of significant levels of carbon monoxide in any combustion system.

2.1.4 The Oxidation of Carbon Monoxide

Carbon monoxide is the unwanted repository of considerable combustion energy in inefficient combustion systems. In many instances where hydrocarbons are burnt, the oxidation reactions proceed rapidly to the point where CO is formed but then slowly until CO burnout is achieved. Carbon monoxide may be further oxidized to carbon dioxide according to the following reversible chemical reaction:

$$2CO + O_2 \leftrightarrow 2CO_2 + 173 \text{ kJ mol}^{-1}$$

The combustion of dry carbon monoxide is extremely slow. However, if hydrogen-containing radicals are present in the flame, the combustion rate of (wet) carbon monoxide increases significantly.

2.2 Combustion Calculations

In the combustion process the masses of fuel, oxygen and combustion products are non-conserved properties. Information regarding the

transformation undergone by these properties is obtained from the reaction equations. Thus if A and B burn to give C and D,

$$aA + bB \rightarrow cC + dD$$

is the general form of the reaction equation.

This reaction equation indicates that molecular transformations take place; represents a balance of the atomic species (conserved properties) involved in the transformation. It should be noted that only the ratios and not the absolute values of the coefficients *a, b, c, d* are fixed. These ratios are termed the stoichiometric proportions for the reaction. In addition, the extent to which the transformation occurs must be known, as reactions do not necessarily always go to completion.

When dealing with chemical reactions, it is convenient to use mole units. We are particularly concerned with combustion reactions, in which carbon and hydrogen (and possibly other trace elements, e.g. sulphur) found in conventional fuels react with oxygen to form their respective oxides. Incomplete combustion of fuels containing carbon is associated with the formation of carbon monoxide, or in extreme cases carbon (e.g. soot, coke). Combustion is said to be complete when the only oxide of carbon present is CO_2 and no elemental carbon remains. The products of combustion which leave the combustion chamber, or furnace, are usually referred to as flue gases.

To achieve complete combustion in practical combustion systems it is almost always necessary to provide excess air. This is the amount of air over and above the minimum required for complete combustion, i.e. in excess of the stoichiometric air requirement. The excess air percentage is defined as

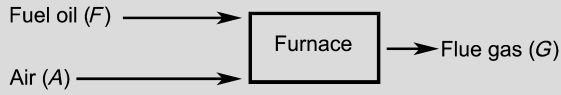
$$\text{excess air } \% = \frac{(\text{total air} - \text{stoichiometric air})}{(\text{stoichiometric air})} \times 100 \qquad (2.1)$$

Example 2.1 Fuel oil with the following ultimate analysis (%w/w basis) is to be burnt with 15% excess air in a furnace.

Element	*% w/w*
Carbon	84.6
Hydrogen	10.9
Sulphur	0.7
Oxygen	3.8
Total	100.0

Assuming complete combustion, determine:

(i) the mass of air required to burn 1 kg fuel oil;
(ii) the mass of flue gas produced from the combustion of 1 kg fuel oil;
(iii) the flue gas composition (%v/v);
(iv) the volume of flue gas produced (at 300 °C and 1 atm) from 1 kg oil.



where *F*, *A*, and *G* are in kg. The composition of air is assumed to be 23.3% weight/weight Oxygen and 76.7% weight/weight Nitrogen.

Basis for the calculation:-	1 kg fuel oil
Total mass balance gives	$F + A = G$
or, as $F = 1$	$1 + A = G$

Complete combustion involves the following reactions:

$$C + O_2 \rightarrow CO_2$$

$$2H + 0.5O_2 \rightarrow H_2O$$

$$S + O_2 \rightarrow SO_2$$

The flue gas will consist of:

carbon dioxide	*c* kmol
water	*w* kmol
sulphur dioxide	*s* kmol
nitrogen	*n* kmol
excess oxygen	*y* kmol

Consider now the steady-state mass balance for individual atomic species:

Mass IN = Mass OUT

Carbon (kg):	$0.846 = 12c$	thus	$c = 0.0705$ kmol
Hydrogen (kg):	$0.109 = 2w$	thus	$w = 0.0545$ kmol
Sulphur (kg):	$0.007 = 32s$	thus	$s = 0.00022$ kmol
Nitrogen (kg):	$A \times 0.767 = 28n$		
Oxygen (kg):	$A \times 0.233 + 0.038 = 32c + 16w + 32s + 32y$		
	$= 3.135 + 32y$		
thus	$A \times 0.233 = 3.097 + 32y$		

Thus the stoichiometric oxygen requirement = 3.097 kg

Total oxygen supplied = $(3.097 + 32y)$ kg

As the excess air required is 15%

$3.097 \times 1.15 = 3.097 + 32y$

thus $y = 0.0145$

The answers are then worked out from the above derived relationships as follows:

(i) the mass of air required for 1 kg fuel oil: $A = 15.29$ kg

(ii) the mass of flue gas produced from 1 kg fuel oil: $G = 15.29 + 1 = 16.29$ kg

(iii) the flue gas composition (%v/v):

Flue gas component	*kmol*	*% mol (= % v/v)*
CO_2	0.0705	12.62
H_2O	0.0545	9.76
SO_2	0.0002	0.03
N_2	0.4188	74.99
O_2	0.0145	2.60
Total	0.5585	100.00

(iv) the volume of flue gas produced (at 300 °C and 1 atm) from 1 kg oil.

The gas laws state that $pV = nRT$

where R (universal gas constant) = 0.03697 $m^3 \cdot atm \cdot K^{-1} \cdot kmol^{-1}$

Thus $V = (0.5585 \times 0.03697 \times (273+300))/1.0 = 12\ m^3$

2.3 Chemical Reaction Kinetics

We have previously considered the basic reactions that summarise the combustion of a hydrocarbon fuel, defined as the Simple Chemically Reacting System (SCRS), but we know that these reactions do not really occur as we have written them. If we just considered the reaction between hydrogen and oxygen, then we should really write (at least) the following:

$$H_2 + OH \leftrightarrow H_2O + H$$
$$H_2O + O \leftrightarrow 2OH$$

$$O_2 + H \leftrightarrow OH + O$$

$$H_2 + O \leftrightarrow H + OH$$

$$H + H + M \leftrightarrow H_2 + M$$

$$O + O + M \leftrightarrow O_2 + M$$

$$O + H + M \leftrightarrow OH + M$$

$$H + OH + M \leftrightarrow H_2O + M$$

Where *M* is any molecule, These reactions do not even consider the additional effect of carbon, where we can also form free radicals like HCO, HCOH etc. In other words, we actually generate a large number of intermediate chemical species, which are unstable, but progress the chemistry to give the overall result of the SCRS. Within our reacting combustion 'soup' we have a mixture of stable and unstable species, so that for instance, an oxy-methane flame which involves over 300 reactions would contain:

Stable specis	CH_4, C_2H_2, CO, CO_2, H_2O, O_2, H_2
Unstable species	H, O, OH, C, C_2, CH, HCO, HCOH, CH_3

Observation of the reactions listed above will show that they all are reversible and involve an unstable species, or free radical. These are often denoted with a *, e.g. H*, to indicate that they are unbalanced between the nucleus and available electrons and are seeking to redress that balance. You will also notice that in some of these reactions free radicals give rise to more free radicals and it is this 'chain reaction' process which results in the rapidity of the combustion process. All we need is an 'initiator' radical to start the process off and it is then self-sustaining. Some materials (*M* in our equations) will break the chain by promoting the formation of stable products, and these are termed 'inhibitors' (e.g. fire extinguishers).

2.3.1 Types of Reactions

All these reactions are not the same, but may be classified into different types. These include:-

(i) Collision controlled bi-molecular reactions

In this type of reaction, which is the most common within the flame, molecules or radicals A and B collide and, if the energy and orientation is right, react immediately:-

$$A + B \leftrightarrow C + D$$

or molecule or radical A collides with an inert molecule M and, if the energy and orientation is right, decomposes immediately:-

$$A + M \leftrightarrow C + D + M$$

Immediately means in a time much shorter that the average time between collisions.

(ii) Decomposition controlled reactions

These are similar to (i) but the reaction or decomposition times are longer.

$$A + B + (AB)^* \leftrightarrow C + D$$

Where $(AB)^*$ is a relatively long-lived activated complex.

(iii) Tri-molecular reactions

The activated complex is formed as in (ii) but decomposes again (i.e. shakes itself to bits) unless an inert third body, M, is nearby to absorb the excess energy.

$$A^* + A^* + M \leftrightarrow B + M$$

The frequency of three molecules meeting is much less than two, and thus these are 'slow' reactions.

2.3.2 Reaction Rate Theory

The rate at which a chemical reaction occurs is a function of the concentration, [*], of the reactants, thus if we consider reaction (i) above

$$A + B \leftrightarrow C + D$$

Then the forward rate $= k[A]\cdot[B]$, and the reverse rate $= k'[C]\cdot[D]$

If the reaction reaches equilibrium then

$$k[A]\cdot[B] = k'[C]\cdot[D] \tag{2.2}$$

thus

$$[C]\cdot[D]/[A]\cdot[B] = k/k' = K \tag{2.3}$$

K is called the equilibrium constant of the reaction. This constant is temperature and pressure dependent. The effect of temperature is generally correlated by the Arrhenius equation, which is derived from the van't Hoff equation:-

$$\frac{\partial \ln K}{\partial T} = \frac{\Delta E}{RT^2} \tag{2.4}$$

Locally within the flame, chemical equilibrium is rarely achieved, so we are interested in the forward, or backward rate of the individual reactions, which leads to an equations of the form:-

$$\frac{\partial \ln k}{\partial T} = \frac{E}{RT^2} \text{ (forward rate Arrhenius equation)} \tag{2.5}$$

or

$$\ln k = -\frac{E}{RT} + C \text{ (integrated form)} \tag{2.6}$$

or

$$k = C\exp\left[-\frac{E}{RT}\right] \tag{2.7}$$

where

E = activation energy (experimentally determined)
R = Universal gas constant
T = temperature (absolute units)
C = constant (experimentally determined)

The Arrhenius equation as it is expressed above, is applicable to homogeneous gas phase reactions, but frequently fails for chain reactions. As the equation presently stands we have also made no provision for the effect of pressure.

If we consider the theory of collisions between molecules (and radicals) we can 'extend' the Arrhenius equation for collision reactions (i) to the following:-

$$R_A = C\cdot p^2 m_A m_B T^{-2/3} \exp\left[-\frac{E}{RT}\right] \tag{2.8}$$

where

R_A = rate of consumption of species A
p = pressure (absolute units)
m_A = mass fraction of A in gaseous mixture
m_B = mass fraction of B in gaseous mixture

If we examine the relationship between the reaction rate and temperature for this equation we get a curve of the form shown in Figure 2.1. If we also consider the effect of the reducing values of m_A and m_B as the reacting components travel through the flame, we can derive a similar relationship between R_A and residence time, as shown in figure 2.2.

In both curves it can be seen that the rate of consumption of species A (and B), and hence the rate of generation of C and D, are highly temperature dependent, and whilst this is beneficial with respect to efficient burning of fuel components, it is the same effect that causes unwanted pollutants such as thermal NO_x.

Within the 'chemical soup' that constitutes the reality of fossil fuel combustion we have an enormous number of competing chemical reactions taking place, see Figure 2.3, but if we just consider the 'overall' reaction of fuel with oxidant, we can gain some important insights

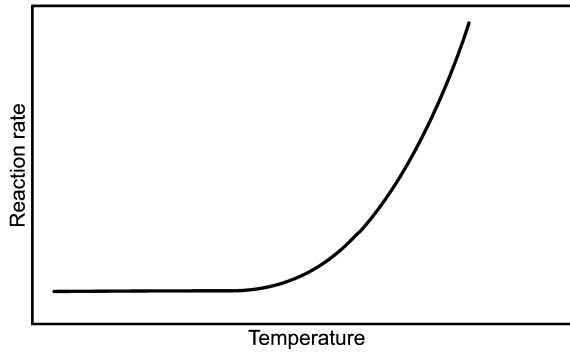


Figure 2.1 Effect of temperature on reaction rate in the extended Arrheneus Equation



Figure 2.2 Consequence of extended Arrhenius equation on temporal consumption of species *A*

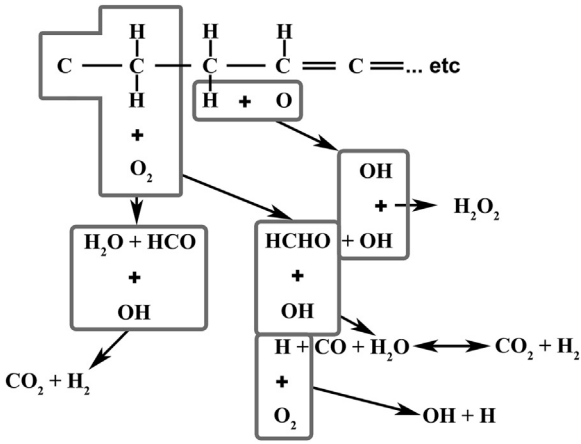


Figure 2.3 Extracted reactions from the 'chemical soup' of fossil fuel combustion

into the processes of ignition, stabilisation, propagation and extinction in a flame.

2.3.3 Reaction Rate Behaviour

Suppose that A and B are our fuel and oxidant respectively, then we can develop an overall rate of consumption of fuel based on the Arrhenius equation. If the subscripts 0 and 1 refer to the initial and completely burnt conditions respectively, then the mass consumption of fuel (m_{fu}) and oxidant (m_{ox}) can be related to the 'reactedness', τ, (i.e. measure of completeness of the reaction). Thus

$$\tau = \frac{m_{fu} - m_{fu0}}{m_{fu1} - m_{fu0}} = \frac{m_{ox} - m_{ox0}}{m_{ox1} - m_{ox0}} \tag{2.9}$$

The progress of the combustion reaction can be thus graphically represented, see Figure 2.4. The Arrhenius equation implies that the rate of reaction of fuel, R_{fu}, is directly proportional to m_{fu}, m_{ox} and T.

$$R_{fu} = C_1 p^{C_2} m_{fu}^{C_3} m_{ox}^{C_4} \exp\left[-\frac{C_5}{T}\right] \tag{2.10}$$

where C_1, C_2, C_3, C_4 and C_5 are constants. As the reaction proceeds, although T rises, the values of m_{fu} and m_{ox} fall, and thus R_{fu} falls to zero as τ tends to unity, as in shown Figure 2.5, which is similar to Figure 2.2.

We have in all the equations thus far presented, used values of p, m_{fu}, m_{ox} and T which are instantaneous but, as we know from other studies, aerodynamic turbulence gives rise to fluctuating values about

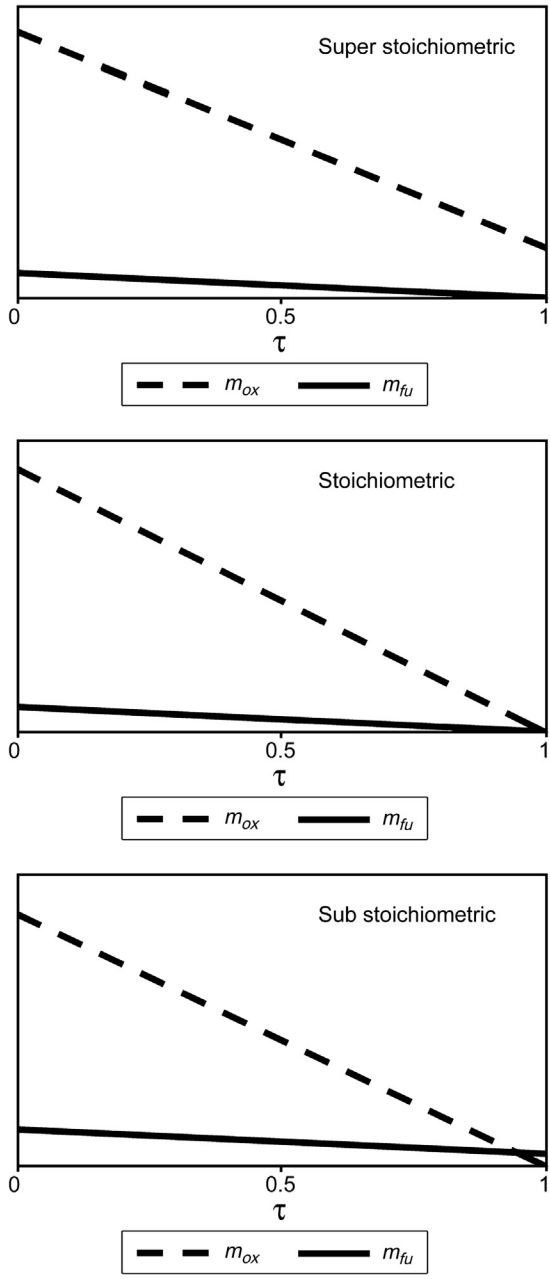


Figure 2.4 Relationship between reactedness and mass consumption of fuel and oxidant

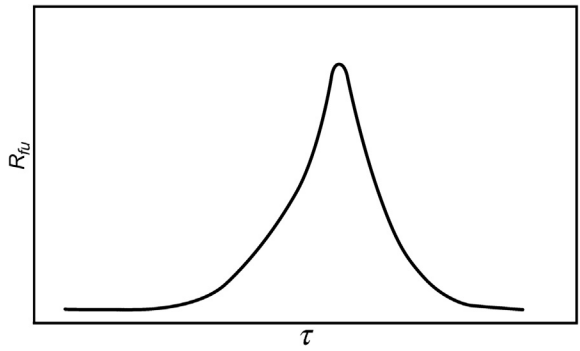


Figure 2.5 Dependence of fuel reaction rate on the reactedness of a flame

a mean at any point within the flame. It is very important to understand that the kinetic equations do not hold true for mean values, thus

$$R_{fu} \neq C_1 \overline{p}^{C_2} \overline{m}_{fu}^{C_3} \overline{m}_{ox}^{C_4} \exp\left[-\frac{C_5}{\overline{T}}\right] \tag{2.11}$$

It is for this reason that all the individual reaction rate experimental data that is generated to give the required values for the constants in these equations are derived from premixed laminar flames. It is also for this reason evident why 'average' values used in chemical kinetic models of flames yield inaccurate predictions of pollutant species such as NOx, CO, and UHCs (unburnt hydrocarbons).

Figure 2.6 shows measured values of the variation of equilibrium constant with temperature for most of the primary reactions occurring within a flame. It should be noted that the axes of this graph are $10000/T$ on the x-axis and $\log_{10}$K on the y-axis. Hence the temperature scale on the x-axis varies from 5000K on the left to 600K on the right, whilst one unit on the y-axis represents an order of magnitude change. From the previous analysis, it is apparent that the higher the value of the equilibrium constant, the greater will be the forward reaction rate relative to the reverse rate. Thus if we wish to compare the propensity of relative reactions to occur at a given temperature, it is generally the case that those with the higher K values will be dominant. Extreme care should be exercised in any 'partial' analysis, as it is quite likely that some other competing reaction may be overlooked, which could in fact swamp the local domain being examined.

2.3.4 Burning Droplets and Particles

The analysis presented so far has assumed homogeneity of the reacting components, and is therefore only truly applicable to the gaseous phase of the flame. Liquid and solid fuels are usually burnt as a

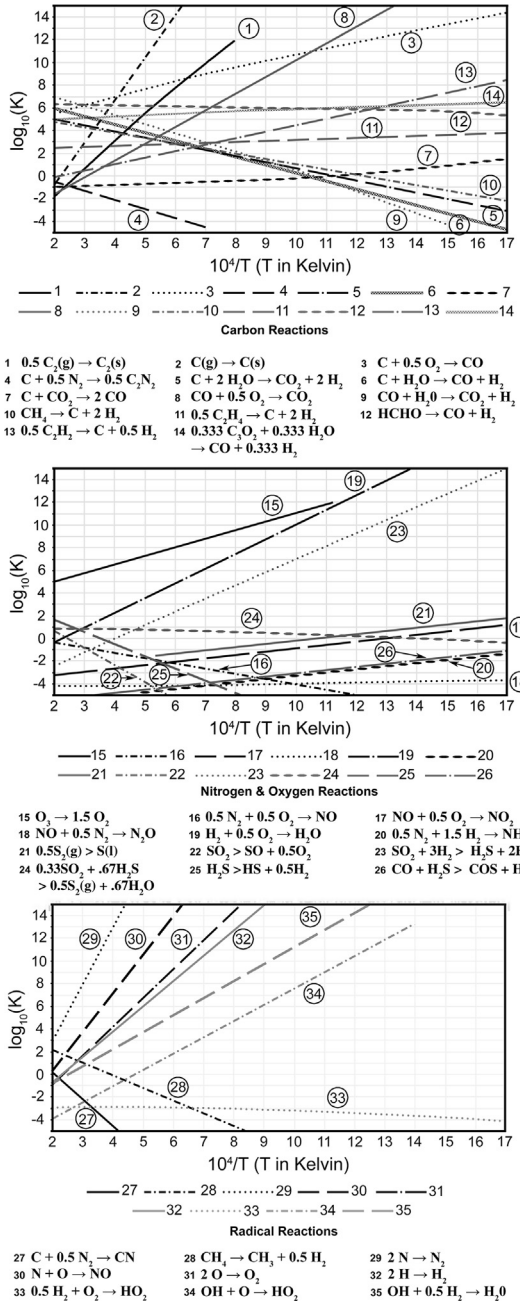


Figure 2.6 Equilibrium rate values for combustion reactions

particulate suspension. Combustion of a particle or droplet may include some or all of the following sequential, overlapping steps

- Particle drying
- Devolatilisation
- Particle swelling/shrinkage and porosity change
- Volatile combustion
- Char combustion

The combustion of the fuel volatiles occurs in the gaseous phase, and will conform to the previous analysis, whilst the residual, carbonaceous char burning occurs on the surface on the particle and is therefore heterogeneous, being controlled by the diffusion rate of oxygen, the chemical reaction rate and the surface.

The classical model of particle combustion is based on a two-stage process, whereby an initial shell of volatiles is created around the fuel particle. This then burns as a shrinking sphere until it is consumed. Char burning then commences at the surface of the particle, giving rise to a sequential burning hypothesis. See Figure 2.7. This analysis has been based principally on observations during single particle burning studies, in which the particle is suspended in stagnant surroundings. Experimental evidence in dynamic flame conditions have

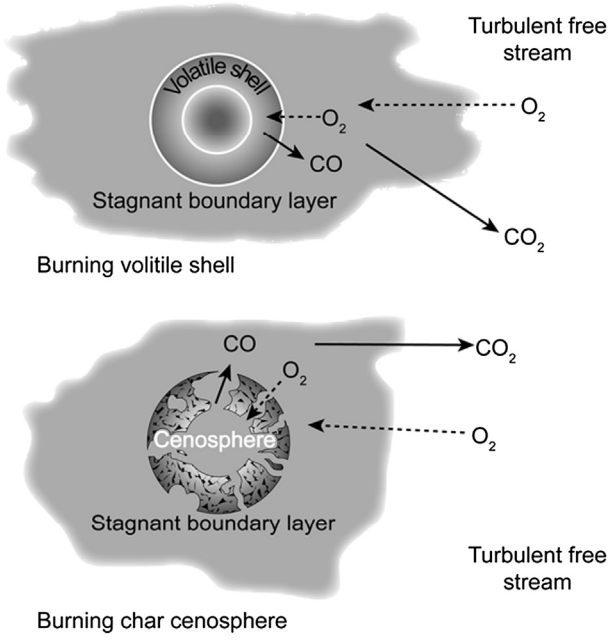


Figure 2.7 Stages in the combustion of a fuel particle

led to a hypothesis that the volatile shell is 'stripped' from the solid char particle, owing to its momentum, and thus the combustion of volatiles and char will occur concurrently in a true flame.

Char combustion is controlled by a combination of gaseous diffusion and surface reaction processes. Depending primarily on the local temperature of the gases and the particle surface, one or other of these mechanisms will be dominant. Analysis of the diffusion process is defined by the equation

$$k_d = \frac{24\phi D}{dR\overline{T}} \tag{2.12}$$

where

k_d - diffusion reaction rate coefficient
ϕ - mechanism factor for $CO_2(=1)$ or $CO(=2)$ transport
D - diffusivity of oxygen in nitrogen at T K
d - diameter of particle

The diffusion rate of oxygen through nitrogen (D) is temperature dependent and can be accommodated into the equation. The mechanism factor (ϕ) is also temperature dependent, and varies between values of 1 and 2 depending on the ratio of CO to CO_2 at the combustion surface.

The char surface reaction coefficient, k_s, is defined by an Arrhenius relationship of the form

$$k_s = A\exp\left(\frac{-E}{R^* T_s}\right) \tag{2.13}$$

where T_s is the char surface temperature. Early comprehensive analyses of char reaction mechanisms, Field et al. (1967), Jenkins and Moles (1987), were based on a limited number of experimental data of mainly British coals. These studies provided quantitative values for A and E. The experimental data indicated that the reaction mechanism is a function of the local partial pressure of oxygen such that the char burning rate, q, is given by

$$q = \frac{p_{O_2}}{\frac{1}{k_d} + \frac{1}{k_s}} \tag{2.14}$$

Thus it is presumed that the reaction is first order with respect to the partial pressure of oxygen. Recent studies, including Hamor, Smith and Tyler (1973), Smith and Tyler (1974), Morgan and Dekker (1988), Knill, Maalman and Morgan (1989), Knill et al. (1990), on a much wider range of coal chars have indicated that k_s is a function of the square root of the partial pressure of oxygen, and thus the overall char burning rate is given by:

$$q = \frac{1}{2}\frac{k_s^2}{k_d}\left\{\left(1 + 4\left(\frac{k_d}{k_s}\right)^2 p_{O_2}\right)^{0.5} - 1\right\} \qquad (2.15)$$

2.4 The Physics of Combustion

None of the chemical reactions can take place until the oxygen in the air is brought into contact with the gas. All combustion processes therefore take place in the following stages:

MIXING → IGNITION → CHEMICAL REACTION
→ DISPERSAL OF PRODUCTS

The rate of combustion is dependent on the slowest of the above stages. In most industrial combustion systems, the mixing is slow whilst the other steps are fast. The time-scale for mixing is typically 1 to 5 seconds, while the time-scale for the processes of ignition and reaction are of the order of a millisecond. Therefore, the rate and completeness of the combustion process is controlled by the rate and completeness of fuel/air mixing. Insufficient fuel/air mixing produces unburnt CO in the flue gases, wasting potential fuel energy.

For good combustion, it is necessary to ensure that adequate air is supplied for complete mixing and that the burner is designed to mix the fuel and air streams effectively and efficiently. In an ideal system, a stoichimetric ratio of air to fuel would be adequate, but in practice a small amount of excess air is necessary, as the diffusional mixing process is not perfectly homogeneous. It is shown later in Chapter 9 that the amount of excess air should be as small as possible to maximize thermal efficiency and minimize the production of some pollutants. The rate and completeness of combustion is controlled by the rate of completeness of the fuel-air mixing. Hence, the saying of combustion engineers:

IF IT'S MIXED, IT'S BURNT

Some small burners are designed to premix the fuel and air prior to ignition, but most industrial burners are designed for diffusion mixing of the combustion air and fuel inside the furnace, See chapter 5. In a diffusion burner, any air that is premixed with, or conveys, the fuel is termed primary air. The balance of the air required for combustion is supplied through one or more separate channels or ducts and, depending on their relative locations with respect to the fuel jet, are termed as secondary, tertiary, etc, air.

In most combustion systems the mass of air required for complete combustion is at least ten times that of the fuel. Consequently the momentum of the air is often greater than that of the fuel alone, in

which case it will probably dominate the mixing between the fuel and air. In some combustion systems, e.g. process heaters, the flow patterns of the air can be controlled reasonably well and swirl is often imparted to the air to control the mixing. In other systems, e.g. rotary kilns, the flow pattern of the air entering the kiln cannot be easily controlled. In this case it is often advisable to increase the effective momentum of the fuel jet by introducing some of the air through the burner nozzle as primary air. Such a configuration allows the momentum of the combined fuel and primary air streams to dominate over the rest of the combustion air. The mixing of air and fuel influences flame stability, emissions, and the thermal release profile. Because each of these parameters depend on the mixing in different ways, it is common to use multiple nozzles to try and optimise the mixing. However, increased complexity does not necessarily improve the performance.

Most burner systems employ some type of jet entrainment device for fuel-air mixing. The principal of jet entrainment is illustrated for a free jet issuing into an ambient environment in Figure 2.8. The initial jet velocity is normally high enough to produce a turbulent flow stream. Friction occurs between the boundary of the jet and its surroundings, causing the surrounding fluid to be locally accelerated to the jet velocity. The accelerated air is then pulled into the jet, thus expanding it. This process is known as entrainment. The momentum flux of the jet controls the amount of air entrained, and the process continues until the velocity of the jet is the same as that of its surroundings. The greater the momentum flux of the jet, the more of the surrounding fluid that will be entrained into it. A free jet can entrain as much of its surrounding medium as is required to satisfy its entrainment capacity, and it is able to expand unimpeded in doing so. The entrainment rate of a free jet is therefore a function of the mass

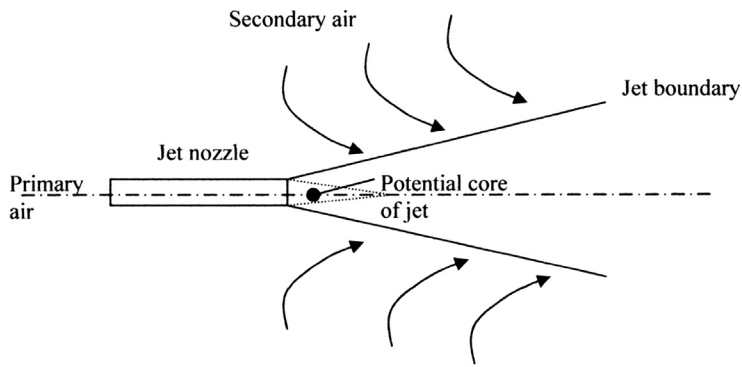


Figure 2.8 Entrainment of secondary fluid into a free jet

flowrate and velocity and has been shown from experimental studies by Ricou and Spalding (1961) to be related by the formula:

$$\frac{m_x}{m_0} = 0.32\left(\frac{\rho_1}{\rho_0}\right)^{0.5}\frac{x}{d_0} \tag{2.16}$$

where

m_0 - mass flowrate of jet fluid at the nozzle
m_x - mass flowrate of jet fluid at distance x from nozzle due to entrainment
ρ_0 - density of nozzle jet fluid
ρ_1 - density of entrained fluid
d_0 - diameter of nozzle

Example 2.2 If we assume 'mixed is burnt' at 10% excess air conditions and ignition occurs at the nozzle plane, what will be the length of a raw natural gas flame issuing into stagnant air surroundings, at the same temperature, at a rate of 1.5 kg/s through a 100 mm diameter nozzle? The stoichiometric air requirement of the natural gas is 9.751 m^3/m^3, with a density of 0.7615 kg/Nm^3.

For complete combustion the jet must entrain the stoichiometric air requirement together with 10% excess air. Thus

$$m_0 = 1.5\ kg/s$$

$$m_x = 1.5 + \left(1.5 \times 1.1 \times 9.751 \times \frac{1.2928}{0.7615}\right) = 28.8146\ kg/s$$

Using equation 2.16

$$\frac{28.8146}{1.5} = 0.32\left(\frac{1.2928}{0.7615}\right)^{0.5}\frac{x}{0.1}$$

$$x = 4.607\ m$$

It should be noted that for these conditions, the exit velocity of the gas from the nozzle is 250.8 m/s.

In the case of a confined jet, which is the normal situation inside a furnace, the jet is now constrained in two ways. The quantity of surrounding fluid being supplied to the furnace i.e. the mass of secondary air, is controlled and limited and the expansion of the jet is now bound by the physical presence of the furnace walls. If the confined jet has momentum in excess of that required for the complete entrainment of the secondary stream, then jet recirculation will occur. In this

case, the secondary air stream is initially pulled into the jet in a similar manner to a free jet. A point is then reached, however, when all the available air has been entrained into the flame. At this stage, the jet will pull back exhaust gases into the flame from beyond its current position in order to overcome the excess momentum flux in the jet, relative to its local surroundings. The jet will continue to recirculate fluid until the momentum is dissipated evenly across the furnace enclosure.

2.4.1 The Role of Primary Air

Primary air has two major roles in jet entrainment burners:-

- It controls the rate of fuel-air mixing.
- It assists with flame stability.

Primary air is often defined as a percentage of the stoichiometric air requirement. The primary air itself is either premixed, or mixes very rapidly with the fuel at the nozzle, but the remaining air (secondary, tertiary, etc. air) must be entrained into the primary air and fuel jet. The rate of entrainment depends on the ratio of the momentum of the combined jet of primary air and fuel, to the momentum of the combined secondary, tertiary, etc. air. Thus, the higher the flowrate and velocity of primary air, the more rapid the fuel-air mixing. The flame characteristics are determined by this momentum ratio, and burners can be designed to give specific flame characteristics by the use of modelling, discussed in Chapter 6.

The presence or absence of recirculation has a great effect on the characteristics of the flame. Figure 2.9 illustrates how external recirculation is created in a confined jet. In furnaces where the flame is not influenced or restricted by the walls, i.e. a free jet, swirled primary

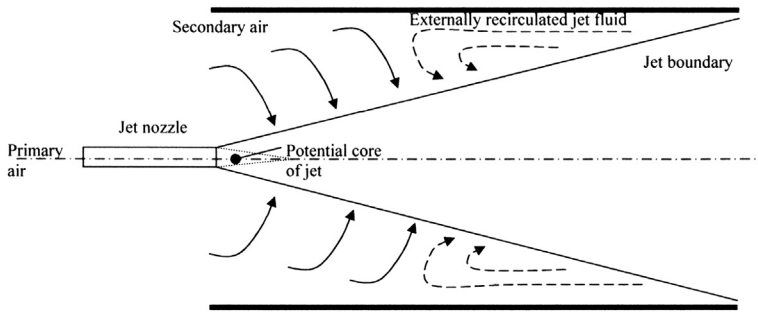


Figure 2.9 Entrainment of fluid into a high momentum confined jet with external recirculation

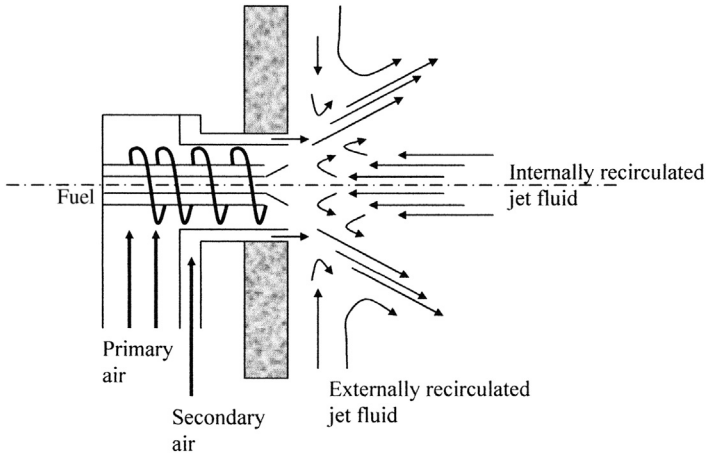


Figure 2.10 Entrainment of fluid into a swirling free jet with internal recirculation

air or a bluff body is used to create an internal recirculation region. See Figure 2.10.

A moderate degree of recirculation is a positive indication that fuel-air mixing is complete, whilst its absence is a clear indication that not all of the secondary air has been entrained into the primary jet. In this case, the production of significant levels of carbon monoxide is normal unless the burner is operating at a high excess air. Furthermore, in confined jets, the absence of recirculation results in a tendency for the flame to expand until it impinges onto the furnace walls or load. Hot reducing gases will then be in direct contact with the refractory brick, tending to "wash them away" and causing their subsequent failure; impinge on heat transfer surfaces e.g. tubes; or may adversely affect the quality of the product. The recirculating gases from a high momentum flame, however, provide a "cushion" of cooler inert flue gases which prevents this direct impingement of the flame. A high momentum, recirculatory burner jet will also produce a responsive and stable flame that is more controllable, hence making the operation of the furnace easier. The characteristics of furnace flames with and without the presence of external recirculation are summarised in Table 2.1.

The furnace flames illustrated in Figures 2.9 and 2.10 are characterized as axi-symmetric enclosed turbulent jet diffusion flames, and there are a number of jet theories that enable us to define their properties. The first useful theory of an enclosed jet, particularly from the aspect of combustion studies, was put forward by Thring and Newby (1953), who made predictions of confined jet properties based on free jet theory. They introduced a parameter, θ', which may be used to determine the point in the downstream jet where recirculation

Table 2.1 The Characteristics of Furnace Flames With and Without External Recirculation

Characteristic of Combustion Process	*Flame With Recirculation*	*Flame Without Recirculation*
Fuel-air mixing	Good	Poor
Reducing/oxidising conditions	Oxidising conditions exist throughout the flame	Strongly reducing conditions occur in fuel rich parts of the flame. Oxidising conditions exist elsewhere.
Flame impingement	None. Recirculating gases protect bricks, walls and product bed from flame impingement.	Flame impingement occurs on the brickwork/product at the point where the jet expands (at ~11°–14°) to hit the kiln wall. Impingement is especially severe where a low primary air/secondary air momentum ratio occurs.
Carbon monoxide level in flue gases	CO only produced at levels of excess oxygen below 0.5%.	CO produced at levels of excess oxygen as high as 2–4%.
NO_x emissions in flue gases	Can result in high thermal NO_x formation if early flame ignition is not achieved.	Low NO_x owing to lower flame temperatures and reducing conditions in the flame.
Heat release pattern	Rapid mixing gives high flame temperature near nozzle.	Poor mixing gives gradual heat release with a long flame.
Flame stability	Good flame shape with stable ignition front and heat release pattern.	Flame shape, ignition front and heat release pattern considerably affected by changes in secondary air temperature, excess air, fuel quality, etc.

entrainment starts, x_n, the core of the recirculation eddy, x_c, and the mass of recirculating fluid, m_r.

$$\theta' = \frac{d_0'}{d_1}\left(\frac{\rho_0}{\rho_1}\right)^{0.5}\frac{m_0 + m_1}{m_0} \tag{2.17}$$

$$x_c = 1.5625(\theta' + 0.9104)d_1 \tag{2.18}$$

$$\frac{m_r}{m_0} = \frac{0.455}{\theta'} - 0.5 \tag{2.19}$$

where

d_0' - equivalent nozzle diameter
d_1 - enclosing chamber diameter (or geometric equivalent)
m_1 - mass flowrate of secondary fluid

The predictions of these equations are some 20% higher than experimental data and the theory is limited to systems where $d_1/d_o'<20$, where

$$d'_0 = \frac{2(m_0 + m_1)}{(\pi\rho_0\{m_0u_0 + m_1u_1\})^{0.5}} \tag{2.20}$$

where

u_o - velocity on nozzle fluid at the nozzle exit plane
u_1 - velocity of secondary fluid at the nozzle exit plane

A more fundamental approach was taken by Craya & Curtet (1955), who used mean integrated values of the Navier-Stokes equations in conjunction with the continuity equation to describe the performance of an enclosed jet. This theory has been further developed, expanded and tested for hot systems by Becker (1961) and Becker, Hottel and Williams (1962). The theory of Craya and Curtet predicts recirculating flow conditions with no limitation of confinement ratio. Craya and Curtet use a similarity parameter, m, which for an enclosed jet in a duct of constant dimension is given by:

$$m = -1.5R^2 + R + K\frac{R^2}{\left(\frac{d_0}{d_1}\right)^2} \tag{2.21}$$

where

$$R = \frac{(u_0 - u_1)\rho_0\left(d_0/_2\right)^2}{u_1\rho_1\left(\frac{d_1}{2} - \delta^*\right)^2 + (u_0 - u_1)\rho_0\left(\frac{d_0}{2}\right)^2} \tag{2.22}$$

K - jet shape factor (K=1 for a round jet)
δ^* - boundary layer thickness (usually negligible except for very small jet nozzles)

Since the derivation of the parameter is based on an assumption of isothermal flow, the densities of the jet and entrained fluids are evaluated at the same temperature. Craya and Curtet also derived an expression for the mass of recirculating fluid, given as

$$\frac{m_r}{m_0 + m_1} = 0.430\left(\sqrt{m} - 1.65\right) \tag{2.23}$$

It has been shown that when the jet is considered as a point source, at its origin

$$\theta = \sqrt{m} \tag{2.24}$$

Table 2.2 The Comparative Characteristics of Simple Enclosed Jet Theories

Parameter	*Symbol*	*Maximum Value*	*Minimum Value*	*Onset of Recirculation*	*Relationship*	*Limitations*
Thring Newby parameter	θ'	0	∞	<0.9	$=m^{-0.5}$	$d_l/d'_o<20$
Craya Curtet parameter	m	∞	0	>1.5	$=0.5(Th^{-2}-1)$	
Becker throttle factor	Th	0	1	<0.4	$=\theta'/(2+\theta'^2)^{0.5}$	
Curtet number	Ct	0	∞	<0.75	$=m^{-0.5}$	

Table 2.2 shows the inter-relationship between the various simple jet parameter values, and their significance. Example 2.3 illustrates the use of these parameters in practical applications

Example 2.3 A 3.5m internal diameter rotary kiln fires 1.5 kg/s of natural gas, with the same properties as in example 2.2, through a burner consisting of a 100 mm diameter gas nozzle, surrounded by a concentric primary air nozzle 110 mm inside diameter and 230 mm outside diameter. The kiln operates at 10% excess air with 15% primary air, the balance of the combustion air being supplied as secondary air around the burner over the whole of its cross section. If the primary air and gas are at 20°C, and secondary air is at 850°C, will the resulting jet be recirculatory?

From the information in example 2.2, the stoichiometric air requirement on a mass basis $= 9.751 \times \dfrac{1.2928}{0.7615}$

$= 16.5543$ kg/kg

The primary air rate $= 1.5 \times 16.5543 \times 0.15 = 3.7247$kg/s

The total air rate including the excess air $= 1.5 \times 16.5543 \times 1.1$

$= 27.3146$ kg/s

Thus secondary air rate $= m_1 = 27.3146 - 3.7247 = 23.5899$ kg/s

The burner is of a composite construction, which for analysis is reduced to an equivalent plain nozzle.

The primary jet rate $= m_0 = 1.5 + 3.7247 = 5.2247$ kg/s

Gas density $= 0.7615 \times \dfrac{273}{293} = 0.7095$ kg/m^3

$$\text{Primary air density} = 1.2928 \times \frac{273}{293} = 1.2046 \text{ kg/m}^3$$

$$\text{Secondary air density} = 1.2928 \times \frac{273}{1123} = 0.3143 \text{ kg/m}^3$$

$$\text{Gas port area} = \pi \times \frac{0.1^2}{4} = .007854\text{m}^2$$

$$\text{Primary air port area} = \pi \times \frac{0.23^2 - 0.11^2}{4} = 0.03204\text{m}^2$$

$$\text{Secondary air entry area} = \pi \times \frac{3.5^2 - 0.23^2}{4} = 9.5796 \text{ m}^2$$

$$\text{Volume flow of gas} = \frac{1.5}{0.7095} = 2.1142\text{m}^3/s$$

$$\text{Volume flow of primary air} = \frac{3.7247}{1.2046} = 3.0922 \text{ m}^3/s$$

$$\text{Volume flow of secondary air} = \frac{23.5899}{0.3143} = 75.0605 \text{ m}^3/s$$

$$\text{Gas velocity at nozzle plane} = \frac{2.1142}{0.007854} = 269.18\text{m}/s$$

$$\text{Primary air velocity} = \frac{3.0922}{0.03204} = 96.50 \text{ m}/s$$

$$\text{Secondary air velocity} = u_1 = \frac{75.0605}{9.5796} = 7.835 \text{ m}/s$$

$$\text{Mass weighted jet velocity} = u_0 = \frac{1.5 \times 269.18 + 3.7247 \times 96.5}{5.2247} = 146.07 \text{ m}/s$$

Mass weighted jet density $= \rho_0$

$$= \frac{1.5 \times 0.7095 + 3.7227 \times 1.2046}{5.2247}$$

$$= 1.0624 \text{ kg/m}^3$$

Secondary air density at primary jet temperature $= \rho_1$

$$= 1.2928 \times \frac{273}{293} = 1.2046 \text{ kg/m}^3$$

Geometric equivalent nozzle diameter $= d_0$

$$= \left(\frac{5.2247 \times 4}{\pi \times 1.0642 \times 146.07}\right)^{0.5}$$

$$= 0.207 \text{ m}$$

Thring Newby equivalent diameter

$$d_0' = 2 \times (5.2247 + 23.5899)/(\pi \times 1.0624 \times (5.2247 \times 146.07 + 23.5899 \times 7.835))^{0.5} = 0.5608 \text{ m}$$

$$\frac{d_1}{d_0'} = \frac{3.5}{0.5608} = 6.24$$

This value is less than 20 and therefor the Thring Newby parameter is not suitable and the Craya Curtet parameter will be used.

Since d_1 is very large compared to the boundary layer thickness, $\delta^*=0$. K=1 as the system is a round jet.

$$R = \frac{(146.07 - 7.835) \times 1.0624 \times (\frac{0.207}{2})^2}{(7.835 \times 1.2046 \times (\frac{3.5}{2})^2) + (146.07 - 7.835) \times 1.0624 \times (\frac{0.207}{2})^2}$$

$$= 0.051619$$

$$m = -1.5 \times (0.051619)^2 + (0.051619) + \frac{(0.051619)^2}{(\frac{0.207}{3.5})^2}$$

$$m = 0.8094$$

The value of the Craya Curtet parameter, m, is less than 1.5 , and the jet will not be recirculatory.

Further calculations can be made to show that the primary air would need to be increased to >20%, or the combined jet velocity increased to >200 m/s to make the jet recirculatory.

2.4.2 The Role of Swirl Flows

Many burner designs utilise air swirl to control the fuel-air mixing. For these burners the presence or absence of an internal, or "central" recirculation zone (Figure 2.10) is controlled by the intensity of the swirl. A dimensionless swirl number, *S*, is used to characterise the amount of swirl, Beer & Chigier (1972). The swirl number is the dimensionless ratio of angular to axial momentum:

$$S = G_\phi / G_x\, r \tag{2.25}$$

Where:

$$G_\phi = \text{Axial flux of angular momentum} = \int_0^{d_o} (Wr)\, \rho U^2 \pi r \partial r$$

$$= \text{constant} \tag{2.26}$$

$$G_x = \text{Axial flux of axial momentum} = 2\pi \int_0^{d_o} \rho U^2 r \partial r \tag{2.27}$$

Although the swirl number is easy to define, it is not so easy to measure. For this reason a "geometric swirl number" is often used which is based on the geometric angles of the swirl generators. Because there are losses in the system, the geometric swirl number is always higher than the real swirl number. Typically an internal recirculation is established for a real swirl number of greater than about 0.5.

2.4.3 Turbulence in Jets

Combustion is not a steady state process, and all the parameters that define its progress are subject to fluctuations. These fluctuations can be attributed to the turbulent structure of the flow in most flames, since we have already noted that the bulk Reynolds Number is typically in the turbulent regime. We have already premised that diffusional mixing rates define the essential characteristics of the flame, therefore computation of these rates should result in a 'complete' flame model. The laminar jet represents steady state conditions throughout the complete domain i.e. no local fluctuations of jet properties, and the basic differential equations for mass, momentum and jet fluid conservation provide the basis for analysis. Thus the normal engineering analogies between mass, momentum and heat transfer are applied. Computational procedures for turbulent flows generally involve the calculation of the 'effective' viscosity, which implies that

turbulent flow is likened to laminar flow with a viscosity correction. This has been shown to be reasonably valid for many 'simple' flow problems, but the interactions of turbulence and chemical reaction e.g. combustion, make this assumption far less certain.

Dimensional analysis of the near field flow of a jet, see Figure 2.8, yields the following:

$$\mu_{eff} = C_1 \rho (u_0 - u_{ax}) \delta \tag{2.28}$$

where $C_1 = 0.0148$ for a free jet, and 0.0102 for an axisymmetrical jet.

$$Re_{turb} = \frac{[\rho(u_0 - u_{ax})\delta]}{\mu_{eff}} \tag{2.29}$$

Thus from equations 2.28 and 2.29, it can be seen that Re_{turb} approximates to a constant value of $\sim$100 for an axisymmetrical jet. If μ_{eff} is connected strictly with 'local' quantities, then the turbulent kinetic energy, k, and the length scale, λ, are relevant. Thus we have:

$$\mu_{eff} = C_2 \rho k^{0.5} \lambda \tag{2.30}$$

where λ is defined by reference to the local rate of energy dissipation, $\varepsilon\rho$, by:

$$\lambda = \frac{k^{1.5}}{\varepsilon} \tag{2.31}$$

and

$$\mu_{eff} = \frac{C_2 \rho k^2}{\varepsilon} \tag{2.32}$$

This is the classic k-ε model, where C_2 has a value of the order of 0.1, and is reasonably valid if the turbulence fluctuations do not vary excessively. If:

$$k^{0.5} = \lambda \frac{\partial u}{\partial y} \tag{2.33}$$

and the value of C_2 is set to unity, then λ is called the Prandtl mixing length, λ_m, thus:

$$\mu_{eff} = \rho \lambda_m \frac{\partial u}{\partial y} \tag{2.34}$$

λ_m is directly proportional to δ, and is typically one tenth of its value ($\lambda_m \sim 0.075\delta$. for an axisymmetrical jet).

Intensification of turbulent mixing by the use of swirl has been shown to be effective in flames, but this generates turbulent fluctuations in both the axial and tangential flow planes. When the swirl number reaches unity (S=1) we can no longer theoretically justify the use of a simple jet correlation, and the k-ε model breaks down.

In practice it is probable that if $S>0.5$ then the tangential fluctuation component exerts sufficient flow distortions that it can no longer be incorporated into the axial component, and thus a theory which embraces (at least) two planes must be used. This leads to the Reynolds stress model, which defines the conservation equations by differential perturbations in three planes. The solution of this fundamental turbulence problem is the basis of computational fluid dynamic models (CFD), which are discussed further in Chapter 6.2.4.

2.4.4 Secondary Flow Aerodynamics

Since the secondary, tertiary etc. air has to be entrained into the fuel-primary air jet, the secondary flow aerodynamics can have a prodigious effect on the fuel/air mixing. The secondary flow patterns in the furnace are considerably affected or determined by the geometry of the inlet(s) and the configuration of the inlet ducting. For many furnace designs, the air ducts, entry ports and the flue gas exit ports are often erroneously determined as much by mechanical and process requirements, as by any aerodynamic considerations. The ideal jet theories discussed in 2.4.1 consider the secondary fluid(s) to be evenly distributed around the jet. This can be achieved if the burner designer has complete control of all of the air flow streams. This situation is typical of a packaged burner used in boilers and process heaters.

However, in many furnaces the burner designer can only control the primary air. A good example of this situation is a rotary kiln, where the secondary air flow is considerably determined by the design of the cooler uptake and hood system, or in the case of planetary coolers, by the cooler elbows. To obtain the optimum potential performance from any kiln, it is absolutely essential that the aerodynamic characteristics of the kiln are taken fully into account when designing the burner. Typical aerodynamics for a grate cooler kiln are illustrated in Figure 2.11, which shows the results of water and air flow modelling patterns for high and low momentum jets. It can be clearly seen that there is a significant difference between the secondary air flows in the two cases, in particular the size and strength of the recirculation zones which decrease with decreasing jet momentum and eventually disappear. The relationship between the jet momentum and the secondary air velocity has a significant effect on the flame length and hence heat transfer. For example, rotary kilns with very low jet momentum suffer from poor fuel/air mixing with long flames and inefficient combustion, leading to increased fuel consumption. This topic is discussed in more detail in Chapter 5.

Similar effects are observed with flash calciners as shown in Figure 2.12. In the first diagram, a right-angled secondary air entry duct to the calciner creates a highly asymmetric airflow, giving poor

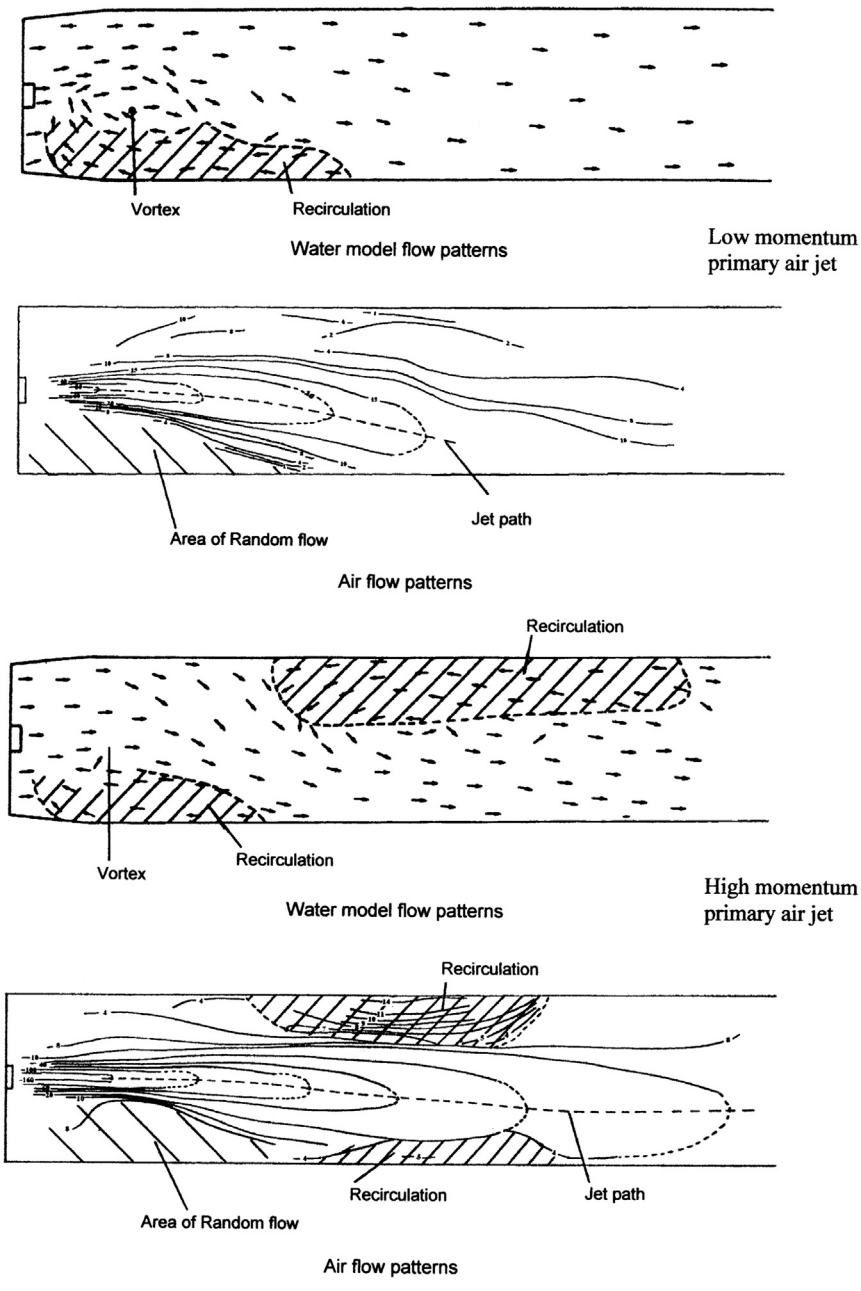


Figure 2.11 Typical aerodynamics in a rotary kiln associated with a grate cooler, obtained by water-bead and air modelling

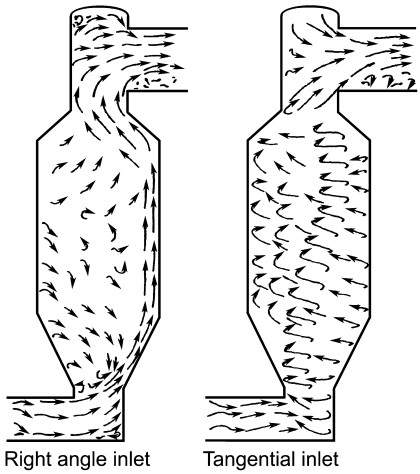


Figure 2.12 Typical aerodynamics in a flash calciner – obtained using water-bead modelling

fuel/air mixing and an intense recirculation zone on one side. For complete combustion excellent fuel/air mixing is required, and this is aided by the good secondary airflow pattern generated by a tangential secondary air entry duct as shown in the second diagram.

2.4.5 Effect of Excess Air on Fuel Consumption

Although the effect of excess air level on overall efficiency for thermal processes has been understood for many years, it is surprising how little attention is paid to this matter even today. A reduction in efficiency occurs as the oxygen level is increased above the optimal value, caused by the requirement to heat the excess oxygen and nitrogen passing through the system. This causes the flame temperature and heat transfer to reduce.

In process plants where the combustion air is preheated, the increased air flow causes a reduction in the secondary air temperature, and therefore a reduction in the flame temperature, thus requiring even more fuel to heat the charge to the required process temperature. The total increase in fuel consumption is much greater than that necessary to heat the excess air to the flue gas exit temperature alone. The effect of excess air on thermal efficiency is very considerable. Figure 2.13. shows the relationship between the flue gas oxygen level and the measured daily heat consumption for a cement kiln. A clear trend is apparent and increasing the excess oxygen level from 1% in the kiln to 5% results in an increase in the heat consumption of more than 10%.

If the excess air level in a flame is reduced below a certain level, carbon monoxide is produced. This in turn also leads to an increase in the

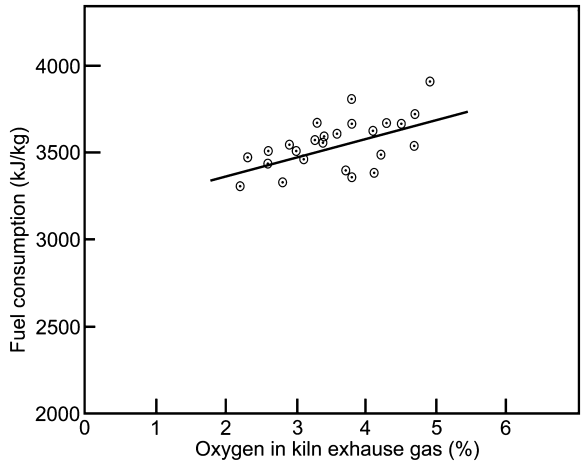


Figure 2.13 The effect of excess air on heat consumption (i.e. fuel efficiency) for a cement kiln

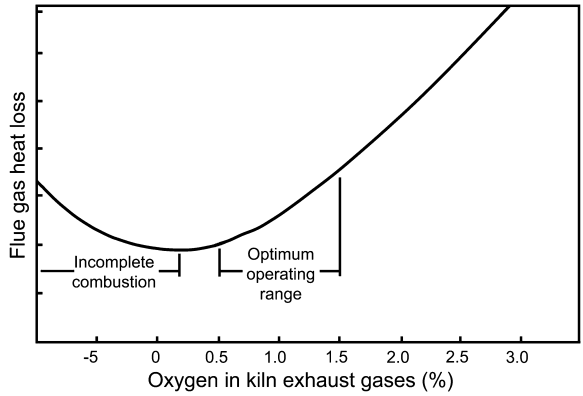


Figure 2.14 The effect of excess air on flue gas heat losses

fuel consumption, due to the incomplete combustion of carbon as can be seen in Figure 2.14. The better the fuel-air mixing, the lower the excess air at which these emissions occur.

2.4.6 Multiple Burner Installations

Many plants such as water tube boilers and petrochemical heaters utilise multiple burners with a common air supply firing into a common furnace. To ensure efficient operation each burner must have a consistent and controlled combustion air supply. Whilst this is obvious for a single burner, it is equally true for a number of burners firing into a common combustion chamber, since little inter-mixing occurs between

the flames in the furnace. Hence, if the airflow to an individual burner is deficient, then the associated flame will be sub-stoichiometric. The significance of poor air distribution is discussed in detail in Chapter 5.

It is particularly difficult to achieve satisfactory air distribution where a large number of burners are supplied by a common air duct. Dampers are often provided to permit 'air balancing' between burners, but in practice it is very difficult to achieve a satisfactory balance, since adjustment of one burner damper influences the air supply to all the other burners. Whilst it may be possible to achieve a reasonable air balance on a furnace with six burners by the use of individual dampers, it is virtually impossible where there are more than ten burners owing to the very large number of adjustments, interactions and re-adjustments which would be necessary.

Nomenclature for Chapter 2

A = reaction rate constant.
C = constant
Ct = Curtet number
d = diameter
D = diffusivity
E = activation energy
G = momentum flux
k = reaction rate constant, turbulent kinetic energy
K = reaction equilibrium constant, jet shape factor
m = mass fraction, mass flowrate, Craya-Curtet parameter
n = moles
p = pressure
r = radius
R = universal gas constant, rate, momentum ratio
q = char burning rate
S = swirl number
T = temperature
Th = Becker throttle factor
u,U = velocity
V = volume
W = tangential velocity
x = separation distance

Subscripts

A,B = chemical species
ax = axial
c = core of entrainment

d = diffusion
eff = effective
fu = fuel
n = start of entrainment
ox = oxidant
O_2 = oxygen
r = recirculation
s = surface
$turb$ = turbulent
x = axial
0 = origin
1,2,etc. = identifiers
Φ = angular

Greek Letters

δ^* = boundary layer thickness
Δ = difference between two values
ε = eddy diffusivity
θ' = Thring −Newby parameter
λ = length
μ = viscosity
π = geometric constant
ρ = density
τ = reactedness
ϕ = mechanism factor for CO_2/CO transport

References for Chapter 2

Becker, H. A. (1961). Concentration fluctuation in ducted jet mixing. *Sc.D. Thesis, Mass. Inst. Tech*.

Becker, H. A., Hottel, H. C., & Williams, G. C. (1962). *Mixing and flow in ducted turbulent jets*, 9th. Symp. (Int.) on Combustion. New York: Academic Press, 7–20.

Beer, J. M., & Chigier, N. A. (1972). *Combustion Aerodynamics* (p. 109). U.K: Applied Science.

Craya, A., & Curtet, R. (1955). On the Spreading of a Confined Jet. *Comptes-Rendus Acad. des Sciences, 241*, 611–622.

Field, M. A., Gill, D. W., Morgan, B. B., & Hawksley, P. G. W. (1967). *Combustion of Pulverised Fuel*. Appendix P. Leatherhead: B.C.U.R.A.

Hamor, R. J., Smith, J. W., & Tyler, R. J. (1973). Kinetics of Combustion of Pulverised Brown Coal Char between 630 and 2200 K. *Combustion and Flame, 21*, 153–162.

Jenkins B. G. & Moles F. D. The Design of Pulverised Coal Firing Burners for the Process Industries, First European Dry Fine Coal Conference, Harrogate, IV/2/1–18, 23–25 June 1987.

Knill, K. J., Maalman, T. F. J., & Morgan, M. E. Development of a Combustion Characterisation Technique for High Volatile Bituminous Coals – Report on the CC4 Trials, IFRF Doc No. F 88/a/10, Int. Flame Research Foundation, IJmuiden, The Netherlands, July 1989.

Knill, K. J., Maalman, T. F. J., Morgan, M. E., & Nel, W., Characterisation of the Combustion Behaviour of Bituminous Coals – Report on the CC6 Investigation, IFRF Doc No. F 88/y/12, Int. Flame Research Foundation, IJmuiden, The Netherlands, Nov. 1990.

Morgan, M. E., & Dekker, J. S. A., Characterisation of the Combustion Performance of a Suite of Pulverised Coals – Report on the CC1 Trials, IFRF Doc No. F 188/a/4, Int. Flame Research Foundation, IJmuiden, The Netherlands, April 1988.

Ricou, F. P., & Spalding, D. B. (1961). Measurement ef entrainment by axisymmetrical turbulent jets. *Jnl. Fluid Mechanics, 11*, 21–32.

Smith, J. W., & Tyler, R. J. (1974). The Reactivity of Porous Brown Coal Char to Oxygen between 630 and 1812 K. *Combustion Sci. and Technol., 9*, 87–94.

Thring, M. W., & Newby, M. P. (1953). *Combustion Length of Enclosed Turbulent Flames*, 4th. Symp. (Int.) on Combustion. Baltimore: Williams & Wilkins, 789–796.

Chapter 3

Fuels for Furnaces

Chapter contents

3.1	Gaseous Fuels	69
3.2	Liquid Fuels	75
3.3	Solid Fuels	77
3.4	Waste Fuels	79
3.5	Choice of Fuel	80
3.6	Safety	85
3.7	Emissions	86
Nomenclature		86
References		86

Choice of fuel is a critical decision in the furnace design process, especially since fuel is one of the highest costs of subsequent furnace operation. Fuel choice also has a major impact on furnace performance and the capital cost of the overall installation. This chapter will consider the various fuels available and how their characteristics influence their suitability as furnace fuels. It should be noted that a fuel that approaches ideal for one process may be less suitable or even totally unacceptable for a different system. Factors affecting the cost of fuel to the user include; abundance or scarcity (both worldwide and locally), ease of extraction or manufacture, ease of use (fuels that are easier to use attract a premium from suppliers), political policy (i.e. taxation), ease of transportation etc. The relative importance of these features changes with time. Between 1965 and 2005, oil, coal and natural gas have each been the cheapest fuel in much of Europe for periods of time. Properties of a fuel that influence its use include:

1. Availability and cost
2. Calorific value
3. Flammability limits
4. Density of the fuel, especially gaseous and liquid fuels
5. Emissivity of flame produced
6. Chemical composition and the products of the combustion process*
7. Ash content and composition (principally for solid fuels)
8. Effect of products of combustion on the product

Given that furnaces have design lives of typically 20 years and are often in use for much longer, choosing a fuel that will be the most economical over the entire life of the furnace is a difficult task and impossible to accomplish with any certainty. Fuel properties are considered in greater detail later in this chapter and throughout the book, to assist designers and users to make the most appropriate choice.

Generally, but not exclusively, fuels are hydrocarbon based. Non-hydrocarbon fuels include hydrogen, carbon monoxide, ethanol, methanol, and many of the so called bio-derived fuels. Other materials such as sulphide ores, while not normally considered to be fuels, release heat when oxidised and contribute significant energy to the process. Fuels may be solids, liquids or gases and may occur naturally or be manufactured, or in the case of so-called bio-fuels, grown. Even naturally occurring fuels generally require some processing prior to use. It is conventional and convenient to classify fuels by their physical state, i.e. gases, liquids and solids. Each type is considered in turn below.

*Including toxicity of the fuel and its products of combustion.

3.1 Gaseous Fuels

Gases may be natural or manufactured, the latter generally from oil, coal or biomass (wood). Both natural and manufactured fuels vary widely in chemical composition and physical characteristics.

Natural gas has been known for many years and may have been used by the Chinese to evaporate salt as early as the second century AD (Donovan & Kirkman 1986); indeed, the burning bush quoted in the Bible was probably the result of a natural gas fire.

Manufactured gases, once dominant in the industrial world, have been losing ground to natural gas, firstly in the USA and Canada, then in the late 1960s, in Australia and Europe following discoveries of local natural gas. The liquefaction and sea borne transportation of natural gas (LNG) was pioneered by British Gas in the mid fifties when Algerian natural gas was transported to Essex by the 'Methane Pioneer' which used tanks insulated with balsa wood. LNG currently forms a very important and growing link in the natural gas transportation system.

3.1.1 Properties of Natural Gas

Although the basis of natural gas is methane, the actual composition depends both on the composition in the reservoir and the degree of treatment that occurs. Natural deposits of gas typically contain higher hydrocarbons, as well as CO_2, N_2, H_2S, etc. Hydrogen sulphide is always removed from gas sold through the public system, owing to both its very high toxicity and the toxicity of its products of combustion (SO_2 & SO_3). Typical natural gas compositions for Australia, Europe and North America are shown in Table 3.1. Gas specifications are normally available from the supplier and should always be obtained prior to developing a furnace design.

3.1.2 Manufactured Gas

Gas has been manufactured since the mid 19th Century and, although manufactured gas is rarely supplied through the public distribution system these days, it is still produced as a by-product of many chemical and metallurgical processes. These off-gases are usually utilised as fuels within the plant, so manufactured gases are of great interest to furnace designers. In addition, propane and butane (LPG), a by-product of oil refining and natural gas treatment, are widely distributed by tanker and used as both transport fuels and furnace fuel. Table 3.2 shows the typical properties of a number of manufactured gases.

Table 3.1 Typical Natural Gas Compositions as Supplied to Customers

Property	North[1] Sea	Groningen[1]	Kansas Missouri[2]	South Australia[3]	Coal Bed Methane[4]
CH_4 (%)	94.4	81.8	84.1	91.25	98.0
C_2H_6 (%)	3.0	2.7	6.7	4.53	—
C_3H_8 (%)	0.5	0.4	—	0.54	—
Higher C_xH_y (%)	0.4	0.2	—		—
N_2 (%)	1.5	14.0	8.4	1.4	1.5
CO_2 (%)	0.2	0.9	0.8	2.0	0.5
Relative Density (air =1)	0.589	0.641	0.63	0.612	0.566
CV gross (MJ/m^3)	38.62	33.28	36.13	38.33	37.0
Air Req (m^3/m^3)	9.751	8.402	9.16	9.644	9.33
Wobbe No (MJ/m^3)	50.322	41.568	45.522	48.87	49.2

[1] Technical Data on Fuel, 7th Ed, p268
[2] North American Handbook, Vol 1, 3rd Ed, pp 36–38
[3] Data provided courtesy of Origin Energy and Santos
[4] Data is for mid life Queensland coal seam, and provided courtesy of Origin Energy

Table 3.2 Raw Compositions of a Few Manufactured Gases

Properties	Blast Furnace Gas	Coke Oven Gas	Producer Coal Gas	Lean Reformer Gas[1]	Lurgi Crude Syngas	Commercial Propane
CH_4 (%)	—	28	2.6	22.7	10.3	—
C_2H_6 (%)				5.0	—	1.5
C_3H_8 (%)				—	—	91.0
Higher C_xH_y (%)	—	2	0.4	0.4	0.6	7.5
CO	24	7.4	29	2.2	24.4	—
H_2	2.5	54	12	53.7	37.3	—
N_2 (%)	56	5.6	52	—	1.8	—
CO_2 (%)	17.5	2	4	16.0	25.6	—
O_2 (%)		0.4	—	—	—	—
Relative Density (real air =1)	1.04	0.38	0.87	0.593	0.732	1.523
CV gross (MJ/m^3)	3.18	19.89	6.14	18.92	11.76	93.87
Air Req (m^3/m^3)*	0.631	4.572	1.28	4.398	2.556	23.762
Wobbe No (MJ/m^3)	3.118	32.266	6.583	27.196	13.745	76.064

* For dry fuel and dry air
[1] CO converted and enriched

For further information on gas manufacturing see Ulmans, 1989, Vol, A12 p169–306.

Comparing the gases in Tables 3.1 and 3.2, it can be seen that there is a wide range of properties for gaseous fuels. This implies that a combustion system designed for one type of gas is unlikely to operate

satisfactorily on a different gas. It is therefore essential that we have a means of classifying gases so that we can assess whether they are suitable for use in a particular appliance. The broadest classification is that of rich and lean gases. While there is no clear demarcation between the two, the former have the higher calorific values generally above 25–30 MJ/m^3, while lean gases occupy the lower end of the scale. This classification is highly subjective and does not allow any quantitative assessment as to whether a gas is suitable for a specific application. The properties outlined in the opening paragraphs influence the choice of gas for an application as they do for all fuels. However for gas, a major consideration is the energy relative to the density because this affects the heat release rate of a burner. This property is encapsulated in the Wobbe Number or Wobbe Index, which is discussed below.

Examination of Tables 3.1 and 3.2 will show that most gases are lighter than air, the exceptions being blast furnace gas and propane. Although not shown, butane is even denser than propane. Light gases tend to disperse following a leak and rarely accumulate in dangerous quantities. However, dense gases do not disperse readily but accumulate in low spots. This factor, together with the extreme toxicity of blast furnace gas and the high energy density of propane and butane, render these gases far more dangerous than most other fuels. While the use of blast furnace gas is largely restricted to the steel industry where its risks are well understood, LPG is widely distributed in the community and used by people who do not always appreciate the risks involved. Anecdotal evidence would suggest that the numbers of accidents involving LPG are significantly greater than represented by its proportion of the market. These issues are considered further in section 3.6 and Chapters 7 and 8.

3.1.3 Wobbe Number or Index

For any combustion system one of the most important parameters is the heat release rate and, if we look at the tables above, we can see that similar volumetric gas flow rates will give wildly different heat release rates for different gases. Furthermore, since most systems supply the gas through a fixed nozzle the flow rate will vary with the density. This problem has been overcome by the use of a parameter know as the Wobbe Number or Wobbe Index.

$$W_I = \frac{CV}{SG^{0.5}} \tag{3.1}$$

Where:

CV = the higher or gross calorific value in MJ/m^3 or BTU/ft^3
SG = the specific density relative to air

The Wobbe Number is not non-dimensional but depends on the units that are used for the calorific value and density.

Gases of similar Wobbe Number will produce the same heat release in a furnace when supplied through the same nozzle with similar supply pressure. (Assuming the furnace chamber pressure is the same in both cases.)

3.1.4 Flammability Limits

For a flame to self-propagate following initial ignition the mixture must be within certain limits. Outside of these limits the reaction does not propagate from the ignition source. These limits are not absolute values and depend on the size and shape for the vessel containing the mixture and the direction of propagation, upward propagation being the most favourable (Rose & Cooper, 1977). Much of the work was undertaken by the US Bureau of mines and published in the Journal of the Institute of Fuel (Bennett, 1933/4) and (Callcott, 1956). The limits of interest are:

- Minimum Flammable Concentration
  The minimum concentration or Lower Limit of flammable material which, when suspended in air (or other oxidant), is capable of ignition and explosion.
- Maximum Flammable Concentration
  The maximum concentration or Upper Limit of flammable material which, when suspended in air (or other oxidant), is capable of ignition and explosion.
- Maximum Permissible Oxygen Concentration to Prevent Ignition
  If the mixture contains insufficient oxygen then an explosion cannot be propagated. The maximum oxygen concentration at which an explosion cannot be propagated is determined by creating a mixture of the flammable substance and an inert gas and adding oxygen until an explosion occurs. The effectiveness of an inert gas or vapour depends on its molar heat capacity, the greater heat capacity, the more effective the inert component in suppressing flammability, hence steam is more effective than CO_2 which is more effective than N_2.

Typical flammable limits at room temperature are given in Table 3.3

Calculation of the Flammable Limits for Mixtures of Gases

The limits of mixtures of gases can be calculated using Le Chatelier's rule. This is based on the empirical observation that the limit of the mixture is proportional to the composition of the individual gases in

Table 3.3 Flammable Limits for Gases at Room Temperature

Property	*Hydrogen*	*Carbon Monoxide*	*Methane (CH_4)*	*Ethane (C_2H_6)*	*Propane (C_3H_8)*	*Butane (C_4H_{10})*
Lower limit (%)	4.0	12.5	5.0	3.0	2.1	1.8
Upper limit (%)	75	74	15.0	12.4	9.5	8.4
Maximum safe oxygen in N_2 (%)	5.0	5.6	12.1	11.0	11.4	12.1

Source: Technical Data on Fuel, 7th Ed, p247–249

the mixture and their individual flammable limits, thus for the lower flammable limit:

$$L_{mix} = 100/(P_1/L_1 + P_2/L_2 + P_3/L_3 + \ldots + P_n/L_n) \qquad (3.2)$$

Where: P_1, P_2, P_3 … P_n are the percentages of gases 1,2,3 etc, and L_1, L_2, L_3 are their lower flammable limits.

Similarly for the upper limit:

$$U_{mix} = 100/(P_1/U_1 + P_2/U_2 + P_3/U_3 + \ldots + P_n/U_n) \qquad (3.3)$$

Where: P_1, P_2, P_3 … P_n are the percentages of gases 1,2,3 etc, and U_1, U_2, U_3 are their upper flammable limits.

The accuracy of the formula has been tested for many mixtures and it holds good for coal gas and water gas, both of which contain substantial proportions of hydrogen but not for hydrogen-ethylene-air mixtures nor for chlorinated hydrocarbons. (Rose and Cooper, p250). Wierzba and Kilchyk (1996) also confirmed the validity of Le Chatelier's Rule for all CO-H_2 mixtures up to 300 °C.

Influence of Temperature and Pressure on the Limits

Limits of flammability for most combustible/oxidant systems widen with elevated temperature and pressure, so the data in Table 3.3 cannot be directly applied to most operating conditions. Pressure seems to exert only a small influence on the flammable limits but there has been limited research into this phenomenon. Since most furnaces operate at or close to atmospheric pressure, the effect of pressure is of limited interest to most furnace designers and operators, so readers interested in the influence of pressure on flammable limits should consult, Rose and Cooper, Lewis and Von Elbe (1961), Wierzba and Kilchyk (1996) and Shebko et al (1995).

Increasing temperature widens the limits until the auto–ignition temperature is reached when almost all mixtures will react without any additional ignition source. Figure 3.1 shows this effect for methane.

The effect of temperature on the lower flammable (lean) limit for simple mixtures in air can be calculated using the Burgess-Wheeler Law.

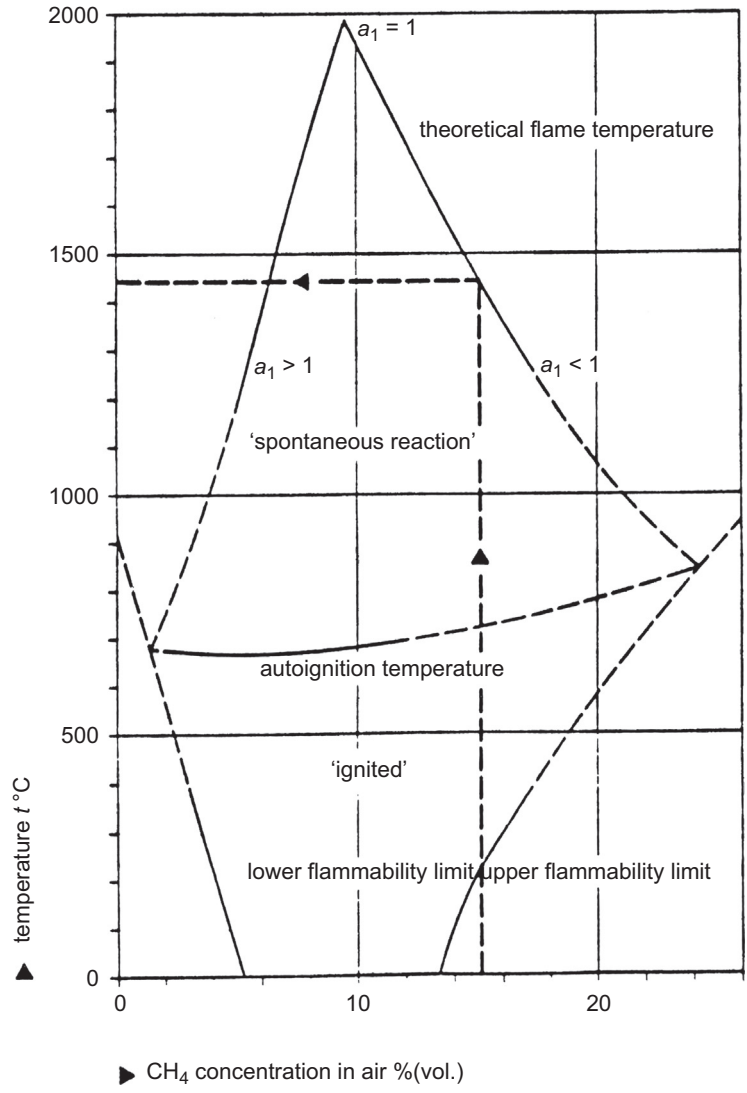


Figure 3.1 Combustion characteristics of methane (Copyright Gasunie BV, reproduced with permission)

$$LT = Lo + \frac{3.14(T - To)}{\Delta Hc} \tag{3.4}$$

Where:

LT = lower limit at temperature T
Lo = lower limit at room temperature To
ΔHc = Enthalpy of combustion in kJ/mole

Note that in this convention ΔHc is negative hence increasing temperature reduces the limit.

The Burgess-Wheeler Law predicts a linear effect of elevated temperature as a ratio of the original limit at room temperature. A similar effect is observed for the upper limit which increases with temperature.

3.1.5 Flame Radiation from Gaseous Fuels

In Chapter 4 the authors discuss flame radiation and its crucially important contribution to heat transfer and furnace efficiency. Radiation is largely the result of the products of partial combustion in the flame, especially carbon in the form of soot, hence the emissivity of a flame is largely dependent on the carbon content of the fuel. Many gases such as natural gas, blast furnace gas, etc., have relatively low proportions of carbon and are therefore poor emitters of radiation and rely on the radiative properties of CO_2 and water vapour for their contribution to radiative heat transfer. This has a detrimental effect on the radiant heat transfer from the flame and can seriously affect the efficiency of the plant, especially high temperature plant such as rotary kilns and metallurgical furnaces. This important phenomenon is discussed later in this chapter and throughout the book.

3.2 Liquid Fuels

Most liquid fuels are based on petroleum and, although in the past, liquid fuels have been produced from coal tars which were a by-product of coal gasification plants, such fuels are nowadays rarely available. More information on these fuels is available in Spiers p272–278 (1962) and Rose and Cooper p293–297 (1977).

Oil fuels are produced by the refining of crude oil. Waste lubricating oil is currently being used as a supplementary fuel in a number of plants, but supplies are limited. Oil fuels are classified as distillate fuels, such as kerosene and diesel oil, or residual fuels. The latter come in a range of viscosities and are classified differently in different countries. Typical characteristics of oil fuels are given in Table 3.4.

Residual fuels such as heavy fuel oil have to be heated to render them pumpable and to reduce the viscosity to enable atomization, see Chapters 5 & 6. Since the viscosity required for satisfactory atomisation is in the order of 15–25 cSt, the heavier the fuel, the more it has to be heated, Figure 3.2.

One of the most common causes of poor oil burner performance is too high an oil viscosity at the burner caused by inadequate heating of the oil, see Chapter 5.

Table 3.4 Typical Properties of Selected Petroleum Based Furnace Fuels

Properties	*Light Distillate*	*Kerosene*	*Gas oil*	*Medium Fuel Oil**	*Heavy Fuel Oil**
C (%)	84.1	85.8	86.1	85.6	85.4
H (%)	15.85	14.1	13.2	11.5	11.4
S (%)	0.05	0.1	0.7	2.6	2.8
O_2, N_2, Ash	—	—	—	0.3	0.4
Flash point (°C)	Below -30	40	70	105	115
Kinematic viscosity (15.6°C) (cSt)	0.5	2.1	5.0	—	—
Kinematic viscosity (82.2°C) (CSt)	—	—	1.4	30	70
Density kg/m^3 (1 atm, 15.6 °C)	0.68	0.78	0.83	0.95	0.96
CV gross (MJ/kg)	47.8	46.5	45.6	43.1	42.9
Air Req (Kg/kg)	15.09	14.69	14.44	13.88	13.84

* These properties are illustrative only; actual properties depend on source of crude oil and refining/reforming processes used.

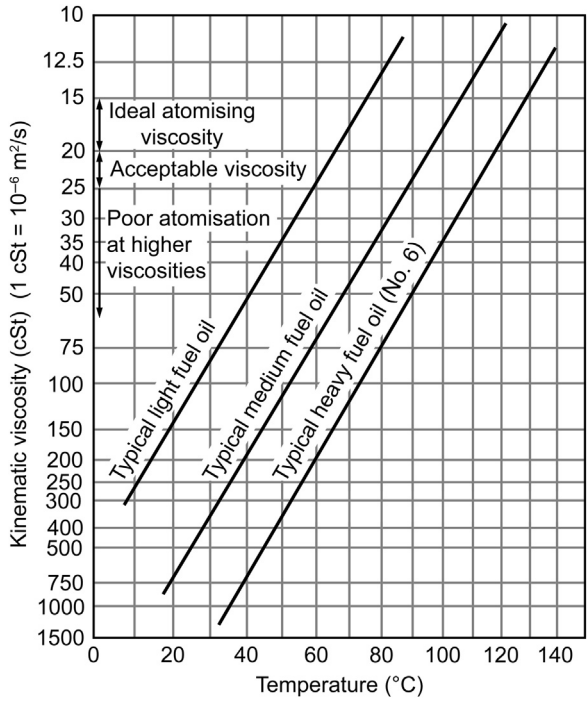


Figure 3.2 Viscosity temperature relationship for petroleum based fuels

Owing to the tendency of heavy fuel oil to solidify when cold, great care has to be taken with the design of oil fuel handling systems to minimize 'dead legs'. Since the lighter 'white' oil products have a higher value than black fuel oils, refineries increasingly manufacture more light products, leading to heavier and heavier black fuels containing increasing quantities of asphaltenes. These augmented refining processes involve 'cracking' the oil and produces black oils which have different characteristics from the former residual oils. These cracked fuels vary in character, depending on the source of crude and the refining process and are not necessarily compatible with each other. Under some circumstances, fuel oils from different sources can form 'gels' in tanks and fuel handling systems with disastrous results. Proposed fuels should therefore always be tested for compatibility with the existing fuel before purchase.

Used lubricating oil is also occasionally available for use as a furnace fuel. Providing excess water is removed and the oil is filtered to minimise the presence of particulate, it burns satisfactorily. Similarly to heavy fuel oil it may need heating, typically to approximately 70°C to ensure that the viscosity is suitable for atomisation (15–25 cSt). Owing to the variability of this fuel, tests may be required to determine the correct temperature for each batch. Waste oils typically contain wear products from bearings such as lead and other heavy metals, so care needs to be exercised to ensure that these do not contaminate the product or cause excessive emissions of these pollutants. This normally means that these fuels may only be used in furnaces where suitable flue gas cleaning equipment is installed.

3.3 Solid Fuels

The first furnaces were fired using solid fuels and they are still an important fuel for many processes, such as blast furnaces and cement manufacture. Solid fuels include charcoal, coke, anthracite, coal, lignite, peat and wood, in order of decreasing calorific value. The complexity and range of solid fuels means that only superficial consideration of their properties is possible here. However, owing to their importance in the past, anyone contemplating the use of solid fuels is referred to the copious volumes of literature on the topic, examples of which are listed at the end of this chapter. Examples of the properties of selected solid fuels are given in Table 3.5.

A glance at Table 3.5 shows the wide range of calorific values for solid fuels; with charcoal formed by carbonising wood having the highest *CV* compared with wood which has the lowest. Calorific value affects the quantity of fuel required; the lower the *CV* the greater mass of fuel required for firing a furnace and also the lower the flame temperature produced. Lower *CV* fuels produce a lower flame

Table 3.5 Characteristic Properties of Selected Solid Fuels

Properties	Anthracite	Bituminous Coal[1]	Lignite[2]	Wood	Charcoal	Industrial Coke
*C (%)	93.0	87.5	70	50.0	93.0	96.5
*H (%)	3.7	5.3	5	6.0	2.5	0.5
*N_2 (%)	1.3	1.9	2	1.0	1.5	2.0–3.0
*S (%)	0.7	1.0	–	trace	trace	Up to 1.0
*O_2 (%)	1.3	4.3	23	43.0	3.0	1.0
*Volatile (%)	5	35	53	80	1.0	1.0
*CV gross (MJ/kg)	36.25	36.05	26.8	18.65	34.75	33.7
CV gross (MJ/kg) (comm.. fuel as fired)	29.0	29.92	21.45	15.8	33.71	27.97
Air Req (Kg/kg)	10.05	9.74	7.09	5.10	11.11	9.58
Moisture (%)	12	9	15–20	15	2	8–12
Ash (%)	8	8	1–5	trace	1	7

* Properties are dry ash free basis, except moisture, ash and air requirements which are for typical commercial fuel.
[1] Mid rank coal (401),
[2] Lignite deposits typically contain 20–65% moisture, commercial form is normally dried and pulverised or briquetted

temperature than would be produced by a higher *CV* fuel under similar conditions. There lower temperatures may result in reduced heat transfer leading to even higher fuel consumption rates. Other than calorific value, the volatile content, ash content, ash composition, reactivity, ease or difficulty of handling and the variability of the fuel all affect their performance in a furnace and severely restrict the use of solid fuels to a small range of furnaces where these properties are either an advantage such as in cement manufacture, or where the lower cost of the fuel outweighs the difficulties.

These limitations have meant that in the past much effort was made to reduce the limitations of solid fuels by upgrading them either by carbonisation or gasification. Attempts to utilise biomass (such as wood) as a furnace fuel is likely to lead to a resurge in the demand for small scale on-site gasifiers. Charcoal burning is one of the earliest and the longest standing techniques for upgrading fuel, having been undertaken since pre-historic times. During charcoal burning the volatiles are driven off and the residual carbon left behind. When done correctly, this residual carbon is highly reactive and burns readily and the calorific value is nearly doubled typically from approximately 18–19 MJ/kg to over 34 MJ/kg, owing to the reduction in volatile content. Unlike bituminous coal, the volatiles in wood have relatively low heating value owing to the oxygen content, which at approximately 43% accounts for over half the volatile mass. Industrial coke formed by upgrading bituminous coal in a similar manner to making charcoal has only just over 80% of the heating value of charcoal. This lower *CV* led to considerable

difficulties in substituting coke for charcoal in iron making, which were finally overcome by Abraham Darby in the early 18th Century (Raistrick 1989).

3.3.1 Ash

Most solid fuels contain ash which is formed during combustion from the inorganic components in the fuel and are typically compounds of aluminium, calcium, iron, magnesium, potassium, silicon, sodium, etc. These components arise from three principle sources, organic cations in the volatiles, inorganic compounds inherent in the fuel structure and inorganic material acquired during fuel processing. The behaviour of ash is a complex topic that has been the subject of much research and is still not well understood. The properties of interest to furnace designers are discussed later in this chapter.

3.4 Waste Fuels

In principle any combustible waste can be utilised as fuel; materials that have been used include paper and cardboard, wood bark, plastic chippings, demolition wood, domestic garbage, recovered solvents, spent transformer oil, sewage sludge, etc. Wastes may be upgraded to improve their combustion and environmental performance or used in their raw state. Except in purpose built incinerators, wastes are rarely burnt alone but in combination with a normal fuel. Factors that need to be considered when evaluating the feasibility of utilising waste include:

- **Effect on furnace air requirement and flue gas volumes**
  At the most basic level furnace firing rate, and hence production, is often limited by the combustion air supply and flue gas handling systems. Many wastes have higher combustion air requirements per net MJ of energy and similarly produce larger flue gas volumes. Unless the furnace can handle these larger volumes a production loss is inevitable.
- **Effect on flame heat release profile**
  Substitution of a waste derived fuel for the standard fuel will inevitably change the heat release profile. Common effects include raising or lowering the peak heat flux, and moving its position in the flame. The waste may also increase or decrease the overall heat transfer. Provided reasonable combustion data is available then these effects can be predicted using the techniques described in Chapters 4 and 5. Failure to make this assessment prior to implementation of a waste fuel burning project will result in

unpredictable furnace performance and can lead to either reduced output or poor product quality. Either way the project fails to deliver its full potential.

- **Waste storage and handling**
  Unless the furnace is located close to the source, a storage and handling system is required and this normally represents a substantial capital investment. There is always pressure to build this system for the lowest cost to improve the financial return, but systems that are poorly designed and constructed rarely perform well and at their worst can be dangerous. It needs to be borne in mind that most wastes are more difficult to handle than conventional fuels, so the relative capital cost of an effective waste fuel handling system will be higher than for a conventional fuel. This is dealt with in Chapter 7.
- **Environmental effects**
  For most plants the operating licence specifies the permitted fuel(s) and a change in the terms and conditions of the licence is normally required prior to installing a waste burning system. This usually involves a full environmental impact assessment of the changes and a period of public consultation; a procedure is intended to ensure that the waste fuel will not adversely affect emissions. The public consultation can be a very challenging task for plant management with emotions running high on all sides, especially for certain wastes such as spent solvents and wastes from the chemical industry. If handled badly, failure is inevitable even if it can be shown scientifically that the scheme will produce an overall environmental benefit. This is especially true of waste solvents, oils and plastics containing chlorine which have the potential to produce dioxins.

3.5 Choice of Fuel

In the authors' experience choosing the most appropriate fuel for a particular furnace application is rarely given the consideration it deserves. Often a fuel is chosen because it is already available on the site; for example natural gas is utilised because it is already available. Whilst such a decision is not necessarily wrong, it is always worthy of a more detailed consideration because choice of fuel significantly affects furnace efficiency and maintenance costs and not always in an obvious way. For example, natural gas is often the default choice yet its low carbon/hydrogen ratio results in low emissivity flames and relatively poor radiant heat transfer. For example, the output of glass production tanks increased when converted from producer gas to oil, owing to the increased emissivity of the oil flame but declined again when converted to natural gas firing despite efforts to increase the emissivity of the

natural gas flame (Rhine and Tucker 1991). Factors that should be considered when choosing a furnace fuel are discussed below.

3.5.1 Furnace Performance

The effect of fuel type on furnace performance is process specific and every case must be considered individually but the need to optimise heat transfer is generally the overriding influence on furnace performance. However for many furnaces, especially metallurgical furnaces, the need to control the furnace atmosphere, such as maintaining an oxygen free environment, may be crucial.

Heat Transfer

Heat transfer affects both furnace efficiency and product quality. Efficiency can be defined as the useful process heat relative to the total heat input. While this is influenced by a number of factors, as will become clearer in the rest of the book, especially Chapters 4 and 9, the primary driving force for high furnace efficiency is effective heat transfer and the heat transfer from flames is largely by radiation. The radiant heat transfer in turn is proportional to the flame emissivity. Figure 3.3 shows the influence of fuel C/H ratio on the emissivity of similar flames.

While there are means of modifying the flame that increase the emissivity of low carbon fuels by changes to burner design to increase soot formation, the increase achieved is relatively small because the soot formation is limited by the fundamental fuel chemistry. Hence a furnace needs to be designed to accommodate the heat transfer characteristics of the chosen fuel; a high emissivity fuel is preferred for high temperature processes because radiation normally contributes the greater proportion of heat transfer under these conditions. Where low emissivity fuels are used then the furnace must be designed to increase the contribution of convective heat transfer. Fuel emissivity also affects the position of the peak heat flux in the flame with peak heat transfer occurring further along the flame for low emissivity fuels such as natural gas, see Figure 3.4 (Jenkins & Moles 1988).

A practical manifestation of the effect of fuel emissivity on furnace efficiency occurred in the European cement industry in the 1960's and 70's. When the price of oil fell below that of coal in the sixties, many kilns were converted to the cheaper fuel but operators found that this also led to a small reduction in output. Some kilns were also converted to gas firing and suffered a larger drop in output. According to Moles (1978), the kilns at the Rhoose plant of the Aberthaw and Bristol Channel Cement Company suffered a 5% drop in output on conversion from coal to oil firing and a further 5% drop in output following

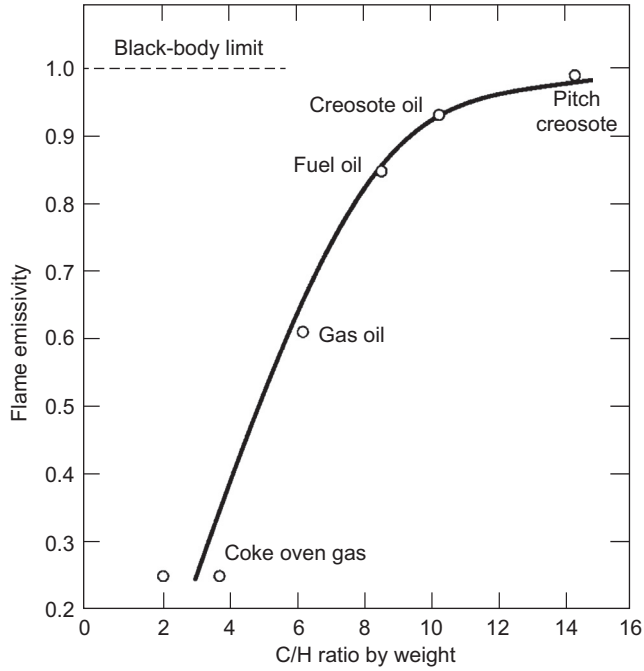


Figure 3.3 Effect of Carbon/Hydrogen ratio on flame emissivity (Weber1998) (Reproduced with permission of the International Flame Research Foundation)

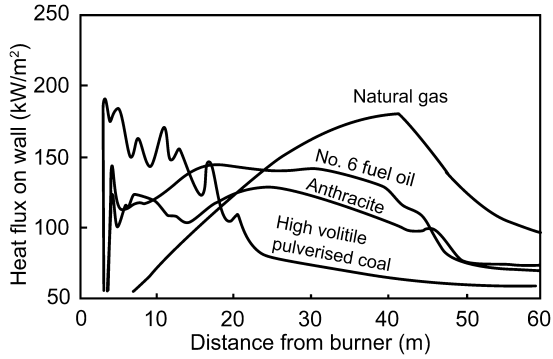


Figure 3.4 Effect of fuel type on heat transfer in a rotary kiln

conversion to natural gas. While some of the drop in the conversion to oil firing can be attributed to the loss of the ash in the coal which becomes part of the product and leads to increased production in cement manufacture, the drop in the conversion to gas firing was caused solely by heat transfer and higher flue gas volumes.

Furnace Atmosphere

Some processes, especially reduction or metal treatment, require close control of furnace atmosphere for optimum process efficiency. This is usually achieved by supplying excess fuel compared with the stoichiometric proportion. This generally requires very close control over fuel and air flow rates to ensure carbon monoxide concentrations are not excessively high, and for this reason gaseous fuel is preferred. However, there are processes that use solid fuel, the most notable being the blast furnace, which contains excess coke and a carefully controlled air supply. However carbon monoxide concentrations are very high, typically above 20%. Another example of furnaces with reducing conditions that use solid fuel are the reduction kilns used in the mineral sands industry and for the reduction of iron sand.

Another factor affecting furnace atmosphere is the sulphur content of the fuel. Sulphur can occur in fuels in a number of forms including, organically bound sulphur, pyrite and as gas (H_2S). Regardless of form, the products of combustion when excess air is present are SO_2 and SO_3. Generally SO_2 dominates but greater concentrations of SO_3 can be formed when the excess air is high, the higher oxygen concentration favouring SO_3 formation. These gases are highly reactive as well as corrosive and can affect product quality by reacting with it, e.g. with lime to form calcium sulphate.

Flexibility of Operation

While many furnaces operate continuously in a quasi steady-state, others are subject to intermittent operation or cyclic operation. For the latter, which may involve a start from cold, a heating up period, followed by a "soak" at temperature and a cooling phase, excellent control over the heat input over a wide range of firing rates is required. Other furnaces may operate with a cold start every Monday morning and hence require a short controlled warm-up time.

To achieve intermittent and cyclic performance, an excellent turndown ratio is required. While this can, in principle, be achieved with solid fuels it requires a complex, and therefore expensive, fuel handling system. Furthermore, most cyclic and intermittent furnaces are relatively small so the complexity and high capital cost is difficult to justify. Hence gas firing with its low capital cost and simplicity of operation is normally preferred for intermittent and cyclic duties. Oil firing is equally suitable on technical grounds but the firing system is more complex than for gas and more expensive, so oil would normally only be used if gas was not available or oil were cheaper and the additional capital could be justified on this basis.

Effect of Ash

Most solid fuels and heavy fuel oil contain ash. While the proportion of ash in fuel oil is generally under 1% that in solid fuels is often substantial, on rare occasions even up to 50%. The behaviour of ash is a complex topic that has been the subject of much research and is still not well understood. Properties of interest to furnace designers and operators are the ash chemical composition and whether this will affect the product and the ash slagging and fouling properties. Slagging and fouling properties need to be determined under conditions that are similar to those that will prevail in the proposed furnace, especially temperature and atmosphere; most ashes tend to melt at lower temperatures under reducing conditions.

Use of fuels containing ash is limited to furnaces where the ash is compatible with the product and becomes part of it, such as cement manufacture, or where the ash is able to be collected and disposed of in an environmentally acceptable manner. Where the ash becomes part of the product then the chemistry of the feed material will need to be adjusted, so that when combined with the ash the final product has the required composition.

Refractory Life

Fuel choice and furnace operating conditions have a major influence on refractory life and hence on operating costs. Refractory is a major component of any furnace and a significant contribution to its capital cost. Furthermore, the life of most refractory is limited, so it needs to be replaced and maintained on a regular basis and this maintenance is one of the larger contributions to operating costs.

It is difficult to be specific regarding the effect of fuel type on refractory life because the interaction is so process specific. Generally gaseous fuels tend to provide longer refractory life than other fuels but this may not always be the case. Where coal and other solid fuels are used ash slagging needs to be considered. Molten ash tends to react with the refractory surface and bond to it. This can provide protection to the refractory but is also a potential source of failure, caused by the different coefficients of thermal expansion. While this is not really a problem with a continuously operating furnace, when the furnace is allowed to cool then the differential contraction causes stress in the near surface zone of the refractory and the top 10–15 mm spalls off and repeated heating and cooling leads to rapid refractory failure.

Fuel Cost and Security of Supply

Except for very small furnaces and those processing very costly materials, cost of fuel would be one of the largest, if not the largest cost of furnace operation. Hence furnace operators are under constant

pressure to choose the cheapest acceptable fuel. At the design stage this means selecting a fuel that will be the cheapest over the life of the furnace, not easy given the volatility of fuel prices and the relatively long life of most furnaces, typically more than twenty years and sometimes approaching fifty years. After a long period of low fuel prices the future prospects are for sustained increases in effective fuel costs as a consequence of more limited supplies, or the imposition of taxes on carbon emissions.

Probably even more important to many organisations is the security of fuel supply, a major disruption to fuel supply having potentially catastrophic effects for most businesses. Almost all fuel supplies are potentially subject to disruption whether by political events, excess demand or technical failure. In the past, natural gas has been considered a secure supply (when contracted as such) however, the depletion of sources close to the point of use and reliance on ever longer pipelines is making such supplies more vulnerable to both technical failure and political events.

Clearly given the complexity of the topic and geographical influences, the authors cannot predict future fuel supply issues. However, in the absence of certainty purchasers of new furnaces would be wise to consider this issue carefully and determine whether provision for alternative fuels is technically possible or economically feasible.

Fuel Handling System Capital and Running Costs

The fuel system and its associated controls are a major part of the capital cost of a furnace system. Generally the lowest costs are associated with natural gas unless the costs of the incoming pipeline have to be borne by the project. Oil, LPG and solid fuel systems are substantially more expensive, owing to the need to store substantial quantities of fuel on-site. Solid fuel handling is the most complex and therefore the most expensive system and this additional cost must be amortised in lower fuel costs or other benefits to justify incurring it. For more information on fuel handling systems see Chapter 7.

3.6 Safety

Safety is a major issue with furnace design and operation and this is extensively covered in Chapter 8. While explosion is a risk with all fuels, a few fuels exhibit additional hazards and need special precautions. These fuels include:

- LPG whose high density leads to accumulation in low spots and the risk of a BLVE (boiling liquid vapour explosion) in the event of a mishap with its storage system;

- Coal, lignite, peat and wood dust which are all subject to spontaneous combustion if incorrectly stored;
- Distillate fuels that are easily ignited and burn very fiercely;
- Certain wastes that may be toxic or otherwise hazardous.

It is not possible to give further consideration to these issues here but designers and operators need to familiarise themselves with the issues and take them fully into consideration when choosing a fuel and designing its handling and storage system.

3.7 Emissions

Choice of fuel has a major effect on emissions and the cost of any flue gas treatment where this is required. Potential furnace emissions include CO_2, CO, NO_x, dust, acid gases (SO_2, SO_3 & H_2S) and toxic by-products from the combustion of waste fuels. The expected pollutants must be taken into account at the design stage and during consideration of any potential process change. This topic is so important that Chapter 10 is devoted to it.

Nomenclature

CV = the higher or gross calorific value in MJ/m^3 or BTU/ft^3
ΔHc = Enthalpy of combustion in kJ/mole
L = lower flammable limit
Lo = lower limit at room temperature To
LT = lower limit at temperature T
P = percentage of specific gas in mixture
SG = the specific density relative to air
U = upper flammable limit

References

Bennett, J. C. J Inst Fuel, 7, p. 109, 1933–34
Callcott, T. G. (1956). *J Inst Fuel, 29,* p. 207.
Donovan, P., & Kirkman, N. (1986). *The Unquenchable Flame, The story of the South Australian Gas Company*. Adelaide: Wakefield Press. page 4.
Jenkins, B. G., & Moles, F. D. (1988). *Design of Burners for Kiln Applications using modelling techniques, Proceedings of the Fifth International Kiln Conference*. London: International Kiln Association.

Kirk Othmer, *Encyclopaedia of Chemical Technology* (4th ed.), (Vol. 12, p. 269), John Wiley & Sons, New York.

Lewis, B., & Von Elbe, G. (1961). Combustion *Flames and explosions of Gases*. New York: Academic Press.

Moles, F. D. (1978). *Private communication*.

Raistrick, A. (1989). Dynasty of Ironfounders. *Ironbridge Gorge Museum Trust,* p. 30–46.

Rhine, J. M., & Tucker, R. J. (1991). *Modelling of Gas-Fired Furnaces and Boilers*. Maidenhead & New York: McGraw-Hill, 354–356.

Rose, J. W., & Cooper, J. R. (1977). *Technical data on Fuel* (7th ed). *British national Committee, World Energy Conference*, London, p. 246–250.

Shebeko, Y. U., Tsarichenko, G., Korolchenko, Y. A., Trunev, A. V., Navzenya, V. Y. U., Papkov, S. N., & Zaitzev, A. A. (1995). Burning Velocities and Flammable Limits of Gaseous Mixtures at elevated temperatures and Pressure. *Combustion and Flame, 102*, p. 427–437.

Spiers, H. M. (1962). *Technical Data on Fuel* (6th ed.). *British National Committee, World Power Conference,* London.

Ulmans. (1989). VCH Verlagsgellshaft. *Weinheim*, Vol. A12, 169–306.

Weber, R. (1998). *The spirit of Ijmuiden, International Flame Research Foundation* (p. 34). The Netherlands: Ijmuiden. ISBN 90-801495-2-7.

Wierzba, I., Bade Shrestha, S. O., & Karim, G. A. (Sep 1996). An Approach for predicting the flammability limits of fuel/diluent mixtures in air. *Jnl. Inst. E.*122–130. Vol. LXIX, No 480.

Solid Fuel Bibliography

IEA Clean Coal Centre publishes many reports on modern coal technologies, available via their website - www.iea-coal.co.uk

Juniper, L. (2000). *Thermal Coal Technology - A Manual for Australian Coal*. Ultra-systems Technology Pty Ltd.

Spiers, H. M. (1962). *Technical Data on Fuel* (6th ed.). *British National Committee, World Power Conference*, London.

Rose, J. W., & Cooper, J. R. (1977). *Technical data on Fuel* (7th ed.). *British national Committee, World Energy Conference*, London, (p. 297–312).

Durie, Ed, The Science of Victorian Brown Coal

The Efficient use of Fuel, HMSO, London 1944

Chapter 4

An Introduction to Heat Transfer in Furnaces

Chapter contents

4.1	Conduction	90
4.2	Convection	99
4.3	Radiation	112
4.4	Electrical Heating	126
Nomenclature		131
References		138

The primary objective of a furnace is to transfer thermal energy to the product, thus before we analyse or design any combustion process equipment we must have a comprehensive knowledge of the fundamentals of heat transfer. If there is a temperature difference (i.e. a driving force) between two parts of a system, then heat will be transferred by one or more of three methods.

Conduction In a solid, the flow of heat by conduction is the result of the transfer of vibrational energy from one molecule to the next, and in fluids it occurs in addition as a result of the transfer of kinetic energy. Conduction may also be created from the movement of free electrons (viz. metals).

Convection Heat transfer by convection is attributable to macroscopic motion of a fluid and is thus confined to liquids and gases. Natural convection arises from density differences caused by temperature gradients in the system. Forced convection occurs due to eddy currents in a fluid in turbulent motion.

Radiation All materials radiate thermal energy in the form of electromagnetic waves. When radiation falls on a surface it may be reflected, transmitted, or absorbed. The fraction of energy that is absorbed is manifest as heat.

We can write a general equation for the heat transfer rate between two parts of a system (net heat flux) as:

$$Q = \Phi(\Delta t)^n \tag{4.1}$$

The origin of Φ and the value of n vary according to the mode of heat transfer

	Φ	n
Conduction	kA/x	1
Convection	hA	1
Radiation	$\sigma\varepsilon A$	4

During convective heat transfer, chemical reactions sometimes occur concurrently at the interface (surface), and in these cases the enthalpy difference is used in place of the temperature difference to account for both sensible and chemical energy components.

4.1 Conduction

When considering conduction, we can rewrite equation 4.1 more correctly as

$$\frac{\partial Q}{\partial \theta} = -kA\frac{\partial t}{\partial x} \tag{4.2}$$

This is the classical Fourier equation, and can be used to analyse two scenarios:

- steady state conduction $-\partial t/\partial x$ is independent of time θ
- transient conduction $-\partial t/\partial x$ depends on time θ

4.1.1 Steady State Conduction

Under these conditions, the temperature gradient through the system remains constant. Thus equation 4.2 becomes:

$$Q = -\frac{kA}{x}\Delta t \tag{4.3}$$

This is the simplest type of problem, and is relevant to calculations of heat loss through furnace walls, optimum lagging thickness etc. A typical example is as follows.

Example 4.1 What is the heat loss per square meter through a furnace wall constructed from 130mm of alumina firebrick (k = 2.5 W/m^{2}K/m) backed with 90mm of insulating brick (k = 0.12 W/m^{2}K/m) and 5mm of steel shell (k = 43.3 W/m^{2}K/m)? The temperature of the hot face of the refractory brick is 1500°C and the outside of the furnace is open to air at 25°C. A diagrammatic representation of the construction is shown in Figure 4.1.

If we define the temperature at the interface between the firebrick and insulation as T_1, and between the insulation and the shell as T_2, then we can write from equation 4.3 that

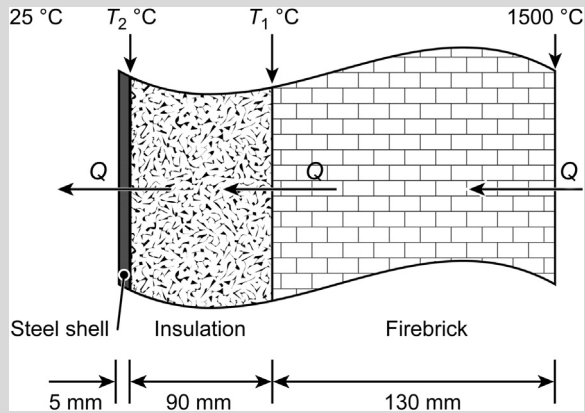


Figure 4.1 Representation of section through compound refractory furnace wall

$$Q = 2.5\%\ 1\%(\{1500 + 273\} - T_1)/0.13$$

and $$Q = 0.12\%\ 1\%(T_1 - T_2)/0.09$$

and $$Q = 43.3\%\ 1\%(T_2 - \{25 + 273\})/0.005$$

thus eliminating T_1 and T_2

$$0.75Q = (1773 - 0.052Q) - (0.000115Q + 298)$$

$$Q = \frac{1475}{0.802115} = 1839\ \text{W/m}^2$$

If we substitute back then

$$T_1 = 1677\ \text{K}$$
$$T_2 = 298.2\ \text{K}$$

From this example we can see that as a general rule

$$Q = \frac{\Delta t}{\sum_{n}^{1} \frac{x_n}{k_n A_n}} \tag{4.4}$$

(Note: If there was no insulating backing in the example then $Q \approx 2.5 \times 1 \times (1773 - 298) / 0.13 = 28365\ \text{W/m}^2$.)

Values of the thermal conductivity vary with temperature to a small extent (±20% over 1000 K), but are extensively documented in most standard reference textbooks, viz. Weast (1988), or manufacturer's literature on refractories, etc. Where temperature effects are significant, they are usually expressed in a temperature dependent form as

$$k = \frac{1}{b_1 t + b_2 + \frac{b_3}{t}} \tag{4.5}$$

Where b_1, b_2 and b_3 are constants

4.1.2 Transient Conduction

Under transient conduction conditions, the temperature gradient through the system varies with time; i.e. Equation 4.2 holds:

$$\frac{\partial Q}{\partial \theta} = -kA\frac{\partial t}{\partial x} \tag{4.2}$$

Problems requiring this type of solution include heating and cooling of objects, typical examples being steel-slab reheating, ingot soaking, space heating / thermal inertia of buildings, vulcanising, and glass cooling lehrs. The solution of these problems is more complex, and is generally developed by two methods:

- Mathematical solution of equation 4.2 for given boundary conditions using calculus.
- Numerical solution by finite difference methods (graphical).

Analytical Approach

The theoretical relations may be expressed in terms of 4 dimensionless groups (these are discussed further in Section 4.1.2.2. of this chapter).

• An unaccomplished temperature change	$Y = (t_a - t)/(t_a - t_b)$
• A relative time	$X = \alpha\theta/r_m^2$
• A resistance ratio	$m = k/r_m h$
• A radius ratio	$n = r/r_m$

A number of writers, see McAdams (1954) have expressed the relationship between X, Y, m, and n graphically, for different systems (slab, cylinder, sphere). The best way of illustrating the use of these charts is by example.

Example 4.2 A forge reheating furnace is standing at 1300°C prior to door opening and the bogie drawn out for addition of a 230 tonne ingot at 650°C. The furnace is 6.1m wide, 5.5m high, and 17m long. Figure 4.2 shows the ingot shape and furnace firing pattern. The maximum thermal input of the burners is 25 MW, firing natural gas. What are the ingot skin and centre time/temperature gradients, and the thermal loading requirements of the furnace to the ingot over the heating cycle?

The heating of the solid ingot is a transient conduction problem. As an example of the solution to this type of calculation we shall in this case use Gurney-Lurie charts. Figure 4.3. shows the chart for a long cylinder, which is the closest approximation to the ingot in question.

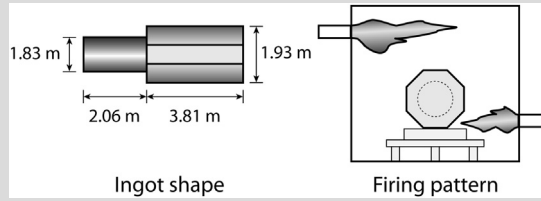


Figure 4.2 Representation of ingot shape and reheating furnace firing pattern

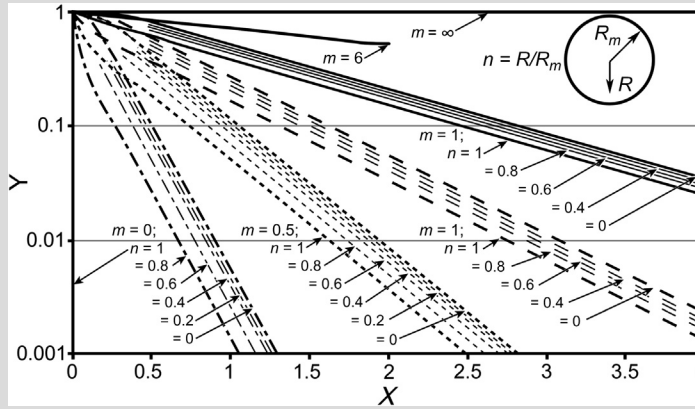


Figure 4.3 Gurnie-Lurie chart for long cylinder (see McAdams for original) Reproduced by kind permission of McGraw Hill and the American Chemical Society

Defining the terms used in the chart:

r_m — mean ingot radius = 1.12m (equivalent based on external surface area)
k — thermal conductivity of steel = 0.0462 kW/m.°C
ρ — density of steel = 7800 kg/m^3
C_p — specific heat of steel = 0.72 kJ./kg.°C
t_a — furnace temperature = 1300 °C
t_b — ingot start temperature = 650 °C
h — overall heat transfer coefficient = 0.4 kW/m^2.°C (this value is derived from the sum of the convective and radiative components at the surface and is calculated later in section 4.2)
θ — time from start
t — ingot temperature at time θ
r — radial distance from centre of ingot
m — $k/r_m h$
n — r/r_m

thus

$$\mathrm{m} = \frac{0.0462}{(1.12 \times 0.4)} = 0.103$$

$$X = \left(\frac{0.0462}{7800 \times 0.72}\right)\frac{\theta}{r_m^2} = 8.2265\mathrm{e}^{-6}\,\frac{\theta}{r_m^2}$$

From the Gurney-Lurie chart we can interpolate for the values of m = 0.1. Thus after any chosen time, θ, for any position within the ingot, r_m, we can calculate X, and for the selected value of n can determine Y and hence the temperature of the ingot, t. Figure 4.4 has been constructed to show the time/temperature history for the ingot at the surface (n=1), mid-point (n=0.5) and centre (n=0).

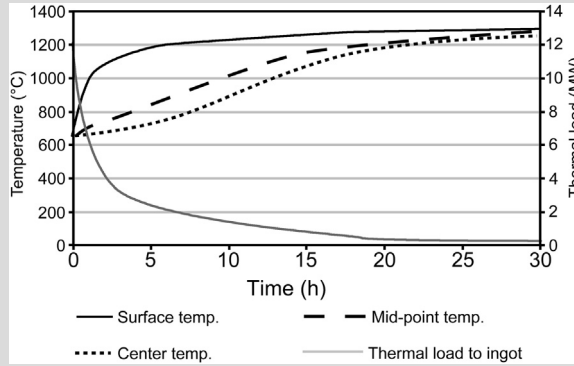


Figure 4.4 Ingot heating predictions using Gurnie-Lurie chart

The energy input required to obtain the heating curve can be calculated from the previously evaluated heat transfer coefficient. Thus, at the start of heating:

$$Q_{start} = h \cdot A \cdot \Delta t.$$

Where A = external surface area of the ingot = 46.68m^2

Thus

$$Q_{start} = 0.4 \times 46.68 \times \frac{1300 - 650}{1000} = 12.14 \text{ MW}$$

After 3 hours, the surface temperature is approx. 1100°C, thus

$$Q_{3\,hours} = 0.4 \times 46.68 \times \frac{1300 - 1100}{1000} = 3.73 \text{ MW}$$

The estimated thermal loading to the ingot in the furnace with time is also plotted in Figure 4.4.

Numerical Approach

In many cases, the operating conditions (e.g. geometry, heat cycles) do not lend themselves to an analytical solution. In these cases the use of a numerical method replaces a continuous process by a stepwise one. These are characterised by dividing the medium being heated or cooled into a number of finite 2-dimensional slabs, or 3-dimensional cubes. The calculation can be explained by the general numerical method developed by Dusinberre (1949).

Assume we have a large slab with a thickness x, with a uniform cross sectional area, A. The solid is divided into a number, n, of equal

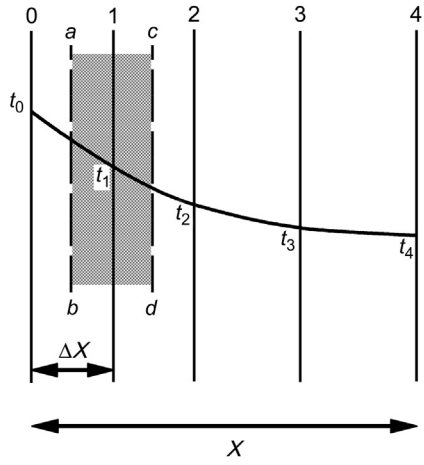


Figure 4.5 Representation of slab showing slice details

finite slices of thickness, Δx by temperature-reference planes, t_n. If we write a heat balance over plane (1) zone abcd, see Figure 4.5, then,

$$\frac{-\partial t}{\partial x}_{\text{at plane ad}} \cong \frac{t_0 - t_1}{\Delta x} \tag{4.6}$$

and

$$\frac{-\partial t}{\partial x}_{\text{at plane bc}} \cong \frac{t_1 - t_2}{\Delta x} \tag{4.7}$$

The temperature at t_1 is the average temperature of the zone abcd, thus a heat balance gives:

$$\frac{kA(t_0 - t_1)}{\Delta x} - \frac{kA(t_1 - t_2)}{\Delta x} = \frac{(A\Delta x)(C_p\rho)(t_1' - t_1)}{\Delta\theta} \tag{4.8}$$

where t_1' is the new temperature at 1 after the elapse of time increased $\Delta\theta$. If

$$\alpha = \frac{k}{C_p\rho} \tag{4.9}$$

and

$$M = \frac{(\Delta x)^2}{\alpha\Delta\theta} \tag{4.10}$$

then equation 4.8 ε

$$t_1' = \frac{t_0 + (M-2)(t_1) + t_2}{M} \tag{4.11}$$

It should be noted that equation 4.9 is a function of the physical properties of the slab, whilst equation 4.10 is essentially user defined through the selection of the time step, $\Delta\theta$, slice thickness, Δx, or the value of M. A simple solution of equation 4.11 can be obtained using the Schmidt (1924) method, which employs a value of $M = 2$. Thus we have:

$$t'_1 = \frac{t_0 + t_2}{2}, \quad t'_2 = \frac{t_1 + t_3}{2}, etc. \tag{4.12}$$

Or more generally

$$t'_{(n-1)} = \frac{t_{(n-2)} + t_n}{2} \tag{4.13}$$

Thus we can solve any problem using a tabular or a graphical approach. By selecting a value of Δx to give the required degree of sensitivity we can calculate the heating/cooling curve for a solid body for any number of time increments, $\Delta\theta$, where

$$\Delta\theta = \frac{(\Delta x)^2}{2\alpha} \tag{4.14}$$

Example 4.3. Calculate the time taken for the distant face of a brick wall, of thermal diffusivity, $\alpha = 0.082$ cm^2/s and thickness 45cm to rise from 20°C to 100°C. The whole wall is initially at a constant temperature of 20°C when the near face is instantaneously raised to 600°C and held at that temperature. Assume that the distant face is perfectly insulated.

Let us choose a value $\Delta x = 5$cm. Using a value of $M = 2$, we can construct a simple graphical solution using equation 4.13, as shown in Figure 4.6.

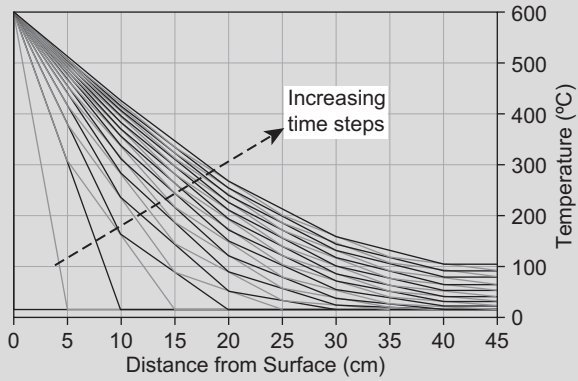


Figure 4.6 Graphical solution of slab heating problem (example 4.3)

Note that the temperature at each slice only changes every other $\Delta\theta$. This is because we have chosen a value of $M = 2$. The graphical method is only possible if $M = 2$, otherwise we must solve the problem using a tabular method. From Figure 4.5 we can see that the far face temperature takes between 25 and 26 time increments to reach 100°C.

$$\Delta\theta = \frac{(\Delta x)^2}{2\alpha} \tag{4.14}$$

Thus

$$\Delta\theta = \frac{(5)^2}{(2 \times 0.082)} = 152.44 \text{ seconds}$$

Thus, time to heat face to 100°C = 25.5 x 152.44 sec. = 1.08 hours

There are several aspects of the last problem that are impractical. The most significant is that the surface temperature of the slab will not rise from 20°C to 600°C instantly. In reality, the heat transfer to the surface will be controlled by some parameters (conduction, convection and/or radiation at the surface) that are external to the problem, but the method may be modified to include these effects. If we write a heat balance on the half slice adjacent to the surface (see Figure 4.7), then:

$$hA(t_a - t_0) - \frac{kA(t_0 - t_1)}{\Delta x} = \frac{(A\Delta x)(c_p\rho)(t'_{0.25} - t_{0.25})}{2\Delta\theta} \tag{4.15}$$

Where t_a is the ambient temperature outside the surface, and h is the overall heat transfer coefficient at the surface. We can define the dimensionless Nusselt or Biot modulus, N, as

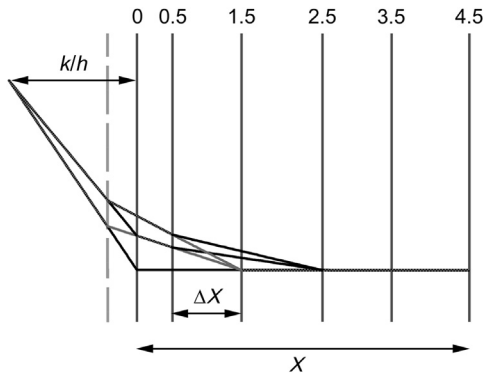


Figure 4.7 Representation of slab showing slice details with surface heat transfer

$$N = \frac{h\Delta x}{k} \tag{4.16}$$

thus, (4.15) becomes

$$t_0' = \frac{2Nt_a + \{M - (2N + 2)\}t_0 + 2t_1}{M} \tag{4.17}$$

This evaluation of t_n may be included in the normal tabular calculation method using 4.11 for the temperature change in the solid. If we use the graphical solution method when $M = 2$ then equation 4.17 becomes

$$t_0' = N(t_a - t_0) + t_1 \tag{4.18}$$

This may be handled graphically, see Figure 4.7, by selecting a starting point at temperature t_a, a distance k/h from the surface, and considering half slices $\Delta x/2$ on either side of the surface.

4.2 Convection

Convective heat transfer is in reality the conduction of heat through a flowing fluid to a fixed surface, whereby the conductivity is defined by a convective heat transfer coefficient, h.

$$Q = hA\Delta T \tag{4.19}$$

Measurement of such systems shows that the temperature gradient in the fluid, and hence the thermal resistance, occurs in a thin layer close to the surface, termed the boundary layer. The thickness of, and flow within the boundary layer, is determined by the flow in the main bulk of the fluid. Additionally we know that the boundary layer is not instantaneously present when a fluid meets a surface but develops as shown diagrammatically in Figure 4.8. Within the boundary layer the flow velocity increases exponentially from zero at the surface to the uniform bulk velocity at the interface.

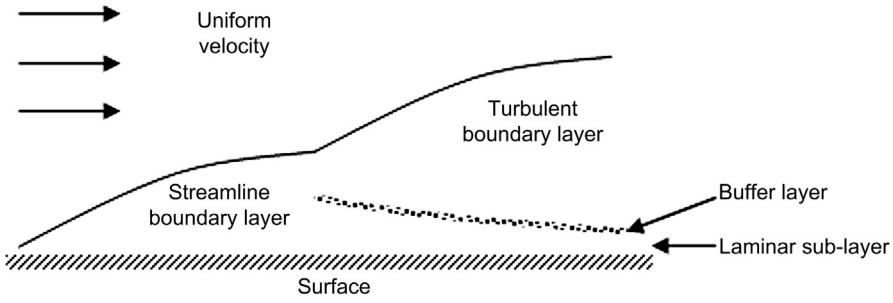


Figure 4.8 Development of boundary layer over a flat plate

The development of the boundary layer will vary with the shape and roughness of the surface, the fluid properties, and the flow velocity. This will in turn determine the rate of heat transfer. For a simple geometry, like the example shown in Figure 4.8, we can analytically determine the convective heat transfer coefficient, which is in fact an 'averaged' thermal conductivity through the boundary layer. For complex geometries, such as flow over a bank of tubes, it is not possible to define either the bulk flow conditions, or the resulting boundary layers, and hence the convective heat transfer coefficient must be measured. The concept of dimensionless groups allows us to extrapolate experimental results to most design problems.

4.2.1 Dimensional Analysis

Since the physical properties of a system are interconnected by a series of mechanical and physical laws, it is possible to regard certain quantities as basic and others as derived. This is an important concept in heat transfer calculations, as it permits us to derive groups of physical properties that may be used to characterise these laws in a general form. Length, L, and time θ are fundamental to all systems of measurement (viz. SI, cgs, fps). Mass, M, or Force, F, is usually taken as the third fundamental. They are related by

$$(\text{Force}) = (\text{Mass}) \times (\text{Acceleration})$$

$$F = ML\theta^{-2} \tag{4.20}$$

Temperature, T, is often regarded as a basic quantity where:

$$T = L^2\theta^2 \tag{4.21}$$

(i.e. the square of velocity).

In heat transfer calculations it is also convenient to regard heat, Q, as a basic quantity, where

$$Q = ML^2\theta^{-2} \tag{4.22}$$

provided that no mechanical or chemical energy is involved in the system.

If some quantity A_1 is a function of physical quantities A_2, A_3, A_4, etc., then these must appear in combinations which have the same dimensions as A_1.

$$A_1 = f_1(A_2,\ A_3,\ A_4\ldots) \tag{4.23}$$

thus,

$$f_2(A_1,\ A_2,\ A_3,\ A_4\ldots) = 0 \tag{4.24}$$

where f_2 is usually the product of a series of powers of A's.viz.

$$K.A_1^a.A_2^b.A_3^c\ldots = 0 \tag{4.25}$$

These physical quantities, i.e. A's, can be combined to form dimensionless groups, π_1, π_2, π_3, etc. thus

$$f(\pi_1,\ \pi_2,\ \pi_3\ldots) = 0 \tag{4.26}$$

The number of dimensionless groups formed is a function of the number of physical quantities (A's) and the number of fundamentals chosen (M, L, T, etc). Each fundamental must be involved in at least one physical quantity. Each fundamental chosen must not be implicit in any other, e.g. Length L and Area L^3. The number of dimensionless groups (π's) is the number of variables (A's) minus the number of fundamentals. This is known as Buckingham's π theorem.

The analytical significance of dimensionless groups is that they enable us to develop generally applicable relationships for different systems that have the same value of dimensionless number. Thus we can study a particular mechanical or physical phenomenon at one scale, and extrapolate the results to a different situation using dimensionless similarity.

4.2.2 Application to Convective Heat Transfer

If we consider a convective heat transfer problem in which fluids are flowing over a surface, we can deduce that the heat transfer rate will depend on the following variables.

$$q \propto \left(u^a, L^b, \Delta t^c, \mu^d, K^e, \rho^f, C_p{}^g, (\beta g)^h\right) \tag{4.27}$$

Choosing the following fundamentals, L, M, T, θ, Q.

q	heat transfer/unit area. unit time (heat flux)	—	$Q\,L^{-2}\,\theta^{-1}$
u	velocity	—	$L\,\theta^{-1}$
L	characteristic dimension	—	L
Δt	temperature difference	—	T
μ	viscosity	—	$M\,L^{-1}\,\theta^{-1}$
k	thermal conductivity	—	$Q\,L^{-1}\,T^{-1}\,\theta^{-1}$
ρ	density	—	$M\,L^{-3}$
C_p	specific heat	—	$Q\,M^{-1}\,T^{-1}$
β	linear coefficient of thermal expansion	—	T^{-1}
g	acceleration due to gravity	—	$L\,\theta^{-2}$

If we equate the powers of the fundamentals on the left and right hand sides of the proportionality equation 4.27:

L	$-2 = a + b - d - e - 3f + h$	(i)
M	$0 = d + f - g$	(ii)
θ	$-1 = -a - d - e - 2h$	(iii)
T	$0 = c - e - g - h$	(iv)
Q	$1 = e + g$	(v)

If we solve these equations in terms of a, g, h, then

(v) $\Rightarrow$	$e = 1 - g$	(vi)
sub (vi) $\Rightarrow$ (iii)	$d = g - a - 2h$	(vii)
sub (vi) $\Rightarrow$ (iv)	$c = 1 + h$	(viii)
sub (vii) $\Rightarrow$ (ii)	$f = a + 2h$	(ix)
sub (vi) (vii) (ix) $\Rightarrow$ (i)	$b = a + 3h - 1$	(x)

Thus from equations (vi) to (x) we can see that there are four power factors remaining, viz. 1, *a, g, h*. These are equivalent to four dimensionless groupings (Note: application of π theorem, viz. 9 quantities $-$ 5 fundamentals $=$ 4 groups). Therefore,

$$Q \propto u^a.L^{a+3h-1}.\Delta t^{1+h}.\mu^{g-a-2h}.K^{1-g}, \rho^{a+2h}, C_p{}^g, \{\beta g\}^h \qquad (4.28)$$

collecting powers:

$$q \propto \left(\frac{\Delta tk}{L}\right)^1.\left(\frac{Lu\rho}{\mu}\right)^a.\left(\frac{C_p\mu}{k}\right)^g.\left(\frac{\beta g\Delta tL^3\rho^2}{\mu^2}\right)^h \qquad (4.29)$$

or

$$\frac{qL}{\Delta tk} = \frac{hL}{k} = C.\left(\frac{Lu\rho}{\mu}\right)^a.\left(\frac{C_p\mu}{k}\right)^g.\left(\frac{\beta g\Delta tL^3\rho^2}{\mu^2}\right)^h \qquad (4.30)$$

Dimensionless analysis arrives at the conclusion that convective heat transfer can be quantified by four dimensionless groups.

$\frac{hL}{k}$	Nusselt Number	Nu
$\frac{Lu\rho}{\mu}$	Reynolds Number	Re
$\frac{C_p\mu}{k}$	Prandtl Number	Pr
$\frac{\beta g\Delta tL^3\rho^2}{\mu^2}$	Grashof Number	Gr

The physical significance of these groups are

Nu	–	ratio of temperature gradient at the surface to some reference temperature gradient
Re	–	ratio of inertia to viscous forces in a fluid
Pr	–	ratio of kinematic viscosity to thermal diffusivity
Gr	–	ratio of buoyant to viscous forces

For natural convection there is a general relationship of the form:

$$Nu = f(Gr \cdot Pr) \tag{4.31}$$

i.e. convection depends on buoyancy.

For forced convection:

$$Nu = f(Re \cdot Pr) \tag{4.32}$$

i.e. buoyancy effects are negligible.

For most gases over a reasonably wide temperature and pressure range, the Prandtl Number is constant (Note. kinetic theory of gases predicts that $k/(C_v \cdot \mu)$ is constant) and can be incorporated into the constant, C, so that:

$$Nu = C' Re^n \tag{4.33}$$

A further dimensionless group is often used in place of the Nusselt Number. This is the Stanton Number, St, where:

$$St = \frac{h}{C_p \rho u} = Nu \cdot Re^{-1} \cdot Pr^{-1} \tag{4.34}$$

This is used because it removes the evaluation of L, which may be difficult for geometrically complex problems. This analysis implies that all convective heat transfer systems can be reduced to an equation of the form of 4.30, requiring suitable numerical values for the constant (C) and powers (*a, g, h*) that are characteristic to each individual system.

4.2.3 Evaluating Convective Heat Transfer Coefficients

There are three approaches to evaluation convective heat transfer coefficients.

1. By analysis of conductive heat transfer through the boundary layer.
2. By analogy between heat, mass and momentum transfer processes; e.g. heat transfer can be predicted from shear stress measurements between a wall and flowing fluid.

3. By direct measurement under limited conditions and extrapolation using dynamic similarity.

It is possible to use the first method for simple geometric systems involving forced convection in laminar flow. The complex geometry of most furnaces, together with the normally turbulent gas flows preclude a complete analytical solution, even using current available computational fluid dynamics (CFD) software and hardware, see Pope (1990). The second method relies on a Reynolds flow analogy, (viz. equation 4.33), providing a semi-empirical method for turbulent flow systems, but this is limited as this requires that the flow measurements for the particular system have been made available. The third method is still the most important source for calculating suitable convective heat transfer coefficients.

There is extensive data in the literature giving correlations based on dimensionless groups for various flow systems. Figure 4.9. shows a typical temperature profile through a boiler tube wall. It can be seen that the temperature gradients occur in the outer and inner boundary layers and also over the scale deposit. It is generally the practice to report dimensionless correlations for such systems using physical constants (i.e. C_p,k,ρ.μ) evaluated at the mean film temperature, which is normally the arithmetic mean of the bulk and wall temperatures. However, some relationships are evaluated at bulk temperature conditions, thus care must be taken in using any correlation to ensure that the correct physical constant values are used. Table 4.1. summarises a number of correlations for the calculation of convective heat transfer systems. All the correlations in the table have been determined using physical values calculated at the film temperature.

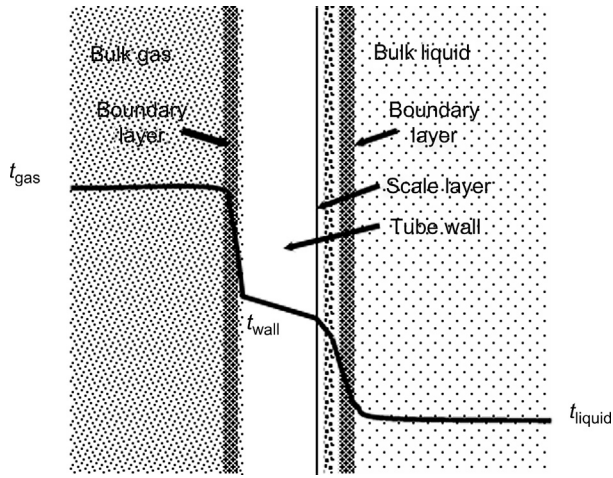


Figure 4.9 Temperature profile through a tube wall

TABLE 4.1 Convective heat transfer correlations for a number of common geometries

General equation is of the form $Nu^a = C\,Re^b\,Pr^c\,Gr^d$						
System	a	C	b	c	d	Limitations
Air to single cylinder, forced	1	0.891	0.330	—	—	$1<Re<4$
Air to single cylinder, forced	1	0.821	0.385	—	—	$4<Re<40$
Air to single cylinder, forced	1	0.615	0.466	—	—	$40<Re<4000$
Air to single cylinder, forced	1	0.174	0.618	—	—	$4000<Re<40000$
Air to single cylinder, forced	1	0.024	0.805	—	—	$40000<Re<250000$
Flow over a cylinder, forced gas	1	0.700	0.500	0.33	—	
Flow inside tube, forced gas	1	0.023	0.800	0.33	—	Re>10000 L>60diameters
Flow over sphere, forced gas	1	0.370	0.600	0.30	—	$25<Re<10^5$
Flow over flat plate , forced gas	1	0.037	0.800	0.33	—	
Flow over tubes, forced gas, in-line	1	0.300	0.600	0.33	—	
Flow over tubes, forced gas, staggered	1	0.380	0.600	0.33	—	
Flow over tubes, forced gas, co-flowing	1	0.037	0.800	0.33	—	
Flow over vertical plate, natural laminar	1	0.555	—	0.25	0.25	$Gr<10^9$
Flow over vertical plate, natural turbulent	1	0.100	—	0.33	0.33	$Gr>10^9$
Flow over horizontal cylinder, natural	1	0.530	—	0.25	0.25	$Pr>0.5\ 10^3<Gr<10^9$
Flow over sphere, natural	1	2+0.45(PrGr)	—	0.25	0.25	
Flow over hot plate, face up, or cold plate, face down, natural	1	0.540	—	0.25	0.25	$10^5<Gr<2x10^7$
Flow over hot plate, face up, or cold plate, face down, natural	1	0.140	—	0.33	0.33	$2x10^7<Gr<3x10^{10}$
Flow over hot plate, face down, or cold plate, face up, natural	1	0.270	—	0.25	0.25	$3x10^5<Gr<3x10^{10}$

Example 4.4 To show how these correlations are used, let us consider again the data in example 4.2, and evaluate the convective heat transfer rates to the ingot at the start and after 3 hours of the heating cycle.

We previously calculated that the thermal input at the start of the cycle is 12.14 MW and 3.73MW after 3 hours. Using data from Chapter 3, table 3.1, for a typical natural gas we can define the following values

Fuel gross CV	– 38.62MJ/Nm^3
Theoretical air requirement	– 9.751Nm^3/Nm^3

For simplicity in the example, as a first approximation we shall assume the flue gases to have the same physical properties as air since over 70% will be nitrogen, although in a rigorous calculation the actual flue gas components should be used.

Fuel rate at start = 12.14/38.62 = 0.3143 Nm^3/s

If we assume complete combustion then flue gas flow rate at start = 0.3143 + 0.3143 x 9.751 = 3.379 Nm^3/s

Similarly, the fuel rate after 3 hours = 3.73/38.62 = 0.0966 Nm^3/s and the flue gas flow rate = 1.038 Nm^3/s

Hence, the true volumetric flue gas flow at start = 3.379 x (273 + 1300)/(273) = 18.232 m^3/s, and after 3 hours =5.983 m^3/s

If we assume that the furnace flue gases leave at the opposite end from the charging door, then the free flow area for the flue gases (excluding the bogie) = (5.5 x 6.1) − (π x 1.12^2) = 29.6 m^2.

Thus mean flue gas velocity at start = 18.232/29.6 = 0.651 m/s, and after 3 hours = 0.202 m/s

At the start the mean film temperature = (1300 + 650)/2 = 975 °C

After 3 hours, the ingot surface temperature has risen to 1100 °C, hence the mean film temperature after 3 hours = (1300+1100)/2 = 1200 °C.

The physical properties of air at the film temperatures are

Property	*@ 975°C*	*@1200°C*
C_p J/kg C	1.18 x 10^{-3}	1.21 x 10^{-3}
k W/m C	0.0664	0.0933
ρ kg/m3	0.2828	0.2396
μ poise (g/cm s)	482 x 10^{-6}	534 x 10^{-6}

To determine the relevant correlation, we must first evaluate the Reynolds number, thus

$$Re_{start} = vL\rho/\mu = \frac{0.651 \times 2.24 \times 0.2828}{482 \times 10^{-6} \times 0.1}$$
$$= 8556 \text{ (turbulent flow)}$$
$$Re_{3hr} = vL\rho/\mu = \frac{0.202 \times 2.24 \times 0.2396}{534 \times 10^{-6} \times 0.1}$$
$$= 2030 \text{ (transitional flow)}$$

From table 4.1, we can use the correlation for air to a single cylinder, forced for the range $4000 < Re < 40000$ at the start.

i.e. $Nu = 0.174\ Re^{0.618}$

$$\text{thus } h_{start} = 0.174\left(\frac{0.0664}{2.24}\right)8556^{0.618} = 1.39\ W/m^{2\circ}C$$

Convective heat transfer at start $= hA\Delta t = 1.39 \times (\pi \times 2.24 \times 5.87 + 2 \times \pi \times 1.12^2) \times (1300-650) = 44452$ W

Likewise, from table 4.1, we can use the correlation for air to a single cylinder, forced for the range $40 < Re < 4000$ after 3 hours.

i.e. $Nu = 0.615\ Re^{0.416}$

$$\text{thus } h_{start} = 0.615\left(\frac{0.0933}{2.24}\right)2030^{0.416} = 0.61\ W/m^{2\circ}C$$

Convective heat transfer after 3 hrs $= hA\Delta t = 0.61 \times (\pi \times 2.24 \times 5.87 + 2 \times \pi \times 1.12^2) \times (1300-1100) = 6001$ W

4.2.4 High Temperature Convective Heat Transfer

Under conditions where high temperature combustion gases are in contact with surfaces (particularly 'cold' surfaces), the normal relationships for convective heat transfer do not hold owing to a number of anomalies.

- The transport properties (i.e., C_p, μ, ρ, k) of the gases cannot be regarded as those of air or normal combustion products.
- The use of the mean film temperature to evaluate physical properties is inadequate.
- Chemical recombination reactions in the boundary layer will change the heat transfer rates.

Because reactions occur within the boundary layer, it is better to use the enthalpy driving force in the heat transfer evaluation rather

than the temperature driving force that will not take into account the energy due to dissociation.

$$q_{conv} = \frac{hA}{C_p}(H_g - H_s) \tag{4.35}$$

$$\text{note } \frac{h}{C_p} = G \cdot St \tag{4.36}$$

The enthalpies, H_g and H_s, are derived by summing the components of the species in the gas phase and at the surface respectively.

$$H_i = \int_{T_2}^{T_1} C_{pi}\partial T + \Delta H_{fi}^0 \tag{4.37}$$

i.e. sensible heat + heat of formation

$$H_g = \sum_i m_i H_i \tag{4.38}$$

where m_i = mole fraction of species i.

Combustion chemistry indicates that there are hundreds of reactions occurring in a flame, all of which are reversible. Whilst the predominant products of combustion are CO_2 and H_2O in simple air/fuel flames, in combustion systems where oxygen is used to replace some of the air, or where the combustion air is preheated to high temperatures (>600°C) this is not the case. Five of the most important combustion dissociation reactions that occur in high temperature flames (viz. >2000°C) are:

Reaction	ΔH_f^o *kJ/kg mole*
$CO_2 \rightarrow \frac{1}{2}O_2 + CO$	283.17
$H_2O \rightarrow H_2 + \frac{1}{2}O_2$	244.15
$H_2O \rightarrow \frac{1}{2}H_2 + OH$	325.00
$\frac{1}{2}H_2 \rightarrow H$	221.46
$\frac{1}{2}O_2 \rightarrow O$	249.34

All of these dissociation reactions will be driven towards the right hand side of the equation in the hottest regions of the flame, which will change the transport properties of the flame gases. The Lewis Number, Le, defines the ratio of atomic diffusion (principally H atoms) to thermal diffusion, and has a value of unity for most combustion conditions since H atoms are not usually present below 1700°K.

$$Le = \frac{D_i}{\left(\frac{k}{\rho C_p}\right)} \tag{4.39}$$

where D_i - diffusion coefficient of species i through the gas mixture

D_i depends on the temperature, for which data is avalable, see Hirschfelder, Curtiss & Bird (1954). If the Lewis Number is $\neq 1$, then the transport properties of the gas are changed, and hence the Prandtl Number will change.

$$Pr_{diss} = Pr\left(1 + (Le - 1)\frac{\Delta H_{chem}}{\Delta H}\right)^{-1} \tag{4.40}$$

where

$$\Delta H_{chem} = \sum_i m_i \Delta H_f^0$$

and is the enthalpy due to chemical dissociation

Thus, the new value of Pr_{diss} is substituted into the standard correlation for the system being investigated to give a modified heat transfer coefficient.

Example 4.5 What are the apparent and true convective heat transfer coefficients for a 2:1 oxy-methane flame impinging on a 10mm diameter steel rod? The following data can be used:

Flame temperature	– 3000°K
Steel rod temperature	– 600°K
Mass velocity of flame gases	– 3.524 kg/m^{2}s

The flue gas composition (mole fraction) of the oxy-methane flame at various temperatures is

Component	*600K*	*1000K*	*1400K*	*1800K*	*2200K*	*2600K*	*3000K*
H_2O	0.6566	0.6566	0.6566	0.6554	0.6405	0.5727	0.4152
CO_2	0.3283	0.3283	0.3283	0.3275	0.3121	0.2428	0.1288
CO	–	–	–	0.0005	0.0126	0.0657	0.1430
O_2	0.0151	0.0151	0.0151	0.0153	0.0218	0.0498	0.0870
H_2	–	–	–	0.0003	0.0049	0.0244	0.0639
OH	–	–	0.00004	0.0009	0.0074	0.0335	0.0892
O	–	–	–	–	0.0004	0.0052	0.0332
H	–	–	–	–	0.0004	0.0060	0.0398

From the above data the following thermal and transport properties can be derived

Temperature °K	*Mean molecular weight g*	*Density kg/m³*	*Specific heat kJ/kg°C*	*Viscosity μNs/m²*	*Thermal conductivity w/m°C*	*Diffusion coefficient of H in oxygen m²/s*
600	26.75	0.5436	1.490	24.47	0.0526	—
1000	26.75	0.3261	1.698	38.25	0.0937	—
1400	26.75	0.2329	1.858	50.26	0.1355	—
1800	26.75	0.1810	1.973	61.09	0.1716	0.002490
2200	26.73	0.1466	2.051	70.63	0.2133	0.003485
2600	25.18	0.1178	2.098	79.85	0.2519	0.004694
3000	22.14	0.0900	2.126	88.43	0.3045	0.006333
Weighted mean	26.01	0.2202	1.914	59.42	0.1741	0.002767

And hence, the weighted mean values of the relevant dimensionless groups.

Temperature °K	*Re*	*Pr*	*Le*
600	1440	0.69	—
1000	921	0.69	—
1400	701	0.69	—
1800	577	0.70	5.18
2200	499	0.68	4.91
2600	441	0.67	4.61
3000	399	0.62	3.98
Weighted mean	676	0.68	4.70

The weighted mean values are calculated using the integrated mean over the temperature range, rather than the simple arithmetic mean used for normal film temperature condition calculations.

The enthalpy difference of the flame gases between 600°C and 3000°C is given by the difference in the heat of formation of the combustion products at 600°C and 3000°C

$$\left(C_p\Delta T + \Delta H_f^0\right)_{600} = 1.490 \times 600 + (0.6566 \times 239.07 + 0.3283 \times 393.40)$$
$$= 1180\ kJ/kg$$

$$\left(C_p\Delta T + \Delta H_f^0\right)_{3000} = 2.126 \times 3000 + (0.4152 \times 239.07 + 0.1288 \times 393.40 + 0.1430 \times 1238.87 + 0.0892 \times 135.23 + 0.0332 \times 1561.76 + 0.0398 \times 1529.02)$$
$$= 6830\ kJ/kg$$

$$\Delta H = 6830 - 1180 = 5650$$

The heat of recombination of CO, OH, O and H at 3000°C is

$$\Delta H_{chem} = 0.143 \times 283.17 + 0.0892 \times 325.00 + 0.0332 \times 249.34 + 0.0398 \times 221.46$$
$$= 86.6\ kJ/kg$$

Correcting the Prandtl number for dissociation gives

$$Pr_{diss} = 0.68/(1 + \{4.7 - 1\} \times 86.6/5650) = 0.643$$

The relevant convection correlation taken from table 4.1 is

$$Nu = 0.7Re^{0.5}Pr^{0.33}$$

Thus, the convective heat transfer coefficient under dissociation conditions is

$$h_{diss} = \left(0.7 \times 0.174 \times 676^{0.5} \times 0.643^{0.33}\right)/0.01 = 273.7\ W/m^2\ ^oC$$

and the heat transferred using equation 4.35 = 273.7 x 5650/1.914 = 0.81 MW/m^2

If we use the mean film temperature data (i.e. 1800°C) then

$$h = \left(0.7 \times 0.1716 \times 577^{0.5} \times 0.70^{0.33}\right)/0.01 = 256.5\ W/m^2\ ^oC$$

and the heat transferred using equation 4.19 = 256.5 x (3000 − 600) = 0.62MW/m^2

Thus the true convective heat transfer rate is approximately 30% greater than that predicted without dissociation effects.

4.3 Radiation

When two solid surfaces are at different temperatures and are separated by a transparent fluid phase, they will exchange thermal energy by radiation. The latter consists of electromagnetic waves of the same character as visible light and its intensity, and visibility due to the wavelength spectrum, increases with the temperature of the radiating surface. See Figure 4.10. Therefore a net amount of energy flows from the warmer to the cooler surface. Particularly at elevated temperatures this type of heat exchange often exceeds conductive or convective transport and becomes the controlling process. In most high temperature furnaces operating at above 1000°C, approximately 90% of the heat transfer is radiative, whilst the balance is convective. Whether one deals with pyro-metallurgical operations, high-temperature chemical reactors or simple combustion chambers to produce thermal energy, a thorough study and understanding of radiation phenomena must precede the actual process investigation or design of equipment. A related field - with growing activities and interest - is the use of solar energy as an alternative energy source.

The physical laws governing thermal radiation are well established but are insufficient to describe technical processes quantitatively. This is largely due to the structure and thermal behaviour of real surfaces as

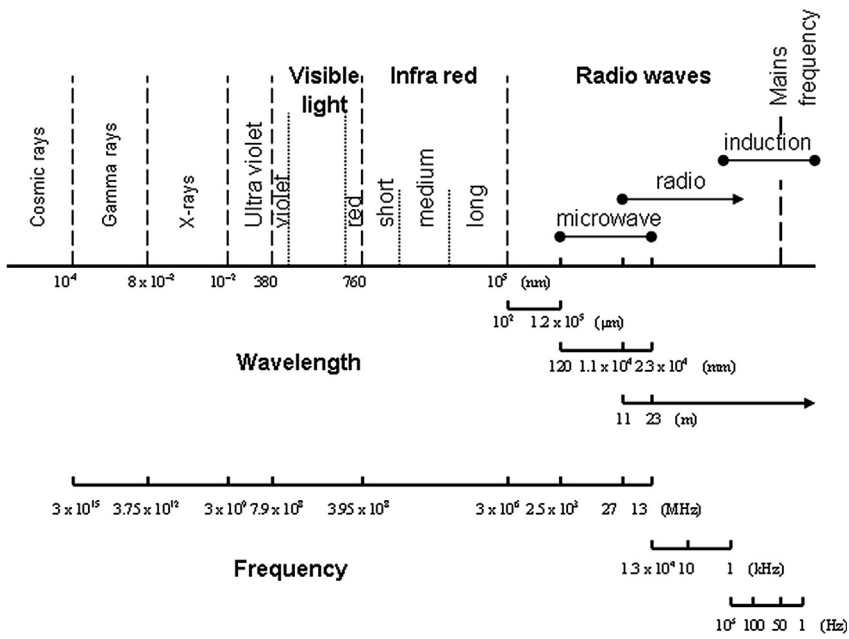


Figure 4.10 The electromagnetic spectrum (note scale not constant)

opposed to ideal surfaces (determination of emissivities), as well as to the interaction between different surfaces and bodies of more or less complicated orientation in space (determination of view factors). The former problem has, to a major extent, been solved experimentally whereas the latter has been, and still is circumvented by devising suitable models. Only with very simple configurations of surfaces can the net energy flux be calculated rigidly.

4.3.1 Physical Basics of Radiative Exchange

Matter that is exposed to radiation can absorb (α), reflect (γ), and transmit (τ). In any case, a balance gives:

$$\alpha + \gamma + \tau = 1 \tag{4.41}$$

where α, γ and τ are fractions of the incident radiation. A body is called black, white or grey when

$\alpha = 1$	black body ($\gamma = 0$, $\tau = 0$)
$\gamma = 1$	white body ($\alpha = 0$, $\tau = 0$)
$\alpha < 1$, $\gamma < 1$	grey body ($\tau \geq 0$)

Most solid bodies, and many liquids, absorb within a thin surface layer in which case

$$\tau = 0 \quad \text{opaque body}, \ \gamma + \alpha = 1$$

In this case, as far as heat exchange is concerned, the main effect consists of an increase in the surface temperature. The mechanisms of radiation and possible convection (or conduction) are decoupled and the corresponding heat flux densities can be added. A surface is called smooth if there is regular reflection of the incident radiation, as with light on a mirror, and is called rough for diffuse reflection going in all directions.

In thermal equilibrium, Kirchoff's law applies, viz.

$$\alpha = \varepsilon \tag{4.42}$$

Where ε, the emissivity of a body, is defined by equation 4.44. The more radiation a body absorbs the more it also emits (viz. conduction of absorbed heat away from the surface maintains a stationary temperature difference between two surfaces). In the limiting case of a black body, which we may use as a reference body or surface,

$$\alpha = \varepsilon = 1.$$

On the other hand black body radiation can be calculated. The energy flux radiated from a black body is a function of temperature only.

Since it is the maximum possible, the surface structure has no effect, and is

$$E_b = \sigma\left(\frac{t}{100}\right)^4 \tag{4.43}$$

Where $\sigma = 5.67$ W/m^{2}K^4, and is called the black body, or Stefan-Boltzmann radiation constant. The actual radiation E of a real surface is always smaller and depends on the physical and chemical structure of the surface. This leads to the definition of emissivity

$$\varepsilon = \frac{E}{E_\mathrm{b}} \tag{4.44}$$

thus

$$E = \varepsilon\sigma\left(\frac{t}{100}\right)^4 \tag{4.45}$$

where ε has to be measured and is discussed in section 4.3.2.

Equation 4.43 yields the total emission from a surface element into the space "seen" by the surface element. Planck has shown that energy cannot be emitted with monochromatic radiation i.e. radiation of one given wavelength. A range of wavelengths is required and one spectral emission (emissive power) is defined as

$$E_{b\lambda} = \int_t \frac{\partial E_b}{\partial \lambda} = C_1 \frac{\lambda^{-5}}{e^{\left(C_2/\lambda t\right)} - 1} \tag{4.46}$$

This is illustrated in Figure 4.11, and is seen to be a strong function of the wavelength λ. Also, with increasing temperature more energy will be emitted in the range of visible light (viz. solar radiation).

The total emission at a temperature, t, is given by the area under the corresponding curve and it is important to note that a "grey" body absorbs, and hence emits, the same fraction of energy at each wavelength. In practice, there are also a number of more or less

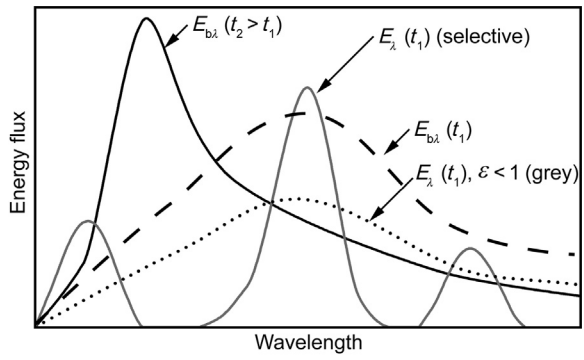


Figure 4.11 Diagrammatic representation variation of E with λ for various types of emitter

'selective' absorbers (e.g. glass, wall plaster, combustion gases) which only absorb in certain ranges of the wavelength spectrum.

Finally, we should note that emitted energy will not be distributed uniformly over the space above the radiating surface. This behaviour becomes important when the energy exchange between finite size surfaces of arbitrary orientation to each other is evaluated. In the ideal case of black body radiation or any other totally diffuse radiation, Lambert's Law applies.

$$E_{b\phi} = E_{bn} \cos \phi \tag{4.47}$$

By integrating over the entire hemisphere one gets:

$$E_b = \pi E_{bn} \tag{4.48}$$

Equation 4.48 explains why a radiating sphere appears as a disk of uniform brightness, viz. the sun. A surface obeying equation 4.48 is called a Lambert surface and the concept provides the basis for most calculations in high-temperature engineering.

So far, we have been dealing with radiating surfaces where $t = 0$. Gases, other than the ideal gases, however, do not absorb and emit in a very thin layer but rather over a volume of certain depth, giving rise to the concept of 'gas-body' radiation. For monochromatic radiation or for total radiation in a grey medium the radiative energy flux decreases exponentially with the travelled distances. This is defined by the Bouguer-Lambert Law.

$$\frac{i}{i_0} = e^{(-KL)} \tag{4.49}$$

where K is the absorption coefficient and has to be measured.

Here we have introduced the intensity, i, to account for the fact that radiation going in different directions may have to pass through gas layers of different lengths and hence will be absorbed to different degrees. In the simplified case of a collimated beam of black body radiation passing through a grey gas column of length L the absorbed energy is equal to the difference in intensities.

$$i_0 - i_L = i_0\left(1 - e^{(-KL)}\right) \tag{4.50}$$

However, from equation 4.42 this energy must also be emitted so that the radiation emitted by the gas body is

$$E_g = E_b\left(1 - e^{(-KL)}\right) \tag{4.51}$$

Hence, we define the emissivity of a gas, in analogy to equation 4.44, as

$$\varepsilon_g = 1 - e^{(-KL)} \tag{4.52}$$

This is known as Beer's law. It can be seen that only an infinite thick gas body can be interpreted as a black body (ε=1). These two concepts of 'solid surface' and 'gas body' radiation are most important even in the simplest engineering problems and will be applied frequently later.

4.3.2 Emissivity and Absorptivity

The understanding of the radiation properties of solid surfaces and gas bodies in particular requires a qualification of Kirchoff's Law, equation 4.42. Strictly speaking, the absorbed fraction, α, of incident radiation is equal to the emissivity, ε, only when the source of incident radiation and the emitting surface have the same temperature, i.e. are in thermal equilibrium with no net heat exchange between the surfaces. However, in practice we are obviously more interested in non-equilibrium resulting in a non-zero heat flux. Under these conditions we find that equation 4.42 still holds for monochromatic radiation of wavelength λ, since it is a general property of materials that their absorptivity, α_λ, is insensitive to large variations in intensity of irradiation. Equation 4.42 also holds for total radiation (integrated over all λ) as long as the surface or body is grey as previously defined. In this case the total absorptivity will therefore not depend on the temperature of the source of irradiation and be equal to the total emissivity. The latter may, however, be a function of the temperature of the emitter since this temperature determines the wave spectrum of emitted radiation (ref. Figure 4.11) and as the solid may be emitting more at one wavelength than at another, its total emissivity may vary with temperature. One of materials that exhibits the strongest selectivity is glass where we find that $\varepsilon = 0.92$ at room temperature, but $\varepsilon = 0.47$ at 800°C (silica glass). Notwithstanding, with most solids it is sufficient to specify one integrated value of the emissivity, if necessary at a number of different temperatures.

The emissivity may also vary with the angle of emission. Most high-temperature furnace materials are diffuse radiators and the emissivity is independent of angular position i.e. they are Lambert surfaces. If that is the case, the specification of a total *(with respect to wavelengths)* normal *(to the radiating surface)* emissivity ε_n is sufficient. This quantity usually has to be measured and extensive data are given in appendix 4.A. at the end of this chapter. The emissivity can be determined by measuring the total radiation from a flat piece of material into the hemisphere above it. This obviously supplies a value of ε integrated over all directions. It is shown that:

with metal surfaces	$\varepsilon/\varepsilon_n \cong 1.2$
and with non-conductors	$\varepsilon/\varepsilon_n \cong 0.95$
whereas, with most rough or oxidised surfaces	$\varepsilon/\varepsilon_n \cong 1$

As far as heat transfer calculations are concerned, we usually assume a uniform emissivity, ε, valid in all directions.

TABLE 4.2 Total emissivity of some common materials at room temperature

Material	ε
Polished copper	0.035
Polished stainless steel	0.15
Cast, oxidised iron	0.63
Fire-clay brick	0.9
Rough steel plate	0.94
Black, oxidised copper	0.8
Cream paint	0.88
Wood	0.92
Water	0.96
Frost	0.98

An impression of orders of magnitude of emissivity may be obtained from table 4.2 (all materials at room temperature). It is noted that in general the metals' emissivity increases with temperature whereas the opposite is true for non-conductors.

The radiation characteristics of gases such as CO_2, H_2O, CO, SO_2, SO_3, NH_3, and hydrocarbons are different and, unfortunately, more complicated. It is well established that these gases only emit and absorb radiation of a specific wavelength or waveband. Therefore, they cannot strictly be interpreted as grey bodies and Kirchoff's law would only hold either in thermal equilibrium or for a given wavelength, but not for total emissivity or absorptivity. However, in most radiant heat transfer calculations for furnace design, we work with integrated values, largely due to a substantial amount of experimental results on virtually all situations of practical interest. This implies that we treat such gases or gas mixtures as grey bodies. However, it should be quite clear from previous remarks that:

- the absorptivity depends on both the gas temperature and the temperature of the radiating source and is not equal to the emissivity
- both α and ε depend on the shape and extent of the gas volume.

In addition, α and ε depend on the system pressure and, more importantly on the partial pressure of the component under consideration as this determines the opacity of the gas mixture. In furnace atmospheres the major radiating components are CO_2 and H_2O. The volumetric CO_2:H_2O flue gas ratios are approximately 1:2 for natural-gas flames, 1:1 for oil flames, and 2.5:1 for coal flames. Emissivity measurements for these two gases have been reported by Hottel and Egbert (1942), who have provided the results in diagrams found in all standard heat transfer textbooks. Once ε is available, the

absorptivity, being only a function of t_w and ε_g can be determined approximately from

$$\alpha_g(t_g, t_w) = \left[\left(1 - \left\{1 - \varepsilon_g(t_w)\right\}\right)^{t_g/t_w}\right]\left[\frac{t_g}{t_w}\right]^n \tag{4.53}$$

Where $n = 0.65$ for CO_2 and $n = 0.45$ for H_2O

The emissive characteristics of combustion flue gases can be reduced into a simplified form as shown in Figure 4.12. This chart provides a rapid method of assessing flame emissivity for use in some of the design methods discussed in later Chapters, and is accurate to ±5% within the ranges shown.

For pressures different from 1 bar further corrections have to be made since the emission bands depend on the total pressure. However, this is usually unnecessary for most furnaces because their operating pressure is generally close to atmospheric. Hottel and Egbert (1942) also provided correction charts for overlapping bands occurring with two or more absorbing gases, where radiation may for example be absorbed by CO_2, which also emits radiation of different wavelengths that is again partly absorbed by simultaneously present H_2O. In design calculations that require more accurate evaluation of gas emissivity and absorptivity, a method involving the weighted sum of a number of fictitious grey gases is often used to simulate the radiative properties of a real gas mixture. A general correlation using a two grey gas model is given by

$$\begin{aligned}\varepsilon_t = &\left(290 + \frac{191}{(A)^{1.3}\left(e^{[0.77/A]} - 1\right)}\right)\left(1 - e^{1.93BL}\right) \\ &+ \left(82 + \frac{374}{(A)^{2.7}\left(e^{[2.5/A]} - 1\right)}\right)\left(1 - e^{28.6BL}\right)\end{aligned} \tag{4.54}$$

where

$$A = P_{H_2O}/P_{CO_2}$$
$$B = P_{H_2O} + P_{CO_2\ (\text{atm.})}$$

The correlation is a good fit to the data within the range $0.03 < BL < 1.0$. For BL values below 0.03, the emissivity of the gas mixture is <0.025 within the normal flame temperature range, and thus makes a negligible contribution to radiative heat transfer.

A final point of importance is the effect of dust or soot particles in the gas. For pulverised coal combustion it has been shown, Thring

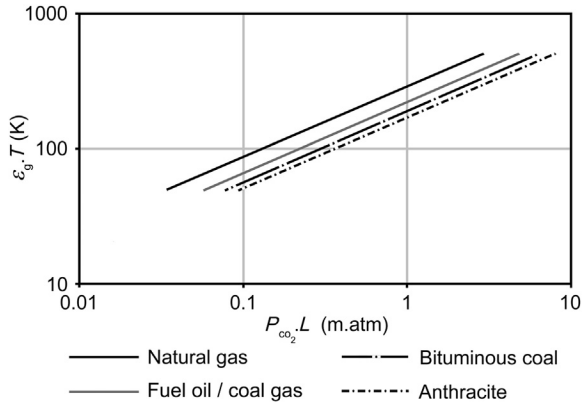


Figure 4.12 Evaluation chart for approximate flame gas emissivity calculations

(1952), that the emissivity of the dust may be expressed approximately as:

$$\varepsilon_d = 1 - e^{\left(\frac{-3c_p L}{2d_p \rho_p}\right)} \tag{4.55}$$

where c_p - particle concentration in gas
d_p - particle diameter
ρ_p - particle density

This relationship is valid where the absorptivity (or emissivity) of the dust typically lies between 0.15 and 0.35.

Soot particles are individually smaller than the wavelength of infra red radiation and thus, even when agglomerated, have different radiative properties to larger dust particles. Experimental studies have shown that the absorption coefficient for soot is related to the wavelength by:

$$k_{s\lambda} = a\lambda^{-b} \tag{4.56}$$

where a and b are constants. Integration of this relationship over all wavelengths leads to k_s. Experimental measurements in gas and liquid fuel flames, Foster (1965), has suggested the following empirical relationship

$$k_s = 1.1 \times 10^6 c_s \ \left(\mathrm{m}^{-1}\right) \tag{4.57}$$

and the total emissivity of soot is given by:

$$\varepsilon_s = 1 - e^{-k_s c_s L} \tag{4.58}$$

where c_s - soot concentration in gas

The overall emissivity of the gas-dust-soot combination is given by the sum of the exponents, to yield:

$$\varepsilon_m = \varepsilon_g + \varepsilon_d + \varepsilon_s - \varepsilon_g \varepsilon_d - \varepsilon_g \varepsilon_s \tag{4.59}$$

whereas

$$\alpha_m = \alpha_g + \alpha_d + \alpha_s - \alpha_g\alpha_d - \alpha_g\alpha_s \tag{4.60}$$

However, in modern pulverised-coal furnaces it is not unreasonable to assume an overall emissivity $\varepsilon_m = 1$, due to luminosity. Similar reasoning may apply to oil fired furnaces. If in doubt, one should always consult actual data taken from industrial flames, since the latter may be considerably influenced by the design of the burner.

4.3.3 View Factors

The prime objective in radiative heat transfer calculations for a furnace design is to calculate the heat flux between two or more surfaces, each having perhaps different absorption characteristics. In an ordinary furnace there are a minimum of six surfaces and a centrally positioned flame all of which emit, absorb and reflect radiation; although the required information may only consist of the net flux from the flame to a block of material or bank of reaction tubes, all the individual exchange rates may contribute and hence must be quantified. This makes a detailed furnace design extremely complicated and, unless some simplifications are introduced, even the simplest individual rates can not be determined numerically. In order to demonstrate the difficulties encountered in these calculations, and also to provide a basis for understanding the models used in design, we shall look at some very simple geometric configurations: starting with two grey Lambert surfaces separated by a transparent fluid. We shall then look at more than two surfaces in exchange, and finally include radiation of gases and flames.

When two grey Lambert surfaces of temperatures t_1 and t_2 ($< t_1$) and emissivities ε_1 and ε_2 are parallel to each other and are large in comparison to their distance from each other (see Figure 4.13) then

$$\dot{Q}_{1\to 2} = \varepsilon_1 E_{b_1 t_1} A_1 \alpha_2 + (\text{reflective terms}) \tag{4.61}$$

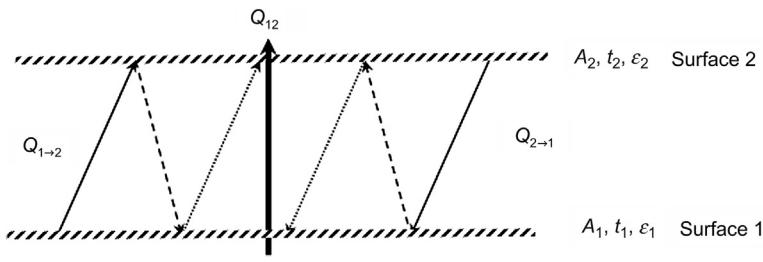


Figure 4.13 Radiative exchange between large, closely spaced parallel Lambert surfaces

and

$$\dot{Q}_{2\to 1} = \varepsilon_2 E_{b_2 t_2} A_2 \alpha_1 + (\text{reflective terms}) \tag{4.62}$$

From Kirchoff's Law, equation 4.42:

$$\alpha_{1,2} = \varepsilon_{1,2}$$

so that the net flux - with the reflective terms small of first order – becomes

$$\dot{Q}_{12} = \varepsilon_1 \varepsilon_2 A \sigma \left\{ \left(\frac{t_1}{100} \right)^4 - \left(\frac{t_2}{100} \right)^4 \right\} \tag{4.63}$$

At high temperatures, as encountered in furnaces, reflection can sometimes be neglected ($\gamma = \alpha - 1, \alpha \to 1$). If this is not the case, we find for the considered example that

$$\varepsilon_1 \varepsilon_2 \;\to\; \frac{1}{\dfrac{1}{\varepsilon_1} + \dfrac{1}{\varepsilon_2} - 1} \tag{4.64}$$

In the case of concentric pipes, of areas A_1 and A_2, equation 4.64 becomes

$$\varepsilon_1 \varepsilon_2 \;\to\; \frac{1}{\dfrac{1}{\varepsilon_1} + \dfrac{A_1}{A_2}\left(\dfrac{1}{\varepsilon_2} - 1 \right)} \tag{4.65}$$

Thus for a hot pipe in a large room ($A_2 \to \infty$), the radiative loss can thus be calculated immediately as

$$\dot{Q}_{12} = \varepsilon_1 \sigma A_1 \left\{ \left(\frac{t_1}{100} \right)^4 - \left(\frac{t_{\text{room}}}{100} \right)^4 \right\} \tag{4.66}$$

Characteristic for these examples are that all the radiation emitted from one surface reaches the other and nothing is lost. This is not so in the general case of two surfaces of finite sizes A_1 and A_2 (see Figure 4.14). Here a fraction of the emitted radiation of A_1 bypasses A_2 and vice versa. A consequence of this is that absorption of reflected radiation can often be neglected even when the surfaces

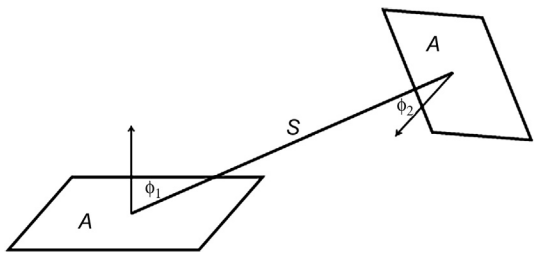


Figure 4.14 Radiative exchange between two finite surfaces

have a substantial reflectivity. One then defines a view factor F_{12}, expressing the fraction of the hemisphere above A_1 that represents A_2 and likewise the fraction of the hemisphere above A_2 that constitutes A_1.

Thus the view factors for Figure 4.14 are given by

$$A_1F_{12} = A_2F_{21} = \pi \int_{A_1} \int_{A_2} \frac{\cos\varphi_1 \cos\varphi_2}{S^2} \partial A_1 \partial A_2 \tag{4.67}$$

so that

$$\dot{Q}_{12} = \varepsilon_1\varepsilon_2\sigma F_{12} A_1 \left(t_1^4 - t_2^4\right) \tag{4.68}$$

It is mainly the evaluation of view factors according to equation 4.67 that complicates radiative exchange calculations. Just to give an example, the view factor for an extremely simple configuration of a differential area ∂A_1 to a parallel plate of area A_2 and dimensions X by Y, separated by a distance Z, is solved by two integrations over X and Y, the final result being:

$$F_{\partial A_1 \to A_2} = \frac{1}{2\pi}\left[\frac{X}{(X^2+Z^2)^{1/2}} \sin^{-1}\left\{\frac{Y}{(X^2+Y^2+Z^2)^{1/2}}\right\} + \frac{Y}{(Y^2+Z^2)^{1/2}} \sin^{-1}\left\{\frac{X}{(X^2+Y^2+Z^2)^{1/2}}\right\}\right] \tag{4.69}$$

Although the limitation to a differential area ∂A_1, may seem a rather theoretical exercise the results provide a good approximation of real situations whenever one of the surfaces, A_1, is much smaller than the other. The case of two areas of similar size involves another two integrations, and equation 4.67 becomes too complex to solve analytically. For the designer, an extensive number of important geometric configurations viz. rectilinear, cylindrical, etc., have already been studied, and values for the view factors can be found in Hottel & Sarofim (1967).

With curved surfaces the integration may become difficult, and here a very simple method, called "crossed-string method" supplies view factors directly as long as we are designing an essentially two-dimensional system, i.e. the surfaces extend in one direction much further than in the others. Typical examples where this type of calculation becomes applicable is the radiation from a fuel-fired furnace chamber to a long row of tubes mounted on the wall, or from long electric resistance rods into a furnace chamber. The general rule of the method is to draw the shortest connections between the four points of the surfaces which just see each other (see Figure 4.15). This results in a pair of crossed and a pair of uncrossed strings. It can be shown that the view factor is

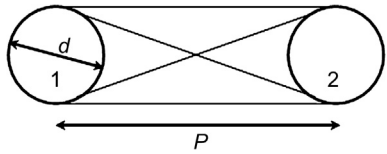


Figure 4.15 Example of crossed string evaluation of exchange area between curved surfaces

$$F_{12} = \frac{1}{A_1}\frac{(\text{sum of crossed strings}) - (\text{sum of uncrossed strings})}{2} \tag{4.70}$$

The view factor for the configuration shown in Figure 4.14 is then:

$$F_{12} = \frac{1}{\pi}\left[\sin^{-1}\left(\frac{d}{P}\right) + \left\{\left(\frac{d}{P}\right)^2 - 1\right\}^{1/2} - \frac{P}{d}\right] \tag{4.71}$$

Before proceeding to radiative exchange between more than two surfaces it is necessary to define some identities, These may be employed to cut short on calculation procedures for complex systems.

- From the definition of the view factor (equation 4.67) it is apparent that:

$$F_{12}A_1 = F_{21}A_2 \quad \text{or generally} \quad F_{ik}A_i = F_{ki}A_k \tag{4.72}$$

  The product, $F \cdot A$, is called the direct exchange area.
- For rectangular plane surfaces which are either perpendicular, adjacent or parallel (see Figure 4.16), it can be shown by extension of equation 4.67 that:

$$F_{13}A_1 = F_{42}A_4 = F_{31}A_3 = F_{24}A_2 \tag{4.73}$$

- In a complete enclosure (see Figure 4.17) obviously

$$\sum_{k=1}^{n} F_{ik} = 1 \tag{4.74}$$

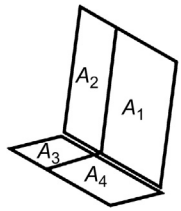


Figure 4.16 Rectilinear surface relationship

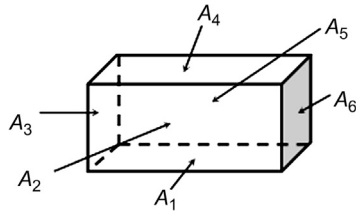


Figure 4.17 Complete geometry system.

This relationship may save the determination of the last of a large number of view factors.

- If a plane surface A_1 is not of a uniform temperature, it can be split up into a number of sub-surfaces A_{1j} each of which is approximately of a constant temperature. In that case (see Figure 4.18) it can be shown that for any angle ω:

$$A_1 F_{12} = \sum_j A_{1j} F_{1j2} \tag{4.75}$$

When a number of surfaces forms a complete enclosure, the simplification of neglected absorption of reflected radiation used for parallel plates would only hold for $\alpha = 1$. Already, with relatively small deviations from $\alpha = 1$, a total energy balance neglecting reflection does not match because the reflected amount must be absorbed somewhere, if not on the original surface then on one of the others completing the enclosure. The analytical treatment of this refined process is rather complicated, and has led to the development of the zone-method, Hottel & Sarofim (1967).

Equivalent Grey Surface

The concept of an equivalent grey surface or plane is often used to simplify the analysis of a composite surface, such as a tube lined refractory wall. See Figure 4.19. The fraction of radiation intercepted and absorbed directly by the tubes is

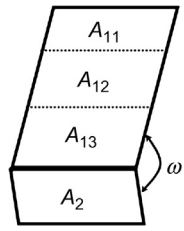


Figure 4.18 Sub division of radiating planes

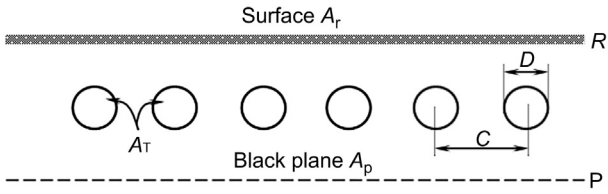


Figure 4.19 A refractory backed row of tubes

$$F_{TP} = \frac{\pi D}{2C} - \frac{F_{TT}}{C} \tag{4.76}$$

where F_{TT} is the exchange area between tubes given by equation 4.71. Thus, $(1 - F_{TP})$ is incident on the refractory surface and is reflected or re-radiated. Thus the total absorbed between the tubes from plane P is given by

$$\overline{F}_{TP} = F_{TP}(2 - F_{TP}) \tag{4.77}$$

The total exchange factor between the plane P and the combined, or equivalent, composite grey plane E formed by the tubes and refractory is given by

$$F_{EP} = \frac{1}{\dfrac{1}{\overline{F}_{TP}} + \dfrac{C}{\pi D}\dfrac{\rho_T}{\varepsilon_T}} \tag{4.78}$$

4.3.4 Mean Beam Length

The emissivity of a gas body according to equation 4.52 only applies to a gas column of differential cross-section and length L, which is a rather hypothetical system. However, the concept is also correct for a hemispherical gas body of radius L being irradiated from (or radiating onto) a small surface ∂A in the centre of the hemisphere (see Figure 4.20). Here all radiant beams would pass through the same length of gas. In comparison, when an absorbing gas lies between two parallel large surfaces the radiation from an element on surface

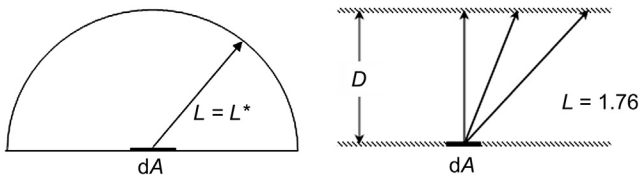


Figure 4.20 Mean beam length values for two geometric systems

1 would pass through different lengths, depending on the angle, before reaching the other wall 2. In that case the characteristic length for absorption or emission would have to be larger than the gap between the surfaces. It is therefore sensible to devise an equivalent mean-beam length, L^*, and write for the emissivity:

$$\varepsilon_g = 1 - e^{(-KL^*)} \tag{4.79}$$

For simple configurations L^* can be calculated and tables are found in Hottel and Sarofim, table 7.3 (1967) (e.g., for the radiating gas between two infinite parallel surfaces one finds that $L^* = 1.76.D$, for a pipe $L^* = 0{,}9.D$). If L^* cannot be calculated from known values we can, as an approximation use:

$$L^* = 0.9\frac{4V_g}{A_g} \tag{4.80}$$

where A_g is the total surface area and V_g is the total volume of the gas body (and of the enclosure).

4.4 Electrical Heating

Heat can be transferred by other parts of the electromagnetic spectrum, particularly in the long wave region, in and beyond the infrared. See Figure 4.10. The primary source of energy for heating in this region is electricity. The are a number of methods used to deliver the electrical energy to the material, principal amongst these being:

- Resistance heating
- Arc heating
- Induction heating
- Dielectric heating
- Infra-red heating

4.4.1 Resistance Heating

The passage of electricity through a conducting material gives rise to the generation of heat in the material owing to its electrical resistance. The power developed is I^2R (watts) where I is the current (amps) and R is the resistance (ohms). The resistance of a conductor is given by:

$$R = \Omega\frac{x}{A} \tag{4.81}$$

where

Ω- resistivity of material
x- length
A - cross sectional area

Most materials, solid, liquid and gaseous conduct electricity, but the value of Ω varies by about 3 orders of magnitude depending on the material properties and temperature, see table 4.3. Metal resistivity normally increases with temperature, whilst it may decrease for non-metallic materials. If the material exhibits a uniform variation, then the temperature relationship is of the form:

$$\Omega_T = \Omega_0(1 + aT) \tag{4.82}$$

Resistance heating can be used to heat the material directly, or can be used to heat a separate conductor or heating element, which in turn heats the material by a combination of conduction, convection and radiation.

Direct Resistance Heating

To efficiently use the electrical power in a direct resistance heating system, a high proportion must be dissipated in the workpiece, which implies that it should have a high resistance, relative to the supply circuit.

TABLE 4.3 Materials used for resistance heating elements

Material	*Maximum operating temperature in dry air °C*	*Resistivity 10^{-12} ohm.m @ 20°C*
Nickel based alloys		
80 Ni / 20 Cr	1200	110
80 Ni / 20 Cr + Al	1250	
60 Ni / 15 Cr / 25 Fe	1100	110
50 Ni / 18 Cr / 32 Fe	1075	110
37 Ni/ 18 Cr / 33 Fe / 2 Si	1050	
54 Ni / 46 Cu	400	49
Iron based alloys		
72 Fe / 22 Cr / 4 Al	1050	139
72 Fe / 22 Cr / 4 Al + Co	1275	145
Refractory materials		
Platinum	1400	11
Molybdenum	1750	5.7
Tantalum	2500	12.5
Tungsten	1800	5.5
90 Platinum / 10 Rhodium	1600	19.2
60 Platinum / 40 Rhodium	1750	17.4
Non-metals		
Silicon carbide	1600	10^5
Molybdenum disilicide	Up to 1800	40
Graphite	3000	10^3

Since the resistivity of most common ferrous and non-ferrous materials is of the same order on magnitude as the copper conductors used in the supply circuit, this limits direct heating to relatively long workpieces, leading to a practical limit of 1:6 width: length ratio. A relatively uniform cross-sectional area is also desirable.

Indirect Resistance Heating

Heating elements are constructed from high resistivity materials to give a high thermal release from the surface, at least equivalent to a flame, and hence permitting compact furnace designs. Some typical materials used, and their heating properties, are given in Table 4.3. The selection of the most suitable material is based on suitability for the furnace atmosphere i.e. oxidizing, carburizing or reducing, and on the degree of cyclic operation. This is discussed further in Chapter 12. Depending on the material used, the elements may be flat panels, or rods.

4.4.2 Arc Heating

Electric arcs are commonly known in engineering from their widespread use in welding. The underlying principle of an arc is that it is composed of gases of elevated to a temperature (typically >6000°C) that makes them highly ionized, The extremely high temperatures attained in an arc permit very high heat transfer rates. A typical fossil fuel flame will have maximum heat transfer rates in the order of 5×10^2 kW/m^2, whilst an oxy-acetylene jet transfers heat at $\sim 5\times10^5$ kW/m^2 and a plasma jet at $<2.5\times10^6$ kw/m^2. There are two basic types of arc heating systems, those with electrodes, and those without, the latter relying on energy transfer to the plasma by induction. Plasma heating efficiencies of between 50% and 80% are typical.

Electrode Devices

Figure 4.21 shows the regions of a typical arc. The arc is struck between the two electrodes and is sustained by either a DC or an AC current. If an AC supply is used the anode and cathode interchange position each half cycle. There are three distinct regions of the arc, the cathode region, the long column and the anode region. There is a potential drop over each of these regions. The power associated with the drops in the anode and cathode regions is generally dissipated as heat to the anode and cathode respectively, whilst the power in the long column region is manifest as an increase in the gas plasma temperature. Thus, if the arc is used to heat an electrically conducting

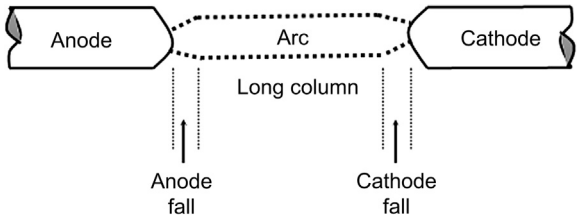


Figure 4.21 Regions of an arc

solid, the workpiece is arranged to be one of the electrodes and the arc is of a short length. Heat transfer from the gas plasma to the workpiece is often achieved by forced convection through an externally generated gas blast flow, or by electromagnetic pumping. Conversely, if the intention is to heat a gas plasma then the arc should be long, to reduce the relative energy losses at the electrodes.

Electrodeless Devices

These devices generate and contain the plasma within a duct constructed from a ceramic insulator. The gas is fed into the bottom of the duct, and heated by a high frequency coil wrapped around the duct. Figure 4.22 shows a typical arrangement. When the oscillator energises the high frequency coil, inserting a conducting rod into the duct ignites the plasma. The plasma discharge then draws power from the circuit by inductive coupling, the plasma acting as the secondary winding of the transformer.

4.4.3 Induction Heating

Induction heating occurs in any transformer system i.e., where a primary winding induces a current in a secondary winding. For conventional transformer design, this heating is both a source of energy loss

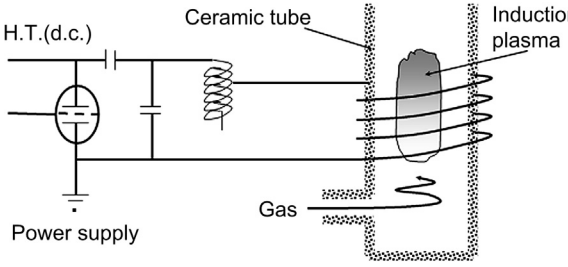


Figure 4.22 Induction heating of plasma

and added design complication in the provision of cooling systems. However, if a conducting workpiece replaces the secondary winding, rapid and controlled heating can be achieved. The electrodeless arc device shown in Figure 4.22 is one application of an induction heating. Lenz's law states that current is induced in the workpiece in such a direction that it attenuates the field of the primary coil. It is this current, flowing through the resistance of the workpiece that generates heat. The induced current in the workpiece decays from the surface inwards according to the equation

$$I_z = I_0 e^{-z/p} \tag{4.83}$$

where I_z is the current at distance z below the surface, I_0 is the surface current density, and p is the penetration depth. The penetration depth (mm) is given by:

$$p = \frac{5}{\pi}\left(10^5 \frac{\Omega}{f\eta}\right)^{0.5} \tag{4.84}$$

where Ω is the resistivity ($\mu\Omega$m), f is the frequency (Hz), and η is the magnetic permeability (H/m). The current falls to 38.6% of its surface value at the penetration depth, and approximately 90% of the induced heat is released within this section. For good electrical efficiency, the penetration depth should not exceed half of the workpiece thickness or equivalent radius, r, and thus for a given workpiece we can determine the minimum frequency required for efficient heating

$$f \leq \left(2\frac{5}{\pi}\right)^2 10^5 \frac{\Omega}{\eta r^2} \leq 1.013 \times 10^6 \frac{\Omega}{\eta r^2} \tag{4.85}$$

Most metals, with the exception of iron and some steels, are non-magnetic, so that η=1. The current in the workpiece lags 45° in phase behind the induced voltage so that for a solid workpiece the power factor (power/{current x voltage}) cannot be better than cos 45° i.e. 0.707. In practice, owing to flux leakage, the power factor usually lies in the range 0.1 to 0.5.

4.4.4 Dielectric Heating

When an electrical field is applied to a dielectric the material becomes polarized. If the field is reversed, the polarization charges reverse their positions. Thus if the field oscillates, the polarization charges oscillate and an alternating current results. Depending on the material, the motion of the charges is resisted, leading to local heating. This effect is particularly strong in materials with a dipole structure e.g. water. The rate of heating per unit volume Q_v, is given by:

$$Q_v = 2\pi f\ \omega_0 \omega_r'' E^2 \tag{4.86}$$

where

E = local peak field strength V/m
ω_0 = permittivity of free space (8.85 x 10^{-12} F/m)
ω''_r = dielectric loss factor

The loss factor is a function of the material being heated, and varies widely with different materials. It is also a function of field direction, moisture and compaction. A major advantage of this form of heating is the ability to rapidly heat throughout the volume of the material without the constraints of the temperature driving force, Δt, required for conventional conductive, convective or radiative heating. The practical limitation to the thickness of material that can be heated uniformly is set by the penetration depth, p, where

$$p = \frac{\frac{(2)^{0.5}\, c}{4\pi}}{f\left\{\omega'_r\left[\left(1+\left(\frac{\omega''_r}{\omega'_r}\right)^2\right)^{0.5} - 1\right]\right\}^{0.5}} \tag{4.87}$$

where

ω'_r = dielectric constant of the material relative to free space
c = velocity of light in free space

4.4.5 Infra-red Heating

The theoretical basis of infrared heating is the same as that already discussed in the previous section 4.3, although the wavelength of the infrared spectrum used lies beyond the shorter wavelength visible light region. The practical construction of infrared heating elements is discussed in chapter 12.

Nomenclature

a = constant
A = surface area, physical quantity, ratio of partial pressures of H_2O and CO_2.
b = constant
B = sum of partial pressures of H_2O and CO_2
c = concentration, velocity of light
C = constant, distance between tubes
C_p = specific heat at constant pressure

d = diameter
D = tube diameter
D = diffusion coefficient
E = energy flux = σT^4
E = local peak field strength
F = force, view factor
f = electrical frequency
g = acceleration due to gravity
G = mass flow/unit cross sectional area = $u\rho$
Gr = Grashof Number = $\beta g \Delta t L^3 \rho^2/\mu^2$
h = convective heat transfer coefficient
H = enthalpy
i = radiant intensity
I = electrical current
k = thermal conductivity
K = constant, absorption coeffcient
L = charateristic dimension, mean beam length
Le = Lewis Number = $DC_p\rho/k$
m = resistance ratio = $R/r_m h$, mole fraction
M = dimensionless group =$(\Delta x)^2/(\alpha \Delta\theta)$, mass
n = radius ratio = r/r_m
N = Biot modulus = $(h\Delta x)/k$
Nu = Nusselt Number = hL/k
p = penetration depth
P = distance between tubes
Pr = Prandtl Number = $C_p\mu/k$
q = heat transfer/unit area. unit time (heat flux)
Q = heat transfer rate
r = distance from midplane to a point in the body, radius
R = electrical resistance
r_m = distance from midplane to surface of body.
Re = Reynolds Number = $Lu\rho/\mu$
S = separation distance
St = Stanton Number = $h/C_p\rho u$
t,T = temperature
u = velocity
V = volume
x = length, width or separation distance of Δt
X = relative time = $\alpha\theta/r_m^2$, separation distance in x plane
Y = an unaccomplished temperature change = $(t_a - t)/(t_a - t_b)$, separation distance in y plane
Z = separation distance in z plane

subscripts

a = ambient
b = black body
$chem$ = chemical reaction
$conv$ = convection
d = dust
$disc$ = chemical dissociation
E = equivalent
g = gas
i = indentifier
k = identifier
n = numerical identifier or value
o = origin or start
p = particle
P = plane
R = refractory
s = soot
T = tube, temperature
v = unit volume
w = wall
z = distance below surface
1.2.etc. = identifiers

Greek letters

α = thermal diffusivity = $k/\rho C_p$, radiant absorptivity
β = linear coefficient of thermal expansion
γ = reflectivity
Δ = difference between two points or values
ε = emissivity
η = magnetic permeability
θ = time.
λ = wavelength
μ = viscosity
π = dimensionless group, geometric constant
ρ = density
σ = Stefan-Boltzmann constant
τ = transmissivity
φ = geometric angle
Ω = resistivity
Φ = heat transfer parameter
ω_0 = permittivity of free space
ω_r' = relative dielectric constant
ω_r'' = dielectric loss factor

Appendix 4 A Tables of Emissivity Data

		$\varepsilon = a + b.10^{-5}.T + c.10^{-8}T^2 + c.10^{-10}T^3$				
Material	*Condition*	a	b	c	d	*Temperature range K*
Alumina	polished @ 3 microns	0.9	0	0	0	298 – 373
Alumina	pure	0.98	−53	10.2	0	300 – 1800
Aluminium	oxidised	0.0463	5.01	0	0	450 – 900
Aluminium	polished	0.0263	5.01	0	0	300 – 900
Aluminium	lightly oxidised	0.11	21	0	0	473 – 873
Ash	coal sintered	0.9	−30	0	0	500 – 1500
Ash	coal powdered 120 microns	0.85	−30	0	0	500 – 1500
Ash	coal powdered 33 microns	0.75	−30	0	0	500 – 1500
Ash	coal powdered 6.5 microns	0.65	−30	0	0	500 – 1500
Ash	coal glassy	1	−40	0	0	500 – 1500
Brass	polished	0.03	0	0	0	473
Brass	natural, unoxidised	0.053	0	0	0	298
Brass	oxidised @600C	0.6	0	0	0	573 – 873
Carbide coating	bonded to refractory bricks	0.99	0	0	0	273 – 1273
Carbon	rough	0.81	0	0	0	300 – 2100
Carborundum	Zirconia based	0.198	32.8	0	0	1073 – 1350
Carborundum	powder based	1.565	−60	0	0	1023 – 1273
Carborundum	silica based	0.906	−7	0	0	950 – 1373
Cement	clinker	0.88	0	0	0	300 – 1750
Cement	concrete	0.63	0	0	0	1273
Ceramic fibre	Saffil (95% alumina, 5% silica)	0.49	0	0	0	1010
Ceramic fibre	Zircar (99% zirconia)	0.51	0	0	0	1080
Ceramic fibre	Kaowool (45% alumina, 55% silica)	0.292	62.5	0	0	173 – 923
Ceramic fibre	Microtherm (65% silica, 3.2% titanium oxide)	0.48	0	0	0	950
Ceramic fibre insulation		0.93	−48.8	0	0	673 – 1023

Ceramic insulation board	(45%alumina,55%silica) fibres normal to surface	1.27	−48.5	2.84	0	600 – 1400
Ceramic insulation board	(45%alumina,55%silica) parallel bonded fibres	1.47	−91.1	14.4	0	600 – 1400
Char	coal	0.9	0	0	0	1000 – 1400
Copper	thick oxide	0.72	20	0	0	400 – 1000
Copper	oxidised @1000K	0	80	0	0	600 – 1000
Copper	polished	0.021	1.98	0	0	300 – 1200
Copper	oxide, red heat form 30 min.	0.06	15.4	0	0	400 – 1050
Dolomite	stabilised with Zr/Fe/Cr oxides	0.98	−4.1	0	0	1273
Firebrick (Al/Si/Fe oxides)	low Al_2O_3 (~25%)	0.9	−10	0	0	673 – 1673
Firebrick (Al/Si/Fe oxides)	high Al_2O_3 (>40%)	0.8	−20	0	0	673 – 1673
Firebrick (Al/Si/Fe oxides)	medium Al_2O_3 (~35%)	0.84	−20	0	0	673 – 1673
Glass	fused silica	0.77	24.8	−31.3	0	70 – 1050
Glass	borosilicate	0.82	28.7	−24.6	0	70 – 750
Glass	Vycor (Corning 7900)	0.85	9.5	−10.8	0	70 – 1050
Glass	Pyrex (Corning 7740)	0.83	14.4	−17.3	0	70 – 1150
Glass	soda	0.8	36.6	−46.8	0	70 – 800
Glass	aluminium silicate	0.84	24.6	−25.7	0	70 – 950
Gold		0.0432	−8.88	7.15	0	600 – 1000
Graphite	polished	0.81	2.2	0	0	0 – 3000
Iron oxide	Fe_2O_3	−0.01	161	−75	0	850 – 1300
Iron/steel	heavily oxidised	0.72	20	0	0	400 – 1000
Iron/steel	molten	0.35	0	0	0	1810 – 1860
Iron/steel	iron oxide, red heat 30 min.	0.173	68.6	−25.6	0	100 – 1050
Iron/steel	polished	0	18.2	0	0	100 – 1050
Magnesium oxide	MgO	0.73	11.8	−65	2.48	50 – 2350
Molybdenum	polished	0.0288	12.7	0	0	100 – 1800
Molybdenum	oxidised	0.82	0	0	0	600 – 800
Nichrome	oxidised	0.71	16	0	0	773 – 1273

(*Continued*)

Appendix 4 A Tables of Emissivity Data—cont'd

		$\varepsilon = a + b.10^{-5}.T + c.10^{-8}T^2 + c.10^{-10}T^3$				
Material	*Condition*	a	b	c	d	*Temperature range K*
Nichrome	clean	0.65	0	0	0	323
Nickel	polished	0.014	12.9	0	0	100 – 1500
Nickel	oxidised	0	60	0	0	400 – 1000
Paint	Aluminium paint (substrate)	0.55	0	0	0	298
Paint	white enamel	0.95	0	0	0	298
Paint	black varnish – matt	0.98	0	0	0	312
Paint	Aluminium coating (in silicone binder)	0.2	0	0	0	298
Paint	black varnish – gloss	0.87	0	0	0	298
Palladium	polished	0.008	10.8	0	0	400 – 1550
Paper		0.94	0	0	0	298
Porcelain	glazed	0.92	0	0	0	298
Refractory coating	Novit (62%zirconia,32%silica)	0.99	−40	0	0	1073 – 1373
Silicon carbide	SiC polished	0.99	0	0	0	298 – 373
Silicon carbide	SiC	0.8	15.4	−9.01	0	400 – 850
Silicon carbide	SiC oxidised @1367K for 1 hour	0.7	−25	0	0	600 – 800
Silicon nitride	Si_3N_4 polished	0.98	0	0	0	73 – 298
Silicon nitride	Si_3N_4	0.86	13.9	−16.3	0	250 – 600
Silver	electrolytic	0.0119	1.9	0	0	400 – 1200
Soot	on a solid surface	0.95	−3	0	0	373 – 1273
Soot	lamp black	0.95	0	0	0	298
Stainless steel	N-155, lightly oxidised	−0.0372	27.8	0	0	450 – 1300
Stainless steel	310, heated in service	0.802	20.1	0	0	490 – 835
Stainless steel	304, heated in service	0.46	32.5	0	0	490 – 835
Stainless steel	oxidised at high temperature	0.42	30	0	0	600 – 1400
Stainless steel	347, heated in service	0.423	19.55	0	0	500 – 1170

Stainless steel	316, heated in service	0.498	14.3	0	0	500 – 1140
Stainless steel	heavily oxidised	0.72	20	0	0	400 – 1000
Stainless steel	301, heated in service	0.584	−2.8	0	0	500 – 1220
Stainless steel	N-155, oxidation retarded	0.0144	17	0	0	100 – 1500
Tantalum	filament	0.11	6.1	0	0	1327 – 3273
Thorium dioxide	ThO_2	1.93	−224.1	74.7	0	1200 – 2250
Tin	polished	0.00846	10.8	0	0	300 – 500
Titanium	lightly oxidised	0.2	61	0	0	673 – 1023
Titanium dioxide	polished	0.955	0	0	0	298 – 373
Titanium dioxide	TiO_2	0.68	−21.2	0	0	850 – 1300
Tungsten	filament	0.003	9.7	0	0	300 – 3590
Tungsten	polished	−0.003	10.5	0	0	550 – 2800
Water		0.95	0	0	0	273 – 373
Zinc	polished	0.04	50	0	0	473 – 573
Zinc	unoxidised	0.05	0	0	0	573
Zirconia	ZrO_2	0.82	6.67	−86.8	4.18	50 – 1600
Zirconia	unstabilised	0.98	0	0	0	813 – 1373
Zirconia coated fibre		1.26	−26.7	0	0	1000 – 1300
Zirconia/Magnesia	50 wt% ZiO_2/50 wt% MgO	0.9	−37	0	0	700 – 1700
Zirconia/Magnesia	polished	0.93	0	0	0	293 – 373
Zirconium carbide	ZrC	0.98	−13.9	0	0	1200 – 2400

References

Dusinberre, G. M. (1949). *Numerical Analysis of Heat Flow*. McGraw Hill, 44–47.

Foster, P. J. (1965). Carbon in Flames. *Jnl.Inst. Fuel, 38*, 297–302.

Hirschfelder, J. O., Curtiss, C. Y., & Bird, R. B. (1954). *Molecular Theory of Gases and Liquids*. Wiley.

Hottel, H. C., & Egbert, R. B. (1942). *Trans. Am. Inst. Chem. Engrs, 38*, 531–565.

Hottel, H. C., & Sarofim, A. F. (1967). *Radiative Transfer*. McGraw Hill.

McAdams, W. H. (1954). *Heat Transmission* (3rd ed.). McGraw Hill. 33–35.

Pope, S. B. (1990). Computations of Turbulent Combustion: Progress and Challenges, 23rd Symposium (International) on Combustion. *The Combustion Institute*.

Schmidt, E. (1924). *Foppls Festschrift*. Springer, 179–198.

Thring, M. W. (1952). *Science of Flames and Furnaces* (1st ed.). Chapman & Hall, (pp. 200).

Weast, R. C. (1988). *CRC Handbook of Chemistry and Physics* (69th ed.). section E.

Chapter 5

Flames and Burners for Furnaces

Chapter contents

5.1	Types of Flame	140
5.2	Function of a Burner and Basics of Burner Design	149
5.3	Gas Burners	155
5.4	Oil Burners	170
5.5	Pulverised Coal Burners	180
5.6	Furnace Aerodynamics	182
5.7	Combustion System Scaling	193
5.8	Furnace Noise	196
Nomenclature for Chapter 5		204
References for Chapter 5		206

The performance of the burners has a huge effect on furnace operation and efficiency, yet it is relatively rarely that burner design is fully integrated with the furnace heat transfer requirements, little wonder then that poor performance is often the result. Burners are often specified and selected from a catalogue based on little more than the estimated heat liberation required for the furnace, the number of burners needed and the price of the burner. Needless to say this is not a reliable method and the purpose of this chapter is to provide the reader with sufficient knowledge to specify burners, critically assess a burner design and to optimise furnace performance and heat transfer.

5.1 Types of Flame

The combustion process was discussed at length in chapter 2 and will not be re-examined here except to remind the reader of the four stages of the combustion process:

$$\textit{Mixing} > \textit{Ignition} > \textit{Chemical Reaction} > \textit{Dispersal of Products}$$

Any one of these processes can determine the rate of combustion. In normal circumstances the fuel/air mixing is the slowest and is the rate controlling step in the process and largely determines the type of flame produced because the chemical reaction is very fast for most fuels. Finally, dispersion of the products is dependent on an effective flue gas handling system. Unless the combustion products are removed from the furnace, the incoming air cannot enter and the reaction is starved of oxygen and the flame extinguished.

Two types of flame are common as illustrated by the laboratory Bunsen burner. Operated normally, with the air holes open, Figure 5.1, the flame is nearly premixed, that is, most or all of the air necessary for combustion is mixed with the fuel prior to the burner port. When the air inlet hole at the base of the burner is shut, all the air for combustion must, of necessity, diffuse gradually into the flame after the burner port and a diffusion flame results. Thus:-

- Premixed flames are short, blue, noisy and the reactions are virtually complete
- Diffusion flames are long, yellow, quieter and the reactions are incomplete

In practice, most flames fall somewhere between these two extreme conditions. If the reactions in diffusion flames are incomplete, then why use them at all? The answer is that, in many practical situations, it is just too hazardous to premix the fuel with air prior to the

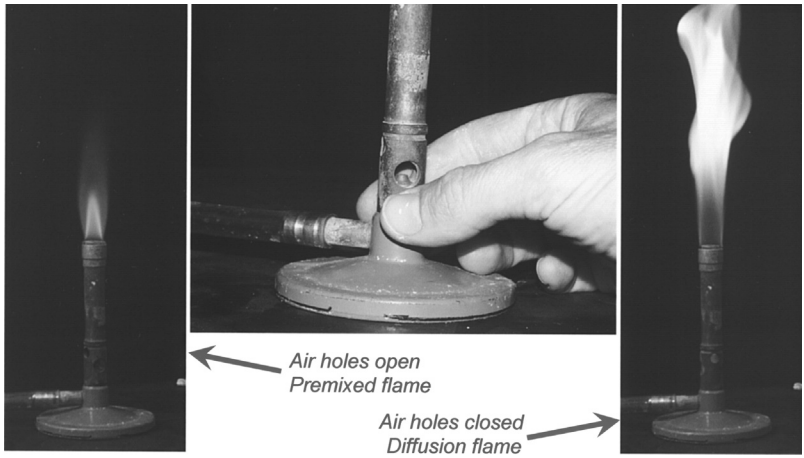


Figure 5.1 Premixed and diffusion flames produced by a Bunsen burner (Photo courtesy of Prof. G.J. Nathan)

combustion chamber. This distinction between flames of premixed gases and flames utilising diffusion at an interface between different gases is both convenient and basic. In the first case, we have essentially an explosion wave travelling through a mixture where fuel and oxygen are in intimate contact. In a diffusion flame, there is no true flame propagation or burning velocity and, in many cases, the fuel has even decomposed thermally before it reaches oxygen, because the fuel and oxygen are separated by a wedge of intermediate combustion products.

When a flame is pale blue and emits only a small quantity of light, it is known as a non-luminous flame. In many flames, however, solid particles of microscopic sized carbon are formed, by the decomposition and cracking of complex hydrocarbons. At flame temperatures these carbon particles become incandescent and radiate. The resulting yellow or white flame is known as a luminous flame.

5.1.1 Premixed Flames

Combustible gases or vapours are capable of burning in air or oxygen, only within closely defined limits of concentration as explained in chapter 3. These flammable limits extend on either side of the stoichiometric mixture to the points where it becomes either too rich or too weak to ignite. The process of ignition proceeds as an accumulation of thermal energy, the precise value of any particular limit will be determined by the physics of the heat loss or gain from that system; outside of these limits the heat loss exceeds the potential thermal

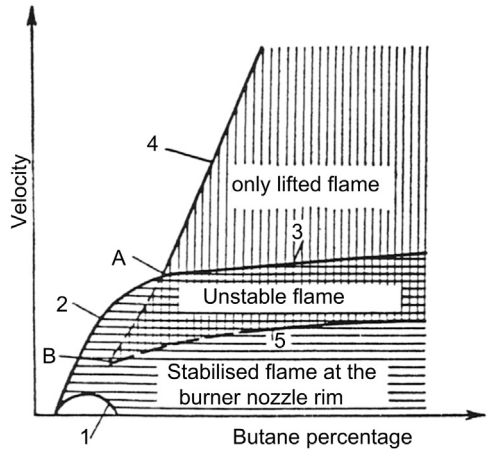


Figure 5.2 Schematic diagram of the stability limits of a premixed flame (Whol, Knapp & Gazley (1949)). Reproduced with kind permission of the Combustion Institute

gain from the reaction. If the limits are wide, the particular mixture is dangerous to handle in a premixed burner. If the limits are narrow, then it is a safer proposition but care still needs to be taken. A premix burner will only operate within these clearly defined limits, Figure 5.2.

The velocity at which a flame will travel through a flammable mixture has an important influence on the design of both burner devices and combustion chambers. Too high a flame speed may lead to flame extinction or light back through the nozzle into the mixing system, causing an explosion. Too low a speed may overheat the burner or cause flame lift off. Measurements carried out in large volumes i.e., rooms rather than pipes, show that the rates at which flames spread in flammable mixtures is roughly comparable with the speed of traffic:-

Propane/air	slow walk at 3 km/h (0.85 m/s)
Hydrogen/air	cycling at 16 km/h (4.4 m/s)
Hydrogen/oxygen	fast car at 130 km/h (36 m/s)

The air/fuel mixture limits within which a gaseous fuel will burn and the velocity with which the flame will propagate are the fundamental design parameters of premixed combustion systems. They determine the degree of safety of the system and the stability of the flame on the burner, respectively. The other critical parameters are the calorific value and specific gravity because these determine the heat release rate. In practice, the calorific value and the specific gravity are linked by the Wobbe Index ($W_I = CV/SG^{0.5}$) and gases of similar

Wobbe Index will provide similar heat release in a burner when supplied at the same pressure. For a full explanation of the Wobbe Index see chapter 3.

5.1.2 Turbulent Jet Diffusion Flames

During the past century, scientists have paid far less attention to diffusion flames than they did to premixed flames, despite the fact that the majority of industrial flames involve the simultaneous mixing and combustion of separate streams of fuel and air. The problem with analysing diffusion flames is that there is no fundamental property, like flame speed, which can be measured and correlated, even the mixture strength has no clear meaning.

When any jet mixes into its surroundings, steep concentration gradients are set-up in the neighbourhood of the orifice as the surrounding atmosphere is entrained, as shown in chapter 2, Figures 2.8 – 2.11. Further downstream, turbulent mixing causes these gradients to become less severe but then rapid and random oscillations and pulsations occur. Only after the jet has largely decayed can any approximation to homogeneity be seen.

A typical example of this phenomenon is the turbulent jet diffusion flame in a rotary kiln. The particular mixing pattern is determined by the mechanical and diffusion flux. Jenkins and Moles (1976, 1981) measured the CO concentrations in a kiln flame, Figure 5.3. The

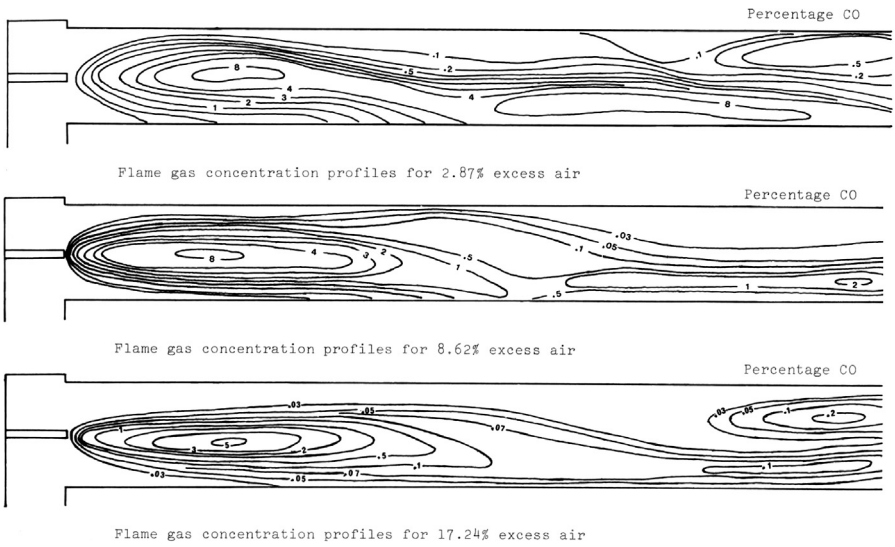


Figure 5.3 Carbon monoxide concentrations in an 8 MW rotary kiln flame (Jenkins 1976)

concentrations change significantly with excess air and the rates of chemical reaction are of little importance except in the tail of the flame.

5.1.3 Heterogenous Combustion

So far we have only considered gaseous mixtures. Where solids and liquids are used as fuels an added complication occurs because we have to achieve mixing between a solid or liquid and the gaseous combustion air. Historically this was achieved by burning these fuels in beds or pools, hence the fuel was in surplus and the reaction rate limited by the air supply. This fact limits the heat release rate that can be achieved and the completeness of combustion, these systems being very smoky. Smoke emissions became a major problem following the industrial revolution and engineers sought ways both to increase firing rates and to reduce emissions. Spakowski had succeeded in burning oil in the form of a spray during the 1860s and patented a commercial oil burner in 1866 (Kelly 2003) but the technique did not see widespread application until the early 20th Century because oil was not readily available, coal still being the predominant fuel.

Attempts to mimic Spakowski's success using powdered coal finally succeeded between 1895 and 1898 with the development of the first successful rotary cement kiln at the Atlas and Alpha cement works in Pennsylvania (Francis 1977). This was the first successful application of burning a solid material in suspension as an aerosol. The development of the rotary cement kiln, the internal combustion engine and the pulverised coal fired power boiler led to a rapid increase in the understanding of aerosol combustion. The invention of the jet engine in the 1940's gave an added stimulus to the development of combustion knowledge which has continued since.

Atomisation of Liquid Fuels and Pulverisation of Coal

Liquids and solid fuels are normally burnt in turbulent jet diffusion flames and need a spray of droplets or dispersion of powder to increase the surface area available for the oxygen and to mix the droplets or particles with the combustion air.

Atomisation and pulverisation are important because the initial particle size determines the surface area available for mixing and the size of the cenosphere or char particle which are formed and, hence the length of time taken for the particle to burn. The oxygen diffusion is dependent on the surface area, but the oxygen demand is dependent on the mass of the particle. Since the surface area is dependent on diameter^2 and the mass on diameter^3, it follows that the larger the drop the longer it takes to burn.

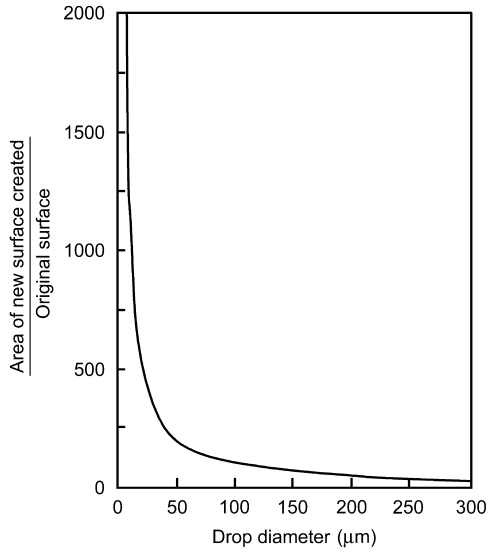


Figure 5.4 Effect of final droplet size on the additional surface area created by atomising a 10 mm sphere

The effect of particle size on surface area is shown in Figure 5.4. It can be seen that the smaller the drops, the greater the surface area that is available for the oxygen/fuel reaction. The effect of particle size and the manner in which this affects the burning time was discussed in chapter 2, where it was shown that for an evaporating drop the burning time is proportional to the square of the initial diameter, whereas for a residual oil drop, or pulverised coal particle, the burning time was proportional to the initial diameter. Hence the size of the droplets or particles and the way they are dispersed critically affects the performance of the burner, since the initial size largely determines the burning time. For liquids, this process is known as atomisation and is generally not well understood by either burner designers or users. By way of contrast, pulverisation of solids is relatively well understood, not least because it is easier to measure the particle size.

The basic mechanism of atomisation is shown in Figure 5.5. Although this particular example shows a twin fluid atomiser, the basic mechanism is similar for most atomisers. Firstly the oil is formed into a thin moving film either by accelerating it though a nozzle (pressure jet type) or by interaction with a high velocity gas jet, usually air or steam (twin fluid type). The oil film is then exposed to shearing forces as it interacts with the surrounding atmosphere and the film starts to form waves. Small drops are formed at the crests of these waves. The film then breaks up into ligaments, which in turn break up into larger drops. The size of these larger drops is determined by

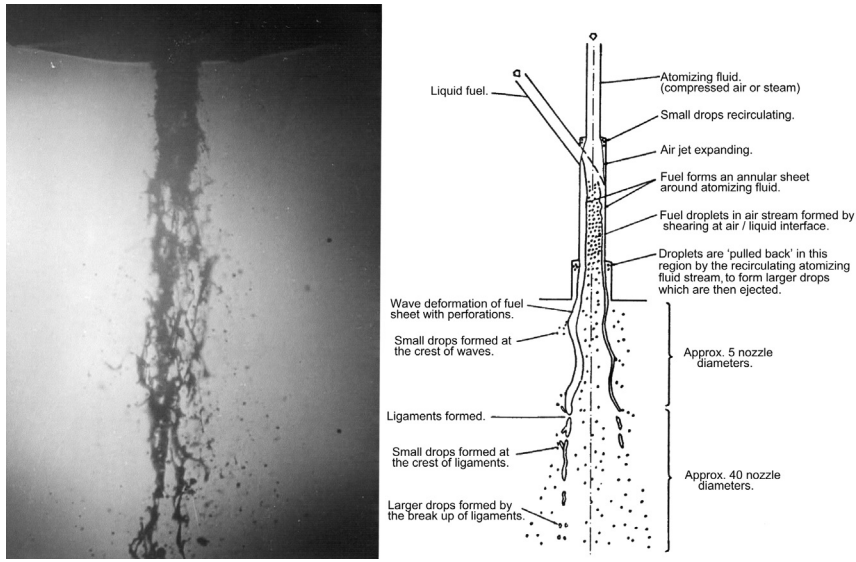


Figure 5.5 Mechanism of spray formation from a typical atomiser (Mullinger & Chigier 1974). Reproduced with kind permission of the Energy Institute

the initial film thickness, the thicker the initial film the larger the final droplets.

The Importance of Drop and Particle Size

Droplet and particle sizes are normally measured in microns, a micron being 10^{-6} of a metre. This means that a 100 micron drop is 0.1 mm and 1000 micron drop is 1 mm diameter. Most atomisers produce a range of drop sizes, with the smallest being in the order of a few microns in diameter and the largest anything from 100 micron to 1000 micron or even more. Significant difficulties occur in attempting to characterise sprays and particle size distributions. For convenience drop and particles are normally measured in size bands, typically of 5–10 micron and can be plotted on a histogram but this is not a particularly convenient way of comparing the performance of atomisers or coal milling systems, nor is the average or mean particle size. The latter is largely meaningless from a combustion perspective because the very large number of small particles bias the arithmetical average to a relatively low value, suggesting that the spray or coal grind is finer than it is in reality. For example, a spray with a substantial number of particles larger than 200 micron can have an arithmetic average as low as 60 micron. To overcome this difficulty, averages based on the mass of the particles, or their surface area,

are often used, for example the Sauter Mean Diameter (SMD), which is the diameter of a droplet that is equivalent to the total mass of spray/total surface area. The SMD is commonly used in empirical expressions for predicting atomiser performance and is equally suitable for particle size distributions, though rarely used for that purpose.

$$SMD = \frac{\sum(\Delta N_i)d_i^3}{\sum(\Delta N_i)d_i^2} \tag{5.1}$$

Where:

d_i = the average diameter of a sub-band of drops
ΔN_i = the fractional count of drops in sub-band d_i

Rosin and Rammler (1933) developed an improved way to describe powdered coal which is equally suitable for sprays. Using the laws of probability they developed an expression for the particle size distribution of ground coal:

$$R = 100 \exp\left[-(x/x_0)^n\right] \tag{5.2}$$

Where

R = mass residue on a sieve of aperture x (oversize)
n & x_0 are constants specific to the particular distribution.

By taking logs twice and turning the left hand side upside down we get:

$$\log\left(\log \frac{100}{R}\right) = n \log x + \text{constant} \tag{5.3}$$

Since equation 5.3 represents a straight line, by sieving the sample of coal with a range of sieves of varying aperture, we can obtain a series of values of R for different sizes (x) which can be plotted on special Rosin-Rammler graph paper (reciprocal log log versus log). An example is shown in Figure 5.6, which shows the drop size distribution of 4 different oil sprays. Note that, while the theoretical expression is a straight line, the line curves upwards at the upper limit of the size distribution and downwards at the lower limit (where applicable) for real sprays and coal samples.

The major advantage of using the Rosin-Rammler distribution is that the spray or particle size distribution can be characterised simply by two measurements. For example, if the mass of particles greater than 50 microns and those greater than 90 microns are determined, then the complete distribution can be characterised and expressed mathematically because the slope of the graph is n, while the diameter that corresponds with 36.8% residue is x_0. It follows that the larger x_0, the coarser the spray and the greater the slope (n), the narrower the size range. Furthermore, all size distributions can be described

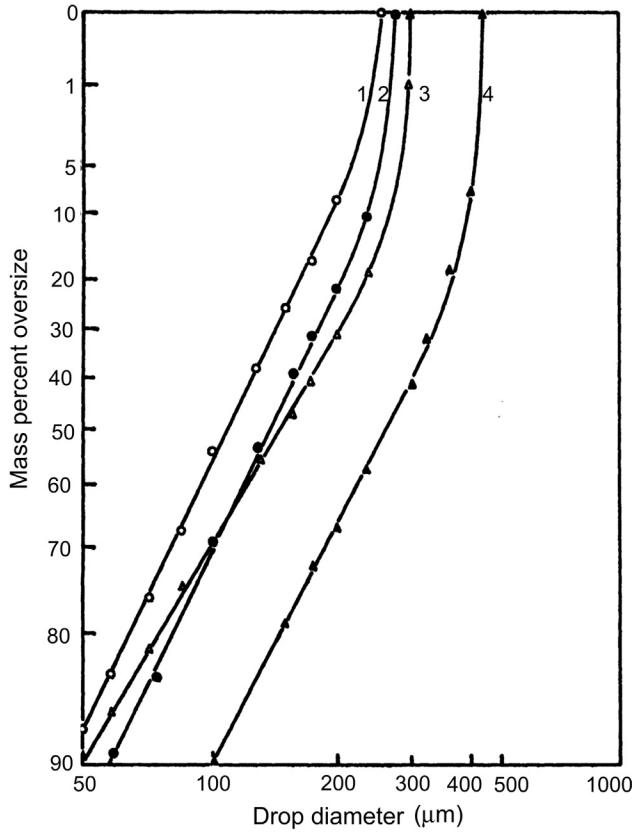


Figure 5.6 Rosin Rammler distribution for four different oil atomisers (Mullinger 1973)

by these two values, x_0 and n. Similarly, if the values of x_0 and n are known, the complete size distribution can be replotted, making characterisation easy. In the case illustrated in Figure 5.6 a number of different atomiser geometries were examined. Since the slopes are all similar the size range of each spray is similar but the spray produced by the geometry represented by line 1 (lowest x_0) is clearly the finest.

Another important parameter that can be determined from the Rosin-Rammler plot but cannot be estimated from any average diameter data is the size of the coarsest drops and particles. This is critically important because, as discussed in chapter 2, the larger particles take longer to burn and are the source of most of the unburnt particulate matter. An indicative "rule of thumb" is that a 100 micron particle of residual fuel oil or coal, takes approximately half a second to burn in a typical industrial flame and a 500 micron particle takes about five times as long and a 1000 micron particle 10 times as long. Since the residence time of a droplet in a flame is typically

1 second or less, it follows that drops larger than about 200 micron will not be fully burnt out at the end of the flame and will either drop into the product as unburnt carbon or end up in the dust collector. Anyone who makes a light coloured product but sees discoloured dust - dark grey or black - is suffering from this problem. Depending on the particular application, the upper limit of drop or particle size should be in the order of 200–250 micron to minimise the risk of unburnt fuel at the tail of the flame.

For optimum combustion performance, an oil sprayer with a range of drop sizes is ideal; fine drops to facilitate ignition and flame establishment with coarser drops needed to maintain a controlled burning rate but, as indicated above, the largest drops in the spray should be no greater than approximately 200–250 micron.

Like oil firing, the particle size of pulverised coal is critical to the process. Fortunately, it is much easier to measure than for oil. It is simply necessary to collect a sample and sieve it. Techniques for pulverising coal are discussed in chapter 7.

5.2 Function of a Burner and Basics of Burner Design

In principle, a burner is a transducer since it transforms one form of energy into another form of energy. In the case of the burner, it transforms the chemical energy in the fuel into heat energy within the furnace using the chemical reactions in a flame. The effectiveness with which this is achieved is a measure of its performance. Despite the apparent simplicity of this statement, burner design is a most complex subject and even today is less than completely understood.

The key objective of a furnace burner is to burn the fuel as efficiently as possible and to produce the optimum heat flux to the product. It should be noted that different processes require different heat fluxes, so a burner that is optimum for one process is not necessarily suitable for a similar process. For example, the authors have found that for a number of rotary kiln processes the optimum combustion intensity was different for each process and varied with the production rate for that process, Figure 5.7.

Although combustion intensity in Figure 5.7 is in similar units to heat flux, i.e. kW/m^2, it should not be confused with heat flux even though the latter is also in kW/m^2. The heat flux is the heat transferred to the product, whereas the combustion intensity is the total heat release in the flame divided by the flame's external surface area and includes all the heat lost to the atmosphere in the flue gases, etc. Combustion intensity can also be quoted as a function of flame volume but is less useful as a comparison for furnace design. Another difference is that the combustion intensity is inevitably an overall average value, whereas the heat flux may either be an average value or a local value.

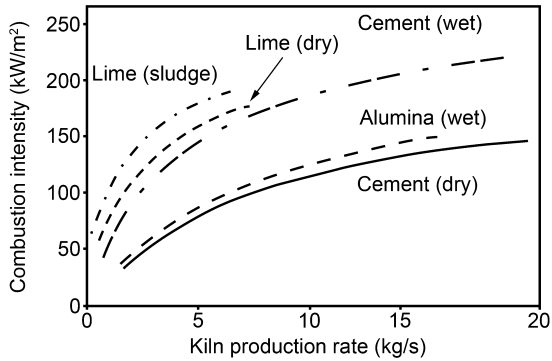


Figure 5.7 Optimum combustion intensities for selected rotary kiln processes

Figure 5.8 shows the flame temperature and heat flux profiles in a petrochemical cabin heater and it can be clearly seen that the peak heat flux can exceed twice the average value. This figure illustrates a number of features relevant to furnace burner performance which are considered in further detail below.

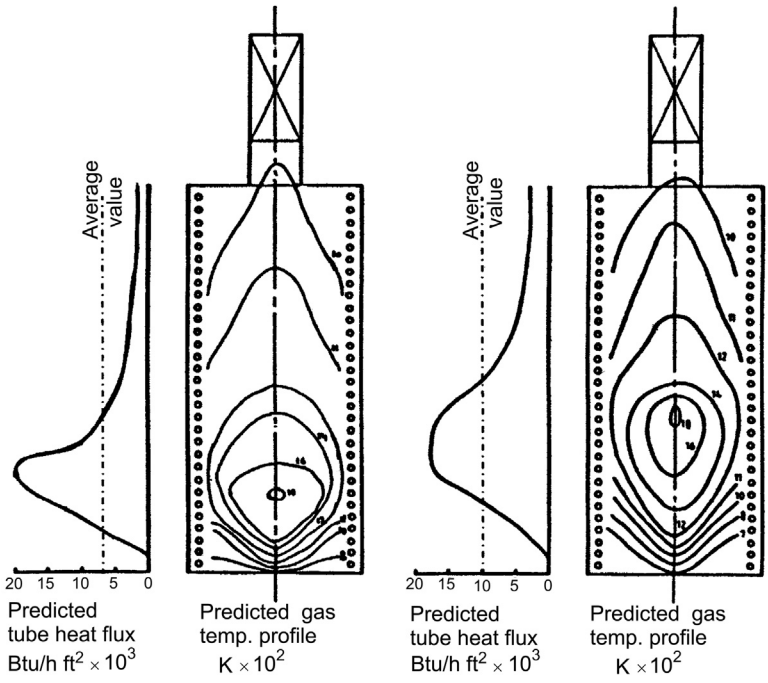


Figure 5.8 Predicted temperatures and heat flux profiles in a cabin heater

The heater in Figure 5.8 was heating heavy residual oil from a refining process prior to further treatment and was fired using refinery gas via eighteen burners in a single row along the bottom. It can be seen that the flame does not have a uniform temperature but exhibits a temperature profile. Furthermore, although flame temperature is related to heat transfer, it is not possible to deduce the heat flux profile simply from knowledge of the flame temperatures. The figure also illustrates the danger of using an average heat flux for design purposes. In the case on the left, the average flux is only 7,000 Btu/h·ft^2 (22.1 kW/m^2), yet the peak is over 20,000 Btu/h·ft^2 (63 kW/m^2) nearly three times the average. In practice the peak heat flux exceeded the safe limit for the process and the heavy residual oil in the tubes cracked and deposited coke on the inner surface. This coke served as an insulating layer and reduced the heat transfer to the fluid and caused the tube wall to overheat. This is a dangerous phenomenon in a fired heater because, in the medium to long term, tube failure will result and oil will spill into the combustion chamber, causing a dangerous fire. As a consequence of these problems, the firing rate had to be reduced to keep the peak heat flux below a safe level and the output of the heater was restricted. Additionally, the availability was poor since the heater had to be shut down and the tubes cleaned to remove carbon deposits at regular intervals.

The problem was resolved by improving the air distribution between the burners and small, but significant, changes to the burner gas nozzle and flame stabiliser. These changes provided a lower air pressure loss and controlled fuel/air mixing. The modifications made to the air duct to improve the air distribution are discussed in section 5.6.3 'Combustion air duct design'. Following these changes the burners produced the heat flux profiles shown on the right. It can be seen that although the peak heat flux is reduced to 18,000 Btu/h·ft^2 (56.8 kW/m^2) the average is actually increased to 10,000 Btu/h·ft^2 (31.6 kW/m^2). The result was that the unacceptable coking was eliminated, the heater output was increased by 4% and it ran continuously between its twenty-four month scheduled outages (Jenkins & Boothman 1996).

5.2.1 The Essential Importance of Heat Flux Profiles

From the foregoing it can be deduced that determining the ideal heat flux profile for the process, then designing a furnace/burner system to produce that profile, is the ideal approach to furnace design. Unfortunately this approach is rarely used, most furnaces are still designed using the time honoured, but in our opinion largely discredited method, of extrapolating from the previous design. The problem with this approach is that not all features scale similarly and unless their relative

contributions are well understood, poor performance is the likely result. There are many examples of the failure of this methodology and probably most readers have personal experience of such a failure. For those who have not, an example of unsuccessful extrapolation used in the cement industry is described later in this chapter.

Average heat fluxes can be calculated using the Hottel well-stirred furnace model as described in the following chapter, while heat flux profiles can be calculated using the long furnace models and/or the two and three dimensional zone models, as appropriate. Note that it is not currently possible to obtain reliable heat flux profiles using computational fluid dynamic modelling because these programs do not close the energy balance and hence do not provide a check on the overall energy balance.

5.2.2 Flame Stabilisation

Once a flame has been ignited on a burner, it will only continue to burn if it receives feedback of heat from the reaction to maintain ignition on, or close to, the nozzle, i.e. the flame is stable, Figure 5.9. Although there are a number of methods for achieving this, only two are of practical significance, re-radiation and recirculation. Since both mechanisms can be present entirely accidentally in any combustion system, it was some time before their real significance was properly appreciated by combustion engineers.

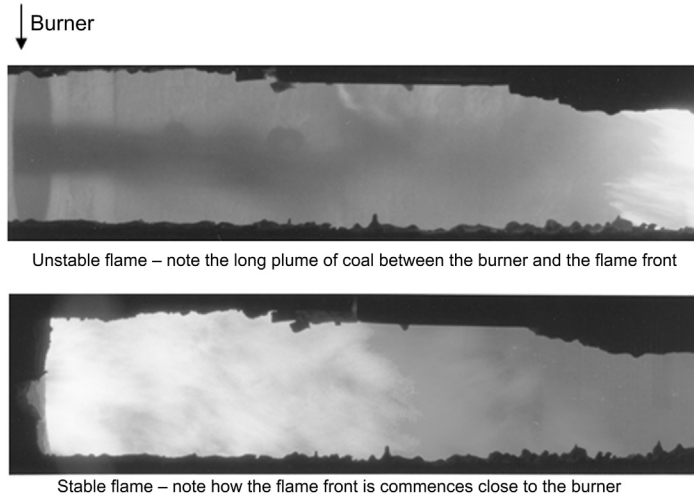


Figure 5.9 Examples of stable and unstable flames on the same burner which is to the extreme left in each photograph (Photos courtesy of Dr Neil Smith)

Re-radiation was the main mechanism of flame stability in steam locomotive fireboxes and open hearth melting furnaces, both playing a major role in consolidating the Industrial Revolution. The vital re-radiation comes back from the high temperature burning zone, either direct from the flame, or reflected from the combustion chamber walls. Except for some relatively primitive burners, such as premix tunnel burners and some rotary kiln burners, re-radiation is rarely used as the primary means of flame stabilisation today; more positive methods using recirculation are preferred.

Flow recirculation occurs when some of the flow in or around the flame is caused to move in the "reverse" direction, i.e. opposite to that of the dominant motion of the jet. In a flame, recirculation transports hot combustion products back to the nozzle or close to it. These hot products raise the temperature of the fuel which ignites and hence "anchors" a flame on, or close to, the burner. It exists, to a greater or lesser extent, in all conventional combustion systems because of the natural phenomenon of entrainment by a turbulent jet.

The dominant flow recirculation can usually be categorised as either "internal", typically along the axis of the burner nozzle, or "external", around the outside of the flame. These two types of recirculation are illustrated in Figure 5.10. Furnaces with a relatively low degree of confinement (i.e. the side-walls are a long way from the flame) tend to exhibit relatively weak external flow recirculation. For these applications burners are therefore usually designed to provide a dominant internal flow recirculation, usually by means of a bluff body or air swirl, see below. In contrast, rotary kiln burners have a much higher degree of confinement and are therefore commonly designed to have external flow recirculation to confine the flame and protect the walls.

The simplest way of achieving recirculation is either by jet entrainment described above or by some form of flow deviation, typically

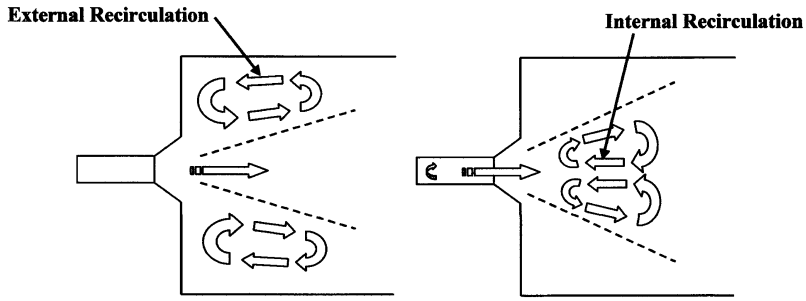


Figure 5.10 Schematic diagrams illustrating the presence of "external" and "internal" flow recirculation

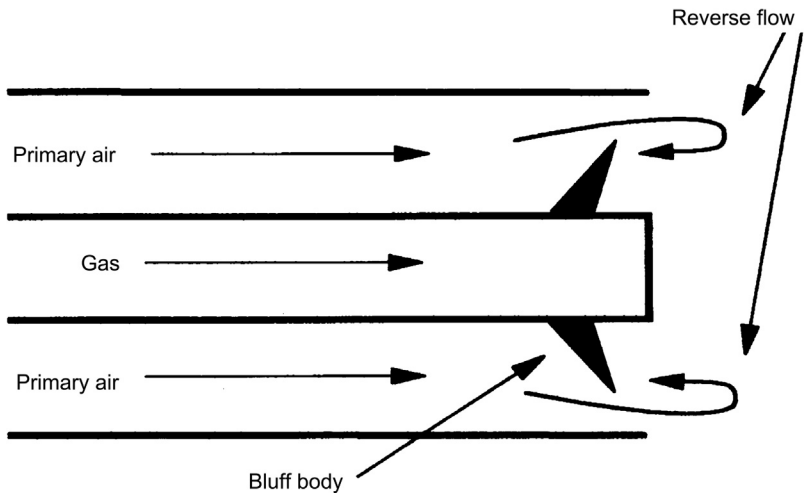


Figure 5.11 Flame stabilisation using flow deviation caused by bluff body

around a bluff body, Figure 5.11. While bluff bodies are quite suitable for gas burners, they can create problems with oil and coal fuels because burning particles are drawn back onto the surface in the wake and often stick creating a carbonised deposit. If this build-up continues to grow, which commonly occurs, the shape of the bluff body is changed by the deposit and the aerodynamics of the burner system are then adversely affected.

To overcome the limitations of bluff bodies, swirl on all or part of the combustion air is frequently used to create recirculation. This excellent method of stabilizing and intensifying combustion became apparent to combustion engineers during the post-1940 development of gas turbine jet engines for aircraft. Many burners now utilise air swirl to stabilise the flame and to control the fuel/air mixing. For these burners the presence (or absence) of an internal, or "central" recirculation zone is controlled by the intensity of the swirl. Increasing swirl intensity also increases fuel/air mixing rates. However, this increased mixing is not "free" because it requires greater fan power to impart the swirl. To characterise the amount of swirl, a dimensionless swirl number, S, is used as described in chapter 2.

Although the swirl number is easy to define, it is not so easy to measure. For this reason a "geometric swirl number" is often used which is based on the geometric angles of the swirl generators. Methods of calculating this value for a range of swirl generators are described in Beer and Chigier (1972). Because there are losses in the system, the geometric swirl number is always higher than the true swirl number. Typically an internal recirculation is established for a real swirl

number of greater than about 0.5. The International Flame Research Foundation, has done most of the work in characterising the different types of swirling flames that can be generated as a function of swirl number. It has also played a leading role in understanding the principals by which low NO_x swirl burners can be designed, see for example, Smart, et al, (1990).

The presence (or absence) of recirculation therefore has a great influence on the characteristics of the flame. A moderate degree of recirculation is usually associated with complete fuel/air mixing and a dramatic increase in flame stability. There are various reasons why this occurs. In some cases, the recirculating flow may bring back hot combustion gases to act as a source of ignition to the reactants. In other cases, it is more associated with the increased rates of mixing, as described above. Flow recirculation can also be used to assist in the development of low NO_x combustion technology since it allows zones of distinct characteristic stoichiometry to be created.

5.3 Gas Burners

In the introduction to this chapter we discussed the four fundamental stages of the combustion process and the fact that we had two fundamental types of flame, premixed and jet mixed and noted that most practical flames fell between these two extremes. Nevertheless gas burners are generally classified as premixed or turbulent jet diffusion burners, as defined below:

Premixed Burners, where the fuel and *most of the air* are mixed together prior to passing through the nozzle. Note that these burners often introduce a small proportion of the air separate from the fuel as *secondary air*.

Turbulent Jet Diffusion Burners, where the fuel and *most of the air* are introduced separately and are mixed within the furnace. Combustion is then controlled by the rate at which the air mixes with the fuel. Note that these burners often mix a small proportion of the air with the fuel as *primary air*.

Burners and furnaces are also classified by the air delivery system as natural draught, forced draught, induced draught and balanced draught. This is discussed further in section 5.6.

5.3.1 Premixed Burners

Premixed burners generally are used where the required heat liberation is relatively small and a high combustion intensity flame is required. Since the slowest of the four steps, mixing, has been accomplished prior to entry into the combustion chamber, the heat release is

controlled by the reaction kinetics instead of the fuel/air mixing. The following characteristics typify premix flames:

- Flames are small in volume relative to heat release rate
- High combustion efficiency i.e. small fraction of un-reacted or partially reacted fuel
- Non-luminous (little soot formation) and low radiant heat transfer efficiency
- Noisy (relative to heat release rate)

The premixing is normally accomplished by either a nozzle mixing system or a venturi injector, Figure 5.12.

The nozzle mixing system requires that both the air and gas are supplied under pressure. Subject to the pressures available, high velocities can be achieved. Indeed high velocities are required to prevent "burn back" into the mixture tube. The mixing is complete prior to the refractory tunnel where the combustion reactions occur. Provided some excess air has been supplied, combustion is also complete or nearly complete at the tunnel exit.

The venturi mixer shown on the right can be used in place of the nozzle mixer. With this device the gas pressure is used to entrain the combustion air from the atmosphere. Since the entrainment rate is a function of the gas momentum, the fuel must be supplied under sufficient pressure to achieve the mixing and overcome any back pressure from the furnace. This tends to limit venturi mixers to furnaces that are under suction or have very low back pressure.

The need to remain within the lower and upper limits of flammability puts a tight limit on the operation of these burners and it is essential that, when varying heat release, the mixture is maintained within the flammable limits at all times. Even momentary excursion outside the limits will result in flame out. This problem is more acute with the internal nozzle mix burner than the venturi type because the latter is effectively self-proportioning, since the air entrained is

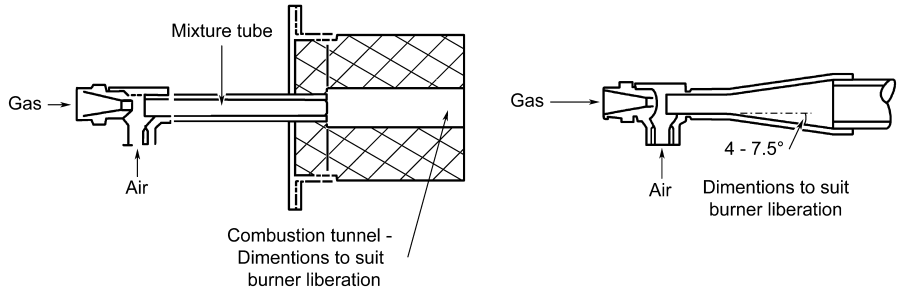


Figure 5.12 Typical nozzle premix as applied to a tunnel burner (left) and venturi mixer

proportional to the gas jet momentum. Hence the air/fuel ratio remains approximately constant for all gas flows. By contrast, the nozzle mix burner requires an effective proportioning control system to achieve turn down.

As noted above, some burners classified as premixed are, in reality, only partially pre-mixed with typically 70–90% of combustion air premixed and the remainder entrained into the premixed jet following ignition of the mixture. Typically, these are burners that use a venturi for mixing because the reduced air volume results in a reduced mixture volume and allows the use of a smaller venturi and gas nozzle.

Another application of partial premixing is to create a reducing atmosphere. By restricting the air supply to less than the full stoichiometric value, combustion is incomplete and a significant concentration of carbon monoxide is formed. Extreme care must be taken when employing this technique since CO is highly toxic. Furthermore, excessive restriction of the air supply will result in unburnt methane and other products of partial combustion. This can increase the concentration of combustibles in the flue gas so that it becomes potentially flammable and imposes and explosion risk in downstream equipment in the event of air in-leakage.

Effect of Excess Air (Mixture Ratio) on Flame Temperature

Owing to the very fast reaction rates achieved following premixing, together with the non-luminous flame, there is very little radiant heat transfer from premixed flames, hence the actual flame temperature approaches the adiabatic flame temperature. Maximum adiabatic flame temperature is achieved at stoichiometric conditions and decreases as excess air is increased, Figure 5.13. Note how even small quantities of excess air reduce the adiabatic flame temperature significantly. This feature can be used by furnace designers to control flame temperatures, providing that the mixture remains within flammable limits at all times. However, using additional excess air to reduce flame temperatures also reduces the heat available for transfer for the product, thus reducing the maximum achievable furnace efficiency, as discussed in chapters 4 and 9.

Premixed flames produce very little soot and therefore have low emissivity and low rates of radiant heat transfer. Furthermore, apart from using excess air to reduce flame temperature, there is very little opportunity to control radiant heat fluxes from pre-mixed flames. Thus, in effect, the tunnel burner is a hot gas producer and the majority of heat transfer is by convection. Since convective heat transfer is dependent on furnace gas velocity, the burner tunnel exit velocity and the flow patterns in the furnace are important design variables.

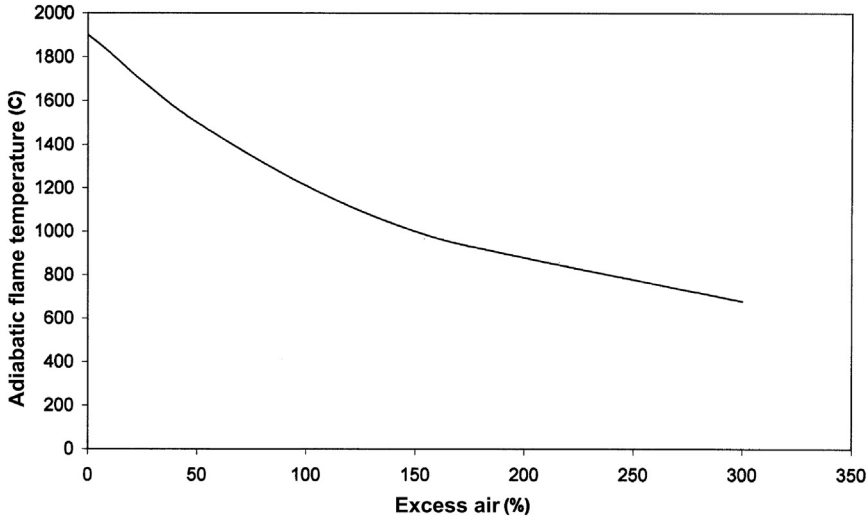


Figure 5.13 Effect of excess air on adiabatic flame temperature for natural gas (37.25 MJ/m^3)

Use of excess air to control flame temperatures always reduces furnace efficiency and is therefore to be discouraged. A better method of controlling furnace temperatures is to use flue gas recirculation, since this recovers heat that would otherwise be lost up the stack but this has a high capital cost and is rarely employed. However, operation at very low excess air in the burner produces a very high temperature within the tunnel which subject the refractory to severe thermal loads and requires very high duty refractory to ensure satisfactory service life.

Radiant Wall Burners

Another application of premix, or partial premix burners, is radiant wall furnaces. These are common in the petrochemical industry where a matrix of burners installed in a refractory wall is used to heat the wall and the hot refractory radiates to the load. A typical example of a burner designed for this application is the Walrad™ burner shown in Figure 5.14. This burner is the partial premix type with most of the combustion air entrained in the venturi by the gas while the remainder enters as secondary air through the air register. The proportion of primary air is controlled by an adjustable damper band to minimise thermal NO_x formation. See chapter 10 for a discussion on NO_x formation and its control.

™Trade mark of Hamworthy Combustion Engineering Limited

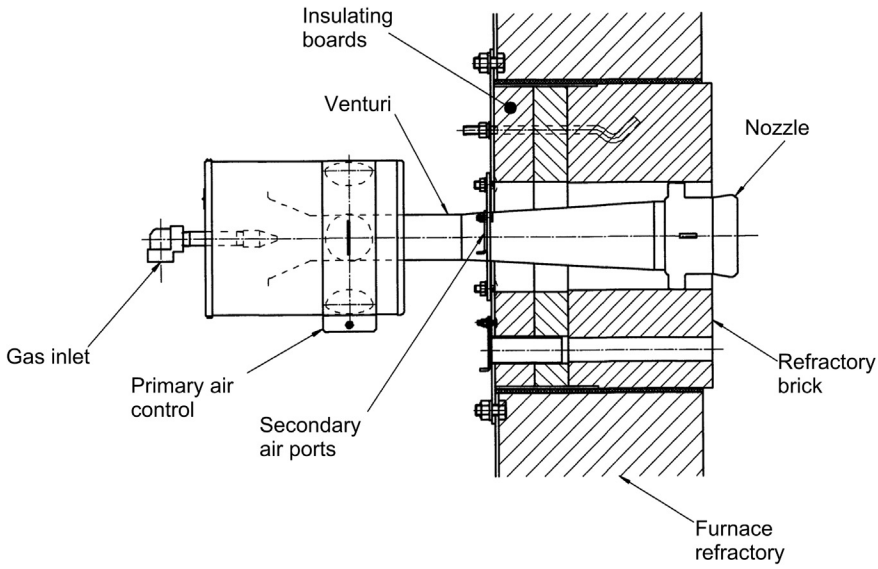


Figure 5.14 Partial premix radiant wall Walrad™ burner (Diagram courtesy of Hamworthy Combustion Engineering Limited)

Use of Premix Burners in Low NO_x Applications

The relationship between mixture fraction and flame temperature, Figure 5.13, implies that burners that operate in the very lean mode (high excess air) have low flame temperatures and hence produce low concentrations of thermal NO_x. This characteristic has resulted in widespread application of premix burners to industrial gas turbines to control NO_x emissions. However, it is not applicable to the majority of furnace applications because the flame temperatures are simply too low for effective heat transfer. This is not the case in a gas turbine where it is desirable to retain all the energy in the hot gas (typically up to 1450°C) prior to expansion through a turbine where the heat energy is converted to mechanical energy.

Safety Issues with Premix Burners

A premix burner will only operate within clearly defined limits, Figure 5.2. Since the mixture is within flammable limits, there is the ever present risk that the flame front will travel back though the nozzle or "flash back". The region in which this can occur is defined by line 1 in Figure 5.2. For butane this risk is low, as indicated by the small area applicable. However, for many gases, especially those mixtures containing hydrogen, the flash back region is much larger and hence the

risk is significantly higher. For these fuels, flash back is prevented by a combination of two techniques:

- Maintaining a nozzle exit velocity that exceeds the flame speed of the fuel;
- Using a nozzle design that is, in effect, a flame arrestor.

Using a nozzle velocity that exceeds the flame speed prevents the flame front propagating against the gas velocity, i.e. the burner is designed to operate above line 1 in Figure 5.2. Using this technique limits the safe turndown ratio because the nozzle exit velocity falls as the mixture flow rate is reduced, so the flame cannot be turned down below the safe nozzle exit velocity.

Flame arrestor nozzles function by reducing the mixture temperature below the ignition temperature, extinguishing the flame front in the event that the flame begins to propagate through the nozzle. A typical nozzle used with premix burners is shown in Figure 5.15. It uses gas ports that are long compared with their diameter and, relative to the burner heat liberation, the nozzle is heavy. If we consider the heat transfer across the nozzle, the flame tends to heat it, however the cool fuel/air mixture passing through the nozzle cools it and counteracts the heating effect of the flame, hence the nozzle remains at a relatively low temperature. It is the low temperature of the metal that ensures its flame arresting capability because a flame front propagating back through the gas port is cooled below its ignition temperature. This is achieved by using gas ports with long length and small diameter, i.e. large L:d ratio. The length L must be greater than the

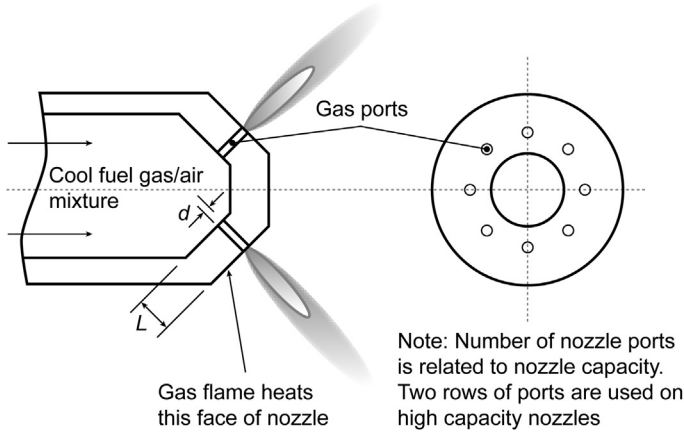


Figure 5.15 Principle of flame arrestor fuel gas nozzle

quenching distance for the fuel and the total volume of the port must be smaller than the fuel's quenching volume. For fuels with very high flame speeds, such as hydrogen, the quenching length is long and the quenching volume is very small, so to ensure safety with hydrogen small diameter gas ports are required (1mm or less) and at least 10 mm long to ensure that the flame is effectively quenched. The length L must be greater than the quenching distance for the fuel and the total volume of the port must be smaller than the fuel's quenching volume. This is considered further under gas nozzle design.

Example 5.1 How to calculate port size to prevent flashback for premixed flames

A premixed flame flashes back into a burner tube of 12.5 mm internal diameter at a mean flow velocity of 1.2 m/s. The mixture density is 1.05 kg/m^3 and its viscosity is 150 $\times$ 10^{-6} micropoise. The minimum operating mixture flowrate for the burner is 15 cm^3/s, thus it is proposed to fit a metal plug to the end of the pipe with four drilled holes of equal diameter. What is the maximum allowable hole diameter?

If the gas flow is laminar, we can use Poiseuille's equation to determine the critical velocity gradient for flashback, g_f.

$$g_r = \frac{4v}{R} = \frac{4x1.2}{\frac{0.0125}{2}} = 768 \ \text{(m/s)/m}$$

Calculate Reynolds Number for burner tube at flashback

$Re = (1.2 \times 0.0125 \times 1.05)/(150 \times 10^{-6} \times 0.1) = 1050$, i.e. laminar flow

Poiseuille's equation states

$$u = 2v\left(1 - \frac{r^2}{R^2}\right)$$

Where

u — velocity at radius r
v — mean velocity
R — tube radius

The critical velocity gradient is given by the differential of this equation

$$g_r = -\frac{\partial u}{\partial r} = -2v\left(-\frac{2r}{R^2}\right)$$

$$g_r = \frac{4vr}{R^2}$$

If we assume that the critical velocity gradient occurs at the wall of the tube, i.e. $r=R$ then assuming that the flow is divided evenly between the four drilled holes,

flow/hole = 15/(4x1000000) = 0.00000375m^3/s. thus if the maximum hole radius is R'

$$\partial R'^2 v' = 0.00000375$$

where v' is the mixture velocity in the hole. By rearranging the critical velocity gradient equation we get.

$$v' = \frac{g_r R}{4}$$

thus

$$\frac{\pi R'^3 g_r}{4} = 0.00000375$$

$$R'^3 = \frac{0.00000375 \times 4}{\pi \times 768}$$

$$R' = 0.00184 \text{ m}$$

Thus the maximum hole diameter to avoid flashback is 3.67 mm.

Size Limitations

While there is no absolute limit for the heat release of premix burners, the volume of the mixture is typically an order of magnitude greater than that of the gas alone and hence the mixing chamber must be of a significant volume and a large nozzle is required. Hence high liberation pre-mix burners are expensive to manufacture because they are physically much larger. Furthermore, this mixture is flammable, so the larger the volume, the greater potential explosive energy release in the unfortunate event of light back.

Premix burners therefore tend to be relatively small, with a large number employed where high heat release rates are required. Turndown is achieved by turning off individual burners or groups of burners.

Many burner designs employ a combination of these techniques to prevent flash back. For fuels with high proportions of hydrogen the burning velocity is very high so the flame arrestor nozzle is the only option.

5.3.2 Turbulent Jet Diffusion Burners

The great majority of industrial furnace burners are turbulent jet diffusion burners. With these burners the combustion air is supplied

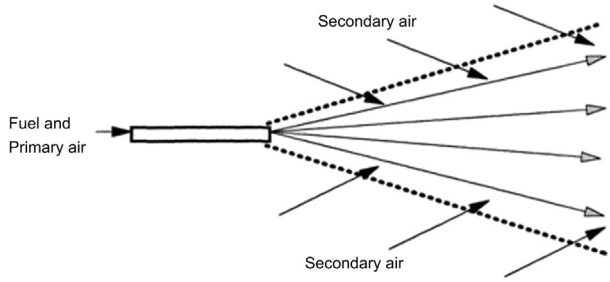


Figure 5.16 Principle of turbulent jet diffusion flame

separately and mixes with the fuel jet within the combustion chamber. The rate of combustion is largely controlled by the rate at which the air mixes with the fuel, Figure 5.16. In the turbulent jet flame the fuel is generally supplied via a central jet and the combustion air is supplied co-axially surrounding the fuel jet. A limited amount of air, known as primary air, may be supplied through the central jet together with the fuel. This jet must have significantly higher velocity and momentum than the surrounding combustion air to create effective mixing.

Friction occurs between the boundary of the high velocity jet and its surroundings, creating large eddies. The surrounding fluid is locally pulled into the eddy and hence accelerated to the jet velocity. The accelerated air becomes part of the jet, thus expanding it. This process is known as "entrainment". The amount of air entrained is controlled to a first order by the momentum of the jet and the process continues until the velocity of the jet is the same as that of its surroundings; the greater the momentum of the jet, the more of the surrounding fluid that will be entrained into it. An unconfined free jet can entrain as much of its surrounding air as is required to satisfy its entrainment capacity and it is able to expand unimpeded in doing so.

In the case of a confined jet however, such as most furnace flames, the jet is now constrained in two ways. The quantity of surrounding fluid being supplied to the furnace, i.e. the mass of secondary air, is controlled and limited. In addition, the expansion of the jet is now bound by the physical presence of the furnace walls. If the confined jet has momentum in excess of that required for the complete entrainment of the secondary stream, then recirculation will occur. The secondary air stream is initially pulled into the jet as described above for a free jet. A point is then reached, however, when all the available air has been entrained into the flame. At this stage, the jet will pull back combustion products into the flame in order to overcome this excess momentum. This causes the external recirculation illustrated

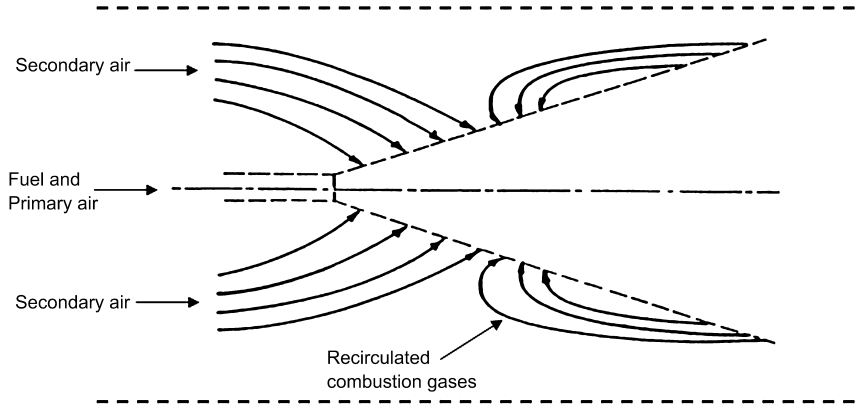


Figure 5.17 Recirculation in confined flames

in Figure 5.17. The onset of recirculation can be estimated by calculating the Craya-Curtet parameter, see chapter 6 section 6.1.2.

The Craya-Curtet parameter must exceed 1.5 for external recirculation to occur. However, it is advisable to use significantly higher Craya-Curtet parameters where feasible (typically 2.0 to 2.4), since flames with parameters close to 1.5 can flip in and out of recirculation and produce unstable heat transfer patterns for quite small changes in operating conditions. Flames with Craya-Curtet parameters above 2.6 produce very intense recirculation that dilutes the oxygen concentration with combustion products and tends to lengthen the flame compared with lower values.

The primary air itself mixes very rapidly with the fuel at the nozzle but the remaining air (secondary air) must be entrained into the primary jet (primary air and fuel) as described above. The rate of entrainment is dependent on the ratio of the momentum of the combined jet of primary air and fuel to the momentum of the secondary air. Thus, the higher the flow-rate and velocity of primary air, the more rapid the fuel/air mixing. The flame characteristics are determined by this momentum ratio and burners can be designed to give specific flame characteristics by the use of combustion modelling to determine the required jet mass flow and velocity, which is covered in the following chapter.

The role of recirculation is discussed also under flame stabilisation in section 5.2.2 but the presence (or absence) of recirculation has a great effect on the characteristics of the flame. A moderate degree of external recirculation is a positive indication that fuel/air mixing is complete, whilst its absence is a clear indication that not all of the secondary air has been entrained into the primary jet. In this case, the production of significant levels of carbon monoxide is normal. In

our experience insufficient primary jet momentum is one of the main contributory causes of poor combustion performance with jet entrainment burners, a condition that can be diagnosed by calculating the Craya-Curtet parameter.

5.3.3 Precessing Jet Diffusion Burners

Researchers at the University of Adelaide discovered that a precessing jet issuing from a nozzle has significantly different mixing characteristics compared with conventional jets. The precessing jet creates rapid large scale mixing of fuel and air in the near field, resulting in early heat release close to the nozzle. However, overall, the flame has lower global mixing rate than conventional and swirling jet flames, resulting in increased soot within the flame, making it highly luminous compared with normal natural gas flames. This facilitates high rates of radiant heat transfer to the furnace load reducing flame temperature and therefore suppresses thermal NO_x formation (Nathan et al, 2006).

The precessing jet is developed within a nozzle employing a rapid expansion into a cavity, followed by an exit orifice, Figure 5.18. The gas issues from a converging nozzle into the cavity and it deflects to the chamber wall before discharging from the exit as a severely deflected narrow jet. The point of attachment inside the nozzle changes constantly and causes the jet to precess rapidly. This nozzle design, and subsequent variants, have been patented by Luxton et al (1988) and is licensed to FCT Combustion, who design and market it as the Gyro-Therm burner. This burner is especially suited to high temperature processes utilising radiant heat transfer. The increased heat transfer, created by the improved emissivity, has been found to increase production by 2–10%, reduce gas consumption by between 2–8% and reduce NO_x emissions by 40–60% on a gas fired cement kiln (Videgar 1997).

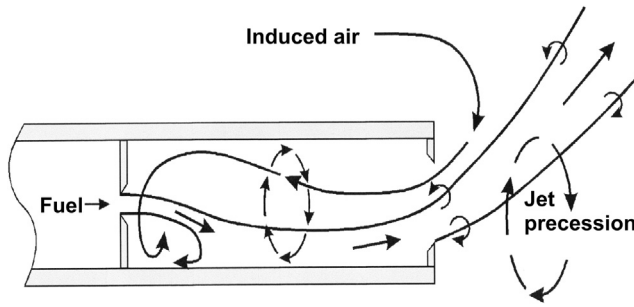


Figure 5.18 Precessing jet gas burner nozzle (Diagram courtesy of Prof. GJ Nathan)

5.3.4 Gas Nozzle Design

The procedure for calculating gas port sizes and arrangements are based on standard fluid flow equations together with experimental experience. Premix burners, except tunnel burners see Figure 5.12, generally have two nozzles, the fuel gas nozzle at the inlet to the entrainment venturi and the mixture nozzle at the exit of the venturi as shown in Figures 5.14 and 5.15. The procedure outlined below deals with each type of nozzle separately.

Determining the Fuel Gas Nozzle Port Area

The flow of a gas or liquid through an orifice is a function of the pressure differential and the physical properties of the gas/liquid. The governing equations are derived from the standard flow analysis (Coulson & Richardson, 1999) and can be generally expressed as:

$$Q = kA\sqrt{\frac{\Delta P}{\rho}} \tag{5.4}$$

where:

Q = the volumetric gas flow
ΔP = the pressure drop across the nozzle
A = the flow area
ρ = density of the gas on the upstream side of the nozzle
k = a constant

Nozzles are normally designed for the maximum liberation (thermal input) required from the burner plus a small design margin, typically 10% above the nominal design liberation. It is critically important that excessive design margins are avoided otherwise the burner turndown ration becomes severely limited. From the specified liberation the gas flowrate, Q, can be calculated using the fuel's calorific value. Note that it is important to maintain consistency in this regard, since the liberation may be specified in terms of either the gross or net heat input. The calorific values of gaseous fuels are normally provided in volumetric units so the flowrate can be calculated using:

$$Q = \frac{H}{CV} \tag{5.5}$$

where:

Q = the volumetric gas flow as before
H = the liberation or thermal input
CV = calorific value (volumetric basis)

If the *CV* is only available in gravimetric units then the gas flow must be converted to volume using its density:

$$Q = \frac{H}{\rho CV_m} \tag{5.6}$$

where:

Q = the volumetric gas flow as before
H = the liberation or thermal input as before
ρ = the gas density
CV_m = calorific value (mass basis)

The available pressure differential, ΔP, at the burner nozzle is limited by the supply gas pressure, the losses that occur in the gas valve train, and the furnace pressure. A gas pressure governor can be used to set a desired pressure at the gas nozzle after taking due account of the former limiting factors.

High differential pressures increase the gas exit velocity and momentum, thus improving gas/air mixing in jet entrainment burners. However, the noise generated by the jet (see section 5.8) also increases dramatically with injection velocity, especially above Mach 0.8. For this reason, most industrial gas burners are designed for subsonic, quasi-incompressible flow. Under these conditions the required nozzle area A, can be calculated using:

$$A = C\frac{Q}{k}\sqrt{\frac{S}{\Delta P}} \tag{5.7}$$

where:

C = a constant
k = the discharge coefficient
S = specific density of the gas relative to air
Q, A and ΔP are as before

The value of the constant C value depends on the units employed for the calculation, North American (1986), while the discharge coefficient, k, is a function of the approach geometry to the orifice, the type of orifice and the exit port geometry. The discharge coefficient must be determined experimentally but typical values range from 0.6 to 0.9.

A small number of specialist burners are designed for sonic or supersonic gas injection velocities. For these cases the gas must be delivered at very high pressure, so that it expands through the nozzle port, then the maximum velocity in the nozzle will be restricted to the speed of sound (in the gas), and the port is 'choked'. It is normal practice to use a convergent/divergent or venturi nozzle design for

this situation so that the gas can expand downstream of the throat and accelerate to supersonic velocity. The throat minimum area is determined using:

$$A = kG\sqrt{\frac{w^{-2/\gamma}}{1 - w^{(\gamma-1)/\gamma}}\frac{(\gamma - 1)S_1}{2\gamma P_1}} \tag{5.8}$$

where:

G = the mass flowrate
w = the pressure ratio of the upstream to downstream pressures P_2/P_1
γ = the specific heat ratio for the gas.

The minimum area, when sonic velocity is attained, corresponds to the critical pressure ratio w_c, where:

$$w_c = \left(\frac{2}{\gamma + 1}\right)^{\frac{\gamma}{\gamma-1}} \tag{5.9}$$

Determining the Drilling Pattern

The flow area, A, determined using equation 5.7, is normally provided by drilling a number of individual ports with a total area equal to A. Most burners feature a central gas gun or multiple gas pokers, Figure 5.19. The latter are particularly popular in boiler and petrochemical applications. Both arrangements allow for oil sprayer installation so that oil can be used as a back up fuel.

Individual jets are preferred over annual gas nozzles for the flowing reasons:

- Each individual jet will entrain air locally from its surroundings until it expands to meet an adjacent jet. Hence the air and gas are more intimately mixed, creating a larger volume of gas/air mixture within flammable limits in the near flame region. This enables the flame(s) to ignite at or near to the nozzle, creating good stable flames.
- A larger jet surface area is created by individual jets, as compared to a single jet thus giving a shorter, hotter flame.
- The flame can be 'shaped' to suit a particular furnace geometry or heat transfer requirement by arranging the jet drillings with differing areas and at compound angles.

The geometric arrangement used for gas burner nozzles are ultimately proven by experimental test firing, although flow modelling

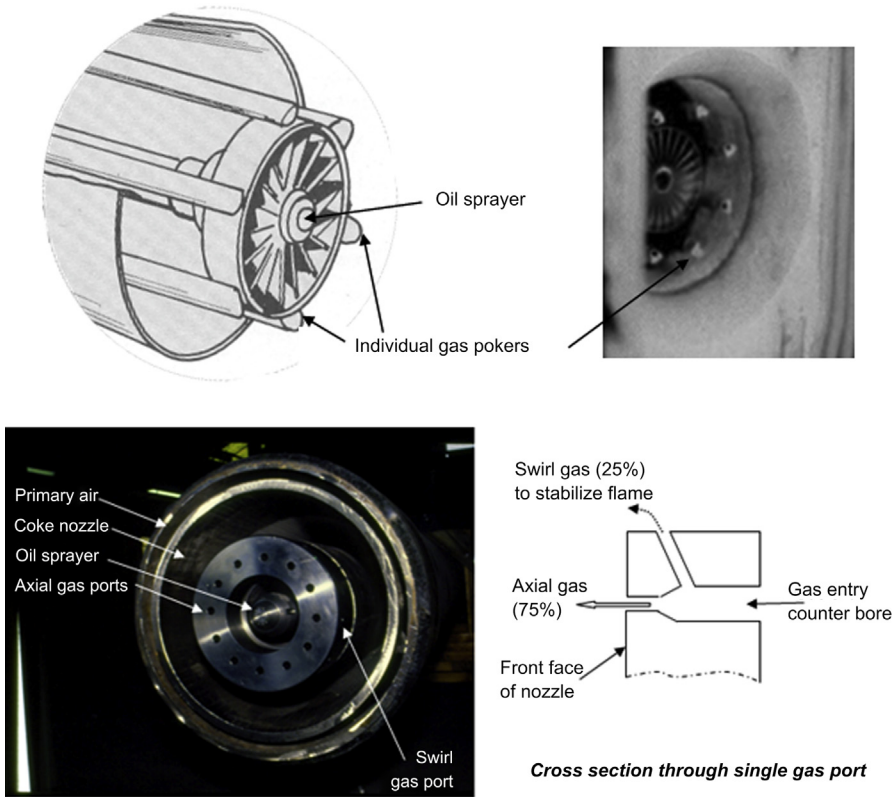


Figure 5.19 Typical industrial turbulent jet burner gas nozzle arrangements with gas pokers (upper) and central gas gun (lower)

can be used as a first stage in the design to examine possible configurations. Experimental results indicate that individual axial jet holes should lie within a range of separation distances relative to neighbouring jets. If the holes are spaced with less than one hole diameter of metal between jets, the resulting flame tends to 'collapse' back to a single jet, resulting in a long flame, that is often inefficient (viz. significant unburnt components in the flue gases). If the holes are spaced with more than four hole diameters of metal between jets, the resulting flame will appear as a distinct array of individual flames in the far field region of the burner, akin to the flames created by a gas cooker head. This is the result of each individual jet entraining sufficient air to attain stoichiometry before impinging with its neighbouring jet. Similarly, angled holes will create a similar result as the jets are directed radially and tangentially away from the axis.

Determining the Gas Mixture Nozzle Port Area for Premix Nozzles

The procedure for determining the nozzle port area is similar to that for the fuel gas nozzle using equation 5.4 except that the properties of the fuel/air mixture rather than fuel alone are applied. Hence, Q becomes the volume of gas/air mixture and ρ is the density of that mixture. The available ΔP is normally small for mixture nozzles, which together with the higher flowrate implies a large nozzle port area. However, the risk of flashback requires a large L:D ratio, Figure 5.15. If the gas flow is laminar, we can use Poiseuille's equation to determine the critical velocity gradient for flashback and ensure that the actual gas velocity is higher than this, see worked example below. The large mixture volume, together with the low pressure drop available and need to use a small hole diameter to prevent flashback, means that a large number of small ports are required for this application.

5.4 Oil Burners

Oil burners have the added complexity of two-phase flow resulting from the spray of fuel. Premix burners are limited to very volatile fuels such as naphtha and kerosene which, owing to their high cost have little industrial application and will not be considered here.

Oil burners consist of an air register to control the combustion airflow, a means of stabilising the flame and the atomiser, figure 5.20.

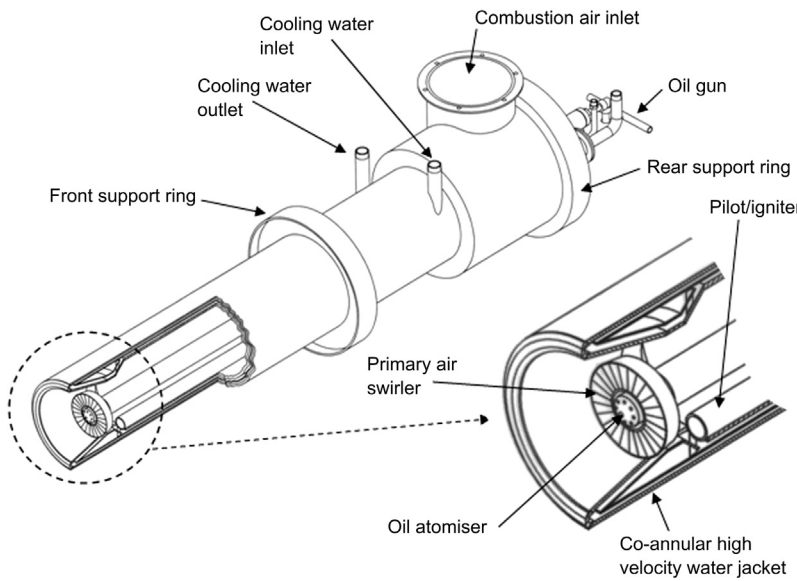


Figure 5.20 The main components of a typical furnace oil burner – Water cooled version shown. Reproduced with kind permission of FCT Combustion Pty.

An igniter may also be provided to assist start-up. The atomiser is a critical component and is considered further below, but before doing so, the general mechanism of spray combustion in an oil burner will be considered.

Figure 5.21 is a simplified illustration of a hollow cone spray burning in the wake of a bluff body flame stabiliser. The airflow is shown to the left of the line of symmetry, while to the right of the line the basic zones within the visible flame are shown. Note the primary reaction zone in the wake of the bluff body that stabilises the flame and the secondary reaction zone where final burnout occurs. Important parameters that affect the completeness of combustion include the size of the drops and their distribution in the airstream (spray angle) together with the aerodynamic flow patterns. The importance of matching the spray pattern with the air flow patterns was established by Drake & Hubbard (1966) but achieving this match is difficult and much full scale testing is often required. Most sprays are conical and two types can be used,

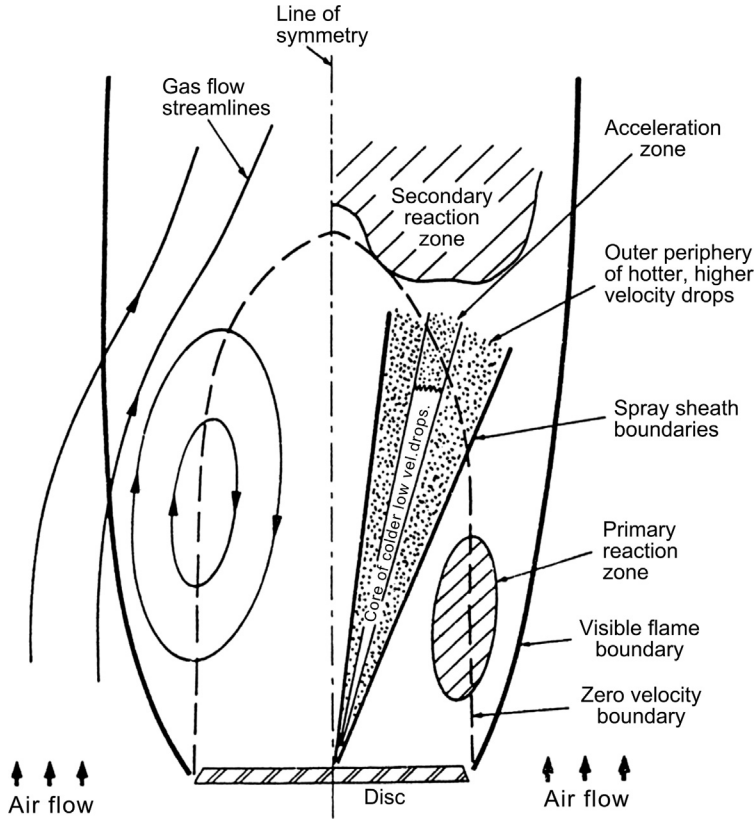


Figure 5.21 General mechanism of spray combustion (McCreath & Chigier, 1973). Reproduced with kind permission of the Combustion Institute

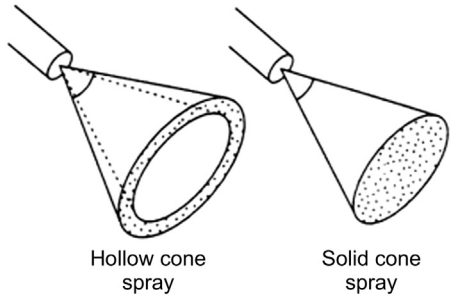


Figure 5.22 Solid and hollow cone sprays

hollow cone and solid cone, Figure 5.22. Hollow cone atomisers are generally preferred, since this enables the air to mix most effectively with the fuel. The small number of drops in the core of a hollow cone spray allows the establishment of an internal recirculation zone which assists in maintaining a stable flame front, Figure 5.23.

The importance of drop size distribution has already been discussed but unfortunately, it is relatively difficult to measure the drop size of

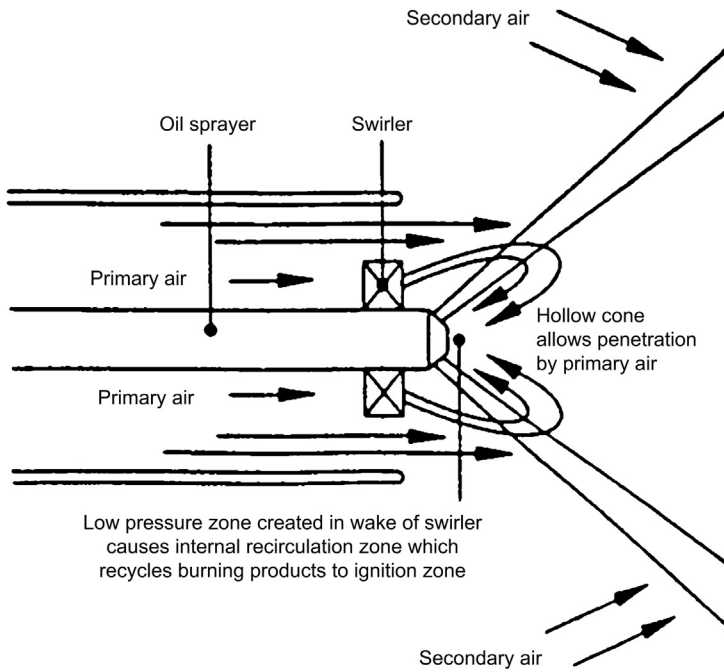


Figure 5.23 Illustration of flame stabilisation by internal recirculation zone caused by air entrainment into a hollow cone spray

an oil spray especially that produced by a large industrial atomiser, so most manufacturers have put this task into the 'Too Hard' category rather than investing the time, effort and money required. This is a great shame, since the atomiser characteristics are the single most important factor in oil burner performance and coarse drops can cause the user many problems with poor product quality and increased fuel consumption, together with excessive particulate emissions, difficult ignition and poor flame stability.

5.4.1 Turndown

Most burners are required to operate over a range of heat liberation and therefore fuel flow rates, since neither process plant nor boilers operate consistently at full load all the time. However, combustion performance of oil burners normally deteriorates under reduced load conditions owing to reduced energy for fuel/air mixing as a consequence of the lower air velocity and, in some cases, larger drops resulting from poorer atomisation, especially where simple pressure jet atomisers are used. For some atomisers the spray angle also changes under turndown conditions. Where large turndown ratios are required (greater than 2:1) it is especially important that the atomiser performance is satisfactory over the entire operating range and this is an important consideration when choosing an atomiser for a particular application. This topic is considered in further detail below.

5.4.2 Atomisers

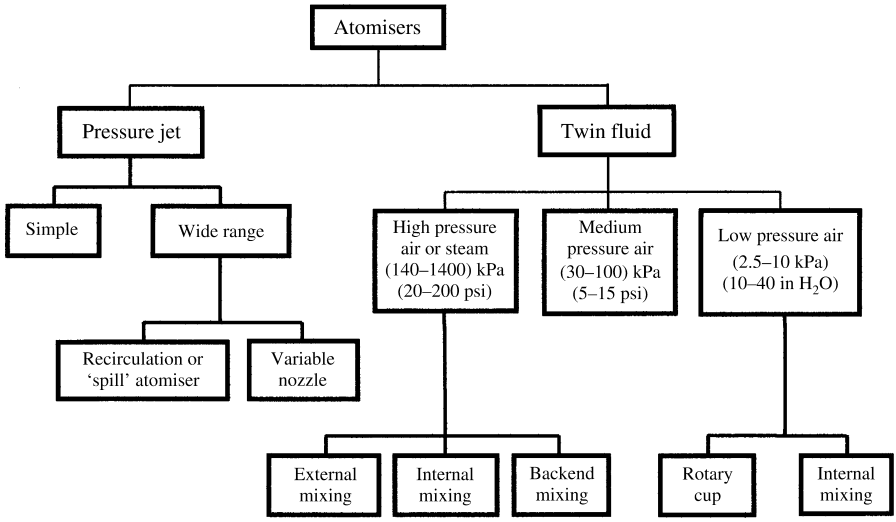
The two principle types of atomiser used in furnace burners are pressure jet atomisers and twin fluid atomisers. These are normally further subdivided into a range of sub-types as shown in Figure 5.24 and oil burners are often classified by atomiser type.

Pressure Jet Atomisers

A diagrammatic representation of a simple pressure jet atomiser is shown in Figure 5.25 (left). Pressure jet atomisers have the advantage of simplicity and the fact that the pressure-flow relationship follows the normal square root law but they suffer from poor turndown. Consideration of the basic pressure-flow and drop size relationships demonstrates this:

The flow through pressure jet atomisers is given by a modified version of Bernoulli's equation:

$$Q = k_1 \times d_o^2 \times p^{0.5} \tag{5.10}$$



Note: There are many commercial variations on these types of atomizers owing to the ad-hoc manner that burner makers undertake their design and development processes

Figure 5.24 Classification of oil burners by atomiser type

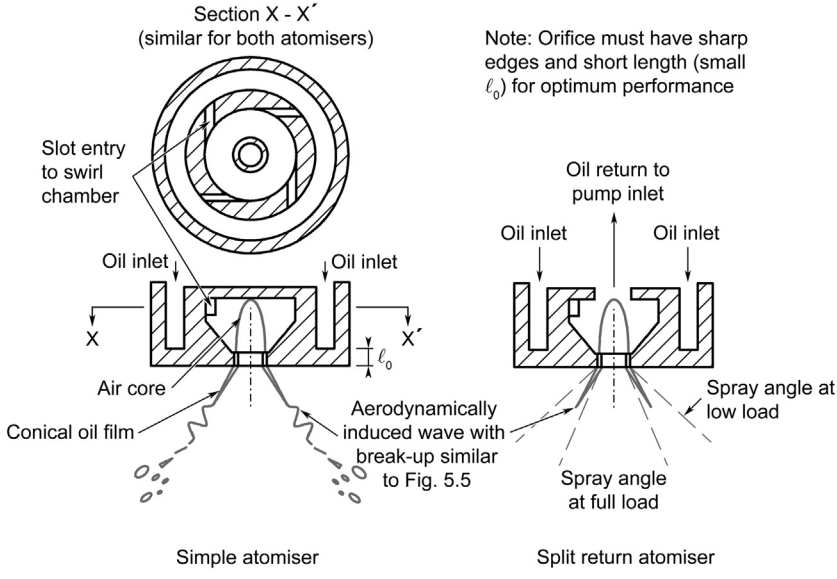


Figure 5.25 Schematic of simple and spill return pressure jet atomisers

Where:

Q = the flow rate
d_o = exit orifice diameter
p = the fuel supply pressure
k_1 = a constant

It is common in the industrial field to combine the constant, k_1 and the orifice diameter, d_o into a single constant that characterises the atomiser. This constant is known as the Flow Number (FN):

$$FN = Q/p^{0.5} \tag{5.11}$$

The Flow Number depends on a large number of factors associated with the geometry and is normally extrapolated by empirical scaling from similar designs or determined experimentally.

The drop size produced by a pressure jet atomiser is strongly dependent on the fuel viscosity and the surface tension. Radcliffe developed an empirical expression for estimating the SMD (Lefebvre 1989):

$$SMD = 7.3\sigma^{0.6}\upsilon^{0.2}m^{0.25}\Delta p^{-0.4}\text{micron} \tag{5.12}$$

Where:

σ = surface tension (N/m)
υ = viscosity (m^2s)
m = mass flow (kg/s)
Δp =pressure drop across atomiser (Pa)

Equation 5.12 implies that for any given atomiser, the fuel viscosity has the greatest effect on drop size and viscosities should be in the range 15–20 cSt (15×10^{-6} m^2/s) for satisfactory atomisation. Atomisers designed for high pressure operation relative to flow, i.e. small FN and orifice diameter produce smaller drop sizes, conversely low pressure atomisers with large orifices (high FN) result in very large drop sizes. High oil pressures and relatively small orifices are essential for effective atomisation. Normally oil supply pressures of 3.5 MPa (500 psig) and above are needed with large burners utilising heavy fuel oil.

Since the oil pressure falls rapidly with reduced flow, the drop size significantly increases under turndown conditions and this limits the practical turndown ratio of a simple pressure jet atomiser to approximately 2:1. The reason for this effect is that, as the oil pressure is reduced, the oil exit velocity decreases and the film thickens. When the ligaments break up, Figure 5.5, they form larger droplets. Special types of pressure jet atomiser can be used to increase the turndown ratio. One example is the spill return atomiser shown on the right in Figure 5.25. This design maintains a thin exit film by keeping the swirl

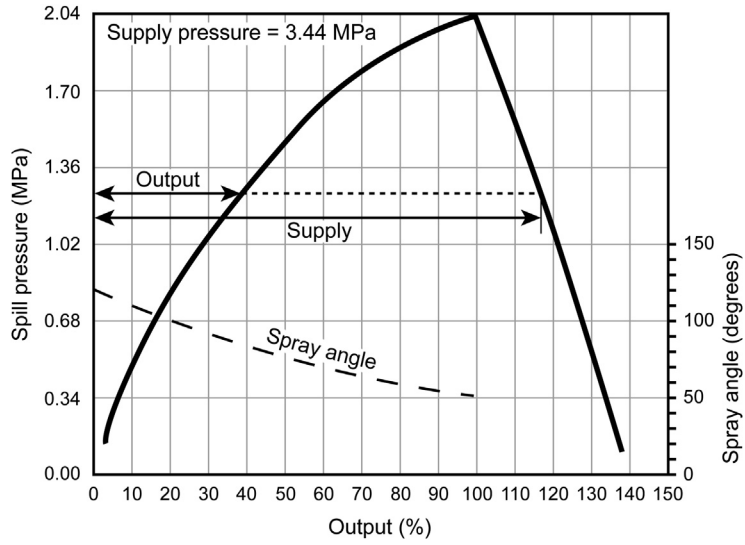


Figure 5.26 Calibration curve for wide turndown spill return pressure jet atomiser

chamber flow, and hence film velocity, constant. Turndown is achieved by returning the excess oil to tank through the back of the swirl chamber when operating under low flow conditions. Unfortunately the spray angle increases under low load conditions with the spill atomiser, Figure 5.26, and this causes difficulties with matching the combustion air to the spray geometry in some applications.

Another way of achieving turndown, while maintaining the spray angle constant, is the duplex atomiser, which is effectively one atomiser within another, Figure 5.27. The inner atomiser, usually known as the pilot, has a low capacity, typically 25 to 30 % of full load while the outer, or main, atomiser carries 70–75% of full load. Maximum output requires both atomisers in use while low load involves the pilot atomiser only with intermediate loads achieved by various combinations of pilot and main, together and alone.

Twin Fluid Atomisers

To overcome the limitations of pressure jet atomisers, and use lower oil pressures with higher turndown ratios, twin fluid atomisers can be used. In this type of atomiser, a second fluid, usually steam or compressed air, provides the energy for atomisation. As a consequence, the energy available is independent of the oil flow rate and drop size is more consistent throughout the operating range. Much higher turndown ratios are achievable, 8:1 being typical with even higher turndown ratios available from some manufacturers. Twin fluid atomisers are available in a wide

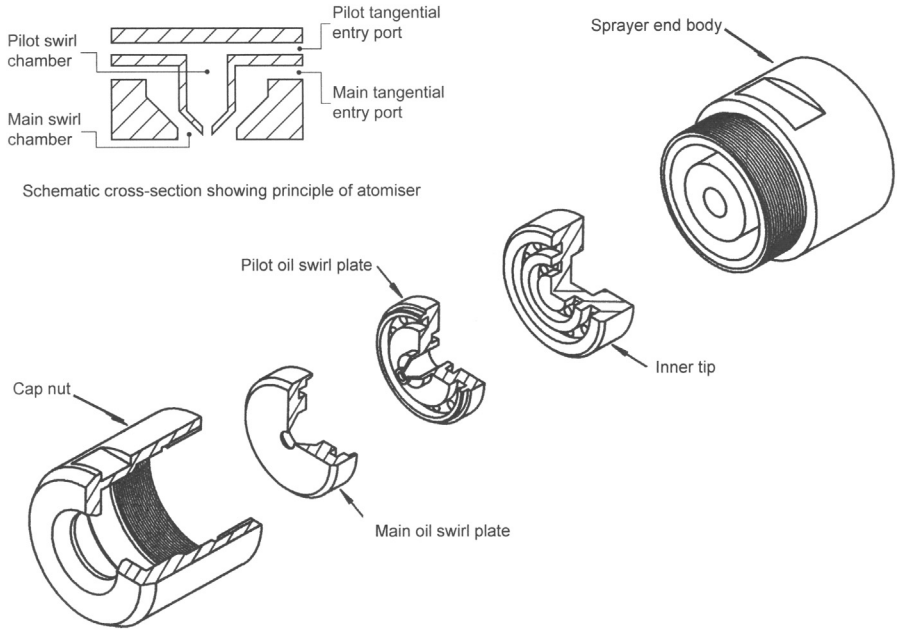


Figure 5.27 Schematic and "exploded view" of duplex wide turndown pressure jet atomiser

range of designs normally classified into low pressure, medium pressure and high pressure atomisers, Figure 5.24.

An example of a low pressure atomiser is shown in Figure 5.28. These atomisers always use the primary air as the atomising fluid with a supply pressure in the order of 8–15 kPa. These burners are versatile and robust and see widespread use on driers and small furnaces where gas is not available. They are supplied fully adjustable and require significant skills to set them up correctly during the commissioning period. It is not practical to use steam instead of air owing to the large quantities required and the cooling effect it would have on the flame.

Examples of medium pressure and high pressure twin fluid atomisers are shown in Figure 5.29. Medium pressure atomisers, Figure 5.29(a), also use air, rather than steam, generally supplied a blower at pressures in the range of 100–120 kPa. These atomisers were very popular in the past but, like the low pressure type, require a great deal of setting up for individual applications and significant energy is consumed by the blower. Atomisation performance can be very good for the better designs, when well set up, but in other circumstances the drop size distribution is far too coarse for efficient operation. Few manufactures currently offer these atomisers so they will not be considered further.

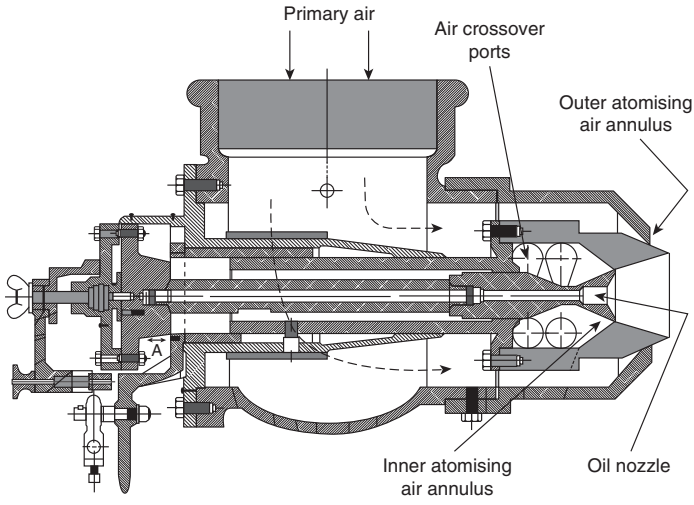


Figure 5.28 A low pressure air atomising burner (Diagram provided by courtesy of NA-Stordy Combustion Ltd.)

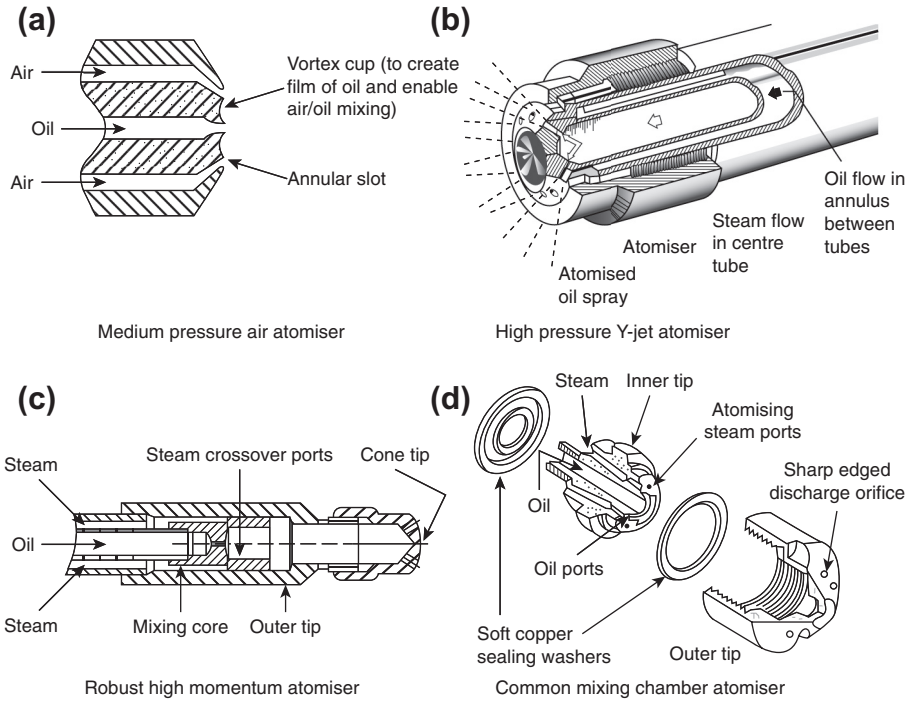


Figure 5.29 Examples of medium and twin fluid atomisers (Figs (b) & (c) courtesy of Hamworthy Combustion Engineering Limited, fig (d) courtesy of FCT Combustion Pty.)

Figures 5.29 b, c & d show the main three types of high pressure atomiser currently available. These are the Y-jet Figure 5.29(b), a high momentum atomiser, Figure 5.29(c) and a high performance common mixing chamber atomiser, Figure 5.29(d). Variations on these designs are available from a number of manufacturers and all can use air or steam as the atomising fluid. They are supplied fully finished and require no further adjustment on site.

The Y-jet has the major advantage of low steam or air consumption (generally less than 0.1 kg steam/kg of oil) but requires low viscosity oil (15–20 cSt) and dry steam. One disadvantage of the Y-jet is the asymmetric oil entry, which gives a stream of larger drops on the side adjacent to the oil port, see Figure 5.5, which shows the cross-section through a single jet of a Y-jet atomiser showing the mechanism of its oil film break-up.

A high momentum atomiser is shown in Figure 5.29(c). These are very robust and relatively tolerant of both poor steam quality and higher oil viscosity but have a high steam consumption of approximately 1 kg steam/kg of oil.

The atomiser shown in Figure 5.29(d) utilises a common mixing chamber with multiple steam and oil ports and eliminates the asymmetry of the Y-jet. This atomiser also requires dry steam and low viscosity oil and consumes approximately 0.25 kg steam/kg of oil but produces a much finer drop size than other atomisers.

Twin fluid atomisers do not follow the normal pressure flow-relationship and each fluid has to be separately controlled. Normally the flow of oil is measured and controlled, with the atomising fluid set to a constant pressure, or controlled to a differential pressure relative to the oil pressure. Each design of atomiser has to be individually calibrated in accordance with the chosen mode of operation. A typical calibration curve is shown in Figure 5.30.

The wide variety of twin fluid atomiser designs has made prediction of their drop size difficult. As a result, the expressions that exist can only be applied to a limited range of atomisers. For example, Wigg's equation (1964) which was developed for internal mixing air blast atomisers with high air/fuel ratios, can also be applied to the conventional Y-Jet type, as well as the atomisers it was originally developed for.

$$D_{md} = \frac{200\, v^{0.5}\, Q^{0.1}\, (1 + Q/A)^{0.5}\, h^{0.1}\, \sigma^{0.2}}{\rho^{0.3}\, V} \qquad (5.13)$$

Where:

D_{md} = mass median diameter of spray (microns)
v = fuel viscosity (cSt)
Q = fuel flow rate (gm/s)
A = air flow rate (gm/s)

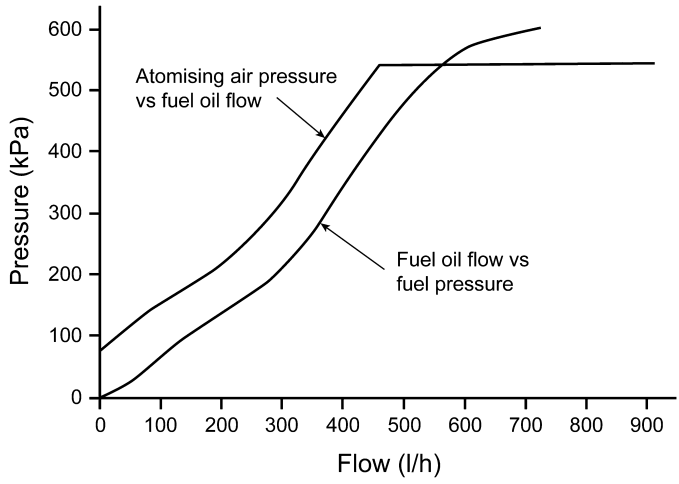


Figure 5.30 Typical calibration curve for a high pressure twin fluid atomiser

h = height of the air annulus (cm)
σ = surface tension of the fuel (dynes/cm)
ρ = atomising fluid density at the mixing point (gm/cm)
V = atomising fluid velocity relative to fuel velocity

This expression shows that oil viscosity, atomising fluid/fuel ratio, density of the atomising fluid and its velocity relative to the fuel velocity, all have a major influence on the drop size. The equation suggests that the effect of geometry is small, being represented by "h". However, in practice, the influence of atomiser geometry is significant because it also affects critical variables such as the atomising fluid density and the relative velocity.

5.5 Pulverised Coal Burners

Pulverised coal firing has many advantages over other forms of coal firing and makes burning coal similar to oil firing from a process viewpoint. Since coal is generally cheaper than either oil or gas it becomes the economically preferred fuel, where the ash and trace chemicals can be accommodated by the process. Pulverised coal firing has grown in importance as power stations and cement plants have grown larger. Despite the resources lavished on so-called "clean coal technology", fluidised beds, coal gasification, etc., have made little real inroad to the quantity of coal burnt in the pulverised form. While this will have to change in the future to reduce greenhouse gas emissions, pulverised coal is likely to remain an important fuel for high temperature

furnace applications, such a rotary kilns, owing to its very high emissivity, which results in high rates of heat transfer to the charge.

Generally, the lower cost of coal gives it a significant economic advantage compared with other fuels. Coal is rather more difficult to handle than oil or gaseous fuels, since it is a solid material of varying composition and calorific value. Furthermore, owing to the high capital cost of pulverised coal grinding plant, its use is normally restricted to relatively large installations. The largest users are power station boilers, cement kilns and steel making. Smaller applications may be economic where pulverised coal is commercially available. In these markets the coal is ground in a central grinding plant and transported to the point of use by road or rail tanker. For more information on coal grinding, see chapter 7.

In many ways burning pulverised coal is similar to burning oil, but the variable nature of pulverised coal requires a flexibility of burner design to allow the use of differing grades of fuel. Even coal sourced from the same mine will vary with time but often the source of coal is changed during the life of the burner, so it is important that this is taken into account at the design stage. Factors that should be considered include; variation of calorific value, moisture content, ash content, ash abrasiveness and ash chemical composition. These factors also influence the design of the grinding system.

Pulverised coal burners are similar to oil burners but the atomiser is replaced with a coal nozzle. The fine coal is air conveyed to the nozzle. An important point, not always effectively addressed, is the tendency of the coal to form localised concentrations in the conveying air. This effect, known as "roping", can cause major problems with fuel distribution in the combustion air, adversely affecting combustion performance. It is desirable that the burner incorporates a means of breaking the rope and improving the coal distribution in the conveying air prior to discharge into the furnace. One way of achieving this is to impart swirl to the conveying air flow at the inlet to the burner.

By far the largest application of pulverised coal in furnaces is for rotary kilns and blast furnaces. In the past, many rotary kiln coal burners were simple open ended pipes. In this case the coal is conveyed by the primary air and the remaining combustion air or secondary air, is provided from the cooler, Figure 5.31. Unlike oil and gas burners, it is quite safe to rely on re-radiation from the kiln walls to stabilise the flame when coal firing, owing to the low ignition temperature of most coals. Apart from the inconvenience of having to insert a temporary oil burner to warm-up the kiln, a plain pipe can give an excellent combustion and heat transfer performance provided the primary air momentum is effectively optimised. The critical performance criteria is that the primary jet momentum is matched to the secondary air momentum to produce the correct rate of fuel/air mixing so that the

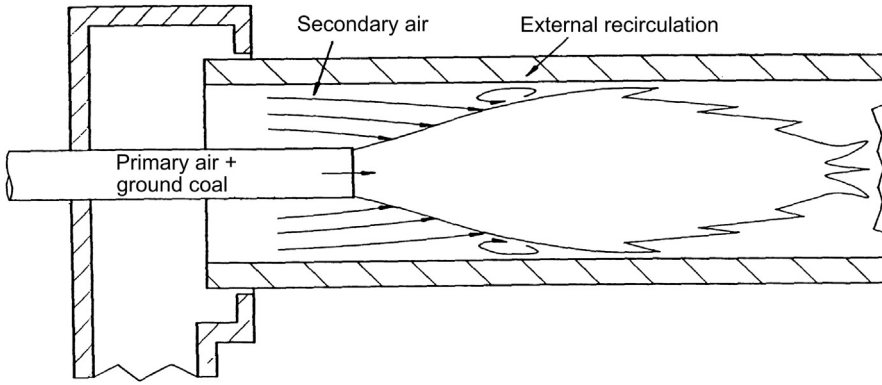


Figure 5.31 Typical open ended pipe kiln burner arrangement.

optimum heat release pattern is produced for the material being processed. For ways of achieving this see chapter 6.

With the conversion of many rotary kilns from oil firing to coal firing in the 1970's, new coal burners were developed based on existing oil burner designs. These burners use less primary air than plain pipe burners and are suitable for use with indirect firing systems where the coal is ground then stored as pulverised coal prior to use, see chapter 7. However, their performance is often very poor because the low primary air jet momentum causes inadequate fuel/air mixing. A major benefit of multi-channel burners is that the start-up oil burner can be permanently installed, minimising additional labour demands during kiln start-up. Significant benefits can also result from the use of multi-channel burners, especially with more difficult low volatile fuels such as petroleum coke, since the fuel can be injected at low velocity to maximise residence time in the flame, while using high velocity primary air to optimise the fuel/air mixing. A typical coal burner incorporating an integral oil start-up burner is shown in Figure 5.32.

5.6 Furnace Aerodynamics

Since fuel/air mixing largely controls the combustion process, the combustion air supply system and resulting airflow patterns have a huge effect on the overall performance. The combustion air may be supplied by four techniques:

- Natural draught
- Induced draught
- Forced draught
- Balanced draught

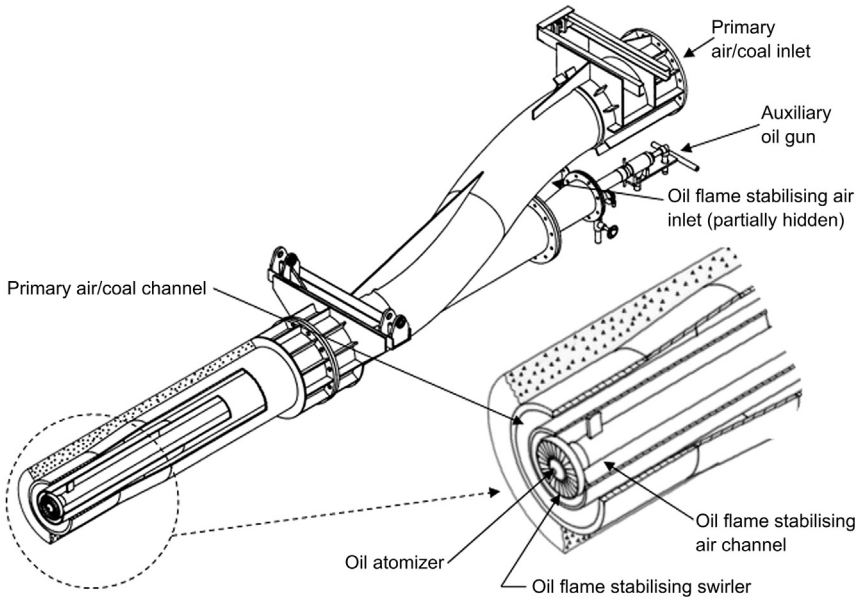


Figure 5.32 Typical pulverised coal burner with auxiliary oil firing for rotary kilns (Diagram courtesy of FCT Combustion Pty)

Simple schematic diagrams of these four draught techniques are shown in Figure 5.33.

Natural draught, Figure 5.33 (a) utilises the buoyancy of the hot gas in the furnace and chimney stack compared with the density of the ambient air to provide flow through the system. It has the advantage that no fans are required but the suction available is small, typically 100–800 Pa, hence the pressure drop through the system must also be small. Furthermore, the need for relatively high flue gas temperatures to create the draught prevents the installation of heat exchangers to recover surplus heat from the flue gases. This limitation becomes even more severe in hot climates or at altitude where the air density is lower and all gas and air passages must be larger. The suction available from a natural draft system in Pascals is given by:

$$p = 9.81\, H(\rho_s - \rho_a) \tag{5.14}$$

Where:

ρ_s = the average density of the stack gas (kg/m^3)
ρ_a = the density of air at ambient conditions (kg/m^3)
H = height of the stack (m)

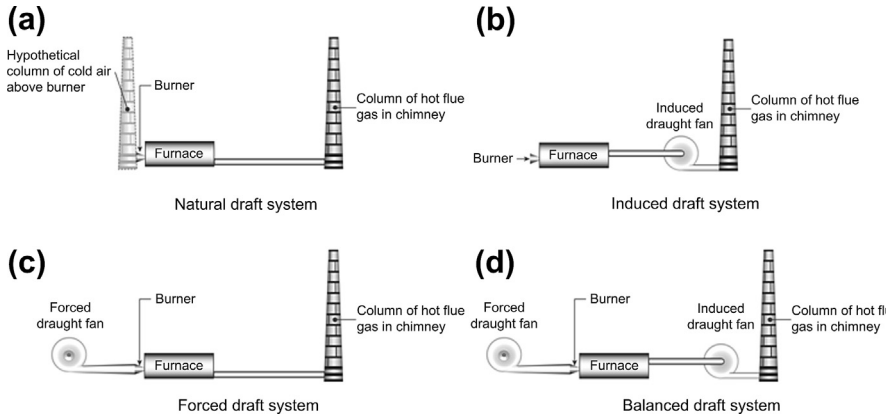


Figure 5.33 Schematic of the principle combustion air supply systems

The density of air and the flue gas can be calculated using the ideal gas laws. The main influence on the available draught is the height of the chimney, the average gas temperature in the stack and the ambient temperature.

Induced draught, Figure 5.33 (**b**) uses a fan in the flue gas system to increase the suction available and therefore allows the use of convective heat exchangers in both the flue gas system and air supply system. The principle disadvantages of induced draught are that the fan is subject to hot and, possibly dirty, gas and that the furnace operates under relatively high suction. This increases the proportion of in-leakage or false air compared with other draughting arrangements.

Forced draught, Figure 5.33 (**c**) uses a fan to blow air through the burner and furnace system. Much higher pressures can be achieved (but have to be paid for in fan power) and therefore relatively high equipment pressure drops are allowable. Therefore higher air and gas velocities can be used, improving convective heat transfer and reducing equipment size. With this system the furnace operates under pressure and any leakage is outwards into the surroundings. This can create safety problems because hot, and possibly toxic, gases may be emitted.

Balanced draught, Figure 5.33 (**d**) uses a fan to blow air through the burner and a second fan in the flue gas system to increase the suction. The normal objective is to achieve the performance of a forced draught system while maintaining the furnace internal pressure at, or very close to, atmospheric pressure thus minimising leakage in or out. Balanced draught systems are the most complex and require sophisticated control systems to maintain stable system pressures and flows.

Burner and Furnace Airflow Patterns

As articulated by Drake & Hubbard (1964), poor airflow patterns have a major detrimental effect on combustion efficiency, heat transfer and flame shape. In the case of very poor aerodynamics severe flame impingement on the furnace walls may result, leading to damage to the refractory walls. The airflow patterns in the furnace are influenced by a range of factors including:

- Design of the burner and the aerodynamic flow patterns that it produces;
- Shape and route of the combustion air supply ducting;
- The number and spacing of burners in multiple burner installations;
- The design of common windboxes and plenum chambers.

Poor flow patterns caused by inadequate combustion air ducting or burner plenums and wind-boxes can ruin the performance of otherwise excellent burners. Poor aerodynamic flow patterns are extremely common and cause problems with both single and multiple burner installations. This is discussed in sections 5.6.1 to 5.6.4.

5.6.1 Single Burner Systems

Single burner installations are rare in furnace applications apart from hot gas generators, dryers and rotary kilns. Air heaters and dryers tend to utilise "package burners" where the whole installation, burner, windbox, ducting and fan are supplied by the burner manufacturer as a bolt-on unit.

Package Burner Installations

The aerodynamics of these systems is normally optimised, or at least the most significant problems resolved, during the design and prototype testing stage. These burners will normally only give problems if the design of the "package" has been modified to accommodate special space requirements, such as may occur when a system is adapted for unusual applications.

An example of the problems that can occur with a modified single package burner system is the case of an air heater installed on an offshore oil rig in the northern North Sea. In this example, restricted head room led to a remote fan installation with an interconnecting combustion air duct. This duct was designed simply to join the fan to the burner while accommodating the structural steelwork, ignoring the aerodynamic characteristics of the design. The duct routeing

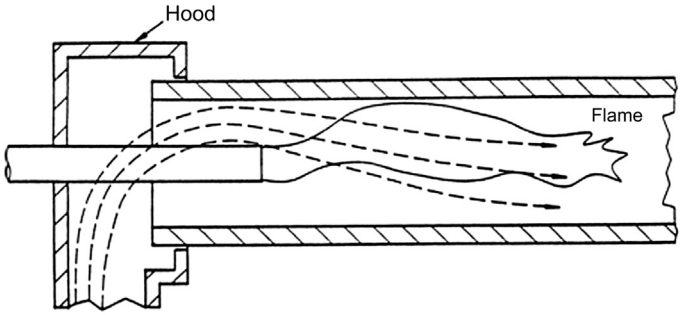
adversely affected the air flow and produced a skewed flow distribution at the inlet to the burner windbox, which it could not compensate for and the flame was deflected over to one side of the combustion chamber, impinging on the ceramic fibre wall. This wall failed during the commissioning period, a particularly dangerous and costly failure for an offshore rig. The unit was repaired but failed again shortly after restarting; causing the gas sweetening plant to be shut down and the associated gas had to be flared. The consequential losses were over US$ 75,000 per day for several weeks (mid 1980s prices) and could have been avoided if the aerodynamic issues had been considered at the design stage. The problem was resolved by undertaking physical modelling of the duct to determine the appropriate size, shape and location of the splitters required to correct the flow. Following their installation the problem was resolved. Millions of dollars could have been saved had this approach been adopted as part of the design strategy.

Rotary Kilns and Driers etc

Rotary kilns and drum driers are one of the most common single burner installations. Rotary kilns are used for processing a wide range of solids including alumina, cement, chrome ore and chrome oxide, clays, lime, petroleum coke, mineral and tar sands, nickel titanium dioxide etc. Rotary kilns are also used to burn the organic matter out of a number of inorganic materials and for the incineration of medical and hazardous waste. The operation of rotary kilns is not easy and some still suffer from combustion problems, despite being a mature technology.

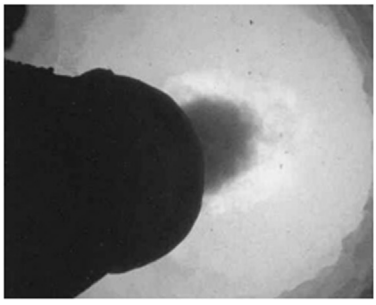
Problems arise with rotary kilns because the burner is usually purchased as an add-on package. Therefore in most rotary kiln systems the aerodynamic design is not under the control of the burner manufacturer but decided by the kiln designer, often without any serious consideration as to the flow patterns that are likely to result. Rotary kilns therefore frequently exhibit very poor aerodynamics, largely because the designers ignore, or are unaware of, aerodynamics and valuable design techniques, such as modelling. The latter is discussed extensively in the next chapter.

Normally all the fuel is injected through the burner jet but only 10–30% of the combustion air passes through the burner. The remaining combustion air enters through the coolers or kiln hood. Thus, the burner supplier only has the control over 10–30% of the air needed for combustion, the remainder coming from elsewhere. This is in contrast to a package burner, where the burner designer has complete control over all the combustion air. In the rotary kiln, the burner designer has to accept whatever secondary air flow pattern is provided by the kiln designer. Figure 5.34 illustrates the type of problems that we have experienced with rotary kilns. In our opinion, many kiln burner designers and manufacturers do not help

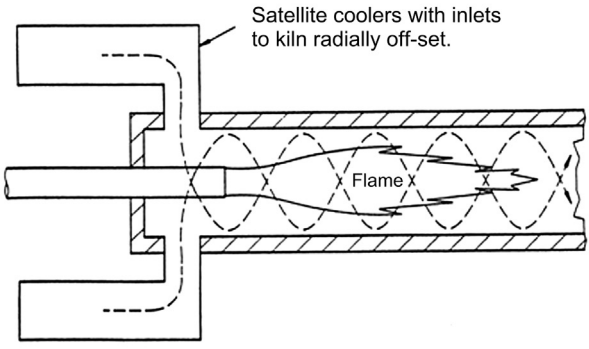




Note how the high secondary air velocity in the narrow kiln hood deflects the flame



Flame following correction of secondary airflow patterns



Fuel/air mixing delayed by strong high momentum swirl induced by satellite cooler inlets

Figure 5.34 Examples of how poor secondary airflow adversely affects kiln flames

themselves, since they regard their burner as an add-on package and do not attempt to ensure that it matches the particular kiln and consequentially problems arise. The majority of these problems can largely be avoided if due attention is paid to the role of combustion and its associated airflows in the performance of the plant. For example, the deflected flame can be avoided by appropriate design of the kiln

chute and hood to ensure a reasonable uniform air velocity profile at the kiln inlet. This can be effectively achieved by using modelling to optimise the design.

5.6.2 Multiple Burner Systems

Multiple burners are used on a wide range of process plant as well as large water tube boilers for power generation. The latter typically use 4 or 6 burners for small units with installations of up to 64 burners relatively common on 600 MWe units. Process plant utilising multiple burners include petrochemical heaters, steel re-heating furnaces, glass tanks, annealing furnaces, brick kilns, etc. As for single burner installations, the effect of poor aerodynamic flow patterns can result in reduced output, poor product quality, higher fuel consumption and excessive emissions and premature failure of the equipment.

Most of the aerodynamic problems experienced with single burner installations also occur with multiple burner installations which have the added complexity of ensuring equal supply of air between the burners, together with minimising any detrimental aerodynamic interference between the flames within the combustion chamber. It should be especially noted that, although the furnace interior may appear to be highly turbulent, intermixing between the flames is quite limited and cannot compensate for poor air distribution between the burners in the windbox or air ducting.

To operate effectively a burner needs the correct mass flow of air to achieve complete combustion. In other words the stoichiometric airflow plus the target amount of excess air, as defined by the burner designer. For example, the air distribution to an array of burners designed to operate at 5% excess air (approx. 1% O_2 in the flue gas) must be better than $\pm 2\%$, otherwise some of the burners will have virtually no excess air while others will have far too much.

5.6.3 Combustion Air Duct Design

An arrangement common in both the petrochemical and metals industries utilises a number of burners supplied by branches off a common

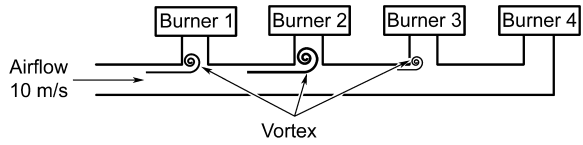


Figure 5.35 Typical combustion air duct supplying multiple burners

air duct, Figure 5.35. In this example burner 4 will probably receive much more air than the other three owing to the effect of increasing static pressure available as the velocity drops along the duct and dynamic pressure becomes converted to static pressure. However, unless the system is modelled, the burner receiving the lowest airflow is unpredictable and depends on the flow regime in the entrance to the burner off-take. Usually a vortex is set up in this area and the size of the vortex determines the effective flow area of the branch. The duct routing and the equipment installed upstream, such as dampers, air heaters, etc., all affect the size of the individual vortices and the location of the largest one. Often the burners nearest to the inlet i.e. burners one and two, receive the least air.

Figure 5.36 shows the measured air distribution in a petrochemical heater with a particularly poor common air supply duct for 18 burners. In this case, the discharge duct from the combustion air heater introduced the combustion air to the burner air supply duct adjacent to burner 8. It can be seen that while this burner receives an excessively high airflow, the burners immediately adjacent to it are very short of air, with No 10 receiving only just over half the average airflow. The burners at the extreme ends of the duct received very high airflows, in the order of 140% and 118% of the average airflow, respectively. The consequence of this appalling air distribution was severely distorted heat transfer profile in the heater that led to reduced output and severe coking of the tube internals as a consequence of overheating of the petroleum feedstock.

Sometimes the vortices in the burner off-takes are unstable and vary in size with time, often flipping between two meta-stable states. This phenomenon can lead to quite puzzling symptoms such as CO excursions and "dancing flames".

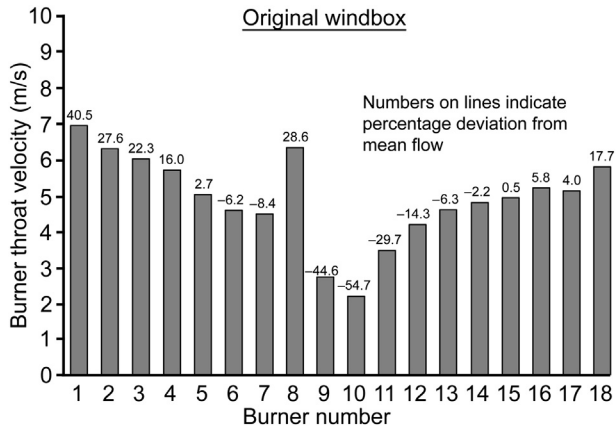


Figure 5.36 Poor combustion air distribution caused by inadequate duct design

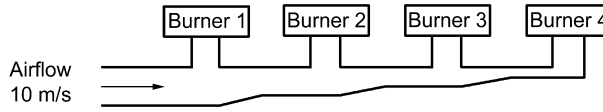


Figure 5.37 Example of constant velocity combustion air ducting

Many designers attempt to resolve the problem of poor air distribution by adopting constant velocity ducts, Figure 5.37. In this arrangement the duct cross-section decreases immediately after each burner combustion air off-take. Whilst this minimises the additional pressure at burner 4, caused by static pressure recovery, it does nothing to eliminate the vortices in the root of the off-take. The air distribution between the burners is likely to remain poor but nothing like as bad as seen in Figure 5.36. However, variations of ± 20% of the mean flow would be typical with this type of duct, making it quite inadequate for low excess air furnace operation.

Good combustion air distribution, better than ± 5% can be achieved by the installation of flow splitters in the various bends in the duct between the fan and the inlet to the first burner. Correctly designed splitters ensure a nearly uniform flow distribution in the duct. However, a suitable velocity profile in the duct does not in itself ensure even air distribution between the burners, owing to the presence of variable sized vortices in the inlets to the burner off-takes, but it is an essential starting point. Once the velocity profile is optimised the flow into each burner duct can be controlled by installing weirs close to the burner air off-take. These weirs are sized to effectively control the size of the vortex so that the flow into each of the burners is equalised, Figure 5.38. Unfortunately, the optimum position of the flow splitters and the size and position of the weirs cannot be determined mathematically but physical modelling is required. This uses water/bead modelling for flow visualisation so that the problem areas can be identified, followed by air modelling to obtain quantitative measurements of the burner airflow distribution. Computer based flow modelling techniques are not yet able to cope adequately with this problem owing to its complexity and the unstable vortex flows that are frequently experienced.

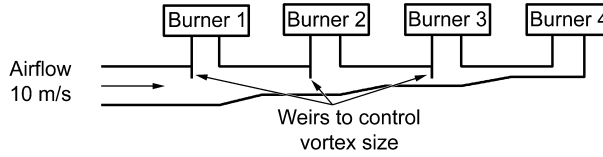


Figure 5.38 Example of constant velocity combustion air ducting with weirs

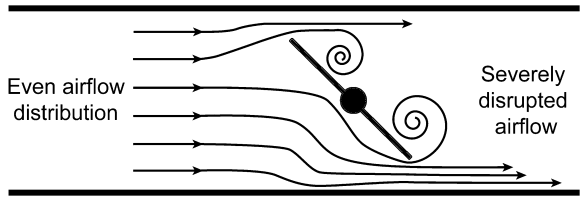


Figure 5.39 Effect of single blade damper/air door on airflow

Dampers, or air doors, provided on burner inlets are often adjusted in a fruitless attempt to correct poor air distribution. Blade type dampers severely affect the air distribution within the burner when partially closed, owing to vortex shedding and the tendency to direct the air across the damper blade to the burner wall, Figure 5.39. Clearly the disrupted airflow created by a single (or even a multiple) blade damper will have a severely detrimental effect on the combustion performance of the burner. Furthermore, adjusting dampers to correct airflow distribution is totally ineffective because adjusting one damper affects the flow to all the other burners in addition to the one being adjusted. Once there are more than two or three burners it becomes impossible to balance the flows, even approximately.

Fortunately it is generally possible to correct the air distribution between burners even after the plant has been put into service by modelling the existing installation using water/bead and air to obtain visualisation of the flow patterns and quantitative measurements of the burner airflow distribution respectively. Once the existing condition has been assessed then flow splitters, weirs, bluff bodies, etc, are installed in the model and the model re-tested until the problems are resolved. It is then simply a matter of preparing suitable engineering drawings and installing the improvements on the full size plant. Even the atrocious airflow distribution shown in Figure 5.36 can be vastly improved. Figure 5.40 shows the combustion airflow achieved on this heater following modelling and the installation of appropriate flow correction devices but with no major changes to the ducting.

5.6.4 Common Windbox and Plenum Design

Achieving good air distribution in plenums or windboxes housing a number of burners is a similar problem to multiple burner air supply ducts but, in addition, burners designed for installation in a plenum or windbox generally need the air to flow radially into the burner from all around the periphery, Figure 5.41. Uneven distribution of the radial flow, or a flow with a significant tangential or swirl component, are both likely to lead to severely distorted flames. Indeed, one of the

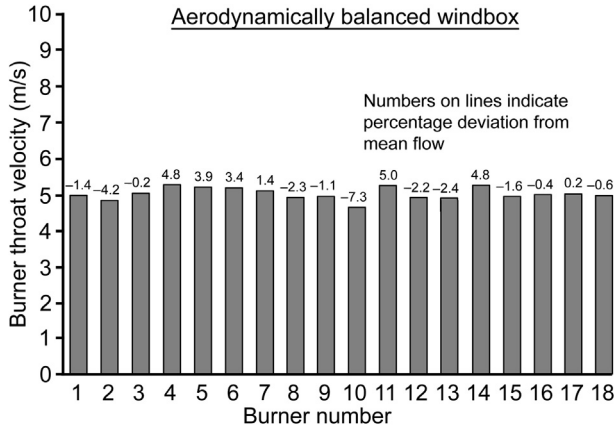


Figure 5.40 Combustion air distribution following modelling and installation of flow correction devices

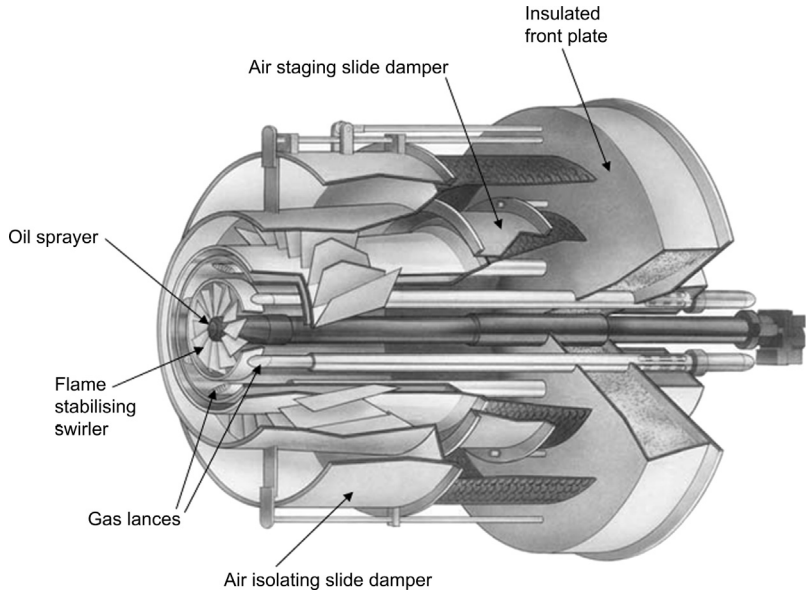


Figure 5.41 Typical Register oil burner - note the radial airflow distribution required for optimum performance

major problems associated with multiple burner windboxes is the formation of swirling vortices around individual burners.

Designing plenums to achieve the required radial airflow is not easy and is generally based on utilising a low air velocity within the

windbox. However, this is not sufficient on its own to ensure good air distribution and flow modelling is required to achieve satisfactory air distribution for low excess air operation. Computational or physical modelling can be used and, in general, the larger the number of burners the more complex and time consuming the modelling becomes. However, it should always be remembered that the cost of modelling represents only a small proportion of the overall installation and saves much time and effort during commissioning by eliminating problems associated with air distribution well in advance. Furthermore, the fuel cost savings arising from improved performance over the life of the furnace are usually hundreds of times greater than the cost of the modelling.

5.7 Combustion System Scaling

Combustion system scaling is required to scale up from lab tests, small scale industrial tests or to scale up from pilot plant. The scaling involved in these processes is often an order of magnitude or more. Such scaling is fraught with difficulties because not all the pertinent features scale similarly; hence the relevant scaling parameters have to be chosen carefully. Failure to choose the correct parameters will result in a furnace that fails to achieve its intended performance. Typical performance shortfalls include reduced output, lower efficiency or inferior product quality. Even scaling up an existing plant to a larger capacity by quite a small factor can cause problems.

The basic scaling techniques are constant velocity scaling, constant residence time scaling and constant combustion intensity scaling. Each is described in more detail below:

- **Constant Velocity Scaling** This technique maintains similar inlet velocities for the small scale and large scale systems. For example, the air discharge velocity from the burner is similar for both the small scale test system and the large system. Sometimes the velocity ratios, rather than the absolute velocities are kept similar in the two systems.
- **Constant Residence Time Scaling** This maintains the gas or particle residence times in the combustion chamber similar between the small scale system and the larger system. It implies that for the larger system, with the larger combustion chamber or furnace volume, the velocities will also be higher. In some systems, where appropriate, the product residence time may also be held constant.
- **Constant Combustion Intensity Scaling** Combustion intensity scaling maintains similar specific heat release rate in the small scale and large scale systems. The heat release is normally chosen to be related to either the internal surface area of the furnace or the

furnace volume. It could also be related to the exposed surface of the product or heat exchange surface. Thus the scaling parameter is usually quoted in kW/m^2 or MW/m^3 ($BTU/hr.ft^2$ or $BTU/hr.ft^3$).

Each method has its advantages and disadvantages and we must choose the appropriate technique for the system being scaled, which requires a fundamental understanding of the limiting factors. The complexity of this topic means that generalisations are not reliable and it is impractical to provide specific guidance for different systems. The appropriate scaling techniques can only be determined by a careful analysis of the system and modelling is a powerful tool to help determine the process limiting factors. Traditional rules of thumb are often used but these tend to become unreliable where large scale-up, beyond previous experience, is involved. For example, rotary kilns have generally been scaled using constant combustion intensity (volume basis) but this method failed for kilns larger than 1500 tonne/d, when constant air velocity and constant product residence time became the more appropriate techniques, see the following example.

5.7.1 Example of Combustion System Scaling

Up until the late 1960s the largest rotary cement kilns typically had maximum capacities of approximately 1000 tonne/day of clinker. A typical dry, or semi-dry, process kiln of this capacity operated with a secondary air velocity of approximately 3–4 m/s and was 4 to 4.5 m diameter inside the refractory and was in the order of 85 m long.

Until this time kilns had been scaled up incrementally over a period of sixty years from the earliest kilns with a typical capacity of 100 t/day to the then current capacity of 1000–1100 t/day. However, the 1960s saw unprecedented economic expansion, and with it greatly increased demand for cement, and soon kilns of 2000 to 3000 t/day were being designed and constructed. During the previous period of incremental size increases, kilns had been scaled up volumetrically; i.e. a constant heat release and clinker production per m^3 of kiln volume, usually keeping a similar length/diameter ratio. This methodology had served the industry well but had resulted in an increase in secondary air velocity from 1–2 m/s for the smaller kilns to approximately 3–4 m/s for kilns of 1000 t/day, depending on the fuel consumption and the secondary air temperature. Scaling up to 2500 tonne/day on this basis gave major problems owing to the increase in secondary air velocity that occurred because the airflow cross sectional area did not increase as much as the firing rate. In reality, the problem was exacerbated because this method of scale-up resulted

Table 5.1 Comparison Between Original and New Scaled-up Kilns

Parameter	*Original Kiln*	*New Kiln*
Production rate (tonne/day)	1100	2500
Specific energy consumption (kJ/kg)	3975	3560
Diameter - inside brick lining (m)	4.6	5.4
Length (m)	85	140
Kiln internal volume (m^3)	1413	3210
Length/diameter ratio	18.5	23
Coal firing rate (tonne/h)	7.2	14.5
Primary air (% of stoichiometric)	20	20
Primary air velocity (m/s)	85	115
Excess air (%)	10	10
Secondary air temperature (°C)	850	1100
Secondary air velocity (m/s)	3.02	5.46
Craya-Curtet Parameter	1.6	1.0

in kilns of over 6m diameter making the tyres very expensive to manufacture, so there was a tendency to increase the *L/D* ratio, further increasing the secondary air velocity. The primary air velocity was increased to compensate, but not sufficiently to maintain recirculatory conditions.

Table 5.1 shows the major operating and design parameters for an existing 1100 t/d kiln and a new kiln scaled on the basis of similar production rate per unit of internal volume. The existing kiln had an internal volume of 1413 m^3, so scaling up to 2500 tonne/day using the basis of constant clinker production per m^3 of kiln volume gave a new volume of 3210 m^3. The designers also increased length: diameter ratio from 18.5 to 23 so the new kiln dimensions were 5.4 m diameter (inside refractory) and 140 m long, compared with 4.6 m and 85 m for the original kiln. Since the specific fuel consumption was reduced by 10% on a kJ/kg basis, the secondary air mass flow increased by a factor of 2.04. However, the increase in flow area was much less, with a new cross sectional area of 1.4 times the original area, hence the secondary air velocity increased from 3.02 m/s to 5.46 m/s. To compensate, the velocity of the primary air was increased to 115 from 85 m/s but this was insufficient to maintain a similar primary/secondary air momentum ratio and the fuel/air mixing deteriorated. This was confirmed by calculation of the Craya-Curtet parameter, which dropped from approximately 1.6 to 1.0, indicating that the flame was now non-recirculatory. With the slower fuel/air mixing, the flame now had lower peak heat fluxes and heat release was delayed, which resulted in a shortfall in output and poor quality clinker. Indeed many large cement kilns based on this scaling technique never achieved their guaranteed production.

The cement rotary kiln is effectively a heat exchange device combined with a moving bed chemical reactor and both functions need to be taken into account during design. To maintain consistent heat transfer patterns requires that constant velocity scaling is used but, to ensure that the sintering reaction is effective requires a constant product residence time. Therefore, in principle, rotary kilns should be scaled up on constant velocity for the combustion with constant residence time for the product. However, this was not practical owing to limits on tyre size and effective compromises had to be found such as reducing the production rate/m^3 of kiln volume. Better still, rather than use empirical scale-up factors, the kiln can be sized on product residence time with the combustion system designed using modelling. For cement kilns the problem was largely resolved by a process change that introduced a stationary pre-calciner furnace to undertake the endothermic calcining reaction and used the rotary kiln to complete the clinker sintering process. In this way, the firing density of the kiln is reduced by approximately 50%, consequentially reducing the secondary air velocity.

Determining the appropriate scale up technique is an important part of the design process and requires that all the relevant controlling parameters are identified before choosing which ones can be relaxed and which must be scaled. This decision can make or break an individual design since different applications require different parameters to be held constant. We can't scale nature; hence all scale up is a compromise and choice of scale up parameters should be made only after careful analysis of the process parameters to determine which of these is the limiting, or most influential, on the operation. Where this analysis cannot be determined theoretically, appropriate modelling can often assist in the choice of scale up parameters and provide for a more rigorous scale up process.

5.8 Furnace Noise

Furnace noise is an important topic because excessive noise is an occupational health hazard and, where it penetrates beyond the site boundary, it is an environmental nuisance. Anyone who has spent time around furnaces will be aware that they tend to be noisy. This noise arises from a number of sources e.g.:

- Fans, pumps, etc.;
- Gas flow though nozzles, valves, hoses, etc.;
- Combustion processes;
- Product movement (where applicable).

Furnace designers have a duty to minimise noise level or limit it to sound pressure levels defined by occupational health and safety

legislation and therefore need to understand how the noise is created and to how to develop a strategy to control it. The objective of this section is to provide an overview of the issues and provide references to more detailed material for those who need it.

The theory of sound was first explained by Lord Rayleigh in the late 19th Century. There is not sufficient space to consider this theory since it requires a book in itself, or at the very least a complete chapter; in any case there are already many excellent texts on the subject. Needless to say Rayleigh's book is long out of print but an excellent text for furnace designers is "Engineering Noise Control, Theory and Practice" by Bies and Hanson (2003). Another useful reference is "Noise Control in Industry" (1991).

Basically, sound is transmitted via wave propagation through gases, liquids and solids, Figure 5.42. It is characterised by the frequency of the wave and its amplitude. Humans can typically hear sound in the range 20 Hz to 20 kHz, with the hearing threshold being at its most sensitive in the 250Hz–16 kHz range. The speed of transmission depends on the density of the medium, with higher velocities in more dense media. Hence, for air and gases at elevated temperature, the speed of sound is lower than for ambient conditions. Sound pressure levels could be measured in SI units, i.e. Pa but this scale is not convenient because it is too compressed, so we use a logarithmic scale known as decibel (dB). However, for occupational exposure limits, we are interested in the response of the human ear so the measurements

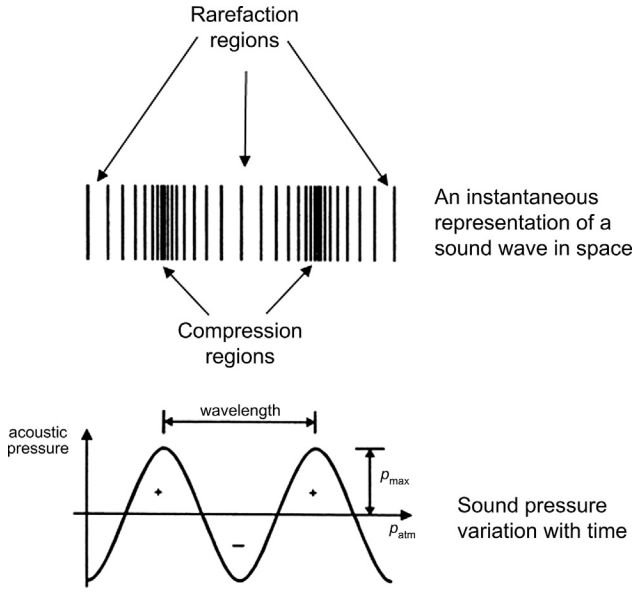


Figure 5.42 Schematic and graphical representation of a sound wave

are weighted using a correction curve. Several correction weightings are available but the most commonly used for human response is the A-weighting and indicated by the symbol dBA or dB(A).

The main duty of furnace designers is concerned with the sound pressure level experienced by people in the vicinity of the furnace and, where appropriate, near the boundary of the plant.

Occupational exposure levels are normally stated as sound pressure levels, e.g. 85 dBA at 1 m from the source. Typical sound pressure levels permitted at the site boundary are in the order of 45 dBA. Noise measurement is particularly difficult since we are rarely measuring just the pressure level from just one source and background noise must be accounted for. Ways of achieving this are explained by Peters (2002).

5.8.1 Combustion Roar

When a flammable gas/air mixture reacts, energy is released and the mixture temperature rises causing it to expand and this expansion creates a pressure wave. Despite the typical appearance of a flame combustion occurs as a series of discrete reactions or flamelets (Turns, 2000). Each of these reactions creates its own pressure wave. The magnitude of the pressure wave is related to the volume of the reacting mixture and the rate of reaction. Larger volumes and more rapid reactions produce bigger pressure waves. Thus the combustion noise arises from the sum of these individual pressure waves. Hence larger and more turbulent flames create more noise. Each reacting flamelet propagates noise in all directions and the sum of all these noise sources produces the combustion roar that we are all familiar with. The randomness of the process produces a wide, low frequency, sound spectrum usually with a single peak, typically in the 200–500 HZ range. Unfortunately, apart from the general trend of larger more turbulent flames producing more noise and pre-mixed flames producing most noise, there is currently no way of predicting the sound power level produced by an individual flame.

5.8.2 Nozzle and Turbulent Jet Noise

Gas issuing from a nozzle at high velocity can create substantial noise and can even be the largest noise source in a combustion system. This source becomes particularly significant if the nozzle velocity exceeds the speed of sound in the fuel, especially for large jets. For this to occur the gas supply pressure must be above the critical pressure which varies with the gas density but is in the order of 110 kPa(g) (15.5 psig). Once the critical pressure is exceeded the jet becomes supersonic and shock waves are established. These compress and expand the

flame gases as they move along the jet and create significant noise. These sources are often at higher frequency than the familiar flame noise and the result is sometimes described as a whistle or screech. Unlike combustion roar, this noise is easily avoided simply by designing for lower gas pressures. While higher gas velocities improve mixing, once the flow becomes sonic there is no further increase in velocity, so only a very marginal mixing advantage is gained compared with using a slightly subsonic nozzle velocity. Hence this shock noise is easily avoided and it is surprising that burner designers continue to size nozzles for pressure drops exceeding the critical value, given that there is so little gain in burner performance but a major increase in noise emissions. Noise is also created by the wave patterns that form in jets. Generally this noise also increases as the jet becomes larger and has a higher velocity and is intimately related to the size of the structures created in the jet. This source of noise can be minimised by using multiple gas ports, instead of one large port, where practical. However, a large number of smaller jets have a lower entrainment capability than a single large jet of the same total momentum, so the fuel/air mixing may be reduced to unacceptable levels if this route is chosen.

5.8.3 Fan Noise

Fans are a major source of noise in industrial plant and can cause nuisance well beyond the site boundary. For example, in the 1980s the noise from an induced draught fan on a rotary kiln, located in a quarry, was creating nuisance in the next valley. The fan concerned was a backward bladed, centrifugal fan and the noise was caused by the fan blades passing the volute throat creating vortex shedding. Although the flue stack was equipped with an attenuator at the top, the tone broke through and could be heard several kilometres away. The problem was eventually solved by cutting a V-notch in the volute throat to minimise the coherence of the vortex shedding. Excellent guidance on the issue of fan noise is provided in Bies and Hanson, pp 511–518.

5.8.4 Pipe and Valve Noise

Fluids, especially gas, air and steam, flowing through pipes also create noise, owing to vortex shedding from internal ridges and flow valve orifices etc. A typical gas valve train is shown in Figure 7.1. Noise is created by flow though valves, filters, flow meters, restrictors, hoses etc and the flow past side branches for pressure gauges and the like. This noise is similar to the nozzle noise discussed above and the sound

power level increases with velocity and pressure drop. This noise can be minimised by designing for lower velocities and by using more pressure reduction stages to reduce pressure. However, this approach involves higher cost because the pipes and valves must be larger and are more expensive. Another technique is to wrap the valves and pipe-work with sound deadening material but this is less effective than low velocity design. Again Bies and Hanson provide guidance on flow through pipes and valves in pages 543–546.

5.8.5 Furnace Noise Attenuation

For a furnace user, the major consideration is the overall noise produced by the system which is the result of all the noise sources, plus the effect of the furnace and duct-work enclosures. The design of the furnace can either reduce the noise emissions or amplify them.

The internal surface of the furnace either absorbs the sound pressure waves or reflects them. The phenomenon of pressure wave reflection is known as reverberation and the total sound within the furnace is a function of both the direct and reverberation sound levels. The topic is complex and extensively covered in Bies & Hanson, chapter 7 but for our purposes, we can consider that the reverberation sound is restricted to a low frequency range and a high frequency range.

The low frequency range is largely influenced by the standing waves which are determined by the dimensions of the furnace. Depending on whether opposing waves meet in phase or out of phase, the pressure is increased by addition, or decreased by cancellation respectively. The point of pressure minimisation is known as a pressure node, whereas the point of pressure augmentation is known as an anti-node. These low frequencies are dominated by the geometry of the furnace. In a limited number of cases this low frequency resonance couples with the burner/flame characteristics and combustion driven pulsations occur, see section 5.8.6 below. By contrast the high frequency sound is more diffuse because at the higher frequency (shorter wavelength) the number of resonant nodes is so large the reverberant field is effectively uniform. The actual noise experienced in the vicinity of the furnace depends on its construction and in particular, the number and size of openings, the ability of the structure to resist excitation, the number and type of burners, the ability of air and flue gas ducting to resist excitation, together with the number and type of extraneous sources.

A practical approach for minimising noise is to ensure that the furnace has heavy construction with the minimum number of openings through which noise can break-out and that these are equipped with heavy, tight sealing doors. This is also important for

minimising in-leakage air. Flat surfaces should be effectively braced or otherwise prevented from excitation. *We must always be wary of inadvertently designing a loudspeaker!* In this respect, cylindrical air and flue gas ducting is preferable to rectangular ducting but is normally more expensive to construct and equip with flow splitters, etc.

Jet noise, another major source can be minimised as described above and by ensuring that furnace openings are not within a region of $\pm 30^\circ$ of the axis of burner jets, although openings facing on to jet axis do not experience excessive noise. This is because jet noise is caused by the entrainment of the surrounding fluid into the jet so is highly directional and the maximum coincides with the jet boundary, shown by the dotted lines in Figure 5.17, i.e. in a region lying between 7° from the axis and 15° from the axis.

Natural draught and induced draught burners present a special problem because the air inlet is very close to the flame and hence there is little attenuation of the noise, such as occurs in the combustion air ducting associated with forced draught burners. Furthermore, most furnaces employing natural draught burners are multiple burner installations, so the additive effect of individual burners needs to be taken into account. These days most natural draught burners need to be equipped with mufflers to meet the required occupational noise exposure levels. The design of suitable mufflers is extensively cover by Bies and Hanson, chapter 9.

5.8.6 Combustion Driven Oscillations

Occasionally, the flame will provide energy to augment the pressure fluctuations at the anti-nodes in the furnace, in the air supply system or in the fuel system and this positive feedback will set up combustion driven, low frequency oscillations. This low frequency noise can be very intense and is very destructive to the furnace structure. In our experience this problem is rare but difficult to resolve when it occurs. It can occur in virtually any type of plant from power station and marine boilers to small premix burners on glass furnace forehearth. Two examples are given below.

In the late 1960s a large natural gas burner being test fired on the large test facility at the Gasunie research station at Groningen in The Netherlands created very severe oscillations when supplied with hot combustion air. The intensity was such that the walls of the furnace pulsated with an amplitude of some 30–40 mm and complaints were received from up to 10km away.

More recently, a pair of flares at the Shell Clyde refinery in Sydney exhibited this phenomenon, but only at high flow rates. When oscillating the flames were highly coherent, Figure 5.43. The oscillations



Figure 5.43 The Clyde Refinery flares in normal mode (left) and oscillation mode (right) (Photos courtesy of Prof. GJ Nathan and Mr A Langham)

could be prevented by reducing the airflow at high gas rates but at the expense of unacceptable smoke emissions. The ambient noise level was over 120 dB at a frequency of 15–20 HZ when oscillating. The cause was traced to flow instability within the gas system in the flare tip, coupling with the resonant frequency of the flare gas supply pipework. Once one flare was oscillating, the sound pressure propagated through the ambient air caused the second flare to oscillate and to lock in-phase. The variation in frequency was caused by the fact that refinery gas varies in its composition and hence its density (molecular mass). The latter affects the speed of sound in the gas and hence the resonant frequency of the gas supply system. The cause was only positively identified after extensive site measurements, followed by a comprehensive and careful analysis of the data, as described by Nathan, et al (2006).

Resolving combustion driven oscillations is often difficult because the acoustic coupling, once established, is normally very strong and difficult to break. For example, in the case of the burner at Gasunie the problem appeared to be related to flame attachment at the gas nozzle, but changes to gas swirl, etc. had no effect on the problem until the conical nozzle was redesigned parallel, with a flat end.

Coupling can occur with the combustion air system or the combustion chamber and, in the case of gas burners, with the fuel supply pipework. The authors have never experienced coupling with coal or oil supply systems. It is probably extremely difficult to couple with an oil supply system since the higher density of oil implies a much higher

sound pressure wave velocity, making low frequency resonance much less likely. Also, the flow-rate of the oil is controlled by the relatively high pressure drop across the atomiser, so that pressure fluctuations in a combustion chamber will not produce oscillations in the fuel flow-rate.

Pulverised coal supply systems are much like air supply systems but the coal particles will modify the characteristics of the system, particularly at the high powder loadings typical with coal conveying systems. It is also likely that the damping effect of the suspended coal particles on pressure oscillations will minimise the risk of coupling.

Today we have more diagnostic tools available to investigate these problems, especially in the analysis of waveforms to enable the identification of the frequencies and their harmonics. These can then be checked against the resonant frequencies of the various chambers, which include the combustion chamber, the fuel supply system and the combustion air system. Calculation of the resonant frequency of pipes and rectangular chambers is relatively straightforward.

For resonant coupling in supply pipework, the chamber is normally very long compared with the diameter. Sharp bends will form nodes while long radius bends significantly less than 90° will approximate to straight pipe, Figure 5.44. For pipes the resonant frequency will be equivalent to the multiples of the wavelength thus a pipe 20 m long could have resonant wavelengths of 20m, 10m, 6.67m, 5m, etc. Hence the resonant frequency can be determined by:

$$F = c/L \tag{5.15}$$

Where:

F = particular frequency (HZ)
c = speed of sound at temperature (m/s)
L= wavelength

For chambers that are relatively wide and deep relative to their length, equation 5.11 can be used to calculate the frequency:

$$F_{\mathrm{n}} = c/2\left[(n_x/X)^2 + \left(n_y/Y\right)^2 + (n_z/Z)^2\right]^{0.5} \text{ HZ} \tag{5.16}$$

Where:

F_{n} = particular frequency (HZ)
c = speed of sound at temperature (m/s)
n_x, n_y & n_z = particular node number (must be a positive integer (inc 0)
X, Y and Z = the furnace dimensions (m)

By comparing the measured frequencies with the calculated resonances, the matching resonance can be identified. An example of a

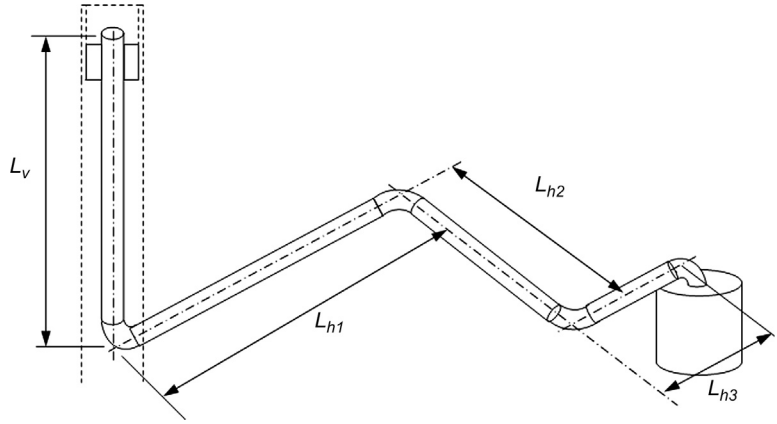


Figure 5.44 Schematic of gas supply pipework for Clyde Refinery flares (Diagram courtesy of Prof. GJ Nathan)

methodical approach to diagnosis of this type of problem is described in Nathan, et al (2006).

Once the matching resonance is identified a strategy for solution of the problem can be developed. However, solving these problems can be very difficult. It is rarely possible to make significant changes to the furnace size or shape and small changes are unlikely to be effective. Changing air ducting or fuel piping is generally easier but still quite difficult and there is no guarantee that the flame would not couple with the new resonant frequency. In our experience almost all effective solutions involve changing the burner to ensure that the new design can't couple with the natural resonance of the system. Generally these changes have been based on trial and error on the full size plant but a recent approach, using physical modelling, to determine the cause of the flow instability within the flare tip installed at the Shell Clyde refinery, is described by Riese et al (2003).

Nomenclature for Chapter 5

A = atomizing air flow rate
A = flow area
c = speed of sound
d_i = the average diameter of a sub-band of drops
d_o = orifice diameter
CV = calorific value of fuel
D_{md} = mass median diameter of spray (microns)
F = frequency (HZ)

F_n = particular frequency (HZ)
FN = Flow number
ΔN_i = the fractional count of drops in sub-band d_i
G = the mass flowrate
$G\varphi$ = Axial flux of angular momentum
$G_x^{'}$ = Axial flux of linear momentum
h = height of air annulus
H = height of the stack
H = liberation of thermal input
k = constant
L = wavelength
m = mass flow
n = constant
n_x, n_y & n_z = particular node number
p = pressure
Q = flow rate
R = Mass residue of particles
R_b = Burner diameter
S = dimensionless swirl number
SG = specific density of gas relative to air
SMD = Sauter mean diameter
V = atomising fluid velocity relative to fuel velocity
w = the pressure ratio of the upstream to downstream pressures P_2/P_1
WI = Wobbe index
x = sieve mesh spacing
x_o = constant
X, Y *and* Z = furnace dimensions

Greek Letters

ΔP = the pressure drop across the nozzle
υ = fuel viscosity
h = height of the air annulus
σ = surface tension of the fuel
ρ = density
Υ = the specific heat ratio for the gas.

Subscripts

m = mass basis
s = stack
a = ambient

References for Chapter 5

Beer, J. M., & Chigier, N. A. (1972). *Combustion Aerodynamics*. Applied Science. pp. 100–146.

Bies, D. A., & Hansen, C. H. (2003). *Engineering noise control, theory and practice* (3rd ed). E&FN Spon.

Drake, P. F., & Hubbard, E. H. (March 1966). Combustion system aerodynamics and their effect on the burning of heavy fuel oil. *Jnl. InstF., 39*, 98–109.

Field, M. A., Gill, D. W., Morgan, B. B., & Hawksley, P. G. W. (1967). *The combustion of pulverised coal*. Leatherhead, UK: The British Coal Utilisation Research Association.

Francis, A, J., The cement industry 1796–1914: A history, David & Charles, p. 255.

Jenkins, B. G. (1976). *Heat Transfer in Rotary Kilns*. PhD thesis. Univ. of Surrey.

Jenkins, B. G., & Moles, F. D. (1981). Modelling of heat transfer from a large enclosed flame in a rotary kiln. *Trans. Inst. Chem. Engrs., 59*, 17–25.

Jenkins, B. G., & Boothman, M. (1996). Combustion science: A contradiction in terms. *Petroleum Tech. Quarterly, Autumn*.

Kelly, N. (Jan 2003). A brief history of oil burning. *Oil heating magazine*. Industry Publications, N.J.

Lefebvre, A. H. (1989). *Atomization and Sprays*. Hemisphere.

Luxton, R. E., Nathan, G. J., Luminis Pty. Ltd., (1988) "Mixing of Fluids", Australian Letters Patent No. 624528, granted 8/1/98, US Letters Patent No. 5,060,867, Granted 29/10/91

McCreath, C. G., & Chigier, N. A. (1973). *14th. Symp. (Int.) on Combustion*. New York: Williams & Wilkins, 1355–1362.

Mullinger, P. J. (1973). *The Design and Performance of Multi-Jet, Internal Mixing Twin Fluid Atomizers*. PhD thesis. Univ. of Sheffield.

Mullinger, P. J., & Chigier, N. A. (Dec 1974). The design and performance of internal mixing multijet twin fluid atomizers. *Jnl of the Inst. of Fuel*, 251–261.

Nathan, G. J., Mi, J., Alwahabi, Z. T., Newbold, G. J. R., & Nobes, D. S. (2006). Impacts of a jet's exit flow pattern on mixing and combustion performance. *Prog. Energy and Combust. Sci., 32*(5-6), 496–538.

Nanthan, G. J., Mullinger, P. J., Bridger, D., & Martin, B. (2006). Investigation of a combustion driven oscillation in a refinery flare, Part A: Full scale assessment. *in Experimental Thermal and Fluid Science, 30*, 285–295.

Peters, R. J. (2002). *The noise and acoustics monitoring handbook*. UK: Coxmoor Publishing Company, Oxford.

Smart, J. P., van de Kamp, W. L., & Morgan, M. E. (1990). The effect of scale on NOx emissions from a swirl stabilised pulverised coal burner. *Fuel, 69*(1111), 1350–1355.

Riese, M., Nathan, G. J., & Mullinger, P. J. (2003). *Flow Visualization in the Scale Model of a Refinery Flare Tip to Identify the Cause of a Combustion-Driven Oscillation*. Australian Symposium on Combustion & The 8th Australian Flames Days, Monash, Vic.

Rosin, P., & Rammler, E. (October 1933). The laws governing the fineness of pulverised coal. *Jnl. InstF.*, pp. 29–36.

The Sound research laboratories Ltd. (1991). *Noise control in Industry* (3rd Ed). E&FN Spon.

Turns, S. R. (2000). *An Introduction to combustion, chapters 12 & 13*. McCraw-Hill.

Whol, K., Knapp, N. M., & Gazley, C. (1949). *The stability of Open Flames*. Third symposium on combustion, flame and explosion phenomena, (pp. 3–21). Baltimore: Williams & Wilkins.

Wigg, L. D. (Nov 1964). Drop size prediction for twin fluid atomizers. *Jnl. Inst.F, 37*, 500–505.

Videgar, R. (November 1997). Gyro-Therm Technology Solves Burner Problems. *World Cement*.

Chapter 6

Combustion and Heat Transfer Modelling

Chapter contents

6.1	Physical Modelling	211
6.2	Mathematical Modelling	217
6.3	Application of Modelling to Furnace Design	238
Nomenclature		239
References		241

Designing an industrial furnace generally requires the simultaneous resolution of transient heat, mass and momentum transfer phenomena in a complex chemically reacting system. It is therefore not surprising that the prediction of the performance of burners, combustion equipment and their furnace environment is extremely difficult, and often imprecise in its execution. For the design engineer, resolution of this intractable problem is to resort to

- Guesswork based on intuition
- simple empirical correlations and extrapolations
- partial modelling.

The first option is the cheapest to implement, but is unreliable, and the implicit uncertainty leads to oversized designs, which are operationally and thermally inefficient. The second option is the product of evolution, and can be used if an existing proven design is being duplicated, but can be very unreliable when scaling up or down, or when changing process demands. Of the three, modelling is indisputably the most reliable technique, relying on the representation of the significant variables of the full size system in a physical and/or mathematical model that is based on sound, proven and validated theory. Modelling is termed as partial because it is not possible to satisfy all the scaling criteria or algorithms required for a complete model. Selecting the significant variables correctly is often termed as the 'art of modelling', and requires the modeller to be skilled in both an understanding of the design objectives, as well as the mechanics of the modelling process. The following quotations taken from Spalding (1979) summarise the designer's dilemma, and some inkling to its solution.

> "To design a combustion chamber it is necessary to at least calculate the flame length, and it would be helpful to know other things, such as velocity profile, temperature profile, radiant heat flux, etc."
> and
> "Generally the chemical reactions are very 'fast', and the flame shape is limited by diffusional mixing of fuel and oxygen"

The methodology of modelling is universal, and consists of five sequential steps:

1. Obtain or derive process and operating data.
2. Design the model(s)
3. Validate the model(s) against measured or design process data
4. Develop an optimised solution using the model(s)
5. Convert the optimised model result to an engineering solution

It is important to understand that any modelling technique will only partially simulate the full-scale system and, as will be explained

in this chapter, it is therefore advisable to use more than one modelling technique to reduce the risk of inadvertently overlooking a significant variable. If we knew what was important when we start, then we would probably not need to model it anyway.

6.1 Physical Modelling

The practice of using isothermal physical scale models to visualise and study furnaces can be traced back to Groume-Grijmailo (1923), although it is through studies carried out between the late 1940's and mid 1960's that most of present physical modelling theory and techniques have been derived. The basic premise that justifies the validity of physical modelling lies in the second of Spalding's statements, that mixing controls the combustion process. This has been discussed in Chapter 2.4, and it is the relative rates of the diffusional processes of mixing and dispersion of products to the kinetics of ignition and reaction that justify the premise that 'mixed is burnt'. This is particularly the case for the turbulent jet diffusion flames encountered in many industrial applications, where jet momentum governs the entrainment and mixing rates.

The mechanics of physical modelling involves the construction of a geometrically scaled model, maintaining faithfully the internal dimensional scale in a clear plastic simulation. Figure 6.1 shows a typical water modelling facility. Models are typically not smaller



Figure 6.1 Physical modelling facility set up for water modelling

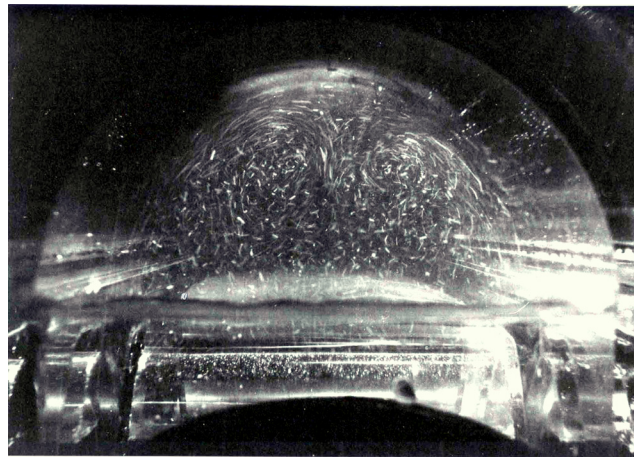


Figure 6.2 Flow visualisation in an arched furnace roof using water bead modelling

than 1/20 full size in order to minimise boundary layer effects in the observed flows. The working fluids in the model are usually water or air. Water is used primarily for visualisation and air for quantitative data collection. For a simple isothermal flow the model is truly similar to the real system if equal Reynolds Numbers are preserved. However it has been shown by Rosin (1936) that true Reynolds similarity is not necessary for scale representations, and a reduced Reynolds number may be used in the model, provided the flow regimes are the same i.e. both fully turbulent. Water modelling aids visualisation since for any given Reynolds number, the velocity of the water flow relative to air is reduced by a factor of ~ 10, making the use of neutral buoyancy tracers, e.g. pre-expanded polystyrene beads, much simpler to 'label' the flows. A typical water flow model is shown in Figure 6.2.

Targeted, pulsed dye injection is used to determine residence time, segregation, etc., giving quantitative information on localised mixing. Acid/alkali modelling, Hawthorn (1939), Ruhland (1965), is used to define the stoichiometric mixing envelope between two or more reacting streams, e.g. fuel and oxidant. Figure 6.3 shows the result of a dynamic simulation of fuel/air mixing in a rotary kiln using the acid/alkali technique. The stoichiometric, or 'mixed is burnt' boundary of the jet is defined by the neutral mixing region, where the pH indicator changes colour. Air modelling is used to measure velocity and/or pressure data over a predetermined grid in some plane of the model using a simple or five hole pitot tube, a hot wire anemometer or laser Doppler velocimetry (LDV). Turbulence and species concentration can be measured in both air and water models using laser

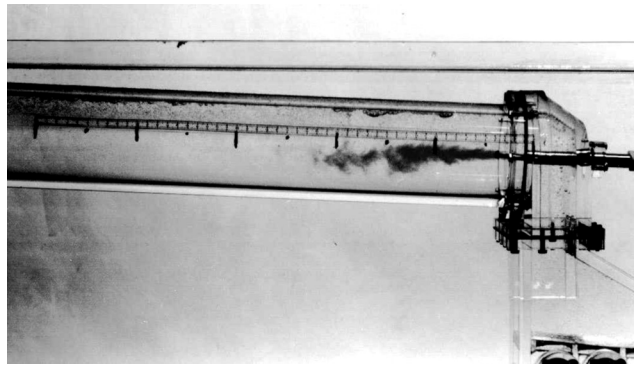


Figure 6.3 Simulation of fuel/air mixing in rotary kiln using acid-alkali modelling

induced Raman or Rayleigh scattering, coherent anti-Stokes Raman spectroscopy (CARS) or laser induced fluorescence (LIF), Goulard (1975).

Physical modelling techniques involve isothermal flows, and can be used directly in the design of ductwork to and from the furnace, and in ancillary equipment (e.g. flue gas filters). This is of particular importance in multiple burner installations fed from a common air supply (e.g. petrochemical process furnaces) where an even distribution of air between burners is an essential prerequisite for efficient operation.

In combusting systems, the generation of heat and molar changes, due to chemical reactions in the combustion process, result in volume changes and buoyant forces in the system. Thus the isothermal model is no longer truly representative throughout the domain, but may be locally correct. The real 'art' is therefore in correctly distorting the flows in the model to generally represent the prototype.

Thus for turbulent jet diffusion flame modelling we must:

- preserve geometric similarity
- use reduced Reynolds similarity for the bulk flow (to enhance visualisation and reduce pump/fan costs)
- apply a suitable jet nozzle distortion parameter

There are four scaling parameters that are most commonly used for jet nozzle distortion in modelling. These are the Thring-Newby (1953) parameter, θ, the Craya-Curtet (1955) parameter, m, the Becker (1961) throttle factor, Th, and the Curtet number, Ct, Becker, Hottel & Williams (1963). These parameters have already been introduced in Chapter 2.4.1.

6.1.1 Thring-Newby Parameter

Using the Thring-Newby parameter as a scaling parameter for non-isothermal jets requires the following relationship to hold true

$$\theta = \left(\frac{(m_o + m_a)r'_o}{m_o L}\right)_{model} = \left(\frac{(m_o + m_a)}{(m_o u_o \pi \rho_e)^{0.5} L}\right)_{system} \tag{6.1}$$

where

$$r'_o = \frac{2m_o}{(m_o u_o \pi \rho_e)^{0.5}} = r_o \left(\frac{\rho_o}{\rho_e}\right)^{0.5} \tag{6.2}$$

Application of the parameter requires that the physical size of the nozzle in the model is equal to r'_o, which is generally larger than the equivalent scaled r_o. This can result in mechanical difficulties in closely confined jets ($r'_o/L<0.05$) where the increased nozzle dimensions distorts the flow channel for the secondary fluid.

6.1.2 Craya-Curtet Parameter

The Craya-Curtet parameter is determined based on the physical conditions of the two fluids where they cross the plane of the end of the nozzle, using the axisymmetric jet derivation. i.e.

$$m = -\frac{3}{2}R^2 + R + k\left(\frac{L}{r_o}\right)^2 R^2 \tag{6.3}$$

where

$$R = \frac{q}{Q} \tag{6.4}$$

$$q = \pi r_o^2 \rho_o (u_o - u_a) \tag{6.5}$$

$$Q = \pi L^2 \rho_a u_a + \pi r_o^2 \rho_o (u_o - u_a) \tag{6.6}$$

For the simple case of an isothermal jet system where both fluids are similar (i.e. as in a water or air model), then $\rho_o = \rho_a$, and this simplifies the derivation. Where the jet and secondary air are of different compositions (e.g. a gas jet), then we need to include the density in the derivation of q and Q. Jet similarity is ensured if the value of m is maintained between the prototype and the model.

6.1.3 Becker Throttle Factor

The self-preserving properties of a jet, whether it is free or enclosed, are used to derive the Becker throttle factor. This relates the dynamic

mean initial jet velocity, u_d, to the kinetic mean initial jet velocity, u_k, where

$$Th = \frac{1}{\sqrt{2}}\frac{u_k}{u_d} \tag{6.7}$$

where

$$u_d = \sqrt{\frac{m_o u_o + \frac{1}{2} m_a u_a}{\pi \rho L^2}} \tag{6.8}$$

$$u_k = \frac{m_o}{\pi \rho L^2} + u_a \tag{6.9}$$

The same criteria for modelling similarity are applied as for the Craya-Curtet parameter.

6.1.4 Curtet Number

The Curtet number also relates the dynamic and kinetic velocities for a jet considered as a point source, and is defined as

$$Ct = \frac{u_k}{u_o^*} \tag{6.10}$$

where u_o^* is the characteristic stream velocity, defined by

$$u_o^* = \sqrt{u_d^2 - \frac{1}{2}u_k^2} \tag{6.11}$$

6.1.5 Relationship Between Scaling Parameters

All of these parameters have been developed from solutions of the basic Navier-Stokes equation, and Table 2.2 shows their numerical range and limitations. θ has only limited application for closely confined flames ($r_o'/D<0.05$), because of excessive distortion at the nozzle, whereas m, Th and Ct are more generally applicable to all confined jets. θ and m are spatially defined, whereas Th and Ct are temporally defined. The value of the scaling parameter must be preserved between the prototype and the model by adjusting the nozzle size or flows. Scaling is only 'true' at the nozzle plane (m, Th, Ct), or in the far field flame (θ)for non-isothermal (combusting) jets. The resulting data must be corrected for temperature and pressure effects.

6.1.6 Determining the Required Model Flows

The volumetric flowrate, $v_{a,}$ of the secondary air stream, which is usually significantly larger than the primary air/fuel stream, is determined for the model by selecting a suitable Reynolds Number, which will ensure turbulent bulk flow throughout the model (viz. $Re \geq 5000$). Thus

$$v_a = 5000 \frac{\pi SL\mu_m}{2\rho_m} \tag{6.12}$$

The stoichiometry of the combustion process will then determine the volumetric flowrate, $v_{o,}$ of the primary fuel stream.

Thus if, for example, we have a fuel which has a stoichiometric air requirement of 10 volumes/volume of fuel, and we are operating at 10% excess air with 20% primary air (of stoichiometric air), then the secondary flow represents

$$10\left[\frac{(100 + 10 - 20)}{100}\right] = 9 \text{ volumes}$$

Thus for this case, $v_o = \dfrac{v_a}{9}$

6.1.7 Applying the Scaling Parameter

The principal of modelling similarity is that the scaling parameter for the full-scale system and model has the same numerical value. Thus we have to calculate the required radii and velocities in the model to meet this demand. As the model scale, S, is fixed, and from section 6.1.6 we have also fixed the volumetric primary and secondary flowrates, the secondary velocity is given by

$$u_a^{model} = \frac{v_a}{\pi(SL)^2} \tag{6.13}$$

The primary velocity is related by a similar equation

$$u_o^{model} = \frac{v_o}{\pi\left(r_o^{model}\right)^2} \tag{6.14}$$

By applying these two velocity relationships into the scaling parameter equation, we develop a polynomial in terms of r_o^{model}, which we can solve to satisfy the scaling criteria. This in practice generally results in a distorted nozzle, which is usually larger than the scale nozzle value.

6.1.8 Applying a Post Measurement Correction

If the jet is a flame, then there will be temperature, and hence density variations throughout the domain of the jet, which will modify the

secondary fluid entrainment and jet geometry. Pressurised combustion also affects the jet mixing process. Experimental work published by Jenkins [1998] indicated that a simple correction factor can be applied to the length scale, X, of any results observed from the model studies such that:

$$X_{system} = X_{model}\ S\left(\frac{\rho_a}{\rho_f}\right)^{0.5}\left(\frac{P_{model}}{P_{system}}\right)^{0.33} \tag{6.15}$$

6.2 Mathematical Modelling

Very early furnace design calculations were based on an initial estimate of convective heat transfer using empirical correlations as discussed in chapter 4.2, with a multiplying factor then applied for the effect of radiation. It was not until the latter half of the 20th century that any form of mathematically rigorous furnace design method was conceivable, when the advent of universally available computation power permitted the solution of the complex radiation flux geometry required to generate local heat balance equations throughout the whole domain of the furnace. Much progress has since been made from the early design equations of Orrok (1925), Lobo and Evans (1939) and Hottel (1954) in developing contemporary zone model methods and computational fluid dynamic (CFD) codes as furnace design tools. One of the earliest attempts at the development of a furnace design formula was that of Orrok who proposed an equation of the form:

$$\frac{Q}{H_F} = \frac{1}{1 + \frac{(\text{Fraction of theoretical air})\sqrt{(\text{Firing density})}}{\text{Constant}}} \tag{6.16}$$

This has been shown by Hottel and Sarofim (1967) to relate crudely to the simple well-stirred furnace model.

Furnace designs can be very simply divided into two basic shapes, rectilinear boxes or right cylinders. In each case their major axis can be horizontally or vertically aligned. This generalisation is particularly true for the radiant sections of at least 80% of all industrial furnaces. It is therefor interesting to examine the influence of furnace dimensions on the thermal efficiency. Figure 6.4 compares the effect of changing aspect ratios for two basic furnace shapes with two types of heat sink, a hearth or bed and refractory backed wall tubes using the Hottel well stirred furnace model described in section 6.2.1. For all the cases, the furnace volume, fuel input rate, combustion air rate, preheated air temperature, and sink volume are held constant.

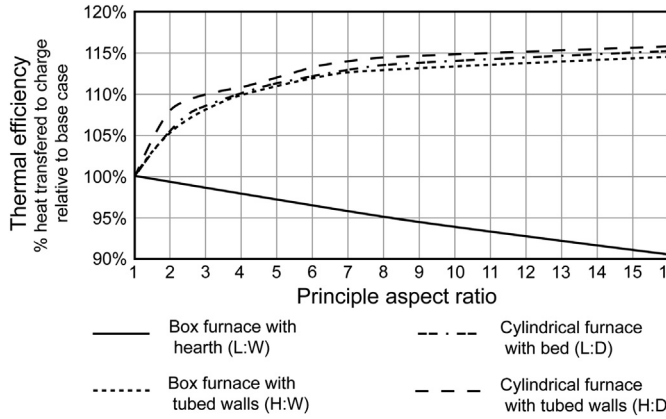


Figure 6.4 Effect of furnace shape on thermal efficiency

Figure 6.4 shows that in all cases except for a box furnace with a fixed hearth, a furnace where the major axis is at least 6 times longer than the minor axis is significantly more effective in transferring heat from the source to the sink. This would therefor imply that furnaces such as glass tanks and open-hearth smelters (box furnaces with a hearth sink) should be square, whilst rotary kilns, boilers and tube-still heaters should be long or high. Examination of such furnaces indicates that this is fairly well borne out in practice; however it is aerodynamically very difficult to achieve well-stirred conditions in a long thin furnace, and thus the potentially beneficial effects of aspect ratios of >6 are not usually completely realised. It should also be noted that these results assume that the sink is assumed to be able to absorb all the incident heat at its surface instantaneously throughout its entire volume.

6.2.1 Simple Well Stirred Furnace Models

The most significant development of a simple furnace model was made by Hottel (1954,1961,1974) and is based on the presumption that many industrial furnaces operate with sufficient momentum in the air and/or fuel streams to create a reasonably well stirred furnace chamber. This assumption allows most of the complex geometric problems associated with radiative heat transfer calculations, see chapter 4.3, to be reduced to a numerically simple solution. For this type of model, the following simplifying assumptions are made

1. Combustion gas mass and flame are assigned a single temperature T_g.
2. Combustion gas is grey with an emissivity ε_g.

3. Surface of heat sink, area A_S, is grey, with an emissivity ε_1, and can be assigned a single temperature T_1.
4. External heat losses and convective heat transfer to the walls (internal and external) are negligible.
5. The sink and refractory wall surfaces are intimately mixed such that the view factors to sink surfaces is the same from all points (speckled wall assumption)
6. The combustion gases leave the radiant section of the furnace at a temperature Δ° below T_g.
7. Convection from the gases to the sink is negligible.

From assumptions 1,2,3,4, and 7 the net heat exchange, Q, from hot gases to the sink is given by

$$Q = (GS_1)_R \, \sigma\left(T_g^4 - T_1^4\right) \tag{6.17}$$

where

$(GS_1)_R$ = total exchange area between gas and sink in radiative equilibrium.

From the assumptions made in 2,3 and 5 this can be calculated from flux geometry as

$$(GS_1)_R = \frac{A_T}{\left(\left[\frac{1}{\varepsilon_g}\right] + \left[\frac{1}{\{C_s\varepsilon_1\}}\right] - 1\right)} \tag{6.18}$$

where

A_T = total internal surface area of furnace (sink[A_S] + refractory walls[A_R])
C_s = cold surface fraction = A_S/A_T

From assumptions 4 and 6 we can write an energy balance

$$\frac{\left(H_f - Q\right)}{H_f} = \frac{(T_g - \Delta - T_o)}{\left(T_{af} - T_o\right)} \tag{6.19}$$

where

H_f = rate of enthalpy derived from fuel + air stream above datum temperature T_o
T_{af} = pseudo-adiabatic flame temperature
$= (H_f/\{mC_p\}) + T_o$
m = mass flowrate of combustion gases
C_p = mean specific heat of combustion gases over range T_{af} to T_o

Eliminating T_g between (6.17) and (6.19) gives

$$\left(\frac{Q}{\sigma(GS_1)_R}\right) + T_1^4 = T_{af}^4\left(1 + \left[\frac{\Delta}{T_{af}}\right] - \left[\frac{Q\left\{T_{af} - T_o\right\}}{H_f T_{af}}\right]\right)^4 \quad (6.20)$$

if we define the following dimensionless groups, we can simplify the above equation

$$Q' = \frac{Q\left(T_{af} - T_o\right)}{H_f T_{af}} \quad (6.21)$$

$$D' = \frac{H_f}{\sigma(GS_1)_R T_{af}^3\left(T_{af} - T_o\right)} \quad (6.22)$$

$$\tau = \frac{T_1}{T_{af}} \quad (6.23)$$

$$\Delta' = \frac{\Delta}{T_{af}} \quad (6.24)$$

thus we have

$$Q'D' + \tau^4 = (1 - \Delta' - Q')^4 \quad (6.25)$$

we can relate Δ' and Q' by the following formula

$$\Delta' = \left(1 - \frac{1}{d}\right)Q' \quad (6.26)$$

where d is a constant of proportionality, thus we have

$$Q'D' + \tau^4 = \left(1 - \frac{Q'}{d}\right)^4 \quad (6.27)$$

It has been further found that for furnaces where $0.02 < D' < 1.0$, d=4/3.

Figure 6.5 shows how the thermal performance of many common furnaces can be related to equation 6.27. It can be seen that analysis of furnaces using this formula implies that the most efficient performance for any given τ is obtained at the largest value of D'. Since D' is a function of $(GS_1)_R$, the implication is that A_T should be as large as possible, i.e. big furnaces are the most efficient. This is an erroneous result relative to practical experience, and is a consequence of assumptions 4 and 7.

If we now make allowance for convective heat transfer, and for radiation losses from furnace openings, we can rewrite equation (6.17) as:

$$Q = (GS_1)_R\sigma\left(T_g^4 - T_1^4\right) + UA_g\left(T_g - T_o\right) + (GS_o)_R\sigma\left(T_g^4 - T_o^4\right) \quad (6.28)$$

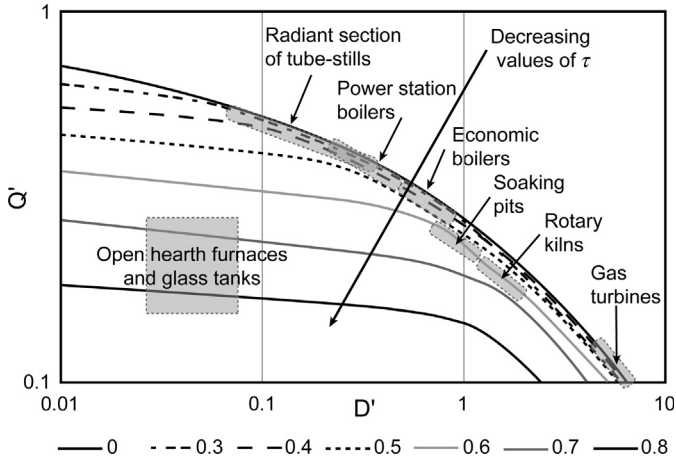


Figure 6.5 Thermal performance of well-stirred furnace chambers

where

U = overall convective heat transfer coefficient
$(GS_o)_R$ = total exchange area between gas and furnace openings, emissivity ε_o, in radiative equilibrium. This can be calculated from flux geometry as

$$(GS_o)_R = \frac{A_T}{\left(\left[\frac{1}{\varepsilon_g}\right] + \left[\frac{1}{\{C_o\varepsilon_{o1}\}}\right] - 1\right)} \tag{6.29}$$

where
C_o = openings fraction = A_o/A_T.

If we eliminate T_g between equations (6.28) and (6.19) as before, and define some extra dimensionless groups as follows

$$\tau_o = \frac{T_o}{T_{af}} \tag{6.30}$$

$$L'_R = \frac{UA_R}{\sigma(GS_1)_R T_{af}^3} \tag{6.31}$$

$$L'_o = \frac{(GS_o)_R}{(GS_1)_R} \tag{6.32}$$

then we can derive a new design equation

$$Q'D' = \left[\left(1 - \frac{Q'}{d}\right)^4 - \tau^4\right] + L'_R\left[\left(1 - \frac{Q'}{d}\right) - \tau_o\right] + L'_o\left[\left(1 - \frac{Q'}{d}\right)^4 - \tau_o^4\right] \tag{6.33}$$

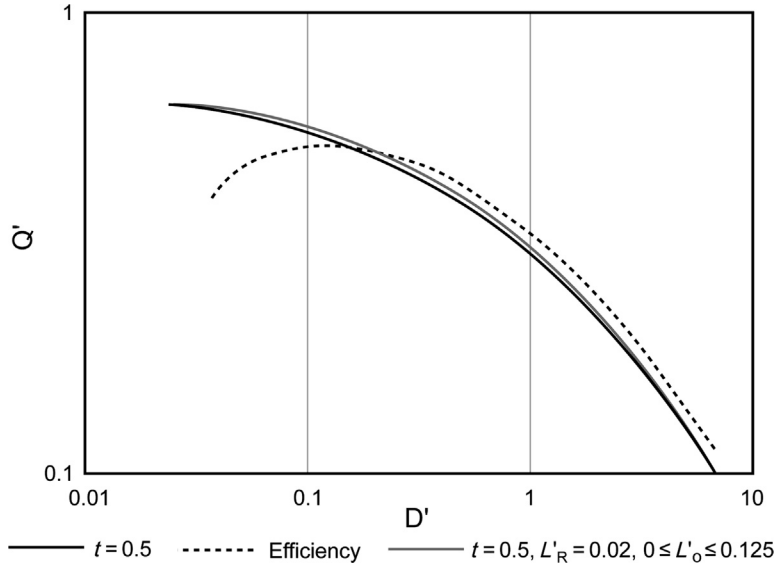


Figure 6.6 Effect of wall loss factor on well-stirrred efficiency equation

the furnace efficiency, η, is then calculated from

$$\eta = \frac{Q - losses}{H_f}$$

$$= \frac{Q'}{1-\tau_o} - \frac{L'_R}{D'}\left(1 - \frac{Q'/d}{1-\tau_o}\right) - \frac{L'_o}{D'(1-\tau_o)}\left[\left(1 - \frac{Q'}{d}\right)^4 - \tau_o^4\right] \tag{6.34}$$

This equation indicates that η reaches a maximum value at a particular D' for any set of τ, L'_R and L'_o conditions, as shown in Figure 6.6, thus we can potentially use equation (6.33) to optimise furnace designs.

Example 6.1 The rotary kiln of a semi-wet process cement plant is 4m internal diameter and 60m long. Process heat is supplied by the combustion of 1.44 kg/s of pulverised coal, conveyed by 1.73 kg/s of primary air at 305°K, and mixed with 10.77 kg/s of secondary air at 1073°K. The net calorific value of the fuel is 30.438 MJ/kg. These figures equate to an excess air rate of 5%.

The material temperature is 750°C, and is 40% calcined, as it enters the kiln from the grate preheater. It leaves the kiln at 1450°C. If the heat loss through the kiln structure is 0.004245 kW/m^2. K and the

charge bed occupies 15% of the total internal surface area, what is the clinker production rate of the kiln?

What would be the effect of changing to natural gas firing (net calorific value 44.59 MJ/kg, stoichiometric air requirement of 13.5 kg/kg)) at the same thermal input and excess air?

Other data

Coal flame emissivity	− 0.9
Gas flame emissivity	− 0.35
Clinker emissivity	− 0.7
Heat of calcination of lime/kg clinker	− 2.11 MW/kg
Heat of formation of clinker	− 1.809 MW/kg
Specific heat of clinker	− 1.089 kJ/kg·K

We will take the datum temperature $T_o = 288$ K (*CV*'s are normally quoted at this temperature)

$$\text{Total internal area } A_T = \Pi \times 4 \times 60 = 754 \text{ m}^2$$

$$\text{Sink area } A_1 = 0.15 \times A_T = 113 \text{ m}^2$$

$$\text{Refractory area } A_R = 0.85 \times A_T = 641 \text{ m}^2$$

$$\text{Cold surface fraction } C_s = 0.15$$

$$(GS_1)_R = \frac{754}{\left(\frac{1}{0.9}\right)+\left(\frac{1}{0.15\times 0.7}\right)-1}$$

$$= 78.26 \text{ m}^2$$

The psedo-adiabatic flame temperature (i.e. neglecting chemical dissociation) is calculated as

$$T_{AF} = \left(H_f / \left[m_f + m_p + m_s\right] \times C_p\right) + T_o H_f$$

$$= \text{Heat of combustion} + \text{Secondary air preheat} + \text{Primary air preheat}$$

$$= 1.44 \times 30438 + 10.7 \times 1.130 \times (1073 - 288) + 1.73 \times 1.005 \times (305 - 288)$$

$$= 53.352 \text{ MW}$$

We need to iterate to a value of T_{af} that agrees with the flue gas C_p.(**note**. this requires a combustion calculation, see chapter 2.2, to determine the flue gas composition).

Guess $C_p = 1.59$ (Flue gases @ 2700K)

$$T_{AF} = \frac{53352}{1.44 + 1.73 + 10.77 \times 1.59} + 288$$
$$= 2695 \text{ K} (\text{this is } \sim 0.2\% \text{ error})$$
$$T_1 = \frac{750 + 1450}{2} + 273$$
$$= 1373 \text{ K}$$
$$\tau = \frac{T_1}{T_{AF}}$$
$$= \frac{1373}{2695} = 0.5095$$
$$\tau_o = \frac{T_o}{T_{AF}} = \frac{288}{2695} = 0.1069$$
$$D' = \frac{H_f}{\sigma (GS_1)_R T_{AF}^3 (T_{AF} - T_o)}$$
$$= \frac{53352}{5.67 \times 10^{-11} \times 78.26 \times 2695^3 \times (2695 - 288)}$$
$$= 0.2552$$
$$L'_R = \frac{UA_R}{\sigma (GS_1)_R T_{AF}^3}$$
$$= 0.004245 \times \frac{641}{5.67 \times 10^{-11} \times 78.26 \times (2695)^3}$$
$$= 0.03133$$

assume $d = \frac{4}{3}$ (Hottel approximation)

$$Q'D' = 1 - \left(\frac{Q'}{d}\right)^4 - \tau^4 + L'_R \left(\frac{(1 - Q')}{d - \tau_o}\right) 0.2552$$
$$Q' = (1 - 0.75Q')^4 - (0.5095)^4 + 0.03133$$
$$(1 - 0.75Q' - 0.1069)$$

rearranging gives

$$0.2787Q' - (1 - 0.75Q')^4 = -0.03752$$

by trial and error for Q' gives

$$Q' = 0.4767$$

but $\quad Q' = \frac{Q(T_{AF} - T_o)}{H_f T_{AF}}$

thus $\quad Q = 0.4767 \times 53352 \times \frac{2695}{2695 - 288}$

$$= 28.11 \text{ MW}$$

From initial equations

$$Q = \sigma(GS_1)_R\left(T_g^4 - T_1^4\right) + UA_R(T_g - T_o)$$
$$28110 = 5.67 \times 10^{-11} \times 78.26 \times \left(T_g^4 - 1373^4\right) + 0.004245 \times 641 \times (T_g - 288)$$

by trial and error for T_g gives

$$T_g = 1732 \text{ K}$$

heat losses $= UA_R(T_g - T_o) = 3.93$ MW

Thus useful heat to charge is $28.11 - 3.93 = 24.18$ MW

The net heat required in the kiln to form 1 kg of clinker is the sum of the sensible heat and reaction energy, thus theoretical process

$$\text{energy} = 1.809 - 0.4 \times 2.11 + 1.089 \times \frac{1450 - 750}{1000}$$
$$= 1.727 \text{ kcal/kg}$$
$$\text{Thus, production rate} = \frac{24.18}{1.727}$$
$$= 14.00 \text{ kg/s} \quad (1210 \text{ tpd})$$

If we convert to gas firing assuming the same thermal input, the gas fuel input rate will be

$$m_f' = 1.44 \times \frac{30.438}{44.59}$$
$$= 0.983 \text{ kg/s}$$

thus the total revised air requirement will be $= 0.983 \times 13.5 \times 1.05 = 13.93$ kg/s

This gives a revised value for the adiabatic flame temperature

Guess $C_p = 1.58$ (Flue gases @ 2500K)

$$T_{AF} = \frac{53352}{0.983 + 13.93} \times 1.58 + 288$$
$$T_{af} = 2552 \text{ K}$$
$$\text{thus} \quad \tau = 0.5380$$
$$\tau_o = 0.1129$$

Substituting the revised value of the flame emissivity into $(GS_1)_R$ gives

$$(GS_1)_R = \frac{754}{\left(\frac{1}{0.35}\right) + \left(\frac{1}{0.15 \times 0.7}\right) - 1}$$
$$(GS_1)_R = 66.25 \text{ m}^2$$
$$\text{and} \quad D' = 0.3775$$
$$L_R' = 0.0436$$

Substituting these values into the design equation, and solving as before gives

$$Q' = 0.422$$
$$\text{thus} \quad Q = 25.38 \text{ MW}$$
$$\text{and} \quad T_g = 1744 \text{ K}$$
$$\text{heat losses} = 3.96 \text{ MW}$$
$$\text{heat to charge} = 25.38 - 3.961 = 21.42 \text{ MW}$$
$$\text{New potential production rate} = 12.4 \text{ kg/s} \quad (1071 \text{ tpd})$$
$$\sim 11.5\% \text{ production decrease}$$

The well-stirred model may also be used to quickly analyse the relative effect of design options such as fuel type and refractory selection, and operating parameters such as air preheating, oxygen enrichment and excess air. As an example, Figure 6.7 shows the combined effects of different fuel options, as defined by their flame emissivity, and the amount of excess air used in the combustion process of a rotary kiln.

6.2.2 Long Furnace Models

The natural progression from the well-stirred model is an extension of the single zone to multiple zones in one, two or three

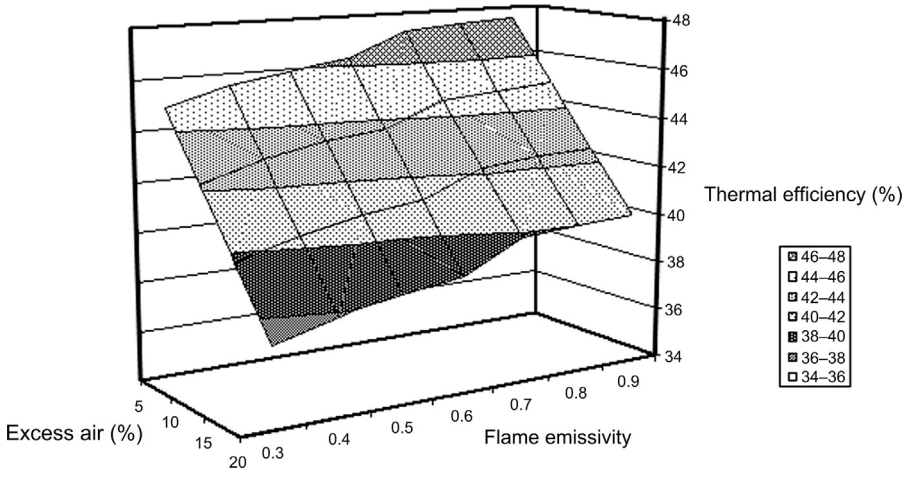


Figure 6.7 The effect of flame emissivity and excess air on furnace efficiency in a rotary kiln

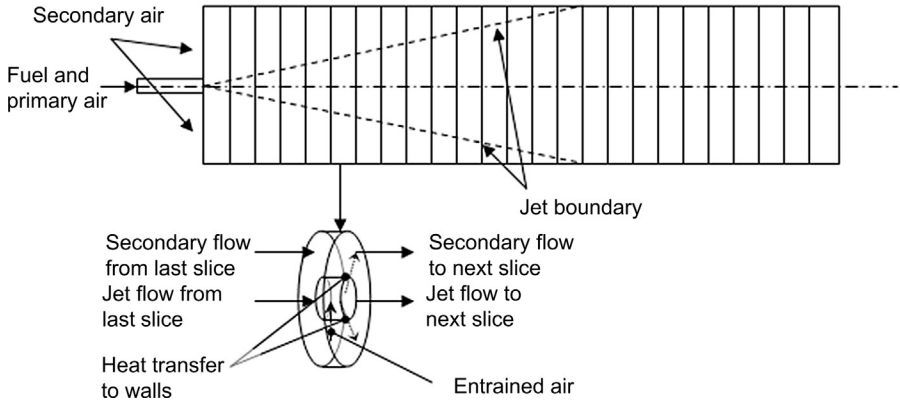


Figure 6.8 Construction of a one-dimensional cylindrical furnace model with jet mixing

dimensions. The one dimensional, or long furnace model is particularly suited to furnace designs with a large length to width ratio, or length to diameter ratio, such as steel re-heating furnaces, or rotary kilns. In this model, the furnace is divided into a series of zones or slices at right angles to the main axis of symmetry as shown in Figure 6.8. Plug flow of gases is assumed, so that mass flow takes place in one direction along the main axis of symmetry. In this geometry, heat transfer occurs predominantly in the radial direction along a central axis of symmetry. Thus a 'marching model' can be used, starting at the end of the furnace where the flows enter, and resolving the mass and heat balance for the first zone, before transferring the resolved flow and enthalpy values to the next adjacent zone. Since longitudinal heat and mass transfer is neglected, the stepping model need only be performed once through the domain to arrive at a solution.

Additional calculation procedures can be included in each zone by introducing radial sub-divisions to model the progress of mixing and combustion, so that a typical model might include:

- Full radiative, convective, conductive heat transfer simulation to the sink in each zone
- A macro-jet entrainment model (chapter 2.4), Ricou & Spalding (1961)
- An internal jet mixing turbulence model (Chapter 2.4.1.2), Pieri (1973)
- Grey gas emissivity approximation for gases, particulates and soot (Chapter 4.3.2)
- An SCRS combustion model (chapter 2.1)

For solid and liquid fuels, the combustion processes are also dependent on the fuel surface and properties, and the SCRS model can be supplemented with:

- A mass weighted multi-band particle size distribution for pulverised coal or liquid fuel
- Volatile and char combustion models (chapter 2.3.4)
- A soot formation/combustion model. Field et. al. (1967), Foster & Howarth (1968)

6.2.3 Two and Three Dimensional Zone Models

The increasing availability of reasonable computational power to academia and industry in the 1970's led to the development of two-dimensional (for symmetrical firing), and three-dimensional (for asymmetrical firing) heat transfer models based on the Hottel zone model, Hottel & Sarofim (1967), flux models, Siddall (1972) or Monte-Carlo models, Steward & Cannon (1971).

The basis of zone models is that the furnace enclosure is divided into volume and surface zones, each having consistent physical and chemical properties (i.e. single temperature, emissivity, chemical composition). From the grid thus generated, view factors and hence direct exchange areas are calculated between each zone and all other zones in the furnace using pre-calculated tables for simple geometries (i.e. rectilinear, cylindrical), or Monte Carlo methods for more complex geometric shapes. From the direct exchange areas, total exchange areas are then calculated, which account for the indirect effect of multiple reflections of radiation at other zones. The radiative and absorptive effects of the combustion gases, soot, particulates, etc, are allowed for by using an approximation based on the weighted sum of a clear plus a number of grey gases (typically 2 or 3). Heat balances can then be formulated for each zone, which also accommodate enthalpy changes due to combustion, flow of gases between zones, chemical reactions, and convective heat transfer.

The first step is to evaluate the direct exchange areas between all surface and volume zones. The calculation methods used are discussed in Chapter 4.3.3. These exchange areas must be evaluated for each absorption coefficient in the grey gas fit as described in Chapter 4.3.2. The next step is to calculate the total radiation incident on/reflected from each zone due to direct exchange and reflected exchange. The leaving flux density, W, at any surface zone is equal to the emitted and reflected fluxes. A radiation balance on surface zone j gives

$$A_j W_j = A_j(\varepsilon_j E_{sj} + R_j) = A_j \varepsilon_j E_{sj} + \gamma_j \left(\sum_k \overline{s_s s_k} W_k + \sum_k \overline{s_s g_k} E_{gk} \right) \tag{6.35}$$

or

$$\sum_k \left(\overline{s_j s_k} - \delta_{jk} \frac{A_j}{\gamma_j} \right) W_k = -\frac{A_j \varepsilon_j E_{sj}}{\gamma_j} - \sum_k \overline{s_j g_k} E_{gk} \tag{6.36}$$

Thus we build up a series of equations similar to equation (6.36) with differing values of flux density for each surface/surface and surface/gas zone pair. From these values of flux density we can calculate the total exchange areas between surface/surface, surface/gas and gas/gas zone pairs, Thus

$$\overline{(S_j S_k)_n} = \frac{A_j \varepsilon_j}{\gamma_j} \left({}_{sj} W_k - \delta_{jk} \varepsilon_j \right) \tag{6.37}$$

$$\overline{(G_j S_k)_n} = \frac{A_j \varepsilon_j}{\gamma_j} {}_{gj} W_k \tag{6.38}$$

$$\overline{(G_j G_k)_n} = \overline{g_j g_k} + \sum_w \overline{g_k s_w}_{gj} W_w \tag{6.39}$$

Where n in the number of absorption coefficients, k_n, in the grey gas fit.

For a given temperature field in the system, the total flux areas for each zone pair are calculated using the temperature dependent grey gas weighting factors, thus for example we have

$$\overrightarrow{S_j S_k} = \sum_n (a_{sn}(T_j)) \overline{(S_j S_k)_n} \tag{6.40}$$

and

$$\overleftarrow{S_j}\, S_k = \sum_n (a_{sn}(T_k)) \overline{(S_j S_k)_n} \tag{6.41}$$

Total energy balances can now be written for all surface and gas zones taking into account convection to surface zones, enthalpy changes in the zone, Q_{ej}, energy release within gas and surface zones, Q_{cj}, and transient terms or storage of energy within gas zones, Q_{ugj}. The basic zone model is not structured to derive the aerodynamic information required for these latter enthalpy factors, and these must be derived from other sources of information such as in-furnace measurements, scaled cold flow models, or computational fluid dynamic simulations (see section 6.2.4). Thus we have for surface zone A_j

$$Q_{jnet} = \sum_k \overrightarrow{S_k S_j} E_{sk} + \sum_k \overrightarrow{G_k S_j} E_{gk} + U_j A_j \left(T_{gk} - T_j \right) - A_j \varepsilon_j E_{sj} \tag{6.42}$$

and for volume zone V_j

$$\sum_k \overrightarrow{G_k G_j} E_{gk} + \sum_k \overrightarrow{S_k G_j} E_{sk} - \sum_n 4 a_{gn} K_n V_j E_{gj} + Q_{ej} = Q_{ugj} - Q_{cj} \tag{6.43}$$

The resulting non-linear heat balances are rapidly converged to a solution using a combination of the Gauss-Seidel and Newton-Raphson methods. The zone method is grid sensitive, but most reasonably sized industrial furnaces would typically require no more than a few hundred volume and surface zones. Provided that the aerodynamic and combustion information is accurate, zone models will provide excellent predictions of the heat transfer processes in a furnace, and there are numerous examples cited in the literature for a wide range of processes.

Figure 6.9. shows gas temperature predictions of a rotary kiln flame, using a three-dimensional (3-D) zone model using 120 gas zones and 46 surface zones. Figure 6.10 show measured flame temperature data for the same kiln, and comparison with the model shows that good agreement for engineering design is achieved.

The applicability of a much simpler 1-D marching model, considering only radial heat transfer from 100mm slices of an axial flame, is compared with the averaged flame gas data from the measured and 3-D models in Figure 6.11. The differences between the 3-D and 1-D models in the 2m to 6m region of the flame are because there

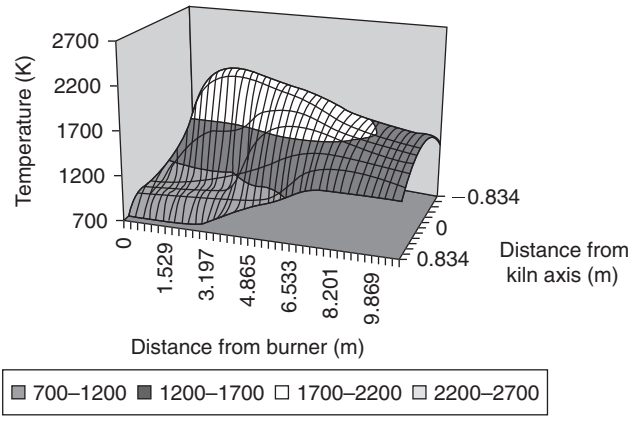


Figure 6.9 Cement kiln flame temperature calculation using 3-D zone model

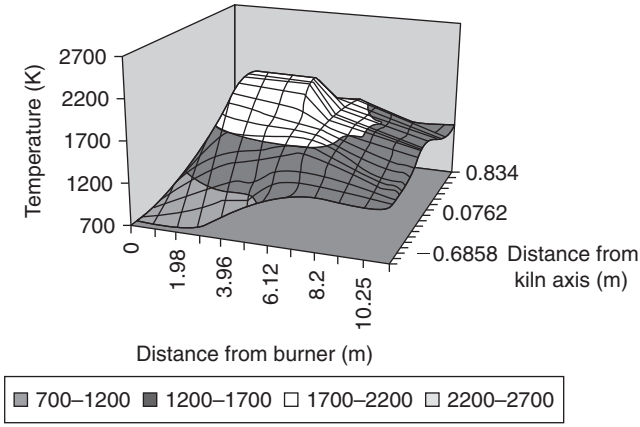


Figure 6.10 Cement kiln measured flame temperatures

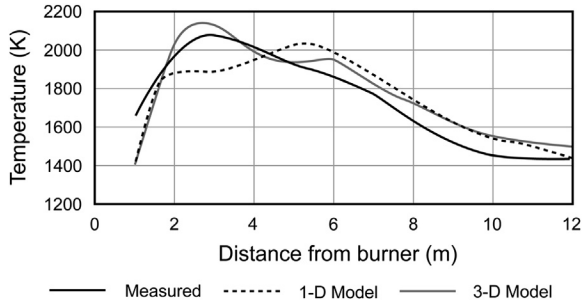


Figure 6.11 Comparison of measured and predicted flame temperatures

is no axial radiation component in the 1-D case. The prediction of wall heat flux, which defines the furnace efficiency, for both the 3-D and 1-D models is presented if Figure 6.12, and compared to a well-stirred furnace prediction using the Hottel model.

It should be noted that the heat flux prediction for the 1-D model is not 'smoothed', like the 3-D model, because these values are only being influenced by the flame temperature in the same vertical plane, and the axial effects of heat transfer from adjacent planes is omitted, however, the predictions for total heat transfer from both models are within ±5%. The well-stirred furnace prediction of 93.5 kW/m^2 is based on the whole kiln (~46m long), and compares favourably with the measured kiln energy consumption (±10%), but gives little indication of the real conditions in the hottest part of the kiln which determines the product quality.

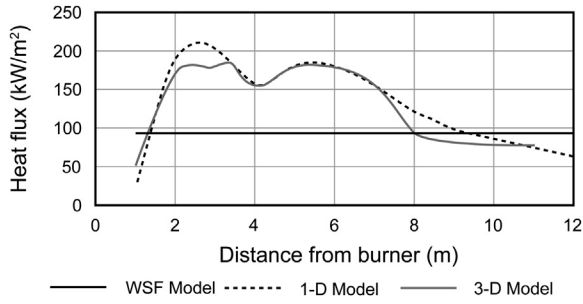


Figure 6.12 3-D, 1-D and well stirred furnace model predictions of wall heat flux

6.2.4 Computational Fluid Dynamics Models

Laws of conservation of mass, momentum, energy, chemical species concentrations, and other physically meaningful quantities and fluid properties govern fluid flow systems. These governing equations can all be expressed in the form of a set of three-dimensional partial differential equations. These equations are given as (6.44) to (6.46). From these differential equations, discretization equations are derived after mathematical treatment. A discretization equation is an algebraic relation connecting the values of a given variable for a group of points within the system.

conservation of mass

$$\frac{\partial \rho}{\partial t} + \frac{\partial \rho V_j}{\partial x_j} = 0 \tag{6.44}$$

conservation of momentum

$$\frac{\partial \rho V_i}{\partial t} + \frac{\partial \rho V_i V_j}{\partial x_j} = -\frac{\partial P}{\partial x_i} + \frac{\partial \tau_{ij}}{\partial x_i} + \rho g_i \tag{6.45}$$

where

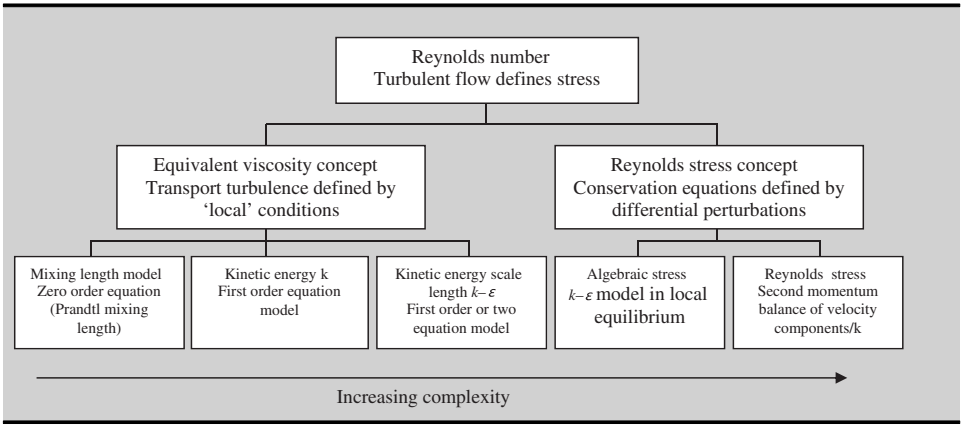
$$\tau_{ij} = \mu \left\{ \frac{\partial V_i}{\partial x_j} + \frac{\partial V_i}{\partial x_i} - \frac{2}{3}\delta_{ij} \frac{\partial V_1}{\partial x_1} \right\}$$

conservation of energy (enthalpy)

$$\frac{\partial \rho h}{\partial t} + \frac{\partial \rho V_j h}{\partial x_j} = \frac{\partial}{\partial x_i} \left\{ \frac{\mu}{\sigma_k} \frac{\partial h}{\partial x_i} + \mu \left(\frac{1}{Sc} - \frac{1}{\sigma_k} \right) \sum_{\alpha=1}^{n} h_\alpha \frac{\partial m_\alpha}{\partial x_i} \right\} + \frac{\partial P}{\partial t} + \dot{q}_{rad} \tag{6.46}$$

All of the variables in these equations are subject to fluctuations about a mean value owing to the phenomenon of turbulence. Turbulence is characterised by a wide spectrum of scales, the smallest of which are very small and cannot be resolved by even the largest computers.

Table 6.1 Hierarchy of Turbulence Models



Turbulence models are therefor required to link the effects of turbulence to the solution of the time-averaged variables. Experience shows that good flow field predictions are only achieved at the expense of very fine grids, and that the more complex turbulence models are more prone to 'instabilities' in the convergence, as well as significantly increasing the time required achieving convergence. Table 6.1 shows the turbulence model hierarchy for CFD modelling. Most recent advances have been made with large eddy simulation models, but theses are still computationally expensive.

The discretized equation conveys the same physical information as, and is solved in place of, the differential equation. The outcome is a theoretical prediction of phenomena involving the flow of heat and material, in terms of distribution in space and time of the temperatures, velocities, pressure, concentrations etc. within the physical system. For a given differential equation the required discretization equations can be formulated in different ways. One of the common methods is the control-volume formulation that can be regarded as a special version of a weighted residuals procedure.

The general form of the discretized steady state conservation equation for a system variable is

$$div\left(R_i\rho_i\overrightarrow{V}_i\Phi_i - R_i\Gamma_{i\Phi}grad\Phi_i\right) = I_\Phi + R_iS_{i\Phi} \qquad (6.47)$$

where

$$\sum R_i = 1$$

R_i is the volume fraction of phase I; ρ_I is the density of phase I; V is the phase I velocity vector; Φ is the conserved property; Γ_Φ is the diffusion coefficient, I_Φ is the inter-phase source term and S_Φ is the source term

Table 6.2 Typical Diffusion Coefficients and Source Terms.

Items	*Conservation of*	*Variable*	Γ_Φ	I_Φ	S_Φ
Mass	Joint continuity equation ⊕ Volume fraction(s) solving.				
Momentum	Gas phase 1	u_1, v_1, w_1	μ_{eff}	$F\vec{i}(\vec{V}_2 - \vec{V}_1)$	$\rho_1 \vec{i}\vec{g} - \vec{i}\, gradp$
	Solid phase 2	u_2, v_2, w_2	0	$-F\vec{i}(\vec{V}_2 - \vec{V}_1)$	$\rho_2 \vec{i}\vec{g} - \vec{i}\, gradp$
Turbulence on continuous phase	Turbulent Kinetic energy	k	μ_{eff}/σ_k	0	G-$\rho\varepsilon$
	Dissipation rate of k	ε	$\mu_{eff}/\sigma_\varepsilon$	0	$(C_1G$-$C_2\rho\varepsilon)\varepsilon/k$
Combustion	Mixture fraction	f	μ_{eff}/Pr	0	0

within a phase. The different values of these quantities for a particular conserved property are listed in Table 6.2.

Gridding of CFD Models

The fine grids required for meaningful CFD solutions present particular problems that are less apparent with zone model grids. The internal surfaces must be accurately defined and these are often complex, and the burner scales are usually much smaller than the furnace. Consequently, complex gridding schemes are required, resulting in long computational times and convergence problems. Pioneers in the use of CFD modelling of furnaces were as severely hampered in the 1980's by the limitations of computer power as the zone modellers were in the 1960's. The validity of predictions was severely compromised by the number of cells used, and grid sensitivity was a major consideration in the modelling process. This is now of less importance, as computational power now allows for grid matrices of $<10^6$ cells on a normal laptop computer. Grids may be

- Structured – These grids are formed from a matrix of standard geometric shapes viz. triangles, rectangles, polygons or cylinders, These may be regularly aligned in a cartesian or cylindrical grid, or 'twisted' into a 'body-fitted' structure.. See Figure 6.13.
- Unstructured – These are inherently 'body-fitted' by using a mixture of cell shapes to best fit the internal geometry and cell interfaces.

The most important factor for grid stability is that the cells can be easily aligned with the flow. Structured grids are generally robust, but whilst triangular cells are easier to fit to complex shapes, they are more difficult to align with the flow. Severe distortion of structured cells in a body fitted shape, e.g. excessive tapering of the cells in the flow

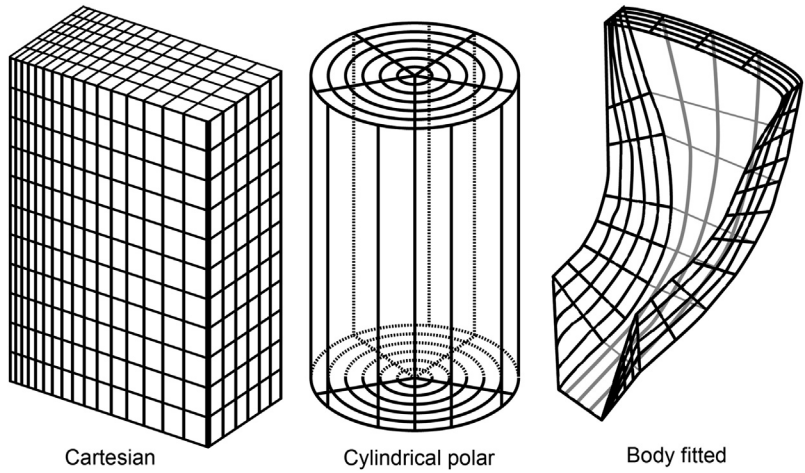


Figure 6.13 Co-ordinate grid systems used in CFD modelling

direction, can lead to numerical instability and drift between the cell interfaces. It is in these cases that an unstructured grid is used.

The obvious desire to minimise the number of cells used in a CFD model has in many cases proved to be the most common source of poor predictions, and resulted in a healthy scepticism of its value by experienced engineers. Axes of symmetry allow the model calculation time to be reduced by resolving one sector and then rotating the result to form a complete model. The danger of this approach lies in the assumption that the system is truly symmetrical, i.e. all physical dimensions have a geometric tolerance of zero, which is never the case in reality. Even small asymmetries, arising from necessary mechanical tolerances during construction will result in asymmetric flows that, depending on the scale, can produce erroneous model results.

Figure 6.14 shows some CFD predictions of flow and temperature distributions in a shaft kiln for the production of high alumina cement. This is an L shaped construction, the lower horizontal section being a molten hearth furnace with burners firing over the surface, whilst the resulting flue gases flow into the vertical packed bed section. The Figure shows two options for the spacing between burners, and it should be observed that even though the two halves of the furnace are effectively symmetric, the resulting flow streamlines and temperature distributions are not. The predictions also serve to show the effect of burner pitch, where the closely spaced burners tend to coalesce into a single forward flowing jet with an external recirculation region, whereas the more widely spaced burners form individual jets surrounded by their own recirculating gas toroid. Experimental evidence of the effect of burner pitching can be seen in chapter 12, Figure 12.20.

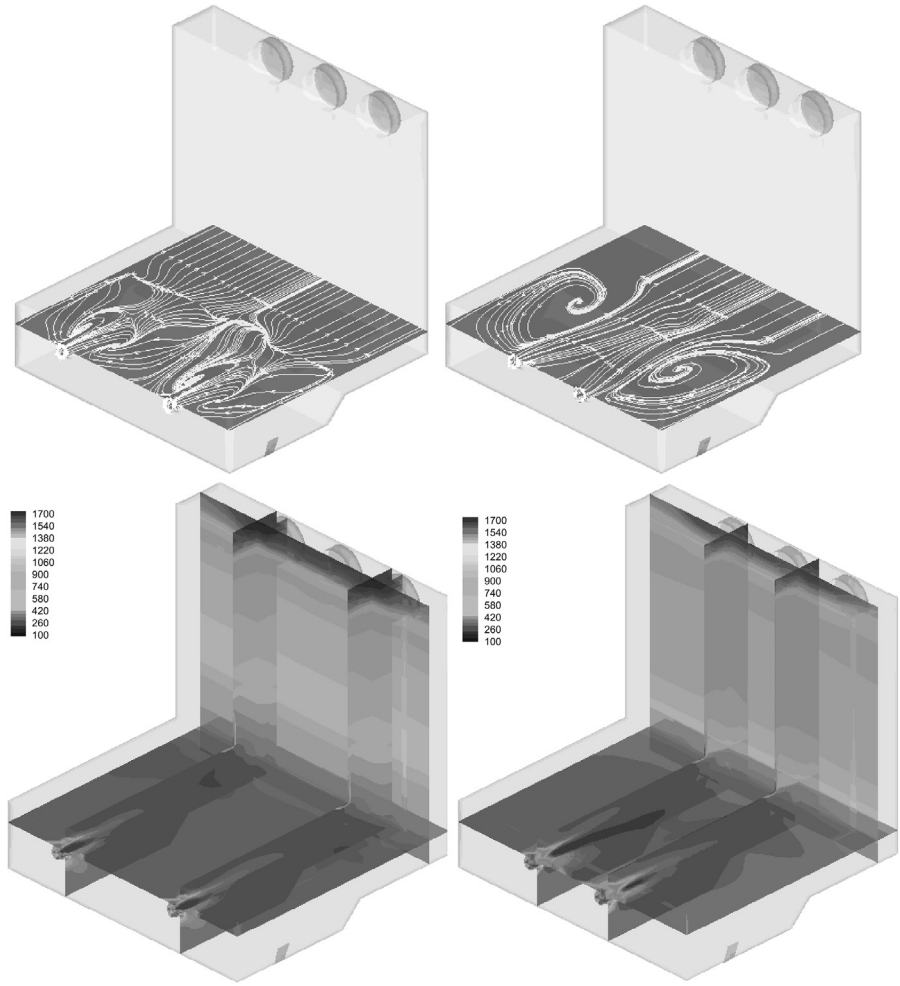


Figure 6.14 Effect of burner spacing in a high alumina cement shaft kiln

Another source of poor predictions is the assumption of even flow distributions at inlet grid points. In chapters 2 and 5 the significance of entry duct flows on the furnace aerodynamics has been illustrated. This is further illustrated in Figure 6.15, which shows how poor wind box design in an existing four burner water tube boiler used for steam raising results in four different flame temperature profiles, lengths and shapes. It should be noted that this CFD model grid included all the air ducting from the fan discharge point, and it was possible to correct the flow using the CFD model in a similar manner to a physical model to determine the size and position of flow deflectors. For a CFD model of a furnace to be valid, the flow fields at all

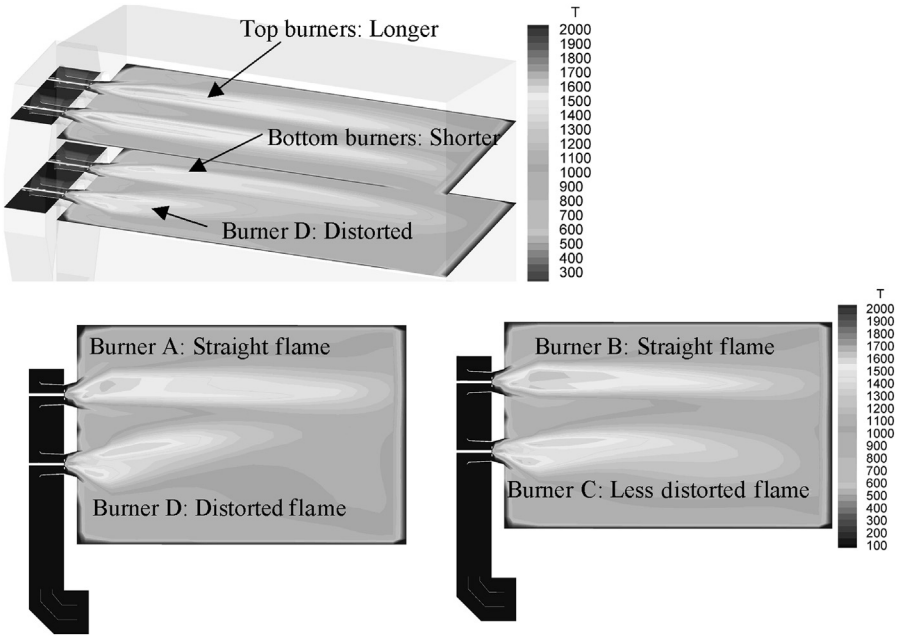


Figure 6.15 Effect of poor windbox design on flames in a four burner water tube boiler

input nodes must be correct. This requires that the flows are physically measured, in the case of an existing furnace, or determined from physical, or CFD modelling of the ductwork back to a known point of even flow, e.g. fan exit, restriction orifice, or flow straightener.

Convergence of CFD Models

All CFD codes use similar calculation methodologies.

- Guess the pressure field throughout the domain
- Solve the discretized equations for the other variables
- Solve the momentum equations
- Compute the field of pressure corrections
- Compute the associated velocity corrections and calculate the velocity field
- Determine the pressure field from the guessed and corrected pressures. Ibid. for the velocity field.
- Treat the new pressure field as the next guesses pressure field. The stored values of the velocity components being used as guessed values in the next iteration.
- Continue iterations until the chosen convergence criteria are met.

It is important in the use of CFD modelling is to ensure that the right convergence criteria are selected. For example for a simple jet,

turbulence is a direct function of the pressure field whereas, for swirling flows turbulence is a function of the [pressure field]^2 and hence a smaller error between values is required for convergence (e.g. if the differential error is set at 10^{-3} for a simple jet it must be 10^{-6} for a swirling jet). A final observation is to note that in cases where the model does not converge this may not be calculation error, but may be an indication of inherent flow instability in the system. Observing the results of each iteration for any cyclic patterns will show this.

6.2.5 Particle Drag in Combustion System

In oil and pulverised coal flames we have to consider the dynamic interaction of the droplet or particle with the surrounding gas. Experimental studies on burning droplets by McCreath, Roett & Chigier (1972) have shown that their trajectories and velocities do not follow the expected paths for non-reacting particles in two-phase flow. It is not possible to physically scale the drag forces on a particle, thus a two phase flow model incorporated into a suitable mathematical model provides a potential tool for simulating the burning particle. This is normally achieved using a slip algorithm to define the relative velocity difference locally between the discrete particles or 'particle clouds' and gas, based on the drag coefficient of the particle and the particle Reynolds Number. By way of example, the inter-phase slip model of Spalding (1981), which considers the slip between two phases (gas and particles) sharing the same space, uses the following equation:

$$F = 0.75 R_1 \frac{c_d}{d_p} \rho u_{slip} \tag{6.48}$$

The selection of the correct slip model is important, since it has been shown that significantly different results can be obtained for the same input parameters, Bertrand, Jenkins & Moles (1997).

6.3 Application of Modelling to Furnace Design

Having reviewed the modelling options in this Chapter, it is evident that there is no complete solution for the design of a furnace. Table 6.3 compares the relative merits and disadvantages of the modelling methods discussed. The correct approach to combustion system modelling is to use as many of these techniques as possible, both to ensure that the individual weaknesses are eliminated, and to internally validate the predictions. The interactions between the various modelling techniques are shown in Figure 6.16.

Combustion engineering has made some remarkable advances in the last fifty years, which have enabled us to predict flames with a

Table 6.3 Comparative Merits of Modelling Methods

Method	*Scaling*	*Turbulence*	*Heat Transfer*	*Mass Transfer*	*Momentum*
Physical	Distortion Parameters Used	Inherently Correct	Isothermal -post corrected	Correct but see heat transfer, no sub-chemistry	Correct but see heat transfer
Mathematical	Coarse grids give 'stepped' answers	'Crude' mixing length models used	Correct	Correct at macro-chemistry scale. Sub-chemistry limited by turbulent model	Relies on other model predictions
CFD	Correct if fine grids are used	Selection of suitable model is critical	Correct	As good as available sub-chemistry data	Correct but see turbulent model

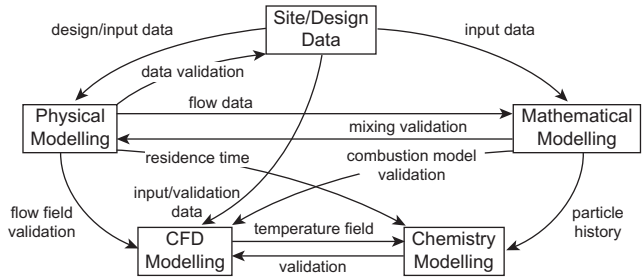


Figure 6.16 Modelling inter-relationship for engineering design

growing degree of confidence. There are still areas where knowledge of the fundamental mechanisms are unclear, particularly turbulent structures in jets and the complex combustion chemistry of pollutant formation, but this should not deter us from trying to implement models to help solve practical engineering problems. The complete process model of a furnace is not yet a universal reality, but the application of good models will always yield better solutions than guesswork or extrapolation.

Nomenclature

A = area
c_d = drag coefficient
C = constant

C_o = furnace openings fraction
C_p = specific heat at constant pressure
C_s = cold surface fraction
Ct = Curtet number
D = firing density
d = diameter, constant of proportionality
E = black body flux density ($=oT^4$)
F = friction force / unit velocity difference
g = gravitational constant
G = generation rate of turbulent energy
$(GS_o)_R$ = exchange area between gas and ambient atmosphere in radiative equilibrium
$(GS_1)_R$ = exchange area between gas and surface 1 in radiative equilibrium
h = enthalpy
H = heat input
I = inter-phase source term
k = jet shape parameter, turbulent kinetic energy
L = half width, heat loss
m = mass flowrate, Craya-Curtet parameter
P = pressure
q = primary jet momentum flux
q_{rad} = energy from thermal radiation
Q = total momentum flux, net heat exchange
r = radius
R = momentum ratio q/Q, volume fraction
S = model scale, phase source term
t = time
T = temperature
Th = Becker throttle factor
u = velocity
U = overall convective heat transfer coefficient
v = volumetric flowrate
V = velocity vector
x,X = length scale

Subscripts

a = secondary
af = adiabatic flame
d = dynamic
e = entrained
eff = effective (also called turbulent or eddy)
f = flame

g = gas
i = refers to phase I
j,k,n = identifiers
k = kinetic
o = starting or ambient
R = refractory
S = sink
T = total
1,2, = identifiers

Superscripts

‘ = dimensionless or normalised
* = characteristic

Greek letters

Γ = diffusion coefficient
Δ = temperature difference
ε = emissivity, rate of energy dissipation
η = thermal efficiency
θ = Thring Newby parameter
Π = viscosity
ρ = density
σ = Stefan-Boltzmann constant
σ_k = diffusion constant
σ_ε = dissipation constant
τ = temperature ratio
Φ = any conserved property

Dimensionless groups

Re = Reynolds Number - $ux\rho/\mu$
Sc = Schmidt Number - $\mu/\rho x$

References

Becker, H. A. (1961). Concentration Fluctuations in Ducted Jet Mixing. *Sc.D. Thesis. M.I.T. Mass*.

Becker, H. A., Hottel, H. C., & Williams, G. C. (1963). *Mixing and Flow in Ducted Turbulent Jets*. New York: 9th Int. Symp. on Combustion. Combustion Inst, 7–20.

Bertrand, C., Jenkins, B. G., & Moles, F. D. (1997). Aerodynamic Simulations of an Industrial Stationary Furnace. *Phoenics Jnl. of CFD and its Applications, 10*(2), 194–211.

Craya, A., & Curtet, R. (1955). On the Spreading of a Confined Jet. *Comptes-Rendus Acad. Des Sciences, 241*, 611–622.

Field, M. A., Gill, D. W., Morgan, B. B., & Hawksley, P. G. W. (1967). *Combustion of Pulverised Coal*. Leatherhead, UK: BCURA.

Foster, P. J., & Howarth, C. R. (1968). Optical Constants of Carbon and Coals in the Infrared. *Carbon, 6*, 719–729.

Goulard, R. (1975). *Combustion Measurements. Modern Techniques and Instrumentation*. Academic Press. Part V.

Groume-Grijmailo, W. E. (1923). *The Flow of Gases in Furnaces*. Wiley.

Hawthorne, W. R. (1939). The Mixing of Gas and Air in Flames. *Sc.D. Thesis. M.I.T. Mass*.

Hottel, H. C. (1954). In W. H. McAdams (Ed.), *Heat Transmission* (3rd ed.). McGraw-Hill. Chapter 4.

Hottel, H. C. (1961). Radiative Transfer in Combustion Chambers. *J.Inst. Fuel, 34*, 220–234.

Hottel, H. C., & Sarofim, A. F. (1967). *Radiative Transfer* (1st ed.). McGraw-Hill. Chapter 11.

Hottel, H. C. (1974). First estimates of industrial furnace performance – the one-gas-zone model re-examined. In Beer Afgan (Ed.), *'Heat Transfer in Flames', Chap.1* (pp. 5–28). New York: Wiley.

Jenkins, B. G. (Feb 1998). *Modelling – it's plastic, mathematic, stochastic, elastic and fantastic. Thermal Energy Engineering and the Environment*. South Australia: Adelaide International Workshop, Univ. of Adelaide, 265–281.

Lobo, W. E., & Evans, J. E. (1939). Heat Transfer in the Radiant Section of Petroleum Heaters. *Trans. A.I.Ch.E, 35*, 743–778.

McCreath, C. G., Roett, M. F., & Chigier, N. A. (1972). A Technique for Measurement of Velocities and Size of Particles in Flames. *J of Physics E: Scientific Instruments, 5*, 601–604.

Orrok, G. A. (1925). *Trans. Am. Soc. Mech. Eng, 47*, 1148.

Pieri, G. (1973). A Mixing Correlation for Annular Concentric Jets. *J Inst. Fuel, 46*, 384--388.

Rosin, P. O. (1936). Aerodynamics as a Basis of Modern Fuel Practice. *J Inst. Fuel, 9*, 287.

Ruhland, W. (1965). The Length of Pulverised Coal Flames in Rotary Kilns. *Schriftenreihe der Zementindustrie, 32*.

Ricou, F. P., & Spalding, D. B. (1961). Measurement of Entrainment by Axisymmetrical Jets. *J Fluid Mechanics, 11*, 21–32.

Siddall, R. G. (1972). *Flux Methods for Analysis of Radiative Heat transfer*. London: 4th Symp. on Flames in Industry. Inst. of Fuel. Paper 16.

Spalding, D. B. (1979). *Combustion and Mass Transfer*. Pergamon Press, 170.

Spalding, D. B. (1981). *Developments in the IPSA Procedure for Numerical Computation of Multiphase Flow Phenomena with Interphase Slip, Unequal Temperatures*. Wimbledon. UK: CHAM Ltd.

Steward, F. R., & Cannon, R. (1971). The Calculation of Radiative Heat Flux in a Cylindrical Furnace usign the Monte Carlo Method. *Int. Jnl. Heat & Mass Transfer, 14*, 245–262.

Thring, M. W., & Newby, M. P. (1953). *Combustion Length of Enclosed Turbulent Jet Flames*. Baltimore: 4th Int. Symp. on Combustion. Combustion Inst, 789–796.

Chapter 7

Fuel Handling Systems

Chapter contents

7.1	Gas Valve Trains	246
7.2	Fuel Oil Handling Systems	249
7.3	Pulverised Coal Handling and Firing Systems	253
7.4	Waste Fuel Handling	283
Nomenclature		287
References for Chapter 7		287

Safe and effective fuel handling systems are an essential requirement of any industrial combustion system. For gas, which is usually provided under pressure at the factory gate, the fuel handling system consists simply of pipework and one or more valve train assemblies. For oil, the system is more complicated and requires storage tanks, normally with heaters, pumping and heating units, pipework and valve train assemblies. Coal handling and firing systems are much more complex than either oil or gas handling systems and require a great deal of mechanical handling plant.

Fuel handling systems, and their components, must comply with appropriate national guidelines and standards such as those promoted by NFPA, DIN, TUV, BSI, ASA, etc. Where local or national standards are not available, the most appropriate of the international standards should be applied.

7.1 Gas Valve Trains

In most countries, prescriptive national standards specify the design of gas valve trains and the components that shall be used. It is important that these standards are referred to when designing or specifying fuel gas systems, since failure to comply can cause significant cost and long delays.

Figure 7.1 shows a process and instrument diagram (P&ID) for a typical gas valve train. The incoming gas is filtered to remove sand and debris to ensure that it does not cause valves to stick or leak. The provision of adequate filtration is essential to maintain the safety integrity of the system. Following filtration, the pressure is reduced and controlled to a constant pressure prior to the flow metering and control system.

The performance of the flow meter and flow control valve are critical where high turndown ratios (>5:1) are required. Particular care has to be taken when selecting and sizing valves for this function to ensure that the required turndown ratio can be achieved.

Probably the most critical part of the valve train is the safety shutoff system. This always consists of two shutoff or block valves and either an intermediate bleed valve or a leak testing system. These systems are described more fully below.

Pipework and valves are sized using normal velocity and pressure drop considerations. Useful information is provided in the *North American Combustion Handbook* (3rd Ed), pp153–199. Higher velocities and pressure drops require smaller valves and pipework and hence results in a cheaper valve train. However, higher velocities and pressure drops also produce higher noise levels, owing to vortex shedding off internal ridges and nozzle noise caused by flow valve orifices, etc. For any particular chosen velocity the noise can be

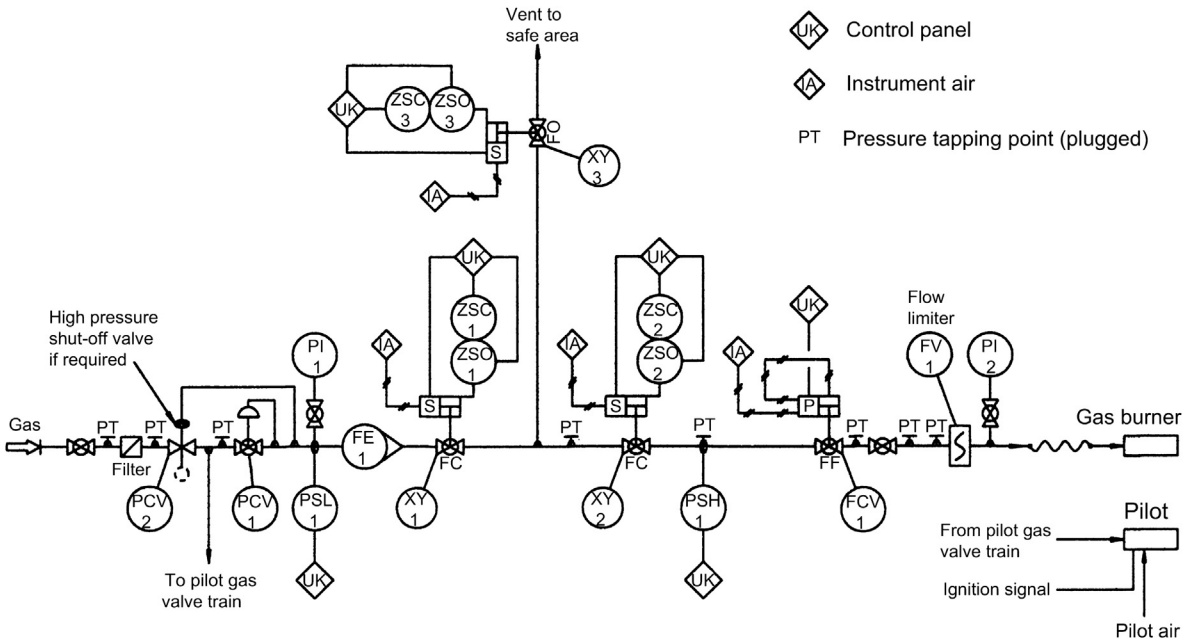


Figure 7.1 Typical Gas valve safety shutoff system - double block and bleed type (Note different requirements apply in different jurisdictions)

minimised by paying close attention to the quality of manufacture, especially ensuring that gaskets fit flush with the internal bore and neither intrude into the pipe, nor create a recessed ridge. All flexible hoses should be smooth bore with corrugated metallic hoses lined using a smooth bore liner. Using this approach, we have utilised velocities around 60 m/s and maintianed acceptable noise levels. Noise can also be attenuated by wrapping the valves and pipe-work with sound deadening material but this is less effective than either low velocity design or minimising vortex generation.

In addition to the main gas valve train most installations require a pilot valve train. This is usually a branch off the main line with its own pressure regulator and double block safety shutoff valves.

7.1.1 Safety Shutoff Systems

The safety shutoff system's purpose is to prevent gas entering the combustion chamber when the burner is shut down. This must be achieved even in the event of a serious malfunction of the shutoff system. A pre-start safety check also normally occurs prior to any attempt to light the burner. The safety integrity is normally achieved by either double block and bleed valves or by using two valves in series with leak testing, together with position proving for the valves. These techniques are described below.

Double Block and Bleed

Figure 7.1 shows the double block and bleed safety shutoff system. It consists of two main block valves in series and a bleed valve between them. When the gas to the burner is shut off both the main valves are closed and the vent valve is open. Thus if gas leaks past the upstream valve it vents safely to atmosphere even if the downstream valve is leaking. When gas is to be supplied to the burner, the vent valve closes and the main valves open. The main gas valves normally have to be proved closed with the vent valve open, before the start up sequence can commence.

Leak Testing and Proving

This system dispenses with the vent valve by undertaking a leak test on both safety shutoff valves during the pre-start purge. The system functions by evacuating or discharging the gas trapped between the valves. The pressure in this part of the valve train is checked for a pre-set period. If the pressure rises, it indicates that the upstream valve is leaking and the start up is abandoned and lockout occurs. Once the integrity of the upstream valve is proven, the space between the valves is

refilled and the pressure again measured for a predetermined time. If the pressure falls it shows that the down stream valve is leaking and again lockout occurs. Thus if a leak is detected in either valve the start-up is aborted.

7.2 Fuel Oil Handling Systems

Despite the high cost of fuel oil, it is still used as a back-up fuel and where natural gas is unavailable. As discussed in Chapter 3, oil fuels are subdivided into distillate fuels, such as kerosene and diesel oil, and residual fuels. In addition, waste lubricating oil is currently being used as a supplementary fuel in a number of plants. While distillate fuels do not require heating, owing to their relatively low viscosities at ambient temperature, residual oils and waste lubricating oils must be heated to reduce their viscosity to approximately 15–25 cSt to achieve satisfactory atomisation and combustion. The only exception to this requirement is the rotary cup atomiser, which can tolerate higher viscosities, up to 40–50 cSt but is rarely used for firing furnaces.

Many fuel oil handling systems installed on existing plants were designed and installed in the 1960s and early 1970s, when fuel oil qualities were much better than they are today. The higher asphaltenes content of today's "cracked" and "reformed" fuels requires better filtration and heating to a higher temperature to reduce the viscosity. Failure of the oil pumping system can cause serious problems since once cold, solidified oil can be impossible to move solely by pumping. Many existing systems would benefit from upgrading. Indeed, upgrading is often essential if newly imposed emission limits are to be achieved.

7.2.1 Storage, Pumping and Heating

Residual fuel oils are far too viscous to pump at ambient temperature, they therefore have to be stored and pumped at elevated temperature in order to reduce the viscosity. Since fuel oil is an emulsion, it should be stored at the lowest practical pumping temperature to prevent it deteriorating. The heaviest oils require continual circulation by pumping to prevent them from solidifying in the pipework. The oil is therefore pumped from the tank to the burner(s) around a lagged and trace heated ring main. For effective atomisation, the viscosity should be less than 25 cSt, preferably 15 cSt at the burner and therefore requires further heating. Steam, electric, or thermal fluid heaters are normally provided for this purpose, see below. A typical ring main with multiple burner off-takes is shown in Figure 7.2. Note the fire safety shutoff valve, which is installed to cut off the oil supply in the event of a fire. It should be installed outside the building where the pipework

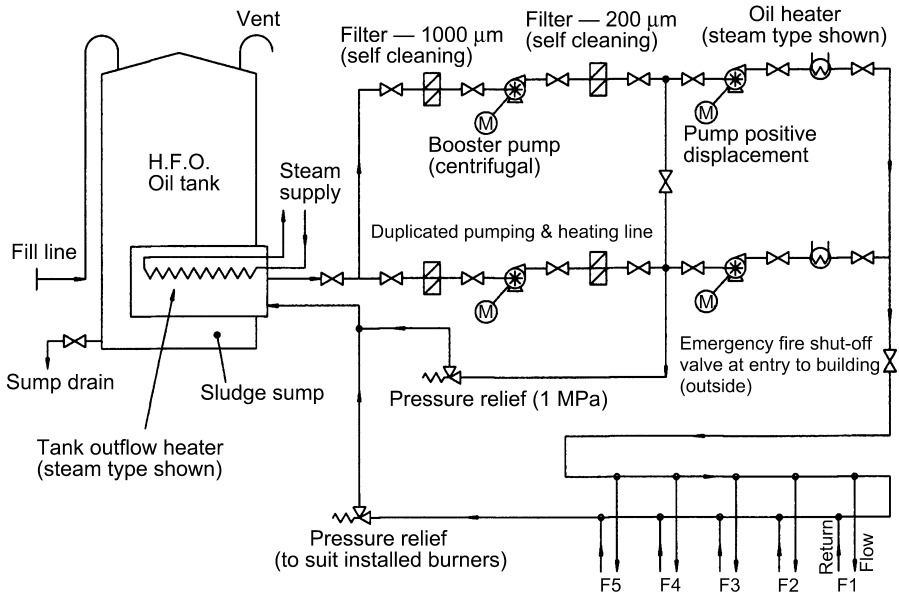


Figure 7.2 Oil system typical ring main with multiple furnace off-takes and steam heating

enters, or in the case of outdoor equipment, just far away from the furnace so that it is not affected by a plant fire. The velocity in the ring main is normally between 1 and 3 m/s depending on the allowable pressure loss. When undertaking pressure loss calculations it is important to use the maximum viscosity of the fuel in the ring main, noting that the viscosity will increase as the distance from the tank increases, owing to the drop in temperature caused by the external heat loss. Pumps, filters, heaters, etc. are normally duplicated to allow servicing while the furnace remains operational.

The pumping and heating unit is a vitally important feature of a heavy fuel oil system and the importance of adequate heating of the oil to the correct atomising temperature cannot be stressed too strongly. The quality of the combustion and the final emissions of unburnt particulates are strongly dependent on the oil drop size, which in turn is dependent on the viscosity of the oil and the atomiser type. The higher the viscosity the larger the oil drops and the greater the particulate emissions. The viscosity/temperature graph for various fuel oils is shown in Figure 3.2. It can be seen that small decreases in temperature cause significant increases in viscosity and hence increased drop size with increased unburnt particulate emissions.

The oil is normally heated by saturated steam or electricity and many heater units incorporate both to ensure the ability to start in the event that steam is unavailable. Steam is the preferred heating

medium because there is reduced risk of local "hot spots" that can occur with electric elements. The latter can cause localised boiling of volatile components combined with the formation of carbon deposits that can lead to downstream blockages and premature element failure, because the deposits reduce heat transfer rates, thus overheating of the electrical element. Steam heaters are conventional shell and tube heat exchangers and for modern oils it is preferable to pass the oil through the tubes and the steam supplied to the surrounding shell. This permits easier removal of sludge deposits from the tube surfaces. The steam condenses in the shell thus giving up its latent heat. Very high heat transfer rates are achieved since liquid to liquid heat transfer occurs and the resulting heat exchanger is therefore relatively small. Provided the steam pressure is controlled so that the steam temperature is a few degrees higher than the target oil temperature, overheating cannot occur. Usually the heaters are factory assembled, together with the filters and high pressure pumps, into a conveniently packaged pumping and heating unit, Figure 7.3.

Many older heaters do not have the heat transfer capacity required to raise high asphaltene, cracked fuel oil to a sufficiently high temperature to achieve acceptable atomisation. This implies that the emissions of oil firing installations are tending to increase owing to deterioration in fuel oil quality, while the environmental requirements are getting stricter. Most old oil firing systems can therefore benefit from upgrading their pumping and heating units to meet the requirements of modern fuel oils. However, the maximum temperature that

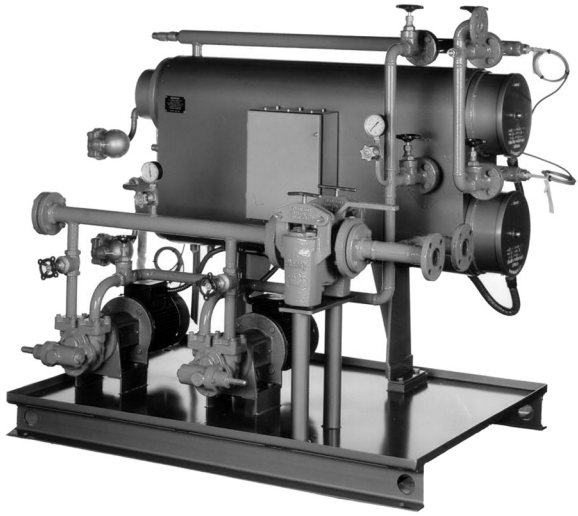


Figure 7.3 Typical pumping and heating unit with shell and tube oil heaters and standby electric heating (Photo provided by courtesy of midland Combustion Ltd.)

can be achieved with steam heaters is dependent on the steam supply pressure, which can make upgrading difficult and expensive if this pressure cannot easily be increased.

On some plants, where steam is not available, or very high fuel temperatures are required, such as for burning bitumen, thermal fluid heating systems are used. Thermal fluids are organic liquids, or silicone based oils, with high flash point and high auto-ignition temperature. Similar shell and tube heat exchangers, such as those used for steam, are employed and the thermal fluid is generally heated in a specially adapted hot water boiler. In all other aspects the fuel handling system is similar to that shown in Figure 7.2.

It is important to note that all pipework needs to be designed and manufactured to the appropriate standards, such as those utilised in the petrochemical industry. This implies using welded and flanged joints and eliminating all screwed joints, except for minor branch connections for instrumentation, such as for pressure gauges, etc.

7.2.2 Oil Valve Trains

The flow of oil to a plant unit, or an individual burner, is normally controlled by a valve train, which allows fuel to flow to the burner(s) only when instructed by the burner management system. The valve train also controls the flow-rate of fuel and hence the heat output of the burner. All valves and components used in the valve train should be "Fire Safe". That is in the event of fire, the valves seal tight and do not leak oil to further feed the fire.

A typical oil valve train arrangement is shown in Figure 7.4. The incoming oil is filtered to remove sand, and debris as well as carbonised oil, to ensure that such debris does not cause valves to stick and leak, or to block atomisers. The provision of adequate filtration is critical to maintain the safety integrity of the system and the performance of the atomiser.

For clarity, the valve train is shown without the trace heating or lagging, both of which are essential to maintain the temperature of the oil and to protect personnel from burns. Great attention must be paid to the elimination of "dead legs" in valve trains and fuel oil systems, since such "dead legs" can cause major problems, especially on start-up from cold. Similarly, provision for automatic purge of oil from the burner is provided to ensure no plugs of cold oil remain after shutdown. For some years tip shutoff burners were used where the hot oil was circulated right up to the atomiser during shut down, eliminating all dead legs. However, tip shutoff atomisers can leak and dribble oil into the furnace providing an explosion risk on the subsequent start-up, so tip shutoff atomisers are now discouraged on safety grounds.

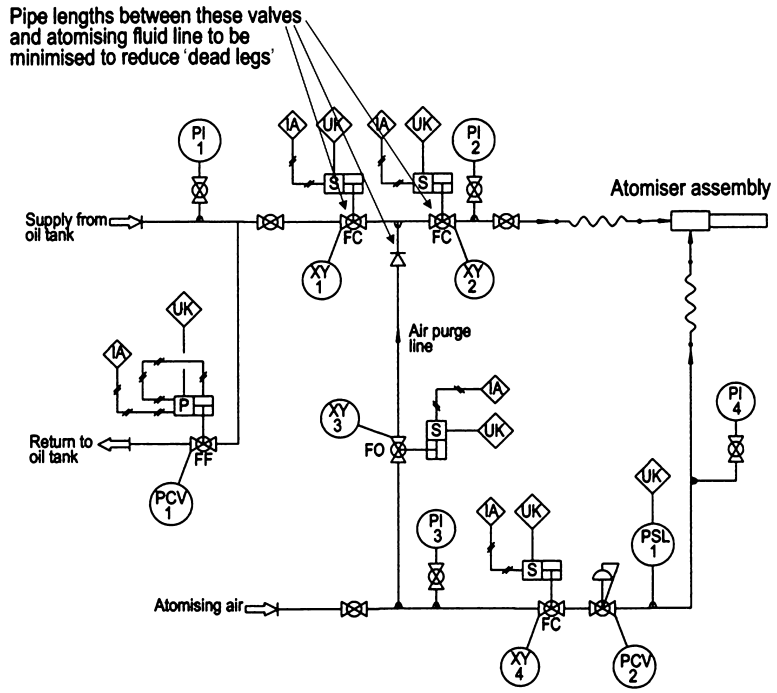


Figure 7.4 Typical oil valve train arrangement

The performance of the flow meter and flow control valve is important where high turndown ratios are required (>4:1). Particular care is necessary when selecting and sizing valves for this function to ensure that the required turndown can be achieved.

In addition to the oil valve train most installations require a pilot gas valve train. This is usually a totally separate unit and generally similar to that used for gas burners.

7.3 Pulverised Coal Handling and Firing Systems

Pulverised coal (PF) firing has many advantages over other forms of coal firing and makes burning coal similar to oil firing from a process viewpoint. Since coal is generally cheaper than either oil or gas it becomes the economically preferred fuel where the ash and trace chemicals can be accommodated by the process. However, a pulverised coal firing system is both more complex, and more hazardous, than other fuel systems. Despite the hazards, few codes and standards are available for PF systems. The most relevant general code is NFPA 8503: Standard for Pulverised Fuel Systems, (1997).

Pulverised coal firing has grown in importance as power stations, steel mills and cement plants have grown larger. Despite the resources lavished on so-called "clean coal technology", fluidised beds, coal gasification, etc., have made little real inroad to the quantity of coal burnt in the pulverised form.

Raw coal reception, storage and handling are a vital part of any coal firing system. Care should be taken to ensure that the coal is not degraded by contamination with soil and rock, nor allowed to degrade by spontaneous combustion. Any deterioration in the coal is a severe, but often unnoticed, financial loss. Most of these problems occur owing to incorrect design of the facility (especially storage) in the first instance rather than errors by the operators. The losses associated with coal degradation can run into hundreds of thousands of dollars per year.

Design of raw coal storage facilities is a specialist topic, not covered here owing to lack of space, but increased complexity does not necessarily imply better storage or reclaiming. Many an open stockpile is a satisfactory store, while spontaneous smouldering and burning often lead to huge losses in covered stores. The most important factor is to use the appropriate technique for the particular application and for the quantity and type(s) of coal stored.

Most pulverised coal firing systems follow a similar basic form, with the raw coal stored in a bunker and fed to the coal grinding mill. The airflow through the mill dries the coal and carries it out of the mill, either directly to the burner, or to a pulverised coal storage facility and thence to the burner. These systems are considered below.

7.3.1 Raw Coal Bunkers and Feeders

The critical issue with designing raw coal bunkers is to ensure mass flow, rather than rat-hole flow, Figure 7.5. Mass flow ensures "first in-first out" utilisation, whereas rat-hole flow implies "last in-first out" and leads to stagnant coal remaining in the bunker indefinitely or for very long periods. This introduces a significant risk of spontaneous combustion, a hazard that must be avoided at all costs.

To ensure mass flow, raw coal bunkers need very steep sides and large discharge openings. Therefore a raw coal bunker is very tall to achieve the required storage capacity. For convenience most bunkers are rectangular and this requires that the resulting valley angle in the discharge chute is large to prevent coal sticking, Figure 7.6. The minimum angle is dependent on the angle of repose of the coal. Tests can be undertaken to determine this factor. Bunkers are usually lined to minimise the friction between the coal and the walls. Glass and basalt tiles, rubber, PTFE and austenitic stainless steel are commonly used

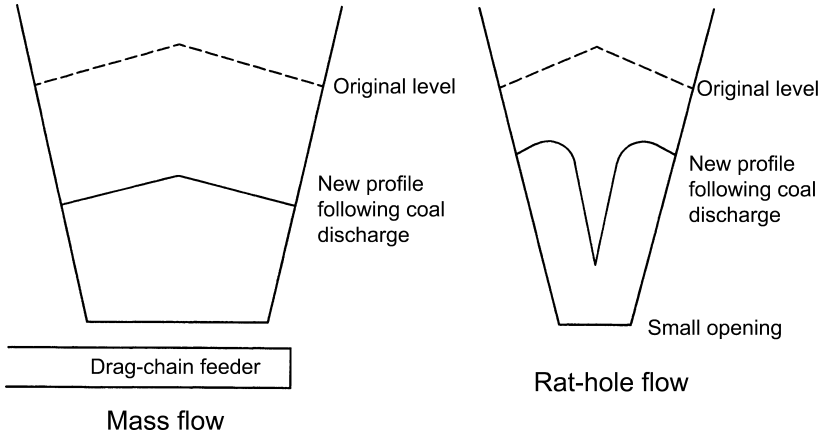


Figure 7.5 Rat hole and mass flow

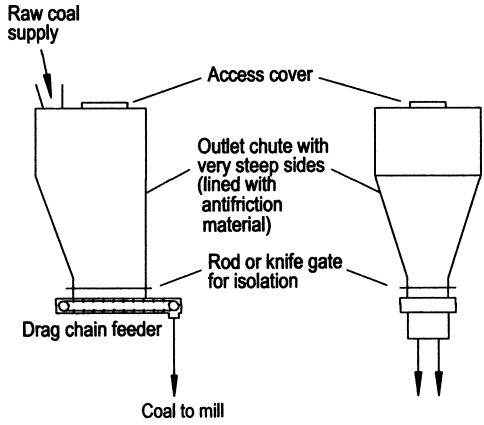


Figure 7.6 Raw coal bunker and feeder

materials. Mass flow hoppers are subject to large lateral forces caused by the movement of the coal during discharge. The calculation of these forces and the sizing of the appropriate steel work is a specialist task (Arnold, et al 1979).

Raw coal can be extracted from bunkers by a variety of devices. Coal mills require a reasonably even feed-rate of coal. This is particularly important with direct coal firing systems, see below. The most suitable feeders are enclosed drag chain type such as the Besta or Redler feeder. Open belt feeders and pan feeders are also used but introduce an increased risk of coal spillage and an associated fire and

explosion risk unless the spilled coal is cleaned up promptly. Screw feeders and table feeders are also found on smaller installations. These feeders are particularly susceptible to hold ups in coal feed owing to their relatively small inlets which limits the size of the bunker outlet; hence they cannot be relied on to give a consistent feed-rate of coal. Sometimes air locks are installed between the feeder and the coal mill and these tend to cause coal hold up, which can result in loss of coal feed to the mill, thus introducing an explosion risk. This is caused by rapid increase in mill temperature that occurs when the heat sink created by the coal drying process is lost.

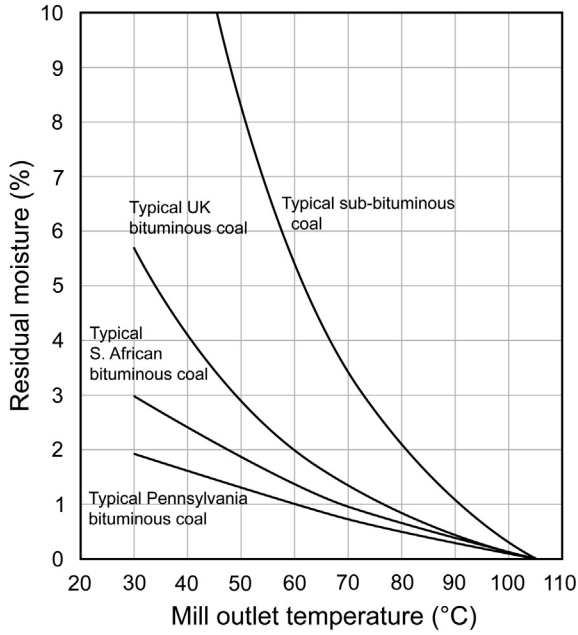
7.3.2 Coal Grinding and Drying

To produce pulverised coal the raw coal must be dried, ground and classified. The coal needs drying so that the particles of fine coal do not stick together and form a coagulated mass. Drying and grinding are both carried out in the mill, normally using a hot air or hot gas stream to dry the coal. We will consider the drying characteristics of coal before describing the grinding mills commonly used for coal firing.

Coal Drying Characteristics

Coal has two types of moisture, surface or free moisture and inherent or hydroscopic moisture. The water is removed by heating the coal to dry it. The surface, or free moisture, evaporates first. Higher temperatures are required to remove the inherent or hydroscopic moisture. The coal should be dried just sufficiently to make it handleable. This involves removing all the surface moisture and, to ensure that this occurs, some inherent moisture is also removed. The temperature required to remove the moisture is dependent on the individual coal, and is characterised by de-watering curves, Figure 7.7. It can be seen from the few examples shown, that different coals have quite different drying characteristics.

Care should be taken not to remove an excessive proportion of the inherent moisture since this increases the fire and explosion risk. This means that the milling system must be designed for the type of coal that is going to be used. If the coal is over-dried it becomes hydroscopic and moisture from the atmosphere recombines with the fine coal. This reaction is exothermic and causes heating of the coal. If sufficient moisture recombines over time, the coal temperature will rise and the coal will spontaneously ignite. We will return to the topic of drying later but before we do we need to consider the coal grinding process, the type coal mills commonly used and the associated firing systems.



Note: These drying curves are illustrative only. The shape of a coal drying curve depends strongly on the seam of origin, the ash content and the physical condition of the coal.

Figure 7.7 Coal drying curves (After FL Smidth)

7.3.3 Coal Mills

The coal mill is the heart of the firing system and the characteristics of the mill determine the types of firing system in which it can be used. The grinding, airflow and drying capacity are critical considerations when selecting a coal mill. It is always necessary to consider the possibility of future fuel changes also; few if any coal firing systems more than ten years old are processing their originally specified coal.

Coal is ground by three basic mechanisms:-

- Crushing between balls cascading in a rotating tube (ball mills)
- Crushing between rollers and a rotating table or bowl (vertical spindle mills)
- Impact with high speed rotating elements (high speed mills)

Following grinding, classification usually takes place with the oversize returned for regrinding. A general comparison between the different types of coal is provided in Table 7.1 and more detailed consideration follows.

Table 7.1 General Comparison Between Ball, Vertical Spindle and High Speed Mills

	Airswept Ball Mill	*Vertical Spindle Mill*	*High Speed Mills*
Drying method	In drying chamber before grinding.	In airstream after grinding.	In grinding chamber.
Drying capacity	10–14% maximum.	20–25% maximum.	8–12% maximum.
Mill airflow range	1.5–2.5 air/kg coal.	1.5–3.5 by air/kg coal.	2.6–4.8 kg air/kg coal
Maximum mill inlet temperature	250–300°C	300–400°C depending on type.	Up to 510°C depending on manufacture.
Classifier	External.	Internal.	None.
Classifier-returns	To mill inlet or outlet.	To grinding zone with raw coal.	–
Turndown ratio	Very restricted.	2:1	Large turndown ratio.
Suitability for direct firing	Possible but poor turndown and low inlet temperatures restrict use.	Suitable except where limited by low mill inlet temperature or high mill airflow requirements.	Suitable but may need external booster fan to obtain adequate primary air momentum.
Suitability for indirect firing	Suitable.	Suitable.	Possible but rarely used in this role.
Wear rates	Low	Moderate but depends on mechanical design.	High.
Typical power requirement for coal	35–55 kWh/t (indirect) 25–30 kWh/t (direct)	18–25 kWh/t (direct)	16–20 kWh/t (direct)

Ball Mills

Many manufacturers produce ball mills, sometimes know as tube mills, for grinding coal. Ball mills are simple and rugged in their design and construction and are particularly suitable for grinding hard and abrasive coals and petroleum coke, but they have a lower drying capacity and higher specific power consumption than vertical spindle mills. A typical ball mill is shown in Figure 7.8. Raw coal is fed through the hollow trunnion into the rotating mill cylinder. It is important that coal does not accumulate in this inlet because the hot airflow will dry it out, presenting a high risk of spontaneous ignition. Although smouldering coal in this region is unlikely to ignite the incoming raw coal, there is significant risk of igniting the dry classifier rejects that are returned to the mill inlet for re-grinding, especially in the event of raw coal flow failure. Ignition of this fine coal will most likely lead to a coal mill explosion. This risk is very difficult to eliminate by improved design of the inlet, so considerable effort needs to be directed towards preventing coal feed failure. In the event that the feed

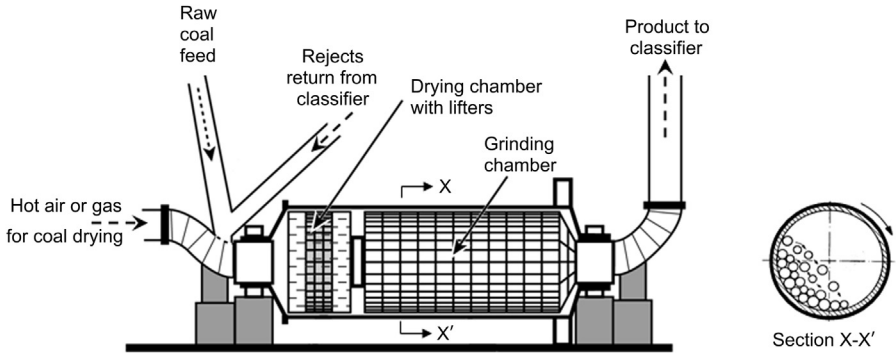


Figure 7.8 Ball mill for grinding coal with integral drying chamber

does fail, the hot air must be immediately cut off and the mill flooded with inert gas (CO_2 or N_2) to minimise the explosion risk. Sometimes, as described later, flue gas is used in place of hot air to reduce the explosion risk.

For coal moistures of 10% or more, a drying chamber is installed before the grinding compartment. The coal is distributed in the hot gas stream by lifters and dried by direct contact with the hot gases. A lifting diaphragm conveys the dried coal into the grinding chamber where it is ground by the combined action of pressure, friction and ball impact. Crushing occurs in the early part of the chamber with fine grinding near the exit. Large balls (75–100 mm) crush the coal and small balls undertake the fine grinding. The chamber section is either compartmentalised to keep the balls apart or fitted with a classifying lining. The mill airflow conveys the ground coal from the mill to the classifier which separates the oversized coal and returns it to the mill inlet for re-grinding. This introduces the risk of spontaneous ignition and explosion discussed above, particularly if deposits are allowed to build up in the mill inlet.

The drying capacity of the mill is limited by the maximum permitted mill inlet temperature and the air velocity through the mill. Normally the mill inlet temperature is limited to 250–300 °C to prevent overheating of the trunnion bearing and for safety reasons. The airflow rate is normally in the range 2.0–2.5 kg air/kg coal. Since the ball mills normally operate under considerable suction, and the seals are difficult to keep gas tight, significant air inleakage is normal with up to 20% false air being common, thus the drying capacity is limited to raw coals with maximum moisture contents of approximately 10–12% (less, if more false air is present).

Vertical Spindle Mills

Vertical spindle mills have a greater drying capacity than ball mills because they can accommodate a higher heat input. Airflows of up to 3.5 kg air/kg coal with up to 400 °C inlet temperature are possible. On the other hand, some vertical mills can operate with as little as 1.8 kg air/kg coal and these are particularly suitable for direct firing of rotary kilns.

A vertical spindle mill is much more complex than a ball mill and therefore there are many more variations in the mechanical design, which in turn, has a considerable influence on the wear rate, availability and maintenance costs of the mill and minor changes in design can have a dramatic effect on these factors. It is therefore advisable to choose a mill which has a good service record on similar applications. Two examples of vertical spindle mills are shown in Figure 7.9, which shows a conventional roller mill and the ball ring mill such as the Babcock E-Mill and the Claudius Peters EM mill. The roller mill employs three or four rollers pressing on a rotating table, while the E-Mill and EM mills employ a number of large diameter hollow steel balls located between two grinding rings to crush the coal.

The grinding table, or the lower grinding ring (ball ring mill), is mounted on a yoke which is driven by the vertical shaft, whilst the rollers or upper grinding ring (E Mill) are held stationary. The

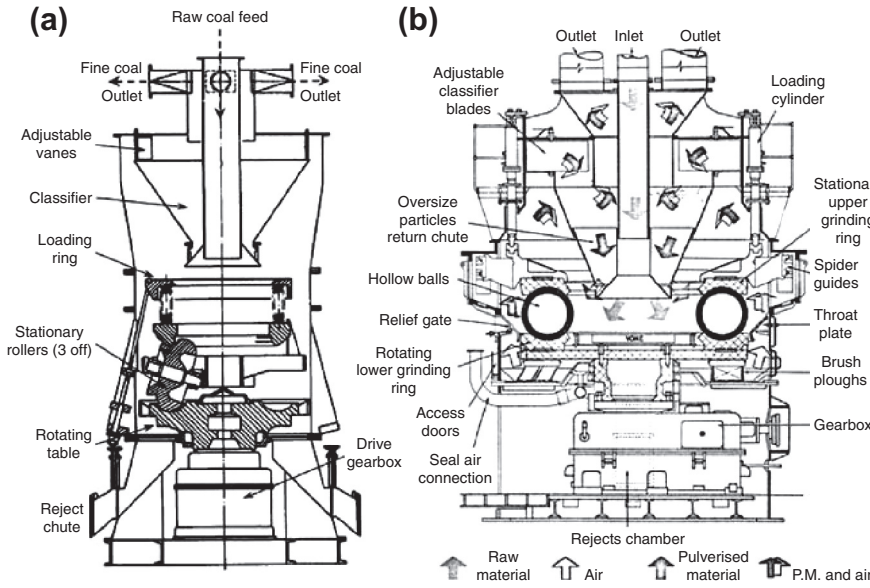


Figure 7.9 Two types of vertical spindle mill for grinding coal

loading pressure is applied by springs, hydraulic cylinders or hydro-pneumatic cylinders loaded by compressed nitrogen stored in cylinders. The latter avoids the expense and complexity of hydraulic pumps.

The basic operation of all vertical spindle mills is similar. In the case of the ball ring mill, the raw coal falls through the stationary grinding ring then onto the rotating yoke and centrifugal force carries it into the grinding zone, where it is crushed between the balls and rings, and then picked up by the hot air stream. The hot air has a maximum permitted temperature of 400°C (lower in roller mills owing to the bearings in the rollers). It enters the mill via a windbox which distributes the air evenly to the throat. The very large particles fall back to the grinding zone and the air flow carries the rest to the integral classifier which separates the fine coal and sends it to the burner, whilst the coarse coal returns to the centre of the yoke for regrinding.

Tramp material, too hard to grind, such as metal or pyrites, is carried round the throat ring until it falls through the relief gate into the reject box. It is important that the reject box is emptied regularly to prevent fires since pyrites is prone to spontaneous ignition. The setting of the classifier blades controls the fineness of the coal. The oversize coal falls down the classifier cone and passes through the ring of plates back into the grinding zone.

Advantages of the ball ring mill, compared with traditional roller mills are that surfaces of the grinding balls wear evenly because, unlike rollers, they do not 'track'. Furthermore, the absence of bearings inside the mill largely eliminates the risk of coal ingress and allows higher inlet temperatures. This results in an unusually long life for the grinding elements which have been known to last many years on some installations.

High Speed Mills

In high speed mills, the coal grinding in the mill takes place by impact between the coal and the grinding elements. A number of designs exist. A common type consists of two grinding zones of beaters, one set of which pass between stationary pegs. A set of swing hammers is optional and assists in dealing with lumps and tramp material. The whole assembly is mounted on a rotating shaft, together with the fan, and driven at 850–1700 r.p.m. The larger machines are slower to restrict the peripheral speed.

Although high inlet air temperatures are generally permitted for high speed mills, in practice, the drying capacity is limited by the heat transfer within the mill and the restricted airflow through it. There is little control over the coal fineness, which tends to be finer at high outputs, while increased airflow makes the coal coarser. Wear rate is high, particularly with hard coals and those containing

quartz in the ash; a life of less than three months being common for the fixed peg grinding elements. Great care must be taken to exclude tramp material; a component as small as a 6 mm nut will cause catastrophic failure of the beaters and pegs.

A more robust high speed mill is the Sardon Saxifrage mill which, instead of having fixed cast iron beaters and pegs, it is equipped with swing hammers, Figure 7.10. It is thus much less vulnerable to tramp material with only the larger material presenting a significant risk of damage. The clearances are greater and the wear parts are made from appropriate wear resistant steels and not being dependent on small clearances, it will last at least twice as long as the peg type mill between overhauls. Furthermore, when maintenance is required it is both quick and easy.

Coal feed to the Saxifrage mill, is through the top and it is impacted by the rotating hammer assembly. The air/coal mixture has a rotating motion imparted by the hammers. The ground product is carried by the airstream into the static vanes where the larger particles are thrown outwards and returned to the grinding zone via a separate passage. The finer coal is carried from the mill in the air stream. The mill has a high turndown ratio and the product fineness varies with throughput, being finer at low throughputs when direct firing and can be controlled adjusting mill rotational speed. This is a major advantage, since small pulverised coal flames are difficult to sustain and the finer particle size will assist flame stability.

High speed mills are inexpensive and particularly suited to small capacity installations, up to approximately 10 tonne/hour of coal.

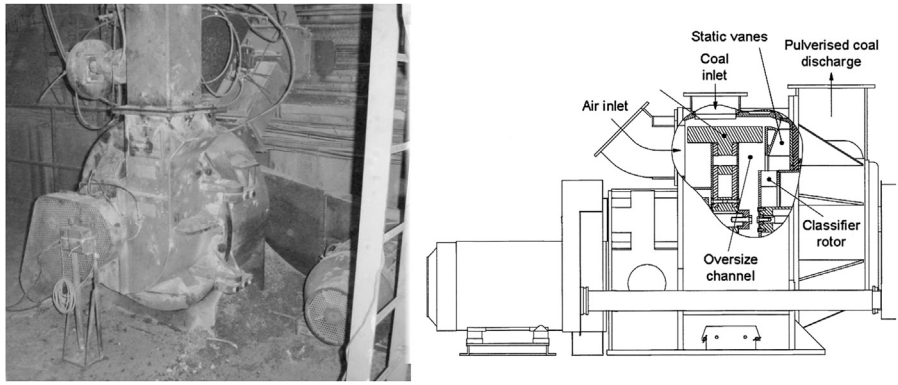


Figure 7.10 Sardon Saxifrage Mill showing a sectional view (Photo provided by courtesy of Sardon International Ltd)

7.3.4 Coal Mill Grinding Capacity

The amount of coal which can be ground in a mill is dependent on the hardness of the coal, its moisture content, the fineness of the product and the drying capacity of the mill; this latter point is considered in section 7.3.6 below.

The measure of grindability in common use is the Hardgrove-Grindability Index. This is an empirical test developed by Hardgrove (1932) and carried out in a small ring ball mill. The procedure is enshrined in ASTM D409-02. A carefully prepared 50 gram sample is ground in the machine for 60 revolutions and then sieved through a 75 micron sieve. The Hardgrove Index is calculated from the equation:

$$Y = a + bX \tag{7.1}$$

Where:

Y = Hardgrove-Grindability Index
X = residue on 75 micron sieve
a & b are constants for the machine determined by a standard calibration procedure

As the coal becomes harder the residue, X is larger and the HI is lower. Therefore the softer the coal the larger the Hardgrove Index, which ranges from approximately 30 for the very hard coals up to 100–110 for very soft coals. The test provides good repeatability except for lignites, sub-bituminous and very high volatile bituminous coals.

For a typical mill, the output is nearly proportional to the Hardgrove Index. Thus, if a mill maximum output is 6 t/h with a coal of 60 Hardgrove, it would be 5 t/h with a coal of 50 Hardgrove and 8 t/h with a coal of 80 Hardgrove. Increasing the coal feed size reduces the mill output because more energy is required to grind the coal. This effect is more pronounced with ball mills than with vertical spindle mills. If the coal is very large (lumps greater than 100 mm) it is more economical to install a pre-crusher than to increase the coal mill size.

The Hardgrove Index is based on a product fineness of 75 micron. If coarser product is acceptable then the mill output is increased while finer size restricts production rates significantly, Figure 7.11.

Coal Fineness

Coal fineness is normally determined by sieving. A useful practical expression for representing the size distribution of powders and sprays is the Rosin-Rammler distribution, previously discussed in

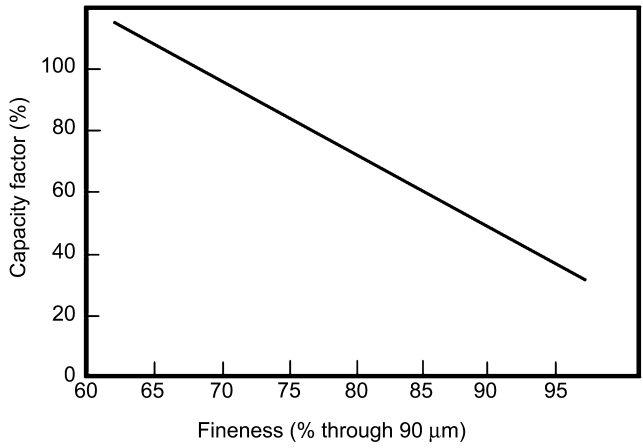


Figure 7.11 Coal mill thoughput vs fineness (After CEGB)

chapter 6. For routine testing, two sieve sizes are often used, 75 or 90 micron and 300 micron. If any doubt arises regarding the performance of a coal mill, five size samples should be taken and the results plotted on Rosin-Rammler graph paper.

Samples of mill product should be taken regularly to determine the residues and fine coal moisture. Obtaining a representative sample can prove difficult and consideration of this point should be given at the design stage. More often than not, the sample is taken by a probe inserted into the pulverised coal delivery pipe. The sampling point should be situated in a straight length of pipe away from bends and from any fan. Several samples should be taken by traversing the pipe.

Coal should not be ground finer than necessary for good combustion since it reduces mill capacity as shown in Figure 7.11 but there should not be more than 1 or 2% retained on a 300 micron sieve, since large particles take a very long time to burn.

Sometimes coal is ground very fine to compensate for poor fuel/air mixing. This is very expensive, both in terms of capital cost (since a larger mill is needed), and subsequent power consumption; furthermore it is also not very effective.

Coal Dryness

Coal drying is carried out in the mill, normally using a hot air or hot gas stream. A number of different arrangements are used to achieve the hot air, or hot gas, stream each of which has advantages and disadvantages and affects both the drying capacity and the interaction with the associated furnace. This means that the milling system must be designed for the type of coal that is going to be used and

the furnace firing requirements. We will return to the topic of drying in section 7.3.6 but before we do we need to consider the coal grinding process systems commonly used.

7.3.5 Pulverised Coal Grinding and Firing Systems

There are number of ways a pulverised coal firing system can be configured. These systems are broadly classified as direct or indirect firing. Not all coal mills are equally suitable for particular firing systems and the characteristics of some mills commonly used for coal grinding have already been described. Coal is liable to spontaneous ignition and when pulverised and blown into a cloud it is explosible. All persons concerned with the design, construction, operation and maintenance of coal firing systems need a good understanding of the fire and explosion characteristics of coal dust and the appropriate safety measures required. For further information on this important subject see Eckhoff (1991), Bartknecht (1981), NFPA 8503, NFPA 68 and the IChemE guidelines.

Direct and Indirect Firing Systems

Over the years there have been considerable differences of opinion regarding the merits of the various types of direct and indirect firing systems. Most of the cement plant equipment manufacturers tend to favour indirect firing systems while boiler manufacturers and suppliers, together with many of the plant operators, favour direct systems. The supporters of indirect firing claim that reduced fuel consumption is obtained in cement kilns when the water vapour is excluded from the kiln and low primary air firing is used. However, this opinion is not supported by combustion theory since lowering the primary air reduces the fuel/air mixing rates owing to the lower jet momentum, see chapter 6; while excluding the water vapour reduces the rate of oxidation of char and carbon monoxide to carbon dioxide (Field et al 1967). Furthermore, the claims for fuel savings with indirect firing are difficult to prove one way or another in practice, since the potential savings are only in the order of a few percentage points, which is generally less than the measurement error.

Confusion exists regarding the definition of direct and indirect systems and their variations. Generally, the term “direct” or “indirect” refers to the coal route:

- **Direct firing** - All systems in which the pulverised coal is fed direct to the furnace following grinding without any form of intermediate storage.

- **Indirect firing** - All systems in which the pulverised coal is stored after grinding and metered to the kiln as pulverised coal from a storage bin.

These systems include:

Direct Firing
Systems in which the pulverised coal is transported direct to the furnace in the mill exhaust which is used as the primary air, Figure 7.12.

Semi-Direct Firing
As for direct firing but a proportion of the gas from the mill exhaust is recirculated to the mill inlet, thus increasing the transport air in the mill and classifier without increasing the primary air, also shown as an option in Figure 7.12.

Indirect Firing
Systems in which the pulverised coal is removed from the mill exhaust gas and stored in a pulverised coal storage bin. The mill gas is exhausted to atmosphere through a filter. Recirculation of

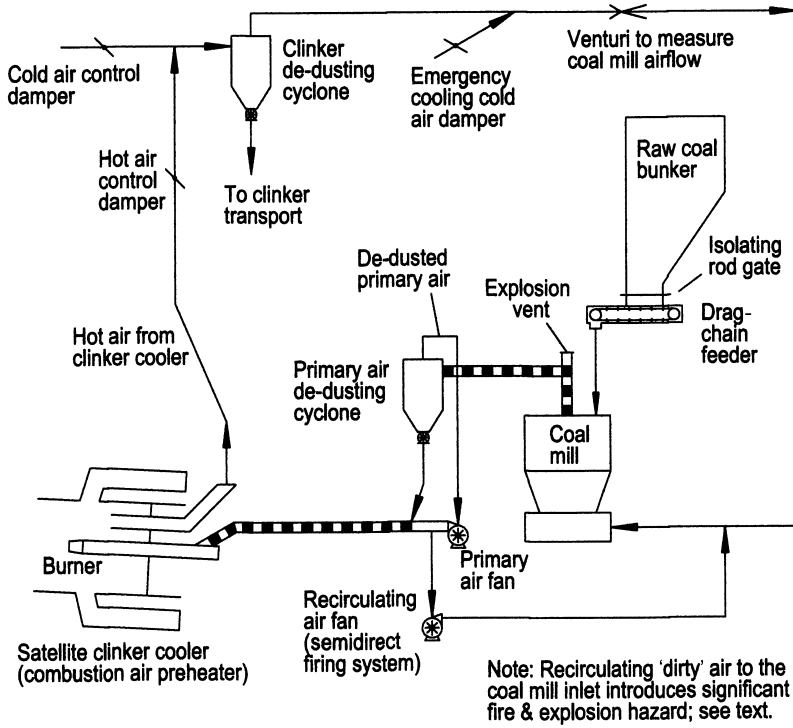


Figure 7.12 Schematic of typical direct firing system applied to a cement kiln

the mill exhaust to the inlet may or may not be used. Furnace exhaust gas or air may be used in these systems, Figure 7.13.

Semi-Indirect Firing
Indirect firing systems are those in which the filter is omitted and the mill exhaust discharged into the furnace as primary air. Recirculation of the mill exhaust may or may not be used.

Discussions regarding the relative merits of direct and indirect firing focus on consistency of the feed of fine coal to the furnace, the effect of primary air on the process and the effect of water vapour. Safety is also a consideration since indirect systems require greater safety precautions to reduce the risk of fire and explosion to an acceptable level.

For a direct firing system a coal mill with a low airflow 1.5 – 2.0 kg air/kg coal with a controllable output and good turndown is required. By contrast for an indirect system no turndown is necessary but a high

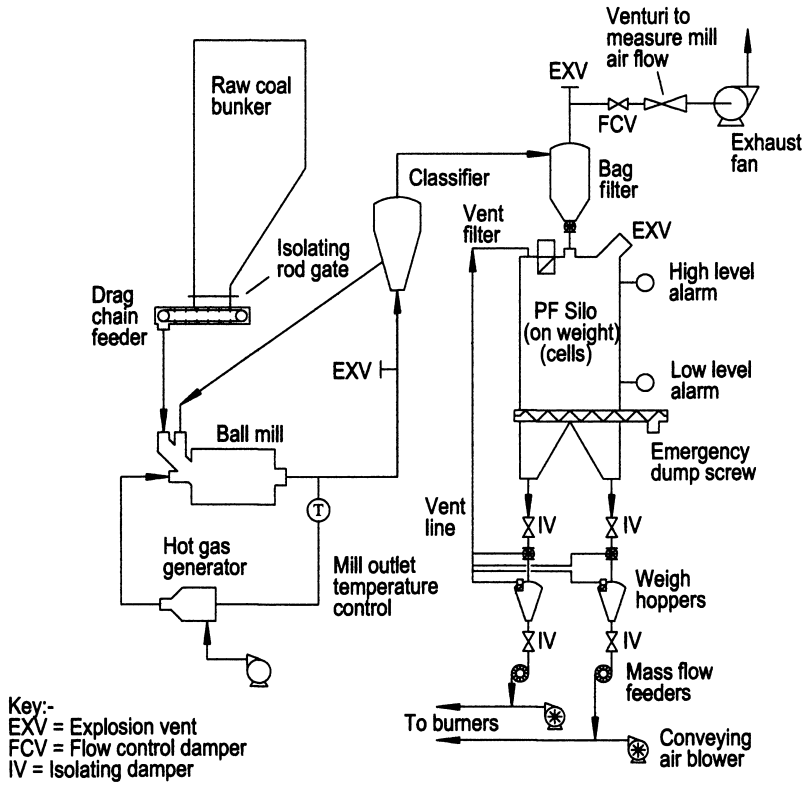


Figure 7.13 Schematic of typical indirect firing system

airflow is preferable to depress the dewpoint temperature and reduce the risk of condensation in the bag filter.

The coal feed to the burner should be steady with very little short term variation. If low excess air operation is required then a short term variation in the coal feed calorific value of less than +− 1% is desirable. Raw coal has a variable calorific value mainly caused by variations in the moisture and the ash content. This variability is reduced in pulverised coal because moisture content is reasonably stable and only ash variation occurs. It should, therefore, be possible to feed pulverised coal to a furnace from a storage hopper with greater consistency than can be achieved by direct firing systems but much is dependent on the accuracy of the feeder. This is considered in more detail below. For direct firing systems the coal mill attenuates the short term variations in the raw coal feed owing to the large recirculating load within the mill. Short term variations in the coal feed caused by changes in the physical characteristics of the coal, such as size or moisture content, can be minimised by using drag chain feeders rather than table feeders, whereas variations in calorific value due to changes in the moisture and ash content tend to be long term. Variation in ash affects both direct and indirect firing systems equally.

Whilst it should theoretically be possible to obtain a more even feed of coal by metering pulverised coal from a storage bin, practical considerations mean that this advantage is not often realised. The best raw coal feeders (in combination with an appropriate coal mill in a direct firing system) can feed coal to the burner just as effectively as most of the pulverised coal feeders.

Another difference between the indirect and the direct and semi-indirect systems concerns what happens to the water which is removed from the coal. In the indirect system the water vapour is exhausted to atmosphere from the mill, whilst in all the other systems it is passed through the furnace, being heated up to flame temperature and finally exhausted to atmosphere at the flue gas temperature. Heat balances calculated for these two situations for a dry process cement kiln with 350 °C exhaust when 15% moisture is removed from the coal, show an increase in the specific heat consumption of the direct system by about 13 kJ/kg of cement clinker. This is less than 0.5% of the total fuel consumption and is therefore undetectable. In any case, there are many operating parameters that have much more influence on the process heat consumption. Furthermore, water vapour plays an important role in the oxidation of char and carbon monoxide to carbon dioxide as mentioned above, so its absence is likely to adversely affect char burn-out.

The principle advantage of direct firing systems is their relative simplicity and enhanced safety (compared with indirect systems). All direct firing systems suffer from the disadvantage that all the air from the coal mill must be supplied to the burner. This can be a major

problem where the coal mill requires a high airflow for coal conveying purposes, since excessive primary air may cause a serious reduction in process efficiency. Most coal mills can be used in indirect firing systems but only a limited number are suitable for direct firing.

Indirect firing systems are much more complex than direct firing systems and have an additional fire and explosion risk, especially in the pulverised coal silo and the bag filter. However, the advantages of increased flexibility of burner design with reduced primary air operation, together with its suitability for multipoint firing, tend to outweigh the increased complexity and higher fire and explosion risk. In any case the latter can be minimised and a safe system produced by good design, operation and maintenance.

Except on a power boiler, or a furnace where all burners require the same fuel rate, it is difficult to fire more than one burner using direct firing, so indirect systems are almost always used where multiple burner firing with different liberations are utilised. The characteristics of direct and indirect firing systems are summarised in Table 7.2.

7.3.6 Coal System Drying Capacity

The drying capacity of the mill is dependent on the heat provided by the hot gas or air, which in turn is governed by its mass flow and temperature difference across the mill. Calculation of the drying capacity is a simple heat balance problem, Figure 7.14. The wetter the raw coal fed to the system the hotter the air or gas needs to be in order to dry the coal effectively. Mills with low air mass flow rates need hotter air than those with high air or gas flows.

Figure 7.15 shows the effect of mill air/coal mass ratio on the inlet temperature required to dry coal with 5%, 10% and 15% initial moisture to 2% moisture. Note how increased mill airflow reduces the mill inlet temperature required to dry any specific coal. Hence, mills capable of higher airflows have greater drying capacity. Inleakage air (false air) requires an increased mill inlet temperature to obtain the same drying capacity and extracts heat that would otherwise have contributed to coal drying. Hence, to maintain the drying capacity of a coal milling system it is essential to keep the inleakage air to a minimum.

The final moisture level of the fine coal is dependent on the type of coal and the mill outlet temperature and this can be deduced from the drying curves (see Figure 7.7) for the particular coal that is used. For mills where the heat transfer is not limited by heat exchange considerations, such as vertical spindle mills, the outlet temperature to achieve an optimum fine coal moisture target is typically in the range of 55–70 °C. For mills with poorer heat exchange characteristics higher outlet temperatures are required, typically 90–110 °C. For these mills the drying capacity often limits their output which drops rapidly as coal

Table 7.2 Comparison Between Direct and Indirect Firing Systems

	Direct Firing	*Semi-Direct Firing*	*Indirect Firing*	*Semi-Indirect Firing*
Coal mill air and gas flows required	Low to keep primary air within acceptable limits	Similar to direct system. Mill airflow may be increased by recirculated air flow	High airflow required to depress dewpoint and prevent condensation in bag filter	Similar to semi-direct system
Drying capacity	Good up to 25% moisture removal with vertical spindle mills	Similar to direct system unless mill inlet temperature restricted by recirculated air flow	Normally good but drying capacity may be restricted by mill inlet temperature or filter dewpoint problems	Normally good — no filter dewpoint problems
Burner performance (Fuel/air mixing)	Good if primary air has sufficient velocity	Similar to direct system	Can be poor if very low primary air is used	Similar to direct system
Consistency of coal feed to burner	Good if drag-chain feeder used owing to attenuation of variations in the mill	Similar to direct system	Needs excellent feeder for consistent feed because of minimal attenuation of variations in the conveying pipe	Similar to indirect system
Multi-burner firing	Difficult to arrange effective splitting of coal/air streams	Similar to direct system	Indirect system is very suited to multi-burner firing	Similar to indirect system
Operation	Simple and easy to operate	More complex than direct system owing to need to balance airflows	Complicated to operate, requires a high standard of instrumentation and operator awareness for safe operation	Similar to indirect system but less complex owing to lack of bag filter
Safety — coal dust explosions and fires	Generally safe — minimal risk of fires and explosions	Higher risk of fires and explosions than direct system owing to recirculation of air/fine dry coal to mill inlet	Moderate risk - fires are common Explosions occur occasionally especially in fine coal bin and bag filter	Similar to indirect system but risks are reduced owing to lack of bag filter
Service availability & maintenance requirements	Depends on mill used but minimal equipment implies high availability and low maintenance	Similar to direct system	Less reliant on mill but more complex system implies lower availability and higher maintenance costs	Similar to indirect system
Running costs	Low power consumption and maintenance costs	Similar to direct system	Higher power consumption (more fans) and maintenance costs than direct system	Similar to indirect system
Capital cost	Low	Moderate	High unless required for multi-burner firing	Moderate

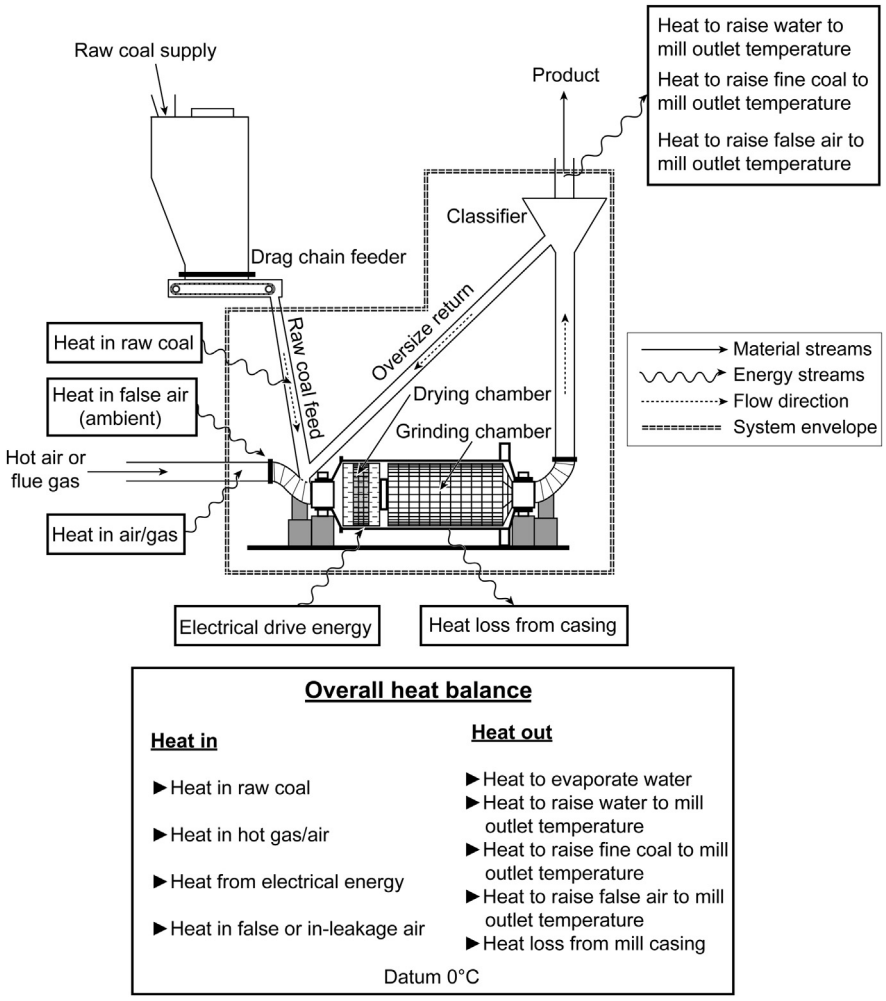


Figure 7.14 Coal mill heat balance

moisture rises, see Figure 7.16 which shows clearly how a ball mill's grinding capacity falls for raw coal moistures exceeding 4%. This is caused by the restricted airflow through these mills owing to the small cross sectional area through the trunnion bearings and the relatively poor contact between the coal and the air in the drying chamber. Vertical spindle mills have greater drying capacity owing to the higher air mass flows but, for coal moistures above 15%, it is still drying capability, rather than grinding that determines their output.

As mentioned above, care should be taken not to remove an excessive proportion of the inherent moisture since this increases the fire and explosion risk. If the coal is over-dried it becomes hydroscopic

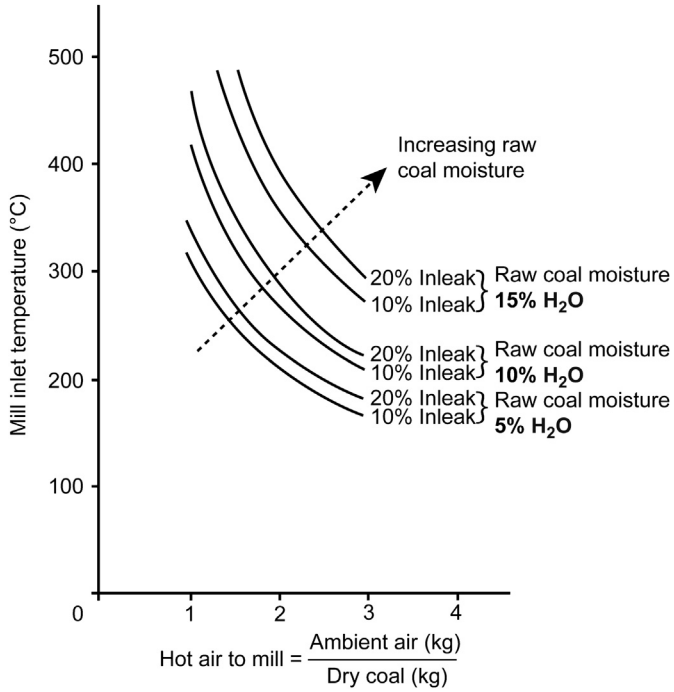


Figure 7.15 Coal mill inlet temperatures required to dry coal from various raw coal moistures to a fine coal moisture of 2% for various mill airflows showing the effect of false air

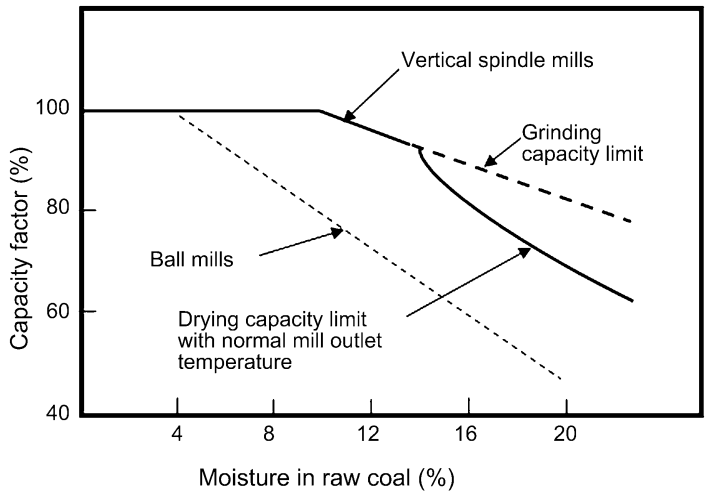


Figure 7.16 Coal mill thoughput vs coal moisture (After CEGB)

and moisture from the atmosphere recombines with the fine coal. This reaction is exothermic and causes heating of the coal which may lead to spontaneous ignition.

The direct contact between fine coal and hot air introduces the risk of fire and explosion, especially for very reactive coals. For these coals, hot exhaust gas from the furnace can be used for drying instead of hot air. This reduces the risk of a coal dust explosion by limiting the oxygen content below the concentration needed to sustain an explosion. Exhaust gas systems can present difficulty in controlling the coal dryness because the temperature of the fresh gas entering the coal mill is approximately constant, typically between 300 & 350 °C and, to maintain low oxygen concentration, the mill inlet temperature is controlled by recirculating cool gas from the mill outlet. This increases the water vapour of the inlet gas and further reduces the drying potential, making the effect highly non-linear and hence difficult to control.

7.3.7 Coal Firing System Fans

Fans handling coal dust in firing systems are a specialist application and few fan manufacturers have the necessary expertise. The fan has to handle coal dust laden air which is explosible and abrasive. The dust loading reduces both the volumetric flow and the pressure developed by the fan. The fan requirements vary depending on whether the fan is intended for a direct or indirect firing system and whether all the pulverised coal passes through the fan or most is removed by a separator. The fundamental requirements are:-

- Wear resistant construction so that coal dust does not cause too rapid deterioration of the fan and create unduly high maintenance costs
- Sufficient clearance between the rotor and the case to prevent the risk of sparking and ignition of the coal dust that could lead to an explosion
- Adequate allowance in the design for the reduced fan capacity caused by the internal friction losses associated with the presence of coal dust
- Dust-tight casing and shaft sealing gland to prevent coal dust leakage
- Strong casing to contain explosion pressures (at least 350 kPa (50 psi))
- Motor adequately protected against dust ingress

Not many fan manufactures fully understand the problem and considerable care must be taken to ensure the fan being offered is adequate for the duty. High efficiency hollow bladed fans and high

speed fans are not suitable for coal firing systems, except when handling clean air downstream of a bag filter.

7.3.8 Fine Coal Storage

Dry ground coal is much more reactive than raw coal and hence more likely to catch fire or explode. To minimise this risk, the capacity of the fine coal storage should be no more than absolutely necessary, typically in the range of 2–12 hours storage. In cases where the plant is taking ready ground coal supplied by road or rail tanker several days storage may be required, increasing the fire and explosion risk, and with it, the safety precautions required. Plant shutdowns are an especially risky time if the coal storage bin is not emptied or inerted.

Like the raw coal bunker it is important to ensure mass flow of coal, rather than "rat hole," Figure 7.5, to ensure an even feed of coal to the burner. Fine coal bins are invariably cylindrical (for strength to withstand an explosion) with a conical outlet, the design of which must be configured to suit the feeder, hence the type of feeder used may have a significant effect on the arrangements at the bottom of the bin. For example, aeration is desirable to assist with the pulverised coal flow but cannot be used with screw feeders owing to the risk of fluidised coal running straight through the screw. This phenomenon is usually known as "flushing". A schematic of a typical fine coal storage bin is shown in Figure 7.17.

Multiple discharge bins, feeding more than one burner, are dangerous when an individual burner is shut down for a prolonged period because the stagnant coal is subject to self-heating, which occurs as a result of slow oxidation. This eventually leads to spontaneous ignition causing fires and explosions. Provision should be made for discharging and recycling the coal from the shut down burner's feeder to minimise the risk of spontaneous heating. Multiple discharge bins feeding more than one process plant are particularly dangerous for the same reason and should be avoided where ever possible. Where it is essential to feed more than one plant from a single bin special safety precautions must be taken, such as providing an inert atmosphere in the bin.

Whilst it is essential that the coal is fed as evenly as possible to the burner this is not just a process requirement, but an essential safety feature to prevent spontaneous ignition. Fine coal bin discharge cones should therefore be designed for mass flow with very steep sides and must be lined with corrosion resistant, low friction material. Glass, rubber, austenitic stainless steel and various plastics have been used. Non-flammable materials are preferred from a safety view point. It is vitally important the bin discharge arrangements suit the fine coal feeder, since any interruption in the coal flow to the feeder has an inevitably detrimental effect on plant performance. Mechanical agitation,

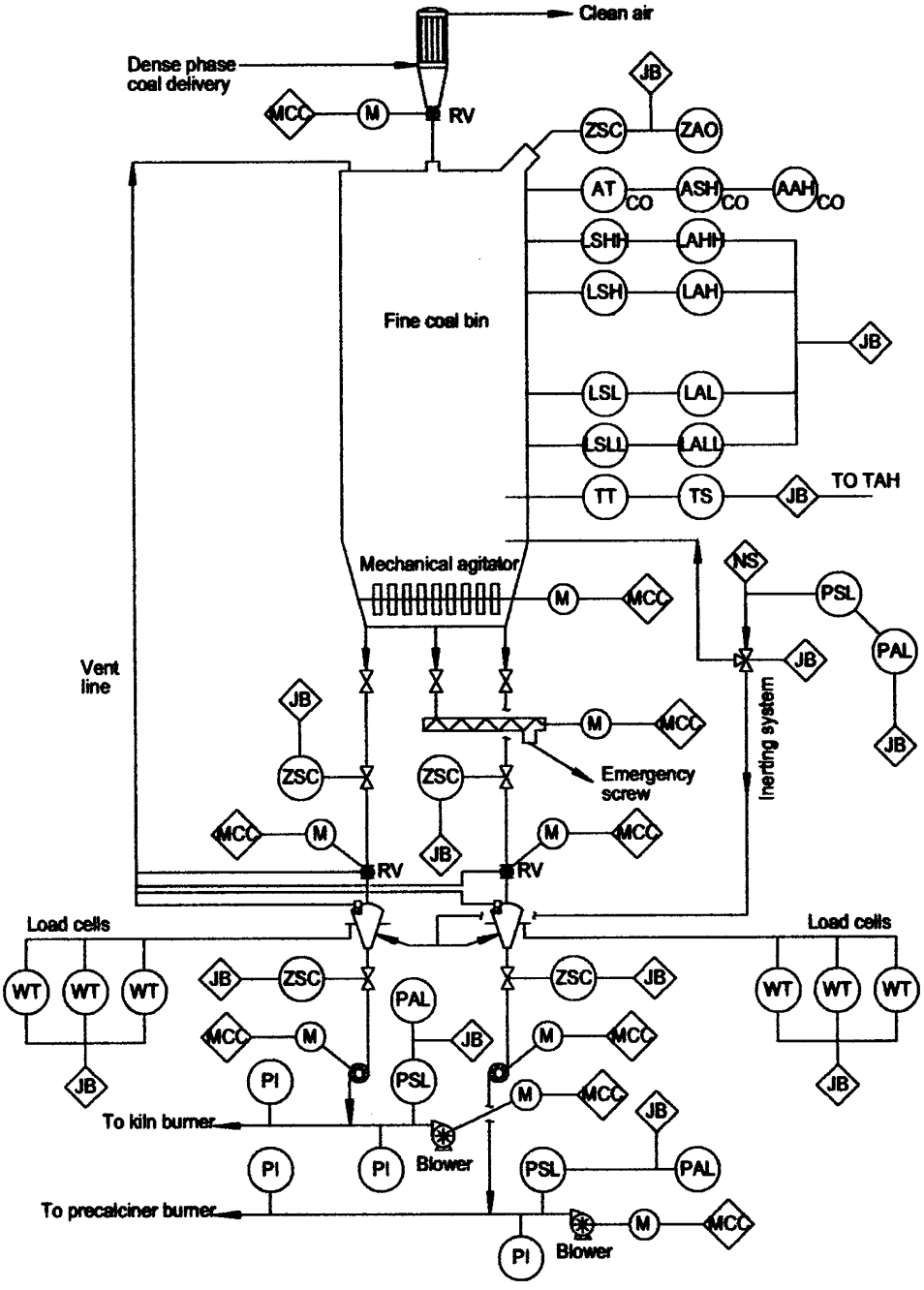


Figure 7.17 Schematic of a typical fine coal storage bin showing the principle instrumentation

or aeration of the fine coal, is essential to ensure free flowing characteristics. The choice will depend on both the type of feeder and characteristics of the coal.

Aeration is simpler with fewer moving parts but is not safe with highly reactive coals because of the risk of fire and explosion, unless inert gas is used. When installing commercial designs of feeder it is vital to follow the recommendations of the supplier. Where this is not possible for physical reasons, any alternative arrangement must ensure the design will still meet the manufacturer's objectives. Mechanical agitation requires slow moving augers of very robust design. Packed pulverised coal at the bottom of even a small bin is extremely resistant to movement and exerts enormous forces on mechanical agitators and their drives.

Fine coal bins require sophisticated instrumentation including level indicators, fire detection and fire fighting systems. High and low level detectors are required, two to indicate high level and two for low level, the first to raise alarm and the second to act as a safety shutdown interlock. Rotating paddle detectors are frequently used for this purpose, the presence of coal causes the paddle to stop rotating and the absence of coal permits the paddle to rotate again.

Fire detection and extinguishing systems are essential to detect the onset of spontaneous combustion. Stored coal emits a low level of CO as an oxidation product. Continuously monitoring this CO emission to detect any increase in CO levels can give an early indication of an increase in oxidation which could lead to a fire. Coal in the lower region of the bin, and especially in the conical section, should be monitored for temperature rise by an array of thermocouples. Fires are normally dealt with by flooding the bin with inert gas (CO_2 or N_2). However, owing to the insulating properties of coal dust the temperature normally remains high, and with it, the risk of re-ignition following exposure to air.

Fine coal bins cannot readily be designed to contain an explosion so must be provided with explosion venting. The vents have to be located on the top of the bin. Their size is very important and the rules for sizing are complex. A number of guides exist for explosion protection, such as VDI 3673, those produced by the IChemE and the NFPA codes. These are listed at the end of the chapter. It is important that the explosion vents discharge direct to the outside atmosphere to avoid risk of injuring people by burning dust and toxic fumes. However, ducts should not be used wherever possible because they reduce the effectiveness of the vent. Where the use of ducts is unavoidable they must not exceed 3m in length and due allowance for the effect of the back pressure must be made. This normally requires larger explosion vents, or a stronger bin. In cold climates designs for explosion vents must prevent snow and ice accumulating on the vents, since the additional mass increases the opening pressure and has caused serious accidents in the past.

7.3.9 Fine Coal Feeding and Conveying

Fine coal feeders control the flow of coal to the burner(s). Coal feed to the furnace should be steady to maintain consistent combustion conditions, with a short term variation in the coal feed calorific value of less than +− 1% desirable. Unfortunately the nature of fine powders makes them very difficult to meter and feed accurately, which together with the lack of attenuation between coal feeder and the burner, makes consistent and accurate fine coal feeding a very difficult problem. There are two basic types of fine coal feeder:

- Volumetric Feeders
- Mass Flow Feeders

The repeatability and consistency of any feeder is equally dependent on the design of the discharge arrangements in the bin. Hence it is possible for a well designed bin with a good volumetric feeder to give a consistent feed, while a poorly designed bin with a mass flow feeder, will give very poor results.

Volumetric Feeders

Typical volumetric feeders include screw feeders, and variable speed rotary valves, Figure 7.18. The former consist simply of a screw conveyer mounted under the fine coal bin. They usually feature a number of "tricks" such as variable pitch on the inlet and "breakers" on

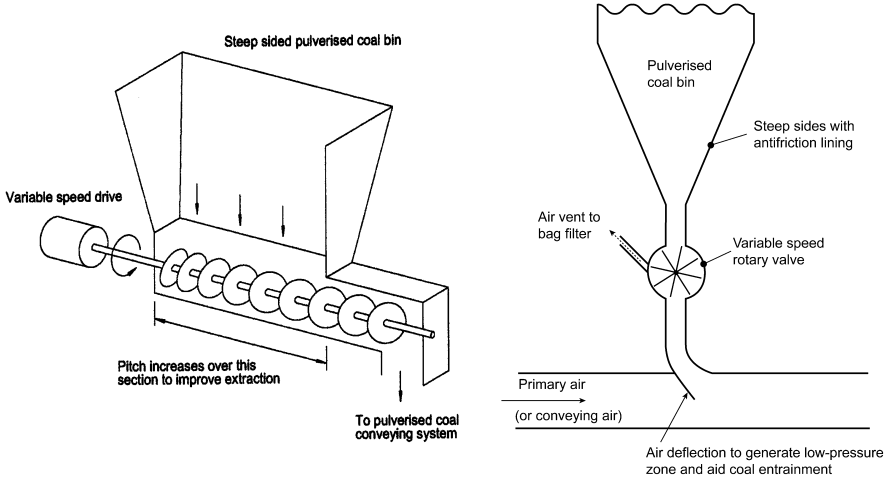


Figure 7.18 Examples of volumetric fine coal feeders showing screw feeder (left) and rotary valve (right)

the discharge in an attempt to achieve a more even feed. Screw feeders were commonly used but suffer from a number of disadvantages including flushing, and bridging in the hopper owing to the flow characteristics into the screw opening. Screw feeders are, however, usually the only practical method of feeding very small flow-rates of fine coal.

A rotary valve is a positive displacement device and, in principle, is capable of giving a consistent volumetric feed. The consistency of the feed provided by a rotary valve can be good, especially if fitted to well-designed hopper with aeration facilities. They are not as sensitive to the dust characteristics as screws. However, variations in density affect the mass flow of coal and incomplete filling of the pockets can be a problem if the design of the bin is incorrect or the valve is running too fast. Owing to the physical size of rotary valves they cannot be used for feeding very small rates of pulverised coal. Generally 0.5/1 tonne/hour is the lower limit.

Mass Flow Feeders

In principle, a mass flow feeder should give a better repeatability and consistency than even the best volumetric feeder but, as discussed above, this is not always the case owing to poor design of the bin discharge. Typical mass flow feeders include variable speed rotary valves with impact weigher, variable speed rotary valves with loss in weight hopper, variable speed belt weigher and propriety mass flow devices, such as the Pfister Feeder; each is considered in turn below.

Impact weighers utilise a variable speed rotary valve to extract the coal from the bin. As the coal is discharged from the rotary valve it slides down an inclined pipe and impinges on a sprung hinged plate, Figure 7.19. The force on the plate and the resultant deflection is proportional to the flow rate of pulverised coal. Normally a feedback loop varies the speed of the rotary valve and attempts to maintain a constant force on the plate and, hopefully a constant mass flow. In practice, there is significant drift about the set point because the coal discharges from the feeder before weighing, so the weigher is always trying to correct the flow after the deviation has already occurred. Impact weighers are simple but difficult to calibrate with any degree of accuracy.

The loss in weight system utilises a variable speed rotary valve to extract the coal from the bin which is located on weigh cells, Figure 7.20. As the coal is discharged from the bin its weight decreases. A feedback loop varies the speed of the rotary valve and attempts to maintain a constant rate of decrease in the weight of the hopper. "Loss in weight" systems are simple and reliable, but the accuracy is poor owing to the small rate of change of mass compared with the overall mass.

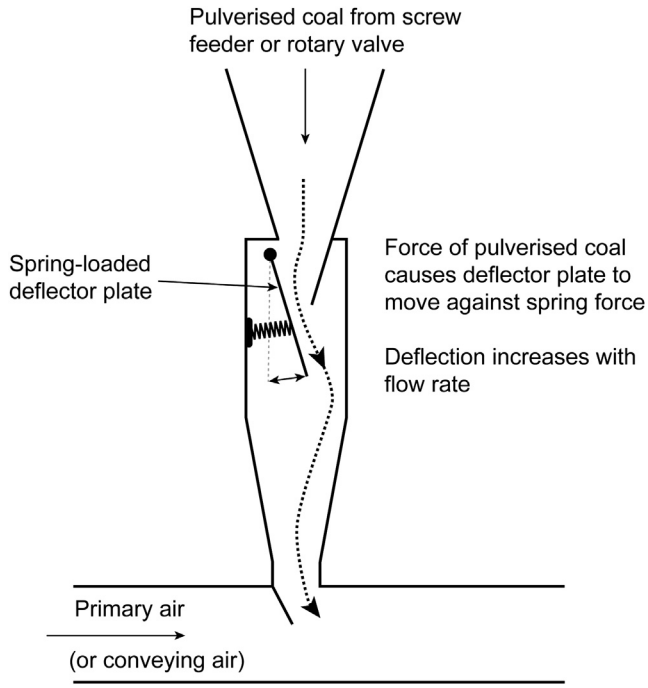


Figure 7.19 Schematic of an impact weigher

The Pfister feeder, Figure 7.21, is a sophisticated weigh feeder incorporating feed-forward control suitable for use in dense-phase conveying systems (see below). The working element is a horizontal rotor divided into cells, enclosed in a casing suspended on load sensors. The coal falls into a cell from the fine coal bin and the turning rotor carries it around to the discharge port. The weight of the coal imposes a load on the casing. The load sensors measure the coal weight half way around between filling and discharging. If the weight varies from the set point the rotor either speeds up or slows down as required, to deliver coal at a constant feed rate to the discharged pipe. Although there are feed variations at the cell change over, similar to the rotary valve, this feeder is, in principle, the most accurate feeder available since there is little drift about the set point because the weighing occurs prior to discharge, so the weigher can correct the flow rate before discharge to the conveying system.

7.3.10 Pulverised Coal Conveying

Pulverised coal is normally conveyed suspended in air or flue gas. Two basic systems are common, lean phase and dense phase; the former

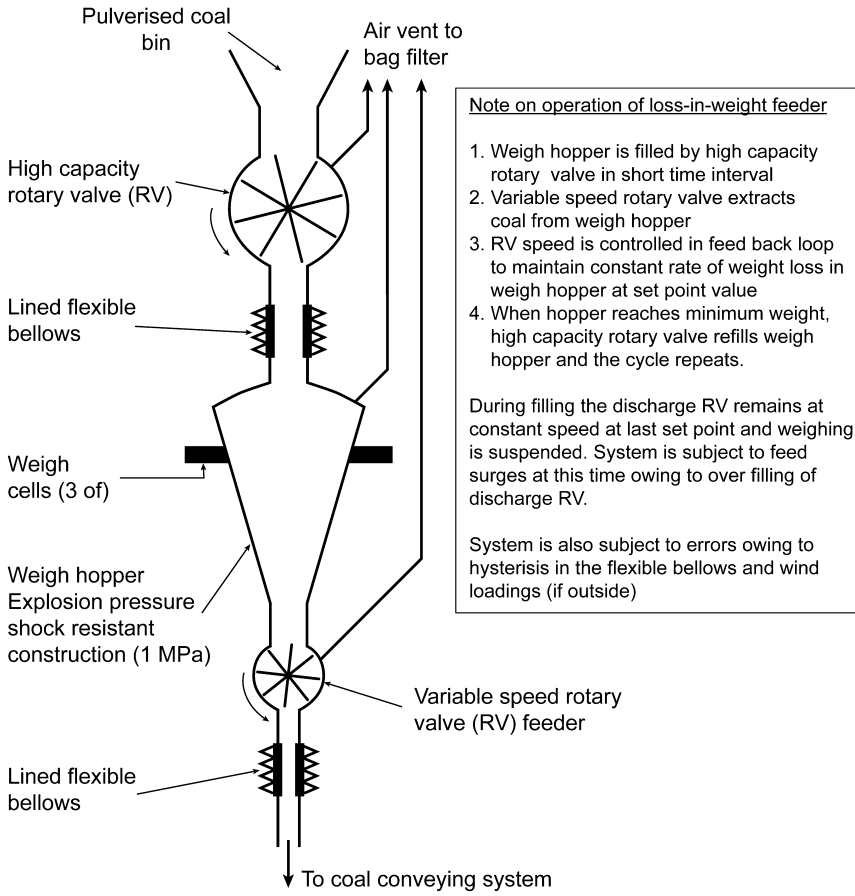


Figure 7.20 Schematic of a loss in weight fine coal feeder system

normally uses the conveying air as primary air in the burner. In this case, the conveying, or coal mill air flow, requirements usually determine the primary air flow. This implies that primary air discharge velocity at the burner nozzle is the only variable which can be used to optimise the momentum and hence the combustion. Dense phase conveying increases the flexibility of burner design since the quantity of primary air is no longer linked to the conveying air requirements. As a result, both the primary air quantity and velocity can be chosen to optimise the fuel/air mixing requirements totally independently of the coal conveying air requirements.

The design of a coal conveying system is critically important, especially in regard to preventing coal "drop out". Therefore dead spaces must be eliminated, bends minimised and adequate conveying velocities provided. Air velocities must be sufficient to maintain the coal

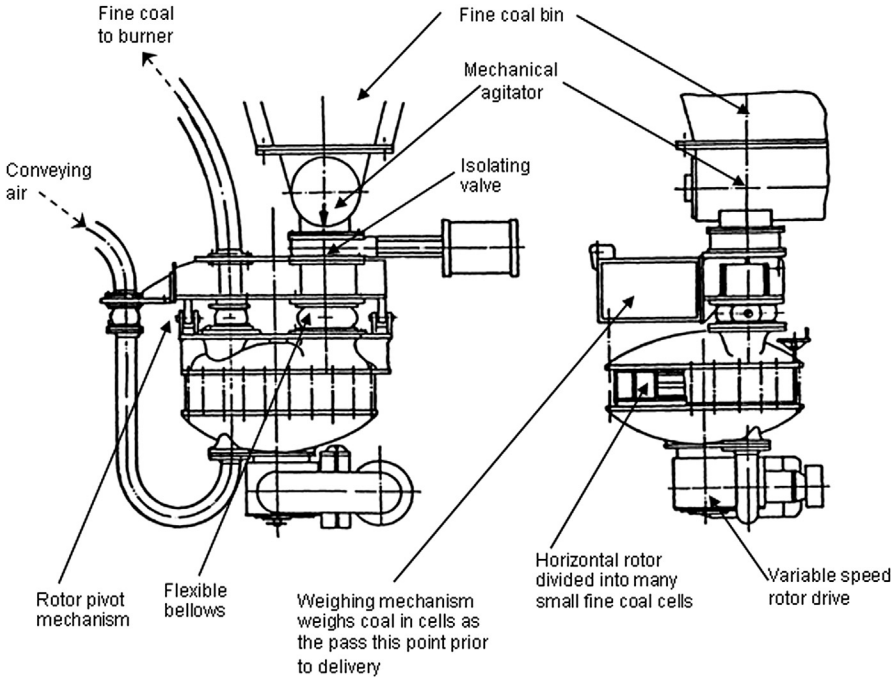


Figure 7.21 Pfister rotor fine coal weighfeeder

in suspension, but not too high since that will cause rapid wear and excessive pressure loss. The minimum recommended conveying velocity is 22 m/s with an optimum of 25 m/s and an absolute minimum of 19–20 m/s. At lower velocities, coal may drop out and accumulate in dead spaces giving rise to a severe fire and explosion risk since the accumulated coal is subject to spontaneous ignition.

Coal dust is not normally evenly distributed in the conveying air within the duct. Often severe mal-distribution of the coal occurs, known as "roping". This is not predictable but tends to become more severe, the more bends there are in the system and the longer the pipe run. Roping is difficult to detect and quantify but adversely affects the performance of the burner with respect to flame pattern and heat release profile. Sometimes severe roping is evident from the appearance of the flame but often it is not that obvious. The problem can usually be detected by sophisticated in-line sampling. To mitigate the effects of roping, burners should always be designed so that an uneven coal concentration at the burner inlet will have minimal effect on the coal distribution in the flame.

Where the system feeds more than one burner requiring that the duct subdivides, achieving an equal pulverised coal split is far from

easy. Whilst it is possible to ensure relatively good air distribution by the use of modelling, it would not be practical to incorporate flow correction devices such as flow splitters, weirs and bluff bodies, owing to the abrasive nature of most coals which would destroy such devices very quickly. In any case, even if the problem of the conveying air distribution is resolved, there remains the problem of the coal distribution within the conveying air stream because of roping. It is important that the coal and air are equally distributed between the various burners; otherwise some will be running fuel lean while others are running fuel rich. While running fuel rich can be used to reduce NO_x, see chapter 10, this has to be carefully controlled to be effective. Riffle boxes; Figure 7.22 are commonly used in an attempt to ensure that the coal and air are split equally at duct junctions.

Dense phase coal conveying systems use less than 1 kg of conveying air per kg of fine coal. The conveying air is normally provided by a blower delivering a pressure up to 150 kPa. A major advantage of dense phase conveying is that smaller pipework can be used than for lean phase owing to the lower air volumes. A potential disadvantage is that flue gas cannot readily be used for conveying. However, the explosion risk is much lower with dense phase conveying compared with lean phase, owing to the low quantity of air used, which reduces the potential energy release.

As for lean phase conveying, velocities must be high enough to always maintain the coal in suspension, with the minimum recommended conveying velocity of 20 m/s. However, unlike lean phase the velocities are not constant throughout the system. As the mixture travels through the pipes, the pressure falls owing to

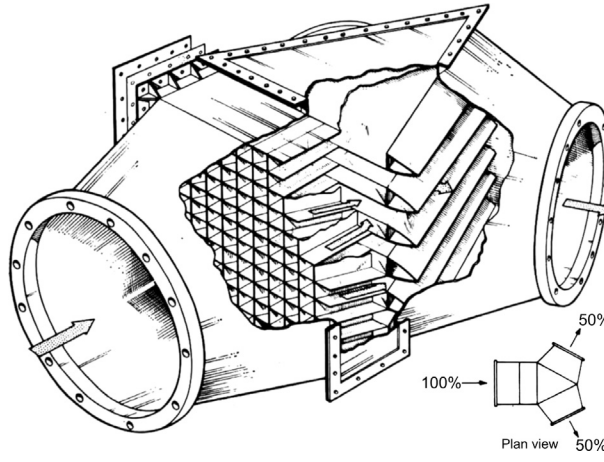


Figure 7.22 CERL Riffle box for Pulverised coal Distribution (Reproduced with kind permission of Elsevier)

friction losses, and the air volume expands, hence the velocity increases. This, together with the two-phase nature of the flow, complicates pressure loss calculations. It is particularly important that parasitic pressure losses are minimised in dense phase conveying systems to ensure that conveying velocities do not become excessively high since they can easily approach 50 m/s as the conveying air expands. If this is allowed to happen equipment wear becomes excessive and coal feed and distribution will be uneven. The system must use the shortest, straightest pipe-run possible and all bends should be long radius type.

7.4 Waste Fuel Handling

Combustible wastes are increasingly used as fuels owing to their low cost. In certain circumstances the furnace user is paid to dispose of the waste, further reducing operating costs. Although wastes include gases, liquids and solids, waste gases are usually consumed on the site where they are produced owing to the difficulty of transporting them. Hence only solids and liquids are normally available for use in industry.

Often the waste is used as a supplementary fuel, and thus only represents a proportion of the total heat input. In these circumstances only limited capital is normally available for the waste fuel handling system. Considerable engineering skill is required to design, manufacture, install and commission a satisfactory waste fuel handling system in these circumstances. While waste fuel handling systems generally follow the basic systems described above for gas, oil and coal, a waste fuel handling system will only be successful if it is designed to accommodate the particular properties of the waste concerned. For example certain liquid wastes can aggressively attack gaskets and seals, or steel pipework, while many solid wastes have very difficult flow characteristics making bunker design especially difficult.

7.4.1 Waste Gas Fuel Handling

Most waste gases have a low energy density and are only available at low pressure, so the valve train pressure loss must be minimised, therefore much larger equipment is required compared with natural gas. For example, coke oven gas and blast furnace gas are normally available at only a few Pa, typically less than 1.5 kPa (6ins W.G.). This requires very large valves to provide sufficient flow and valves as large as 12–24 inches may be required. Such large valves introduce potential issues with the response time for emergency closure owing to the inertia of the mechanism.

Another constraint is the flow capacity of the valve train and supply pipework. As mentioned above, the designer is always under pressure to minimise costs and the price of valves escalates rapidly with increasing size. However, if the system is undersized then furnace output cannot be achieved. We remember being asked to assist with increasing the output a lime kiln installed in a steelworks. The kiln utilised a mixture of coke oven gas and blast furnace gas that was transported several hundred metres in a 22-inch pipe. Owing to limited supplies of coke oven gas, a small proportion of natural gas was blended in near the coke ovens at the inlet to the pipeline. The process engineer hoped to increase the kiln output by using advanced heat transfer modelling. However, the kiln was not limited by heat transfer but by the transport capacity of the pipeline, a factor that became obvious when it was found that the control valve was always fully open. A simple, medium cost solution would have been to add the make-up natural gas at the burner via a separate small diameter pipeline with a separate valve train at the burner thus providing more pipeline capacity. However, this was not implemented because the steelworks closed 18 months later.

7.4.2 Waste Liquid Fuel Handling

Compared with solids and gases, waste liquids are relatively easy to handle. The main issues include ensuring that potential contaminants such as grit, fibres, etc are either separated by filtration, or that the downstream equipment, including valves, atomisers, etc., can handle these materials. Corrosion, together with chemical attack of non-metallic components such as seals, gaskets, etc, is a risk with some liquid wastes, especially spent solvents. To address these issues an analysis of the fuel is required together with a good knowledge of the properties of materials. Many fuel system designers will need additional, specialist advice to address these issues.

7.4.3 Solids Waste Fuel Handling

Combustible solid wastes encompass a very wide range of materials including vegetable matter, wood waste, plastics, garbage, carbon dust, petroleum coke, etc. Characteristics that influence the design of the waste handling system include the size distribution, the flow characteristics, abrasiveness, explosibility and the waste's propensity for degradation. Each of these is considered in more detail below. When I (Peter M) joined the cement industry in the late 1970s, the British industry was attempting to utilise garbage as a supplementary fuel to reduce its high coal costs. One scheme, to use raw garbage, was

moderately successful but the costs incurred were so high that the promised savings were never realised. Many of these unexpected higher costs were caused by the additional labour required to overcome engineering difficulties with the handling system. My employer initiated a scheme to utilise composted garbage, which was chosen over raw garbage because it had a higher and, more consistent, calorific value. It was intended to use a small redundant high speed coal mill fed by a screw feeder from a small hopper. I inherited 300 tones of this material that was stored in the works quarry. The initial trials resulted in the screw feeder seizing solid and shearing its drive. It required complete dismantling to free it, a very unpleasant experience for the fitters responsible for this task. After a few more attempts, it was realised that the material was not usable, unless a substantial capital investment was made and the remainder was left to rot in the quarry.

Size Distribution

The first consideration is the size distribution of the material and whether the material can be burned "as received", or needs further size reduction. If the particles are small, the material can often be burned without further processing, especially if the waste is reactive and burnt as a supplementary fuel. In that case all that is required is a handling system similar to a pulverised coal storage bin and fine coal conveying system. Care will be required in designing the storage bin to ensure that the waste can be reliably extracted and specialist advice may be required to optimize the design.

One of the most important considerations is the explosion risk since most carbonacous materials are explosible and many develop significant electrostatic charges, which provides a powerful built-in ignition source. Most plastics and wood dust are in this category, making them particularly hazardous. In this case all the equipment must be electrically bonded and earthed (grounded) to ensure all static charges are safely dissipated.

If the waste is too large to burn without further size reduction, then its grinding characteristics are important. Many waste materials, such as plastics and wood waste are difficult to grind because they exhibit plastic deformation, stretching molecular bonds rather than fracturing them, rendering conventional ball and roller mills unsuitable. In these cases, hammer mills or "chopper fans" may prove suitable but the choice of pulveriser should be established by careful experimental tests.

While materials such as carbon dust and petroleum coke have similar flow characteristics to raw and pulverised coal, many other waste materials are less easy to handle. As indicated above, an area that causes the greatest difficulty with many waste fuels is storage

and extraction. Waste vegetable matter, wood-waste, shredded plastic, garbage, etc., have very poor flow characteristics making them difficult to extract from hoppers. Furthermore, some of these wastes are biodegradable so for these, ensuring mass flow is even more crucial than for coal. If biodegradable material hangs in bins, it will become putrescent and noxious, representing a serious health hazard.

Biodegradable wastes should not be stored for prolonged periods. Ideally they should be burned within a few hours of delivery. All bins need large outlets and very steep, vertical or even divergent sides and large extractors. Belt and pan feeders are preferred; table feeders and conveying screws should be avoided at all costs. The inlet to most table feeders is simply too small for effective extraction from the hopper while screw feeders also suffer from the small inlet but, in addition, they tend to compress the waste material. When this happens the torque required to turn the screw increases dramatically and either the motor stalls, or the drive suffers a mechanical failure as a result of overloading.

7.4.4 Environmental Benefits and Health Hazards of Waste Fuel Utilisation

Waste fuels can be used to reduce primary fossil fuel consumption, thus saving resources as well as cost. Where wastes are vegetable in origin, such as wood waste, greenhouse gas emissions are also potentially reduced. Furthermore, many wastes are potential health hazards and their use as supplementary fuel in high temperature furnaces is beneficial for the environment, enabling the complete destruction of a potentially hazardous material while simultaneously reducing fossil fuel use. However, their safe utilisation requires that the potential health hazards are carefully assessed and the issues addressed so that the material can be used without adversely affecting the health of employees or the public. For example, waste oils often contain heavy metals, such as lead, resulting from bearing wear. Petroleum coke usually contains vanadium so the ash and particulate are potentially toxic. Where these materials are burnt, excellent dust collection from the flue gases is mandatory. Most petroleum coke contains substantial quantities of sulphur, which may have a detrimental effect on the process and/or the atmospheric emissions. The composted garbage described above is a potential harbourer of Legionella bacteria and other biohazards. Other materials, such as some waste solvents, may be potentially carcinogenic.

Great care needs to be taken to understand the risks and address the potential health issues accordingly. Failure to do so is likely to result in significant penalties and compensation costs that will far outweigh any fuel cost savings.

Nomenclature

a = constant for the Hardgrove machine determined by a standard calibration procedure
b = constant for the Hardgrove machine determined by a standard calibration procedure
X = mass residue on 75 micron sieve
Y = Hardgrove-Grindability Index

References for Chapter 7

Arnold, P. C., McLean, A. G., & Roberts, A. W. (1979). *Bulk Solids: Storage, Flow and Hadling, TUNRA Ltd*. NSW, Australia: Univ. Of Newcastle.

Bartknecht, W. (1981). *Explosions, course, prevention, protection*. Berlin & New York: Springer-Verlag.

Eckhoff, Rolf K. (1991). *Dust explosions in the process industries*. Oxford: Butterworth-Heinemann.

Field, M. A., Gill, D. W., Morgan, B. B., & Hawksley, P. G. W. (1967). *Combustion of pulverised coal*. Leatherhead: BCURA. pp201–207.

FL Smidth & Co. (May, 1982). *Course notes from The Cement Production Seminar*. Denmark: Rungstedgaard Seminar Centre.

CEGB. (1971). *Modern power station practice,* vol 2, (2nd ed.). Oxford: Pergamon Press.

Hardgrove, R. M. (1932). Grindability of coal. *Trans ASME, 54*, F.S.P., 37.

Applicable Codes and Standards

Some of the codes and standards that apply to combustion installations are listed below. This list is not exhaustive and you should check for any applicable codes and standards that apply to the location of the installation. Codes and standards are regularly updated and you must ensure that you are using the current version.

AS 3814–2005 (AGA 501–2005), Code for industrial and commercial gas fired appliances, The Australian Gas Association, Braeside, Vic

AS5601–2001(AGA 601–2001), Gas installations, The Australian Gas Association, Braeside, Vic

ASTM D409–02 "Standard test method for grindability of coal by the Hardgrove-machine method", ASTM D409–02 "Standard test method for grindability of coal by the Hardgrove-machine method", ASTM International

BS EN 161:2002, Automatic shut-off valves for gas burners and gas appliances
BS 799–41991, Oil burning equipment. Specification for atomizing burners (other than monobloc type) together with associated equipment for single burner and multi burner installations
BS EN 1854:1997, Pressure sensing devices for gas burners and gas burning appliances
EN 14797, Explosion venting devices (2003)
IChemE Guide to dust explosion and protection:
Part 1 Venting
Part 2 Ignition prevention, containment, inerting, suppression and isolation
Part 3 Venting of weak vessels and the effects of vent ducts
NFPA 68 "Guide to venting of deflagrations", 2002NFPA 68 "Guide to venting of deflagrations", 2002 Edition, National Fire Protection Association, Quincy, MA, USA (Due for revision in 2006)
NFPA 85: Boiler and combustion systems hazards code, 2001 Edition
NFPA 8501: Standard for single burner boiler operation, 1997 Edition
NFPA 8503: Standard for pulverized fuel systems, 1997 Ed., National Fire Protection Association, Quincy, MA, USA
VDI 3673 Blatt 1, Pressure venting of dust explosions, 2002–11 Ed., VDI Verein Deutscher Ingenieure, Düsseldorf, Germany

Chapter 8

Furnace Control and Safety

Chapter contents

8.1	Process Control	290
8.2	Furnace Instrumentation	292
8.3	Flue Gas Analysis	302
8.4	Combustion Control	313
8.5	Ensuring Furnace Safety	315
8.6	Burner Management Systems	321
Nomenclature		333
References		334

This chapter concentrates on the special features of furnace control and assumes a basic knowledge of process control systems. For more information on the design of process control systems see Dorf & Bishop (2005) or Johnson (2006).

Furnace control systems perform two basic functions, controlling the furnace process and ensuring safe operation. In the past these two functions were undertaken by two totally different systems, generally a pneumatic based system for process control and a fail-safe relay and cam timer based system for safety management. The latter is widely known as a Burner Management System (BMS). This arrangement had a very good safety record, danger-side failures being very rare, with the physical separation of the two systems being a major contributor to this safety record.

With the advent of Programmable Logic Controllers (PLCs) in the 1980s many control engineers were tempted to include both systems in the same unit, losing both the element of redundancy and the fail-safe nature of the previous systems. While the PLC systems were generally more reliable than the old relay based systems, failures were no longer restricted to the fail-safe mode; despite claims by the manufacturers that safety was assured by the watchdog timer. Possibly the worst installation of this type that the authors encountered was a plant with a large number of rotary kilns, each with a 100 MW gas burner that had all the process controls and safety interlocks in the same computer and did not even have a hard wired shutdown button for each kiln.

Despite claims by the manufacturers and control engineers, most of these PLC based systems never complied with the intent of the various burner and furnace safety codes and many dangerous incidents occurred, of which several resulted in explosions. As a consequence, codes such as NFPA 86 now specifically require physical separation of the control and BMS functions and interposing safety relays in critical BMS functions, such as flame failure and fuel safety shut-off valves. Owing to the different functions and compulsory separation of the control system and burner management system, these will be considered separately below.

8.1 Process Control

Pneumatic systems are obsolete, and all new furnaces and retrofits either utilise PLCs for individual furnace control, or the furnaces are controlled through the overall plant Distributed Control System (DCS). Whatever hardware is used, the process control system is required to meet one or more of the following objectives:

- Maximising furnace production capacity;
- Ensuring satisfactory product quality;

- Minimising fuel consumption;
- Minimising emissions;
- Controlling furnace warm-up;
- Enabling smooth change-over between different products.

Furnace control systems typically attempt to meet these objectives by controlling one or more of the following parameters:

- Fuel flow rate(s) or heat inputs to the furnace;
- Combustion air flow rate or air/fuel ratio(s);
- Combustion air temperature;
- Furnace temperature(s);
- Furnace exit gas composition;
- Furnace exit gas temperature;
- Feed rate of raw material to the furnace;
- Physical and chemical composition of raw material to the furnace;
- Product exit temperature.

Note that, direct measurement of product quality is extremely rare because of the great difficulty or impossibility of making such measurements for many processes and, while product quality is often related to temperature, that relationship is often highly non-linear. This means that furnace control is usually based on an interpretation of product quality based on a raft of secondary measurements, which when occurring in the appropriate combination, provide conditions conducive to optimum product quality.

8.1.1 Basic Furnace Control Strategies

A range of strategies are common to many furnaces and these include:

Control of Product Temperature

This strategy is common in furnaces where the product temperature measurement is practical. The temperature is then controlled by either increasing or reducing the heat input (firing rate) or changing the feed rate to the furnace and the residence time of the product in the furnace.

A typical strategy is to continue to increase firing rate until the product reaches the target temperature. If the furnace is not at full firing rate when product reaches target temperature, then feed is also increased until full firing rate and product temperature are achieved simultaneously. If product temperature then falls, feed-rate is reduced and product residence time increased. This strategy maintains maximum possible furnace production rate but can have a detrimental effect on product quality if the feed rate is increased, such that the residence time becomes too short. For example, steel slab reheating

furnaces are often controlled by measuring the surface temperature of the slab, but for rolling it is the temperature profile within the slab that is important and the rate of internal heating is slow compared to the rate of surface heating owing to the former being conduction limited. Hence if the residence time is too short, the slab surface temperature will be achieved but not the core temperature and the quality of the rolled product will be poor.

Fuzzy Logic and Rule Based Systems

Many furnaces have very long time constants and no single variable that can be used to control the process. For these furnaces rule-based expert systems and fuzzy logic control systems are commonly used. These systems use inputs from a wide range of measurable furnace parameters, such as fuel input, exit gas temperature, exit gas oxygen, exit gas CO, exit gas NOx, feed rate, firing rate, feed/product residence time, etc, to infer the furnace operating conditions. The control system then adjusts the furnace inputs to obtain a set of parameters most conducive to optimum product quality and production rate. These systems effectively mimic the best human operators but do so with greater consistency than real operators are able to maintain.

Owing to the complexity of the processes involved, these systems are expensive to install, commission and tune. However, the increased production, improved product quality and reduced specific energy consumption ensures that the return on investment is very good.

8.2 Furnace Instrumentation

Good instrumentation is an essential component of the furnace control system. If the furnace performance parameters cannot be measured reliably, then the furnace cannot be effectively controlled. Techniques for measuring the most important parameters are discussed below.

8.2.1 Temperature Measurement

Gas and product temperature are probably the most useful but also misunderstood and abused parameters of furnace performance, so it is worth considering their measurement in some detail. In our opinion it is vitally important that furnace designers and operators understand the basics of temperature measurement and the limitations of currently available techniques.

Furnace temperature can be measured by a number of contact and non-contact devices, including:

- Thermocouples;
- Resistance thermometers;

- Ultrasonic acoustic devices;
- Radiation pyrometers.

It is important to be aware that these instruments suffer from a number of measuring errors that are fundamental to the technique, regardless of the accuracy of the instrument calibration. For example, when measuring gas temperatures using thermocouples or resistance thermometers, radiation to and from the enclosing sheath can cause major errors in the measurement, especially at higher temperatures, Figure 8.1.

In most industrial situations the wall is cooler than the gas so the sensor is heated by convective heat transfer from the gas:

$$q_{conv} = hA\left(T_{gas} - T_{sensor}\right) \tag{8.1}$$

Where:

A = surface area of the sensor sheath and
h = the gas to sheath convective heat transfer coefficient

Heat loss by radiation is:

$$q_{rad} = \varepsilon \Omega A\left(T^4{}_{sensor} - T^4{}_{wall}\right) \tag{8.2}$$

Where:

ε = emissivity of sensor sheath
Ω = Stefan's constant (6.67×10^{-8} $W^{-2}K^4$)
A = surface area of the sensor sheath and

For steady state conditions: Heat gain = heat lost, therefore:

$$q_{convection} = q_{radiation}$$

Hence:

$$\left(T_{gas} - T_{sensor}\right) = K\left(T^4{}_{\text{sensor}} - T^4{}_{wall}\right) \tag{8.3}$$

Where:

K = constant

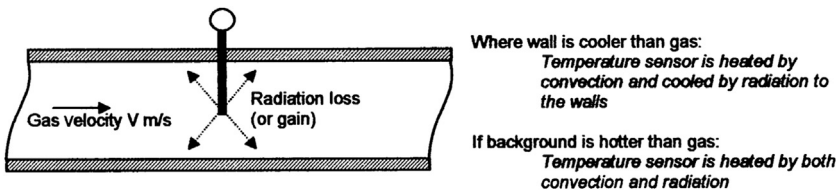


Figure 8.1 Sources of error in temperature measurement using thermocouples and resistance thermometers

Unfortunately, in most circumstances not enough information is available to determine K, so the error remains unknown but wherever the wall temperature is lower than that of the gas the sensor reads lower than the true gas temperature. The error increases with actual gas temperature since loss is proportional to T^4 while the gain is only proportional to T. The errors can be more than 100 °C at temperatures above 1100 °C. The error is therefore a serious problem in high temperature furnaces, which is further exacerbated by low gas velocities since the convective heat transfer coefficient is also lower. In circumstances where the background temperature is higher, such as where a sensor can "see" a flame the radiative and convective heat transfer components both heat the sensor and therefore it reads a higher temperature than the true gas temperature.

True gas temperatures (up to 1450 °C) can be measured by a suction pyrometer. This instrument was developed by the International Flame Research Foundation (IFRF), Figure 8.2. In this instrument, radiation gain to and loss from the thermocouple, is minimised by surrounding it by radiation shields and drawing a sample of gas at high velocity across the thermocouple. Heat transfer to the thermocouple from gas is entirely by convection. By varying the gas flow, the convective heat transfer changes and the temperature indicated by the thermocouple increases with increasing gas velocity, even for a constant gas temperature. If the gas flow across the thermocouple is measured for each condition then the convective heat transfer can be calculated. Since the radiation gain or loss is constant, the true gas temperature can be determined by extrapolation. At gas velocities of over 150 m/s the error is small and makes correction unnecessary for most practical purposes.

For even higher temperatures, up to 2400 °C the venturi-pneumatic pyrometer is used, Figure 8.3. This is essentially a suction pyrometer with the thermocouple mounted in the throat of a venturi. A second

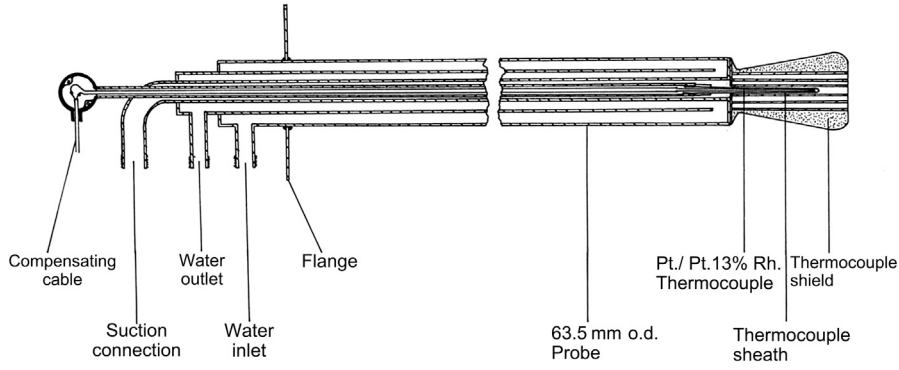


Figure 8.2 Suction pyrometer

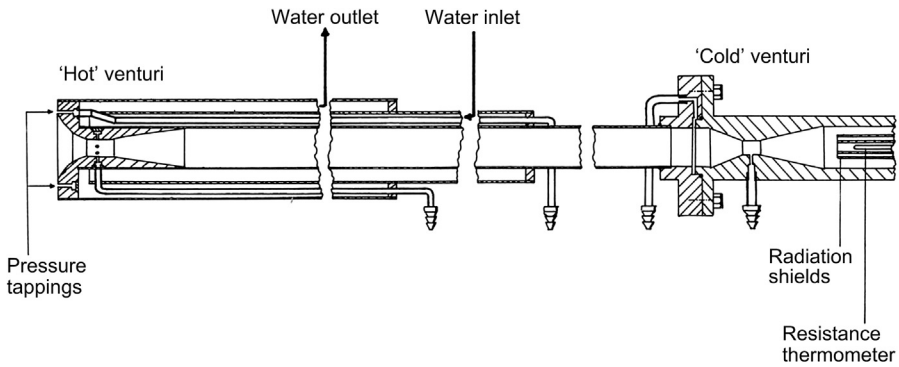


Figure 8.3 Venturi-pneumatic pyrometer

venturi is installed at the working end of the instrument. Hot gas is drawn through this venturi and the pressure drop measured. The sample then flows down the water cooled tube and through the second venturi where the pressure drop and gas temperature are measured simultaneously. Using the ideal gas laws, the volume of gas passing through the first venturi gas can be calculated and hence its temperature determined.

Neither of these instruments is suitable for permanent installation and continuous monitoring owing to difficulty in maintaining the required aspiration rate and problems with blocking, etc, but they are useful for evaluating furnace performance as part of an on-site investigation.

Non-contact temperature measurement normally uses infrared radiation emitted by the object being measured, Figure 8.4. Simple instruments measure the power radiated by the surface using equation 8.2, which in this application becomes:

$$q_{radiation} = \frac{\varepsilon \Omega A_t}{Z^2}\left(T^4{}_{surface} - T^4{}_{sensor}\right) \text{ watts} \qquad (8.4)$$

Since the target surface area increases with the distance of the sensor from the target A/Z^2 reduces to a constant and because the temperature of the sensor is known, the temperature of the surface can be calculated from $q_{radiation}$ received by the sensor, provided the emissivity is also known. This technique requires matching the instrument to the emissivity of the target and if the emissivity is set incorrectly a substantial error occurs, see appendix 4A for emissivity data for common furnace materials.

Setting the instrument to the correct emissivity is difficult, since even if the emissivity of a sample of the material is measured, this value can change with both temperature and surface condition, so substantial errors are inevitable. To improve accuracy, more sophisticated

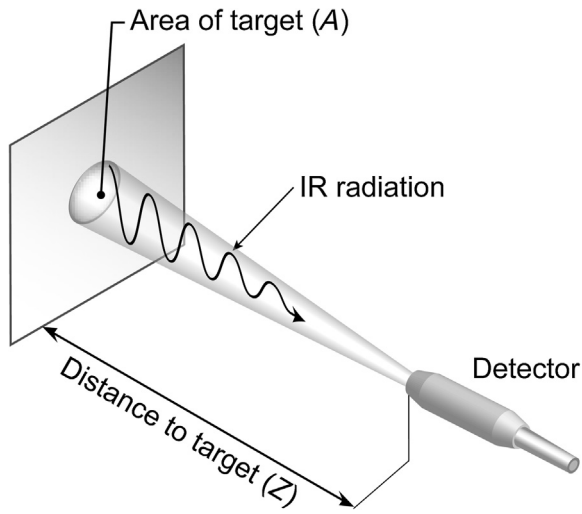


Figure 8.4 Principle of remote temperature measurement using infrared radiation

instruments utilise the fact that the frequency of the radiation increases with temperature and utilisation of this property reduces the effect of emissivity. Infrared instruments are also affected by furnace atmosphere with CO_2, H_2O, soot and dust absorbing and re-radiating infrared radiation. To reduce the effect of these difficulties, sensors responding to specific wavelengths most suited to the application are often chosen. In some cases two sensors, each responding to a single waveband, are used to produce a two-colour instrument. The latter reduces the error caused by suspended dust, etc; but does not eliminate it.

Ultrasonic temperature measurement, Figure 8.5, depends on the relationship between the speed of sound and the density of the medium it passes through. The speed of sound is measured by determining the time taken for the sound wave to cross the duct and then the density is calculated. For gases, density is related to temperature and, providing the gas composition is known, the temperature can then be calculated using the ideal gas laws. This instrument is also used for measuring gas velocity and is considered in further detail under section 8.2.2, below.

8.2.2 Heat Input Measurement

One of the most important parameters for efficient furnace operation is measurement and control of the heat input, both overall heat input and, where appropriate, the heat input to each burner or each zone.

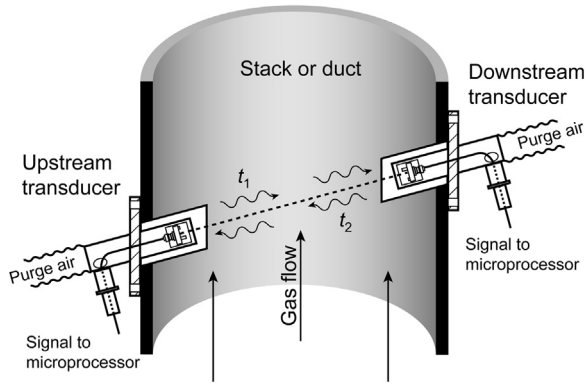


Figure 8.5 Principle of ultrasonic temperature and flow measurement

For fuels of constant, or relatively stable chemical composition and calorific value, this can be achieved by measuring the flow but, for fuels of differing composition such as recovered process off-gases, for example, refinery gas, the calorific value also needs to be measured or assessed.

Flow Measurement of Liquid and Gaseous Fuels

For oil and natural gas, most conventional flow measurement systems are suitable, including orifice plates, vortex shedding devices, corriolis mass flow meters, turbine flow meters, etc. However, flow rates of "dirty" gases, such coke oven gas, are more difficult to measure owing to the adverse effect that impurities, such as suspended particles and tars, have on many flow measuring systems. For example, pressure differential devices tend to suffer from rapid blocking of the tapping points whereas devices that are dependent on specific shapes, such as orifice plates and vortex shedding meters, suffer drift owing to sensor wear caused by particle attrition or deposit build up owing to condensation of tar, etc.

One technique that has been successfully applied to measure the flow of dirty gases is ultrasonic flow measurement, Figure 8.5. An ultrasonic pulse is projected across the duct from left to right and the transit time measured (t_1). A second pulse is sent from right to left (t_2). Since the gas is moving up the duct, t_2 is longer than t_1 and the velocity is directly related to t_2 - t_1 and is independent of gas composition, temperature and dust loading. The volumetric flow can then be calculated using the cross sectional area of the duct. Gas density can be measured using the same instrument, since the speed of sound in the gas is proportional to the density. The average transit time can

therefore be used to calculate the density. Hence from knowledge of the volume flow rate and density, the mass flow is calculated.

This technique is equally applicable to combustion air flow measurement and flue gas flow measurement.

Calorific Value Measurement

Calorific Value (CV) of gases can be continuously determined by an on-line calorimeter or on-line gas-chromatograph; however the latter is very expensive. On-line calorimeters work by burning an accurately metered sample of gas in a controlled airflow under closely controlled standard conditions. A constant exhaust temperature is maintained by carefully regulating both combustion and cooling air flows. The changes in air flow required to achieve the constant exhaust gas temperature is used to calculate the Wobbe Index or Calorific value of the gas. For many practical applications, especially where the range of gas composition is reasonably predictable, measurement of gas density and calculation of the expected CV gives sufficient accuracy for furnace control.

Solid Fuels

The heat input from solid fuels is difficult to measure. As for manufactured gases, both flow rate and calorific value need to be evaluated. Since most solid fuels require size reduction the flow rate can, in principle, be measured before or after size reduction. When the mass flow is measured prior to grinding, the normal method is a belt weigher, Figure 8.6. This technique is really only applicable to the supply to the fuel storage bin, so cannot provide on-line indication of firing rates but is useful for measuring fuel consumption over a longer period, say

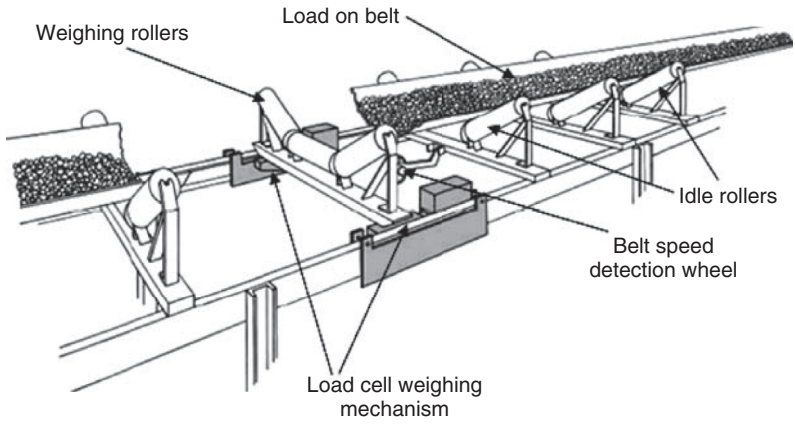


Figure 8.6 Schematic of a Schenck type belt weigher

24 hours or a week. While the manufactures claim accuracies of better than ±1%, this is often not achievable in practice owing to a number of reasons, including the tension in the belt which reduces the load on the weighing roller(s), the inertia of an unevenly distributed load and variations in the speed of the belt.

The most practical way of determining solid fuel flow rates prior to grinding is the use of calibrated volumetric feeders, such as drag chains, see chapter 7. These devices can be calibrated by belt weighers on the bunker feed, loss in weight systems in the bunker or by filling a truck with a sample over a measured time period and taking the load to a weighbridge for checking.

Where the fuel is stored after grinding, there are more options for determining flow rates, including loss-in-weight systems, impact weighers and weighing feeders such as the Pfister feeder described in chapter 7. The complexity of this equipment takes it beyond the realm of simple instrumentation and beyond the scope of this book.

Apart from fuel flow rate, calorific value is also required to determine heat input. This is normally impractical to measure on-line for solid fuels and has to be determined periodically by taking samples and analysing the fuel in a bomb calorimeter. Obtaining a representative sample is particularly important and ways of achieving this are described in various national standards, such as AS 4264:1995 Coal and Coke Sampling. This standard is in four parts, each dealing with a different topic, see references at the end of the chapter. Equivalent national standards exist in most countries.

8.2.3 Determination of Excess Air

For many furnaces, excess air has an important effect on furnace efficiency and is therefore one of the important parameters in furnace control. Too much excess air results in excessive heat being lost in the flue gases since the additional air has to be heated to flame temperature which is reduced as a consequence, adversely affecting heat transfer, This additional air then leaves the system at the exhaust gas temperature. Extra fuel has to be burnt to compensate for these flue gas losses and the reduced heat transfer caused by the lower flame temperature. In addition, the extra fuel required has even more flue gas losses associated with it so the effects are cumulative, and the reduction in efficiency far greater than predicted just from the increased flue gas associated with the excess air.

Figure 2.13 shows the effect of daily average fuel consumption of a semi-dry process cement kiln measured over a six month period. The fuel consumption at 2% oxygen is 3430 kJ/kg of clinker while that at 5% oxygen is 3770 kJ/kg, a 10% increase. This is approximately

twice that which would be predicted from calculating the increased flue gas losses. For a typical cement kiln producing 4000 tonne/day of clinker using thermal coal at US$70 per tonne, this represents an additional fuel cost of over US$1 million per year. On the other hand, too little excess air results in incomplete combustion and increased flue gas losses caused by carbon monoxide and, with solid and liquid fuels, unburnt particulate, see Figure 2.14.

Quite small variations either side of the optimum level (a few percentage points) result in significant reductions in efficiency, so accuracy of excess air determination is important. Three techniques are commonly used:

- Fuel and airflow measurement with calculation of air/fuel ratio or excess air levels;
- Flue gas analysis for excess oxygen with optional calculation of excess air levels;
- Fuel and airflow measurement with calculation of air/fuel ratio together with excess air trim based on flue gas analysis using O_2 or CO concentration.

Calculation of the air/fuel ratio or excess air from the individual flow measurements is rarely satisfactory owing to the significant errors inherent in these measurements. Errors of $\pm$ 10% are common with flow measurement which potentially introduces errors of up to $\pm$ 20% in the air/fuel ratio calculation. Translated to excess air terms, this can result in either sub-stoichiometric operation or operation at very high levels of excess air. The risk of sub-stoichiometric operation is a problem that is usually overcome by establishing a very conservative set point, resulting in operation at excess air levels of 40–50%, together with the corresponding waste of energy. If temperature and pressure correction are incorporated and extreme care is taken with the calibration of the instruments, the air/fuel ratio determined this way can be within $\pm$5%, but such accuracy is extremely rare.

In most applications, the most convenient and accurate method of controlling air/fuel ratio is by measuring the oxygen content of the flue gas. This can be achieved by either in-situ or sampling analysers. Sampling systems draw a small proportion of the flue gas from the exhaust ducting then filter, dry and condition the gas before it enters the analyser. The oxygen reading provided by a sampling analyser is therefore normally a proportion of the total dry gas i.e. oxygen, nitrogen, CO_2 and CO, whereas in-situ analysers measure the oxygen as a proportion of the wet gas, so include the water vapour and any other gases that would be removed in a gas conditioning system, such as SO_2. For a dry gas sample the excess air can be calculated using:

Table 8.1 Typical Flue Gas Analysis for Heavy Fuel Oil Showing the Difference Between Wet and Dry Oxygen Proportions

	CO_2	H_2O	SO_2	N_2	O_2	*Total*
Wet gas (as Measured)	12.62	9.76	0.03	74.99	2.6	100
Wet gas (minus the water)	12.62	—	0.03	74.99	2.6	90.24
Equivalent dry gas composition	13.98	—	0.03	83.10	2.88	100

$$\text{Excess air} = \frac{100x}{(20.9 - x)}\% \tag{8.5}$$

Where x is the oxygen content of the flue gas %

Hence 1% oxygen is equivalent to 5% excess air and a reading of 2.6% oxygen in a dry flue gas sample represents 14.2 % excess air.

For a wet gas sample the water vapour must be accounted for. For most fuels, the SO_2 is a very small proportion of the fuel gas and can normally be ignored for analysis purposes. A typical wet gas composition is shown in Table 8.1, in this case for a heavy fuel oil.

From Table 8.1 it can be seen that 2.6% oxygen on a wet gas basis is equivalent to a dry gas analysis of 2.88% oxygen. Thus for a measured oxygen concentration of 2.6% (wet basis) the excess air is 16% compared with 14.2% for 2.6% O_2 on a dry gas basis. It can be seen that the small proportion of SO_2 would have a negligible effect on the excess air calculation. However, for processes where significant quantities of gas are evolved, such as cement and lime making, equation 8.5 is not applicable owing to the dilution effect caused by the evolved gas.

Determination of excess air from oxygen analysis is much more accurate than using flow measurement because the effect of errors is much smaller. For example, a 10% error in the oxygen reading would change the excess air by one or two percentage points, whereas a 10% in the total airflow reading would change the excess air by approximately 10 percentage points.

The major source of inaccuracy with gas analysis is air in-leakage, either into the flue gas ducting where this operates below atmospheric pressure, or into the sampling system. This leads to a higher oxygen concentration than appropriate for the excess air level in the furnace. If the dilution is significant there is the risk that the resulting false reading will lead to operation at very low levels of excess air, or in extreme cases, even sub-stoichiometric operation. This risk can largely be avoided by also measuring carbon monoxide, which will rapidly increase as soon as the excess air is too low for satisfactory combustion.

8.3 Flue Gas Analysis

Flue gas analysis is used for a wide range of processes. It is widely used to control and monitor excess air in combustion systems, as described above and is useful even where air/fuel ratio control is feasible because it is more accurate and maintains a check on the flow instrument calibration. Where carbon monoxide is also measured, flue gas analysis also provides an indication of combustion efficiency. Hence flue gas analysis is a very important measurement for many furnaces and other combustion plants. Gases such as NO_x, SO_x and CO_2 may also be measured to confirm that the emissions are within the limits prescribed by environmental regulations.

Furnace gas analysis is also used to monitor reducing conditions in a wide range of metal heating and treatment furnaces and for ensuring the integrity of inert atmospheres in processes that require such atmospheres, whether for safety or product quality reasons.

Currently a wide range of techniques is available for flue gas sampling, ranging from intermittent sampling and wet chemistry analysis to all-electronic devices with almost instant read-out and automatic calibration. The choice of analyser is dependent on a wide range of conditions, including cost, outputs required, gas temperature and contamination, operating environment, etc. The considerations are application specific and far too wide ranging to be considered here but the capability of most currently available analysis techniques is summarised in Table 8.2.

As indicated in Table 8.2, flue gas analysers may be mounted directly in the stack (in-situ) and hence measure a wet gas sample or mounted remotely and draw a gas sample from the flue which is filtered and normally dried prior to analysis, hence producing an analysis of the dry gas components. Both systems have advantages and disadvantages as shown in Table 8.3.

8.3.1 Extractive Gas Sampling Systems and Analysers

The basics of a conventional flue gas sampling system are shown in Figure 8.7. It comprises a probe located in the stack, a sample line, filter, and gas conditioning unit, pump and the analyser. More than one analyser may be used to measure a range of components.

A difficulty experienced with extractive sampling systems is achieving a sufficiently rapid response time. The analyser response is generally fast but the transit time of the sample in the sample line is often too long for process control and this relegates the system to a passive monitoring role. Every effort should be made to reduce the gas transit time in the sample line by maintaining adequate gas velocities and using as short a line as practical. Sample response times of

Table 8.2 Summary of Flue Gas Species Analysis Techniques

Technique	*Sample Method*	*O_2*	*CO*	*CO_2*	*H_2O*	*NOx*	*SOx*	*Hydro-Carbons*
Infra-red cell	In-situ or remote	X	✓	✓	✓	✓	✓	✓
Electro-chemical cell	In-situ or remote	0–25%	0–100000 ppm	X	X	NO 0–5000 ppm NO_2 0–1000 ppm	0–5000 ppm	0–55 methane
Para-magnetic meter	Remote	0–21%	X	X	X	X	X	X
Chemical absorption Dräger tube	Remote	0–21% in ranges	✓	✓	X	✓	✓	✓
Wet chemical Orsat analyser	Remote	0–21%	✓	✓	X	X	X	X
Wet chemical Dwyer tube	Remote	X	X	✓	X	X	X	X

Table 8.3 Comparison Between Basic Extractive Gas Sampling and in-situ Gas Analysis Systems

Extractive Gas Sampling Analysers		*In-situ Analysers*	
Draw a sample of gas via from the flue gas system via a small tube. The sample is normally filtered dried and cooled prior to analysis. Because the water vapour is removed, the reading is related to the dry gas components only.		These are mounted local to the stack and have the sensor either in the stack or are close by coupled to a very short probe. The gas is sampled hot and conditioning is either not required or limited to filtration for particulate removal.	
Advantages	**Disadvantages**	**Advantages**	**Disadvantages**
The analysers can be located in a clean environment.	Sampling systems are costly to install and maintain.	Non-sampling systems are cheaper to install and maintain.	For most gases in-situ analysers are less accurate than remote units.
The analyser has a clean sample.	Sampling system design is a specialist skill not normally available on a plant.	Skills required to install the systems are normally available on a typical plant.	Apart from oxygen, only the gases that absorb infra-red radiation can be analysed in-situ.
Greater accuracy can often be achieved with remote mounted analysers.	The instrument supplier may not have sufficient process knowledge to design an appropriate sample system.	Maintenance is normally reduced owing to the absence of a complex sampling system.	The wet gas analysis makes calculation of true excess air levels more difficult.
The same sample can be analysed by a number of different analysers for a wide range of gas components.	Even small leaks in the sampling system can create large errors in the readings, especially for oxygen.	Errors caused by leaks in the sampling system are absent.	The analyser is more vulnerable to damage owing to its location.

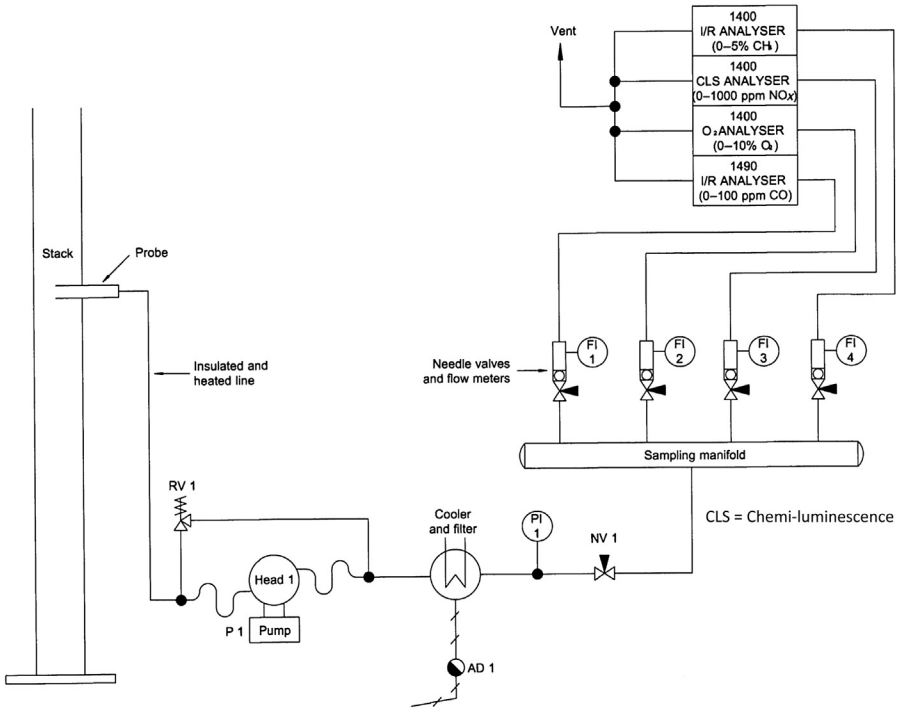


Figure 8.7 Schematic of a conventional flue gas sampling system

10–15 sec are desirable with up to 30 sec being acceptable. Response times longer than one minute become problematic for control purposes and times of 5 min or more are useless.

The two major problems are dust and water vapour that cause blocking of the probe and/or sample line. Dust loadings vary from light loadings, such as the ash from coal combustion which are easy to sample, to very heavy dust loadings with high water contents such as occurs with alumina calcination, cement manufacture, flash drying processes, etc. These gases, with heavy dust loading with high water content, are very difficult to sample reliably. As a result significant variations on the basic system shown in Figure 8.7 have evolved. These are:

- Cold dry extractive systems;
- Hot wet extractive systems with heated sample line to prevent condensation;
- Dilution extractive systems where the sample is diluted with a known proportion of clean dry air to lower both the dust concentration and the dew point.

Sample Probe Installation

Sample probe design and installation will depend on the flue design, the gas temperature and the associated sample system. A critical feature is the probe entry location which must draw a representative sample of flue gas. To achieve this, the probe should be located upstream of any potential air inleakage, wherever possible, with the sample entry towards the centre of the flue away from the walls avoiding the boundary layer, Figure 8.8. Wherever possible the probe should be in a straight duct several diameters downstream of any bends. Where this is not possible, a trial should be undertaken with a portable probe to find a representative sample point prior to design for the permanent installation.

Simple stainless steel probes will suffice for many installations, especially where the flue gas temperature is below 500 °C. Above this temperature water or air cooling may be required. Water cooled probes can be permanently installed in ducts with gas temperatures up to 1450 °C and used for short term trials at much higher temperatures such as direct in-flame sampling. Design of cooling water jackets is very important to ensure effective cooling. This requires sufficient water flow, evenly distributed through the probe to ensure that the cooling water temperature is maintained below 70°C at the outlet

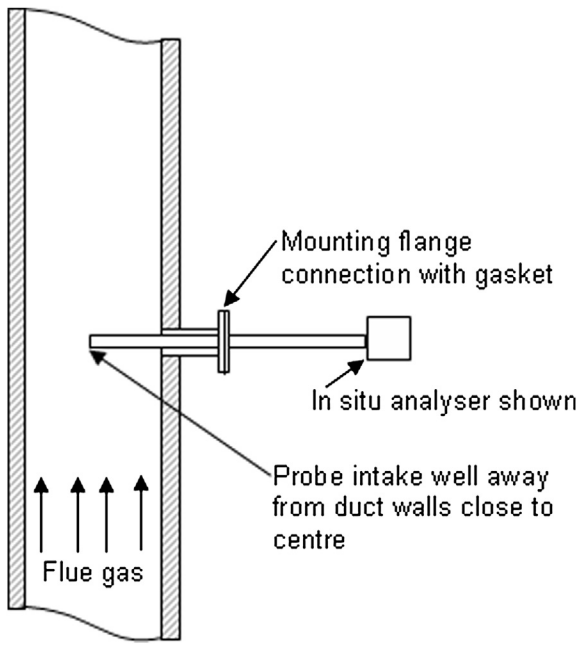


Figure 8.8 Typical flue gas sampling probe installation

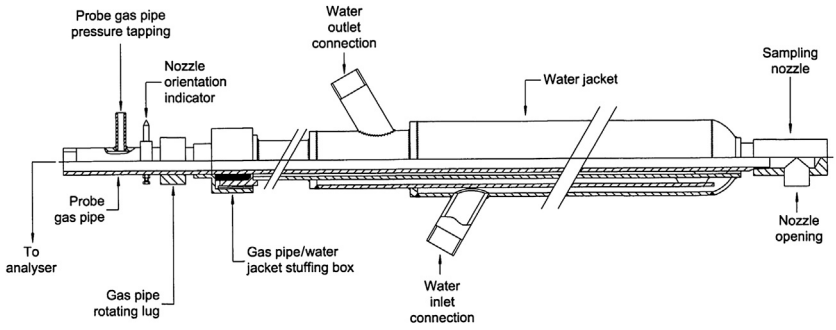
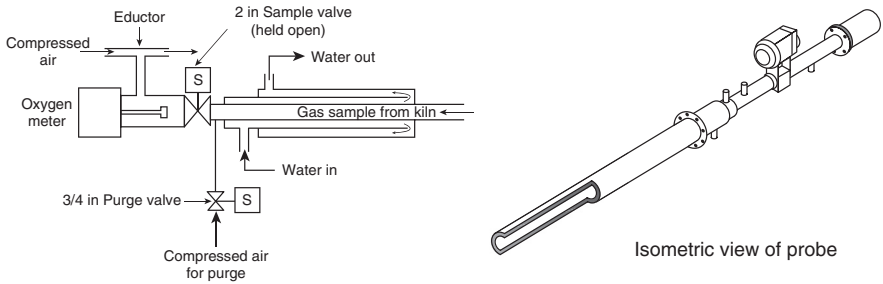


Figure 8.9 Water-cooled hot gas portable sampling probe designed by the authors

to minimise the risk of localised boiling and vapour locking. The authors have found a design based on tangential water inlet and double concentric water space, with water flow proving on the outlet, totally reliable, see Figure 8.9.

If the gases are dusty, or otherwise contaminated, such as with condensable alkali compounds, provision must be made for probe cleaning; otherwise it will become blocked with time. This cleaning can be done manually where the time taken to block the probe is sufficiently long; otherwise automatic pneumatic cleaning is required. A water-cooled probe employing automatic pneumatic cleaning is shown in Figure 8.10.

When a temporary probe is inserted, such as during performance investigations, the sample probe should be inserted well into the duct and, if possible, the gap around the probe at sample hole temporarily sealed to prevent any ingress of air.



Note: During normal sampling the 2 in sample valve is open and the 2/4 in purge valve is closed. For the purge, the 2 in sample valve closes before the 3/4 in purge valve opens for 20 s. The purge valve then closes before the sample valve re-opens to avoid over-pressurising the oxygen meter.

Figure 8.10 A water-cooled probe employing automatic pneumatic cleaning

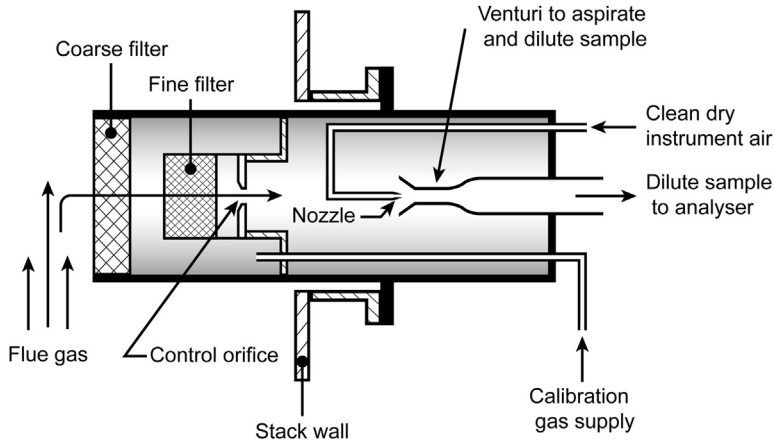


Figure 8.11 Dilution extractive gas sampling system

Cold Gas Extractive Systems

These systems were originally designed for use with paramagnetic oxygen analysers and, since the water vapour condenses in the sample line, it must have a continuous fall to the moisture trap. The sample must be dried and filtered before analysis so the analysis is based on a dry gas sample. These systems are not suitable for measuring gases with significant solubility in water, such as CO_2 SOx or NOx, which must use either hot gas or dilution sampling to preserve sample integrity but can be used for CO since its solubility in water is low.

Hot Wet Gas Extractive Systems

In these systems, the flue gas sample is maintained above its dew point from the sample point to the analyser by using a heated sample line. The sample is cooled, filtered and dried before being fed to the instrument(s) for analysis, so as for a cold gas system, the analysis is based on a dry gas sample. The absence of condensate in the sample line makes these systems suitable for sampling SOx, CO_2 and NOx.

Dilution Extractive Systems

Dilution probe systems use dry contamination-free compressed air fed to an eductor that entrains the sample and conveys it to the analyser. This technique has the advantage that, within reasonable limits, the mass of sample entrained is proportional to the mass flow of dilution air. Hence, small variations in dilution air flow have a negligible effect on the gas sample/dilution air ratio. The diluted sample is well below the dewpoint so that there is no risk of condensation in the sample line

and therefore heated sample lines are not required. The gas sample flow from the flue through the filter is much lower than for non-dilution systems, typically an order of magnitude lower, hence reducing problems with filter blockage. Dilution probe systems offer lower maintenance costs than hot, wet gas systems and are widely used on coal fired power stations but have seen little use on furnaces.

8.3.2 In-Situ Systems

In-situ analysis has the potential benefit of being simpler than remote sampling and easier to maintain. The absence of a sample line also offers the potential benefit of faster response times. The major problem, which has prevented in-situ analysis completely displacing flue gas sampling, is the fact that many gas ducts are hostile environments for a delicate electronic instrument. Whilst boiler flue ducts, the largest market for flue gas analysers, are relatively clean, the conditions in most direct contact processes (e.g. cement kiln, alumina calciners, etc.) are extremely arduous, with temperatures of up to 1200 °C with very high dust loading that sometimes include alkali vapours. These are not the ideal conditions for any instrument.

Dust Monitors

The first in-situ instruments on flue gas stacks were cross-duct optical dust monitors, Figure 8.12. The early units were unreliable and suffered from dust obscuring the windows, calibration drift etc. Great efforts have been made to improve their reliability, which have been generally successful and they are now in widespread use. However,

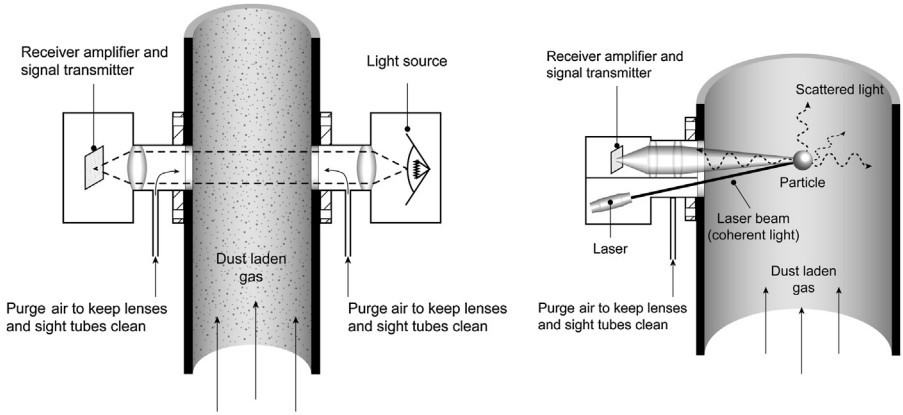


Figure 8.12 Schematic of cross-duct optical obscuration dust monitor (left) and backscatter device (right)

there is a major misconception, promoted by some manufacturers and accepted by many environmental regulators, that these instruments can be calibrated to give a gravimetric (weight based) readout.

These instruments utilise obscuration which results in beam attenuation that provides a signal related to the obscuration caused by the dust. More sophisticated instruments use backscattering of laser light which don't rely on obscuration and eliminate the need for accurate alignment. Both types of instruments are sensitive to the characteristics of the dust including:

- Reflective, refractive and diffractive properties of the particulate;
- Density;
- The number of particles;
- Particle size distribution;
- Particle shape;
- Wavelength of the illuminating source.

Only the wavelength of the illuminating source is under the control of the instrument manufacturer and likely to remain constant with time. Note the absence of mass in the properties influencing instrument calibration.

For many processes, the dust properties remain approximately constant and quasi-calibration against mass flow is possible. However, this is not the case where the dust arises from multiple sources since the dust properties will change according to the relative contribution of each source. For example, cement production has two principle sources of dust; raw meal which is light and reflective and clinker which is dense and has much lower reflectivity. Additionally the shape and size distribution will be different; clinker is predominantly spherical whereas raw meal has been ground and is fractured along cleavage planes. Clinker particles also have a greater mass than raw meal particles of similar size.

It is therefore only possible to reliably calibrate these instruments where the characteristics of the dust remain constant. A good example of where this applies are coal fired power stations where the fly ash size distribution is mainly related to the performance of the coal mill which only changes slowly with time. Despite this, owing to the prevailing ignorance of the characteristics of these instruments, operators of process plants are often required to calibrate their instruments as if the calibration was viable. Occasionally plants are even prosecuted for breach of emissions regulations on this basis.

Oxygen Analysers

The first in-situ gas analyser available was the zirconia oxygen analyser, Figure 8.13, which was available from the mid 1970s. The major

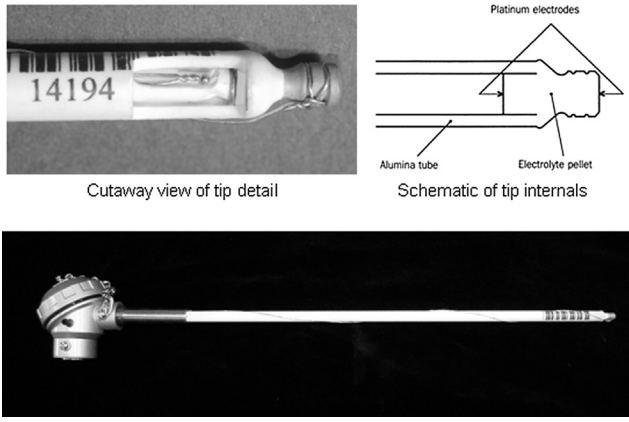


Figure 8.13 A high temperature (700–1700°C) zirconia analyser for flue gas oxygen measurement showing a cross section of the cell (Reproduced by kind permission of Australian Oxytrol Systems)

advantages of this instrument are its ability to function at high temperatures and its very fast response time compared with that using a sampling system, together with its relative simplicity and good accuracy at low oxygen levels. This is a consequence of its operation, in that it compares the oxygen concentration in air with that in flue gas and provides an electrical output related to the concentration difference by the Nernst equation:

$$E = \left(\frac{RT}{nF}\right) \mathrm{In}\left(\frac{pO_2}{pO_2{}^R}\right) \tag{8.6}$$

Where:

E = sensor electromotive force, (mV)
R = gas constant
T = temperature, (Kelvin)
n = number of charges per reactant species
F = Faraday constant
pO_2= mole fraction of oxygen in the sample gas
$pO_2{}^R$ = mole fraction of oxygen in the reference gas (atmospheric air)

Since at low oxygen concentrations in the sample gas $\ln(pO_2/pO_2{}^R)$ is large, this sensor has the largest signal output at low oxygen concentrations making it ideal for flue gas analysis at low excess air. Zirconia oxygen analysers intended for low temperature use enclose the cell in a heated chamber to maintain the sensor temperature at 650–700 °C.

Cross Duct Analysers

Early CO/CO_2 Analysers

Open cross-duct analysers utilising a similar arrangement to the dust monitors have been developed for measuring CO and CO_2 utilising the radiative and absorptive properties of these gases in the infra-red band as a means of detection. These appeared in the early 1980s but suffer from a number of significant disadvantages that has led to limited application. An infra-red beam is sent across the duct and the CO and CO_2 absorb infra-red radiation in specific wave-bands. This property is used to detect the proportion of these gases present. Before transmission, the beam passes through a rotating wheel containing each gas sample to be analysed and a blank window. This creates a reference signal for each gas which is compared with the signal through the clear window. Software is then used to interpret the signals received by the detector and the concentration of each gas is calculated, displayed and recorded.

Folded Beam Analysers

The main problems with cross duct analysers have been related to the effect of dust on the infrared beam which is similar to its effects on visible light; hence cross duct analysers were restricted to relatively clean installations such as oil and gas fired boiler flue ducts. Difficulties were also experienced in maintaining the transmitter and receiver in alignment. These difficulties led to the development of the folded beam unit, Figure 8.14. In this device, an infra-red beam is sent across the duct within a self-contained housing, after passing through a rotating wheel similar to that used in the cross duct system. The flue gas diffuses through a pair of sintered metal pads so that the gas seen by the infra red beam is clean. This unit can measure up to five dipole gases such as CO_2, CO, H_2O, SO_2 and NO_x. Since the dust is removed from the gas as it diffuses in through the sintered pads, the beam passes through clean gas and this overcomes the problem of dust interference. These analysers have been successfully applied on a range of dusty plants such as cement kilns.

Modern Emissions Monitoring Analysers

Recent developments in cross duct analysers have overcome many of the problems of the early units to provide reliable multi-component gas analysers capable of measuring all gases that respond to electromagnetic radiation, such as CO, CO_2, NO, SO_2, H_2O, etc., with a single instrument. These modern instruments use Differential Optical Absorption Spectroscopy. This technique utilises an emitter on one side of the stack that projects a beam of light to a receiver on the other side. Specific gases absorb light from known parts of the spectrum, in

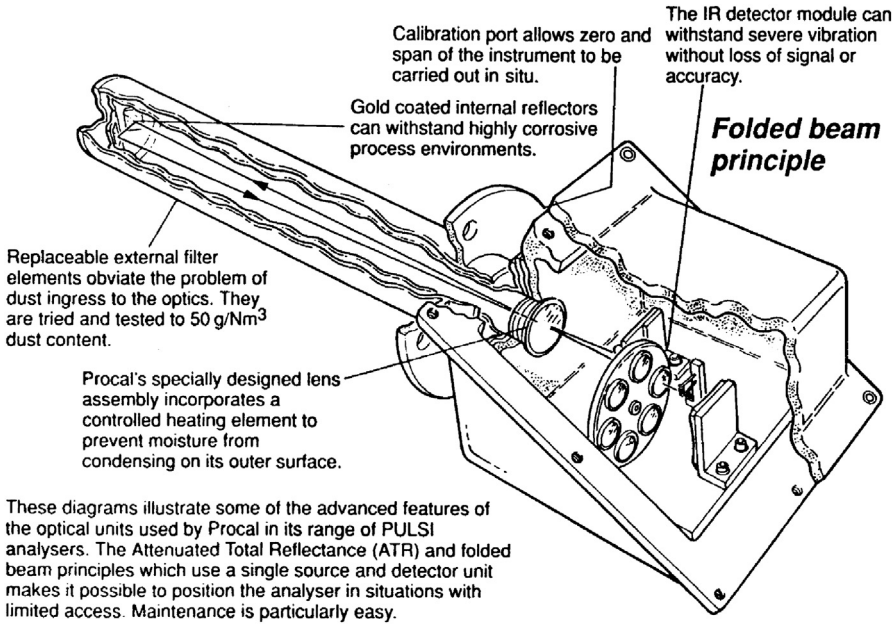


Figure 8.14 Procal folded beam in-situ flue gas analyser (Reproduced by kind permission of Procal Analytics Ltd.)

the UV, visible and infra red frequency ranges. The resulting spectrum is collected and transferred to the analyser through a fibre optic cable, Figure 8.15. The received signals are de-coded using complex software.

These instruments have received widespread approval for pollution monitoring and are generally stack mounted, hence in a relatively clean gas stream. The authors are unaware of how these instruments would respond in a dusty gas stream.

8.4 Combustion Control

Combustion control systems are used to control the operation of combustion plant, including the firing rate and airflow, and to maintain the air/fuel ratio required to meet the desired process conditions such as production rate, furnace temperature, product temperature, etc. The provision of combustion control improves process efficiency by maintaining an approximately constant air/fuel ratio under changing load conditions and relieving the operators of this task. This allows them to devote more time to the matters that really need their

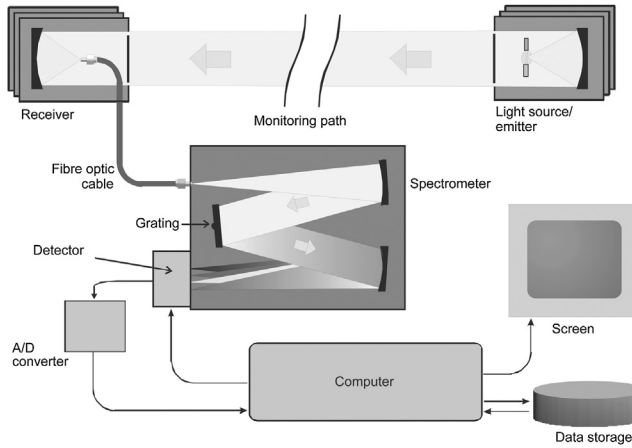


Figure 8.15 An Opsis cross-duct multi-component optical gas analyser (Reproduced by kind permission of Opsis AB)

attention and hence achieve more consistent process operating conditions.

Combustion control is quite distinct from burner management which concerns the start-up, shut-down and supervision of burners and combustion equipment to ensure safe operation. Like the burner management system, the combustion control system has an important safety function since it should prevent the burner from operating sub-stoichiometrically unless it is required to do so for process reasons.

In the past air/fuel ratio was often controlled by a mechanical linkage between the air damper and fuel valve with a characterising cam to compensate for the different valve flow/position relationships. These systems were difficult to set up and have almost been entirely superseded by electronic systems, except on some small burners/furnaces.

In order to maintain the safety integrity of the combustion system, the combustion control function should be kept entirely separate from the burner management system. As far as practical, the combustion control system should be designed to fail to a safe condition i.e., to maintain current flows, reduce the fuel flow to minimum and/or increase the airflow to the burner(s) in the event of any equipment failure, including the failure of field mounted instruments or the interconnecting wiring.

Control of the air/fuel ratio is one of the most important functions of the combustion control system. It must ensure that sufficient excess air is maintained at all times, except where a reducing atmosphere is employed for process reasons, in which case the combustion control system has to maintain a consistent air deficiency, typically 5–10%.

Maintaining the excess air or the sub-stoichiometric margin during firing rate changes is especially important, but also difficult, because of the different response times of the fuel control valves, combustion air dampers and fans, which can result in wide variations in air fuel ratio during load changes.

With normal excess air operation, the risk of sub-stoichiometric operation can be reduced by increasing the airflow before the fuel (air lead) when increasing the firing rate. Similarly when reducing firing rate, the fuel should reduce first, leading the air. It is important to note that the lead of airflow over fuel flow when increasing load should be minimal to maintain efficiency and minimize emissions.

For furnaces with reducing atmospheres, maintaining a consistent air deficiency of 5–10% is more difficult since the different response times of fuel valves and air dampers can cause large changes in air/fuel ratio. This requires that firing rate changes are made slowly at the speed of response of the air damper to ensure that the air/fuel ratio remains approximately constant.

Occasionally excess air is controlled by using air and fuel flow measurements, together with oxygen and carbon monoxide analysers to trim the air fuel ratio. The normal strategy is to choose an air/fuel ratio set point then, if the oxygen level is deemed too high, the air/fuel ratio set point is trimmed to a lower value. This trimming is often continued until the CO threshold is reached as shown in Figure 2.14. The control system then "backs off" to a slightly higher air/fuel ratio set point. In principle this technique is suitable for all furnaces but in practice it is very difficult to set up for furnaces with varying in-leakage air or those with long response times.

8.5 Ensuring Furnace Safety

In any fuel using plant the risk of an explosion is ever present. It is critical that both furnace designers and users understand the sources of risk and take adequate steps to minimize them. Modern furnaces are normally equipped with safety interlock systems, known as Burner Management Systems (BMS). In this section we shall initially consider the conditions that give rise to potential risk of an explosion and then later how to protect against this risk with an effective BMS systems.

8.5.1 Risk Factors in Furnace Operation

During normal operation, the supply of fuel and air, together with the burner design, ensure consistent supply of the incoming fuel and a continuous chemical reaction (burning) clearly illustrated by the fire triangle, Figure 8.16.

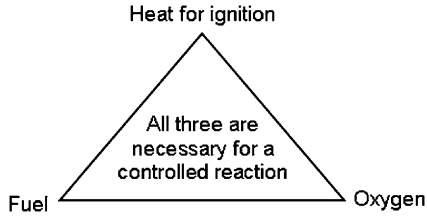


Figure 8.16 The fire triangle

If one of the three components in the fire triangle is missing the reaction cannot be sustained. If fuel is the missing component then the system is safe. However if air, or heat for ignition, is missing the situation is potentially dangerous but for an explosion to occur the fuel/air mixture must be within the flammable range as explained in chapter 3, section 3.1.4.

The basic strategy most commonly adopted for minimizing the explosion risk in furnaces and other fuel using plant, except within coal firing systems, is based firstly on ensuring flammable mixtures do not accumulate anywhere within the plant and taking care to ensure that, when there is a risk of a flammable mixture being present, all ignition sources are eliminated.

There are a number of potential sources of flammable mixtures in a furnace or process plant. These include:

- Oil or gas leaking into the combustion chamber through the burner as a result of leaking fuel shut off valves;
- Deposits of coal or oil from previous firing periods, not properly purged from the system;
- Operation of the plant with insufficient combustion air (sub-stoichiometric operation), resulting in CO and unburnt fuel in the downstream ducting and dust collector;
- Quenching of the flame by cold dust entering the furnace. Cold dust can reduce the temperature in parts of the flame below the ignition temperature. Gas flames are particularly vulnerable to this problem, owing to the high ignition temperature of natural gas;
- Fuel entering the furnace as a result of repeated, unsuccessful ignition attempts. This is a significant risk with oil firing, particularly where the oil is not sufficiently hot to ignite easily. A typical cause is cold oil remaining in pipes during shutdown. This is admitted to the furnace with each ignition attempt but fails to ignite and sticks to the walls. When hot oil finally arrives at the burner, ignition is achieved and the cold oil on the furnace walls is vapourised and ignited by the radiant heat from the flame, the oil burns very rapidly and a damaging pressure increase occurs.

Destructive explosions have resulted from all of these causes of flammable mixtures, with subsequent ignition sources typically being the igniter, main flame or by a spark in the dust collector. Sparks are present in electrostatic precipitator dust collectors (ESPs) during normal operation but can also be generated in bag filters from the build-up of electrostatic charges on the bags, unless anti-static bags are used.

8.5.2 Furnace Start-up

For most furnaces the greatest risk occurs during start-up. A typical simplified start-up sequence is shown in Figure 8.17. The explosion risk arises from failure of the fuel to ignite and/or the risk of ignition of fuel that has accumulated during the shut down. Before attempting to light the burner after a shut-down, the system should be subjected to an air purge to remove any flammable gas or vapour which may have accumulated. This air purge should be long enough to ensure a minimum of 4–5 volume changes of the whole system. The air flow-rate should be at least 25% of the full air flowrate. During this purge it is essential that any electrostatic precipitator (ESP) is de-energized to ensure no spark can ignite any gas or vapour present. Alternatively the ESP can be protected by combustible gas analysers, in which case it can remain energised during the purge provided no flammable gases are detected.

The combustion air pre-purge is one of the most important procedures in the start-up of any combustion plant. It should always be carried out and NEVER neglected or shortened. It should be enforced by both written procedures and effective controls and interlocks, see below.

Deposits of coal and oil should never be allowed to accumulate in combustion chambers or flue gas ducts. The most common cause of such deposits is unstable or sub-stoichiometric operation, followed by a burner trip. These deposits are not always removed by the combustion air pre-purge, especially cold viscous oil, so that in the event that they do accumulate, they may need to be removed by manual cleaning.

Unreliable igniters usually require repeated attempts to obtain ignition of the main flame. With each unsuccessful attempt, fuel enters the plant. Provided a full air purge occurs before the next ignition attempt, no danger arises, unless cold oil is deposited on the furnace walls.

Another danger arises on plants where manual start-up is used or where the operators and/or maintenance staff can access and adjust the BMS timers. In the case of repeated failures to ignite, they may be tempted to shorten the purge time to reduce lost production costs owing to the length of time the purge takes (typically 10–20 minutes).

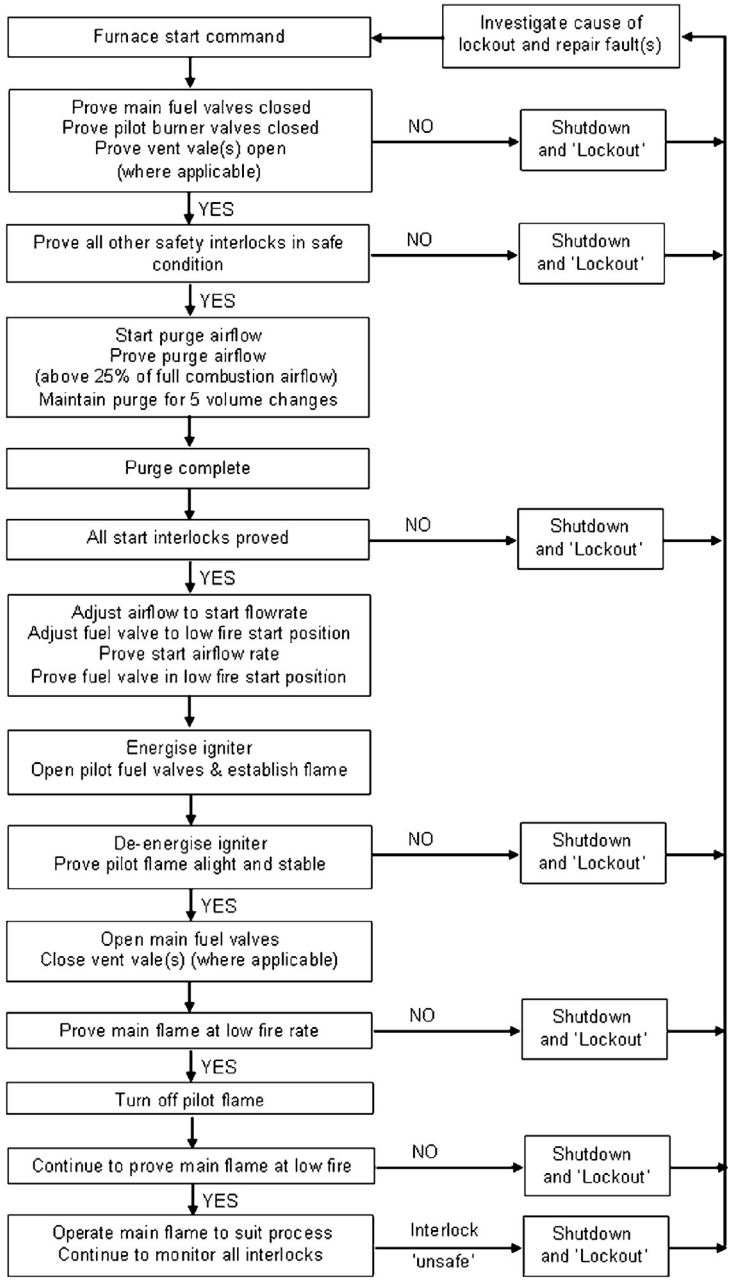


Figure 8.17 Typical furnace start sequence – actual configuration will vary with furnace application and compliance requirements

It is under these very dangerous circumstances that the operator is most likely to reduce the purge time to try and light-up the burner as soon as possible, increasing the risk of an explosion.

There is generally no risk if the ignition attempts are only for the pilot burner with the main fuel valves closed and purge airflow is maintained, because the volume of gas entering the furnace from the pilot alone is normally well below the lower flammable limit in these circumstances.

Critical Time for Ignition During Furnace Start-Up

An important consideration during start-up is how much fuel may be safely admitted to the furnace before posing a risk of damaging the casing by delayed ignition. Useful guidance is provided in Australian Standard AS1375–1985 SAA Industrial Fuel Fired Appliances Code, Appendix D. Three limiting cases are identified:

- Case A: An enlarging pocket of fuel/air mixture progressively filling the furnace
- Case B: An incoming fuel/air mixture mixed continuously with incoming air progressively reaching 50% of the lower flammable limit (LFL)
- Case C: As case B but fuel input too low to reach 50% of LFL

Case A is the most common scenario encountered during furnace start-up. For this case the critical time can be calculated using:

$$t = \frac{5P_p V_c}{I} \tag{8.7}$$

Where:

t = time to reach critical pressure in seconds
P_p = highest pressure that the furnace can withstand without failure in Pascals
V_c = volume of combustion space in m^3
I = thermal input rate in Watts

Assumptions:

Hydrocarbon fuel with stoichiometric mixture CV of 4 MJ/m^3
Maximum potential explosion pressure produced by the mixture = 800 kPa

This equation shows that strong furnaces enjoy longer critical times than weak furnaces and in the case where the furnace can withstand 800 kPa the critical time is infinite. However, as noted previously, strong furnaces are rare and most furnace casings can only withstand a pressure rise of 1 or 2 kPa before sustaining damage.

Case C effectively poses little risk since at 50% of LFL the combustion reaction is not self-sustaining. For more information and Case B, please consult the standard.

8.5.3 Operation with Insufficient Combustion Air

If the flame is not supplied with enough air, not all the fuel can burn. This results in unburnt hydrocarbons and carbon monoxide being formed. While this is normal operation for reducing atmosphere furnaces, it is highly dangerous on furnaces intended to operate with excess air.

The objective of the combustion control system is to prevent this happening. However, not all plants are equipped with combustion control systems because they are not effective for all processes but the operators still need good, reliable instrumentation and adequate training. In the absence of a combustion control system the gases leaving the plant should be analysed for oxygen, carbon monoxide and combustibles. This system must be maintained in excellent condition to ensure that it is operational at all times, with alarms and, where appropriate, shut-down trips for low oxygen, high CO and high combustibles. Unless a full risk scenario study is undertaken, these trips must be configured to operate at approximately 25% of LFL. If they are set to a more sensitive setting (lower % of LFL) then nuisance trips will be a problem leading to more start-ups, with all the associated hazards. If they are set to a higher proportion of LFL then the risk of an excursion into the flammable range is higher.

The operators should be trained to look for inconsistencies in the instruments and ensuring that such inconsistencies are investigated and rectified. For example, both high O_2 and high CO simultaneously could indicate a burner problem or an instrument or sampling system fault. Another factor to watch for is that the airflow into the process is consistent with the oxygen indicated at the exhaust. Again, any inconsistency should be investigated immediately.

Corrective Action for Unintentional Sub-Stoichiometric Operation

In the event of seriously sub-stoichiometric operation leading to generation of combustibles close to, or above, the LFL, the correct action is not to simply trip the fuel supply, since this will allow air into the system and provide the oxygen required to initiate an explosion. While the system is sub-stoichiometric there is no oxygen available to initiate an explosion and, although the presence of flammable gases represents a hazard, no explosion can occur unless oxygen is admitted. The correct action is to slowly reduce the fuel flowrate until the stoichiometric condition is reached then to continue to reduce the

fuel flow slowly until the target excess air is achieved. In this way combustibles and oxygen are not present simultaneously.

8.5.4 Flame Quenching

The risk of flame quenching occurs mainly with gas fired processes where the product is directly heated by the flame. The risk is much higher in gas fired plant than with coal or oil, owing to the much higher ignition temperature of natural gas compared with these fuels. The highest risk occurs during warm-up, when the system is relatively cool or during serious process upsets. When dust (raw feed or product) below 500° C is entrained in the combustion air, its thermal mass reduces the flame temperature. If the amount of dust is excessive, it can cool parts of the flame, principally the edge, below the ignition temperature of natural gas (510–550 °C). If this occurs, unburnt gas is present in the combustion gases, and there is the risk of an explosion in the dust collector. Little carbon monoxide is formed when flame quenching occurs, so this event can only be detected by a combustible gas or methane analyser or the operator's awareness of fuel input/temperature imbalances in the system.

8.5.5 Eliminating Ignition Sources

Despite the best efforts of furnace operators to prevent flammable mixtures forming, they will occasionally do so as the result of instrument or control system failure or flame quenching. When this occurs, it is essential that extraneous ignition sources are eliminated until the risk of explosion has passed. The main risk occurs on plant fitted with electrostatic precipitator dust collectors, which should be de-energized and the high voltage electrodes earthed as soon as possible, whenever there is a risk of a flammable mixture being present. Such action tends to bring conflict with the pollution inspectors and enforcement agencies but safety should always take priority. Tripping of the electrostatic precipitator should be automatic via the burner management system and not left to the discretion of the operator, whose response time is far too slow to prevent danger occurring.

Bag filters also present a potential ignition source owing to the risk of sparks caused by the build-up of electrostatic charges on the bags and there have been a number of explosions from this cause. This risk can be effectively eliminated by the use of anti-static bags.

8.6 Burner Management Systems

Burner management systems are used to control the start-up, shutdown and to supervise the safe operation of burners and combustion

equipment. The burner management system performs a vital safety function preventing operator error, leading to danger and causing the safe shut-down of the burner in the event of other equipment malfunction. It is a basic principle of burner management system design that it should fail to a safe condition i.e. shut-off the fuel(s) to the burner in the event of any equipment failure, or system failure, including the failure of field mounted instruments and equipment or the interconnecting wiring.

Guidance in the functional requirements of burner management systems is provided in the relevant codes and standards, such as NFPA, FM, AGA, ASA, TUV, BSI, IGE, etc. These codes have evolved over the years and originated from the time when all BMS systems were relay based and fail-safe design was easily achieved. But it should be noted that, in general, they only cover the function aspects of the system and not the risk of failure. In some jurisdictions and for some fuels, especially natural gas, the relevant local codes may be mandatory and all such fuel burning installations subject to approval by a government appointed inspector.

8.6.1 Safety Requirements for Burner Management Systems

The design of burner management systems requires appropriate knowledge, since it is equipment of a specialised nature with serious safety implications. Design should only be undertaken by experienced engineers with the appropriate specialist knowledge and experience of combustion systems and the relevant codes and standards. Nevertheless it is vitally important that all plant owners and operators have appropriate knowledge of the functional and safety requirements of BMS systems. The following sections are intended for that purpose, not to provide the reader with design expertise.

The vital safety function of the BMS means that failure can result in an explosion that may cause death or severe injuries with widespread and costly damage to equipment and on-going consequential losses. Two types of failure concern us:

1. Failure to shut off the fuel supply when a dangerous situation arises, for example, failure to close the fuel valves following loss of flame;
2. Equipment failure that causes a dangerous function to occur, for example, a broken wire opening the fuel valves prior to the pilot burner being proved alight.

For many years, this level of safety was achieved by the use of hard-wired relay logic with solenoid or pneumatically operated valves. Conventional relay based systems are relatively easily to design for "fail safe" operation and are a cost effective way of achieving safe

control of a small number of burners. Relay based BMS systems have a proven track record with many thousands still in use supplied by a large number of manufacturers. Relay interlock circuits were designed such that loss of power initiated a shut down, Figure 8.18. In this circuit, the combustion airflow must be proved by energising relay coil AFR before the start button can energise relay FVR and start the timer T1, which closes contacts T1 for 5 secs and holds in the relay for this time. This opens the fuel valve FV via contacts FVR1. If ignition occurs and is detected by the flame detector, contacts FR1 close and energise relay coil FPR which maintains the fuel valve open via FV1 even after the timer has timed out and contacts T1 have opened. Loss of flame detection, combustion airflow or a broken wire, all de-energise FVR and the fuel valve closes.

In relay based BMS systems, all interlock sensors were digital devices such as pressure switches, flow switches, etc. These required the contacts closed and the relay energised to permit fuel to the burner, so failure of any wire, contact or connection led to de-energising of the relay and fuel shut-off. Timers were electro-mechanical, again designed to fail to a fuel valves closed mode. Where solenoid valves were employed as fuel valves the solenoid was energised to open so loss of power closed the valve. Electro-pneumatic valves required both power and compressed air to open against a spring and loss of either air pressure or power resulted in closure and fuel cut-off.

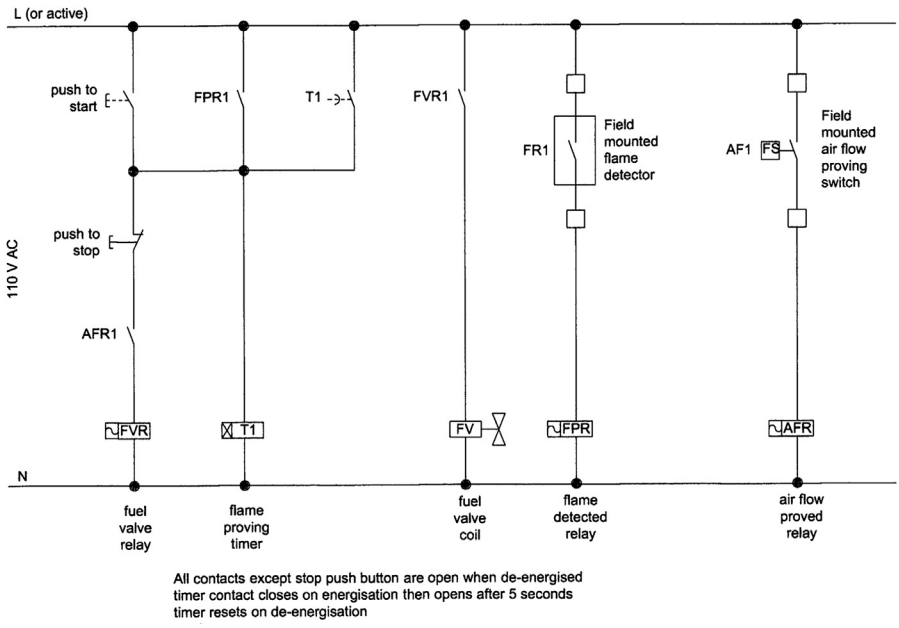


Figure 8.18 Principle of fail safe relay logic employed in BMS systems

The only plausible cause of danger-side failure of a correctly designed relay based system was welded relay contacts and this risk was minimised by ensuring that the relay contacts were not overloaded. The use of AC mains power in the majority of units further reduced the risk of welded contacts, since currents were low and AC inherently creates less contact burn than DC. In addition, circuit redundancy was usually employed on vital circuits, so that if one relay suffered welded contacts a second relay would initiate shut-down, e.g. two relays connected with contacts in series to power open a fuel valve.

Traditionally, only steam boilers in utility power stations were allowed an exemption to the fail-safe requirement that any failure must shut off the fuel. This was the result of an assessment that the risk of minor equipment failure causing spurious boiler and turbine shutdowns exposed the public to unacceptable risk. Consequently, these boilers tended to use power-to-open, power-to-close control functions, so in the event of failure the system remained in the same state, i.e. burner firing or burner shut down as the case may be. The reduced risk to the general-public resulting from minimising spurious power failures was considered to more than off-set the increased risk to the power station operators created by these systems. However, these systems are never acceptable in industry since in this environment the increased risk to operators is not offset by any reduced risk elsewhere. Indeed, in industry, an increased risk to operators also implies an increased risk to the public.

8.6.2 False Trips

False trips are system shut downs that occur in the absence of an unsafe condition. They are normally initiated by either an equipment failure (in a fail safe system) or a process excursion that is not actually dangerous, but the trip occurs because the sensor's trip point is set too close to normal operating conditions. False trips are costly owing to the lost production but introduce a danger of their own because they increase the number of start-ups which, as discussed above, is the riskiest time of plant operation. The other problem is the risk that frequent trips and starts will lead to confusion as to their real cause and mask a real danger. It is very important therefore that false trips are minimised for both economic and safety reasons.

8.6.3 Achieving Acceptable Safety Standards with Programmable Logic Controller Burner Management Systems

Programmable logic controller (PLC) burner management systems offer a number of advantages compared with relay systems, especially

where large numbers of burners are used. However, the fail safe characteristics are more difficult to achieve because PLCs can fail in a number of modes whether caused by hardware failure, software errors, software corruption etc. Unfortunately, in the past, the risk of danger-side failure was largely ignored by the PLC manufactures and many of the PLC based safety systems have an unacceptably high risk of danger side failure. Indeed, in some systems, this risk is much higher (several orders of magnitude) than for the fail-safe relay systems that they supplanted.

I remember visiting one plant in the early 1990s that had a number of rotary kilns, each with a 100 MW burner where the same DCS controlled all the kilns and provided all the BMS functions, so equipment failure left all kilns vulnerable. In addition there were no hardwired emergency shut-down buttons for the kilns in the control room. When I asked the operator to demonstrate an emergency shut-down, he scrolled though 4 pages of display on the VDU and then shut down the primary air fan and relied on the DCS logic to close the gas valves. His only option in an emergency involving a computer malfunction was to use the emergency stop that stopped the gas supply to the entire site and, in that event, it required a call-out to the gas company to re-set the valves and restore the supply. Notably, this system was not installed by a small local company but by one of the major global suppliers of boiler and process control systems.

The failure of designers to appreciate the wide range of failure modes possible with PLC systems or to understand the fundamental BMS fail-safe requirements has led to a number of serious accidents caused by the application of PLCs to burner management and other safety systems. These incidents led to the introduction of guidelines by Health and Safety Executive (HSE) in England and NFPA/FM in the USA aimed at improving the safety of PLC based safety systems. The effect of these guidelines is to require that the BMS system uses a separate safety PLC which does not perform any other control function and is equipped with a separate safety back-up system, such as safety relays to prevent dangerous failures. Further work, by organisations such as the International Electrotechnical Commission (IEC) and the American National Standards Institute (ANSI), has led to the development of standards for the reliability of safety systems. This reliability factor is expressed as the Safety Integrity Level (SIL). The safety integrity level is scaled on a level of 1 to 4 with 1 being the lowest and 4 the highest. The definitions are given in the Table 8.4.

With this philosophy, the concept of fail-safe operation is replaced by the PFD (probability of failure to act on demand), i.e. the risk that the system will fail to shut down the burner when a dangerous or potentially dangerous system arises. Whilst more flexible than the old "fail-safe" concept, this standard puts the onus on plant owners and management to both determine the level of SIL required, then

Table 8.4 Safety Integrity Level Defined by IEC Standard 61508

SIL	*PFD*	*Availability Required*	*1/PFD*
4	10^{-5} to 10^{-4}	>99.99%	100,000 to 10,000
3	10^{-4} to 10^{-3}	99.90—99.99%	10,000 to 1,000
2	10^{-3} to 10^{-2}	99.90—99.99%	1,000 to 100
1	10^{-2} to 10^{-1}	99.90—99.99%	100 to 10

PFD = Probability of failure to act on demand

demonstrate that the safety system achieves this SIL. Note that the SIL applies to the complete safety system, including the dedicated PLC, all associated instrumentation, valves and field wiring which must all achieve the appropriate SIL. This time consuming, and hence expensive, task has led to a massive increase in the cost of installing and owning burner management systems. If your plant is equipped with a PLC based BMS system installed prior to the new requirements, Scott (2003) provides a methodology for assessing its SIL and hence allowing management to determine the need (or otherwise) for replacement.

8.6.4 Choosing an Appropriate Safety Integrity Level

When specifying or designing a new burner management system it is essential to choose the appropriate Safety Integrity Level. If too low a SIL level is chosen staff and equipment will be exposed to an unacceptably high risk but, if too high a level is chosen, then the cost of the system will be excessive. This is not an easy decision, but in principle, the more people exposed to danger and the higher the value of plant, equipment and the production at risk, the higher the SIL required. In some jurisdictions, where statutory approval is required, the risk adverse characteristics of the inspectors may insist on the highest level of SIL despite no personnel being routinely exposed to danger.

Unfortunately there is insufficient space to provide any more than an outline to choosing an appropriate level of SIL but essentially we are seeking the answer to the following equation:

$$\text{HOW CAREFUL} = \text{HOW BIG?} \times \text{HOW OFTEN?}$$

In other words the more frequent the dangerous occurrence and the larger the effect, the more careful we need to be and hence the higher SIL required. Excellent guidance on this determination is provided by Scot (2002). He proposes selection of the SIL based on a quantitative calculation of 'Consequence and Likelihood'. In this method the first calculation is to determine the effect zone based on:

- The vapour or gas cloud explosion effect zone;
- The physical explosion effect zone;
- Pool fire effect zone (for liquid fuels only, including LPG).

These calculations are standard risk assessment procedures for petrochemical plants with methodologies, such as provided in Tweedale (2003). These calculations tend to be quite complex and hence time consuming and therefore expensive. Scott proposes an alternative method based on the simplified protocols developed by the US Environmental Protection Agency (EPA 1999). These protocols are based on converting the total heat released in an explosion to the equivalent amount of TNT using an 'explosive factor' that the EPA have determined. Once the 'effect zone' has been calculated the personnel density is estimated, followed by a determination of the frequency of each hazardous event. Determination of the frequency of the hazardous events is potentially the most difficult part of deciding the appropriate SIL but guidance is provided in publications available from a number of organisations including The Institution of Chemical Engineers (UK) and the American Institute of Chemical Engineers, Center for Chemical Process Safety.

Following determination of the frequency of the hazardous events and the number of personnel affected, acceptable frequency target is determined by dividing the individual risk by the probable number of fatalities. This then permits calculation of the maximum permissible PFD (Probability of Failure on Demand) and hence the SIL. Many furnace owners and operators will find that even Scott's simplified method is very demanding and time consuming to apply and hence seek outside help. If that route is chosen it is critically important that the process owners are involved to ensure that realistic inputs are provided for the calculation, especially those regarding the number of personnel at risk and the field of effect since these both have a massive effect on the outcome of the calculations.

While the codes are based entirely of human safety and environmental protection, in circumstances were few or no people are at risk, it may still be wise to choose a higher level of SIL than safety alone requires if the cost of equipment repair or the consequential losses from lost production are very high. In this calculation the cost of the additional SIL relative to the cost of repair and the consequential losses is the major consideration.

8.6.5 Determining the Safety Integrity Level of the BMS System

As mentioned above, the SIL must apply to the whole system, not just the PLC, in other words just using a safety PLC does not guarantee a safe system. To achieve a safe system all the associated sensors and actuators must also meet the SIL requirements together with the field wiring. The SIL achieved by the system is determined by a fault tree analysis, Figure 8.19. Note how the probability of failure on demand

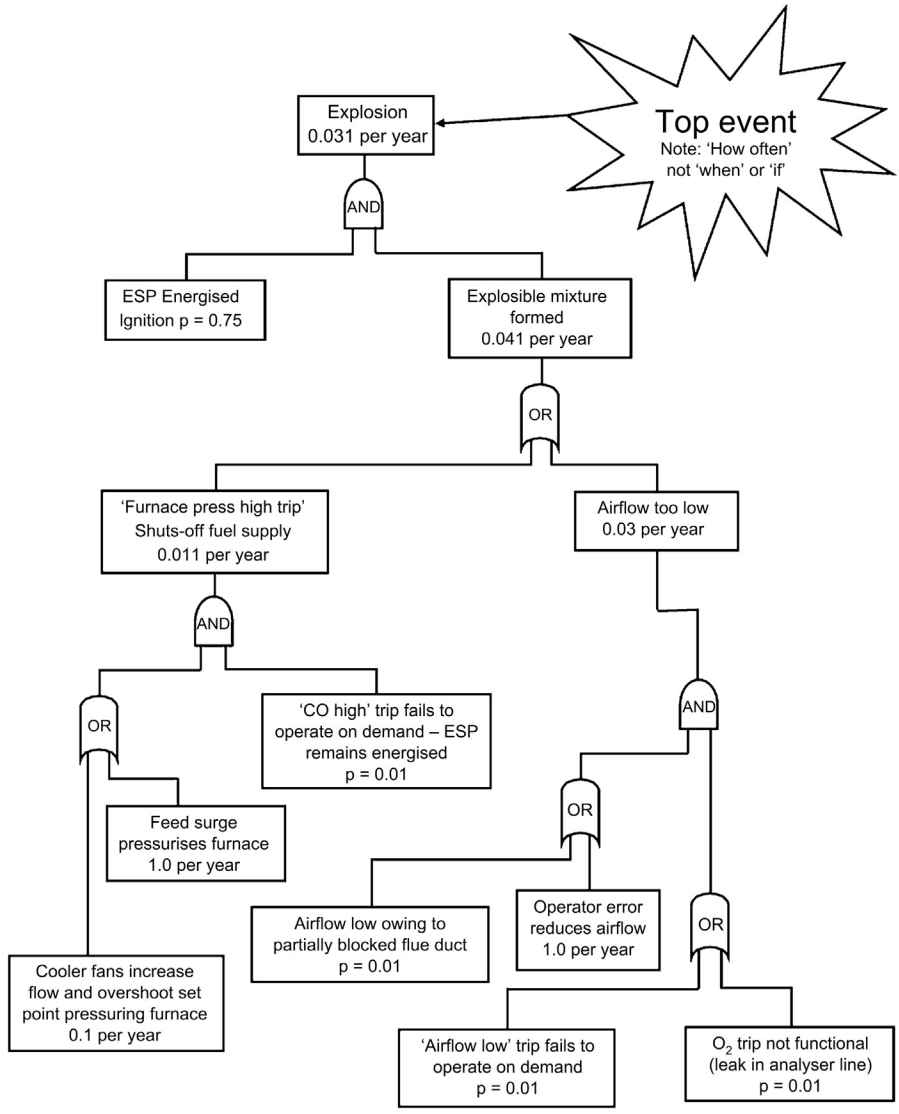


Figure 8.19 Example of fault tree analysis. Note: In this example the dangerous condition arises from the low airflow and failure of the trips to detect this. However, the explosion is initiated by the correct operation of the "furnace pressure high" trip.

(PFD) of the individual system components feeds into the final PFD and hence the SIL that is achieved.

In the fail-safe relay based systems all critical sensors, apart from flame scanners, were switches such as flow switches, pressure switches, etc. These were wired in a fail-safe mode but these devices

were subject to mechanical failure and the additional reliability required was achieved by using two or more devices wired in series or parallel depending on failure modes required. This provided the required level of safety but increased nuisance trips caused by switch failure when no hazard was present.

The introduction of PLCs and their associated signal processing capability has encouraged the replacement of switches by transducers with 4–20 mA signal transmitters, which of course have multiple failure modes. Since the SIL applies to the whole system these transmitters must contribute to achieving the appropriate SIL as shown in the fault tree analysis. Sensors intended for safety systems are often referred to (incorrectly) as SIL devices but the SIL applies to the whole system and, as demonstrated above, the performance criteria of interest for individual components is the PFD. In reality, because the failure of many instruments is subject to statistical scatter it is the average probability of failure on demand (PFD_{avg}) that we consider and the mean time to failure – spurious ($MTTF_s$). To achieve the required PFD_{avg} for safety systems implies $MTTF_s$ in the order of 20 years. Since a requirement of the SIL evaluation is that all safety equipment is 'Proven in Use' this can only be demonstrated by extensive testing, usually by the manufacturer or an accredited laboratory, such as FM Global & UL in the USA or TUV in Germany.

If the required SIL is not achieved when the fault tree analysis in undertaken, then assuming the SIL of the safety PLC is adequate, the SIL of the whole system can be increased by using instruments with lower PFD_{avg} or by building redundancy into the logic. Even when using appropriative safety function components it is unlikely that the appropriate level of SIL can be achieved without redundancy.

For example, where transmitters are used to prove combustion air flow, Figure 8.20, both FTA and FTB must sense air flow and provide a 'flow proved' signal to the PLC. In the event that either fails to provide a signal a safety shut down occurs. If each sensor has a PFD_{avg} of 4×10^{-2} and both have to sense the flow to prove the flow then we have an AND gate i.e. FTA and FTB must fail to produce a system

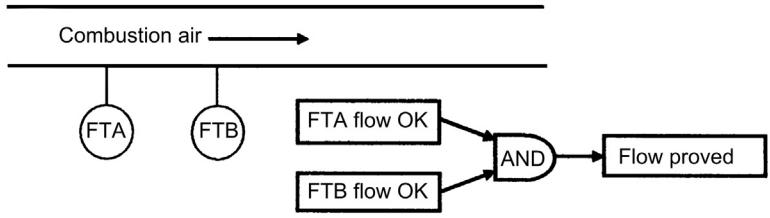


Figure 8.20 Example of two flow transmitters (4-20 mA) are used to prove combustion air flow using redundancy

failure. For AND gates we multiply the probabilities so the new PFD becomes:

$$4 \times 10^{-2} \times 4 \times 10^{-2} = 1.6 \times 10^{-5}$$

Hence we have achieved a significant reduction in the PFD but the downside is that failure of either instrument will cause a safety shut-down. i.e. if FTA or FTB fails to provide a 'flow proved' signal to the PLC a shut down occurs, so now we have an OR gate. With OR gates we add the probabilities so the probability of a spurious trip is:

$$4 \times 10^{-2} + 4 \times 10^{-2} = 8 \times 10^{-2}$$

The number of spurious trips is doubled by introducing redundancy. This is an unacceptable cost for most operators, so three sensors are used with a voting system and the resulting logic is shown in Figure 8.21. Hence both the required PFD_{avg} and the required plant availability are achieved. Usually a warning regarding the dissenting instrument is provided to the DCS control system to allow on-line repair, further improving both the PFD and the plant availability.

While on the topic of links between the BMS safety system and the distributed control system (DCS), it must be emphasised that no safety interlock may pass through the DCS. However, signals from the BMS system can normally be relayed to the DCS provided that there is no possibility of false signals being transmitted back from the DCS to the BMS safety system.

8.6.6 Flame Detectors

Flame detectors provide a signal to the operator or BMS to show whether the flame is alight or not. It is therefore essential that flame detection systems are reliable and fail to a safe condition, that is, provide a 'flame out' signal in the event of any equipment malfunction. For burner management, the flame-off signal is the fail-safe condition because it is always used to initiate a burner shut down.

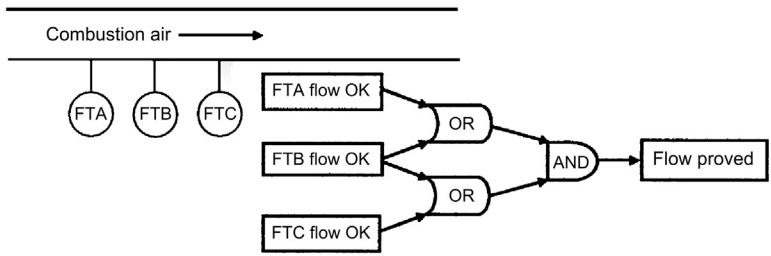


Figure 8.21 Logic associated with three flow transmitters (4-20 mA) used to prove combustion air flow and reduce spurious trips

Flame detectors must achieve the appropriate average probability of failure on demand (PFD_{avg}) and mean time to failure – spurious ($MTTF_s$). Flame detector manufactures have long experience in designing and producing devices to meet the required PFD and this is normally achieved by the use of fail-safe or self-checking circuitry. Fail-safe circuitry typically uses features such as the voting system described in section 8.6.5 above to determine safe/unsafe conditions and/or signals derived from the natural flicker in the flame with a steady signal indicating an unsafe or flame-off condition. In cases where self-checking is provided by a rotating shutter between the sensor and the flame, the sensor sees an alternating flame-on, flame-off signal which is processed to provide a flame-on signal with any other condition being flame-off, hence the unit becomes fail-safe.

Except for small flames, the hostile nature of flames with regard to instrumentation requires optical devices for flame detection. Visible light is rarely used because, if the detector is removed from the furnace, daylight can provide a flame-on signal. Therefore flame detectors must use a unique property of the flame to provide the signal. Three types of detector in common use are described briefly below. These are:

- Ultra-Violet Radiation Detection;
- Infra-Red Radiation Detection;
- Flame Ionisation Detection.

Flames produce ultra-violet (UV) and infra-red (IR) radiation. Both are outside of the visible spectrum with a comparison of the UV, visible light and IR spectrum shown in Figure 8.22, together with the response ranges of typical UV and IR cells.

UV radiation is produced by the ionization within the root of the flame. This UV radiation is detected by a UV sensitive vacuum tube which typically responds to radiation of wavelengths 150–250nm. Unfortunately, the UV signal tends to be very weak and has to be

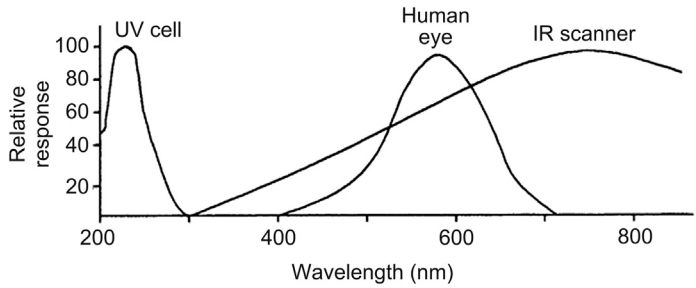


Figure 8.22 Ultra-violet and infra red wavelength compared with visible light

focused onto the detection tube by a quartz lens. The signal is also absorbed by dust which tends to make this technique unreliable for any application where significant dust is present since it can cause many nuisance trips.

UV detector tubes can fail in the 'flame-on' or 'flame-off' mode, so these units must be made self-checking. This is normally achieved by fitting a rotating vane between the cell and the detector tube. Rotation of the vane gives an alternative 'flame-on/flame-off' signal which is processed by electronic circuitry to give a flame on signal output via a relay. In the event of a continuous signal of either mode a 'flame-out' signal is generated by the circuitry which causes the output relay to de-energize.

Unfortunately UV radiation is also emitted by fluorescent and discharge lighting and some operators have been tempted to remove the detector from the furnace and expose it to a lamp, especially in the case of unreliable flame detection. Needless to say if this is done all protection is lost. The mounting collar should be designed to make this impossible by installing proximity switches or the like, so that removal of the detector head from the furnace produces a flame-off signal that cannot be over ridden.

Infra-red radiation (IR) is also emitted from flames. It cannot be seen but is felt in the form of heat on the skin. Large quantities of IR are emitted from oil and coal flames with smaller quantities from gas flames. The use of infra red signal for flame detection overcomes the difficulties caused by the weak UV signal and is therefore suitable for dusty plants. Since infra-red radiation is also emitted by hot refractory, commercial flame detectors are made fail-safe by detecting the characteristic flicker frequency of the flame which is processed electronically to produce a 'flame on' signal via an energised relay. A continuous infra-red signal or no infra-red signal gives a "flame out" indication and the output relay is de-energised. Unlike UV detectors the infra red cells fail to a flame off condition so, provided the circuitry is designed to fail to a flame off condition these devices do not need to be self checking in the same manner as the UV units.

The reacting gases in a flame are ionised as a result of the combination of the hydrogen from the fuel with the oxygen from the air. When an AC voltage is applied across a flame by two electrodes, a very small current is transmitted. Provided the two electrodes have significantly different surface areas (at least 4:1), then a half wave rectified current is produced, Figure 8.23. This signal is then processed to provide a relay output, with the relay energised for 'flame on', de-energised for 'flame off'. The detector circuitry can be made fail safe, since:

- No current = no flame.
- Full wave current = short circuit = no flame.

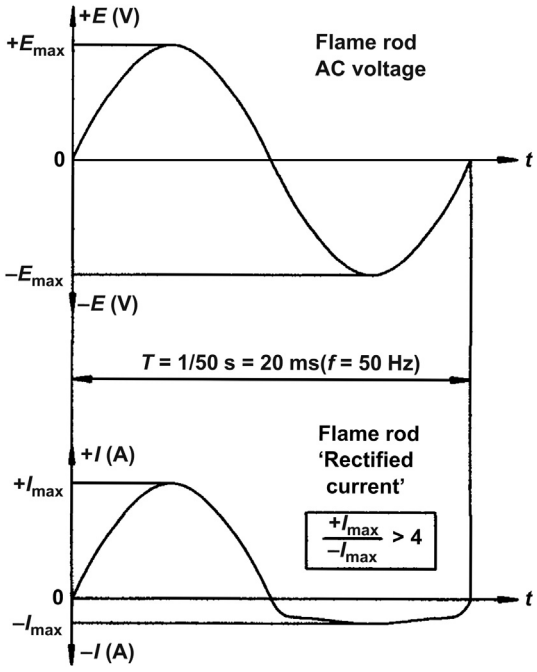


Figure 8.23 Principle of flame ionisation showing half wave rectification of the current

Flame ionization detection is inexpensive, but is generally only suitable for small gas burners, such as domestic and commercial heating. However, it is widely used on industrial pilot burners. The main disadvantage is that the electrodes are susceptible to contamination by moisture, which creates a short circuit and provides a failure signal.

Nomenclature

A = surface area
E = sensor electromotive force, (mV)
F = Faraday constant
h = the gas to sheath convective heat transfer coefficient
I = thermal input rate in Watts
K = constant
$MTTF_s$ = mean time to failure − spurious
n = number of charges per reactant species
pO_2 = mole fraction of oxygen in the sample gas
pO_2^R = mole fraction of oxygen in the reference gas (atmospheric air)

P_p = highest pressure that the furnace can withstand without failure in Pascals
q = heat transferred
R = gas constant
T = temperature K
t = time to reach critical pressure in seconds
V_c = volume of combustion space in m^3
x = oxygen content of the flue gas %
z = distance to target (for optical temperature measurement)

Greek letters

ε = emissivity
Ω = Stefan's constant (6.67×10^{-8} $W^{-2}K^4$)

Subscripts

$conv$ = convection
rad = radiation
t = target

References

American Institute of Chemical Engineers, 3 Park Avenue, New York, NY 10016–5991, http://www.aiche.org, Center for Chemical Process Safety, http://www.aiche.org/ccps/

Australian Standard: AS1375–1985 SAA Industrial Fuel Fired Appliances Code, Appendix D. Australian Standard: AS 4264.1-1995 – Coal and Coke Sampling
Part 1: Higher rank coal – Sampling procedures
Part 2: Coke – Sampling procedures
Part 3: Lower rank coal – Sampling procedures
Part 4: Determination of precision and bias
Standards Australia Limited, Sydney, NSW, Australia, www.standards.org.au

BG paper on BMS systems (details requested from Neil Fricker)

Dorf, R. C., & Bishop, R. H. (2005). *Modern Control Systems* (10th ed.). Pearson-Prentice Hall.

IEC standard 61508, Functional safety of electrical/electronic/ programmable electronic (E/E/PE) safety-related systems, International Electro-technical Commission, GENEVA, Switzerland, website www.iec.ch

Institution of Chemical Engineers, Rugby, UK, http://www.icheme.org/

Johnson, C. D. (2006). *Process Control Instrumentation Technology* (8th ed.). Pearson-Prentice Hall.
NFPA 86: Ovens and Furnaces. (2003). Edition, National Fire Protection Association. Boston USA, www.nfpa.org.
Scot, & Michael, D. (2003). *What's the Safety Integrity of my Existing Burner Management System*. TX: ISA EXPO Houston.
Scot, & Michael, D. (2002). *Burner Management System Safety Integrity Level Selection*. Chicago, IL: ISA EXPO.
Tweeddale, M. (2003). *Managing Risk and Reliability of Process Plants* (pp. 87–187). Gulf Professional Publishing.

Certification and Testing Organisations

Australian Gas Association, Braeside, Vic., Australia, http://www.aga.asn.au/index.html
FM Global Research Campus, West Glocester, R.I., USA, http://www.fmglobal.com/about/campus/campus.asp
TÜV Rheinland, Cologne, Germany, http://www.tuv.com/de/en/index.html
Underwriters Laboratories Inc., Northbrook, IL, USA, http://www.ul.com/

Chapter 9

Furnace Efficiency

Chapter contents

9.1	Furnace Performance Charts	340
9.2	Mass and Energy Balances	343
9.3	Energy Conversion	360
9.4	Heat Recovery Equipment	365
9.5	Identifying Efficiency Improvements	371
Nomenclature for Chapter 9		374
References		375

The concept of efficiency is straightforward. An analysis of the efficiencies, and inefficiencies, of a system can be used to identify where the greatest opportunity for gains can be derived. It can also be used to benchmark the performance of one system against another.

The thermal efficiency of any furnace system is defined as the useful energy derived from the system relative to the energy input:-

$$\eta = \frac{\text{useful heat}}{\text{total heat}} \tag{9.1}$$

Since all systems have losses, the efficiency of any system is always less than one.

In considering a furnace system involving combustion, the primary energy input to the system is ultimately derived from the fuel. However, depending on how the system is defined, it may also include the energy required to pre-heat the combustion air. If we consider the air fans and furnace drive motors we must include the electricity used, in which case the efficiency of the generation system would need to be included. Likewise the energy out may also include waste heat recovery in the form of steam or electricity in addition to the primary product.

A schematic diagram of a generic furnace system is given in Figure 9.1. We can measure the total energy into the system from the fuel, electricity, air and feedstock. We can likewise measure the energy leaving the system in the product, flue gases and exhaust air from the cooler. It should be recognised that these will nor balance, as some

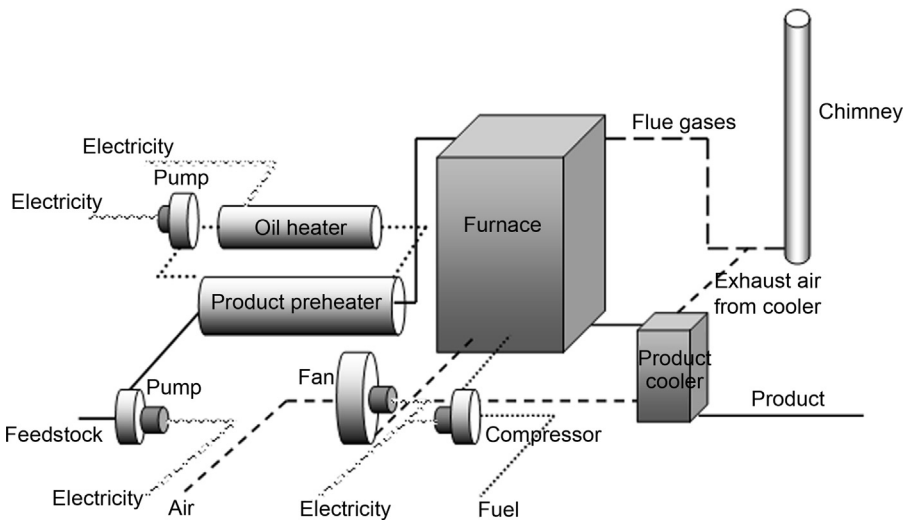


Figure 9.1 Schematic diagram of a generic furnace process showing flows through the system.

energy may be used to process the feedstock (i.e. a chemical or physical change), some will be lost as heat from the structures and interconnecting ducts, some as a pressure drop in flows though the system and some in converting electrical to mechanical power in the motors. However, it is not necessary to measure the energy that is lost through the walls of the furnace etc. to calculate the efficiency. It is only necessary to know the useful energy out, which is usually relatively easy to determine, as it will be directly related to the production rate. However, an estimate of the energy which is wasted can provide a useful cross check. Table 9.1 gives some values of energy flows related to Figure 9.1, (refer to example 9.1 later for the derivation of this information). These energy flows are always expressed relative to datum conditions, which are usually 0°C (NTP), 15.6°C (60°F) (STP), or 25°C (Standard temperature for measurement of fuel CV).

From the data in Table 9.1, the total energy input is ~48MW, of which ~21MW is useful. Thus the overall efficiency of the process is ~43%. If we subtract the output and useful energy from the input energy we have a deficit of ~6MW. This equates to the unaccounted energy components in the system as a result of heat, pressure and electrical conversion losses. The 0.5MW of electrical energy to the pumps and fan is primarily absorbed as motor losses and in pressurizing the fluids, so we could assume as a first approximation that the heat losses from the system are ~5.5MW.

The efficiency of a furnace system depends on each step by which the energy is transferred from the chemical fuel energy and the electrical energy to the process energy contained in the end product. The

Table 9.1 Energy flows relating to Figure 9.1

Energy flow	*MW*	*Direction*
Fuel	41	Input
Air	1	Input
Feedstock	1	Input
Flue gases	14	Output
Cooler exhaust air	5	Output
Product	2	Output
Oil heater electricity	5	Input
Oil heater pump electricity	0.1	Input
Feedstock pump electricity	0.2	Input
Fuel compressor electricity	0.1	Input
Fan electricity	0.2	Input
Theoretical energy in product (chemical and physical)	21	Exchanged

total efficiency is dependent on the efficiency of each operation in the process i.e. pump, preheater, furnace, and cooler. Within each of the various operations are the efficiency with which the fuel is burned, the efficiency with which the heat is transferred into the product and the efficiency with which any waste heat is recovered. It is therefore the case that the least efficient operation in the whole process will have the greatest effect.

9.1 Furnace Performance Charts

Most furnaces, as opposed to boilers, have a low thermal efficiency, typically in the range 5% to 35%. This is because the average temperature of the charge in the furnace is higher than in a boiler, hence the temperature difference between the charge and the heat source is less and heat transfer is reduced. By comparison, in the radiant section of a boiler the thermal efficiency is typically 50% to 60%.

Most furnace systems make use of heat recovery from the flue gases and/or the product to improve the thermal performance. These heat recovery systems usually involve the preheating of combustion air, and/or preheating of the charge. Thus reported thermal efficiencies of furnace systems are usually higher and can be on a par with boilers, as they are based on the heat transferred to the charge relative to the thermal input from the fuel. The lower the furnace efficiency, the greater the potential for heat recovery.

For any furnace in steady state operation we can write a simple heat balance.

$$H_f = H_c + H_s + H_g \tag{9.2}$$

where

H_f = Heat supplied by fuel
H_c = Useful heat to charge
H_s = Furnace structure losses
H_g = Heat loss in flue gases
H_t = depends on the type of fuel and the burner design and is quantified as

$$H_f = Q_f \times CV \tag{9.3}$$

where

Q_f = Fuel flowrate
CV = Calorific value of fuel

The useful heat to the charge is quantified as

$$H_c = Q_c \times (Cp_c \times \{T_c - T_a\} + H_r) \tag{9.4}$$

where

Q_c = Charge flowrate
Cp_c = Mean specific heat of charge
T_c = Outlet temperature of charge
T_a = Ambient temperature
H_r = Reaction energy

The furnace structure, or standing, losses occur because heat is transferred by conduction through the furnace hearth, walls and openings, and then by convection and radiation from the outside to the atmosphere. H_s is therefore quantified as

$$\begin{aligned} H_s &= A_i \times k \times (T_i - T_o) \\ &= A_o \times \left(h \times (T_o - T_a) + \sigma \times \varepsilon \times \left(T_o^4 - T_a^4\right)\right) \end{aligned} \tag{9.5}$$

where

A_i = Inside area of walls
A_o = Outside area of walls
k = Thermal conductivity of walls
h = Convective heat transfer coefficient
T_i = Hot face temperature
T_o = Cold face temperature
ε = Emissivity of walls
σ = Stefan-Boltzmann constant

Heat loss in the flue gases is quantified as

$$H_g = Q_g \times Cp_g \times \left(T_g - T_a\right) \tag{9.6}$$

where

Q_g = Flue gas flowrate
Cp_g = Mean specific heat of flue gas
T_g = Flue gas exit temperature

In addition to the thermal quantities defined above, there is a further thermal input required to heat the structure of the furnace (i.e. refractory, steelwork, internal supports etc.) up to the operating temperature. This energy is input to the furnace during start up, and is lost when the furnace is shut down. Hence, continuous processes are more fuel efficient than batch or intermittent operations.

Examination of furnace performance data can help to usefully identify the relative contributions of these thermal quantities. If the production rate is plotted against thermal input then, allowing for a reasonable degree of scatter owing to other influences, a straight line relationship is usually observed. Figure 9.2 presents some production data for the generic system defined in Figure 9.1, and Table 9.1. The thermal input value where the extrapolated line intercepts the zero production axis quantifies the structure, or standing losses of the furnace.

Figure 9.2 can be split into the thermal components as shown in Figure 9.3. The standing heat loss of 10MW is composed of the

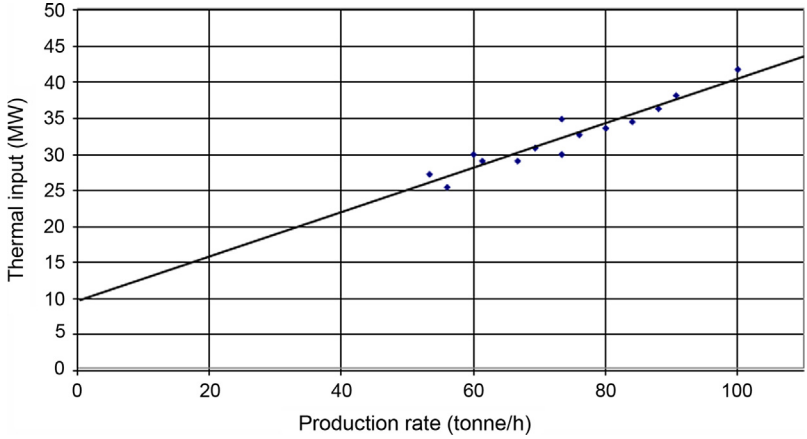


Figure 9.2 Plot of typical furnace performance

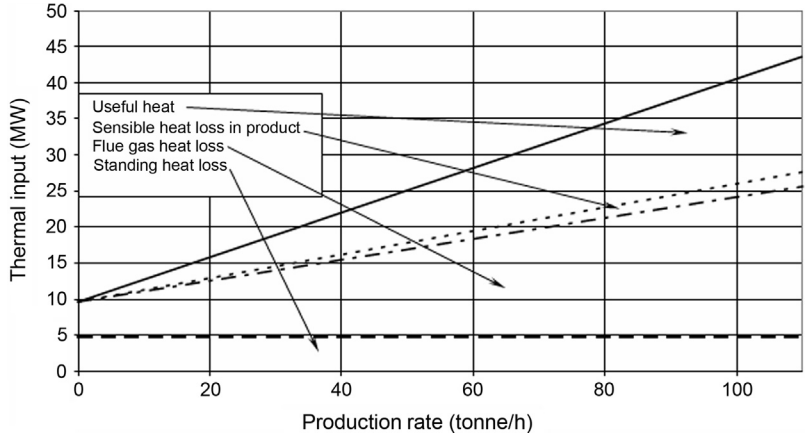


Figure 9.3 Distribution of thermal quantities data

10.5MW of electrical power and 5.5MW of heat losses as previously determined, together with 4MW of flue gas losses, since fuel must still be used to maintain the system 'at load', even with no production. Figure 9.3 also illustrates why the thermal efficiency of a furnace increases with increasing production, since the proportion of useful heat in relation to the total input increases.

9.2 Mass and Energy Balances

> "A material balance of an industrial process is an exact accounting of all the materials that enter, leave, accumulate or are depleted in the course of a given time interval of operation. The material balance is thus an expression of the law of conservation of mass in accounting terms. If direct measurements were made of the weight and composition of each stream entering or leaving a process during a given time interval and of the change in material inventory in the system during that time interval no calculations would be required. Seldom is this feasible and hence calculation of the unknowns becomes indispensable."
> Hougen, Watson & Ragatz (1966).

The above quote perfectly sums up the reasons for, and pitfalls of, a process mass and energy balance. The fundamental objective of the process engineering design of any industrial operation is to draw up process flowsheets that balance gravimetrically and thermally. Only then can the individual process streams be sized and mechanically designed to accommodate the expected flow conditions. Why, therefore, do we not carry out similar mass and energy balances as routine on operating plant?

The simple answer is because it requires a considerable deployment of resources, specialized measuring equipment, analytical back-up and luck! Given these difficulties it is not unreasonable to ask the question, what benefits do I gain anyway? If you really do have a good appreciation of the complete plant operation, then the answer is probably none save the satisfaction of confirming what you already know. If, however, there are parts of the process that do not work as they were designed to, then the effort would almost certainly be rewarding and often revealing.

The first step in the process of constructing mass and heat balances is to draw up an accurate process flow diagram. This should be based on the plant as it is now operating, and not on the original process flowsheet, since this may have considerably altered since the plant was first built. It is particularly important to try and identify recycle flows, as these will affect the heat balance. The next step is to identify the 'process envelopes' which are significant. The 'process envelope' is

a fundamental cornerstone of the calculation procedure and is developed by creating an imaginary boundary around an item (e.g. the furnace) or a group of connected items (eg. the cooler, kiln, suspension preheater and gas cleaning equipment in a cement plant) on the flowsheet. Once you have selected the envelope, this defines the measurement task, since by some means you have to quantify the flows along all lines which cross the boundary of the envelope. If you can achieve this then you will be able to develop a mass balance over the envelope. If there are recycle flows totally contained within the boundary of the envelope, then these flows will have to be quantified before a heat balance can be derived.

9.2.1 On-site Measurement

Having defined the measurement task, the next step is to select the most suitable instrumentation required to collect the data. The general requirement is to measure the mass or volume flowrate, temperature and, if necessary, pressure of each solid, liquid and gaseous stream. Process plants are rarely, if ever, provided with sufficient instrumentation to allow realistic on-line mass and energy balances, as this would generally require more process measurements than those required for control and operator information; incurring additional capital and maintenance costs. To undertake a complete mass and energy balance therefore typically requires additional on-site measurements using portable instrumentation, Figure 9.4. Typical plant instrumentation usually includes the easy to measure items such as:

- Temperatures - using thermocouples;
- Pressures - using pressure differential transmitters;
- Flows of liquids and gases - using a range of devices such as orifice plates, venturis, vortex shedding flow meters, etc.;
- Gas composition - using a range of techniques such as electrochemical cells, infrared absorption, etc.

Whilst the process variables rarely measured by plant instrumentation include

- Flows of suspended powders and dusts;
- Solids concentration within powder and dust suspensions;
- Mass flow of solid feeds and products;
- Temperatures of beds of solid materials;
- Flame temperatures.



Figure 9.4 Plant trials using a suction pyrometer to measure combustion air temperature and an optical pyrometer to measure product discharge temperature

Typical instrumentation required for a mass and energy balance would include most of the following

- **Gaseous streams**
  - Air, flue or inert gas flow - If no existing flow element such as an orifice plate, venturi, etc. is installed, then use a pitot tube and portable manometer in the most suitable section of straight duct, (a minimum of one pipe diameter upstream and half a pipe diameter downstream from any bends, valves, dampers or other obstructions). A vane anemometer can be use to measure air flows at fan inlet ducts where a pitot tube is unsuitable.
  - Fuel or toxic gas flow – In-line flow element (e.g. orifice plate, turbine meter, etc.)
  - Temperature – Thermocouple (<400°C), Suction Pyrometer (>400°C).
  - Pressure – Pressure gauge
- **Liquid streams**
  - Water or inert liquid flow – Portable manometer or pressure gauge.
  - Toxic or hot liquid flow – In-line flow element or 'bucket and stopwatch'
  - Temperature – Thermocouple
  - Pressure – In-line flow element

- **Solid streams**
  - Powder or granular flow – Belt weigher, load cell, calibrated rotary valve, timed or measured section of belt, chute, etc., with weighing scales.
  - Suspended solids flow – Dust collection and sampling probe
  - Temperature – Thermocouple, infra-red pyrometer, disappearing filament pyrometer
- **Surface Heat Loss**
  - Temperature – Infra-red pyrometer, surface thermocouple or line scanner
- **Other equipment**
  - Rotating equipment – Tachometer (shaft speed for fans, rotary feeders, conveyor belts, etc.)

Additionally, samples of each of the streams must be collected and analysed to determine their composition. The fuel must be analysed to determine its proximate (moisture, volatiles, char and ash) and ultimate analyses (C, H, O, N, S), and calorific value, and the feed and product to determine the amount of conversion that has occurred.

Flue Gas Sampling and Analysis

Gas analysis is required for a wide range of processes. It is widely used to control and monitor excess air in combustion systems. Gas analysis is also used to monitor reducing conditions in a wide range of metal heating and treatment furnaces and for ensuring the integrity of inert atmospheres in processes that require such atmospheres, whether for safety or product quality reasons. Flue gas analysis is useful even where air/fuel ratio control is feasible because it maintains a check on the flow instrument calibrations and, where carbon monoxide is also measured, it provides an indication of combustion efficiency. There are two principal ways of continuously analysing the flue gas:

- Sampling the flue gas followed by remote analysis;
- In-situ analysis.

Flue gases are usually measured to determine the oxygen, carbon dioxide, carbon monoxide, water vapour and unburnt hydrocarbons. These measurements are required for both process control and emissions monitoring, but in-situ equipment is often only located at the base of the exhaust stack. It is usually necessary to sample gases at several positions through the process for mass and energy balance calculations and there are a variety of portable flue gas analysers that are commercially available, Table 8.2 summarises the various

analytical techniques used for flue gas analysis. The most commonly used units are those based on electrochemical cells, but care must be taken when using this equipment, as most require a dry gas sample, using a water trap and absorption filter to condition the gas sample before being admitted to the analysis unit. Most of these units give a CO_2 reading, however this is not usually measured, but calculated from a pre-programmed input of the type of fuel. Cross-sensitivity can also be a problem if the cells are not correctly selected (e.g. incorrectly specified NO_x cells will also measure some of any CO in the gases as NO_x). Infra-red detection cells will measure water vapour and, it is usually a required component, as it is often used for calibration checking.

Where remote portable analysis is used, the design of the flue gas sampling probe and sample lines is as important as the analysis equipment. It is vital that the flue gas sample is maintained above its dew point from the sample point to the analyser, since any condensed water will also absorb SO_x, CO_2 and NO_x. If the flue gas is hot, and the detector is within a metre of the sample point, then a heated line is usually not required but, for all other circumstances, a heated sample line should be used. The sample probe should be inserted well into the duct and, if possible, the gap around the probe at the sample hole temporarily sealed to prevent any ingress of air. Figure 8.7 shows a flowsheet for a typical flue gas sampling train. Gas is drawn from the duct via a probe. The sample is cooled, washed and dried before being fed to the instrument(s) for analysis. The design of sampling systems is discussed more fully in section 8.3.

For sampling in hot gases above 500°C water cooled sample probes are generally required. Where the gases are also dusty or otherwise contaminated the provision must be made for probe cleaning; otherwise it will become blocked with time. This cleaning can be done manually where the time taken for the probe to block is sufficiently long; otherwise automatic pneumatic cleaning is required. A water-cooled probe employing automatic pneumatic cleaning is shown in Figure 8.10.

In-situ analysis has the potential benefit of being simpler than remote sampling, and easier to maintain. These analysis systems are discussed in detail in section 8.3.2.

Calibration and Errors in Plant Instrumentation

Great care has to be taken when using data from plant instrumentation for process analysis because plant instruments are rarely calibrated accurately and even the simple and humble thermocouple can have significant errors, especially where it is indicating the

temperature of high temperature gases. Some of the more common issues are:

- Gaseous Flow Meters Uncorrected for Gas Density (temperature and pressure) – Few orifice plate or venturi based flowmeters, especially those indicating ambient air or gas flows, are equipped with temperature or pressure correction. A variation in ambient temperature of as little as 10–15°C (not uncommon even in a single day) introduces an error in the order of 3–5%, which could be highly significant when trying to undertake mass and energy balances.
- High Temperature Thermocouples – The reading indicted by thermocouples located in high temperature gas streams is subject to significant error owing to the effect of radiation from, or to the thermocouple, see section 8.2.1.

9.2.2 Constructing Mass and Energy Balances

Having collected the plant process data, reference to suitable textbooks will provide most of the basic chemical and physical data needed to carry out the mass and energy balance calculations. This data would include specific heat, thermal capacity, reaction energy and temperature, latent heat, and reaction mechanisms. It may also be necessary to use some 'in-house' data for the particular process if it is not a well documented operation. If it is possible to measure all of the input and output stream data then the construction of the mass and energy balance is a relatively simple exercise based on the inviolate laws of mass and energy conservation: 'What goes in must come out'. However, as is the nature of life, it is very rarely possible to accurately measure all of the process flow parameters and in such cases the logic of the detective comes into play.

We can use the generic process depicted in Figure 9.1 as the basis for an example of a mass and energy balance calculation, and demonstrate some of the techniques that can be used to determine values from incomplete information.

Example 9.1 The following process measurements and information has been monitored and samples collected during an operating period of one hour for the process shown in Figure 9.1. Draw up suitable mass and energy balances for the whole process, and also for the furnace.

Fuel used – Algerian *LNG* (analysis supplied)
Chemical reaction energy for process – 0.76 MJ/kg product
Specific heat of feedstock/product at T°C – 2.24 + T / 7500 kJ/kg°C

Table 9.2 Process measurements

Measurement	*Value*		*Measuring device*
Feedstock flowrate	108 tonnes/hr		In line turbine flow meter
Product flowrate	107 tonnes/hr		In line turbine flow meter
Fuel flowrate	3380 m^3/hr		Utility gas meter reading
Furnace air flowrate	590 m^3/min		In duct venture
Cooling air flowrate	3200 m^3/min		Pitot traverse of duct
Preheater Thermex flowrate	9 kg/s		Calibrated in line orifice
Stack gas flowrate	5600 m^3/min		Pitot traverse of duct
Ambient temperature (feedstock and air)	30°C		Thermocouple
Gas temperature	60°F		Utility gas meter reading
Thermex oil temperature into heater	115°C		In line thermocouple
Thermex oil temperature out of heater	352°C		In line thermocouple
Feedstock temperature into preheater	33°C		In line thermocouple
Feedstock temperature into furnace	97°C		In line thermocouple
Product temperature into cooler	117°C		In line thermocouple
Product temperature out of cooler	45°C		In line thermocouple
Air temperature out of fan	32°C		In line thermocouple
Air temperature out of cooler	85°C		In line thermocouple
Flue gas temperature out of furnace	485°C		In line thermocouple
Stack gas temperature	165°C		Thermocouple
Flue gas analysis (volume basis)	*Furnace*	*Stack*	
CO_2	8.35%	1.68%	Infra red analyser
O_2	3.01%	17.38%	In line zirconia probe
N_2	72.73%	77.74%	By difference
CO	1750vppm	350vppm	Portable electrochemical cell
H_2O	15.74%	3.17%	Infra red analyser
Electrical power to heater	5.02 MW		Local sub-station meters
Electrical power to Thermex fluid pump	0.1 MW		Local sub-station meters
Electrical power to fuel compressor	0.05 MW		Local sub-station meters
Electrical power to feed pump	0.23 MW		Local sub-station meters
Electrical power to fan	0.2 MW		Local sub-station meters
Product purity	93%		Laboratory sample analysis

Table 9.3 Selected fuel data

Fuel property	*Value*
Gross calorific value	43.16 MJ/m^3
Stoichiometric air requirement	16.73 kg air / kg gas
Fuel Nitrogen	0.3 vol. %

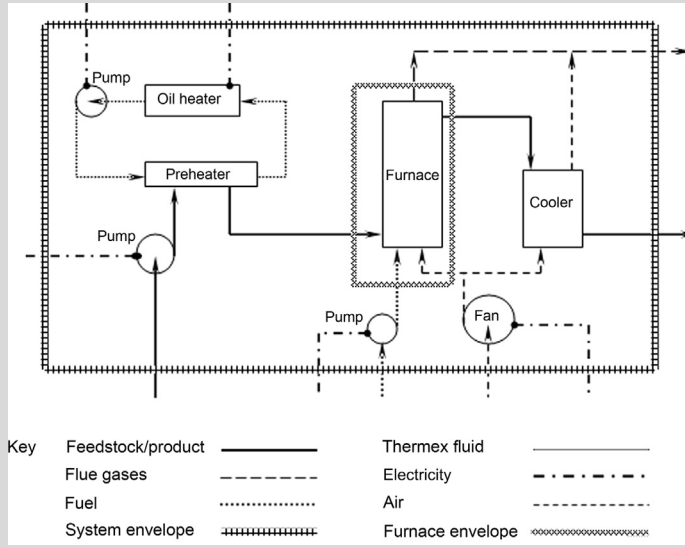


Figure 9.5 Process flowsheet with envelopes

The first step is to draw up a process flowsheet. This s shown in Figure 9.5, together with the process envelopes for the whole process and the furnace. By tracking the system envelope boundary, we can draw up mass and energy balances as follows

Mass balance

IN		*OUT*	
Stream	*Flowrate*	*Stream*	*Flowrate*
Feedstock		Product	
Fuel		Stack gases	
Air			
TOTAL		**TOTAL**	

Energy balance

IN		*OUT*	
Stream	*Energy*	*Stream*	*Energy*
Feedstock		Product	
Fuel		Product (reaction)	
Air		Stack gases	
Thermex heater power			
Thermex heater pump			
Feed pump			
Fuel compressor			
Air fan			
TOTAL		**TOTAL**	

The data is presented as measured, and must be brought to a common set of units relative to datum conditions. The fuel flowrate in measured by the gas meter supplied by the utility company, which is generally calibrated at STP i.e. 15.56°C(60°F) and 1 atmosphere. We will use this as the datum conditions for the calculations. The mass balance will be in kg/s and the energy balance in MW.

$$\text{Feedstock flowrate} = \frac{108 \times 1000}{3600} = 30.00 \text{ kg/s}$$

$$\text{Product flowrate} = \frac{107 \times 1000}{3600} = 28,72 \text{ kg/s}$$

From data on fuel, relative density = 0.6435, thus,

$$\text{Density of fuel gas at } STP = \frac{0.6435 \times 1.2928 \times 273}{273 + 15.56} = 0.787 \text{ kg/m}^3$$

$$\text{Fuel flowrate} = \frac{3380 \times 0.787}{3600} = 0.74 \text{ kg/s}$$

$$\text{Density of air at measurement point} = \frac{1.2928 \times 273}{273 + 32} = 1.1572 \text{ kg/m}^3$$

$$\text{Air flowrate} = \frac{(590 + 3200) \times 1.1572}{60} = 73.58 \text{ kg/s}$$

From the stack gas analysis, we can calculate the weighted mean density.

Component	*Volume fraction*	*Density at NTP*	*Fractional density at 165°C*
CO_2	0.01680	1.9631	0.02056
O_2	0.17380	1.4278	0.15467
N_2	0.77735	1.257	0.60903
CO	0.00035	1.2492	0.00027
H_2O	0.03170	0.8039	0.01588

Weighted mean density $= 0.80041$ kg/m^3

$$\text{Stack gas flowrate} = \frac{5600 \times 0.80041}{60} = 74.71 \text{ kg/s}$$

Table 9.4 Mass balance for the process

IN			*OUT*		
Stream	*Flowrate kg/s*		*Stream*	*Flowrate kg/s*	
Feedstock	30.00	28.73%	Product	29.72	28.46%
Fuel	0.74	0.71%	Stack gases	74.71	71.54%
Air	73.58	70.46%			
Unaccounted	0.11	0.11%			
TOTAL	104.43		**TOTAL**	104.43	

The mass balance is in good agreement, with a 0.11% error, but it should be noted that small flows, such as the fuel flowrate, could vary considerably without affecting the mass balance significantly. It is only when the energy balance is completed that errors in the mass flow measurements may be recognised.

From data on fuel gross $CV = 43.16$ MJ/m^3 (Standard conditions)

$$\text{Energy from combustion of fuel} = \frac{3380 \times 43.16}{3600} = 40.52 \text{ MW}$$

Sensible heat in feedstock above datum

$$= \frac{30 \times \left(\left[\left\{ 2.24 + \frac{30}{7500} \right\} \times 30 \right] - \left[\left\{ 2.24 + \frac{15.56}{7500} \right\} \times 15.56 \right] \right)}{1000}$$

$$= 0.97 \text{ MW}$$

Specific heat of air at T°C can be correlated by $-1.288 + T / 8390$ kJ/kg°C

Sensible heat in air above datum

$$= \frac{73.58 \times \left(\left[\left\{ 1.288 + \frac{30}{8390} \right\} \times 30 \right] - \left[\left\{ 1.288 + \frac{15.56}{8390} \right\} \times 15.56 \right] \right)}{1000}$$

$$= 1.37 \text{ MW}$$

Sensible heat in product above datum

$$= \frac{29.72 \times \left(\left[\left\{ 2.24 + \frac{45}{7500} \right\} \times 45 \right] - \left[\left\{ 2.24 + \frac{15.56}{750} \right\} \times 15.56 \right] \right)}{1000}$$

$$= 1.97 \text{ MW}$$

$$\text{Chemical reaction energy used} = 29.72 \times 0.76 \times 0.93$$

$$= 20.01 \text{ MW}$$

The stack gas analysis shows that there is some CO present, the consequence of which is that some of the fuel combustion energy is not released. The gross CV of CO is 11.97 MJ/m^3 (STP), thus energy loss due to incomplete combustion

$$= \frac{11.97 \times 5600 \times 0.00035 \times (273 + 15.56)}{(273 + 165) \times 60} = 0.26 \text{ MW}$$

From the stack gas analysis, we can calculate the mass fraction of each component (see Chapter 2, example 2.1 for method, or later in furnace mass balance) and hence the weighted mean specific heat.

Component	*Mass fraction*	*Specific heat correlation*
CO_2	0.0257	$1.6824 + T / 1766$
O_2	0.1932	$1.3059 + T / 5726$
N_2	0.7609	$1.2882 + T / 9448$
CO	0.0003	$1.2980 + T / 8400$
H_2O	0.0198	$1.4717 + T / 4204$

Weighted mean specific heat $= 1.3053 + T / 7486$ kJ/kg°C

Sensible heat in flue gases

$$= \frac{74.71 \times \left(\left[\left\{ 1.3053 + \frac{165}{7486} \right\} \times 165 \right] - \left[\left\{ 1.3053 + \frac{15.56}{7486} \right\} \times 15.56 \right] \right)}{1000}$$

$= 14.84$ MW

The latent heat of evaporation of water is taken at the datum temperature as 2.455 MJ/kg. Thus the latent heat in flue gases

$$= 74.71 \times 0.0198 \times 2.465 = 3.65 \text{ MW}$$

Table 9.5 Energy balance for the process

IN			*OUT*		
Stream	*Energy MW*		*Stream*	*Energy MW*	
Feedstock	0.97	2.01%	Product	1.97	4.06%
Fuel	40.52	83.60%	Product (reaction)	21.01	43.34%
Air	1.37	2.84%	Stack gases (sensible)	14.84	30.62%
Thermex heater power	5.02	10.36%	Stack gases (latent)	3.65	7.54%
Thermex heater pump	0.10	0.20%	Incomplete combustion	0.27	0.56%
Feed pump	0.23	0.47%			
Fuel compressor	0.05	0.11%			
Air fan	0.20	0.41%	Unaccounted	6.72	13.88%
TOTAL	48.46		**TOTAL**	48.46	

Mass and Energy Balance of the Furnace

From Figure 9.5, the furnace envelope gives the following balances

Mass balance

IN		*OUT*	
Stream	*Flowrate*	*Stream*	*Flowrate*
Feedstock		Product	
Fuel		Flue gases	
Air			
TOTAL		**TOTAL**	

Energy balance

IN		*OUT*	
Stream	*Energy*	*Stream*	*Energy*
Feedstock		Product	
Fuel		Product (reaction)	
Air		Flue gases	
TOTAL		**TOTAL**	

In the mass balance, the feedstock, fuel and product flowrates are the same as the previous calculation, but the air and flue gas mass flows are different.

$$\text{Air flowrate} = 590 \times \frac{1.1572}{60} = 11.38 \text{ kg/s}$$

The stoichiometric air required to completely burn the fuel $= 0.74 \times 16.73 = 12.38$ kg/s

Since the supply of air from the fan is less than the stoichiometric requirement, and there is excess oxygen in the flue gases, there must also be an in-leakage of air to the furnace.

The flue gas flowrate is not measured, but if we assume that the furnace has X kg/s air in-leakage, then we can use the nitrogen flow through the furnace as a **key component**. Nitrogen is not involved in any of the combustion reactions (other than in the formation of nitrous oxides, which are not significant in mass balance terms), and therefore the mass flow of nitrogen into the system is equal to the mass flow leaving the system. In this case, nitrogen enters the furnace with the combustion air (76.8% by weight) and the fuel (0.3% by volume), together with any in-leakage air (76.8% by weight).

$$\text{Mass flow of } N_2 \text{ in combustion air} = 11.38 \times 0.768 = 8.7389 \text{ kg/s}$$

$$\text{Mass flow of } N_2 \text{ in fuel} = \frac{\left\{3380 \times \frac{0.003}{3600}\right\} \times 1.257 \times 273}{273 + 15.56} = 0.0033 \text{ kg/s}$$

$$\text{Mass flow of } N_2 \text{ in in-leakage air} = X \times 0.768$$

$$\text{Total mass flow of } N_2 \text{ into furnace} = 8.7389 + .0033 + 0.768X$$

$$= 8.7422 + 0.768X \text{ kg/s}$$

$$= \text{mass flow of } N_2 \text{ in flue gases}$$

From the flue gas analysis, which is volumetric, we can calculate the mass analysis.

Component	*m^3/ m^3 of flue gas*	*Density at NTP kg/m^3*	*kg/m^3 of flue gas*	*Flue gas analysis (mass basis)*
CO_2	0.08350	1.9631	0.1639	0.1312
O_2	0.03010	1.4278	0.0430	0.0344
N_2	0.72725	1.257	0.9142	0.7315
CO	0.00175	1.2492	0.0022	0.0017
H_2O	0.15740	0.8039	0.1265	0.1012
Total	1		1.2498	1

Thus 73.15% by weight of the flue gases are N_2.

$$\text{Mass flow of flue gasses} = \frac{8.7422 + 0.768X}{0.7315}$$

$$= 11.95 + 1.05X \text{ kg/s}$$

An oxygen balance will provide a second equation involving X, since the flue gas oxygen is related to the excess air.

The oxygen required for **complete** combustion of the fuel

$$= 0.74 \times 16.73 \times 0.232 = 2.8722 \text{ kg/s}$$

Since there is some CO in the flue gases, the oxygen actually used in combustion

$$= 2.8722 - \frac{0.0017 \times 16}{28} = 2.8712 \text{ kg/s}$$

$$\text{Thus air used in combustion} = \frac{2.8712}{0.232} = 12.3760 \text{ kg/s}$$

$$\text{Thus excess air} = 11.38 + X - 12.3760 = X - 0.996 \text{ kg/s}$$

$$\text{Excess oxygen} = \text{oxygen in flue gases, thus}$$

$$(X - 0.996) \times 0.232 = 0.0344 \times (11.95 + 1.05X)$$

$$\text{In-leakage air flow } X = 3.28 \text{ kg/s}$$

$$\text{Flue gas flow} = 11.95 + 1.05 \times 3.28 = 15.39 \text{ kg/s}$$

Table 9.6 Mass Balance for the furnace

IN			*OUT*		
Stream	*Flowrate kg/s*		*Stream*	*Flowrate kg/s*	
Feedstock	30.00	66.09%	Product	29.72	66.47%
Fuel	0.74	1.62%	Flue gases	15.39	33.90%
Air from fan	11.38	25.07%			
In-leakage air	3.28	7.23%	Unaccounted	0.29	0.62%
TOTAL	45.40		**TOTAL**	45.40	

As previously calculated, the energy from combustion of fuel = 40.52 MW

Sensible heat in feedstock above datum

$$= \frac{30 \times \left(\left[\left\{2.24 + \frac{97}{7500}\right\} \times 97\right] - \left[\left\{2.24 + \frac{15.56}{7500}\right\} \times 15.56\right]\right)}{1000}$$

$$= 5.51 \text{ MW}$$

Sensible heat in air from fan above datum

$$= \frac{11.38 \times \left(\left[\left\{1.288 + \frac{32}{8390}\right\} \times 32\right] - \left[\left\{1.288 + \frac{15.56}{8390}\right\} \times 15.56\right]\right)}{1000}$$

$$= 0.24 \text{ MW}$$

Sensible heat in in-leakage air above datum

$$= \frac{3.28 \times \left(\left[\left\{ 1.288 + \frac{30}{8390} \right\} \times 30 \right] - \left[\left\{ 1.288 + \frac{15.56}{8390} \right\} \times 15.56 \right] \right)}{1000}$$

$$= 0.06 \text{ MW}$$

Sensible heat in product above datum

$$= \frac{29.72 \times \left(\left[\left\{ 2.24 + \frac{117}{7500} \right\} \times 117 \right] - \left[\left\{ 2.24 + \frac{15.56}{750} \right\} \times 15.56 \right] \right)}{1000}$$

$$= 6.81 \text{ MW}$$

As previously calculated, chemical reaction energy used = 21.01 MW

The stack gas analysis again shows that there is some CO present, thus energy loss due to incomplete combustion

$$= \frac{11.97 \times 15.39 \times 0.0017 \times (273 + 15.56)}{273 \times 1.2492} = 0.27 \text{ MW}$$

The weighted mean specific heat of the flue gases is calculated as previously.

Component	*Mass fraction*	*Specific heat correlation*
CO_2	0.1312	1.6824 + T / 1766
O_2	0.0344	1.3059 + T / 5726
N_2	0.7315	1.2882 + T / 9448
CO	0.0017	1.2980 + T / 8400
H_2O	0.1012	1.4717 + T / 4204

Weighted mean specific heat = 1.3591 + T / 5116 kJ/kg°C

Sensible heat in flue gases

$$= \frac{15.39 \times \left(\left[\left\{ 1.3591 + \frac{485}{5116} \right\} \times 485 \right] - \left[\left\{ 1.3591 + \frac{15.56}{5116} \right\} \times 15.56 \right] \right)}{1000}$$

$$= 10.52 \text{ MW}$$

Latent heat in flue gases = $15.39 \times 0.1012 \times 2.465 = 3.84$ MW

Table 9.7 Energy balance for the furnace

IN			*OUT*		
Stream	*Energy MW*		*Stream*	*Energy MW*	
Feedstock	5.51	11.89%	Product	6.81	14.69%
Fuel	40.52	87.46%	Product (reaction)	21.01	46.34%
Air from fan	0.24	0.52%	Flue gases (sensible)	10.52	22.71%
In-leakage air	0.06	0.13%	Flue gases (latent)	3.84	8.29%
			Incomplete combustion	0.27	0.58%
			Unaccounted losses	3.88	8.39%
TOTAL	46.33		**TOTAL**	46.33	

This example demonstrates that even for a relatively simple system, the calculations required are not trivial, and usually involve a significant amount of data manipulation. The mass balances for both envelopes are good, giving confidence to the data, but we should assess the accuracy of each instrument, and apply error bands to both the mass and energy balance values before finally accepting the results. This is particularly highlighted by the identification of in-leakage air into the furnace, which was not evident in the overall mass balance. We should, of course recalculate the overall balance to include the in-leakage air, as this stream also crosses the envelope boundary, albeit invisibly. The derivation of the flue gas mass in the furnace balance by the use of a key component demonstrates an important tool that can be used where the data available is incomplete. It is often the case in practice that measurement of hot furnace flue gas flows is difficult owing to temperature limitations, dust and particulates, condensation of water or corrosive gases in probes, and limited access.

The example shows that there are a number of inefficiencies relating to the performance of the system. The thermal efficiency of the process, assuming that the sensible heat in the product is ultimately rejected to the atmosphere is 43.34% (viz. 21.01MW / 48.46MW), whilst the thermal efficiency of the furnace is 46.34% (viz. 21.01MW / 46.33 MW). The presence of CO in the flue gases means that the combustion process is incomplete, and the combustion efficiency is 99.33% (viz. {40.52MW – 0.27MW}/ 40.52MW). The data also indicates that the product is not fully processed, giving a conversion efficiency of 93%.

Table 9.8 Energy balance for the process with reduced in-leakage and balanced burner flows

IN			*OUT*		
Stream	*Energy MW*		*Stream*	*Energy MW*	
Feedstock	0.97	2.02%	Product	1.97	4.08%
Fuel	40.22	83.41%	Product (reaction)	21.01	43.58%
Air	1.43	2.96%	Stack gases (sensible)	15.09	31.30%
Thermex heater power	5.02	10.42%	Stack gases (latent)	3.84	7.95%
Thermex heater pump	0.10	0.21%	Incomplete combustion	0.00	0.01%
Feed pump	0.23	0.47%			
Fuel compressor	0.05	0.11%			
Air fan	0.20	0.41%	Unaccounted	6.32	13.10%
TOTAL	48.22		**TOTAL**	48.22	

There is obviously scope for improvement in the thermal efficiency of the process in the example, through a number of operational and design changes. It is usually most cost effective to implement process changes first, before considering design changes, as these usually involve both capital investment and lost production time during installation. An obvious process improvement in the example would be to eliminate the energy lost from incomplete combustion. The furnace balances show that the ratio of air to fuel ratio through the burner is 11.38:0.74 , i.e. 15.92 kg air / kg fuel, which is less than the stoichiometric air requirement for the fuel (16.77 kg/kg), indicating that whilst the furnace is running with an excess of air of ~18.5%, the burner(s) are operating sub-stoichiometrically. Chapter 5 has already discussed the importance of good air fuel mixing. By the simple expedient of correctly balancing the air fuel ratio to the burners and eliminating air in-leakage by blocking up openings etc., the CO level is reduced to 20vppm at the furnace exit (4vppm at the stack). The revised energy balance for the process is shown Table 9.8, which indicates that the process efficiency can be increased from 43.34% to 43.58%, and the fuel consumption reduced by 0.75%.

We will return to this example later in this chapter to explore the effect of other design changes.

9.3 Energy Conversion

Any process that uses energy involves its conversion from one form to another. Figure 9.6 is an adaptation of Thring's energy triangle, Thring (1973) and Sunavala (1982), showing the relative interchange of different energy forms, together with best available practice conversion efficiency estimates. This diagram provides a quick reference for

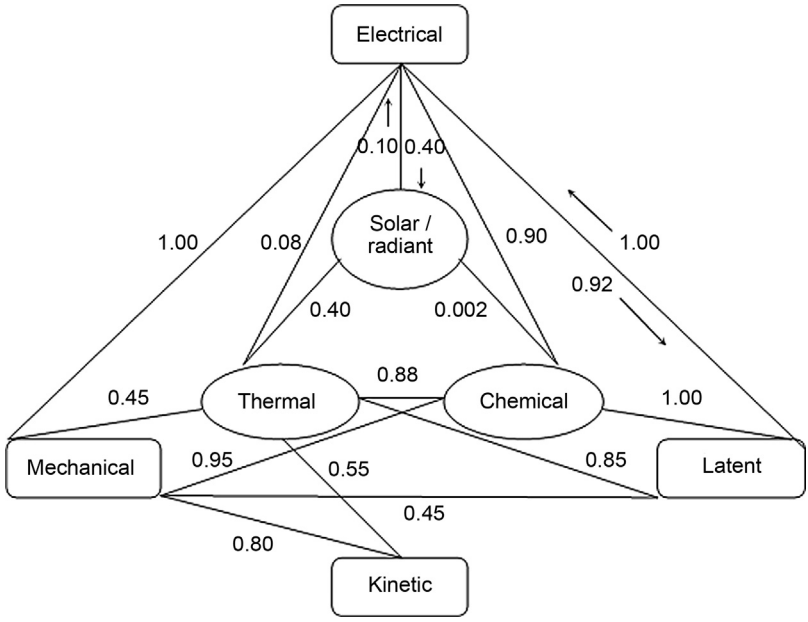


Figure 9.6 Energy conversion trianges (after Thring and Sunavala)

the estimation of maximum efficiency of a particular energy conversion process. For example, the generation of electricity from coal involves

1. chemical energy to thermal energy (combustion) $\eta = 0.88$
2. thermal energy to mechanical energy (steam turbine) $\eta = 0.45$
3. mechanical energy to electrical energy (generator) $\eta = 1.00$

Thus the overall maximum efficiency $= 0.88 \times 0.45 \times 1.0 = 0.396$
Similar analysis gives the results in Table 9.9.

The laws of thermodynamics govern energy conversion processes. The first law, which states that energy is neither created nor destroyed, is the basis of the heat balance and, whilst this quantifies the energy flows, it does not provide a representation of the effectiveness of the system design. The second law provides a means of assigning a quality index to energy. Real processes are irreversible, and the transfer of heat and work from one form to another always results in the loss of some available energy. The second law, which states that the entropy, S, of an isolated system can only increase (in an irreversible change) or stay constant (in equilibrium), evaluates the loss of energy, entropy production or irreversibility of the process. For example, consider a system of two parts, A and B in thermal contact. If a

Table 9.9 Maximum energy conversion for various processes based on Figure 9.12

Process	*Steps*	*Maximum efficiency*
Fossil fuel power station	Chemical – thermal – mechanical – electrical	0.396
IC engine	Chemical – thermal – mechanical	0.396
Aircraft engine	Chemical – thermal – mechanical – kinetic	0.318
Liquid fuel rocket	Chemical – thermal – kinetic	0.485
Incandescent lamp	Electrical – thermal – radiant	0.03
Wind electricity	Kinetic – mechanical – electrical	0.80
Solar thermal electricity	Radiant – thermal – mechanical – electrical	0.18
Solar cell	Radiant – thermal – chemical – electrical	0.317
Steel production	Chemical – thermal – latent	0.748
Aluminium production	Chemical – thermal – mechanical – electrical – latent	0.364

quantity of heat δQ ($=Cp\delta T$) passes from A at a temperature T_A to B at a temperature T_B, where $T_A > T_B$. The entropy of A falls by $\delta Q/T_A$, and that of B rises by $\delta Q/T_B$. The total entropy change is

$$\delta S = \frac{\delta Q}{T_A} - \frac{\delta Q}{T_B} \tag{9.7}$$

and is positive, becoming zero only when $T_A = T_B$, i.e. when thermal equilibrium is reached.

9.3.1 Low and High Grade Heat

We have observed that the efficiency of any thermal process not only depends on the quantity of heat supplied, but also on its quality. The quality is often referred to in terms of low and high grade heat, although the division between the grades is somewhat arbitrary. Notwithstanding, we can reasonably define low grade heat as enthalpy contained in material at low temperature (<400°C), and high grade heat as enthalpy contained in material at high temperature (>400°C). For any given thermal process we can construct an enthalpy-temperature diagram that describes the heating requirements. In some cases, there may be a large demand for heat at a relatively low temperature, owing to endothermic reactions, and only a small amount of additional enthalpy input is required to complete the process. Ideally, in this case low grade heat should be used to carry out the bulk of the heat transfer requirements, and then a smaller quantity of high grade heat should be supplied to achieve completion of the process.

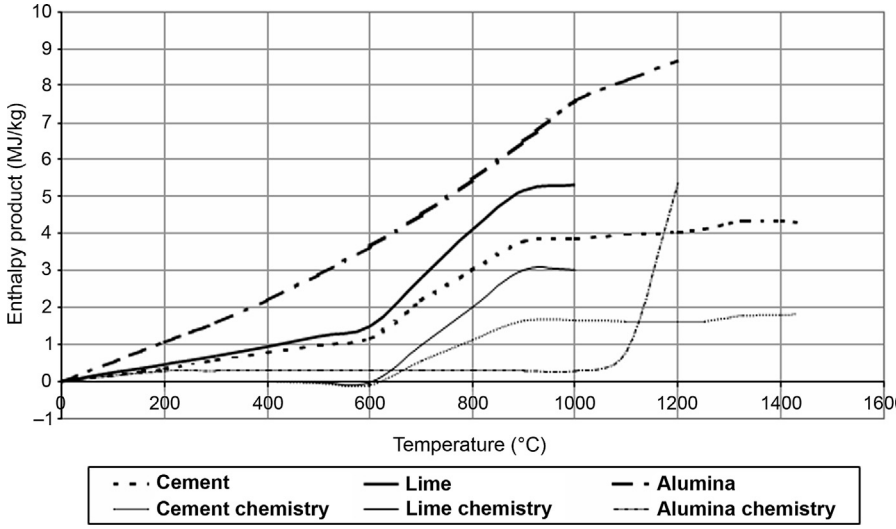


Figure 9.7 Temerature–enthalpy data for cement, lime and alumina production

As an example, Figure 9.7 shows some enthalpy temperature profiles for a number of mineral production processes. The enthalpy that is required for the processing of each of the minerals is the sum of the chemical reactions and the sensible heat to raise the material to the reaction temperature. In the case of cement and lime the majority of heat is required between 600°C and 900°C, where the chemistry curves show endothermic reactions involving the decomposition of calcium carbonate occurring. In the case of cement, the material must be further heated to ~1400°C, where a number of exothermic reactions occur during the final chemical combinations required to produce cement. Conversely, for alumina there is a fairly steady demand for heat throughout the process as sensible heat to raise the alumina hydrate temperature to 1100°C. The endothermic reaction, involving the release of the bound water molecules, only occurs at 1100 °C to 1200 °C.

In practice, most high grade heat is generated from the primary energy source, i.e. combustion of fuel or electrical heating. The first source of low grade heat should be 'recovered' from the exit flows from high grade heat transfer vessels e.g. furnace flue gases and product. If there is insufficient recovered heat available, or the process conditions preclude economic recovery, then boosting with additional primary energy is required. Pinch point analysis provides a structured methodology for optimizing an integrated process design based on minimum cost and energy targets.

9.3.2 Exergy and Pinch Point Analysis

Integrated process design methods adopt a holistic approach to design, retrofitting and operations planning. Cost and energy design targets - typically a minimum values for each objective - can be calculated based on pinch technology, which defines the enthalpy at which the hot and cold process streams are separated by the minimum temperature difference. The ethos of the pinch point approach is to achieve optimal energy utilisation in a process by interconnecting material flows requiring heating (so called cold flows, requiring an increase of enthalpy flow) with those requiring cooling (so called hot flows, requiring a decrease of enthalpy flow). Pinch analysis calculates the target figures for minimal heat expenditure with a given minimal driving temperature difference for the heat transfer. This divides the process into two distinct systems at the "pinch point", and heat/energy flows are optimally interconnected in pairs. Design layouts of the process are thus identified and the optimum network of heat exchangers, heaters, and coolers can be calculated with respect to annual operating and capital costs.

By approximating hot and cold streams as linear correlations, they can be illustrated in enthalpy-temperature diagrams as straight lines, as illustrated in Figure 9.8, which represents the process described in example 9.1. Since only changes of enthalpy are relevant and enthalpy has no absolute zero point, the flows can be moved horizontally in the diagram. In order to construct the hot and cold flow curves, the individual hot and cold flows are divided into temperature intervals, whose limits are chosen so that one interval boundary lies on every entry and

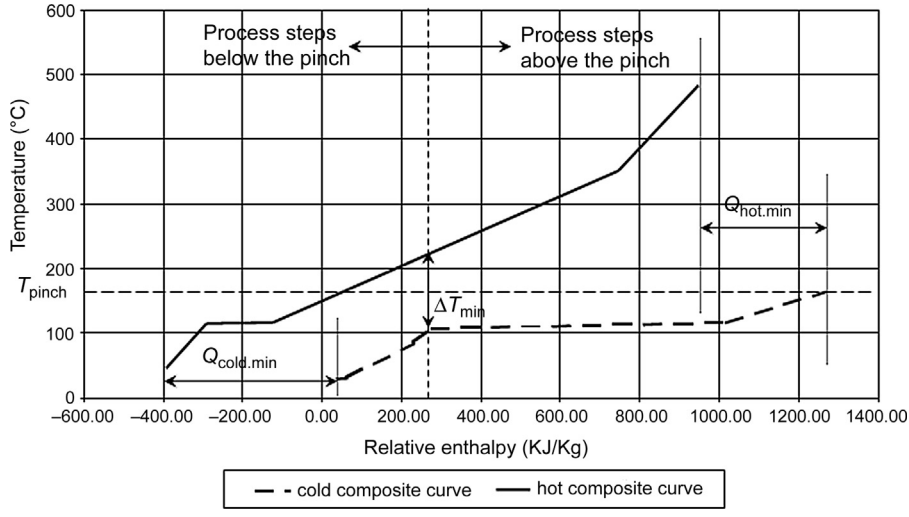


Figure 9.8 Composite curves for hot and cold streams for pinch analysis

exit temperature. In each temperature interval individual hot and cold heat capacity flows are added and displayed together as lines in the H-T diagram. Together they represent the entire heat balance of the system. These merged curves are referred to as the composite cooling and composite heating curves. The points of discontinuity in the composite curves indicate the start or the end of one flow or the onset of a phase change, Peters, Timmerhaus & West (2003). In order to ensure heat transfer between cold and hot flows, the combined curves of the hot material flows must lie above those of the cold flows at all points, and are thus moved horizontally until this condition is met. The constraint set by ΔT_{min} is defined as the minimum temperature difference between the flows. The pinch point, where the distance between the hot and cold curves is minimal, then denotes the possible optimal internal heat transfer between the hot and cold flows.

By decreasing ΔT_{min} the composite curves can be shifted closer together, where $\Delta T_{min} = 0$ is the ultimate limit. $Q_{hot;min}$ is the minimum amount of additional energy demanded for heating, which cannot be covered by utilising the hot flows, whereas $Q_{cold;min}$ represents the amount of heat which must be dissipated by external cooling. The process streams on the right side of the diagram above the pinch temperature require heating (these streams constitute the heat sink), whereas the process streams below the pinch temperature need to be cooled (these streams are referred to as the heat source). Additional heating of $Q_{hot;min}$ would lead to additional cooling of $Q_{cold;min}$ at the end of the process steps. This is an indication of sub-optimal energy use or mismatched energy demand. A surplus of heat below the pinch point cannot be balanced with heat demand above the pinch, since energy would have to be transferred against the temperature gradient. Incorporating these observations three rules, valid for any pinch problem, can be identified, Linnhoff, Manson & Wardle (1979), Peters, Timmerhaus & West (2003):

- no heat dissipation above the pinch,
- no heat supply below the pinch,
- no heat transport across the pinch.

The matching of hot and cold process streams can be done graphically by plotting the composite curves, or by using optimisation algorithms.

9.4 Heat Recovery Equipment

Heat recovery is undertaken in equipment that is generally classified by the term heat exchanger. Whilst they all perform the same function, there is considerable variation in the design of such equipment,

primarily governed by the physical and chemical properties of the hot and cold fluids. Notwithstanding this variety, there are some general observations that can be made about the design methodology of heat exchangers. They can be divided into two major groups, recuperative and regenerative. Recuperative exchangers transfer heat continuously between two fluids, either by direct contact or through a 'thermally thin' dividing medium. Regenerative exchangers use a thermally absorbent sink to store heat from the hot fluid and then release heat to the cold fluid in a cyclic mode. Thus, recuperative heat exchangers operate in a steady state mode, whilst regenerative heat exchangers operate in an unsteady state mode.

9.4.1 Recuperative Heat Exchangers

For recuperative units, the general design equation for the heat transferred, Q, can be written as

$$Q = UA\Delta T_{lm} \tag{9.8}$$

where

$$\text{The overall h.t.c, } U = \frac{1}{\frac{1}{h_{inside}} + \frac{x}{k} + \frac{1}{h_{outside}}} \tag{9.9}$$

and the log mean temperature difference,

$$\Delta T_{lm} = \frac{\Delta T_{out} - \Delta T_{in}}{ln\left(\frac{\Delta T_{out}}{\Delta T_{in}}\right)} \tag{9.10}$$

There are four basic configurations for the arrangement of the flows into and out of recuperative exchangers. These are shown in Figure 9.9. In co-current, or parallel-flow units the two fluid streams enter together at one end, flow through in the same direction, and leave together at the other end (i.e. $\Delta T_{in} = T2_{in} - T1_{in}$, $\Delta T_{out} = T2_{out} - T1_{out}$); whereas in counter-current or counter-flow units the two fluid streams move in opposite directions (i.e. $\Delta T_{in} = T2_{out} - T1_{in}$, $\Delta T_{out} = T2_{in} - T1_{out}$). In single-pass cross-flow units, one fluid moves through the heat transfer matrix at right angles to the flow path of the other fluid. In multi-pass cross-flow units one fluid stream shuttles back and forth across the flow path of the other fluid stream, usually giving a cross-flow approximation to counter-flow.

The most important differences between these four basic types lies in the relative amounts of heat transfer surface area required to produce a given temperature rise for a given temperature difference between the two fluid streams where the primary fluid enters the heat exchanger. Figure 9.10 shows the relative area required for

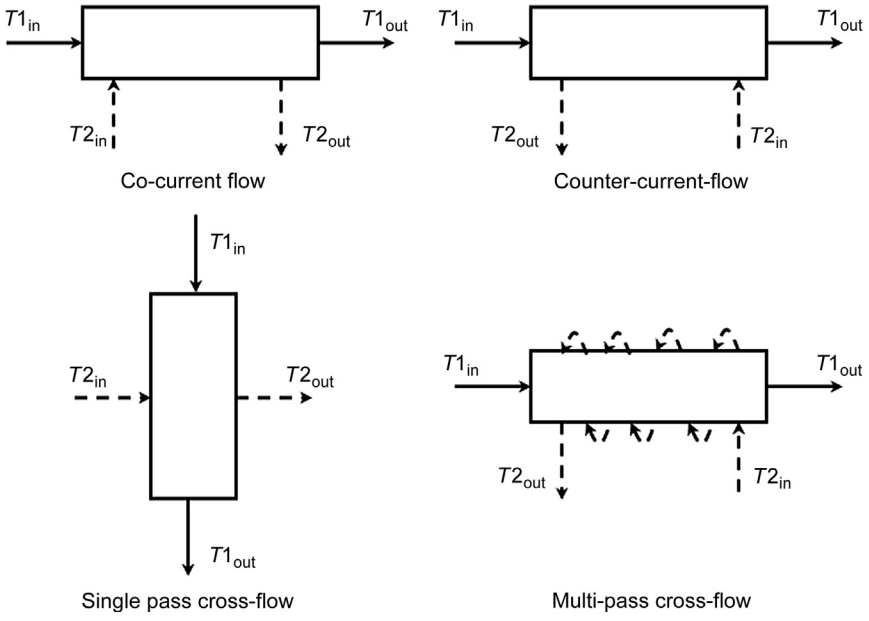


Figure 9.9 Types of flow path configurations through recuperative heat exchangers

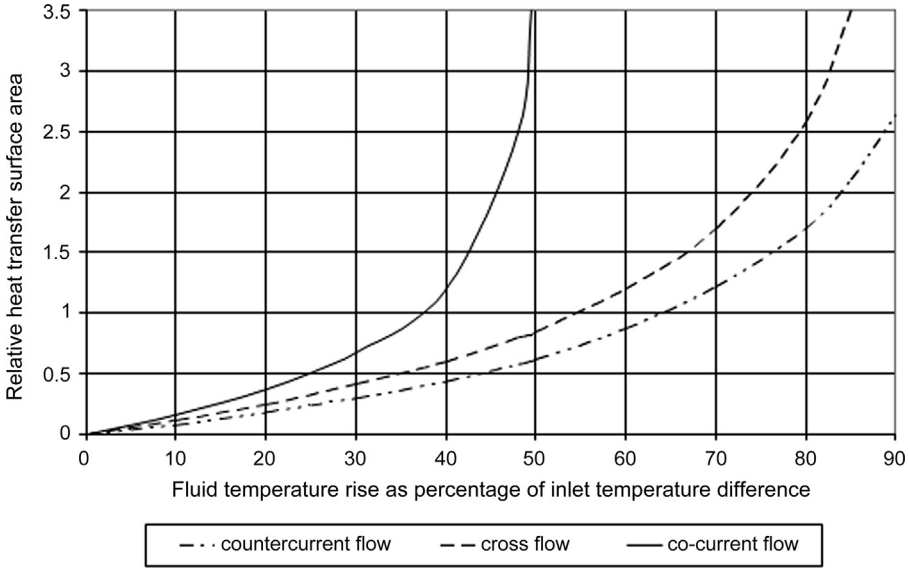


Figure 9.10 Relationship between heat transfer rate and surface area for different recuperative heat exchanger flow regimes

each type, as a function of the change in temperature of the primary fluid for a typical set of conditions. In the region where the primary fluid temperature change across the heat exchanger is a small percentage of the difference in temperature between the two entering fluid streams, all the designs require approximately the same surface area for heat exchange. Table 9.10 summarizes the most common recuperative heat exchanger designs used in furnace operations, together with their operation modes.

9.4.2 Regenerative Heat Exchangers

Regenerative heat exchangers operate over a timed cycle, using a high heat capacity thermal medium as an intermediate exchanger. The general design procedure for this type of unit is based on the transient Fourier equation for conduction into and out of the thermal medium, together with suitable values for the Biot Modulus for heat transfer to and from the surface. This method is explained in Chapter 4, section 4.1.2.2. Cyclic operation can be achieved by either, reversing the flow of the two fluids over the intermediate exchange medium at regular intervals, or by using a closed loop flow of the intermediate material between the two fluids. The most common thermal medium used in regenerators are ceramic, although in lower temperature operations metallic elements and thermal fluids can be used. Reverse flow designs requires that there are at least two equally sized thermal storage units. Figure 9.11 shows the two basic regenerative design configurations. Table 9.11 summarizes the most common recuperative heat exchanger designs used in furnace operations.

9.4.3 General Heat Exchanger Design Procedure

The procedure for designing a heat exchanger depends on the design conditions. Usually, the inlet and outlet temperatures and flowrates of the two streams are fixed by the process requirements, and the design involves the correct sizing of the heat exchanger areas required. It is also usually the case that there are pressure drop limitations for the fluids, governed by economic pumping or fan power considerations. Since the pressure drop depends on the fluid velocity, the flow channel equivalent diameter, and the channel length, the resulting design equations involve six independent variables. Thus there are an infinite number of solutions, but only one optimum design.

The simplest approach is to assume a particular design matrix (i.e. fix the tube channel size and spacing) and velocities for the two fluids. The heat transfer area required and pressure drops for the two fluids are then calculated using the basic design equations. The resulting

Table 9.10 Common types of recuperative heat exchangers used in furnace operations

Description	*Modes*	*Primary fluid*	*Secondary Fluid*	*Common applications*
Tubular array – smooth	co-, counter- or cross- flow	Liquid or vapour (e.g. water/steam)	Low pressure liquid or gas	waste heat boiler (steam plant), process heater (petrochemicals) stack recuperator (steel, non-ferrous metals, glass)
Tubular array – finned	co-, counter- or cross- flow	Liquid or vapour (e.g. water/steam)	Low pressure liquid or gas	air heater, (most industries), process heater (oil & chemicals)
Shell and tube – 1 pass	co- or counter- flow	Liquid or vapour (e.g. water/steam)	Medium/high pressure liquid or gas	Multiple applications (petrochemicals, pharmaceuticals, food processing)
Shell and tube – 2 pass	co- and counter- flow	Liquid or vapour (e.g. water/steam)	Medium/high pressure liquid or gas	Multiple applications (petrochemicals, pharmaceuticals)
Plate and frame	Cross- or multi pass- flow	High pressure liquid	High pressure liquid	Multiple applications (petrochemicals, pharmaceuticals, food processing)
Cooler / condenser	counter-flow	Liquid	Gas	cooing tower (steam plant)
Stack recuperator	Counter-flow	Gas (flue gases)	Gas (air)	Steel re-heating furnace, process heater
Packed bed	cross- flow	Solid	Liquid or gas	Sinter bed (steel), grate cooler (minerals)
Fluid bed	co- or cross-flow	Solid	Liquid or gas	Fluo-cooler (alumina, titanium dioxide), AFBC (incineration)
Cascaded bed	cross- flow	Solid	Liquid or gas	Rotary cooler (metals & minerals)
Suspended bed	co- flow	Solid	Liquid or gas	Preheating cyclone vessel (cement), flash heater/cooler (alumina)

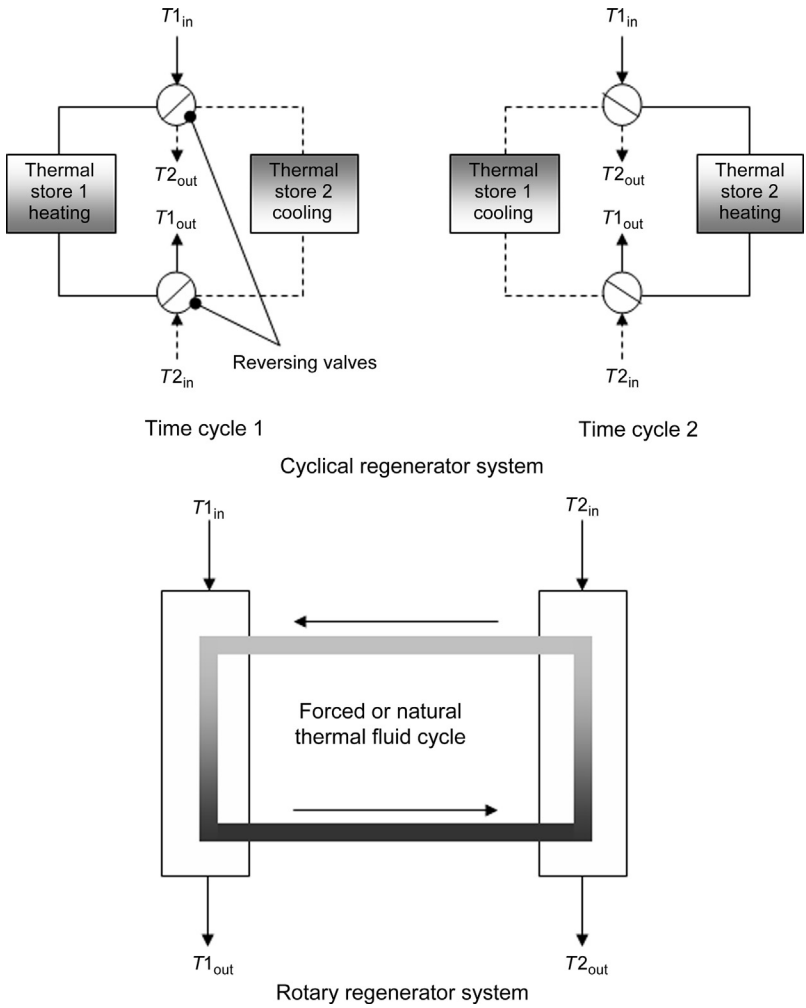


Figure 9.11 Types of flow path configurations through regenerative heat exchangers

design is then considered, in the light of existing design knowledge, and a second design approximation carried out to improve the first estimate. Thus by a series of iterations, the optimum design is fixed. This is a relatively easy, but tedious design procedure.

More rigorous design procedures can be developed, using basic heat transfer and pressure drop equations as functions of tube length, diameter, fluid properties and flowrate. A generalised calculation procedure, yielding simultaneous equations for heat transfer and pressure drop can then be solved analytically, graphically or by computation. This design option requires a significant development investment of

Table 9.11 Common types of regenerative heat exchangers used in furnace operations

Description	*Modes*	*Primary fluid*	*Secondary fluid*	*Common applications*
Brick checker-work	cyclic	Gas (flue gases)	Gas (air)	Open hearth furnace for ferrous and non ferrous smelting, glass tank
Pebble bed	cyclic	Liquid or gas	Liquid or gas	Integral preheat, and flamless combustion burners
Thermal wheel or rotary regenrator	rotating	Gas (flue gases)	Gas (air)	Water tube boiler, glass tank, gas turbine air heater
Heat pipe	Closed loop	Liquid, vapour or gas	Liquid, vapour or gas	Multiple small scale applications (pharmaceuticals, food processing)

manpower to ensure the stability and reliability of the procedure over the design range.

9.5 Identifying Efficiency Improvements

Some of the potential efficiency improvements that can be achieved by good design and operating practices have already been demonstrated in this chapter. Amongst the most common are

- Minimising air in-leakage
- Operating the burners at low excess air to maximise heat transfer
- Recover heat from the products and flue gases

In order to appreciate the potential operating advantages of heat recovery, we will re-examine the process used in example 9.1. This indicates that there are two possible process modifications that could be implemented to utilise waste heat. The simplest modification is to use some of the hot air from the product cooler as preheated combustion air, as shown in Figure 9.12. Using a well-stirred furnace model to study the effect of air preheating on the furnace performance and a simple recuperative heat exchanger equation to simulate the product cooler, a revised heat balance for the system in shown in Table 9.12. Even the small effect of using preheated air at 85°C, rather than ambient air at 32°C reduces the fuel consumption from 40.52MW to 38MW, which is equivalent to a 6.2% fuel saving. The process efficiency is also increased from the original value of 43.34% to 45.93%.

A more radical modification would be to install a convective heating section into the upper part of the furnace to heat the thermal fluid,

replacing the electrical oil heater during normal operation, as shown in Figure 9.13. The required design for the convection section would be equivalent to the 5.02MW of electrical heating duty. Consideration must also be given to the final stack gas temperature to ensure that it is above the acid dew point. For the given example, a lower stack gas temperature limit of 130°C has been used. Using a number of

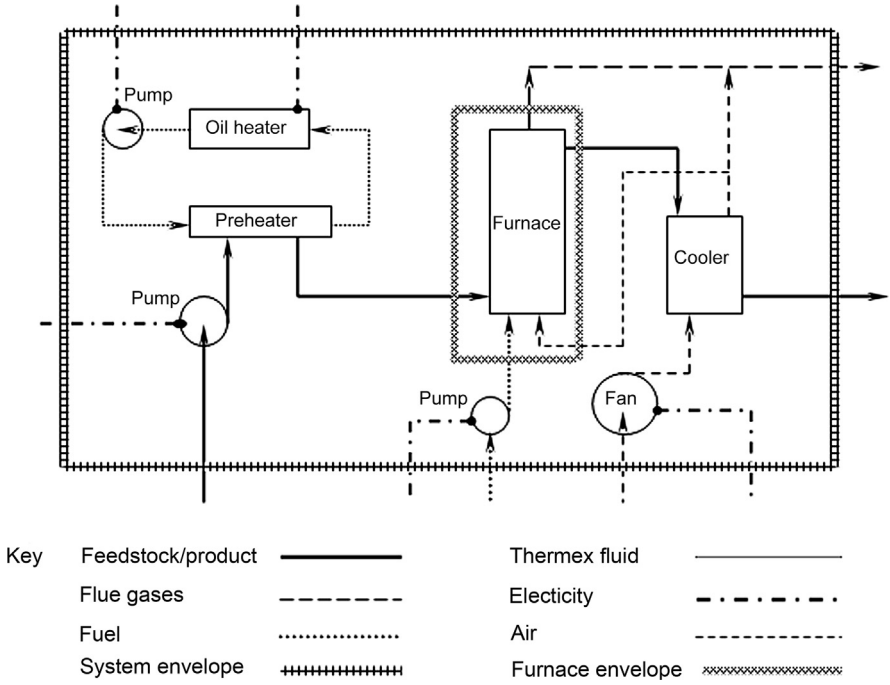


Figure 9.12 Process flowsheet with air preheat option

Table 9.12 Energy balance for the process with combustion air preheating

IN			*OUT*		
Stream	*Energy MW*		*Stream*	*Energy MW*	
Feedstock	0.97	2.13%	Product	1.97	4.30%
Fuel	38.00	83.09%	Product (reaction)	21.01	45.93%
Air	1.16	2.54%	Stack gases (sensible)	13.60	29.72%
Thermex heater power	5.02	10.98%	Stack gases (latent)	3.13	6.84%
Thermex heater pump	0.10	0.22%	Incomplete combustion	0.00	0.01%
Feed pump	0.23	0.50%			
Fuel compressor	0.05	0.12%			
Air fan	0.20	0.43%	Unaccounted	6.04	13.20%
TOTAL	45.74		**TOTAL**	45.74	

iterations, the convective section design is determined, giving a flue gas exit temperature from the furnace after the convection section of 278°C. This requires a small increase in the thermal input to the furnace, relative to the preheated air modification, to provide both the existing process heating duty and the additional thermal fluid heating duty. The resulting analysis is summarised in Table 9.13. This

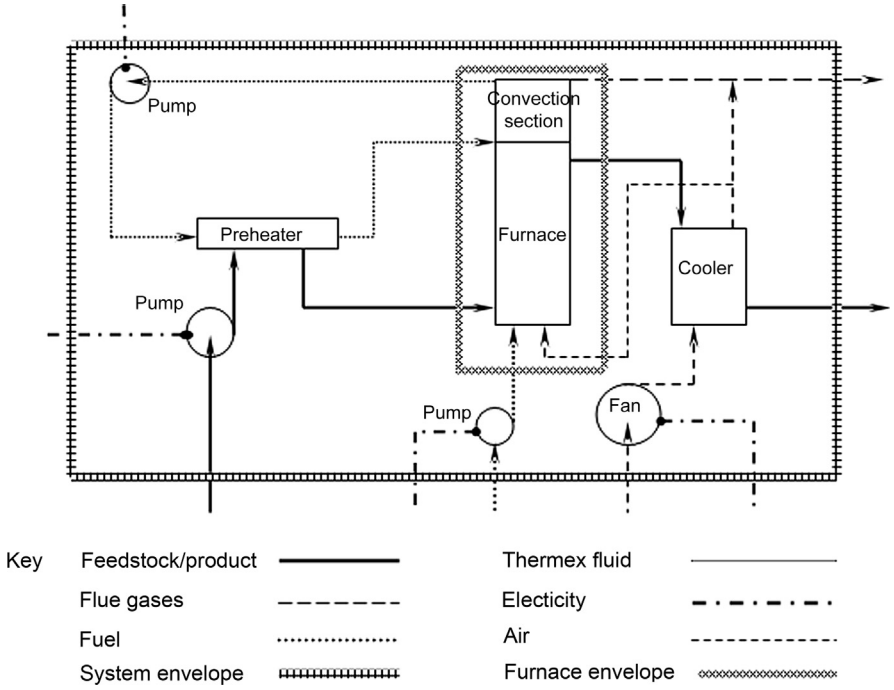


Figure 9.13 Process flowsheet with air preheat and convection section options

Table 9.13 Energy balance for the process with combustion air preheating

IN			*OUT*		
Stream	*Energy MW*		*Stream*	*Energy MW*	
Feedstock	0.97	2.30%	Product	1.97	4.66%
Fuel	39.50	93.57%	Product (reaction)	21.01	49.76%
Air	1.16	2.75%	Stack gases (sensible)	9.60	22.74%
Thermex heater power	0	0%	Stack gases (latent)	3.13	7.42%
Thermex heater pump	0.10	0.23%	Incomplete combustion	0.00	0.01%
Feed pump	0.23	0.54%			
Fuel compressor	0.05	0.32%			
Air fan	0.20	0.47%	Unaccounted	6.54	15.41%
TOTAL	42.22		**TOTAL**	42.22	

shows that the process efficiency is increased from 43.34% to 49.76%. Fuel energy consumption is reduced from 40.52MW to 39.5MW, a 2.5% saving, and electrical energy consumption is reduced from 5.6MW to 0.58MW, an 89.6% saving.

These calculations provide the basis for an economic evaluation of the process modifications to be undertaken. The relatively inexpensive reengineering of the air ductwork to use preheated air, compared to a >5% fuel saving would probably be easily justified. However, the more complex and expensive furnace modifications required to install a convection section would probably be more marginal, when compared to the fuel and electrical energy savings, and would need to be considered more closely.

Nomenclature for Chapter 9

A = area
C_p = specific heat at constant pressure
CV = calorific value
h = convective heat transfer coefficient
H = heat input/output
k = thermal conductivity
Q = flowrate
S = entropy
T = temperature
U = overall convective heat transfer coefficient
x = width

Subscripts

A, B = identifiers
a = ambient
c = charge or sink
f = fuel
g = flue gas
i = inside
lm = logarithmic mean
o = outside
r = reaction
s = structure

Greek Letters

Δ = temperature difference
ε = emissivity

η = thermal efficiency
σ = Stefan-Boltzmann constant

References

Hougen, O. A., Watson, K. M., & Ragatz, R. A. (1966). *Chemical Process Principles, Part 1- Material and Energy Balances* (2nd ed.), Chapter 7, pp. 196, New York: Wiley International.

Linnhoff, B., Manson, D., & Wardle, I. (1979). Understanding heat exchanger networks. *Computers and Chemical Engineering*, (3), 259–302.

Peters, M. S., Timmerhaus, K. D., & West, R. E. (2003). *Plant Design and Economics for Chemical Engineers* (5th ed.). New York: McGraw Hill.

Sunavala, P. D. (Nov 1982). Energy proficiency. *Jnl. Inst. Energy, 55*, 153–159.

Thring, M. W. (1973). *Man, Machines and Tomorrow* (pp. 87). London: Routledge & Kegan Paul.

Chapter 10

Emissions and Environmental Impact

Chapter contents

10.1	Formation of Carbon Monoxide	379
10.2	Formation of Nitrogen Oxides	380
10.3	Formation of Sulphur Oxides	386
10.4	Formation of Intermediate Combustion Products	387
10.5	Particulate Emissions	391
10.6	Environmental Control of Emissions	398
References		411

The latter part of the twentieth century has seen increasing scrutiny and regulation with respect to the environmental impact of industrial operations. However, the history of pollution legislation has been very much led by an 'only what we can see, feel or smell' philosophy. The industrial revolution in Western Europe resulted in severe atmospheric pollution, most visibly from particulate emissions, and very obvious physiological effects from poisoning by lead, arsenic, mercury and phosphorous laden dusts resulted in legislation to the Factories Acts in the UK as early as 1878. Fogs, resulting in unacceptable levels of mortality, caused by particulate emissions from coal fires culminated in Clean Air Acts in the 1950's in most industrialised societies. The harmful gases we cannot see were added to the lists of pollutants in the 1960's, only when we were able to see their effects. Thus nitrogen dioxide only became apparent as a significant pollutant when smog in large conurbations replicated the respiratory problems of fog, or when the combined effects of sulphur and nitrogen oxides created sterile areas of land and water and eroded the exterior of buildings, through the action of acid rain. Forensic medicine has long provided us with comprehensive information on materials that are harmful or fatal, and defined with a high degree of reliability the concentrations of such materials that can be tolerated. Our increasingly sophisticated ability to detect and measure very small quantities of chemicals through the advancement of instrument technology means that we can now 'see' almost everything on a chart, dial or electronic display. This has also enabled us to increase the legislated, or proscribed, range of pollutants. The latest manifestation of pollution is that of climate change, brought about to a greater or lesser degree by human activity contributing to an increase of radiatively absorbent gases in the atmosphere, principle amongst these being methane and carbon dioxide. Legislation for the emission of these gases has taken a different course, being driven by increasing fiscal penalties related to the amount of gases released, rather than the traditional proscriptive approach. Not all pollution comes from the combustion of fossil fuels, but it must be considered as the primary source of nitrogen oxides, sulphur oxides, and carbon oxides from human activity.

Most fuels consist of carbon and hydrogen with small quantities of sulphur, chlorine, phosphorous and nitrogen etc., together with traces of metals. We have seen in chapter 2 that whilst these elements combine in complex organic compounds, for our purpose the principal pollutant chemistry can be reduced to a few simple equations

$$C + O_2 \rightarrow CO_2$$

$$CO_2 + C \rightarrow 2CO$$

$$2C + O_2 \rightarrow 2CO$$

$$N_2 + O_2 \rightarrow 2NO$$
$$2NO + O_2 \rightarrow 2NO_2$$
$$Cl_2 + H_2 \rightarrow 2HCL$$
$$S + O_2 \rightarrow SO_2$$
$$2H_2S + 3O_2 \rightarrow 2H_2O + 2SO_2$$

With the exception of water vapour, all of the compounds on the right hand side of the equations are designated pollutants. Most of these reactions are reversible and depend on the concentration of the species and the temperature for their equilibrium state. High temperature and/or the presence of oxygen drive most of these reactions to the right. In addition to the above reactions, there are some compounds, formed during intermediate reactions, which may persist in the flue gases under certain combustion conditions. Typical of these are volatile organic compounds (VOC's), dioxins and furans. A further source of emissions comes from the mineral matter contained primarily in solid fuels but also in heavy fuel oil fractions and some waste liquids. These minerals are usually converted to metallic oxides and emitted with the flue gases as fly ash, or deposited in the furnace as residual ash.

Carbon, nitrogen and sulphur each have more than one oxide but the two oxides of carbon have a special importance, since the concentration of CO present in the final flue gas is a very good indicator of combustion performance, whilst CO_2 has been identified as a primary cause of global warming. The oxides of nitrogen are precursors in the formation of atmospheric smog and together with the oxides of sulphur give rise to acid rain.

10.1 Formation of Carbon Monoxide

Carbon monoxide (CO) is highly toxic and is the result of incomplete combustion. There is always some residual CO in furnace flue gases because mixing processes are not perfect and the reaction between CO and oxygen to produce CO_2 is reversible. CO is usually formed as the first step in the oxidation of carbon char, and as one of the primary products of fuel pyrolysis during rapid heating of solid and liquid fuels. It is normally subsequently oxidised to CO_2 in a gaseous reaction with atmospheric oxygen. The primary oxidation reaction is

$$CO + OH \leftrightarrow CO_2 + H$$

The reaction rate for the oxidation of CO by O_2 is slow, particularly in 'dry' conditions since water vapour catalyses the oxidation reaction. This can result in residual CO in well-mixed flames if the end of the

flame is rapidly quenched. In good combustion systems, CO should be limited to a few parts/million (ppm), normally in the range of 20–50 ppm. Slightly higher levels may be tolerated in specific circumstances, but levels of 1,000 ppm or more usually result from poor fuel/air mixing or air starvation (high fuel/air ratio) and are the symptoms of serious problems within the combustion processes.

Unfortunately, CO tends to increase when NO_x reduction techniques are applied, since these generally achieve their objectives by delays in fuel/air mixing discussed later in section 10.6.1.2.

10.2 Formation of Nitrogen Oxides

Nitrogen oxides formed during the combustion process are designated as NO_x emissions. Nitric oxide, NO, is initially formed, and most of this is subsequently further oxidised to nitrogen dioxide, NO_2, on contact with further oxygen, either within the furnace or after discharging in the flue gases into the atmosphere. The resulting mixture of oxides is normally reported as NO_x, which is the sum of the NO_2 and the NO as if oxidised to NO_2. The formation of nitrogen oxides in flames is generally controlled by three routes, referred to as thermal, fuel and prompt NO_x.

- Thermal NO_x - formed from atmospheric nitrogen and oxygen and is a function of combustion temperature
- Fuel NO_x - formed from nitrogen in the fuel and is a function of fuel composition
- Prompt NO_x - formed from atmospheric nitrogen and fuel and is a function of mixture stoichiometry

Owing to the very high temperatures that occur in most fossil fuel flames, i.e., above 2000°C, thermal NO_x is generally the dominant mechanism. In gas fired plant, fuel NO_x is absent so all the NO_x comes from the thermal route. However, it should be noted that the absence of fuel NO_x in gas fired plant does not necessarily imply that gas fuels will have lower NO_x emissions, since their flame temperatures are often higher.

Thermal NO_x is formed by the combination of atmospheric nitrogen and oxygen at very high temperatures. The reactions only occur at high temperatures because of the high activation energy of the reaction and it is therefore highly temperature dependent. The reaction takes place between oxygen radicals, nitrogen radicals and molecular nitrogen in what is termed the Zeldovich (1947) reaction couple. Apart from temperature, the in-flame oxygen concentration and the residence time in the high temperature zones influence the final thermal NO_x emissions.

Most fuels, other than gas, contain nitrogen bound as an organic compound in the structure. When the fuel is burnt this organic nitrogen becomes converted into a range of cyanide and amine species, which are subsequently oxidised to NO_x, depending mainly on the local oxygen availability. This mechanism is only weakly dependent on temperature.

The third mechanism of NO_x formation has been identified that involves the fixation of nitrogen by hydrocarbon compounds in fuel rich areas of the flame. This mechanism is known as prompt NO_x.

10.2.1 Thermal NO_x Formation

The generally acknowledged understanding to the formation of thermal NO_x is based on the theory of two coupled basic Zeldovich reactions.

$$O + N_2 \underset{k_{1b}}{\overset{k_{1f}}{\leftrightarrow}} NO + N \tag{10.1}$$

$$N + O_2 \underset{k_{2b}}{\overset{k_{2f}}{\leftrightarrow}} NO + O \tag{10.2}$$

If we assume that the reactions are first order and that the concentration of [N] is steady (i.e. $\partial[N]/\partial t = 0$), then a general rate equation for [NO] can be written in the form

$$\frac{\partial[NO]}{\partial t} = 2[O]\frac{k_{1f}[N_2] - \left(k_{1b}k_{2b}[NO]^2/k_{2f}[O_2]\right)}{1 + \left(k_{1b}[NO]/k_{2f}[O_2]\right)} \tag{10.3}$$

If $K_{p,NO}$ is the equilibrium constant for the reaction

$$\tfrac{1}{2}N_2 + \tfrac{1}{2}O_2 \rightarrow NO$$

where

$$\left(K_{p,NO}\right)^2 = \frac{[NO]^2}{[N_2][O_2]} = \frac{k_{1f}k_{2f}}{k_{1b}k_{2b}} \tag{10.4}$$

then equation (10.3) becomes

$$\frac{\partial[NO]}{\partial t} = \frac{2k_{1f}[O][N_2]\left(1 - \left\{[NO]^2/\{K_{p,NO}\}^2[N_2][O_2]\right\}\right)}{1 + \left(k_{1b}[NO]/k_{2f}[O_2]\right)} \tag{10.5}$$

This is the standard form of the reaction equation for thermal NO formation from atmospheric nitrogen in combustion processes. k_{1f} is strongly dependent on the local temperature. The molecular

concentrations of nitrogen and oxygen, $[N_2]$ and $[O_2]$, are traditionally set to the equilibrium conditions at the prevailing temperature. However, in coal flames the temperatures are probably too low for this equilibrium assumption to be valid for $[N_2]$ and it is virtually impossible to measure the radical oxygen concentration, [O], using currently available techniques. [O] is normally derived to be the equilibrium concentration of the reaction

$$\tfrac{1}{2}\,O_2 \;\rightarrow\; O$$

defined by

$$[O] = \frac{K_{p,O}[O_2]^{0.5}}{(RT)^{0.5}} \tag{10.6}$$

Thus equation (10.5) becomes

$$\frac{\partial[NO]}{\partial t} = \frac{2k_{1f}K_{p,O}[O_2]^{0.5}[N_2]\left(1 - \left\{[NO]^2/\{K_{p,NO}\}^2[N_2][O_2]\right\}\right)}{(RT)^{0.5}\left(1 + \left(k_{1b}[NO]/k_{2f}[O_2]\right)\right)} \tag{10.7}$$

In a more detailed analysis, where in most turbulent diffusion flames some local flame conditions may be sub-stoichiometric, the following reaction becomes important

$$N + OH \;\rightarrow\; NO + H$$

Leading to the inclusion of an [OH] forward reaction component into equation (10.7).

$$\frac{\partial[NO]}{\partial t} = \frac{2k_{1f}K_{p,O}[O_2]^{0.5}[N_2]\left(1 - \left\{[NO]^2/\{K_{p,NO}\}^2[N_2][O_2]\right\}\right)}{(RT)^{0.5}\left(1 + \left(k_{1b}[NO]/(k_{2f}[O_2] + k_{3f}[OH])\right)\right)} \tag{10.8}$$

Table 10.1. gives some values of the rate constants proposed by Bowman (1975) and Westenberg (1971) that can be used in equation (10.8).

The above is a limited and simplified approach to the theory of thermal NO_x formation and is included to allow an appreciation of the complexity of the theory and the difficulty of making theoretical predictions of thermal NO_x emissions.

10.2.2 Fuel NO_x Formation

As has been discussed in chapter 2, heavy liquid and solid fossil fuels generally contain bound nitrogen within their chemical composition.

Table 10.1 Rate Constants for Thermal NO_x Equations

Reaction rate Constant	*Value*	*Units*	*Temperature Range K*	*Ref.*
k_{1f}	$7.6 \times 10^7 \exp(-38000/T)$	$m^3/mol \cdot s$	2000 – 5000	[1]
k_{1b}	1.6×10^7	$m^3/mol \cdot s$	300 – 5000	[1]
k_{2f}	$6.4 \times 10^3\ T \exp(-3150/T)$	$m^3/mol \cdot s$	300 – 3000	[1]
k_{1b}	$1.5 \times 10^3\ T \exp(-19500/T)$	$m^3/mol \cdot s$	1000 – 3000	[1]
k_{3f}	3.3×10^7	$m^3/mol \cdot s$	300 – 2500	[1]
$K_{p,O}$	$3.6 \times 10^3 \exp(-31090/T)$	$atm^{0.5}$		[2]
$K_{p,NO}$	$20.27 \times \exp(-21650/T)$			[1]

[1] Bowman [1975], [2] Westenberg [1971]

The mechanisms by which NO_x is formed from the chemically bound nitrogen in solid and liquid fuels is extremely complex. Even the structure in which the nitrogen is bound in the fuel is subject to considerable conjecture and is strongly dependent on the individual fuel. The nitrogen is believed to be commonly in the form of pyridine, pyrrol and amine type structures, as shown in Figure 10.1. The pyrrolic and pyridine forms are dominant in most coals and the amount of the former tends to decrease with increasing coal rank, whilst approximately half the nitrogen found in crude oils is in predominantly pyrrolic with some amine forms, the balance being as basic nitrogen. However, at present, the importance of the structure of the nitrogen in the coal and oil on the final NO_x emissions is not well established.

When solid and liquid fuels are burnt in suspension they are heated very rapidly to high temperatures and pyrolysis occurs, producing solid and gaseous products. The nitrogen present will divide between the solid and liquid with typically 20% of the nitrogen in the char and 80% in the gaseous phase, the latter both as the light fractions and tars. For any given fuel, the distribution of nitrogen between the gaseous phase and char is heavily dependent on the conditions in

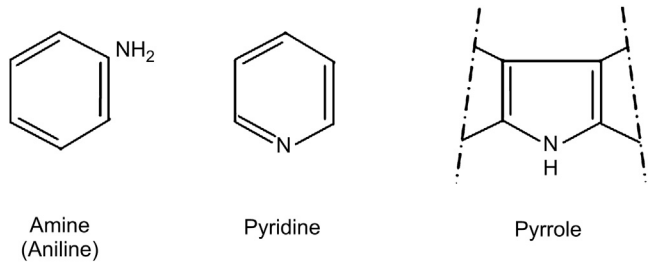


Figure 10.1 The structures in which nitrogen is commonly bound in heavy oil and coal fuels.

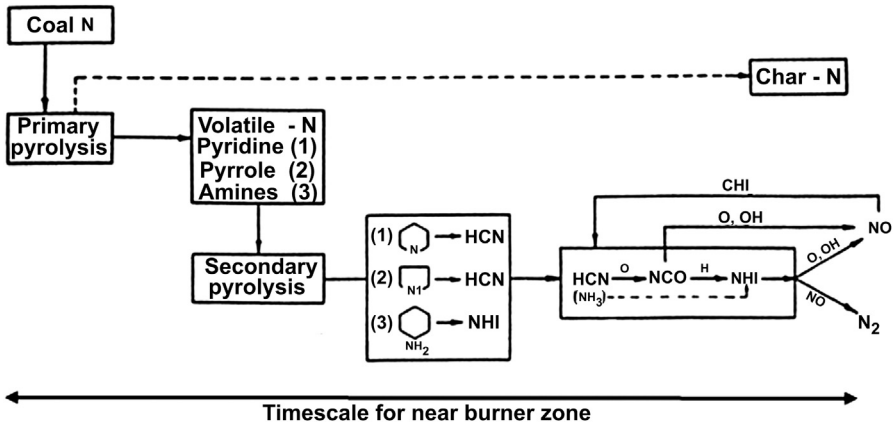


Figure 10.2 A simplified schematic representation of the paths of NO_x formation

the flame such as heating rate, peak temperature, and residence time at high temperature, Niska & Kerstein (1987), Freihaut, Proscia & Seery (1987), and Okazaki et. al. (1984).

A simplified NO_x formation path is shown in Figure 10.2. Most of the gaseous nitrogen pyrolyses either directly or indirectly to HCN. This complex process is not instantaneous but dependent on the conditions in the flame. The HCN then oxidises to NO, Figure 10.3, with this reaction being both temperature and time dependent, as can be seen in Figure 10.4.

10.2.3 Prompt NO_x Formation

In low temperature, fuel rich flame zones, NO is found to form more rapidly than predicted from considerations of the thermal NO

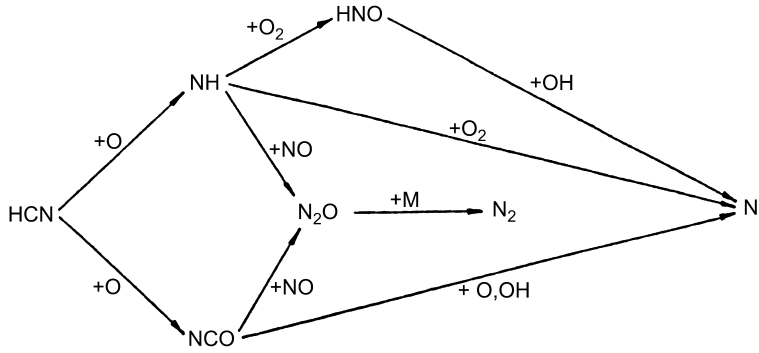


Figure 10.3 A schematic representation of the role of HCN in the NO_x formation process

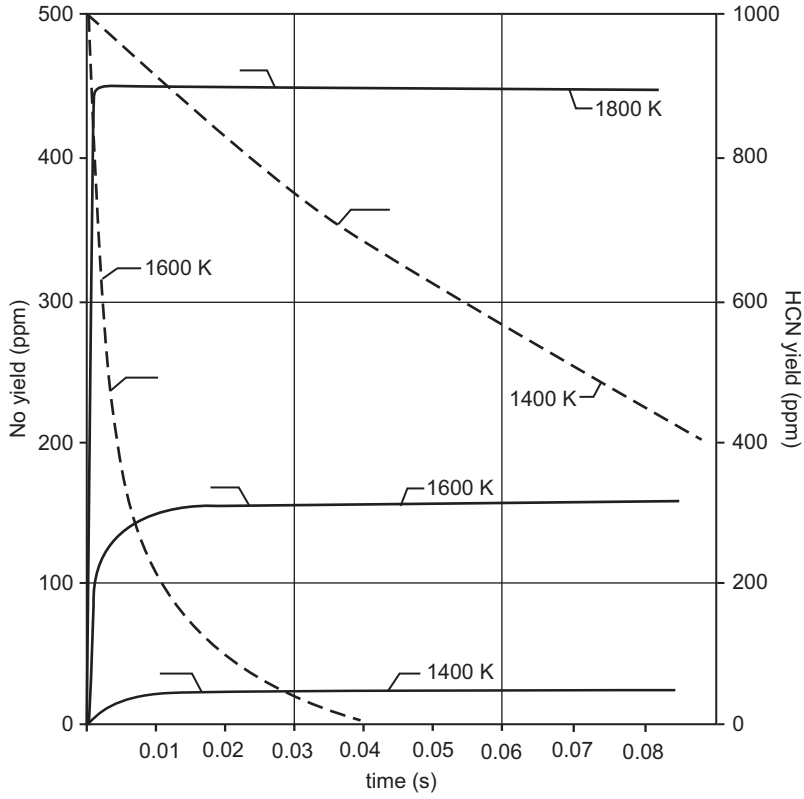


Figure 10.4 The temperature dependence of the NO_x formation process

mechanism alone. The difference is due to the so called 'Prompt NO' formation mechanism. Prompt NO is formed by the rapid fixation of atmospheric nitrogen by gaseous hydrocarbon fragments. Reactions of the following form are involved.

$$CH + N_2 \leftrightarrow HCN + N$$
$$C + N_2 \leftrightarrow CN + N$$

NO is subsequently formed from the oxidation of the nitrogen atom:

$$N + O_2 \leftrightarrow NO + O$$
$$N + OH \leftrightarrow NO + H$$

HCN and CN also react to form NO by reactions important in the fuel nitrogen conversion mechanism discussed in section 10.1.2. Prompt NO is formed in all combustion system but its contribution to the total NO_x emission is combustion system and fuel dependent. Estimates of the contribution to total NO_x emissions from the prompt route for a range of processes is given in Table 10.2

Table 10.2 Occurrence of Prompt NO_x for Some Combustion Processes

Device	*Fuel*	*Percent NO_x Due to Prompt Mechanism*
Utility Boiler	Natural gas	17
Gas Turbine	Natural gas	30
Utility Boiler	Coal (1%N)	<5

10.2.4 NO_x Modelling

The above descriptions of NO_x formation via the thermal, prompt and fuel NO_x routes are only a précis of processes, which are extremely complex and not yet well understood. It therefore follows that modelling these processes is very difficult. Some of the currently available models are capable of predicting the trends of NO_x formation with changes in flame conditions and fuel type, but the reliability of predictions is poor and sometimes little better than orders of magnitude. Computational NO_x models are usually included in commercial CFD modelling packages as a post processor option. These models use the final converged data calculated for the main species concentrations, temperatures etc. in a subsequent sub-routine, using chemical reaction mechanisms such as those outlined in the preceding sections. Currently, the most reliable methods of estimating NO_x emissions from full-scale flames is by scale-up from test flame data using either empirical correlations, or validated NO_x models, but even this has its limitations, particularly in multiple burner furnaces.

10.3 Formation of Sulphur Oxides

Sulphur compounds are emitted where sulphur-bearing fuel (oil, coal etc.) is burnt or where sulphur-bearing materials are processed. The reaction kinetics are such that it is generally the case that all sulphur is oxidised, except under severe reducing conditions when H_2S is formed. Since most furnaces operate most efficiently at reasonably low excess air levels sulphur dioxide, SO_2, is the primary oxide of sulphur found in the flue gases. It is acidic and corrosive, and causes major problems with metal and refractory corrosion in cooler areas of the plant and in the surrounding environment (viz. limestone building erosion). Where conditions in the furnace are favourable (viz. high oxygen concentrations and moderate temperature) sulphur trioxide, SO_3, can be formed. There is also evidence that the presence of heavy metal catalysts such as vanadium, which is present in heavy fuel oils, will increase the conversion of SO_2 to SO_3, Lightman & Street (1981). SO_3 is even more corrosive than SO_2 and leads to sulphuric acid

Table 10.3 Chemical Pathways to the Formation of Acid Mist (James 1984)

Reaction Type	*Reaction*	*Catalyst / Special Sonditions*
Indirect photo-oxidation	$SO_2 \xrightarrow{\text{Free radicals}} H_2SO_4$	smog, sunlight, water vapour, HO, HO_2, CH_3O_2 radicals
Heterogeneous catalytic oxidation	$SO_2 \xrightarrow{O_2} SO_4^{=}$	liquid water, metal ions
Heterogeneous oxidation by strong oxidants	$SO_2 \xrightarrow{O_3H_2O_2} SO_4^{=}$	water droplets
Heterogeneous oxidation in the presence of ammonia	$SO_2 \xrightarrow{H_2O} H_2SO_4 + NH_3 \rightarrow NH_4^{+} + SO_4^{=}$	water droplets
Surface catalysed reactions	$SO_2 \rightarrow SO_4^{=}$	soot

formation with the water from combustion, at the so-called acid dew point. This gives rise to severe corrosion in flue gas ducting, air heaters and economisers of oil fired boilers and, with unburnt carbon, causes acid smuts, James (1984). A significant amount of the SO_2 discharged to atmosphere in the flue gas is further oxidised to SO_3 on mixing with air, and then combines with water vapour to create a persistent visible plume (i.e. acid mist). A number of possible chemical mechanisms exist for this oxidation process, as shown in Table 10.3.

Hydrogen sulphide (H_2S) is extremely toxic and has a nauseating smell, even with concentrations as low as 2–3vppm. It is formed by reducing conditions in the flames of sulphur bearing fuels, or is driven off at low temperatures from sulphur-bearing feedstocks, such as some clays. H_2S is a by-product in the paper pulping process and is combusted in special incinerators or in the lime recovery kiln.

10.4 Formation of Intermediate Combustion Products

All the compounds under this heading could be termed the products of incomplete combustion or PICs, although not all of them arise in flue gas emissions as a direct result of the inefficient combustion of fuel in the furnace.

10.4.1 Volatile Organic Compounds (VOCs)

These are compounds containing hydrogen, carbon and oxygen. VOC emissions arise primarily from internal combustion engines, and have been identified as a significant pollutant, as they contribute to the formation of low level ozone, a respiratory irritant, and for their generally offensive smell. Various, generally expensive, techniques are available for controlling VOC emissions such as incineration, condensation, absorption, or catalytic combustion.

They do not normally result from the combustion process in furnace operations but are driven off from the raw feed in plants where feedstock materials, including solid fuels, containing organics are being processed. They are emitted to atmosphere in processes such as drying, milling or preheating, where the temperature is too low for them to burn.

10.4.2 Polycyclic Aromatic Hydrocarbons (PAH)

The simplest compound in this category is naphthalene, which contains two benzene rings. Naphthalene can occur in the combustion products of some petroleum-derived fuels. Other examples of PAH occurring in combustion processes include anthracene and phenanthrene (three rings), pyrene (four rings), etc. Most of the PAHs are known to have serious effects on health so attention has to be given to their formation even in trace amounts. One of the earliest reported identifications of a substance believed to cause cancer was soot, in 1775, and it is now known that PAH deposited on soot is largely responsible for the carcinogenic activity.

Petroleum-based fuels contain PAH compounds, so one source of PAH is unburnt fuel. Another is what is sometimes possibly erroneously referred to as fuel pyrolysis, but which would perhaps better be termed PAH synthesis. For example, acetylene, when heated to 973 K under conditions precluding combustion, produces pyrene at a yield of 6.5% as well as smaller quantities of other PAH including chrysene. Toluene, butadiene and styrene also yield significant amounts of PAH when heated in this way. More surprisingly, polycyclic organic matter has been found in the effluent from boilers burning natural gas.

Current experimentation has not determined whether such pollutants arise from, for example, the hydrogenation of soot (which has a complex, six-member ring structure) or from trace hydrocarbons in the fuel. PAH can also be formed in the pyrolysis stages of coal during combustion.

10.4.3 PCBs, Dioxins and Furans

Another class of PIC pollutants includes the carbon-hydrogen-oxygen-halogen compounds such as polychlorinated biphenyls (PCBs), dioxins (polychlorinated dibenzene-para-dioxins – PCDD's) and furans (polychlorinated dibenzofurans – PCDF's). PCB's comprise a family of 209 organic compounds based on two partially chlorinated benzene rings linked by a single bond, Erickson (1985), whilst dioxins and furans are oxygenated organic ring compounds containing chlorine, as shown in Figure 10.5.

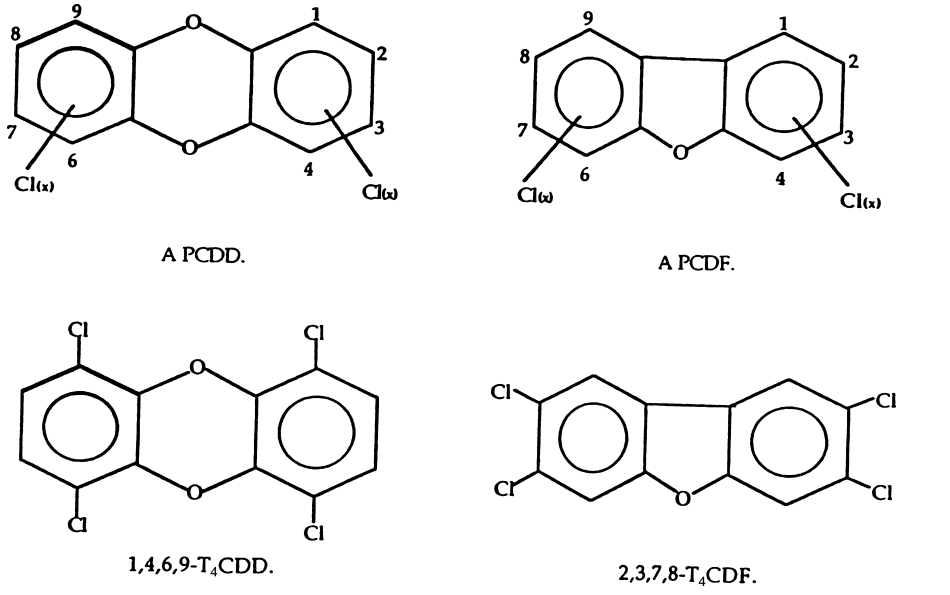


Figure 10.5 The structure of Dioxins

These pollutants have been shown to be extremely toxic to some laboratory animals, but their effect on humans is not fully understood. Human exposure is generally from the soil via the food chain, especially via eggs and meat. They are of particular importance as a pollutant, owing to their chemical and physical stability. They do not readily degrade in the environment and have a tendency to bioaccumulate. They have been identified as occurring in most human and animal tissue, although their toxicity is highly dependent on both the degree of chlorination and isomeric arrangement. From some 419 identified types of dioxin related compounds, only 29 are currently considered to have significant toxicity, with 2,3,7,8-T_4CDD being the most toxic. Table 10.4 gives current World Health Organisation guidelines for toxic equivalence factors. The toxic equivalence factor is an assign value, describing how toxic each dioxin and dioxin-like compound is compared to the most toxic members of the category: 2,3,7,8-T_4CDD and 1,2,3,7,8-PnCDD. To account for how emissions vary in toxicity, we use a weighted value called the toxic equivalent (TEQ).

Dioxins and furans can form in any combustion process where chlorine and fluorine are present. PCB's are normally found in waste incineration and coal combustion processes. However, the mechanisms of their formation are not well understood, owing to the enormous difficulties encountered in sampling and analysing these compounds. As with PAHs, synthesis rather than pyrolysis is more

Table 10.4 World Health Organisation Total Equivalence Factors for Human Risk Assessment of PBCs, Dioxins and Furans.

Congener	*TEF Value*	*Congener*	*TEF Value*
Dibenzo-p-dioxins		*Non-ortho PCB's*	
2,3,7,8-TCDD	1	PCB 77	0.0001
1,2,3,7,8-PnCDD	1	PCB 81	0.0001
1.2.3.4.7.8-HxCDD	0.1	PCB 126	0.1
1,2,3,6,7,8-HxCDD	0.1	PCB 169	0.01
1.2.3.4.6.7.8-HpCDD	0.01	*Mono-ortho PCB's*	
OCDD	0.0001	PCB 105	0.0001
Dibenzofurans		PCB 114	0.0005
2,3,7,8-TCDF	0.1	PCB 118	0.0001
1.2.3.7.8-PnCDF	0.05	PCB 123	0.0001
2,3,4,7,8-PnCDF	0.6	PCB 156	0.0005
1,2,3,4,7,8-HxCDF	0.1	PCB 157	0.0005
1,2,3,6,7,8-HxCDF	0.1	PCB 167	0.00001
1,2,3,7,8,9-HxCDF	0.1	PCB 189	0.0001
2,3,4,6,7,8-HxCDF	0.1		
1,2,3,4,6,7,8-HpCDF	0.01		
1,2,3,4,7,8,9-HpCDF	0.01		
OCDF	0.0001		

likely to be the route of the formation of these pollutants in the combustion process. Of the various mechanisms proposed, four of the more likely are,

- Pre-existing PCB's, dioxins and furans that have been generated from other sources and deposited from the atmosphere onto the fuel and/or feedstock being volatilised at low temperature and released into the flue gases;
- Gas phase formation from chloro-phenol groups inherent in the fuel in the temperature range 500–700°C;
- Reaction of benzene type ring structure in the fuel (e.g. lignin) with chlorine in the temperature range 500–700°C;
- Heterogeneous catalytic formation promoted by heavy metals present in the fly ash in the temperature range 150–400°C (often termed 'de-novo' synthesis).

De-novo synthesis is considered to be the most important as the temperature window corresponds to that used by most high efficiency flue gas cleaning equipment e.g. electrostatic precipitators, bag filters. Flow bypassing, quenching (by contact with cool surfaces or admixture with cold gases) of the flue gases in the 800–400 °C temperature window may also contribute to the formation of PCBs, dioxins and furans by one or more of the above mechanisms. The residence time in the

Table 10.5 Estimated Dioxin and Furan Emissions in the UK, (Harrad 1993)

Source	*Estimated Annual Emissions.*
Municipal Waste Incinerators	10.9 kg
Chemical Waste Incinerators	Minimal - "a few grams of TCDDs". (DoE,1989).(See text)
Clinical Waste Incinerators	1.7 kg
Domestic Coal Combustion	5.1 kg
Industrial Coal Combustion	7.7 kg
Coal Combustion for Power Generation British Purposes	No precise figures. DoE (1989) estimates emissions to be about 5% of total emissions for all UK combustion sources - 1.3 kg.
Leaded Petrol Combustion	0.7 kg
Volatilisation from Chlorophenol Treated Substrates	1.7 kg
Secondary Releases from Chlorophenol Treated Substrates.	No precise figures. Best estimate is 17 kg.

temperature windows defined above has been shown to have a significant effect, with emissions increasing with increasing residence time.

In the most industrialised societies, the greatest measured sources of dioxins and furans are the combustion of coal and municipal waste incinerators, both of which have significant quantities of metallic ashes, see Table 10.5. In more primitive societies they arise from inefficient combustion of wood, etc in open fires. It should be noted in the table that the estimate for chemical waste incinerators is based on a single survey of one UK chemical waste incinerator, conducted by the incinerator's operators. A study of a similar incinerator in the USA reported PCB emission spikes of between 500 and 2500ng/g of fly ash, although variations of individual measurements by a factor of 3 were also noted in the report, Haile et.al. (1983). Given the interdependence of incinerator emissions and parameters such as feedstock and operational conditions, it is possible that typical emissions from chemical waste incinerators may be higher than those reported in the UK study, Harrad (1993).

10.5 Particulate Emissions

Particulate emissions arise from ash in the fuel (coal and oil), and in the case of direct contact processes also from the feedstock/product. Typical of these contact processes are cement and lime manufacture, alumina calcination, ferrous and non-ferrous metals production and glass manufacture. Combustible particulates, such as soot and sub-micron unburnt carbon, may also be emitted from combustion of gaseous hydrocarbons as the products of incomplete combustion (PICs).

10.5.1 Formation of Soot

Soot may form in all combustion systems but it is especially common in those using diffusion flames. Most furnaces operate using this type of flame as it has the advantages of a large stability range. The time taken for soot to form is in the order of milliseconds. It is formed from fuel in the gaseous phase, burning in the absence of sufficient oxygen to produce heavy hydrocarbons, which in turn condense as liquids, and then become solid as soot.

A great deal of work has been conducted on the formation of soot from hydrocarbon fuels and many mechanisms for soot formation have been proposed. There is general agreement that soot formation involves several steps and all of the theories advanced may be summarised as some combination of the following:

1. an initial stage in which the first particles, solid or liquid are formed
2. coalescent collision of these species to form larger spherical particles
3. surface growth on species formed in stages 1 and/or 2 from the complex gas phase hydrocarbon soup of the flame
4. carbonisation of the spherical particles after which further collisions will result in chain structures
5. surface growth onto the chain structures
6. oxidation

Stage 1 corresponds to nucleation, stages 2 and 3 to the formation of the primary spheres and stages 4 and 5 to the formation of the characteristic soot structure. Stages 2 and 4 are agglomerating processes. Foster (1965) and subsequent workers, Lahaye & Prado (1981) and Tesner et.al. (1971), have explained the spherical nature of the elementary soot particle by considering the initial phase of formation, that of nucleation, to be liquid. In this view it has been speculated that the chemical nature of the liquid droplets are large PAH molecules. Homann (1972) calculated that for typical flame temperatures the mass of these primary molecules would have to be more than 2700 atomic mass units (a.m.u.). It is the nucleation stage of soot formation that is least understood.

Graham, Homer & Rosenfeld (1975) have studied the growth of soot particles early in the flame using light scattering techniques. They have determined that coalescence does occur in the first 1-2 milliseconds after nucleation. Particle nucleation and growth are spatially well separated in a flame. Lahaye & Prado (1981) proposed a reason to explain this, in that once the first particulate phase is formed, enough solid surface is available for surface growth, and the probability of generating new particles is greatly reduced. They described

surface growth as a process involving the deposition and attachment of gas phase molecules to the surface of a particle and their incorporation into the particulate phase. The surface growth mechanism is responsible for the majority of the soot mass.

Haynes et. al. (1981) seeded sooting acetylene flames with various metals, and observed how some of these additives could strongly reduce the final soot size, by reducing coagulation. The presence of metal promotes sufficient charging of the small soot particles that subsequently resist coagulation by repulsion.

Experiments on the oxidation of soot have shown that it is similar to the oxidation of graphite. Field et. al. (1967) have calculated from experimental data that there is a marked degree of chemical control of the combustion process within the normal range of flame temperatures, indicating that the burning time of a 500 Å particle of soot in a 0.05bar atmosphere of oxygen varies as shown in Figure 10.6.

Clarke, Hunter & Garner (1946) studied the effect of fuel type on soot formation. Their findings are shown in Figure 10.7. Once soot has left the hot flame zone and is no longer affected by the processes described above, it may continue to agglomerate by sticking together. This is dramatically illustrated by burning most liquid fuels in a laminar diffusion flame, such as a candle flame. If sooting is promoted by increasing wick length, particles that are millimetres in length can be seen to emerge.

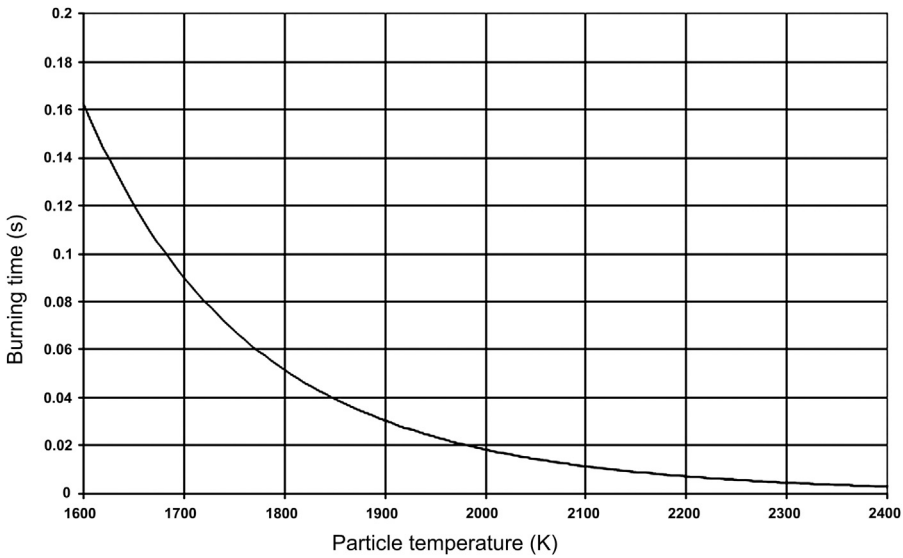


Figure 10.6 Soot burning times for 500 Å particle at an oxygen partial pressure of 0.05 bar

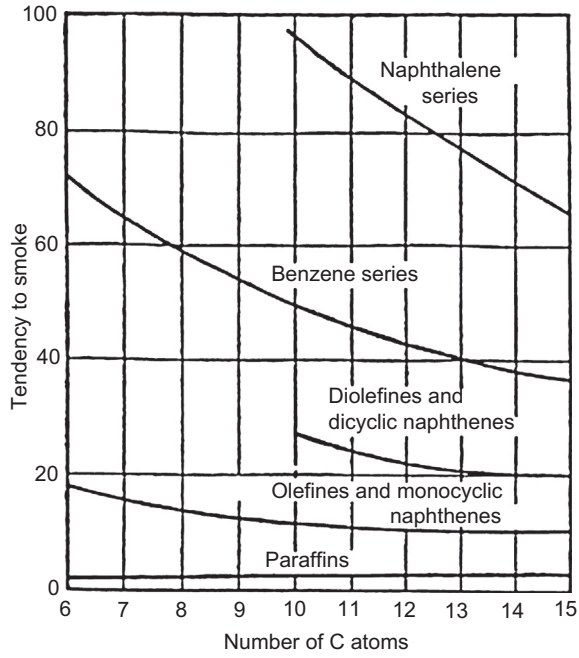


Figure 10.7 Tendency of fuels to smoke in relation to their composition

It is known from studies of premixed flames that the critical amount of oxygen required to suppress soot formation is less than the stoichiometric quantity for complete combustion, but considerably more than is required for carbon to exist in equilibrium. For aromatic hydrocarbons, the stoichiometry lies between 0.75 and 0.8, whilst for aliphatic hydrocarbons with 6 to 16 carbon atoms it is between 0.67 and 0.74. General observations indicate that increasing temperature allows richer mixtures to burn without forming soot, and that reducing pressure also has a similar effect. Figure 10.8 shows a schematic mechanism for soot formation, including the influence of reaction time and temperature, based on experimental observations by Duggal, Preile & Khan (1978).

10.5.2 Formation and Composition of Fuel Ash

Fuel ash is the residual incombustible material remaining after the combustion of char particles. The mineral matter in the original fuel is usually a combination of adventitious or excluded (i.e. discrete mineral particles) and inherent or included (i.e. chemically bonded into the organic fuel structure) material. This mineral matter contains some or all of the following elements, Al, Ba, Ca, Cr, Cu, Fe, Hg, K, Mg, Mn,

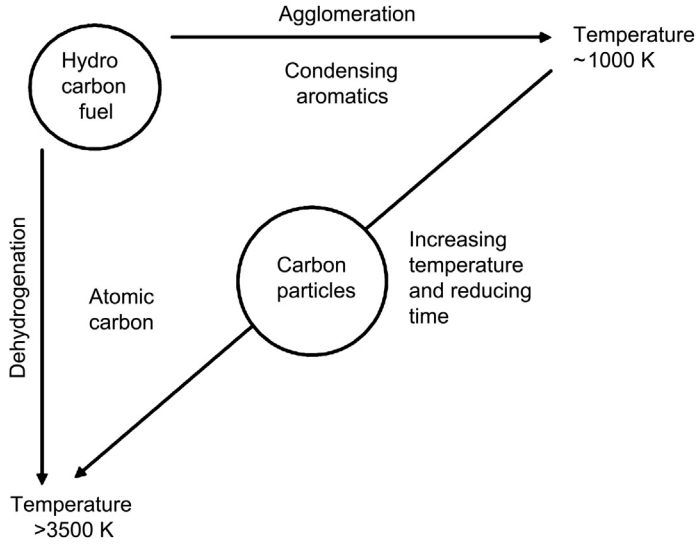


Figure 10.8 Schematic mechanism for soot formation, showing the influence of reaction time and temperature

Na, Ni, S, Si, Sr and Ti as salts, or complex organo-compounds. As char combustion proceeds, the carbon matrix is oxidised and the mineral inclusions melt. As more of the carbon surface is removed, the molten mineral matter agglomerates with other molten ash particles. The resulting melt is primarily an Al-Si-Fe-Ca-O complex. The physical appearance of ash particles is dependent primarily on the specific fuel properties and combustion temperature, and falls into one of three structures.

- solid fused ash particles
- fused cenosphere containing some blowholes
- loose lacy structures

Examples of these three structures are shown in Figure 10.9. The pathways to these ash structures are complex, but a simplified mechanism proposed by Wibberley & Wall (1986) is shown in Figure 10.10. It is apparent from Figure 10.10 that the size range of ash particles is large, varying from 0.02 μm (sub-micron) to 90 μm particles. Flagan (1978) has shown that the distribution is bi-modal, the larger particles being formed by coalescence, fragmentation and shedding of inorganic components, whilst the sub-micron particles are produced by vaporisation and condensation of volatilised species. Fuel ashes also act as absorbents for some of the gaseous species, such as sulphur oxides and chlorine, forming metallic sulphates and

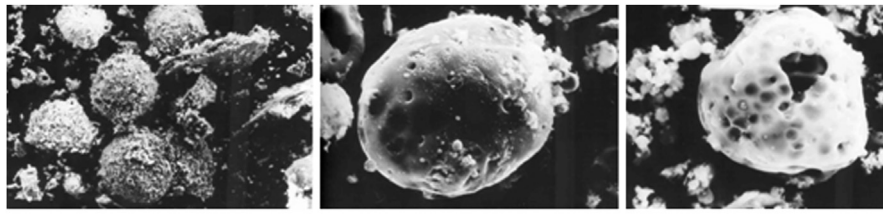


Figure 10.9 Typical ash structures.

chlorides, and as a condensing surface for volatile alkaline metals and mercury. These volatile cycles are discussed in the next section.

10.5.3 Non-combustible Volatile Cycles

Inorganic alkaline metal species, such as sodium and potassium organic acid salts in the fuel are readily vaporised in the flame as hydroxides and chlorides at temperatures above 950°C. The vaporisation route of included minerals in Figure 10.10 represents this process. In the cooler parts of the furnace these alkali metals recondense reacting with mainly sulphur dioxide to form sub-micron sulphate particles (<1100°C) or dissolve into the surface of silicate particles (1200–1600°C), Raask (1985). Evidence of these sulphates can be seen on the surface of the ash particles as small spheres in Figure 10.9. These sulphates will also react with the aluminosilicates in the ash at temperatures above 750°C to form cementaceous compounds, giving rise to the build up of severe hard ash deposits on surfaces in the furnace and downstream equipment and ductwork.

A method of predicting the fouling tendency using the analysis of the ash has been proposed by Winegartner (1974) and is expressed as a Fouling Index.

$$\text{Fouling Index} = \frac{Na_2O + K_2O + Fe_2O_3 + CaO + MgO}{SiO_2 + A1_2O_3 + TiO} \text{ X } \%Na_2O \text{ in ash}$$

With the fouling potential classified by the Index value as

Low	<0.2
Medium	0.2 – 0.5
High	0.5 – 1.0
Severe	>1.0

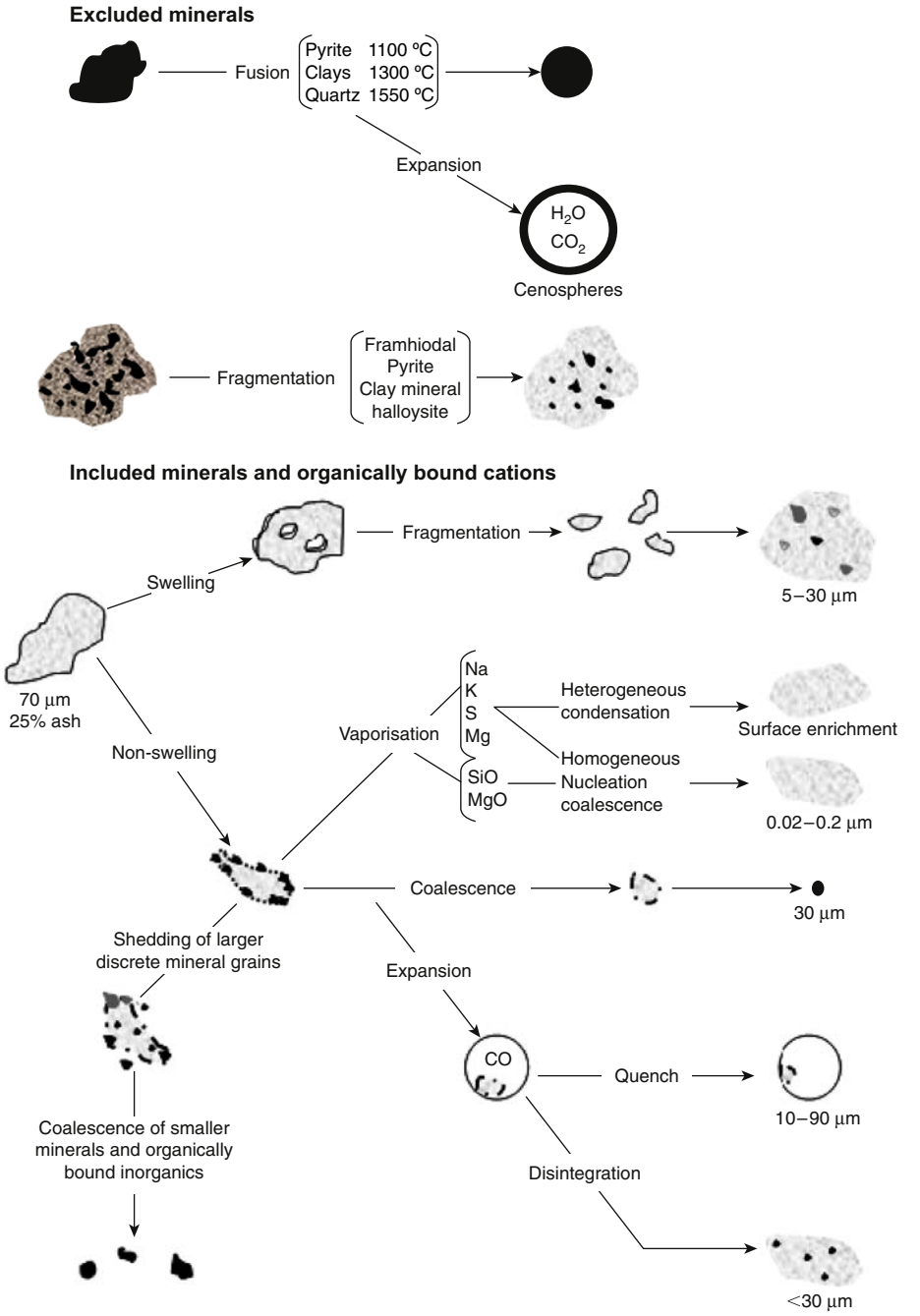


Figure 10.10 Mechanisms for ash formation

This Fouling Index is based on experience of coal firing in boilers. It is therefore important to remember that in direct contact processes, where many of the same basic and alkaline metals may be present in the dust generated from the product, that these should also be accounted for in the assessment of fouling.

10.6 Environmental Control of Emissions

The operation of almost any furnace will be subject to either regulatory or voluntary environmental control by local, national and sometimes international bodies. In many cases, the furnace is considered as part of a wider industrial site operation, the 'bubble' principle, and regulation is based on the emissions at the periphery of the site, rather than on individual unit operations. Whereas, traditionally monitoring of furnace operations were reported regularly to a designated agency with local knowledge to meet local standards, newer controls are based on integrated pollution and prevention legislation covering whole industry sectors, both nationally and internationally. Thus factors such as energy efficiency, noise, raw materials, health and safety, site remediation etc. are covered within the legislation, as well as the monitoring of emissions. The emphasis has moved to providing a high level of protection for the whole environment, based on the concept of best available techniques not entailing excessive cost (BATNEEC). Industrial operators are expected to monitor all inputs to, and releases from the process, provide an environmental impact statement and monitor its effectiveness, calibrate monitoring instruments and validate their accuracy, report all emissions as concentrations and/or mass releases and keep records for external scrutiny. The wider implications of such requirements, together with carbon taxing etc. require acceptance and practice of energy management by the whole organisation, not just a devolved technical responsibility. However the implementation of such management structures is beyond this book, therefore the remainder of this chapter will focus on best available techniques for pollutant reduction and control.

10.6.1 Prevention and Abatement of Emissions

Of the emissions considered in the previous sections, some may be controlled by adjusting equipment design and operation to avoid their formation (viz. pre-flame and in-flame techniques), some may be chemically modified or destroyed within the furnace (viz. reburning, and catalytic reduction) and some may only be captured by treating the flue gases prior to discharge to atmosphere (viz. end–of-pipe treatments). It is important, when considering abatement techniques to take a holistic view, as some of the available technological solutions

may just 'shift' the pollutant problem to another part of the process. Some pollutants, such as sulphur oxides and ash, will be the inevitable result of the burning process, whilst others, such as CO, VOC's, PAH and NO_x, can be minimised or avoided by design and/or operational changes.

The viability of the most suitable emissions control strategy must be considered on a case-by-case basis. However, most furnace operators will chose one of the first two options, since end-of-pipe treatment is usually more expensive, and provides no potential benefits.

Pre-Flame Control

Any process that improves the quality of the fuel, usually termed as beneficiation, will reduce emissions by removing potential pollutants and/or by improving the thermal efficiency. The latter point is important, and improved energy consumption in the process is not always recognised as an effective emissions control strategy within some of the more poorly drafted of the legislative frameworks. However, a cleaner fuel does not always result in higher efficiency owing to changes in flame emissivity etc., as discussed in detail in other chapters of this book.

Pre-flame treatment of the fuel is an effective method of controlling the impact of pollutants such as ash and sulphur, which would otherwise require end of pipe control equipment. It has long been a common practice to wash coals, usually at the pit head, to remove as much of the excluded mineral matter as is commercially practicable. This is a relatively simple technology, relying on the density difference between the heavier mineral matter and the coal to separate the materials. The residual material, or slag, is either returned to the mine, or can be used as raw material in other applications such as the cement making process, brick-making, etc. More advances techniques, such as froth flotation can be used to deep wash the fuel, or even reclaim coal from old slag heaps, but the application will depend on the commercial market value of the coal relative to oil, gas or other energy sources.

There are no commercially viable processes for the removal of sulphur from coal, but desulphurisation of fuel oil is a well-established technology within the normal commercial refinery process, and is required to avoid catalyst poisoning in the cracking and reforming processes. Further desulphurisation processes can produce very low sulphur oils but as with coal ash removal, the market value of the fuel determines the application of the technology.

The removal of other potential sources of pollution, such as fuel bound nitrogen and included minerals by pre-treatment of the fuel is much more difficult, generally involving technologies that modify the fuel composition by chemical or physical processing, principally

by gasification or liquifaction. Such processes are prohibitively expensive even in a rising energy price market, and are only generally viable in unusual circumstances, but the fundamentals for these technologies have been well established and demonstrated, Muir (1977). An example is hydrogenation of coal to produce synthetic gas or oil. The only current commercially operating process of this type is run by SASOL in South Africa, using a pressurised Lurgi gasifier, followed by conversion to oil using the Fischer-Tropsch process. This is a good example of development through adversity, as the expansion of the SASOL operation in 1974 was driven primarily by the imposition of world trade sanctions on oil imports to the South African apartheid regime, whilst the Fischer-Tropsch process was originally developed by Germany during the Second World War to supplement their dearth of oil supplies, before they invaded the Balkans.

It is generally the case that the fuel supplier, rather than the furnace operator caries out pre-flame fuel treatment, and fuel selection for the furnace is based on a commercial cost-benefit analysis. It is inevitably the case that the more beneficiated the fuel, the higher its cost. However, all such processes (viz. liquefaction, gasification, catalytic cracking) tend to produce an expensive high quality fuel stock, and a cheap residual, which is usually almost pure carbon with a significant proportion of the original impurities. For some furnace processes e.g. cement and refractory production, this later fuel can be used owing to the high temperatures, long residence times and inclusion of the mineral ash into the chemical bonding of the product.

In-Flame Control

In Chapter 2 we discussed the importance of mixing and turbulence in the combustion process and concluded that for most industrial flames, these processes control the rate of combustion. Most of man's research efforts in the first part of the 20th century were directed towards intensifying the combustion process through an understanding of the mixing process. This led to groundbreaking advances such as the development of the jet engine by Whittle, and the application of swirl to flames to intensify thermal release rates, giving rise to a new generation of smaller, more efficient furnace designs. However, intense, highly turbulent flames provide ideal conditions for the generation of NO_x, and molten ash. Hence, from the 1960's to the 1990's, world-wide funding for combustion research was directed towards understanding the flame processes that generate pollutants and developing techniques to modify the flame to minimise pollutant formation. Primary amongst this work has been the control of NO_x. During this period a wide range of 'Low NO_x' combustion technologies have been developed. These include flue gas recirculation, combustion staging and re-burn, Bowman (1992). In general NO_x control requires control

of one or more of the parameters which effect NO_x generation in a flame, which are:

- flame temperature
- residence time of hot gases in the flame
- oxygen availability – especially in the hottest parts of the flame

The choice of which combination of the above parameters is best to target depends upon the type of fuel and the type of combustion system. For example, control of the temperature has limited effectiveness if the dominant source of NO_x derives from the nitrogen in the fuel.

It is also important to note that each of these parameters is interdependent, fluctuating and plant specific. For example, changing the oxygen availability will change the temperatures in the flame. Unfortunately the reaction rates associated with the oxidation of the fuel, and notably of CO, also depend upon the same parameters. That is, if the residence time, the oxygen availability and the temperature are reduced, the formation rates of both NO and of CO_2 will be reduced. This gives rise to a dilemma, in that most changes to a system which reduce NO, also increase CO emissions. This is illustrated by Figure 10.11, which is taken from an internal combustion engine, which operates under pre-mixed combustion conditions, Heywood (1976). Although most industrial combustion systems operate with diffusion flame combustion systems, the trends are similar. However, pre-mixed systems e.g. internal combustion engines and some gas turbines, can operate with low NO_x in the very lean region, as shown in Figure 10.12, while diffusion flames cannot. Diffusion flames cannot achieve very lean local combustion because, even though the overall air/fuel ratio may be lean, local reactions tend to occur near to stoichiometric conditions. This is because the flame speed is highest under those conditions.

Reducing the flame temperature will reduce NO_x formation by the thermal route, but is less effective at reducing fuel NO_x. Reduced flame temperature is normally achieved by:

- The addition of an inert species - Most commonly achieved by flue gas recirculation (FGR). However, since heat transfer depends upon the temperature differential, FGR will also alter the heat-transfer characteristics of a system, and will usually reduce the efficiency. In some cases it is possible to redesign the system to compensate for this.
- Increasing the flame emissivity - Since the temperature of a flame depends on the amount of heat extracted from it, increasing the radiant heat loss by increasing flame emissivity will reduce the flame temperature and hence NO_x emissions. This can be achieved

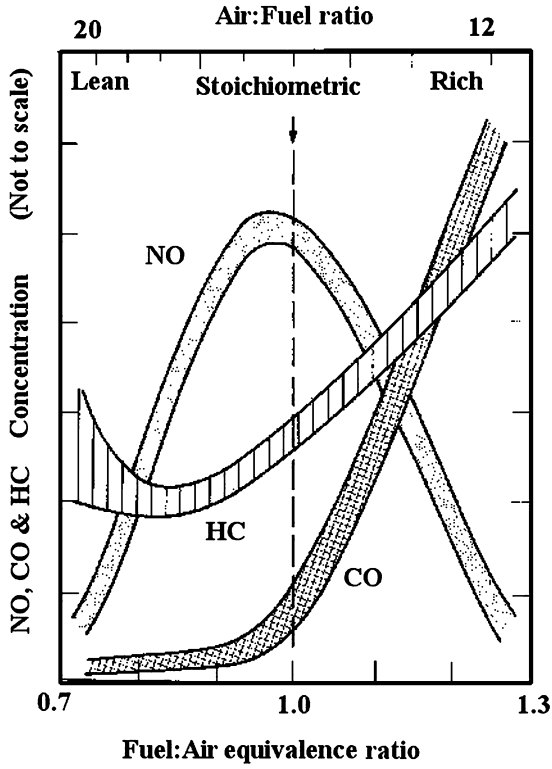


Figure 10.11 An example of the trade-off between NO and CO emissions, here from an internal combustion engine, which operates as pre-mixed flame. [Glassman (1972)]

either by changing the fuel (typically to a higher hydrocarbon) or by modifying the mixing. Since this acts to increase radiant heat transfer, it will increase the efficiency of those systems where radiation is the primary mode of heat transfer.

- Reducing the amount of air preheat - This will almost certainly reduce the efficiency of the system, and so is usually only used as a short-term measure of control until a better system can be installed.
- Increasing the amount of air preheat – This requires a redesign on the furnace system, and process operation to use very high air preheating with delayed fuel mixing to give an even temperature environment in the furnace.

In using flue gas recirculation (FGR), some of the warm flue gases are returned to an injection point behind the flame front, and added into the flame. Strictly FGR is the term used when the flue gas is either added to the combustion air or injected directly into the root of the flame. However, it is also possible to add the flue gas to the fuel.

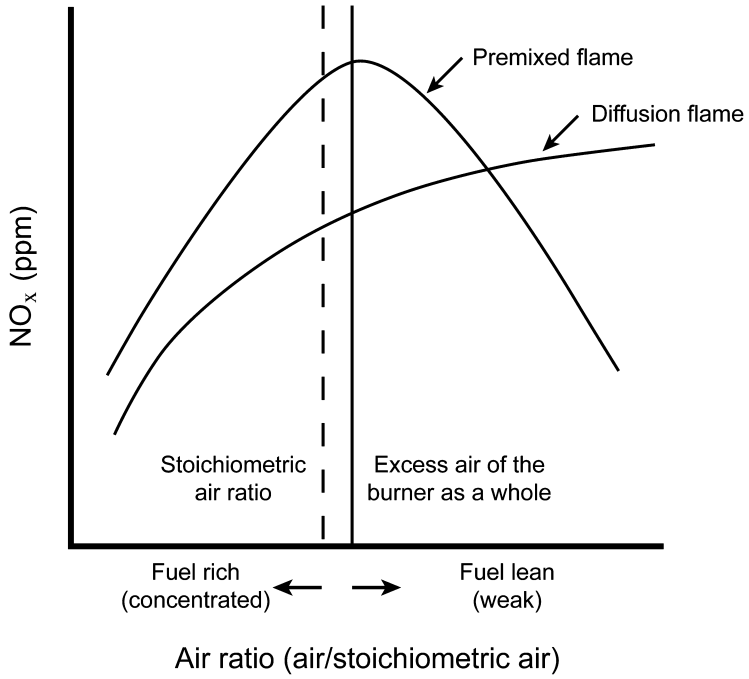


Figure 10.12 Effect of stoichiometry on NO_x emissions for diffusion and premixed flames

This is called fuel injection recirculation, and can be more effective at reducing NO_x emissions than conventional FGR.

FGR has been shown to achieve a 60%–70% NO_x reductions in boilers, (Mansour et al 1995) as shown by the example presented in Figure 10.13. This is usually achieved with 25%–35% of the flue gas recirculated by mass. It is possible to achieve a greater reduction under controlled conditions in the laboratory. For example, reductions of up to 90% have been achieved in a small-scale laboratory furnace firing natural gas with 45% of the mass recirculated.

With careful control of mixing it is possible to simultaneously increase radiant heat transfer and reduce NO_x emissions. Several pilot-scale studies of furnaces equipped with recuperative and regenerative burners at the International Flame Research Foundation have demonstrated that careful choice of port locations and angles can significantly alter NO_x emissions and heat transfer, Nakamura, Smart & van de Kamp (1993) and Webber (2001). However, this requires an air preheat temperature of 1200 °C, which is much higher than achieved in most conventional combustion systems. In these systems, often referred to as flameless oxidation (FLOX) or high efficiency combustion (HEC), the fuel and preheated air/flue gases are injected through separated ports and mixing and combustion proceed evenly

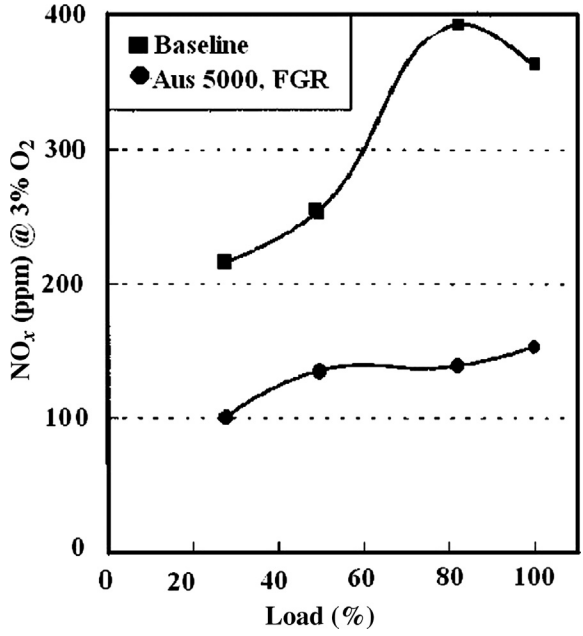


Figure 10.13 The effect of FGR on NO_x emissions in an oil fired boiler (Collins, Unit 3)

throughout the furnace enclosure. Thus there are no significant peak temperatures and the furnace corresponds closely to the well-stirred model discussed in chapter 6.2.1. Likewise control of the mixing characteristics using a precessing gas jet has been shown to provide a simultaneous reduction in NO_x emissions by 30–50% and an increase in heat transfer by 2–10%, (Nathan, et al 1992) and Parham et al. (2000).

Most of the 'low NO_x' burner technologies that are commercially available use combustion staging. The mixing of the fuel and air in the flame is delayed in a controlled manner to create zones of characteristic air/fuel ratio. The zones can either be created within individual flames, as in low NO_x burners or, in the case of multi-burner systems, can be generated within different regions of the furnace. A two-stage combustion system, proposed by Smart & Webber (1989) is illustrated in Figure 10.14. The fuel gun is pushed into the burner quarl so that the fuel is injected directly into the central recirculation region, causing it to be fuel rich. In this way the first stages of combustion (especially devolatilisation in the case of oil and coal) occurs under fuel rich conditions. This acts to drive the fuel NO_x toward formation of N_2. Burnout occurs as the partially reacted products leave the central recirculation zone and mix with the rest of the combustion air.

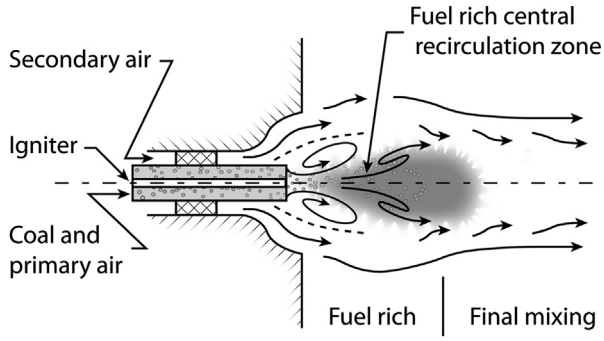


Figure 10.14 An aerodynamically air staged burner

It is a general requirement for a low NO_x burner that all of the combustion air is controlled, so it is not possible to fit low NO_x burners to furnaces where the secondary air is uncontrolled (e.g. rotary kilns, flash furnaces). In multi-burner furnaces burner biasing may be used to create the required zones, whereby some burners are operated in a fuel rich mode and others are operated with additional excess air to compensate.

Even greater reduction of fuel NO_x can be achieved using the "reburn" technique, which has three stages of combustion. This is illustrated schematically for a single burner flame in Figure 10.15. The first stage of combustion is operated with normal amounts of excess air and will therefore produce normal amounts of NO_x. However, these hot products of combustion are fed directly into a zone of secondary fuel-rich combustion by adding more fuel. There is

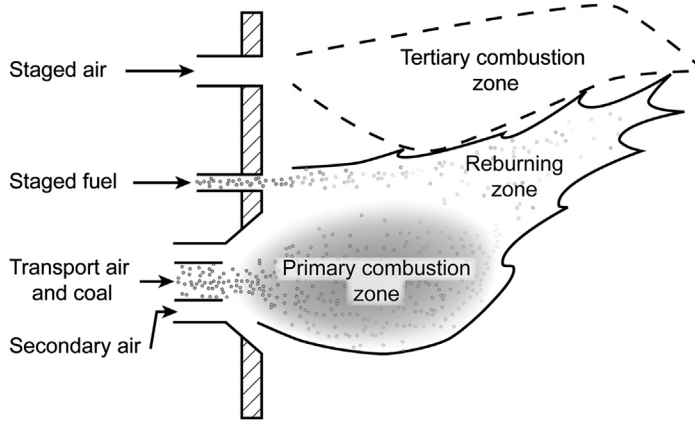


Figure 10.15 The principal of "reburn" illustrated schematically

sufficient oxygen in the secondary region for the mixture to burn, but the fuel-rich conditions again drive the NO reaction scheme back to the formation of molecular nitrogen. The final stage occurs with a low mixing intensity as air is added to complete the combustion.

In general, the fuel used for the re-burn stage is natural gas. This is because the fuel-rich conditions mean that reaction rates are slower, and solid and liquid fuels require longer to burn than gas. If coal is used as the re-burn fuel, there is usually insufficient residence time for it to burn out properly within the furnace. Usually about 15% of the fuel is added as gas in the re-burn stage. Thus re-burn is only really viable when a large supply of natural gas is readily available.

The principal of creating zones of different stoichiometry within a multi-burner system is illustrated in Figure 10.16. In this case the re-burn gas is added through an additional row of gas-fired injectors

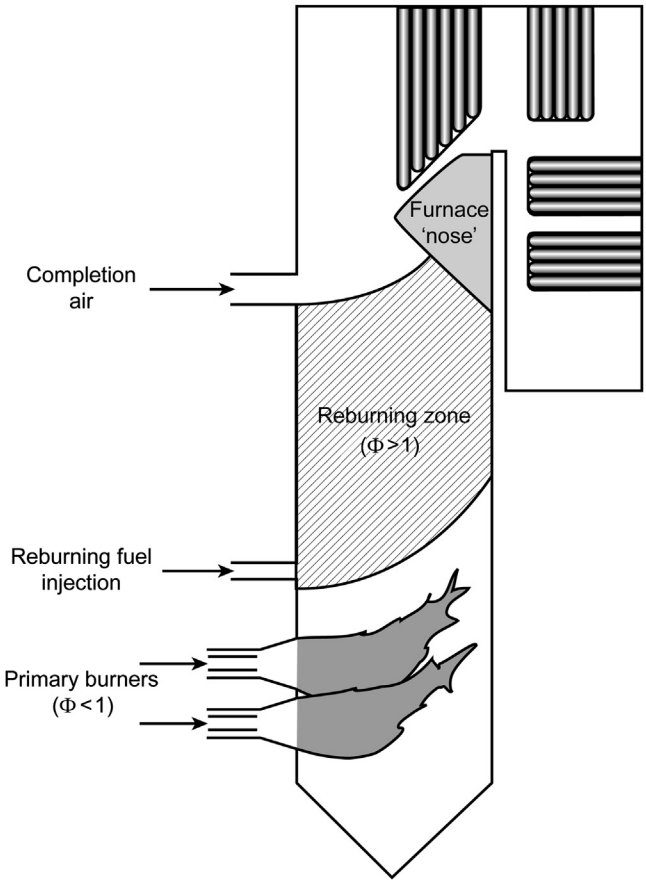


Figure 10.16 The principal of reburn applied to an entire boiler

above the rows of coal-fired burners. Over-fire air is then injected even higher into the boiler again. The principal of staging the entire furnace can also be applied by burner biasing.

Combustion staging may also affect heat transfer and flame volume. Typically the reaction rates in a secondary burn-out zone are lower than those operated under conventional conditions. Hence the volume of staged flames tends to be larger than that of conventional flames. Usually the addition of re-burn fuel and over-fire air at the top of the furnace will increase the total flame volume and may possibly cause problems with overheating of the super-heater tubes. Associated with a change in flame volume, there may also be a change in heat transfer.

The essence of most in-flame emissions control technologies is to design a burner and furnace system that does just enough to meet the process demands, whilst satisfying emissions legislation. If the combustion process is 'too' good then NO_x regulations are likely to be exceeded, whilst if the performance is not quite good enough then PIC's will be the inevitable consequence. Such performance can be achieved on a fully instrumented and monitored test furnace, but to translate this to a production furnace requires equivalent monitoring instrumentation, accurate control of the fuel, air, etc. inputs, and flexibility in the burner design to perform over the required operating range.

End-of-Pipe Control

End-of-pipe control techniques and equipment are primarily concerned with the capture of sulphur oxides and particulates, although there are also techniques available for the reduction of NO_x and CO_2 capture.

NO_x control techniques involve the injection of ammonia or urea into the flue gases to reduce NO_x to nitrogen under controlled temperature conditions. This may be carried out by passing the treated flue gases over a catalyst at a controlled temperature (selective catalytic reduction, or SCR), or within a carefully controlled time and temperature window in the flue gas ducting (selective non-catalytic reduction or SNCR). Both these techniques involve considerable additional cost for the ammonia or urea, and the SCR route has the additional cost of the catalyst, which is subject to poisoning and fouling.

Particulates emissions can be minimised by the use of dust control equipment (cyclones, electrostatic precipitators and bag filters). The application of such equipment is well established but the designs are generally based on somewhat loose empirical rules. This is particularly the case with electrostatic precipitators where the resistivity of the dust is an important parameter. Unfortunately, the resistivity can vary with process conditions leading to excessive emissions under certain

circumstances. The gas velocity is recognised as an important parameter in both electrostatic precipitators and bag filters, but rarely is adequate attention given by designers to ensure a satisfactory velocity distribution. Often local high velocities cause a serious deterioration in performance, despite the average gas velocity being satisfactory.

Dust emission limits are being progressively reduced from, in the order of 200 mg/Nm^3 in the 1960's, to current requirements of less than 50 mg/Nm^3. These new limits raise the prospect of dust collectors being required for oil fired boilers, especially in Europe. It is also important to appreciate that both bag filters and electrostatic precipitators can introduce an explosion hazard to fuel burning plant, owing to the risk of ignition of flammable mixtures by electrostatic discharges.

Sulphur oxides are captured either by wet or dry scrubbing. Wet scrubbers, generally consisting of a water spray tower through which the flue gases are passed, are highly efficient in the removal of SO_x, as these gasses are extremely hygroscopic. They will also remove a significant quantity of NO_x from the flue gases, sufficient to meet most regulatory requirements. The drawback is that the resulting effluent water from the spray tower is itself a hazardous acidic waste. If this effluent cannot be reused within the process, or used to produce commercially saleable sulphuric acid, then it must be neutralised with an alkaline chemical (usually lime or caustic soda) before it can be safely discharged. Dry scrubbing is carried out using either granular limestone, or lime as an absorbent. Two basic methods of absorption are used; in-flight techniques where the absorbent is 'blown or sprayed' into the flue gases either in the furnace, or in the downstream ductwork and captured in the dust filtration equipment, or fixed bed absorption, where the flue gases pass through a packed bed of the absorbent. This latter method requires the bed material to be replenished on a continuous basis. Irrespective of the delivery method, the sulphur is absorbed to form calcium sulphite or sulphate. This material may be regenerated in a separate by-product process to recover SOx (usually as an acid) and recycle the absorbent, or marketed as synthetic gypsum.

Carbon dioxide has been identified as the primary greenhouse gas responsible for climate change. Although VOC's, and in particular methane, are an order of magnitude more damaging to the environment, their much lower emission rate reduces their impact, relative to CO_2. At the time of writing this book, there are no commercially installed control or capture installations for CO_2, but increasing international governmental pressure, through primarily fiscal penalties, will inevitably lead to an economically viable market for CO_2 control. Current legislation has been directed towards large, fossil fuel powered stationary plant (viz, power generation and industrial furnaces). Sequestration, which is the liquefaction of CO_2 from the flue gases, is a technically proven method for CO_2 capture, and is the only viable

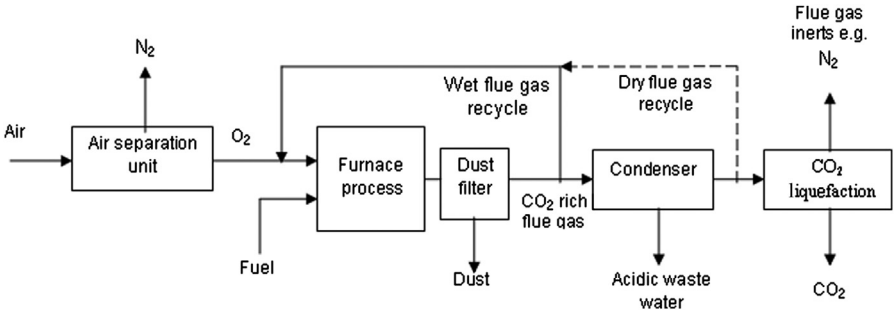


Figure 10.17 The principal of CO_2 sequestration using oxy-fuel combustion

end-of-pipe control method currently available for large flue gas volume discharges.

Liquefaction plant, used for production of bulk and bottled gases such as CO_2, O_2 and N_2 is a mature technology, but to be efficient for sequestration the CO_2 content of the flue gases must be >40% and preferably as high as possible. To achieve this in most furnaces will require a conversion to oxy-fuel combustion with flue gas recirculation to control the temperature, heat transfer etc. as shown in Figure 10.17. This would raise the flue gas CO_2 content to above 90% if dry flue gas is used as shown in Figure 10.18. Tan, Corragio & Santos (2005). Ultimate disposal of the liquid CO_2 is a subject for further discussion, current proposals being to inject into depleting oil wells to enhance oil recovery, Storage in exhausted oil wells or deep mines, or deep sea injection. It should be noted that the major repository of atmospheric CO_2 is as dissolved gas in the earth's oceans, hence rising ocean temperature cause less CO_2 to be dissolved. An advantageous by-product of oxy-fuel combustion technology would be a reduction of NO_x, as there is only a minimal amount of atmospheric nitrogen present, thus eliminating NO_x formation by the thermal route. See also section 15.2 for more information on future prospects for carbon capture.

10.6.2 Dispersion Modelling

We would not complete this chapter without a discussion of atmospheric dispersion modelling, as this is now a commonly required prerequisite for the permitting of new or upgraded industrial installations. The development of mathematical modelling techniques in the field of meteorology has been as rapid as those discussed in Chapter 6 with respect to combustion. The normally accepted calculation procedure until as late as the 1980's involved simple plume

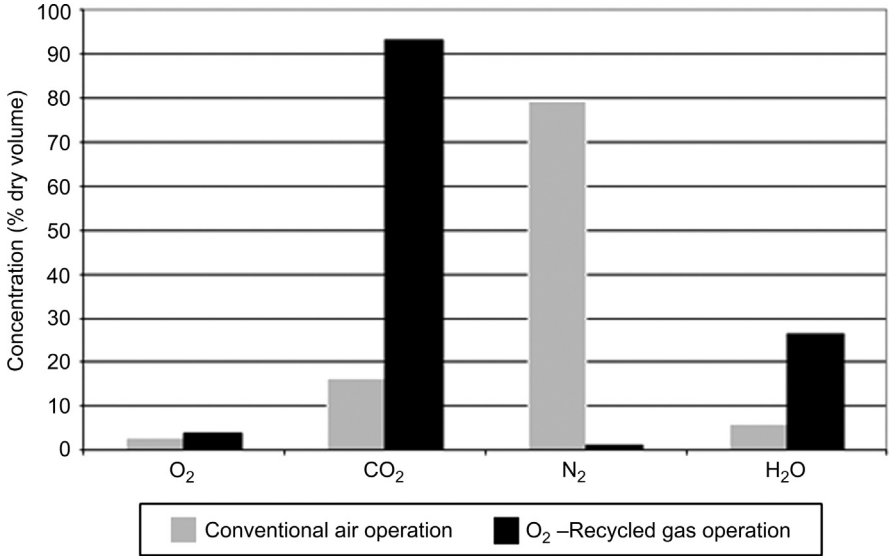


Figure 10.18 Post-combustion gas composition from coal burned in a mixture of oxygen and recycled flue gas

rise and dispersion formulae, which may have been supplemented by physical three dimensional terrain models in wind tunnels for applications of a particularly sensitive nature. e.g. emissions from nuclear installations. These have been supplanted by 'large' three-dimensional mathematical models, Olsen (2001) using similar methodologies to those summarised for CFD modelling, see section 6.2.4. The key parameters to be considered in the use of these models are,

- Emission characteristics – these include mass emissions rates, stack height, efflux velocity and efflux temperature.
- Meteorology – the primary factor to be included is inter-year variations.
- Atmospheric chemistry – chemical reaction rates are dependent on the temperature and atmospheric composition and this will influence the meteorological data used or number of years that may be required to be modelled.
- Terrain – terrain is an important factor in elevated dispersion modelling. However, the techniques used to 'describe' the terrain or boundary in these models is limited by the fineness of the grid and the estimation of surface roughness. This requires the model to be tested for its sensitivity to these factors as part of the process.
- Buildings – any building that fall within a five stack height radius of the emission point will cause wake effects. As with terrain

modelling, the ability of the dispersion models is limited owing to the grid fineness required to mimic the complexity of the building shape, and hence requires a sensitivity analysis.
- Coastal effects – e.g. wind changes due to tidal flows, these must be included in sensitivity analysis.
- Receptor spacing – this refers to the output data grid required, and will define both the grid size and area.

Where these models are used to meet local or national permitting requirements, the presented results generally require a statement or evidence confirming that all of the preceding considerations have been accounted for in the analysis.

References

Bowman, C. T. (1975). Kinetics of pollutant formation and destruction in combustion. *Prog. Energy Combust. Sci., 1*, 33–45.

Bowman, C. T. (1992). Control of Combustion-Generated Nitrogen Oxide Emissions: Technology Driven by Regulation. *Transactions of the Combustion Institute, 24*, 859–878.

Clarke, A. E., Hunter, T. G., & Garner, F. H. (1946). *J.Inst Petrol., 32*, 627.

Duggal, V. K., Priele, T., & Kahn, I. M. (1978). A study of pollutant formation within the combustion space of a diesel engine. *SAE Technical Paper, 780227*.

Erickson, M. D. (1985). *Analytical chemistry of PCBs*. Butterworth.

Field, M. A., Gill, D. W., Morgan, B. B., & Hawksley, P. G. W. (1967). *Combustion of pulverised coal*, 183–184. BCURA.

Flagan, R.C., Proc. of 17th Symp. (int.) on combustion, 97, Leeds, U.K., 1978

Foster, P. J. (1965). Carbon in flames. *Jnl. of Inst. of Fuel, 38*, 297–302.

Freihaut, J. D., Proscia, W. M., & Seery, D. J. (Mar, 1987). *Fuel bound nitrogen evolution during the devolatilisatiion and pyrolysis of coals of varying rank*. New Orleans, U.S.A: Proc. of the 1987 Joint Symp. on stationary combustion.

Graham, S. C., Homer, J. B., & Rosenfeld, J. R. J. (1975). The formation and coagulation of soot aerosols generated by the pyrolysis of aromatic hydrocarbons. *Proc. R Soc. London A, 344*, 259–285.

Haile, C., Stanley, J., Lucas, R. M., Melroy, D., Nulton, C., & Yauger, W., Jr. (1983). *Comprehensive assessment of specific compounds present in combustion processes, EPA-560/ 5-83-04, Office of toxic substances*. Washinton DC: U.S. Environmental Protection Agency.

Harrad, S. J. (May 1993). British Flame Research Committee AGM. *Technical Topic Session*.

Haynes, B. S., Jander, H., Matzing, H., & Wagner, H. G. (1981). The influence of various metals on carbon formation in various flames. *Combustion and Flame, 40*, 101–103.

Heywood, J. B. (1976). Pollutant formation and control in spark-ignition engines. *Prog. Energy Combust. Sci., 1*, 135–164.

Homann, K. H., (1972). Carbon formation in premixed flames, NBS The mechanisms of pyrolysis, oxidation and burning of organic matter. (pp. 143–151), N73–17125 08-06, USA.

James, P. (1984). *The future of coal* (2nd ed.). Macmillan Press.

Lahaye, J., & Prado, G. (1981). *Morphology and internal structure of soot and carbon blacks, 'Particulate carbon formation during combustion'* (3rd ed.). Plenum Press.

Lightman, P., & Street, P. J. (Nov. 1981). The chemistry and physics of heavy oil combustion, The heavy end of the barrel – Future trends in oil firing symposium. *Inst. of Energy,* UK Portsmouth.

Mansour, N. M., Kwan, Y., & Grant, M. P. (1995). *US Experience with Advanced Low NO_x Burners for Electricity Utility Boiler Applications*. Combustion and Emissions Control II, (pp. 285 – 294). Pergamon Press.

Muir, W. L. G. (1977). *The conversion of coal to gas and oil, Progress report No.1*. UK: Coal Industry Information Service.

Nakamura, T., Smart, J. P., & Van de Kamp, W. L. (1993). *The Effect of Fuel Air Mixing on NO_x Reduction and Heat Transfer in High Temperature Gas Fired Glass Melting Furnaces, Combustion and Emissions Control*. The Institute of Energy, 213–230.

Nathan, G. J., Luxton, R. E., & Smart, J. P. (1992). *Reduced NO_x emissions and enhanced large scale turbulence from a precessing jet burner*, 24th Symposium (International) on Combustion, 1399–1405. Sydney, Australia: The Combustion Institute.

Niksa, S., & Kerstein, A. R. (1987). On the role of macromolecular configuration in rapid coal devolatilisation. *Fuel, 66*, 1389.

Okazaki, K., Shishido, H., Nishikawa, T., & Ohtake, K. (1984). *Separation of the basic factors affecting NO formation in pulverised coal combustion*. Proc. of 20th Symp (Int). on Combustion, Michigan, USA. The Combustion Institute

Olsen, H. R. (May 2001). *Ten years of harmonisation activities: past, present and future*, 7th Conf. on Harmonisation and Atmospheric Dispersion Modelling for Regulatory Purposes, Belgirate, Italy.

Parham, J. J., Nathan, G. J., Smart, J. P., Hill, S. J., & Jenkins, B. G. (2000). The relationship between heat flux and NO_x emissions in gas fired rotary kilns. *Jnl. Inst. of Energy, 73*, 25–34.

Raask, E. (1985). *Mineral impurities in coal combustion*. New York: Hemisphere Publishing.

Smart, J. P., & Webber, R. (1989). Reduction of NO_x and optimisation of burnout with an aerodynamically air-staged burner and an air-staged precombustor burner. *Jnl. Inst. of Energy, 62*, 237–245.

Tan, R., Corragio, G., & Santos, S. (2005). *Oxy-coal combustion with flue gas recycle – A literature review*. IFRF Doc. No. G 23/y/1, Sept.

Tesner, P. A., Tsygankova, B. I., Guilazeldinov, L. P., Zuyev, V. P., & Loshakova, G. V. (1971). The formation of soot from aromatic hydrocarbons in diffusion flames of hydrocrabon-hydrogen mixtures. *Combustion and Flame, 17*, 279–285.

Webber, R. (2001). *Combustion of natural gas, oil and coal with air preheated of temperatures in excess of 1000°C*. paper 9, 13th IFRF Members Conference. The Netherlands: Noordwijkerhout.

Westenberg, A. E. (1971). *Combust. Sci. Tech., 4*, 59.

Wibberley, L. J., & Wall, T. F. (1986). *Combustion Science and Technology, 48*, 177.

Winegartner, E. C. (1974). *Coal fouling and slagging parameters*. ASME.

Zeldovich, Y. R., Sadovnikov, P. Y., & Frank-Kamenetski, D. A. (1947). *Oxidation of nitrogen in combustion*. Acadamy of Sciences of USSR.

Chapter 11

Furnace Construction and Materials

Chapter contents

11.1	Basic Performance Requirements of the Furnace Structure	416
11.2	Basic Construction Methods	417
11.3	Practical Engineering Considerations in the Use of Refractories	433
11.4	Ceramic Refractory Materials	435
11.5	Heat Resisting and Refractory metals	440
11.6	Practical Engineering Considerations in the Use of High Temperature Metals	445
11.7	Concluding Remarks	447
References		447

Design of the furnace structure and choice of construction materials is a complex topic that probably deserves a book of its own. In this chapter and the one that follows there is opportunity to alert the reader to the more important issues.

As noted in Chapter 1, the principle objective of a furnace is to achieve controlled heating of the product at higher temperature and lower fuel consumption than could be achieved in the open air. Fuel economy will become increasingly important in a world of diminishing fossil fuel reserves that is also constrained by carbon emission limits.

Early furnaces consisted of brick and stone structures such as the beehive pottery kiln shown in Figure 1.4 and Abraham Darby's blast furnace shown in Figure 1.9. As furnaces increased in output and became physically larger, the brick and stone structures became vulnerable to failure and steel reinforcing bands were often added externally to strengthen the structure. Such reinforcing was used in the beehive kiln shown in Figure 1.4 to prevent the roof from "spreading" the walls and around the doors. Then the steel reinforcing became part of the initial design but the basic brick structure remained.

The invention of the rotary kiln in the late nineteenth century required that it had an outer steel tube with a brick lining thus a new form of construction was developed which in time spread to most other furnaces. Nowadays, most furnaces consist of a steel outer structure with a heat resistant lining. The advantages of a steel casing compared with a steel reinforced brick structure include:

- Reduced gas and air leakage - gas out or air in;
- Easier and lower cost maintenance – relining is cheaper than rebuilding;
- Improved safety – flying debris is reduced in the event of an explosion;
- Greater design flexibility - in terms of shape and size and type of lining.

In this chapter we shall examine the function and principle requirements of the furnace structure together with the materials available for furnace construction. It will of necessity be very brief and can only highlight the issues that need consideration. Design methodologies to determine furnace size, shape, etc., are considered in the next chapter.

11.1 Basic Performance Requirements of the Furnace Structure

In its simplest form a furnace consists of a casing with a heat source, usually a flame, to provide the process energy. Where flames are employed the heating may be direct using radiation from the flame

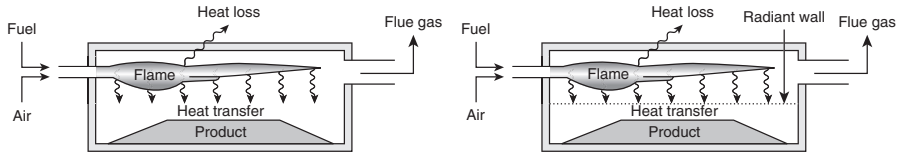


Figure 11.1 Basic types of furnace showing direct fired (left) and indirect fired (right)

and /or convective heat transfer from the combustion products or indirect via radiant heat from a heated wall, see Figure 11.1.

Whichever method of heating is chosen, the furnace structure is required to perform the following functions:

- Provide a controlled environment for the process;
- Provide optimum shaped space for the combustion process and for effective heat transfer;
- Safely contain, and in some cases transport, the product;
- Minimise air and gas leakage in or out;
- Minimise radiation and convection losses;
- Provide the optimum space and shape;
- Have a long life and be easy to maintain.

The need for furnaces to accommodate a wide temperature range, from ambient to, in some cases, up to 2000 °C provides a significant challenge to both design and maintenance engineers. Critical aspects that need to be considered in the design are:

- Accommodating differential thermal expansion;
- Accommodating irreversible expansion caused by structural changes in the refractory during initial heating;
- Minimising high temperature corrosion;
- Need for adequate strength under load;
- Potential for chemical reaction between the feed/product and furnace lining.

Resolving these issues is one of the designer's principle responsibilities and requires careful consideration of all the issues, including choice of materials such as which ceramic refractories are appropriate, methods of accommodating differential expansion, etc.

11.2 Basic Construction Methods

As stated previously most, but not all, furnaces are nowadays steel shells with a refractory lining. This lining can be of three basic types, namely individual bricks positioned against the lining, Figure 11.2, a

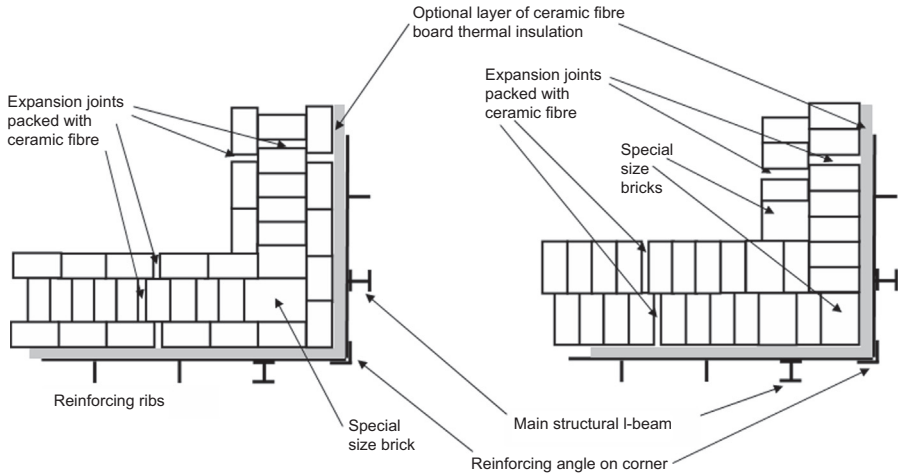


Figure 11.2 Typical brick lining construction showing alternative layers of bricks and expansion joints with casing reinforcing

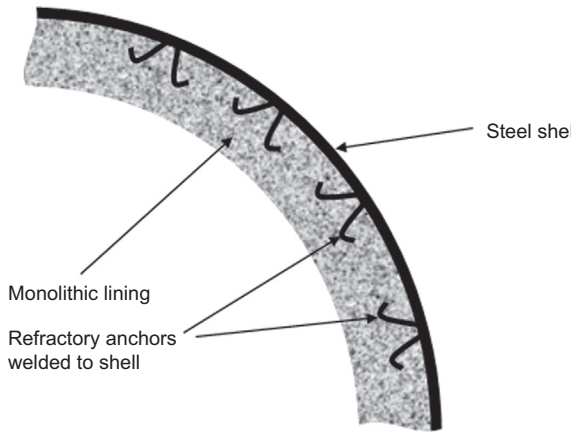


Figure 11.3 Typical monolithic lining held to the shell by anchors

monolithic lining held to the shell by anchors, Figure 11.3 or a ceramic fibre lining, Figure 11.4. In the context of the thousands of years the refractories have been used, monolithic linings are a relatively recent development and, since the late 1960s, have been gaining market share at the expense of traditional brickwork. This trend is likely to continue owing to the reduced time and skill required for installation and the lower cost. Ceramic fibre linings are an even more recent development that started gaining popularity in the early 1980s but

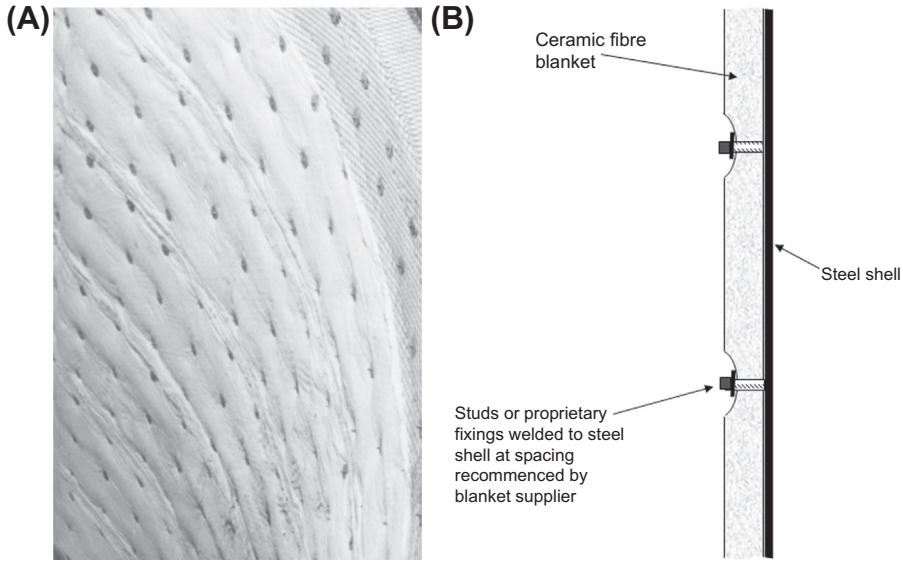


Figure 11.4 Typical ceramic fibre lining showing fixing details on the right (Photo reproduced by kind permission of David Haig)

their lack of durability restricts their use to relatively light duty applications, such as backing insulation and gas fired furnaces.

11.2.1 Brick Lining

This traditional lining technique is a development of the old self-supporting brick built furnace and allows significant flexibility in design. Normally few or no fixings are used to anchor the bricks to the shell but the brick structure is designed to be interlocking often, but not always, using modified traditional bricklaying bonds. In Figure 11.2 alternative layers of bricks are shown; that is, the layer on the right would overlay the layer on the left with all joints staggered, so any one brick is in contact with at least four other bricks (two above and two below). The friction between these surfaces maintains the wall stability. The joints between bricks are staggered so that there is no direct gas path from the hot gas side to the shell.

Dense refractory brick is required in most furnaces to withstand the high internal temperature but dense brick has a relatively high conductivity, so most modern furnaces utilise a layer of ceramic fibre board, or insulating bricks, to provide an insulating layer. Ceramic fibre has a very low thermal conductivity and hence reduces the conduction heat losses substantially. The technique for estimating the effect of an insulating layer is shown in Chapter 4, section 4.1.1.

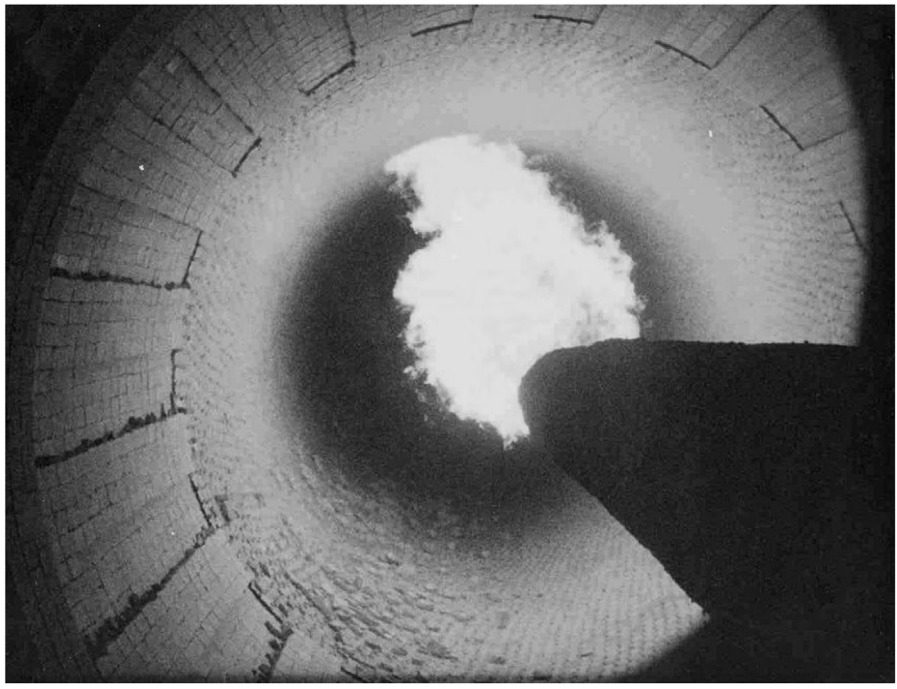


Figure 11.5 Brick failure caused by inadequate allowance for expansion

Expansion joints need to be provided at regular intervals to avoid over stressing the bricks at elevated temperature. These expansion joints also need to be staggered to prevent hot gas reaching the steelwork. In the past these joints were left as gaps, or packed with asbestos rope (no longer permitted), but are now normally packed with ceramic fibre.

The bricks may be assembled dry or use high temperature mortar based on high alumina cement. The mortar is normally weak and compresses when the bricks expand but where they are assembled dry, cardboard spacers or steel can be used between bricks during installation to accommodate any irreversible expansion that occurs during heat up following installation.

All refractory must be heated slowly from cold owing to the need to minimise the stresses created by differential thermal expansion. If the hot side of the brick heats too rapidly compared with the cooler side, the hot side will expand and put the cooler side under a tension stress. Most ceramic materials are weak under tension and if the ultimate strength is locally exceeded a crack will develop, often leading to the hot face becoming detached from the rest of the brick, a process known as "spalling", which can also be caused by failure to allow



Figure 11.6 Tapered brick being installed in a rotary kiln; note the purpose built support frame to facilitate quick and accurate installation (Photo courtesy of Brokk Bricking Solutions Inc.)

adequate room for expansion, Figure 11.5. In this case the bricks failed at less than 250 °C despite being heated at less than 50 °C per hour.

Complex shapes, such as found in rotary kiln firing hoods, can be accommodated by using special profile bricks but their installation requires careful planning and considerable bricklaying skills and is rarely seen today. A "gunned" monolithic lining is preferred as it is simpler and cheaper to install, see later.

Bricks are available from many manufacturers and can be manufactured from most refractory materials, see section 11.4. Bricks based on fireclay are normally pre-fired in a kiln at temperatures up to 1400 °C, the actual firing temperature depending on the material used. Other bricks use chemical bonding agents and may also be pre-fired but are also sometimes supplied "green". Bricks are available in a wide range of shapes and sizes, such as tapered bricks for arches and rotary kilns, Figure 11.6. It should be noted that some special shapes tend to be on long delivery, several months in some instances, especially where new moulds are required.

Despite the higher installation costs, bricks are still used where specialist materials are required, such as in rotary cement kilns and glass tanks. They are also preferred where high rates of expansion need accommodating and where the superior strength and thermal shock resistance of the interlocking bonding system is required.

11.2.2 Monolithic Linings

Monolithic linings are a relatively recent development and consist of a refractory material graded to a range of sizes to reduce voidage together with a bonding agent. There are two basic types of monolithic lining, castable refractory and plastic refractory. Within these two groups there are significant variations depending on the final application.

Castable Refractory

Castable refractory consists of a graded refractory material and a bonding agent which is normally based on high alumina cement, hydratable aluminas or colloidal silica. They are supplied dry but ready mixed in paper sacks. When required for use they are mixed with the correct portion of water and either cast into moulds or gunned in place, as described later. Castable refractories can be considered analogous to concrete and indeed are sometimes called refractory concrete. As for concrete, the cement content affects the properties and much effort has been directed towards the development of additives that allow the cement content to be reduced. This has resulted in refractories with cement as low as 3–10% cement which are known as low cement castable, while those with less than 3% are known as ultra low cement castable. The principle advantage of reducing the cement content is that the water demand reduces with it. Since evaporating water leaves voids, and hence reduces strength, water content is critical and too much water severely degrades the strength.

Unlike conventional concrete, which is generally stronger than its brick counterpart, monolithic refractories are rarely as strong as their brick equivalent. This is largely because the warming up process in a furnace is rarely as well controlled as the firing that occurs in a brick kiln. Furthermore, while the kiln burnt brick generally achieves an even temperature throughout, in a monolithic lining a temperature gradient is developed with the hot side at a much higher temperature than the ambient side, hence the monolithic lining is subject to a range of curing temperatures, as described later.

In certain circumstances castable refractories are reinforced with small fibre like needles, typically up to 2–6% by weight, turning the castable refractory into a fibre reinforced composite. This technique

is critically dependent on the fibre's ability to resist high temperature corrosion and the needles are normally made from rapidly cooled austenitic and superferritic stainless steels to maximise their resistance to high temperature corrosion. For further information on stainless steels and their properties see section 11.5.

Traditional Installation of Castable Refractory

Owing to its relatively poor strength, the durability of a monolithic lining is heavily dependent on the design and installation of the anchors, Figure 11.3. These are available from the refractory supplier and normally consist of a heat resistant stainless steel, Figure 11.7. The refractory supplier's instructions should be carefully followed and in most cases they are welded to the furnace shell or bolted through a hole in the shell. The latter is generally superior, because it allows movement of the anchor to accommodate both shell and refractory expansion. Drilling the holes and bolting the anchors in place is labour intensive and most installers use weld-on anchors. This eliminates the flexibility inherent in the bolted arrangement and, depending on the anchor material, may make it vulnerable to "weld decay", a major cause of anchor failure, see section 11.5.2. When welded, the expansion forces tend to stress the rigid weld, in time also causing fatigue failure. A large proportion of the failures associated with monolithic linings originate with failure of inappropriate anchor fixing welds.

Monolithic linings are installed by casting the refractory in a mould or by spraying it onto the furnace shell. When casting, formwork is used similar to casting concrete in civil engineering applications but, owing to its high costs compared with gunning, formwork is rarely used for furnace linings today being reserved for smaller high precision items such as burner quarls and casings. Figure 11.8 shows a typical set up for casting a refractory coating on the outside of a burner pipe. After placement the material must be vibrated to compact

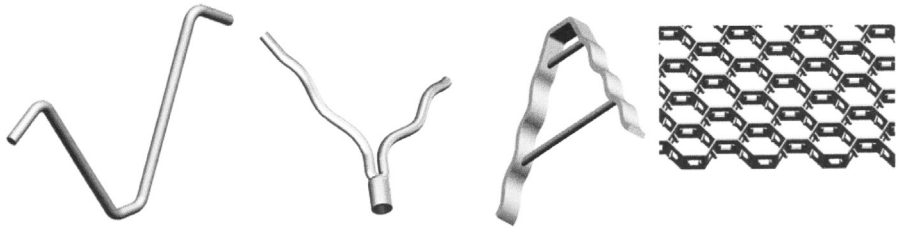


Figure 11.7 Typical anchors for installation of castable refractory as manufactured by Refractory Anchors Inc.

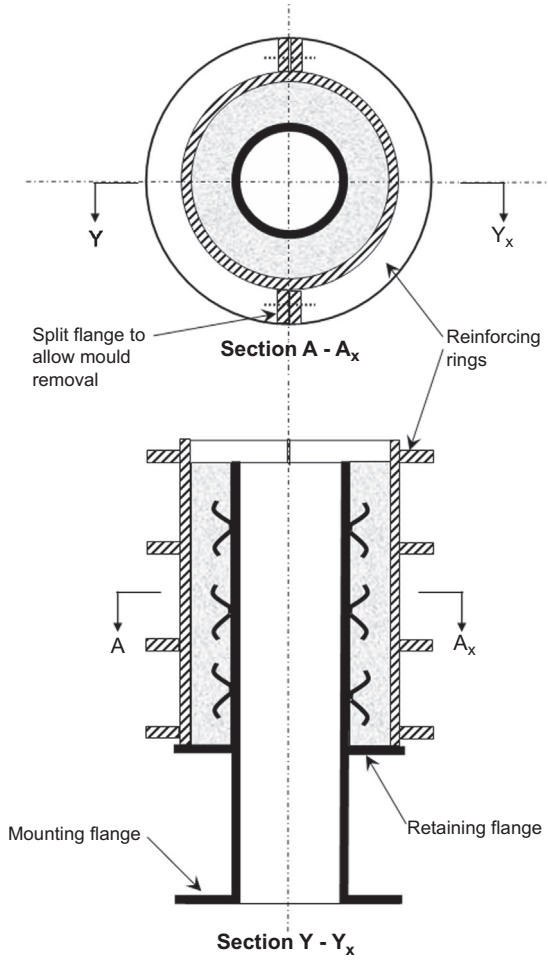


Figure 11.8 Use of split mould formwork to cast refractory on a burner pipe

it and reduce voids, except for specialist free flowing materials that have special additives that improve the flow characteristics of the mix and allow the use of even less water.

Installation of Castable Refractory by Gunning

A selected range of castable refractories can be applied by spaying. This technique, normally known as gunning, eliminates the need for formwork and hence is especially suitable for use in complex shapes where formwork is very difficult to make and it is difficult to ensure effective compaction. It is also very quick allowing large areas to be



Figure 11.9 Gunning refractory into place in a rotary kiln (Photo courtesy of REED Gunite Equipment)

coated in a few hours. For gunning, dry material is air conveyed to the nozzle where it is mixed with the required proportion of water. In some cases accelerators are also added to promote rapid setting and hardening. The resultant mix is ejected from the gun at high velocity and deposited on the surface where hydration commences. The high velocity encourages compaction of the material. During installation the operator commences by depositing material in the lowest elevations and gradually working upwards, building up layers until the required thickness is achieved, Figure 11.9. The surface of gunned refractory tends to be rougher than for cast and only limited surface finishing techniques are available.

Gunning is especially suitable for repair work of damaged monolithic linings and damaged brickwork owing to the need for minimal cutting back of the adjoining lining together with rapid installation.

Drying and Curing of Cast and Gunned Refractory

One disadvantage of cast and gunned refractory is that it must be heated even more carefully than brick because, in addition to the need to minimise the stresses created by differential thermal expansion, the surplus water must be permitted to evaporate and diffuse to the surface in a controlled way and the ceramic bond must be formed. The warming up schedule therefore has two phases; drying and curing.

During drying, the lining is warmed slowly; say 10–30 °C per hour then held at a soak temperature of 100–200 °C for several hours to allow the water to evaporate and diffuse to the surface. Too rapid heating makes the material vulnerable to spalling owing to the risk of an internal steam explosion. If this occurs, catastrophic failure of the lining is the result. Low cement castable is less vulnerable to explosive spalling owing to the lower water content. Explosive spalling is not well understood and can occur even when the refractory manufacturer's instruction have been carefully followed.

Following drying, the lining is warmed slowly to cure the material. The cement has little strength at normal service temperatures and during the curing process the binder, filler and aggregate sinter together to form a strong ceramic bond. As the process proceeds the cement bond tends to weaken prior to the ceramic bond forming producing a minimum strength part way through the process, Figure 11.10. If this minimum coincides with high internal stress caused by evaporating water or thermal expansion, catastrophic failure is again likely.

Another disadvantage of cured in-situ material is that, owing to the significant temperature gradient through most furnace linings, the cooler material never reaches a sufficiently high temperature to fully form the ceramic bond. Consequentially there is a layer of weakness running through the material. It is critically important that the anchors protrude through this layer and into the fully bonded material to avoid risk of premature failure. Needle reinforcing helps to reduce the effect of this weakness and is used especially where the refractory is subject to intense heat, fluctuating temperatures or abrasion, such as steel furnaces, rotary kilns and high temperature fluid bed reactors.

Choice of needle material is important and unsuitable steel will not improve the durability of the refractory and, in the authors' experience, can even reduce the life compared with the un-reinforced variety. While knowledge of the properties of stainless steels helps, needle

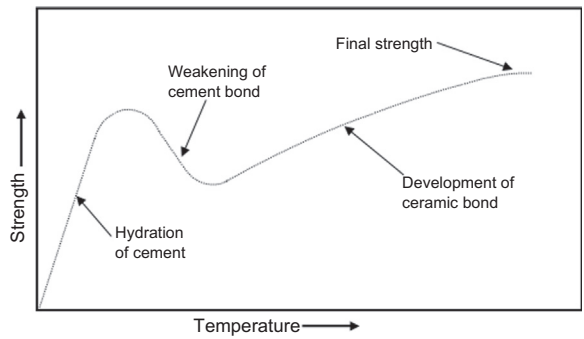


Figure 11.10 Strength development during curing of castable refractory

choice is not an exact science and trial and error and experience still play a role in needle material selection. Needle reinforced refractory can be cast or gunned as for the base material.

Mouldable and Rammable Refractories

These refractories are similar to castable but have a smaller maximum particle size and a binder that allows them to be troweled and tamped into place. The difference between the mouldable and the rammable material is that the latter is a stiffer mix making it more self-supporting. This allows it to be used in areas where the more plastic mouldable material would sag.

Mouldable and rammable refractories are normally used for small awkward areas such as irregular shapes, where their unique properties allow installation without special bricks or formwork. Their properties make them especially suitable for repair work and some plastic refractories are available with very soft plasticity specifically for repair, their softness allowing them to be pounded into gaps left by failed bricks, etc.

11.2.3 Furnace Steelwork

The steelwork consists of the steel shell or plate work and the load bearing frame. In some designs, such as rotary kilns and shaft furnaces, the shell carries the entire load and no frame is used. Even where a frame is employed, the shell contributes to the load bearing capacity. Refractory failure can rapidly heat the shell and reduce its load bearing capabilities and in this event the furnace must be shut down and the lining repaired, unless the frame is designed to accommodate the additional load.

The principle loads are taken by the steel frame and its design is relatively conventional once the loads are determined. However, determining the loads can be difficult since they arise from a number of sources, including static loading created by the refractory lining and differential thermal expansion together with live loadings caused by product transport (including impact in some instances). While the static loadings caused by the mass of the bricks are easy to determine, the loads created by differential thermal expansion are quite another matter. This arises from two distinct causes. Firstly, it is relatively difficult to determine during design the various temperatures that will be experienced by the structure when it is new, let alone as it ages. A second problem is that over time the material of the internal lining may be changed or installed differently leading different expansion characteristics imposing different loads on the external shell.

Product transport has the potential to apply both varying loadings and impact loadings and while these are generally quite small, they

can impose a significant fatigue potential over a prolonged period. An example is a rotary kiln, typically rotating at 1–5 rpm and lasting for 40 years, will undergo millions of loading cycles during its lifetime. Add to this the fact that many of the stressed metallic components are high alloy materials the potential for fatigue failure is significant. While failures such as broken support roller shafts, split shells and dropped satellite coolers are rare, they occur and are potentially dangerous.

As eluded to in the preceding paragraph, many load bearing furnace components operate at elevated temperature. For these applications the choice of material is crucial for safe operation and long life. Factors that require consideration include operating temperature range, the presence of cyclic loads, surrounding atmosphere, etc. Most heat resisting components are based on stainless steels and the properties of these materials are reviewed briefly in section 11.5. High temperature applications of stainless steel are frequently misunderstood by designers and maintenance engineers despite the properties being well documented. These misunderstandings of the properties have led to failures caused by loss of passive oxide layer, phase changes, carbide precipitation, etc. These failures are common and can often be attributed to incorrect choice of material. In the authors' experience, failure is usually followed by a search for a "better" material, which can normally be interpreted as a higher service temperature material, rather than an investigation as to the true cause followed by a revised choice.

For example, Figure 11.11 shows the failure experienced by a burner in a rotary kiln. The main primary air pipe was manufactured from spun cast A316 stainless steel with the intention of resisting scaling corrosion by the hot combustion air at 850 °C as well as heat radiation from the flame. However, the primary air is at 20 °C and provides some cooling so that the burner tube typically operates at 650–750 °C. The burner was designed for a 20 year life but after only 3 months of operation the burner pipe failed by splitting longitudinally as shown. At the operating temperature, A316 stainless steel is vulnerable to chromium carbide precipitation that leaves the grain boundaries deficient in chromium. As a result the oxide layer is destroyed and the material is no longer stainless and the exposed

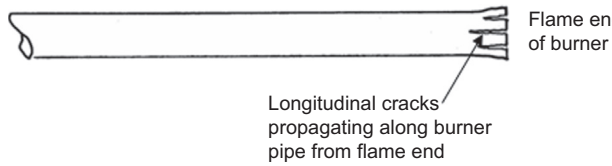


Figure 11.11 Failure of an A 316 spun cast burner tube

iron becomes vulnerable to rapid oxidation. In the face of significant opposition from both maintenance staff and the burner supplier, the burner pipe was replaced with the "lower grade" A304L stainless. This material is low in carbon reducing the ability to precipitate chromium carbides so protection was maintained and a life of over ten years was achieved.

11.2.4 Furnace Roof Construction

For furnaces, roof design is especially problematic since, unlike a conventional building roof where the supporting structure is below and hence can support the roof, the high temperature inside a furnace requires that the structure is external. This potentially puts the refractory material under tension, its weakest property, as it hangs from the structure.

All early furnaces used a brick arched roof, or modification of the arch, such as the beehive kiln shown in chapter 1. In the arch, Figure 11.12 tapered bricks are used and the arch is built on a temporary frame. Once complete the weight of the bricks creates a downwards force that translates into a sideways force on the walls. If unchecked this force would spread the walls and the roof would fall in, so the walls are braced by double I-beams connected together by the buckstay which prevents the walls moving outwards. Thus the roof is supported by the tension in the steel buckstay and compression in the bricks. Similarly in the beehive kilns, the strapping around the top of the walls serves a similar function to the I-beams and buckstay and prevents the walls spreading.

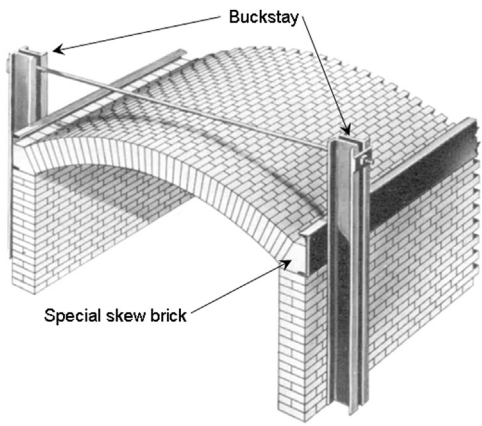


Figure 11.12 Typical furnace arch roof construction (From *Modern Refractory Practice*, Harbison-Walker Refractories)

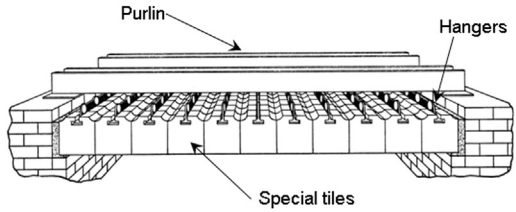


Figure 11.13 An example of an internally tiled furnace flat roof

While the arch is mechanically sound, it requires a varying height above the furnace floor and this may not suit the process operation, owing to its effect on gas velocities etc. Arches are also expensive to design and install. Furthermore, more complex shapes such as compound curves, while possible in arch designs, are both expensive and still limited to relatively simple shapes.

Owing to the limitations of arches, considerable effort has been directed to alternative designs. One alternative is the internally tiled flat roof, Figure 11.13. In this design, special bricks with retaining lugs cast on the top, are hung from stainless steel hangers with the whole assembly supported from external purlins. The principle weakness of this approach is that the lugs on the bricks are in tension, the weakest stress mode for any ceramic; hence the failure risk is high. Failure of just one tile would shut the furnace down, since continuing operation would risk catastrophic failure of the whole roof, so reliable operation can only be achieved by ensuring the highest standards of brick design, manufacture and installation. Special care has to be taken to ensure that no micro-cracks are present in the lugs prior to installation since these are the principle pre-curser to brittle failure. The bricks must be installed carefully without creating any cracks and adequate allowance must be provided for expansion but gas leakage into the steel structure above must be minimised.

Castable refractory can also be used for lining roofs with holes in the steel shell to allow poring of the castable and formwork underneath to support the castable during setting. Anchors are used to support the castable but are normally closer spaced than for other applications. The loads on the formwork are considerable and care has to be taken in its design to prevent collapse, both while pouring, and during subsequent removal. Purpose designed steel formwork is preferred since it can be reused many times and is worth the initial higher investment. Castable can also be gunned onto roofs but losses caused by splashback are normally higher than that for walls and the risk of total collapse is not trivial. Therefore safety issues need careful consideration during design of the gunning operation. Drying and

curing of castable roofs requires even more care than for walls since the tension forces in the refractory increase the risk of spalling.

11.2.5 Furnace Cooling Systems

It was shown in Chapter 9 that only a proportion of the energy into the furnace was utilised in heating the product, the remainder was lost heating the flue gas and the furnace structure. Under steady-state conditions the energy that heats the furnace structure is lost as surface radiation and convection losses. If the heat gained by the furnace structure exceeds that lost from the surface, the structure's temperature will continue to rise and premature failure will result. Where the heat gains are relatively evenly distributed this could cause complete failure of the furnace lining or structure but local heating and subsequent failure is the more normal result.

To prevent these problems cooling is required and generally uses either water or air. With air cooling the opportunity is often taken to preheat the combustion air, increasing the overall furnace efficiency and this should always be the first choice. However, the cooling ability of air is limited owing to its low density and the relatively low temperature differential achievable between the surface being cooled and the air stream. Furthermore, the combustion air mass flow is limited, further restricting its cooling ability. Where the cooling requirement exceeds the capacity of the combustion air, either more air can be used and the excess heat wasted, or cooling water can be utilised. Either technique is a parasitic heat loss, to be avoided whenever possible.

Water cooling has a much higher capacity to remove unwanted heat than any gas and is available on most sites. Its high density and thermal capacity means that relatively small flows are required compared with air and it is frequently used for localised cooling of areas subject to intense heating such as skids in pusher furnaces, burner blocks, burner tubes and components in metallurgical furnaces, etc. The flow needed depends on the inlet temperature of the water and the heat removal required. The outlet temperature is typically limited to approximately 70 °C to prevent vaporisation in low pressure regions and the creation of high temperature "hot spots". The hotter the return cooling water at the equipment discharge, the higher this risk. Higher return temperatures can be tolerated with excellent flow distribution within the cooling water jacket. Unfortunately good flow distribution is rarer than it would be if CFD or physical modelling were used to design cooling jackets, thus optimising flow distribution.

Cooling water systems are either "open circuit" or "closed circuit". In the former cooling systems the water is drawn from a large

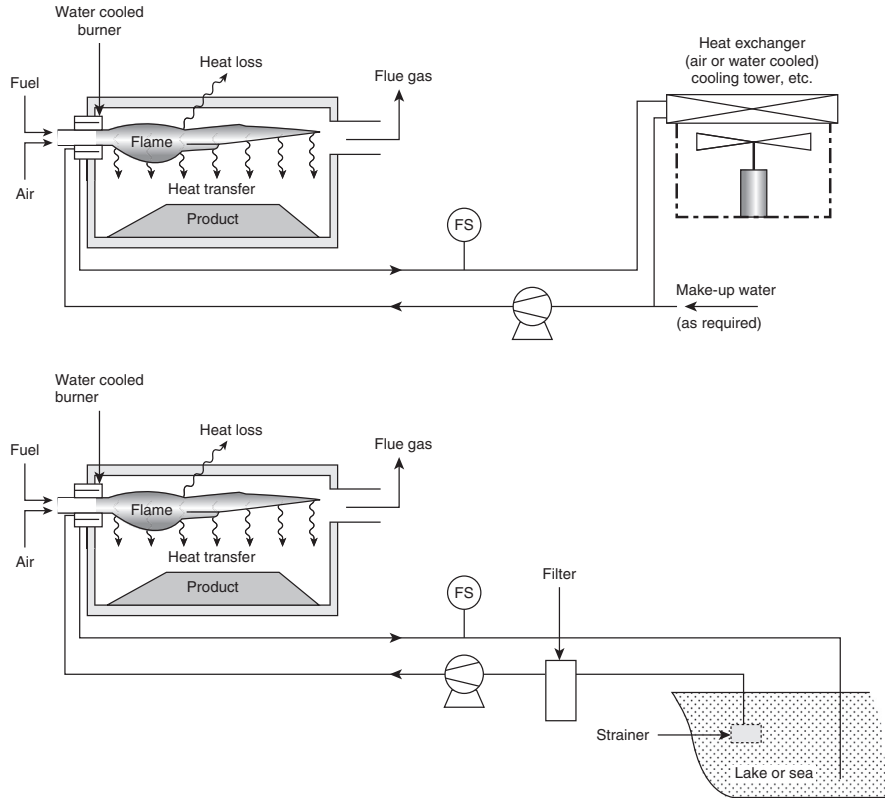


Figure 11.14 Simplified schematic of closed cooling system (top) and open circuit cooling system

reservoir, typically a river or a lake, used for cooling and then returned to the source, Figure 11.14. The permitted temperature rise in open circuit systems is normally very low (1–5 °C) to minimise detrimental environmental effects, hence flows are large. In closed circuit systems, the cooling water is reused continuously and cooled before reuse by heat exchange in a cooling tower or with a separate open circuit system. Where sea water is used, it is normally as the heat sink in a closed circuit system, rather than in open circuit, owing to the corrosion issues associated with its use.

Cooling water should be cool and clean with relatively low levels of dissolved or suspended solids. Suspended solids should be removed by filtration but excessive levels of dissolved solids can cause scale formation within cooling water jackets especially at local hot spots. Once scale is formed it reduces heat transfer and the metal temperature of the cooling jacket increases, leading to water jacket failure if left unchecked. To prevent failure, the scale must be removed using acid cleaning. This tends to be a more significant problem with open circuit

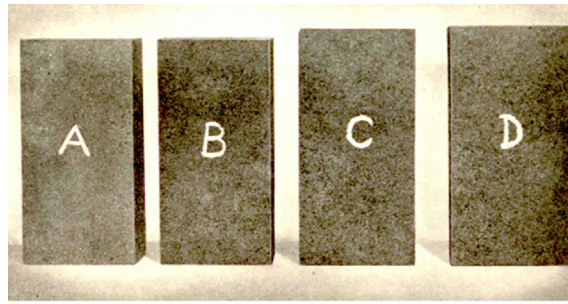
systems and water treatment is required where dissolved solids are excessive. This can take the form of water softening or dosing with chemical additives to flocculate calcium compounds and prevent scale formation. Where the latter is used, the excess flocculated solids must be purged from the system or they will tend to concentrate owing to water loss, especially where evaporative cooling is used.

11.3 Practical Engineering Considerations in the Use of Refractories

There are a huge range of ceramic refractory materials available and these materials are described briefly in section 11.4 but before examining the properties of the various types of refractory we will consider some of the practical issues that need to taken into account during the selection process.

Refractories, particularly those exposed to the inner surface or hot face of the furnace are generally consumed during the normal operating cycle or campaign. Indeed, it is generally the case that refractory failure through erosion, thermal destruction or mechanical collapse determines the operational campaign of a furnace. Therefore the design of the furnace must allow replacement of the refractory material during its life. Depending on the process application, this replacement may be six-monthly, annually or bi-annually. However, in some cases the furnace may operate for much longer periods between refractory replacement. For many processes, refractory replacement is the next highest operating cost after energy, therefore selection of the correct refractory and avoiding premature failure is critically important. Refractory failures can be divided into three main categories, incorrect choice of material, poor installation, and those caused by normal or adverse operating conditions.

Furnaces are generally constructed using a number of different types of refractories, matching the local furnace environment in any particular region with the most suitable refractory and construction method. Selecting the correct refractories for a particular furnace should be carried out in conjunction with the refractory suppliers, since they have specific technical data on their products and the background experience of the performance history of their products. It should be emphasised that the data given in Tables A11.1 to A11.8, in appendix 11A, are only typical values taken from a number of manufacturers' information sources, but since many refractories are made from naturally occurring deposits, there will inevitably be geographical mineral variations that can affect the properties of the refractory. Figure 11.15 shows how differing raw material sources can affect the brick properties. It is also important as an operator to keep a



A – Original 'green' moulded brick
B – Fired brick using Grecian chrome ore
C – Fired brick using Zimbabwean chrome ore
D – Fired brick using South African chrome ore

Figure 11.15 Effect of raw materials on refractory properties (Photo courtesy of Vesuvius Refractories Ltd.)

comprehensive record of refractory performance in each furnace, since this will provide the best guide to optimising the most economical selection of refractories.

Refractory bricks are installed using a thin (1–3mm) layer of the correct bonding cement between each brick, or are laid together with dry, tight fitting faces. Dry face bricking is often employed to form arches, or in rotary kilns, where a wooden or steel former, bent to the correct internal curvature, is used to support the bricks as they are laid. Arches and brick rings should be formed from custom tapered bricks of at least two different tapers to ensure a tight fit. If the external furnace structure is constructed from steel, then allowance should always be made for the bricks to expand in all directions to their operating dimensions. This is generally achieved by putting thin spacers of cardboard, wood of mild steel plates between brick layers at regular intervals. The number and thickness of the spacers can be calculated from knowledge of the thermal expansion and permanent linear change on heating of the refractory. As the furnace heats up the spacers burn away, allowing the refractory to expand into the resulting gap.

Furnaces are usually slowly heated, after the installation of new brickwork and the refractory supplier should supply information on the required rate of heating. This may be achieved using the furnace burner(s) at a low firing rate, or may require special warm up burners that are temporarily inserted into the furnace. Refractory bricks that are incorrectly installed or heated too rapidly to duty temperature will fail very quickly, either by falling out or spalling. Bricks fall out owing to the use of incorrect spacers or too rapid heat up. Spalling, where a layer of 25–100mm breaks away from the working surface of individual bricks, is caused either by insufficient allowance for

expansion, or too rapid heat up which results in excessive stress at the hot face.

The installation of monolithic refractory sections that are cast, rammed or sprayed from refractory cement is more critical than that of bricks. Using the correct water content in the refractory cement mixture is critical, since this affects the bonding, workability and ultimate strength. Once the green refractory is installed it must be cured and heated to duty temperature according to the manufacturers instructions, otherwise early failure will result.

All refractories have a finite life. Depending on the furnace duty and mode of operation, they are subject to wear, surface slagging/coating and attack by corrosive/reducing gases or materials that reduce their strength or refractoriness e.g. iron oxide. Operational temperature excursions beyond the refractory temperature limits will result in melting, usually recognised by a glassy hot face surface. Refractory bricks have a tendency to bond together over a period of time under hot operation owing to migration and changes to the granulation on the material. These changes may also adversely affect the porosity, making the surface more susceptible to corrosive attack.

11.4 Ceramic Refractory Materials

Refractory materials are generally specified according to the predominant ceramic material in the mixture. Hence we have a general classification of furnace refractories into a number of groups, most common amongst these being:

- Silica, Siliceous 97–70% SiO_2, 0.5–15% Al_2O_3
- Alumina, Aluminous 90–20% Al_2O^3, 5–70% SiO_2
- Chromite, Magnesite/Chromite, Magnesite 40–0% Cr_2O_3, 13–90% MgO
- Dolomite ~40% MgO, 40–50% CaO
- Zircon, Zirconia ZiO_2:SiO_2, >95%ZiO_2
- Carbon, Silicon Carbide >99%C, >90%SiC
- Insulation materials, Diatomite, Vermiculite, Calcite, Ceramic fibre
- Sands for foundry casting Silica, Bonded

Trace metallic elements, such as TiO_2, Fe_2O_3, FeO, and MnO, are also present in most of these refractories and can have a significant effect on their properties. They also provide a flux bond in the fired material.

Manufacturers supply refractories in a number of forms for use in furnaces. The most common is as a shaped brick, having either parallel sides for flat surfaces or tapered sides for arch constructions. Bricks

may be pre-fired by the manufacturer in a kiln prior to installation, chemically bonded or simply pressed. In the case of the latter two brick types, they must be cured in-situ in the furnace after installation according to a strict heating cycle, supplied by the manufacturer, before they can be subjected to normal operational duty. Refractory is also supplied as ground material in bags. Depending on the grade, ground refractory is used as an air setting, non-air setting or hydraulic setting cement for bonding bricks, as a spraying or gunning material for hot repairs (spraying), or to form difficult internal furnace shapes e.g. a hot cyclone (gunning), or as a castable or rammable material for the construction of monolithic linings and burner quarls.

Insulating materials are generally supplied as lightweight bricks, sheets, or as loose material suitable for dry filling or spraying. Ceramic fibre sheets and calcite blocks can be surface treated to harden the face, making it impermeable to moisture etc. and thus allowing the material to be used for certain duties in place of a conventional refractory.

11.4.1 Testing of Refractories

Selection of the correct refractory for a particular duty relies on information supplied by the manufacturer and from prior experience. Refractory testing is carried out according to national or international standards (ASTM, BSI), and a number of important test results are used to enable the correct refractory to be selected. These include:

- **Density** - the bulk density, expressed in weight/unit volume including the pore spaces;
- **True Specific Gravity** - the weight of unit volume of crushed material relative to the weight of unit volume of water;
- **Apparent Specific Gravity** -the weight of unit volume of refractory brick relative to the weight of unit volume of water;
- **Porosity** - the ratio of porous volume to total volume, usually expressed as a percentage. The true or apparent porosity relates to the specific gravity value used in the calculation;

$$\text{Porosity} = 100\left(1 - \frac{\text{bulk density}}{\text{Specific gravity}}\right)\%$$

- **Refractoriness** - a measure of the heat resisting properties of refractories. It is determined by testing a cone of the refractory against a set of standard Pyrometric Cones (Seger or Orton) of known refractoriness in a test furnace, where the temperature is raised by 10 °C/min (Seger) or 5 °C/min (Orton) until the tip of the cone is level with its base. The result is expressed as a cone number or pyrometric cone equivalent (PCE) temperature;

- **Refractoriness under Load** - the refractory is heated at 10 °C/min whilst being subjected to a loading (usually tension or sheer) of 0.194 or 0.346 MN/m^2 (28 or 50 psi). The result is expressed as the temperature at which the material fails;
- **Cold Crushing Strength** - standard mechanical strength test of a cube in compression. Expressed as force/unit area;
- **Thermal Conductivity** - is normally reported at a number of temperatures since it is usually temperature dependent;
- **Specific Heat** - this is normally reported as a single value, since it is relatively insensitive to temperature;
- **Thermal Shock Resistance** - this is expressed as the number of times a test piece of the refractory will undergo a cycle of heating to 1000 °C and then shock cooled in air before failure occurs, i.e. test piece pulls by hand into two or more pieces. This is sometimes referred to as the spalling resistance index;
- **Thermal Expansion** - the reversible expansion/contraction that takes place on heating/cooling to 1000 °C;
- **Permanent Dimensional Change on Heating** - the irreversible expansion/contraction that occurs on heating to 1500 °C for 2 hours and cooling. Usually expressed as a percentage of the original length or volume.

11.4.2 Properties and Uses of Refractories

Silica and Siliceous Refractories

Silica refractories are generally lime bonded with a silica content of >93%. Table A11.1 shows the various sub-divisions and typical properties of these materials. This refractory was used extensively in the steel and carbonising industries until LD convertors and natural gas superseded these processes. They are still used in the glass industry for the upper sections of regenerators, blast furnace stoves and arc furnace roofs.

Siliceous refractories, sometimes termed as semi-silica, contain a minimum of 80% silica and 10–15% alumina and their typical properties are also shown in Table A11.1. They are extremely resistant to ash and slag by forming a viscous glaze, and are volume stable. They are used in the lower sections of regenerators and re-heating furnaces.

Alumina and Aluminous Refractories

Alumina refractories are made from high alumina content minerals, Al_2O_3>60%, such as bauxite or fused alumina with various bonding minerals. Their typical properties are shown in Table A11.2. These refractories are resistant to attack by iron oxide and basic slags, and are

used in high temperature areas (>1700 °C) in glass tanks, ceramics kilns, tunnel kilns and alumina smelters.

Sillimanite refractories contain 50–60% Al_2O_3 and 45–35% SiO_2 and are made from naturally occurring Sillimanite, Kyanite or Andalusite fired at 1500–1800 °C. Refractories made from these materials have similar properties as alumina refractories, but slightly poorer mechanical strength and thermal conductivity. They are widely used in blast furnace linings and stoves, arc furnaces, ladles, soaking pits, re-heating furnaces, glass tanks, rotary kilns and boilers.

Firebricks are the most common refractory, and contain 20–40% Al_2O_3 and 70–50% SiO_2. They are made by dry pressing the material into bricks, termed green bricks, and then firing them in long tunnel kilns at 1000–1200 °C. The operational duty temperature rises with increasing alumina content. They are used extensively in most combustion chamber construction including kilns, boilers, and process heaters. Low alumina content bricks are used for the bottom sections of refractory regenerator chequer-work and stacks.

Chromite/Magnesite/Alumina Refractories

Chromate refractories are composed of Chromate ore (35–40% Cr_2O_3) with not more than 25% MgO. They may be fired or chemically bonded, but are not commonly used as they have a low hot strength and a tendency to bursting in contact with iron oxides.

Chromite-Magnesite bricks are composed of a mixture of Chromate ore and fired magnesia with a predominance of Cr_2O_3. In the fired state the magnesia content, some as free Periclase, is between 25% and 50%. These refractories have excellent hot strength, good thermal shock resistance, volume stability, good slagging resistance and are neutral to oxidising atmospheres. They are used for roof construction in basic steel making furnaces, copper converters and reverbatory furnace linings, glass tanks, burner quarls and cement kiln burning zones. Magnesite-Chromite, often termed Magchrome, bricks are fired to contain 55–80% MgO. They have a higher refractoriness under load, up to 1650 °C, and thermal shock resistance than Chromite-Magnesite bricks, and are used in the same applications, but for more severe duties.

Magnesite refractories are made from dead burnt magnesia. Dead burning requires the magnesia, either from natural deposits or sea water extraction, to be fired as a finely divided material to >2,000 °C in a kiln, rendering it resistant to moisture and free from irreversible expansion/contraction. The magnesia content is >80%, and forms the basic content of the brick. These refractories have a high refractoriness under load, >1750 °C, and excellent slag resistance. Major applications are in hot metal mixer linings, basic oxygen steel converters, arc furnaces, furnace hearths, copper, lead and nickel furnaces and converters.

The typical properties of this group of refractories are shown in Table A11.3. There is a preference to use alternative refractories to those that include chrome if possible, since any waste material generated from relining or replacement is classified as a hazardous waste, incurring significant additional disposal liabilities and costs. The most common alternative is to replace the chromite with up to 15% alumina, the properties of which are shown in Table A11.4.

Dolomite Refractories

These refractories are made from calcined or dead-burnt naturally occurring dolomite or limestone deposits. Their typical properties are shown in Table A11.5. The bricks are commonly bonded with tar or pitch, with approximately 5% tar content, which burns off when first fired. They have a high cold crushing strength and reasonable refractoriness under load. They are used extensively in fettling hearths of open-hearth furnaces, linings of oxygen steel converters and electric furnace bottoms.

Zircon and Zirconia Refractories

Zircon is a naturally occurring material, $ZiSiO_4$, and is found in heavy mineral deposits such as illmanite, rutile, monazite and garnet as river or beach sands. High-grade zircon melts at about 2190 °C, softens between 1600 °C and 1800 °C and is volume stable up to 1750 °C. In addition to a high melting point it has very low thermal expansion and good resistance to abrasion. Zircon is used when acidic refractory is required. A cheaper type of zircon-refractory is prepared by mixing zircon with alumina. It is reported to have refractory properties as good as those of zircon. At high temperatures the following reaction takes place: The dissociation of zircon starts at 1400 °C and at about 1600 °C a complete reaction takes place forming a stable product of zirconia and mullite. High-grade zircon sand is largely used in the foundry industry for moulding. It does not wet the molten metal, thus giving a better and smoother surface to the casting.

Zirconia occurs naturally as baddeleyite, or is prepared from zircon. Pure zirconia has a low thermal conductivity and high volume change on heating, about 9% contraction at 1000–1100 °C, giving rise to poor thermal shock resistance. A small amount of MgO, CaO or Y2O3 is generally added to stabilise the material, giving it relatively linear expansion characteristics and this is termed as stabilised cubic zirconia. Zirconia refractories are considered to be basic and find specialist applications in induction furnace linings, crucibles, and casting or pouring nozzles. Table A11.5 summarises the typical properties of zirconia based refractories.

Carbon Refractories

Pure carbon refractories are made from hard metallurgical grade coke, dead burnt petroleum coke or naturally occurring graphite. They are usually bonded with tar or pitch. They have very high refractoriness and high strength and rigidity and are inert to slags, metal and reducing atmospheres. They react and gasify above 350 °C with oxidizing atmospheres and metal oxides. They are used in blast furnace hearths and acid pickling baths (usually metallurgical coke) and electric furnace electrodes (petroleum coke or graphite). Silicon carbide refractories are made from clay bonded silicon carbide, or by sintering at high temperature. They have very high thermal conductivity, mechanical strength, corrosion resistance and thermal shock resistance. Silicon carbide is used for casting high temperature burner nozzles, furnace beams, crucibles and ignition dishes. They generally have a working temperature of ~1600 °C in oxidizing atmospheres, and up to 2,000 °C in reducing atmospheres. Table A11.5 summarises the typical properties of carbon based refractories.

Insulating Refractories

Most of the refractory materials so far reviewed in this section are characterised by high thermal conductivity, resulting in a potentially significant loss of heat though the furnace walls. Insulating refractory materials are typified by high porosity, low crushing strength, relatively low refractoriness and low thermal conductivity. They may be used as hot-face insulators (i.e. as a stand-alone refractory) or as a backing material behind a higher duty refractory, depending on the severity of the conditions, the fuel and the physical and chemical nature of the insulator. Tables A11.6 and A11.7 summarise the significant typical properties of these materials. The use of asbestos as an insulation material is now prohibited owing to the health hazards involved in its application and removal.

11.5 Heat Resisting and Refractory metals

As noted above in section 11.2, it is not always possible to make all the heat resisting components in a furnace from ceramic refractories and heat resting metals perform a crucial function in most furnaces. The principle properties required from metallic furnace components include:

- Resistance to high temperature corrosion
- Sufficient strength at operating temperature
- Need to maintain dimensional stability at operating temperature

- Resistance to creep under load
- Resistance to degradation under cyclic heating and cooling regimes

11.5.1 Effect of Elevated Temperature on Metal Properties

Metals owe their strength to their ordered crystal structure and in particular the presence of alloying elements of different atomic size that distort the structure and hence give it rigidity, Figure 11.16. Pure metals tend to be very soft because the crystal structure is not distorted and the atoms can move relatively easily in relation to each other. Another factor that affects rigidity is the phase of the metal crystal, different phases being stable in different temperature ranges. A good example to illustrate this point is copper. Impure copper is hard and difficult to work whereas annealed pure copper which is so soft, it can be bent by hand. However, repeated bending causes the atoms to move relative to each other and the structure changes and becomes hard. If it continues to be bent in this condition then the crystal bonds and the surface will crack but if the metal is re-heated and re-annealed the soft structure is restored. All practical metals that are used for structural applications are alloys and, as engineers, we owe a great debt to metallurgists and material scientists who have spent a great deal of effort in developing improved alloys. Much of the effort has been directed towards improved performance at high temperature.

As metals are heated, the atomic bonds in the crystal become weaker and the metal softens. Softening increases with increasing temperature until the metal melts. As inferred above, many alloys also undergo phase changes as temperature increases which also affects the properties. As a consequence of these changes, all metals become weaker with elevated temperature, either softening to the point where they cannot resist the forces imposed on them and fail, or they slowly elongate under tensile stress, a process known as "creep".

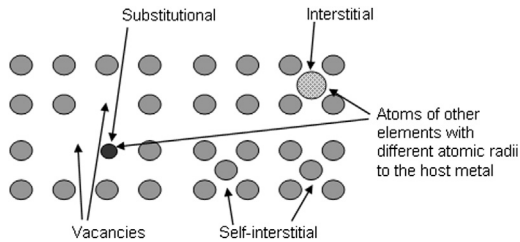


Figure 11.16 Example of alloying element providing strength to a metal by distortions of the crystal structure

In nature, most metals occur combined with other elements, especially oxygen or sulphur and these are the most stable forms. Hence there is a tendency for most metals to oxidise but the reaction needs activation energy to trigger it. Since elevated temperatures provide this energy many metals, including iron, are subject to rapid oxidation under typical furnace conditions. This results in rapid loss of metal mass as the metallic crystal becomes an amorphous oxide that contributes nothing to the strength of the parent metal. For example, carbon steel normally used for the furnace shell and support framework, forms oxide scale on the surface at temperatures over 200–250 °C and rapidly loses strength above 300 °C resulting in a maximum practical service temperature 300–375 °C. However, there are many furnace components such as burner nozzles, air registers, swirlers, hot air ducting, tube hangers, support brackets, etc, that need to operate at much higher temperatures.

Some metals, such as aluminium, chromium, etc, are so reactive that they react with oxygen at room temperature to form an oxide layer which is so stable that it becomes an impenetrable barrier preventing further contact between the parent metal and its environment, Figure 11.17. In this condition the metal is very resistant to further oxidation and is said to be passivated. Aluminium, Chromium and Magnesium all exhibit this phenomenon. Chromium readily alloys with iron and when added in sufficient quantity (>12%) the oxide layer developed by the chromium is sufficiently stable to cover the iron also and passivate the combined alloy, which is known as stainless steel.

11.5.2 High Temperature Alloys

Owing to its ability to passivate iron, chromium is a basic component of most high temperature alloys. Nickel is also very important

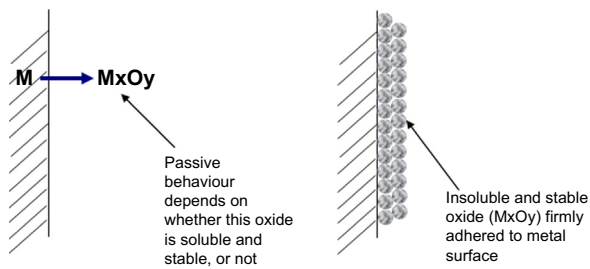


Figure 11.17 Schematic illustration of how a passive oxide layer protects the metal

because, while it does not as readily from an oxide layer like chromium, it is very resistant to oxidation owing to its relatively low reactivity. In practice most heat resisting stainless steels are alloys of iron, chromium and nickel with other trace components such as molybdenum, titanium, silicon and nitrogen added to modify the properties and provide improved performance under specific conditions. Stainless steels are classified into five distinct family groups according to the chromium and nickel content. Each of these groups exhibit distinct properties which are summarised in Table 11.1.

Within these five family groups are an enormous range of individual alloys and an almost bewildering classification system comprising the original AISI, DIN and manufacturers' propriety classifications, together with the new UNS and Euronorm systems.

Within the austenitic group are special heat resisting grades with increased chromium and nickel content than the standard grades (Cr: 20 – 24 % & Ni: 10 – 35 %). Carbon content is low at <0.2% and for the S grades, carbon is less than 0.08%. This is important because, as noted earlier, chromium carbide precipitation at moderate temperatures is one of the main failure modes of stainless steel. These steels exhibit good resistance to oxidation (scaling) at high temperatures (950 – 1100 °C) and good high temperature strength. Common grades are 309, 310 and 30815, while S30815 (extra low C) has high resistance to sigma phase precipitation. These heat resisting

Table 11.1 Characteristics of the Main Classifications of Stainless Steels

Stainless Steel Group	*Cr (%)*	*Ni (%)*	*Other*	*Characteristics and Typical Uses*
Austenitic	>18	>8	C, Mo	Excellent corrosion resistance in the range −200 °C to + 900 °C. Widely used in furnaces, food applications, etc.
Ferritic	12−18	−		Moderate corrosion resistance. Used for fume extraction systems, chutes and hopper liners, etc.
Duplex	18−28	4.5−8	Mo, N	Mixed ferritic/austenitic crystal structure. Has a higher tensile and yield strengths than either parent material and a high resistance to stress corrosion cracking
Martensitic	12−18	−	C	High strength and hardness can be developed but poor weldabiliy. Used for knife blades, shafts and spindles, nozzles, springs, etc.
Precipitation hardening	>17	>4	Cu, Ni	Very high strengths with moderate to good corrosion resistance. Good strength at high temperature (950−1100 °C). Used for high strength shafts, valve spindles high strength wire, etc.

austenitic steels are used for muffle liners, radiant tubes and other furnace parts.

Service Temperature

The service temperatures quoted are based on a corrosion rate of 10 mg/cm^2 per 1000 hours of operation in hot air but the actual atmosphere has a major effect on service life. For example, sulphur bearing gases and reducing gases CO, H_2, etc, shorten the life significantly since they attack the passivating oxide layer or prevent its renewal after loss. Where these and other gases are present it may be necessary to undertake tests to determine most suitable material. These tests are based on uniform corrosion over the surface of the test specimen but in real applications the risk of more rapid, localised corrosion is significant. This occurs as result of local surface conditions preventing the oxide layer from regenerating. These conditions can arise externally as a result of local shielding of the steel preventing oxygen from reaching the surface, or by internal changes in the metal that destroy the oxide layer and result in intergranular corrosion. The former can be prevented by appropriate design, minimising the risk of oxygen starvation at the surface, while the latter is dependent on appropriate material selection. This is considered in further detail in the following section.

Intermittent duty is more onerous than continuous duty and both maximum service temperature and life are reduced as a result of shedding of passive oxide skin during cooling and reheating (spalling). This is caused by differential expansion between oxide film and metal loosening the former's adhesion. The higher nickel content of austenitic stainless steels increases spalling resistance.

Intergranular Corrosion

Any metal with intermetallics or compounds is susceptible to intergranular corrosion and it is common in austenitic stainless steels but also occurs in ferric & two-phase stainless steels as well as nickel based corrosion resistant alloys, Figure 11.18. It is a significant problem from an engineering viewpoint, even at ambient temperature and often follows heating of the steel by welding during the fabrication process and hence is sometimes called "weld decay" (Tretheway and Chamberlain 1998). In this case, it is caused by carbon in the steel reacting with chromium to form chromium carbide which is precipitated at the grain boundaries, and in-turn results in chromium metal content at the boundary being effectively reduced below the minimum required to maintain the oxide layer which locally breaks down. The material is said to be sensitised and is locally no longer "stainless" and with time corrosion occurs at the boundary and whole grains of metal can become detached.

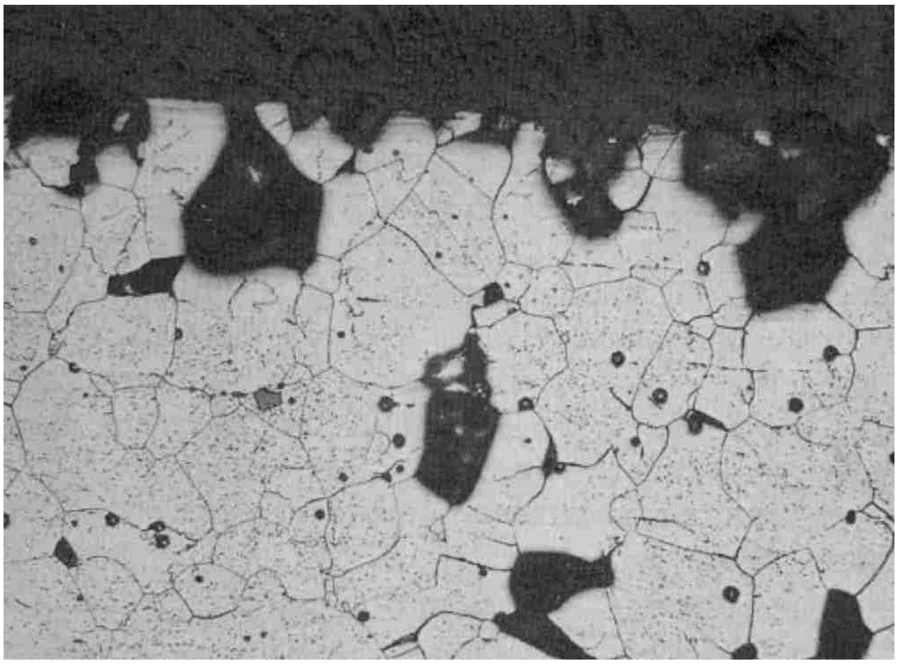


Figure 11.18 Example of intergranular decay in austenitic stainless steel (A304) (From Tretheway and Chamberlain, reproduced with kind permission of Pearson Education)

Proprietary High Nickel Alloys

In addition to the stainless steels considered above, a range of proprietary high nickel alloys are available with service temperatures up to 1150 °C. These alloys are commonly known by their trade names such Hastelloy, Inconel, Incoloy, and Nimonic, each representing a family of proprietary alloys. The service duty cannot be deduced from the chemical composition alone since many of these alloys undergo complex heat treatment regimes to optimise the structure for the intended duty and it is essential that performance specifications are obtained from the manufacturer.

11.6 Practical Engineering Considerations in the Use of High Temperature Metals

The first requirement is to understand the service duty required from the individual component. This includes:

- Operating temperature range;
- Static stress loading (tensile, compressive or shear);

- Dynamic stress loading (tensile, compressive or shear);
- Frequency that loads are applied/removed or cycled (fatigue considerations)
- Expected life in years and furnace warming and cooling cycles

While all these are important and most are relatively straightforward to calculate or estimate, the operating temperature range is frequently misquoted. This normally arises from the assumption that the component will operate at the temperature of its immediate surroundings. Errors arise from two principle sources, either the effects of radiative heating are underestimated or the effect of localised convective cooling is ignored. Radiative heating serves to increase the temperature of the component, while localised convective cooling reduces its temperature. In practice most components have a temperature gradient within them, and this knowledge is an important input into material choice. Owing to the fact that most high temperature materials have an optimum temperature operating window, choosing a material for too high a temperature may be as inappropriate as specifying one for too low an operating temperature. This is because changes can sometimes occur at intermediate temperatures. For example ferritic & duplex steels undergo a structure change at 370 – 540 °C that gives an increase in hardness and a reduction in toughness known as 475 °C embrittlement. In addition, ferritic steels undergo sigma phase embrittlement at ~560 °C. Failure to consider these types of changes can result in premature failure of the component.

The tensile, compressive or shear stress loadings, both static and dynamic, can be calculated from the furnace duty requirements. Permissible loads for stainless steels at temperature are provided in various standards such as AS 1202 and for, special alloys, they are available from the manufacturer. The frequency that loads are applied and removed (for fatigue considerations) can also be determined from the furnace duty. However, care needs to be taken not to overlook the obvious, for example the fatigue loading of a rotary kiln rotating at 1 rpm and operating 320 days per year is 460,800 cycles per annum (60 × 24 × 320) but for a kiln with ten satellite coolers as shown in Figure 1.6, the annual loading is over 4.6 million cycles. This is because each cooler also imposes a cyclic loading in addition to the kiln rotation so the fatigue cycles increase tenfold.

The expected life in years and furnace warming and cooling cycles is another important factor when defining the material specification. A shorter life can be accepted from small easily replaced components than required from large expensive difficult to replace items that form an integral part of the furnace structure.

11.7 Concluding Remarks

It can be seen that although most of this book is concerned with furnace process design, the mechanical design of furnaces and the choice of materials, especially refractories and high temperature metals is complex and this chapter can only provide a flavour of the issues that need consideration. Even materials with nominally similar specifications can vary in their in-service performance owing to different source of raw materials, in the case of refractories, and different heat treatment processes in the case of sophisticated high performance alloys. To achieve optimum furnace performance, and long life between repairs, it is essential to fully understand the duties required from both refractories and high temperature metals. It is then necessary to select appropriate materials to meet these duties. It is unlikely that any individual engineer has all the necessary knowledge and experience to make these decisions in every case and help should be sought from advisory services and research associations such as, CERAM Research (refractories) and the Stainless Steel Advisory Service (high temperature metals). Individual suppliers will also advise on their own materials but such advice is unlikely to be unbiased.

References

Richards, P. K. (1990). A design guide for the refractory linings of vessels and transfer lines. *Proc. Instn. Mech. Eng., 204*, 51–67.

Tretheway, K. R., & Chamberlain, J. (1998). *Corrosion for science and Engineering* (2nd ed, pp. 144–149). Longmans.

Selection of Relevant Standards

ASTM C1054-03, Standard Practice for Pressing and Drying Refractory Plastic and Ramming Mix Specimens

ASTM C865-02, Standard Practice for Firing Refractory Concrete Specimens

ASTM C201-93. (2004). *Standard Test Method for Thermal Conductivity of Refractories*.

ASTM C134-95. (2005). *Standard Test Methods for Size, Dimensional Measurements, and Bulk Density of Refractory Brick and Insulating*.

ASTM C874-99, Standard Practice for Rotary Slag Testing of Refractory Materials

ASTM C874-99, Standard Practice for Rotary Slag Testing of Refractory Materials

ASTM C863-00. (2005). *Standard Test Method for Evaluating Oxidation Resistance of Silicon Carbide Refractories at Elevated Temperatures*.

BS. (1902). *Methods of testing refractory materials*. Note: This standard has many parts covering a wide range of refractory properties.

BS EN 993–12:1997, BS 1902-5.2:1997, Methods of test for dense shaped refractory products. Determination of pyrometric cone equivalent (refractoriness)

BS EN 993–4:1995, BS 1902-3.9:1995, Methods of test for dense shaped refractory products. Determination of permeability to gases

BS EN 993–6:1995, BS 1902-4.4:1995, Methods of test for dense shaped refractory products. Determination of modulus of rupture at ambient temperature

BS EN 993–8:1997, Methods of test for dense shaped refractory products. Determination of refractoriness-under-load

BS EN 993–9:1997, Methods of test for dense shaped refractory products. Determination of creep in compression

BS EN 993–3:1997, Methods of test for dense shaped refractory products. Test methods for carbon-containing refractories

Advisory Organisations

CERAM, Queens Road, Penkhull, Stoke-on-Trent, Staffordshire ST4 7LQ, United Kingdom, Web: http://www.ceram.co.uk/

Stainless Steel Advisory Service, $^{C}/_{O}$ British Stainless Steel Association, 59 Clarkehouse Road, Sheffield S10 2LE, UK, Web: http://www.bssa.org.uk/index.php

Appendix 11A

Table A11.1 General Properties of Silica and Siliceous Refractory Materials

Type			Silica				
			Super Duty	*High Duty*	*Medium Duty*	*Low Duty*	*Siliceous*
SiO_2		%	96—00 — 97.30	95.00 — 96.00	94.00 — 95.00	93.00 — 94.00	88.9
TiO_2		%	0.12	0.10	0.20	0.20	0.40
Fe_2O_3		%	0.93	0.75 — 1.00	1.00 — 1.50	1.20 — 1.80	1.00
Al_2O_3		%	0.30 — 0.50	0.75 — 1.00	1.30 — 2.00	2.00 — 2.55	9.30
MnO		%	Trace	Trace	Trace	Trace	Trace
CaO		%	1.55	1.63	1.90	1.90	0.20
MgO		%	0.15	0.20	0.30	0.20	0.30
K_2O/Na_2O		%	0.10	0.15	0.30	0.35	0.40
Loss on ignition		%	0.22	0.20	0.10	0.25	0.30
Density		kg/m^3	1880 — 1760	1800 — 1670	1820 — 1630	1860 — 1750	1860
True porosity		%	19 — 23	24 — 27	24 — 30	22 — 25	23.6
Apparent porosity		%	18.5 — 23	23 — 26.5	23 — 29.5	21 — 24	20
Specific gravity			2.30 — 2.35	2.32 — 2.37	2.32 — 2.38	2.34 — 23.9	2.39
Refractoriness (PCE temperature)		°C	1720 — 1730	1710 — 1730	1700 — 1710	1700 — 1710	1630
Refractoriness under load		°C	1670 (50psi)	1640 (50psi)	1630 (50psi)	1450 (50psi)	1450 (25psi)
Cold crushing strength		MN/m^2	36.0	29.0	24.5	20.0	10.2
Thermal expansion		$X\ 10^{-5}$	1.1 — 1.3	1.1 — 1.25	1.0 — 1.25	1.0 — 1.1	0.66
Permanent dimensional change on heating		%	+0.1 — +0.5	+0.3 — +1.0	+0.2 — +1.2	+0.4 — +1.5	0
Thermal shock resistance			4 — 6	4 — 10	4 — 10	10 — 15	>10
Thermal conductivity	0—500°C	W/m°C	1.16	1.16	1.16	1.16	0.87
	500—1000°C	W/m°C	1.44	1.44	1.44	1.44	1.16
	1000—1500°C	W/m°C	1.73	1.73	1.73	1.73	1.44
Specific heat		kJ/kg°C	1.11	1.11	1.11	1.11	1.09

Table A11.2 General Properties of Alumina and Aluminous Refractory Materials

			Alumina						*Silimanite*			*Firebrick*			
Type			*A*	*B*	*C*	*D*	*E*	*F*	*G*	*H*	*I*	*J*	*K*	*L*	*M*
SiO_2		%	4.50	13.41	23.82	32.01	38.42	43.44	34.44	39.84	45.00	52.56	57.32	60.40	68.88
TiO_2		%	2.05	1.79	2.00	2.18	1.85	1.74	1.50	1.50	2.30	1.24	1.15	1.15	1.24
Fe_2O_3		%	1.80	2.08	1.85	2.02	2.34	2.62	0.90	1.02	1.82	2.57	2.66	2.01	2.67
Al_2O_3		%	91.32	82.04	71.86	63.26	56.20	51.10	63.05	56.88	49.87	42.02	37.08	34.50	24.03
MnO		%	Trace	Trace	Trace	Trace	Trace	Trace	Trace	Trace	Trace	Trace	Trace	Trace	Trace
CaO		%	0.20	0.30	0.36	0.29	0.42	0.37	0.12	0.20	0.35	0.56	0.58	0.37	0.50
MgO		%	0.10	—	Trace	0.11	0.28	0.16	—	Trace	0.21	0.20	0.24	0.46	0.42
Na_2O		%	—	—	0.15	0.14	0.12	0.25	0.08	0.23	0.20	0.30	0.35	0.30	1.11
K_2O		%	—	—	—	—	—	—	—	—	—	0.40	0.52	0.45	0.90
Loss on ignition		%	0.10	0.10	0.12	0.20	0.15	0.15	0	0.05	0.13	0.15	0.10	1.12	0.20
Density		kg/m^3	2950	2730	2380	2350	2310	2380	2350	2300	2250	2030	2000	2020	2120
True porosity		%	23—27	23—28	25—30	25—30	24—28	23—24	22—24	22—24	20—22	22	22	21	20
Apparent porosity		%	22—25	22—27	24—29	24—29	23—27	21—23	21—23	21—23	19—21	20	20	18	18
Specific gravity			3.90	3.65	3.18	3.00	3.00		2.90			2.60	2.56	2.56	2.65
Refractoriness (PCE temperature)		°C	1880	1850	1825	1805	1790	1780	1805	1790	1780	1740	1720	1690	1610
Refractoriness under load		°C	1550	1500	1560	1530	1500	1500	1620	1610	1580	1510	1500	1400	1220
Cold crushing strength		MN/m^2	100.0	85.0	70.0	70.0	60.0	65.0	70.0	60.6	65.0	50.0	22.2	40.0	20.0
Thermal expansion		$X\ 10^{-5}$	0.80	0.75	0.70	0.68	0.62	0.55	0.45	0.47	0.48	0.57	0.58	0.61	0.68
Permanent dimensional change on heating		%	0	0	+0.2	+0.3	+0.5	−0.3	−0.2	−0.2	−0.3	+0.5	−0.75	−1.00	+0.5
Thermal shock resistance			>30	>30	>15	>15	>20	>30	>30	>30	>30	30	30	26	15
Thermal conductivity	0—500°C	W/m°C	2.31	2.02	0.87	0.87	0.87	1.00	1.15	1.15	1.01	0.58	0.58	0.58	0.58
	500—1000°C	W/m°C	2.45	2.31	1.15	1.15	1.15	1.10	1.44	1.44	1.30	0.87	0.87	0.87	0.87
	1000—1500°C	W/m°C	2.74	2.45	1.44	1.44	1.44	1.20	1.73	1.73	1.59	1.15	1.15	1.15	1.15
Specific heat		kJ/kg°C	1.13	1.13	1.05	1.05	1.05	1.10	1.13	1.13	1.09	1.11	1.11	1.11	1.13

A – 90% Al_2O_3 B – 80% Al_2O_3 C – 70/73% Al_2O_3 D – 60/65% Al_2O_3 E – 53/57% Al_2O_3 F – 48/50% Al_2O_3 G – super duty H – high duty I – standard duty J – high duty K – medium duty L – general duty M – low duty

Table A11.3 General Properties of Chromite/Magnesite Refractory Materials

			Chromite		*Chromite - Magnesite*		*Magnesite - Chromite*		*Magnesite*	
Type			*Fired*	*Bonded*	*Fired*	*Bonded*	*Fired*	*Bonded*	*Fired*	*Bonded*
SiO_2		%	4.0–6.0	4.0–6.0	4.0–6.0	4.0–6.0	3.0–4.0	3.0–5.0	2.0–3.0	2.0–3.0
TiO_2		%	0.2	0.2	0.2	0.2	0.1	–	0.1	0.1
Fe_2O_3		%	12.0–15.0	0.5	10.0–14.0	–	4.0–6.0	4.0–5.0	2.0–5.0	2.0–5.0
FeO		%	–	11.0–14.0	–	10.0–14.0	–	–	–	–
Al_2O_3		%	16.0–20.0	16.0–20.0	14.0–20.0	15 0–18.0	4.0–6.0	3.0–4.0	1.0–3.0	1.0–3.0
Cr_2O_3		%	36.0–40.0	36.0–40.0	28.0–30.0	22.0–28.0	6.0–10.0	3.0–4.0	–	–
MnO		%	0.2	0.2	0.1	0.1	0.1	–	0.1	0.1
CaO		%	1.0–2.0	1.0–2.0	1.0–2.0	1.0–2.0	1.0–2.0	2.0–3.0	1.0–3.0	1.0–3.0
MgO		%	13.0–20.0	18.0–22.0	38.0–40.0	30.0–35.0	66.0–76.0	78.0–84.0	85.0–90.0	85.0–90.0
Density		kg/m^3	3000	3200	2850	3200	3200	3100	2940	2840
True porosity		%	22–24	15	22–25	16	15–16	22	15–16	20–22
Apparent porosity		%	20–22	14	22–24	15		20		19–21
Specific gravity			4.00	3.80	3.80	3.75	3.65	3.61	3.50	3.55
Refractoriness (PCE temperature)		°C	1730	1700	>1880	1780	1750	1860	1780	1860
Refractoriness under load		°C	1350	1350	1610	1400	1400	1500	1400	1500
Cold crushing strength		MN/m^2	>41.5	>41.5	20.7	31.0	31.0	34.5	70.0	70.0
Thermal expansion		$X\ 10^{-5}$	0.9	0.9	1.0	0.9	1.0	1.1	1.2	1.2
Permanent dimensional change on heating		%	−0.2		0	−0.7	−0.4	−0.2	−1.0	−0.2
Thermal shock resistance			4	>10	>30	>10	>20	>30		4
Thermal conductivity	0–500°C	W/m°C	1.44	1.16	2.16	1.73	2.60	3.61	4.33	5.77
	500–1000°C	W/m°C	1.73	1.44	2.16	1.73	2.16	2.74	2.89	4.33
	1000–1500°C	W/m°C	1.59	1.44	1.59	1.44	1.88	2.02	2.89	3.61
Specific heat		kJ/kg°C	0.75		0.84	0.84	0.84	0.92		0.94

Table A11.4 General Properties of Magnesite/Alumina Refractory Materials

Type			*Magnesia Fused Spinel*	*Magnesia Fused Spinel*	*Magnesia Spinel*	*Magnesia Spinel*	*Magnesia Spinel*
SiO_2		%	0.40	0.50	0.50	0.40	0.90
TiO_2		%	—	—	—	—	—
Fe_2O_3		%	0.50	0.50	0.50	0.50	0.80
Al_2O_3		%	9.00–12.00	9.00–12.00	9.00–12.00	11.0–14.00	11.00–14.00
MnO		%	Trace	Trace	Trace	Trace	Trace
CaO		%	1.00	1.10	1.00	0.80	1.4
MgO		%	85.00–89.00	84.00–88.00	85.00–89.00	83.00–87.00	82.00–87.00
K_2O/Na_2O		%	0.10	0.10	0.10	0.10	0.10
Density		kg/m^3	2950–3100	2900–3050	2850–3000	2850–3000	2850–3000
Apparent porosity		%	13–15	15–17	16–18	16–18	15–17
Refractoriness (PCE temperature)		°C	>2150	>2150	>2150	>2150	>2150
Refractoriness under load		°C	>1700	>1700	>1700	>1700	>1700
Cold crushing strength		MN/m^2	70.0	70	50	45	65
Thermal expansion		$X\ 10^{-5}$	1.17	1.17	1.17	1.17	1.25
Thermal shock resistance			100	100	100	100	100
Thermal conductivity	0–500°C	W/m°C	4.2	4.1	4.0	4.0	0.87
	500–1000°C	W/m°C	3.2	3.1	3.0	3.0	1.16
	1000–1500°C	W/m°C	2.9	2.9	2.7	2.8	1.44
Specific heat		kJ/kg°C	1.0	1.0	1.1	1.1	1.1

Table A11.5 General Properties of Dolomite, Zirconia, and Carbon Refractory Materials

			Dolomite		*Zirconia*		*Carbon*	
Type			*Stabilized*	*100%*	*Zircon*	*Stabilized*	*100%*	*Silicon Carbide*
SiO_2		%	15.10	3.00–5.00	32.50	1.00–3.00	0.25	4.50
TiO_2		%	–	0.2	0.3	–	–	–
Al_2O_3		%	2.00	1.00–3.00	–	–	0.25	1.40
Fe_2O_3		%	3.20	1.00–3.00	.07	–		1.00
MnO		%	–	0.1	–	1.00–3.00	–	–
CaO		%	39.10	48.0–50.0	–	1.00–3.00	–	–
MgO		%	40.6	36.0–40.0	–	–	–	–
C		%	–	–	–	–	99.5	–
SiC		%	–	–	–	–	–	93.2
ZrO2		%	–	–	66.50	94.00–96.00	–	–
Density		kg/m^3	2710	2520	2850	3200	1450–1550	2500
True porosity		%	20	24–25			20–25	15
Apparent porosity		%		23–24				
Specific gravity			3.39	3.35	4.56	5.49		3.1
Refractoriness (PCE temperature)		°C			>1900	>2000	>3000	>1850
Refractoriness under load		°C	1460	1500			>1700	>1700
Cold crushing strength		MN/m^2	>55.2	>27.7			>27.7	>55.2
Thermal expansion		$X\ 10^{-5}$	1.3	1.1	0.45		0.55	0.45
Permanent dimensional change on heating		%	+0.4	+0.3	−9.0	−9.0	+0.15	
Thermal shock resistance			2	>15	>20	5		>30
Thermal conductivity	0–500°C	W/m°C	2.16	1.44	10.05		5.21	18.61
	500–1000°C	W/m°C	2.16	1.73	10.05		5.21	7.61
	1000–1500°C	W/m°C	2.16	2.16	10.05		5.21	5.26
Specific heat		kJ/kg°C		0.25	0.84	0.84	0.71	0.66

Table A11.6 General Properties of Insulating Refractory Bricks

Type			*Hot Face*		*Hot Face / Backing*				*Backing*	
SiO_2		%	50.4	47.9	38.3	34.1	26.3	24.8	26.3	24.8
Fe_2O_3		%	1.7	1.8	6.4	6.6	9.9	10.8	9.9	10.8
Al_2O_3		%	41.0	41.7	42.1	44.1	46.3	42.0	46.3	42.0
Density		kg/m^3	900	800	720	650	500	450	700	600
Porosity		%	66	65	68	70	73	77		
Service temperature		°C	1650	1540	1430	1260	1100	870	1100	870
Cold crushing strength		MN/m^2	4	3	3	2.8	2	1.5	3	2.8
Permanent dimensional change on heating		%	−1.0	−1.0	−1.0	−1.0	−0.5	−0.5	−0.5	−0.5
Thermal conductivity	0−500°C	W/m°C	0.36	0.31	0.30	0.25	0.18	0.12	0.25	0.15
	500−1000°C	W/m°C	0.48	0.45	0.43	0.33	0.26	0.17	0.30	0.19
	1000−1500°C	W/m°C	0.61	0.58	0.56	0.40			0.35	

Table A11.7 General Properties of Insulating Refractory Board, Blanket and Loose Fill

Type			*Insulation Board (Calcium Silicate)*			*Ceramic Blanket*			*Loose Fill*		
									Diatomite	*Perlite*	*Vermiculite*
SiO_2		%	35.00	35.00	35.00	56.0	50.0	44.5	86.0	70.0—75.0	
Fe_2O_3		%	—	—	—	0.9	0.4	0.06	2.0	0.5 — 2.0	
Al_2O_3		%	—	—	—	41.0	48.0	50.0	—	12.0 — 15.0	
CaO/MgO		%	65.00	65.00	65.00	0.2	0.2	0.2	3.0	0.5 — 2.2	
TrO_2		%	—	—	—	1.5	1.0	0.06	—		
Na_2O/K_2O		%	—	—	—	0.4	0.4	0.18	5.0	3.0 — 9.0	
$(Mg.Fe.Al)_3$ $(Al.Si)_4O_{10}(OH)_2$		%									100
Density		kg/m^3	850	360	120	64/96/128	64/96/128	96/128	400	500	120
Service temperature		°C	1000	1000	1000	1050	1260	1450	870	1000	1100
Cold crushing strength		MN/m^2	9.8	4	0.5	0.02 (128)	0.04 (128)	0.023 (128)			
Permanent dimensional change on heating		%	−0.5	−0.5	−1/0	−3.0	−3.0	−3.0			
Thermal conductivity	400°C	W/m°C	0.12	0.07	0.05	.095/.095/.076	.097/.082/.075	.092/.082	0.12	0.17	0.06
	800°C	W/m°C	0.12	0.12	0.12	.245/.220/.170	.245/.205/.170	.205/.179	0.16	0.22	0.12
	1000°C	W/m°C	0.12	0.12	0.12	.326/.285/.237	.333/.270/.220	.268/.234			

Chapter 12

Furnace Design Methods

Chapter contents

12.1	Introduction	458
12.2	Conceptual Design	462
12.3	Furnace Sizing	481
12.4	Burner Selection	498
12.5	Detailed Analysis and Validation of the Furnace Design	501
12.6	Furnace Instrumentation and Controls	503
Nomenclature for Chapter 12		505
References		506

12.1 Introduction

A new furnace is a major investment, with a typical design life of 20 years and an operating life of probably twice that, so decisions made during the design stage will have implications for the furnace owner(s) for decades.

The past few decades have seen fuel prices at historically low levels and despite price spikes in the 1970s and 1980s caused by short term political activity and until very recently, overall prices have been falling. With low fuel costs, other factors, such as capital cost, achieving maximum production capacity and reliability, together with low maintenance costs, have dominated the design process with less emphasis on fuel efficiency. These factors, together with high interest rates meant that minimising capital cost was a major driver in furnace design.

However, the last few years have seen that trend reversed as the local on-shore oil and natural gas, and hence low cost fuels, have become depleted. Off shore oil and gas is inevitably more expensive, as are fuels that originate in remote and inhospitable places, such as Alaska and Siberia. This factor, together with concerns about global warming and the increasingly widespread taxation of CO_2 emissions, is likely to make fuel and emissions costs the dominant costs of future furnace operation. Although coal will probably remain relatively cheap to purchase, the associated carbon dioxide emissions will probably attract higher emissions taxation.

Capital cost, while continuing to remain important, will be less of a constraint allowing the design of more fuel efficient furnaces. At this point it is worth emphasising that, although improved fuel efficiency may cost more if it is achieved with add-on equipment, such as larger more efficient heat recovery equipment, this is not necessarily the case if the need for excellent fuel economy is addressed at the conceptual design stage. The principle objective of this book, and especially this chapter, is to assist future furnace designers to focus on and achieve that objective, i.e. fuel efficient, low cost design.

A good example of fuel efficient low cost design achieved in the past was the work undertaken by the former Midlands Research Station of British Gas. This work was executed during the period from the late 1940s until the 1990s when engineers at MRS Solihull (as the research station was commonly known) utilised most of the then available modelling techniques to develop a range of low cost, energy efficient furnace concepts that led to low cost designs. These concepts included the development of self-recuperative burners, regenerative burners and load recuperation.

As the name implies, self-recuperative burners preheat their own combustion air by recovering heat from the flue gases within the burner. They improve efficiency by eliminating the radiation and convective losses and the air ingress associated with the flue gas ducting, and also eliminate the capital cost of the recuperator in return for a modest increase in the cost of the burner. Consequentially furnace capital cost was reduced simultaneously with improved efficiency. Furthermore, recuperative burners can be fitted, and have been fitted, to many existing furnaces to improve their efficiency.

Another concept developed by MRS was recuperation of heat from the flue gases to preheat the load. This was applied to billet rapid heating furnaces, which are briefly described in chapter 1. The concept led to smaller more efficient furnaces that are price competitive with the older designs that they replaced.

These examples are described to demonstrate that great advances in furnace efficiency that have been achieved using innovative thinking and scientific methodology to develop high efficiency furnaces that are also cost competitive in the market.

There are two major phases of designing a furnace:

- The process design
- The mechanical design

The mechanical design is always undertaken in great detail to produce fabrication drawings for the workshop that will build the furnace, and will not be considered further in this book. However, in our experience, the process design is often skimped and may even consist of little more than modifying the mass and energy balance for the last similar design to suit a proposed new duty. While this approach minimises design costs, it is unlikely to deliver the most cost effective design over the projected life of the furnace, given the foreseeable increases in costs associated with fossil fuel utilisation. We consider that a more rigorous approach is required and this chapter concentrates on process design techniques that can potentially yield a more efficient furnace, which is also cost competitive from a capital investment viewpoint.

Overall process design is well covered in two excellent texts, Sinnott (1999) and Peters et al (2003) so, in this chapter we will limit our discussion to the process design of furnaces and how the furnace is integrated with the rest of the process. The mechanical design of furnaces will not be covered beyond the construction outline provided in chapter 11.

Such a wide range of chemical and physical processes are undertaken in furnaces that it is impossible to cover them here, besides the authors anticipate new processes will be developed over the next

few years that require fundamental thinking. In any case it is important to undertake a thorough analysis of the physical and chemical processes to understand the ideal rates of heating and cooling to achieve the ideal or optimum product. Unless this is done, the furnace design may be unwittingly compromised potentially reducing output and leading to a higher energy consumption and possibly poor quality product. Within this section therefore we will mainly consider the design process as if this was a new process and that only laboratory and small scale pilot data is available for developing a conceptual design; thus the data available to the design team is minimal. Normally far more data is available, together with operating experience of existing units, but this can serve to mask serious shortcomings in current practice that designers have never questioned and that operators have learnt to live with. In our view, it is always worthwhile revisiting the basic concepts when designing a new furnace unless the existing design is achieving optimum product quality with very high energy efficiencies and with low capital and maintenance costs.

12.1.1 Design Constraints

Design is a creative activity that, even in engineering, continues to be an art; albeit an art that uses science and mathematics as tools. There is no single correct answer to a design problem and in principle the designer has a massive number of potential solutions. However, unlike the artist, engineering designers are subject to a wide range of constraints such as the physical laws, government regulations, availability of resources, etc. This is clearly illustrated in Figure 12.1, which shows two rings of constraints. The outer polygon represents the physical, legal and economic constraints on the designer, so designs that are outside of this polygon would either be illegal or would not function effectively.

Occasionally designers unwittingly produce designs that are beyond the outer polygon and the results are economically catastrophic for the owners. Many of these plants also have serious safety issues. The problems are often so severe that few operate beyond their commissioning period. We expect most readers will be able think of examples within their own experience. Unfortunately, the prospect of defending potential libel actions prevents us from quoting specific examples.

Within the outer polygon is the region of "possible designs", that is designs that will operate and be safe but may not achieve the lowest costs or optimum efficiency. While these designs are possible, they are not necessarily efficient or cost effective and might exhibit poor availability and high maintenance costs, so the designers impose additional constraints indicated by the inner polygon that encloses a region

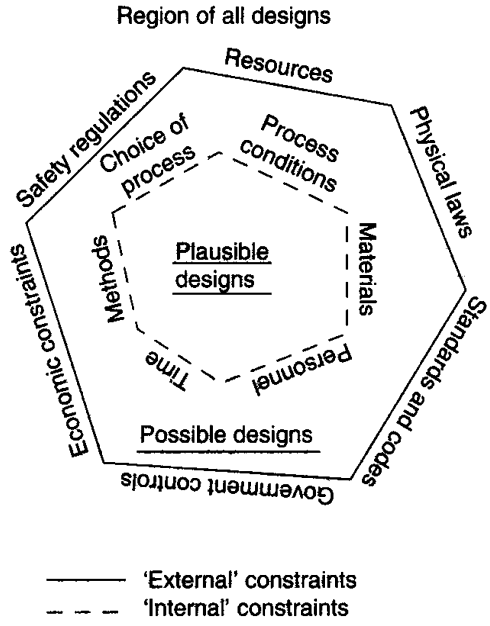


Figure 12.1 Design Constraints (From Sinnott 1999, Reproduced by kind permission of Elsevier)

of plausible designs. It is within this region that the most efficient designs reside.

12.1.2 Cost of Design Changes

Decisions made during the design process have a huge impact on downstream costs. Design changes cost money and correcting a mistake becomes more expensive the later this correction is attempted. An estimate as to how the cost of a design change is affected by its timing is given below:

Change introduced at the conceptual design stage	\$100
Same change introduced at the basic design stage	\$500
Same change introduced at the detail design stage	\$1,000
Same change introduced at the fabrication workshop	\$10,000+
Same change introduced during site erection or commissioning	\$100,000+

Late design changes are a major cause of cost "blow outs" in any project. In some cases, the mistake may be so expensive to correct

once the plant is completed that it is impractical to do so. As a result the plant has to run in sub-optimal mode or is shut down and abandoned.

12.2 Conceptual Design

Usually the furnace is one step in a manufacturing process that involves a series of processes that may include more than one furnace. The seemingly obvious first step is to describe as accurately and succinctly as possible the transformations that are to be undertaken in the furnace and how these relate to the rest of the process, especially the preceding and subsequent steps. Furnaces are used to promote changes such as physical alteration, for example, change of state and phase changes within solids, chemical reactions such as decomposition of one substance into two or more components, multiphase and single phase chemical reactions, physio-chemical reactions such as sintering, etc. The furnace may act simply to separate two components in a mixture, combine two or more components chemically and produce a product with a waste stream, etc., the range is enormous.

To achieve a cost effective design process, it is critically important that the conceptual design is undertaken thoroughly. Time, intellectual effort and especially critical thinking spent on this part of the design process is repaid many times over by cost savings later. By conceptual design, we mean developing a thorough understanding of the furnace functions and how these functions are to be undertaken. For example, what will be the fuels, the heat transfer mechanism(s), whether the feed or product will in be suspension, in a bed, in a molten bath, or a combination of these, etc. This exercise has to be undertaken for new processes, even if only intuitively but, as mentioned above, it is well worthwhile for existing processes, especially where capital costs are high and efficiencies relatively low. For example, in the cement industry which had successfully used the long rotary kiln for many years, a re-examination of the process in the 1920s led to separation of the preheating process from the kiln, making it a two stage process. Later the cyclone suspension preheater joined the grate preheater and a second change of concept occurred in the 1970s that led to the separate calcining furnace, Figure 12.2. The result was a 45% reduction in energy consumption and a lower capital cost per tonne of production capacity compared with the long kiln.

However, owing to the open-ended nature of the task, design is not straightforward, starting at a beginning with the design objective and arriving at the optimum design in one linear process. In reality, design usually involves a number of iterations where the preliminary design is changed as a consequence of feedback from the results of the preliminary efforts, and/or the designers becoming aware of other possibilities, Figure 12.3.

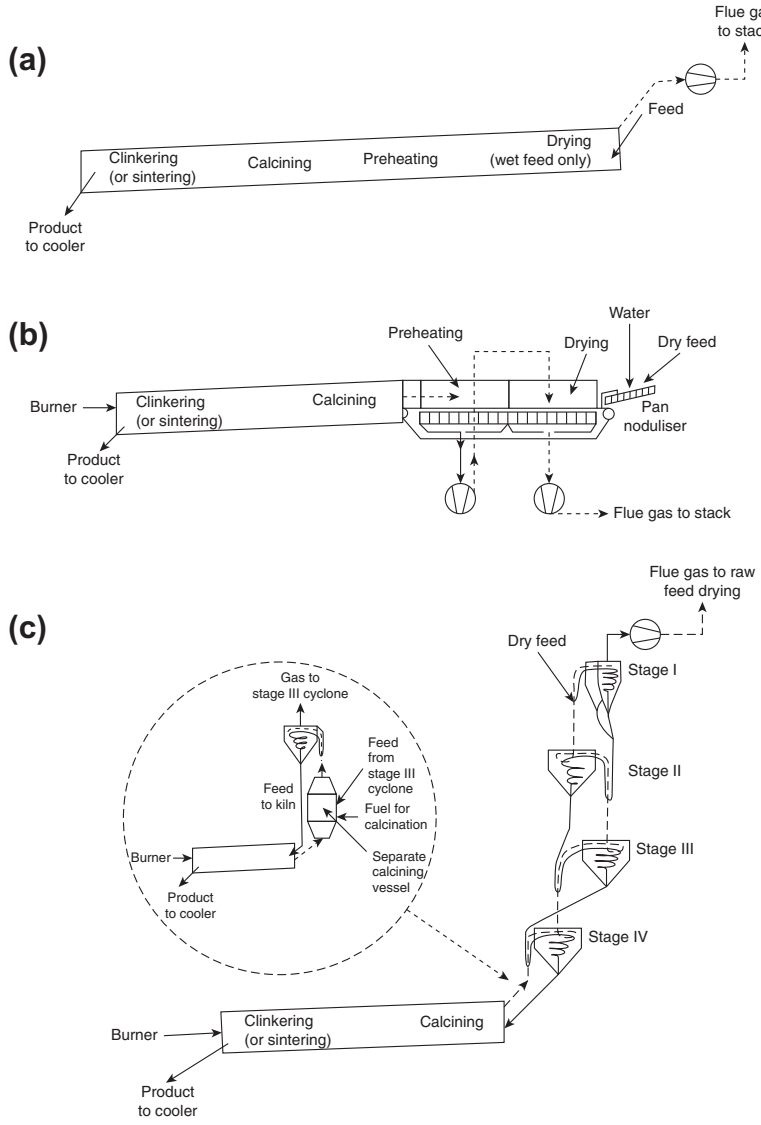


Figure 12.2 Evolutionary development of the rotary kiln cement making process. (a) Long wet or dry process kiln – typical energy consumption 6900 kJ/kg (wet) and 5850 kJ/kg (dry). (b) Lellep's semi-dry grate preheater kiln – typical energy consumption 4200 kJ/kg. (c) Cyclone preheater and precalciner kiln (inset) – typical energy consumption 3600–3200 kJ/kg

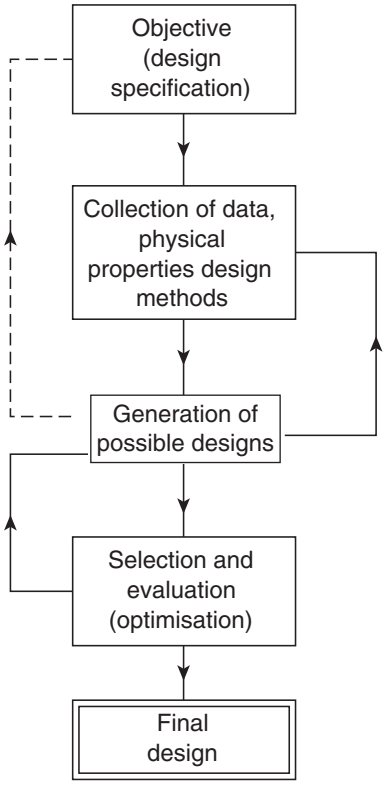


Figure 12.3 The design process (From Sinnott 1999, Reproduced by kind permission of Elsevier)

12.2.1 Process Functions

Before commencing furnace conceptual design it is essential that the function of the furnace is well understood. The overall process design, at least to a preliminary flow sheet and mass and energy balance should have been completed and some data regarding the furnace duty established. If this process is being scaled up from laboratory or pilot plant data then this information might be rudimentary. The first step is to clearly state the expected furnace duty:

- Feed rate & temperature
- Product rate and temperature ex-processing zone(s)
- Feed-product transformations - physical & chemical
- How many transformations are required?
- What is the heat absorbed or released by each transformation?
- Does this suggest more than one furnace zone? If yes, how many?
- What is the function of each zone?
- Product temperature rise/reduction

- Heat released/absorbed
- Physical separation
- What are the limiting parameters?

Heat transfer, cooling rates, heating rates, reaction rates gas/solid mixing, solid-solid mixing, gas solid separation, liquid/liquid separation, solid/solid separation, etc.

The concept of furnace classification in terms of the heat source and sink was introduced in chapter 1, Figure 1.3. These furnace processes will be undertaken in the context of the overall manufacturing process which will most certainly involve both upstream and downstream processes requiring four basic variations on how the heat sink behaves, as shown in the block flow diagrams in Figure 12.4, these are:

- Straight through furnace system
- Separation furnace system
- Combining furnace with downstream separation
- Combining and separation furnace system

Straight through Furnace System

In this type of furnace a single component feed or a fully mixed multi-component feed is provided to the furnace, which then processes the feed to produce a single product, which may or may not be subject to further processing. Metal reheating furnaces are typical of this type of furnace.

Separation Furnace System

In a separation furnace one feed stream enters the furnace and becomes two or more product/waste streams. An example of this type of furnace is a copper flash smelter which receives a single stream of sulphide ore and produces blister copper with a slag waste stream and SO_2 rich off-gas that is further processed to produce sulphuric acid.

Combining Furnace with Downstream Separation

In this type of furnace two or more feed streams enter the furnace and become a single stream which is then separated into two or more product/waste streams by further downstream processes. An example of this type of furnace is a copper reverbatory furnace which receives streams of sulphide ore and recycled converter slag and produces copper-iron matte with a slag waste stream and SO_2 rich off-gas that is further processed to produce sulphuric acid.

Combining and Separation Furnace System

Two or more feed streams enter the furnace where they are combined to make one or more products or a product stream and a waste stream. An example of this type of furnace is a blast furnace which

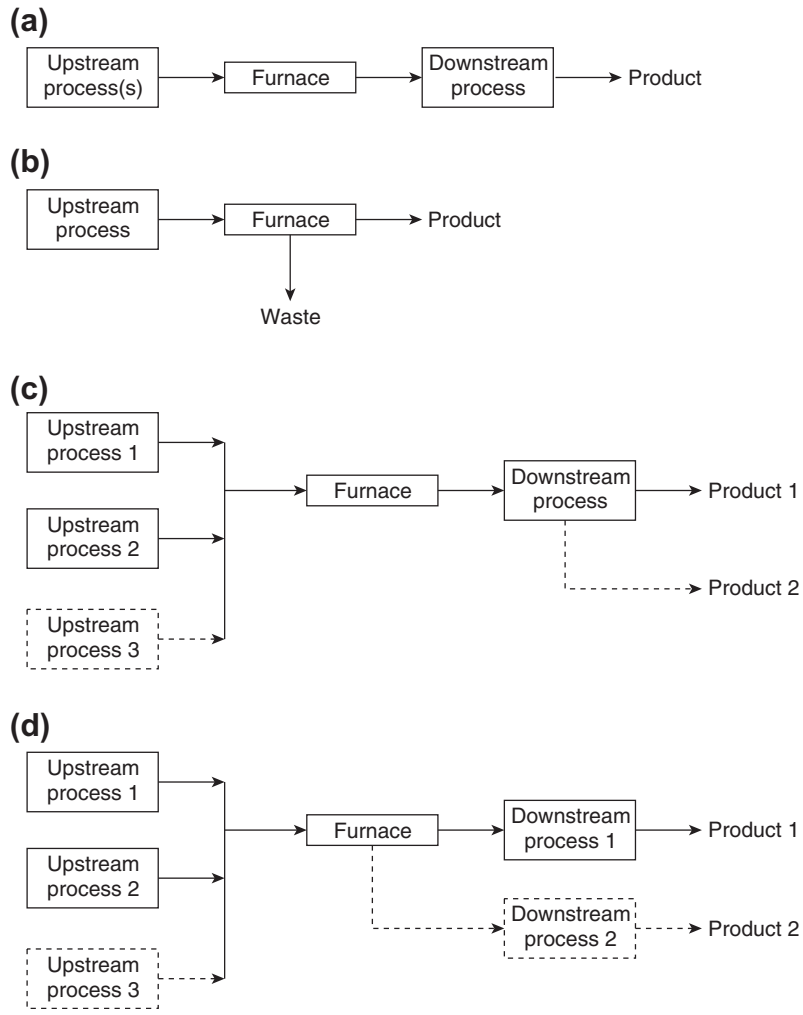


Figure 12.4 Furnace process functions within the overall manufacturing process. (a) Straight-through furnace system. (b) Separation furnace process. (c) Combining furnace process with downstream separation. (d) Combining and separation furnace processes

receives a feed of ore, coke and lime and produces molten iron with a slag which can be further processed to make slag cement.

12.2.2 Defining the Physical and Chemical Changes

These combining and separation processes are a combination of physical and chemical changes. For example, in the flash copper smelter the iron sulphide is oxidised to iron oxide and the copper

sulphide reduced to copper simultaneously while producing SO_2. This is possible owing to the position of iron and copper in the electrochemical series with copper being above iron and hydrogen, hence copper is easily reduced to the metallic form. Together with the other components in the ore, the iron oxide forms a slag which is lighter than the molten copper so floats to the surface and separates physically. However, this physical separation process is less than optimal owing to the turbulence of the molten copper bath, so a significant amount of copper remains entrained in the slag which is sent to another furnace to complete the separation process. Defining these physical and chemical changes and understanding the most effective manner of undertaking them is a critical part of the conceptual design process.

The chemical reactions may absorb heat (endothermic) like lime making where CO_2 is driven off to leave CaO or release heat (exothermic) such as smelting of copper sulphide ores, where the sulphur is oxidised to SO_2 and SO_3. In the latter case, the feed materials need to be raised to a relatively high temperature to trigger the reaction owing to the relatively high activation energy, but the overall heat input required is small and heat transfer is rarely the limiting factor. By contrast, endothermic reactions require a high thermal input and these furnaces are frequently heat transfer limited.

Some processes combine both types of reaction, e.g. Portland cement manufacture involves the physical processes of drying and preheating followed by the endothermic decarbonation of limestone and finally an exothermic clinkering reaction which also combines chemical and physical processes, such as reactions between the lime, silica and alumina components of the feed together with a sintering reaction to develop the crystal structure. Clinkering has a high activation energy and requires heating rapidly to approximately 1490°C to trigger the reaction, followed by rapid cooling to optimise the final crystal size. The drying, preheating, decarbonation and clinkering processes require quite different thermal inputs, yet for decades all were undertaken in the same furnace, namely a long rotary kiln. As early as the 1920s, Lellep realised that the preheating process was dependent on convective heat transfer and that the rotary kiln was ineffective for this, so he developed the grate preheater that reduced fuel usage by 25% (Martin 1932). However this process, although used extensively, did not become popular owing to high capital and maintenance costs. In the 1940s Lellep's grate preheater was joined by the cyclone preheater. The cyclone preheater was simpler than the travelling grate and reduced fuel consumption by approximately 30% compared with the long kiln but made little impact on the capital cost owing to the structure associated with the preheater tower.

In the late 1970s the seemingly obvious step of separating the two chemical reactions was taken, with the first kilns employing a separate

furnace to undertake the endothermic calcining reaction being introduced with an even smaller rotary kiln to complete the exothermic sintering reaction, Figure 12.2. The result was a further 12% reduction in energy consumption and a lower capital cost per tonne of production capacity compared with the preheater tower. Furthermore, this was the only practical way of achieving production capacities of over 4000 tonne/day.

12.2.3 Preliminary Mass and Energy Balances

The development of mass and energy balances was fully covered in chapter 9 and the purpose of this section is to draw attention to improved ways of using these balances in furnace design. Mass and energy balances should be undertaken at the earliest possible stage of the overall process design to provide basic process information. The reliability of the mass and energy balance will be dependent on the reliability of the input data, which may be quite poor for a new process, see below. Nevertheless, trial balances need to be developed early since they will be the only quantitative data initially available to the furnace design team. The mass and energy balance should be constantly refined as the design develops, especially immediately before and after the furnace sizing is undertaken, and again before and after design validation.

In the past, mass and energy balances were usually only undertaken for the design capacity and possibly one or two turndown conditions. This does not provide any insight into off specification operation. Given that virtually no plant operates exactly as designed, it is very worthwhile to use the mass and energy balance to examine the changes in furnace duty that would be imposed by upstream process upsets. This is easy to do with modern computer programs and simulation software and should provide significant insight into how the furnace might cope with such upsets.

Of course, the mass and energy balance will only provide steady-state scenarios but this should give some clues as to how the furnace might function under these conditions. In practice, real process upsets occur under dynamic conditions and they will have a far greater detrimental effect on furnace operation than indicated by a steady state calculation, but building a dynamic model of the system is still very difficult and outside of the resources of most furnace design teams. Further consideration of the important, and oft neglected issue of process upsets, occurs later in this chapter.

12.2.4 Reliability of Available Process Knowledge

A design is only as reliable as the input data. That old saying regarding computing, namely: “rubbish in rubbish out” is equally valid for

design, yet as engineers, we are always required to prepare designs with incomplete information. If Abraham Darby had waited until he had all the information needed to design his coke fired blast furnace we would probably still be using charcoal to smelt iron. The important issue is to understand the reliability of the data and to develop strategies to minimise the risks associated with the errors and gaps in the data.

Existing Processes

For existing processes a great deal of operational experience is available. However, this does not necessarily translate into reliable process knowledge unless the data has been analysed and thoroughly understood and all process anomalies explained, both in physical conceptual terms and modelled either physically or mathematically. This will usually require further on-site measurements as explained in chapter 9, since plant instrumentation rarely provides the data required for an in-depth analysis of the process. This additional data can then be used to develop a process model, either using one of the commercially available packages where available, or by developing the model from scratch. The latter is a time consuming exercise and may require special skills that are not readily available in-house so the earlier this exercise is started the better. Whether all the skills are available in-house or not, it is very useful to have outside process analysts, not totally familiar with the process under examination. The questions they will ask while familiarising themselves will usually reveal many gaps in knowledge not previously recognised.

It is not sufficient to merely build a process model or models but it is critical that the models are validated against real operational data. Again this is not easy, owing to the usual lack of operational data of the type needed to rigorously validate the model, but significant confidence can be gained if the model can be used to predict changes in process output on the basis of the input changes that mimic operational experiences. The models can then be used to investigate the effect of process changes, such as product heating and cooling rates, heat transfer, heat recovery, furnace zoning, etc.

New Processes and Pilot Plants

Few, if any new processes are developed purely from theory, so it is probable that even for entirely new processes some laboratory data is available that provides some insight into the process required. However, owing to the quite different mechanisms by which laboratory tests are undertaken compared with a full size process, this laboratory data may be of limited use when contemplating a furnace design.

For example, most laboratory trial heating and cooling experiments are undertaken either in muffle furnaces or autoclaves. In the former, owing to the lack of gas or air flow, heat transfer is largely by radiation, natural convection and conduction through still air while in the latter the heating is by natural convection and conduction through steam. Translating these laboratory tests into a furnace design is not a trivial exercise since the furnace conditions will be quite different from the laboratory tests. Other data, such as specific heat, density, heat of formation, coefficient of expansion, latent heat of melting or evaporation over a range of temperatures and pressures may be available from the literature or may also need to be determined by laboratory tests.

Inevitably, the data available for design of a new process will fall short of that required for the optimum furnace design. Even where the process is not entirely new but utilises natural raw materials of differing composition, such as smelting non-ferrous ores, each ore deposit is unique and its behaviour has to be investigated thoroughly before the furnace design can be attempted. Indeed some ores are unsuitable for normal thermal processing but must be treated by solvent extraction techniques, known as hydrometallurgy. However, even in hydrometallurgy, furnaces have a role to play in ore drying and roasting, calcination and sulphur removal, etc, despite not being used for smelting.

In these circumstances, while a process model can usually be developed, it cannot be validated until the full size pant is constructed unless a pilot plant is built to test the model's predictions and gain practical operational experience. Construction of a pilot plant significantly delays the introduction of the new process but greatly reduces the risk. In the event that the pilot plant does not perform as expected, changes to the full size plant can be incorporated at the design stage. Furthermore, commissioning times for the full size plant are greatly reduced owing to the transfer of operational experience from the pilot plant. These savings, both in terms of cash and time, are frequently much greater than the money and time spent proving the process in this manner.

While pilot plant is in itself a substantial investment it can be viewed as an insurance premium, since in the rare event that the process fails completely, or proves so difficult to operate as to be impractical, further work can be abandoned and the detail design and construction costs associated with the full size plant saved.

12.2.5 Effect of Upstream and Downstream Processes

Where the furnace is integrated into a larger overall process the furnace design cannot be undertaken in isolation since the performance of

upstream processes will affect the furnace and likewise the furnace performance will affect downstream processes. Since no process runs under optimum conditions at all times it is important that the effect of sub-optimal performance of upstream processes affect the furnace performance. Three conditions need to be examined:

- Reduced output from the upstream process;
- Off-specification product from the upstream process as furnace feed;
- Unstable operation of upstream process leading to both fluctuating output and product quality;

Of these three process issues, reduced output is probably the easiest to cope with provided that the furnace can operate reasonably well under turndown conditions. However, there is always a significant cost associated with this problem, both in terms of the lost production and the higher energy cost.

Off-specification feed to the furnace can rarely, if ever, be accommodated by the furnace and almost always results in off-specification product unless further downstream processes are incorporated to further refine the product.

Unstable operation of the upstream process leads to unstable furnace operation and difficulties with maintaining both product quality and furnace output. Needless to say under these conditions fuel efficiency will also suffer, typically increasing by 10–20%. Unfortunately in our experience, these types of issues are rarely understood, or even considered, at the design stage and are usually discovered during commissioning, when it is usually very difficult to implement an effective cure. Common problems include poor design of upstream blending processes that provide feed to the furnace, with variations in feed composition causing major problems with unstable furnace operation. Often the cause of this instability is misdiagnosed and is seen as a furnace control problem rather than a feed quality variation. As a result, hundreds of thousands of dollars are spent on improving the furnace controls to no avail, while a similar or even smaller sum spent of resolving the feed issues would have resulted in a complete solution.

Unless the issues of poor upstream performance are considered during the design phase it is often difficult to recognise the true cause of furnace operational difficulties. Unfortunately the time constants of furnace processes are such that they can rarely compensate for unstable operation of upstream plant, despite sophisticated control systems. In extreme cases process instability can even lead to safety issues and we are aware of several furnace associated explosions that have been triggered by upstream process instability.

12.2.6 Fuel Choice

The preferred fuel is normally chosen at the conceptual stage, since this decision can have a major influence on the rest of the design. This topic has already been introduced in chapter 3 and this section will be restricted to consideration of the issues affecting fuel choice. It is currently the case that oil is rarely used as a furnace fuel, owing to its high cost and its use is normally restricted to plants that cannot tolerate the ash in coal but which do not have a natural gas supply available. Hence, the majority of modern furnaces in the industrial west use natural gas. However, that was not always the case and there are still many industrial regions that do not have significant supplies of natural gas available at present, including much of South America, India, South East Asia, China and most of Japan.

Fuel choice is critically important and depends on a wide range of factors, including cost, availability and security of supply. In a competitive world most furnace operators will seek to minimise costs so will choose the lowest cost fuel in the local market that is compatible with the process. However, besides cost, there are a number of other factors that need consideration. Overall the following factors need to be considered when selecting furnace fuels:

- Cost
- Availability and security of supply
- Chemical compatibility with process
- Heat transfer characteristics
- Ease of handling
- Environmental issues, NO_x, SO_x, CO_2, etc.

While most furnace operators would like to use the cheapest suitable fuel, energy costs have been volatile for many centuries, influenced by local supply and demand. Although the current market is more global, issues such as the anticipated decline in oil production and concerns over climate change and potential carbon taxes, suggest that the market uncertainties will continue and the current lowest cost option now may not be the lowest cost over the life of the furnace.

Currently fuel cost is largely related to global supply and demand with the cheaper fuels usually being so because of reduced demand relative to their availability owing to difficulties in their utilisation. This results in wastes being the cheapest fuels with distillate oils currently the most expensive. Coal and natural gas are somewhere in between with local cost dependent on availability and supply. It is important to remember that neither absolute cost, nor relative cost is static, but is in a constant state of flux. In this context, it is important to consider the likely future trends in fuel costs at the design stage and, given the unknowns, to build in fuel flexibility, if possible.

This will be easier to achieve with some processes than with others. With the current pressures to reduce carbon dioxide emissions to the atmosphere, it is probable that the real cost of coal will increase significantly in future years. This will in turn increase the demand for natural gas and possibly organic wastes, driving up their costs also.

Fuel Chemical Compatibility with Process

The two principle considerations are chemical compatibility and physical intrusion of the ash, where present.

Ash is the non-combustible residue that arises from most solid fuels and from heavy fuel oil. In the latter it is mainly catalyst residue from the refining process and, to a lesser extent, metallic organic compounds in the oil. It is present in very small quantities (usually less than 0.1%) and does not cause a significant problem for most processes. Coal, wood and wastes such as straw, paper, cardboard, etc. contain significant quantities of mineral matter (2–60%) that is both physically intrusive and potentially chemically reactive. Where it is merely physical intrusion that is the issue, the fuel suitability will mainly be determined by the quantity of the ash. However, physical intrusion alone is unusual, except in low temperature processes because the ash is highly reactive at typical furnace operating temperatures.

Every fuel and waste has its own unique ash and the chemical analysis is normally quoted in the form of its oxides, Table 12.1. Unfortunately this form of ash analysis does not tell the whole story since the compounds shown in the table do not exist in the ash but are merely a convenient way of expressing the analysis. The real ash is much more complex than indicated by the oxide analysis.

Most ashes contain SiO_2, Al_2O_3, CaO, Fe_2O_3 and SO_3. The latter is a good example of how the analysis does not represent the true compounds in the ash because SO_3 is a gas and could not remain in the

Table 12.1 Ash Analysis for Several South Australian Lignites

Ash		*Kingston*	*Lochiel*	*Bowmans*
SiO_2	%	33.8	31.4	17.4
Al_2O_3	%	14.2	8.3	5.3
Fe_2O_3	%	1.4	4.1	7.0
CaO	%	12.4	10.0	8.0
MgO	%	14.6	8.6	11.8
Na_2O	%	5.7	8.7	15.1
K_2O	%	0.5	0.3	0.35
TiO_2	%	0.4	0.5	0.1
SO_3	%	16.3	27.5	33.0

fuel, except by dissolving in the water to form sulphuric acid, something that clearly does not occur. In practice, the sulphur is partially combined with the iron as FeS in the ash and with organic compounds in the volatiles. The ashes shown in Table 12.1 are not typical for traded coals but have been included here because of the presence of the alkali earth elements, sodium and potassium, that also occur in wood and other organic wastes.

Ash reactivity is dependent both on the ash composition and the product chemistry. Some clues may be gained from the ash analysis such as shown in Table 21.1. For example, these lignites would clearly not be suitable for direct firing into furnaces that are making products that cannot accommodate sulphur or sodium. However, as already discussed, the ash chemistry is more complex than that indicated by the analysis and the overall effect of the ash on the process can only be determined by a thorough understanding of both the ash chemistry and the process chemistry which will often require tests specifically designed for this purpose.

Other ash properties commonly quoted are the ash softening and fusion temperatures. These are mainly of interest for firing boilers and other plant where ash is likely to stick to cooler surfaces. In this case, the main risk arises with the lower temperature melting ashes that are therefore still likely to be soft as they approach a cool surface and stick whereas a solid particle would impact and be deflected.

In high temperature furnaces, ash may also react with the furnace lining causing build ups and potential premature failure owing to chemical attack on the refractory, modifying the brick surface physically and chemically by forming a glassy layer. It also has the potential to facilitate spalling because the glassy layer has a different coefficient of thermal expansion than the parent brick with a plane of weakness at the interface. On cooling, the glassy layer falls off leaving fresh brick exposed to further attack. After a few operational heating and cooling cycles the brick is so thin it is unserviceable.

Sulphur occurs in most fuels, except piped natural gas, from which it is removed. It is prevalent in heavy fuel oil as well as coal and some wastes. It is mainly attached to organic compounds and easily oxidised to SO_2 in the flame and under certain circumstances may even form SO_3. The latter is especially common in heavy oil flames where the catalytic properties of the ash facilitate SO_3 formation, especially at excess air levels above 3–5%. Both gases are highly reactive and a potential problem for many products including, cement, copper, lime, nickel, steel, etc.

Chlorine compounds are also present in a wide range of fuels including coal, some woods and waste liquids. It may occur as organo-chlorine compounds or as saline water absorbed into the fuel. Chlorine is detrimental to many processes, even those which are tolerant of the ash. It also has the potential to form dioxins in

the combustion gases if they remain for a significant time (several seconds) in the 400–800 °C range.

Heat Transfer Compatibility with the Process

As discussed previously, heat transfer from the flame in a furnace is by both convection and radiation. At higher temperatures the latter dominates and flames with reduced emissivity can adversely affect furnace performance unless that reduced emissivity is taken into account during design.

Figure 3.3 shows the effect of C:H ratio on the flame emissivity, while Figure 3.4 shows the resulting heat transfer from a flame for different fuels. While this effect has been know for many years, Figure 3.3 dates from flame radiation trials undertaken at Ijmuiden in the mid 1950s (Weber 1998), few furnace designers take fuel flame emissivity fully into account and regard fuels as fully interchangeable when clearly that is not the case.

The difficulties of utilising coal, and the high cost of oil, lead to natural gas being the preferred fuel for many processes on the basis of both cost and convenience but its relatively low carbon content reduces its flame emissivity and reduces radiant heat transfer from the flame to the product. This has led to considerable efforts over the years to increase the emissivity of gas burners, commencing with Shell's Egham luminous flame burner developed in the 1960s, but this quest has achieved limited success owing to the difficulty of producing significant in-flame carbon from the very stable CH_4 molecule. Most of the burners developed to meet this objective have been unduly bulky and expensive to buy and maintain. The newly developed Gyro-Therm burner holds promise to change this scenario, being only marginally more expensive than conventional gas burners and much more compact than previous high emissivity natural gas burners.

Unless enhanced emissivity burners such as Gyro-Therm are used, high temperature furnaces using natural gas must be designed with higher temperature re-radiating refractory surfaces and a significantly greater contribution from convective heat transfer, otherwise their fuel efficiency will suffer and the flue gas heat losses will be much higher than expected. The magnitude of these changes is significant. In the case of the lime kiln represented in Figure 3.4, conversion from natural gas firing to petroleum coke (equivalent to low volatile anthracite) but with no other changes, reduced the fuel consumption by more than 25%. High temperature furnaces designed for natural gas firing therefore need to utilise a higher proportion of convective heat transfer in the furnace than for other fuels, or be equipped with larger external heat recovery systems. This latter approach will lead to a significant increase in capital cost and increased on-going maintenance costs.

While waste fuels are becoming increasingly attractive to owners of processes that can tolerate their particular characteristics, little heat transfer data is available for such fuels. However wastes of various types have seen widespread use in rotary kilns for manufacture of both cement and light aggregate. Little hard data is available on their performance, but we are aware of one case where substitution of a waste organic liquid of moderate calorific value reduced both kiln output and increased fuel consumption to such an extent its use was not viable. One friend in the USA who had a similar experience dubbed the phenomena "BTU deception". Owing to the paucity of data for many wastes, each application needs to be considered carefully and, where feasible, plant trials or other suitable tests such as pilot plant trials undertaken prior to committing to using these materials as furnace fuel.

At the time of writing there is much hype concerning the potential for the "Hydrogen Economy". The gasification of coal and subsequent conversion of the CO component to CO_2 via the water-gas shift reaction and separation of the CO_2 for storage, leaving hydrogen as a fuel gas, is one route being promoted for the manufacture of the fuel. However, hydrogen flames have a very low emissivity owing to the complete lack of carbon with the only radiating component in the flame being water vapour. Therefore any furnace designed to use hydrogen as a fuel will need to rely almost entirely on convective heat transfer. Furthermore, owing to the lack of heat transfer from the flame by radiation, the gases produced by a hydrogen flame are very close to the adiabatic flame temperature and the thermal NO_x will be very high unless special precautions are taken. Failure to understand these issues will lead to an unusable furnace plant.

Hydrogen produced by modern high temperature gasification processes should not be confused with gas producers used in the past that operated at lower temperatures and produced a gas that contained many of the tars and higher hydrocarbons distilled from the coal. Hence this gas had significantly higher emissivity than hydrogen on its own.

Finally, it is worth noting that different fuels can often be used in different zones of a furnace system to maximise fuel efficiency and minimise fuel costs. While this complicates the design, many existing plants are being converted to this mode of operation using cheaper fuels, such as wastes, in parts of the plant that can tolerate them, restricting the premium fuels to zones where their use is essential. While this increases the complexity of the fuel systems, it can significantly reduce operating costs.

12.2.7 Potential for Heat Recovery and Choice of Equipment

It is critically important that this is considered early since early integration within the design allows maximisation of process efficiency

together with minimising capital cost. The preliminary mass and energy balance will allow a first approximation of the overall energy demand and indicate the potential and need (or otherwise) for heat recovery. If the potential need exists, it is appropriate that it is considered at the conceptual stage so that any opportunity to incorporate the heat recovery in the process fundamentals can be taken advantage of. Incorporating heat recovery into the furnace design is almost always cheaper and more effective then purchasing add-on equipment. Three principle opportunities for heat recovery exist:

- Recovery from hot product;
- Recovery from hot flue gases;
- Recovery from shell losses or cooling water.

Heat in hot flue gases and product tends to be high grade heat and is almost always worth recovering, while that in cooling water or arising from shell losses, is low grade heat and its recovery is not only more problematic but is only viable where there is a local demand for the energy. It has little or no effect on furnace efficiency and can only really be considered at part of the detail design, so each case will need to be examined on its merits.

Estimating the Potential for Heat Recovery from Hot Product

The potential for heat recovery from the product exists in most furnaces where the product is required at ambient temperature but not for those furnaces where the material is needed hot for further processing, such as a steel reheating furnace or a melting furnace in a casting plant. In theses cases, the hot product in normally removed from the immediate vicinity of the furnace for further processing and any form of heat recovery is effectively impractical.

Where the heat can be recovered, the available heat in the hot product can be estimated from the sensible heat if it is a solid and from both the sensible and latent heats if it is a liquid, equation 12.1. For solid materials the first two terms equal zero so the equation reduces to the single term.

$$h_c = Cp_L \Delta T + H_m + Cp_{sd} \Delta T \tag{12.1}$$

Hot product is usually used to preheat combustion air by direct contact heat exchange. For a high temperature product, this technique has the potential to recover 70–80% of the sensible heat in the product, provided that sufficient combustion air is available. In these cases, up to 50% of the process heat requirement can be recovered, leading to a significant reduction in fuel consumption, sometimes exceeding 50%. Hence, the capital cost of the fuel supply system and storage (where required) is significantly reduced. Methods of assessing

the potential fuel savings are described in chapter 9 but typically 1 kJ of energy recovered from 1 kg of product normally results in fuel savings of 1.5 to 2.0 kJ/kg of product owing to the corresponding reduction in flue gas heat losses.

Direct heat recovery from hot product to combustion air requires intimate contact with the product and is unsuitable for materials that are sensitive to oxidation. Other methods of cooling are required for these materials and there is generally little opportunity for cost effective heat recovery under these conditions.

Estimating the Potential for Heat Recovery from Hot Flue Gas

Normally the combustion products leave the high temperature zone of the furnace at well over 1200 °C and present a significant opportunity for heat recovery. This is normally achieved by preheating the feed or combustion air and, in some cases, both. Preheating the feed offers significant opportunity for integration into the furnace design by direct heat exchange, whereas preheating the combustion air almost always requires significant add-on equipment. The heat available in the flue gas can be calculated from the mass flow, composition and temperature. The expected composition and mean specific heat can be calculated from the fuel analysis and the anticipated fuel usage using methods described in detail in chapters 2 and 9.

Feed preheating is undertaken by direct contact and can be achieved in several ways, such as an extended furnace zone as in the billet rapid heating furnace shown in Figure 1.18, by gas flow through a packed bed, such as in the lime kiln, Figure 1.5 and 1.6, or by direct exchange in suspension as in the cyclone preheater cement kiln Figure 1.7 and 12.2. If correctly designed, all these techniques are very effective ways of achieving high efficiency heat recovery and significantly reducing furnace fuel consumption. It also has only marginal effect on furnace capital cost since the feed must be heated to achieve the process objective and, if it is not done in a dedicated preheater, it must be undertaken in a larger furnace as in the case of the cement kiln in Figure 12.2.

Using hot flue gases to preheat the combustion air is almost always undertaken in dedicated add-on equipment. This may be stand alone equipment such as an air preheater or in some cases, incorporated into the individual burners. Two basic techniques are utilised, recuperation and regeneration.

Recuperation employs conventional heat exchanger techniques with the flue gas separated from the combustion air by a metallic wall. Designs vary and schematics of two examples are shown in Figure 12.5. In these designs the hot flue gas flows across the outside of the tubes while the combustion air flows through the tubes.

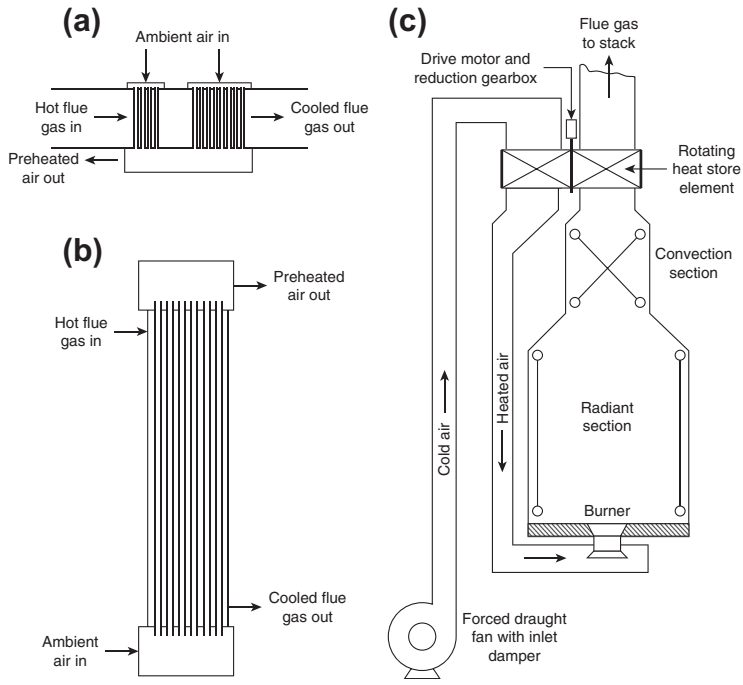


Figure 12.5 Schematics of cross flow and counter flow recuperators and regenerative heat wheel for preheating combustion air. (a) Cross-flow recuperator. (b) Counter-flow recuperator. (c) Regenerative heat wheel applied to a petrochemical furnace

The major limitations of recuperators are their inability to handle dirty gases, owing to the risk of fouling, and the relatively low maximum permitted hot gas inlet temperature. Few designs are capable of accepting inlet flue gas at temperatures higher than 850–900 °C. Even at those temperatures, the recuperator materials are under significant risk of high temperature corrosion and stress corrosion cracking as a consequence of the stresses introduced by differential expansion and CO, SO_2 and water vapour in the flue gas. These factors result in leakage between the air and gas sides of the recuperator and a significant fall in efficiency relatively early in its life. Since the cause of this leakage is corrosion that attacks both the tube and tube-plate, repair is difficult, if not impractical and replacement is both expensive and difficult within the timescale of a typical furnace shut down. Recuperator performance therefore tends to fall significantly as the furnace ages with the accompanying increasing fuel consumption tolerated because the alternative of recuperator replacement is too difficult to contemplate.

Regenerative heat recovery involves the use of heat storage with the hot flue gas transferring heat to a high thermal mass store which then transfers the heat to the combustion air, both by direct contact heating. Two techniques are employed, the thermal wheel, also shown in Figure 12.5 and the double refractory store. Thermal wheels are only suitable for moderate temperatures, such as the flue gases from boilers, owing to material service temperature and differential expansion limitations while the double refractory store technique is suitable for very high temperatures for dirty gases. This system, which is shown on the glass tank in Figure 1.8, operates on a heating/cooling cycle with one store heating the combustion air while the second store is being reheated by the flue gas. When this second store is hot combustion air is passed through it to preheat the air, while cooling the store and the flue gas is switched to the first store to reheat it. The major disadvantages of this system are the cyclic operation, which gives rise to a varying combustion air temperature, the large volume and mass of the regenerators, the more complex furnace design with double the number of burners needed, the design of an efficient hot valve, and the complex flue gas and combustion air ducting required. All of these features impose a significant increase in capital cost. However, the regenerative double refractory store technique remains the only practical way of preheating combustion air by recovering heat from very high temperature flue gas and dirty flue gas.

In certain circumstances, it is not practical to utilise the excess heat in the flue gas to improve furnace efficiency, for example, where the combustion airflow is low or negligible owing to the use of oxyfuel firing, or where for process reasons the flue gas contains high levels of combustibles. In these circumstances, consideration should be given to heat recovery by steam generation in a waste heat boiler. Again, this is a high capital cost add-on technique that will only be economic if there is a process use for the steam. Waste heat boiler design is a specialist skill and furnace designers should talk with engineers from the appropriate specialist companies as soon as it becomes apparent that this method of heat recovery may be appropriate.

Estimating the Potential for Heat Recovery from Shell Losses or Cooling Water

Calculation of the heat losses from the furnace surface or in cooling water is straightforward and involves the use of techniques already described in chapters 4 and 9, but recovery of that heat for further use is complex owing to its low temperature, and would need to be the subject of a specific engineering study to consider the practical aspects. We know of a number of cases where this has been attempted but the results have been uniformly disappointing. Owing to the lack of opportunity for this technique to make significant improvements in furnace efficiency, it will not be considered further here. Where used,

cooling water is typically available in the region of 60–70 °C, higher temperatures being impractical unless pressurised system is used owing to the risk of localised boiling. This is very low grade heat and is mainly a nuisance, requiring a cooling tower to cool the water for reuse rather than being of any practical use. In principle, this water could be used to preheat domestic hot water (via an indirect heat exchanger to prevent contamination of the domestic supply) or for space heating in cooler climates, but normally the furnace is too far away from the potential heat load for this to be worthwhile.

Economic Considerations

Heat recovery is capitally intensive and therefore increases the price of the overall furnace system, even after allowing for the reduction in capital cost of the smaller fuel system, so it increases the costs of the furnace supplier. In a competitive environment where purchasing decisions are based on price this tends to put those suppliers who maximise heat recovery at a disadvantage compared with those who skimp in this area. Hence it is essential that the furnace user and purchaser is able to make his/her own assessment of this feature and ensures that the enquiry documents do not adversely affect the higher priced tenders of suppliers offering higher levels of heat recovery. This is especially important, given that most furnaces will consume fuel worth many times their capital cost in the first few years of operation and for very energy intensive processes, even in the first year of operation.

It is often quite difficult and always very expensive to improve the heat recovery later, so it is better to err on the side of greater, rather than lesser, heat recovery at the design stage given that the trend in energy prices for the foreseeable future is upwards. In our opinion this trend is likely to be sustained and the trend may steepen as natural gas resources become depleted and greenhouse gas (carbon emission) reduction policies bite harder. Hence, if carbon emissions become a cost for furnace users then energy efficiency will become even more important. Given that furnace life typically exceeds 40 years, process design and purchasing decisions need to account for this scenario.

12.3 Furnace Sizing

Determining the size of a furnace for a given production rate depends on one or more of the following:

- Heat transfer rate to product, which will determine the product quality
- Product residence time, which will determine the production capacity

- Combustion space, which will determine the combustion efficiency
- Air, combustion gas and product flowrates and velocities, which will determine the system pressure losses, dust entrainment etc.
- Any environmental restrictions that might require the application of, for instance in-flame NO_x control, flue gas recycling, or oxy-fuel flames, which would modify some or all of the above factors

When considering the design of a furnace for a new process, only laboratory and pilot plant data is available. The first step in the furnace sizing design is to develop from that data an optimum time-temperature-enthalpy diagram for product. This should consider the complete heating and if applicable cooling cycle for the product. In many processes, the furnace may only be part of the complete production cycle and we must determine where to 'fit' the furnace into the diagram. In such systems we also need to carry out a first iteration of an integrated process analysis, as discussed in chapter 9.3, to optimise the overall thermal efficiency. To illustrate the design process, three different processes that require a furnace to heat the product will be considered:

- Continuous controlled heating of metal slabs to a set temperature prior to hot rolling and shaping;
- Heating of a multi-component oil based liquid to evaporation point prior to some chemical transformation over a catalyst;
- Heating and chemical decomposition/transformation of a mineral aggregate.

Whilst these processes may be recognisable as existing industrial furnace operations, in order to illustrate the design process we will consider them as 'new'. Figures 12.6, 12.7 and 12.8 show the time-temperature-enthalpy curves for the three processes derived from laboratory or pilot plant measurements. The first two processes require the process material to be heated to a design temperature prior to further production stages. The third process involves heating, chemical reaction and cooling of the process material. A comparison of the temperature-enthalpy relationships for these processes in Figure 12.9 illustrates this clearly. The first two plots are linear, indicating that the transferred heat to the material is all in the form of sensible heat, and that the specific heats of both are not significantly temperature dependent. Thus we have the simple relationship

$$h_c = \overline{Cp}\ \Delta\ T \tag{12.2}$$

Where h_c is the heat required to process unit mass of product. In the third case the plot is non-linear, particularly in the region from 400 °C to 900 °C, indicating that a large proportion of the transferred heat is absorbed in the chemical reactions. The curved sections from

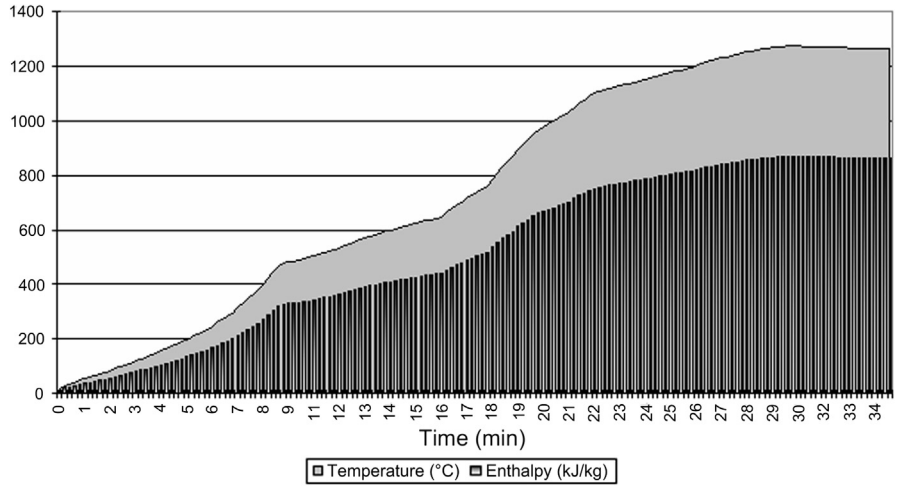


Figure 12.6 Time-temperature-enthalpy diagram for metal slab heating

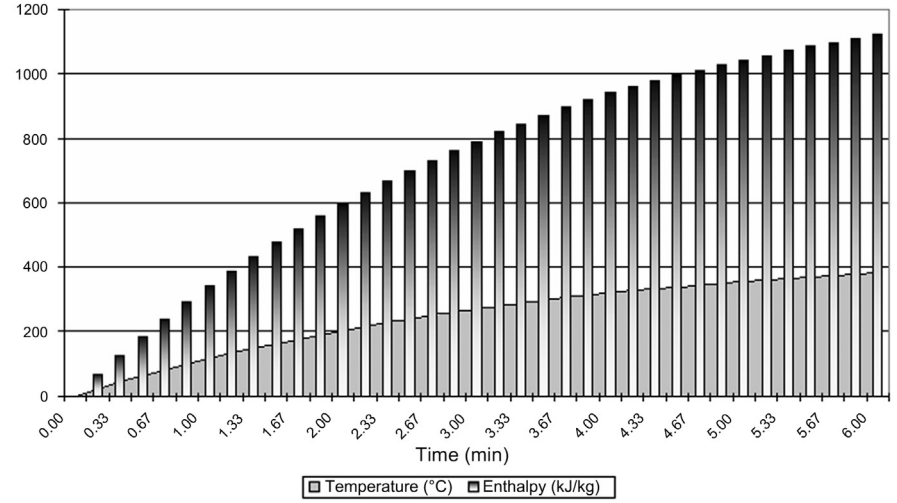


Figure 12.7 Time-temperature-enthalpy diagram for multi-component oil heating

0 °C to 200 °C (heating), and from 1000 °C to 140 °C (cooling) indicate that the material specific heat is temperature dependent. Thus we have (viz. Chapter 9 equation [9.4]).

$$h_c = \{\overline{Cp}\,\Delta T\}_{\text{heating}} + h_r - \{\overline{Cp}\,\Delta T\}_{\text{cooling}} \qquad (12.3)$$

It is important to understand that in the third case, the furnace must be designed to be able to transfer the energy required to heat the material

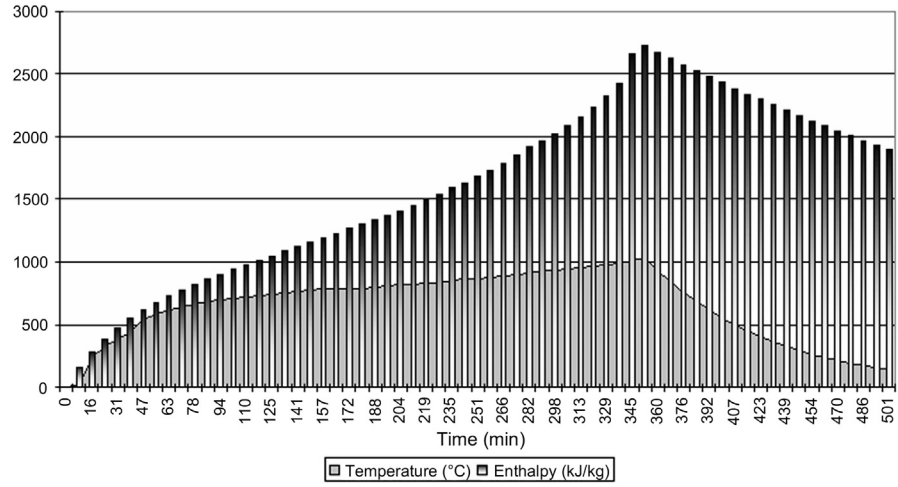


Figure 12.8 Time-temperature-enthalpy diagram for mineral aggregate processing

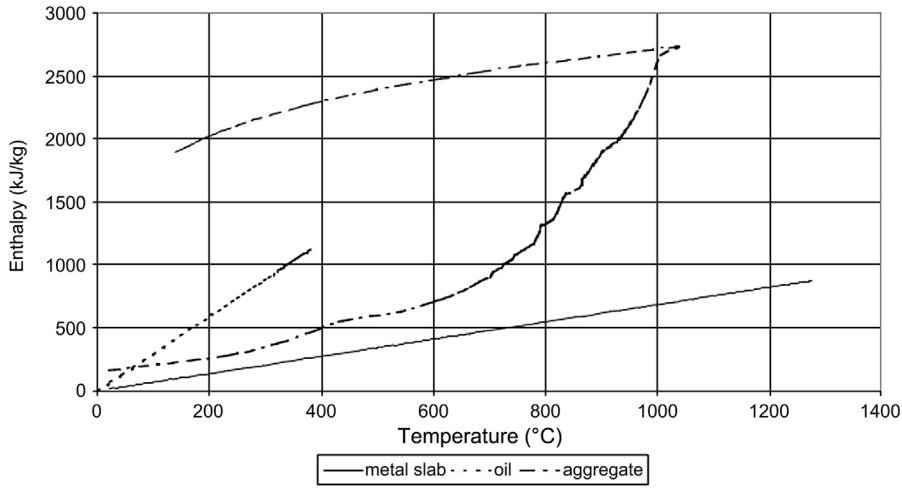


Figure 12.9 Temperature-enthalpy relationships for metal slab. Oil and aggregate heating processes

and carry out the chemical reactions up to the maximum temperature of the product (i.e. >1000 °C), and not just to meet the energy calculated by equation (12.3).

As previously discussed, the requirement to cool the product may be integrated within the furnace design, incorporating some heat recovery, or may be carried out in a separate piece of equipment.

The thermal input required/unit mass of product and average sink temperature for each process can be readily derived from the data. The thermal input/unit mass of product is the difference between the feed and product enthalpies, whilst the average sink temperature is the time mean average of the material temperature between the feed and product enthalpies. See Table 12.2 for the values calculated for the three examples from Figures 12.6, 12.7 and 12.8. Thus for a given production rate, Q_c, the theoretical thermal load of the furnace (i.e. theoretical amount of heat to be transferred) can be calculated.

$$H_c = Q_c h_c \tag{12.4}$$

The physical state of the feedstock and product i.e. gas, liquid or solid, determines the way it is presented in the furnace. This in turn determines the product mass to heat transfer surface ratio. For example liquids or gases are generally contained in tubes or annular ducts, finely divided solids in fluid beds or gaseous suspensions, lumps in packed beds or on hearths, large solid blocks on a support frame, and smelt beds on the furnace floor. For our three example furnaces the following data has been derived from the laboratory and pilot plant tests.

- **Slab heating.** The slab thickness, b, will be 100 mm. The length, l, and width, w, can be varied to suit any commercial or mechanical constraints, although the normal delivered length of feedstock would be between 0.5 and 1.5 m. Metal slab density is 7800 kg/m^3.
- **Oil heating.** Laboratory tests show that the viscosity of the oil is such that it cannot be easily pumped at temperatures below 155 °C. It is therefore likely that the feedstock to the furnace would be delivered pre-heated, and stored at this temperature, splitting the process into two steps. Pilot plant studies indicate that excessive heat fluxes are critically detrimental to the product quality and the minimum diameter pipe that the oil should be heated in to avoid excessive coking of the internal tube surfaces is 2 inch, schedule 40 pipe (d_i = 52.5 mm, d_o = 60.5 mm.). Oil density is 980 kg/m^3.

Table 12.2 Furnace Design Data Derived From Figures 12.6, 12.7 and 12.8

Process	*Furnace inlet temperature °C*	*Furnace outlet temperature °C*	*Time mean average temperature °C*	*Furnace inlet enthalpy kJ/kg*	*Furnace outlet enthalpy kJ/kg*	*Thermal duty (h_c) kJ/kg*	*Residence time (τ) minutes*
Metal slab heating	20	1263	756	13.7	862.6	848.9	34
Oil heating	155	382	279	340.5	1123.1	782.6	4.5
Aggregate processing							
heat	20	1037	739	164.1	2727.9	2536.8	353
cool	1037	140	456	2727.9	1894.7	−833.2	147

- **Aggregate processing.** Quarrying and size reduction tests indicate that the most economic feedstock will be in a range from 25 mm to 200 mm, with a mass mean average equivalent diameter, d, of 100 mm. Aggregate density (apparent) is 1400 kg/m^3. Voidage for loosely packed material is 0.35.

From this information the mass to heat transfer surface ratio for each process can be determined, as shown in Table 12.3. This, together with data from Table 12.2, enables the calculation of the average heat flux to be made.

In order to progress the design of the three example processes, we need to make some further design decisions. The first of these is to determine the desired production rate Q_c. A production rate of 2 kg/s has been selected for all three examples. The second is to select the type of fuel source. The criteria for fuel selection has been discussed in the previous section and since the slab heating, and aggregate processing furnaces will involve direct flame contact with the product, a 'clean' fuel is required. For simplicity and continuity in the example designs, we will therefor consider all the furnaces to be fired with natural gas, using the data from Table 3.1 for North Sea natural gas as the basis.

Using the source-sink concept illustrated in Figure 1.3, the type of furnace designs that are most suited to the requirements can select from Table 1.1. This provides conceptual information in respect of the general shape and hence enables the initial design geometry for the furnace to be calculated. For the three examples:

- **Slab heating.** From Table 1.1, this is a type 15 furnace, which includes open hearths, glass tanks and metal re-heating furnaces.

Table 12.3 Calculation of Heat Transfer Areas and Average Furnace Heat Flux for Design Examples

Property	*Thin slab*	*Tube filled with liquid*	*Sphere*
External surface area	$2.1 \cdot w \cdot$ (where $b << 1 \cdot w$)	$1 \cdot \pi \cdot d_o$	$\pi \cdot d^2$
Internal surface area	—	$1 \cdot \pi \cdot d_i$	—
volume	$1 \cdot w \cdot b$	$1 \cdot \pi \cdot d_i^2/4$	$\pi \cdot d^3/6$
Heat transfer area/unit mass	$2/(\rho \cdot b)$	$4 \cdot d_o/(\rho \cdot d_i^2)$	$6/(\rho \cdot d)$
b m	0.1	—	—
d_i m	—	0.0525	—
d_o m	—	0.0605	—
d m	—	—	0.1
ρ kg/m^3	7800	980	1400
Heat transfer area/unit mass (a) m^2/kg	0.002564	0.089592	0.042857
Thermal duty (Table 12.2) kJ/kg	848.9	782.6	2536.8
Residence time (τ) (Table 12.2) s.	2040	300	21180
Average heat flux kW/m^2	162.3	29.1	2.8

These are characterised by a generally rectangular box shape, where the length and width are greater than the height. The general concept is to contain the flame(s) in a narrow space between the roof (and floor in the case of re-heating furnaces) and the surface of the sink, to maximise the amount of direct and reflected radiation, (see Figure 4.12). Heat transfer within the material is by the process of transient conduction discussed in section 4.2.

- **Oil heating.** From Table 1.1, this is a type 13 furnace, which includes water-tube boilers, tube-still heaters and reforming furnaces. These are characterised by vertical tube-lined walls, which may be backed by a refractory (see Figure 4.19), or joined together by welded metal plates to form a membrane. The general concept is to distribute the sink surface evenly around the walls, and create a combustion space that gives an even thermal release, usually by means of multiple burners. The furnace may be rectangular, or cylindrical with the height generally greater than the length/width or diameter.
- **Aggregate processing.** From Table 1.1, this is a type 14 furnace, which includes rotary kilns, fluidised beds, flash heating furnaces, shaft kilns, moving and rotary hearths. The general concept is to maximise the exposed surface area of the sink, thereby enhancing both radiative and convective heat transfer through close contact between the flame and sink. These furnaces are generally cylindrical (although some smaller fluidised beds are rectangular), with the length greater than the diameter.

Having determined the general shape of the furnace, design options with respect to relative principal dimensions (height, length, width, diameter) can be tested and optimised using the well-stirred furnace model equations (12.5) and (12.6) described in section 6.2.1.

$$Q'D' = \left[\left(1 - \frac{Q'}{d}\right)^4 - \tau^4\right] + L'_R\left[\left(1 - \frac{Q'}{d}\right) - \tau_o\right] + L'_o\left[\left(1 - \frac{Q'}{d}\right)^4 - \tau_o^4\right] \tag{12.5}$$

$$\eta = \frac{Q - \text{losses}}{H_f} = \frac{Q'}{1 - \tau_0} - \frac{L'_R}{D'}\left(1 - \frac{Q'/d}{1 - \tau_o}\right) - \frac{L'_o}{D'(1 - \tau_o)}\left[\left(1 - \frac{Q'}{d}\right)^4 - \tau_0^4\right] \tag{12.6}$$

This will determine the required fuel rate to achieve the production rate, examine options for air preheating, product preheating etc. and optimise the thermal efficiency of the process. The following analysis

Table 12.4 Input Data for Well-Stirred Furnace Model Analysis

a		*Slab heating*	*Oil heating*	*Aggregate processing (heating only)*
Ambient (datum) temperature K	T_o	293	293	293
Production rate kg/s	Q_c	2.0	2.0	2.0
Mass of product in furnace ($Q_c \cdot \tau$) kg	m_c	4080	600	42360
Theoretical heat required ($Q_c \cdot h_c$) kW	H_c	1697.8	1565.2	5073.6
Sink area ($m_c \cdot a$) m^2	A_s	10.46	44.80	1815.42
Sink temperature K	T_s	1029	552	1012
Sink emissivity	ε_s	0.8	0.8 (tube)	0.5
Fuel properties				
Calorific value kJ/kg	C_v	50730	50730	50730
Air requirement kg/kg	*SAR*	16.56	16.56	16.56
Flame emissivity (based on natural gas combustion using equation [54] in Chapter 4)	ε_g	0.3	0.3	0.3
Design variables				
Excess air %	*XS*	10	10	10
Adiabatic flame temperature at design excess air K	T_{af}	1949	1949	1949
Overall htc based on insulation backed refractory (see example 4.1) kW/m^2K	*U*	0.00125	0.00125	0.00125

of the three example furnaces serves to illustrate this stage of the design process. Table 12.4 summarises the input data required for the well-stirred model. For each of the furnaces, the principal dimensions are inter-related to each other and the sink. Thus the first step is to fix the critical dimensions for each design. The following sections demonstrate how this may be achieved for each of the example furnaces.

Slab Heating Furnace Design

The slab heating furnace would be of a pusher design, see Figure 12.10, whereby slabs are pushed side-on into the furnace onto water cooled skids at a controlled rate to give the desired residence time. Slabs are heated on both sides by flames and combustion gases. The design options specified for the feedstock length ranges from 0.5 m to 1.5 m, thus for a given feedstock length, the furnace length is fixed by the already calculated required heat transfer area. The furnace width is designed to suit the length of slabs, thus if an

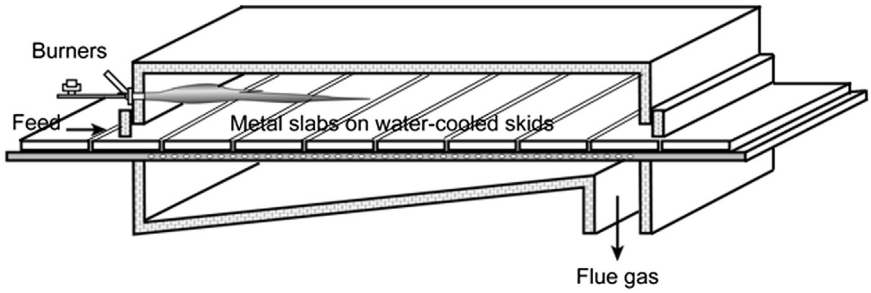


Figure 12.10 Schematic diagram of a typical single zone re-heating furnace

allowance of 200 mm is made on each side of the slabs, the width will range from 0.9 m to 1.9 m to accommodate the range of feedstock sizes. The final dimension to be fixed is the furnace height. The minimum distance required between the sink and the roof/floor to achieve efficient combustion is the factor that determines this dimension. An initial value of 1.5 m between the roof (and floor) and the slabs has been selected, giving an internal furnace height of 3 m. Optimisation of this variable will be discussed in more detail later in this section when considering the burner design. Table 12.5 shows the results of well-stirred furnace analyses using equation (12.5), for a range of furnace widths. In each case, the fuel rate has been iterated by successive calculations of Q' and η to match the value of Q in equation (12.6) to the theoretical heat requirement H_c.

Figure 12.11 illustrates how the effect of the slab length, and hence furnace width, changes the furnace length, thermal efficiency, average heat flux and flue gas exhaust temperatures. The calculations indicate that a wider furnace is slightly more thermally efficient, where the reducing aspect ratio between the width and length reduces the internal refractory surface and results in lower heat losses, This is in agreement with the trend shown in Figure 6.4. A converse consequence of the smaller furnace dimensions, and hence volume is an increasing firing density. This indicates that there will be fewer, larger burners, and they must be designed for higher combustion intensities, where the impact of environmental requirements, such as increased NO_x emissions, must be considered.

Another consideration concerns the charging of the furnace. Whilst the operation is deemed as continuous, it is in fact a semi-batch process, since slabs must be pushed into the furnace at regular intervals. The smaller the slabs, the more frequently they must be 'pushed', thus if the slabs are 250 mm wide, 0.5 m slabs, weighing $\sim$100 kg, would be charged into the furnace every $\sim$50 seconds, whereas 1.5 m slabs would be pushed every $\sim$145 seconds. Each time a slab is pushed, the burner firing rate must be reduced to a low fire rate

Table 12.5 Well-Stirred Furnace Analysis of Slab Heating Furnace Designs

Slab length m	l	0.5	1	1.5
Furnace width m		0.9	1.4	1.9
Furnace length ($A_s/2l$) m		10.46	5.23	3.49
Furnace height m		3	3	3
Refractory area m^2	A_r	87.0	54.4	45.6
Openings area m^2	A_o	0	0	0
Furnace volume m^3	V	28.24	21.97	19.89
Well stirred furnace model results				
Fuel rate kg/s	m_f	0.116	.112	.112
Mass of combustion gases ($m_f(1+SAR \cdot (1+XS/100))$) kg/s.	m	2.2342	2.1571	2.1571
Thermal input ($m_f \cdot C_v$) kW	H_f	5585	5682	5682
Dimensionless firing density	D'	1.17	1.21	1.25
Dimensionless efficiency	Q'	29.72	28.54	27.96
Heat losses kW		382.25	238.52	200.38
Thermal efficiency	η	28.5	29.4	29.4
Average furnace gas temperature °C	T_g	1575	1572	1561
Flue gas temperature °C		1207	1278	1304
Average heat flux kW/m^2		196.8	182.5	178.7
Firing density kW/m^3		197.8	258.6	285.7

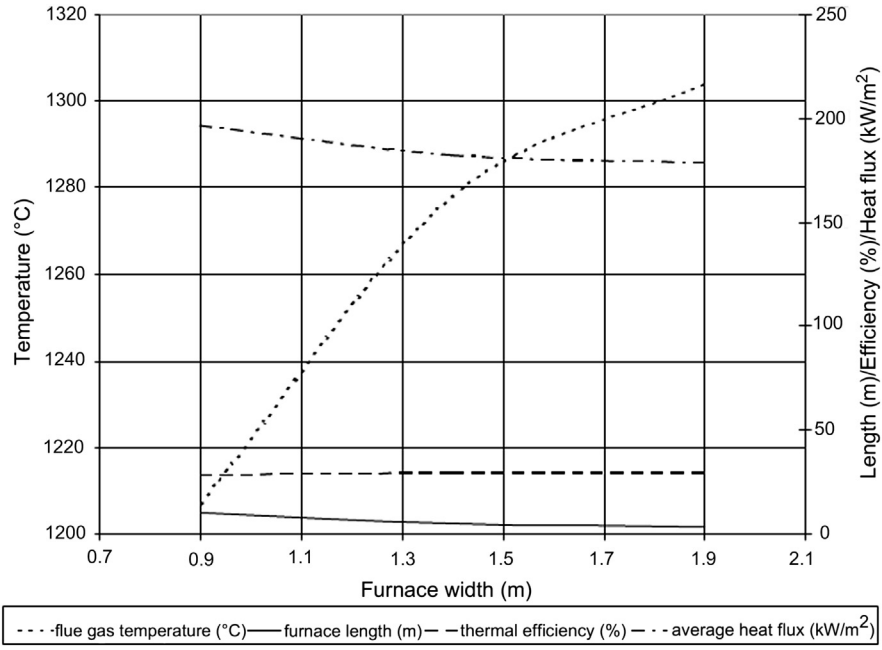


Figure 12.11 Effect of slab length on principal parameters in the design of a heating furnace

for safety reasons, the feed and discharge doors must be opened, the slab pushed, the doors closed and the burners returned to the duty firing rate. This would typically require 10–15 seconds, during which time heat is lost by radiation through the openings and the residence time for each slab in the furnace increased by the cumulative charging times. Once the slab length is determined, a second round of calculations would therefore be required to resize the furnace to meet the production rate including the charging time and calculate the charging heat losses by setting the value of A_o to the charging door areas in the design equation (12.5).

Oil Heating Furnace Design

The oil heating furnace would be of a tube-still design, see Figure 12.12, where the oil passes through a continuous serpentine of vertical or horizontal pipes arranged against the furnace walls. Two basic furnace shapes can be considered, rectangular and cylindrical. The pilot plant data has recommended that as a minimum, 2 inch pipe should be used for the oil. The serpentine formation of the pipework in the furnace involves the use of 180° bends, which from simple constructional considerations would be 'standard' short or long radius 2 inch bends. The bend radius will therefore fix the tube spacing. The velocity of the oil in the tubes would normally be governed by a calculation of the economic pumping pressure requirements. For this type of application, flow velocities in the range of 0.5 to 3.0 m/s are typical, Nelson (1949). Thus for a given velocity, the total length of tube is fixed by the residence time, individual tube lengths by the height (vertical tubes) or length (horizontal tubes) of the furnace, number of tube runs by the total length divided by the individual tube length, and the furnace length, height or diameter, depending on the tube orientation, by the product of the tube spacing and number of tubes. These calculations are shown in Tables 12.6 and 12.7 for vertical tubes in rectangular and cylindrical furnaces of different heights, together with the results of well-stirred furnace analyses for each design. In the case of the rectangular furnace an initial furnace width of 2 m has been chosen to allow for the burner flames. Optimisation of this variable will be discussed in more detail later in this section when considering the burner design.

Figures 12.13 and 12.14 illustrates how the effect of the furnace height changes the furnace length or diameter, thermal efficiency, average heat flux and flue gas exhaust temperatures for both rectangular and cylindrical furnace designs. Comparison of the calculated data indicates that a cylindrical furnace is more thermally efficient than a rectangular design. However, the firing density is a factor of 2–3 times higher in a cylindrical furnace, with the same implications for the burner design as discussed in the previous section on the slab

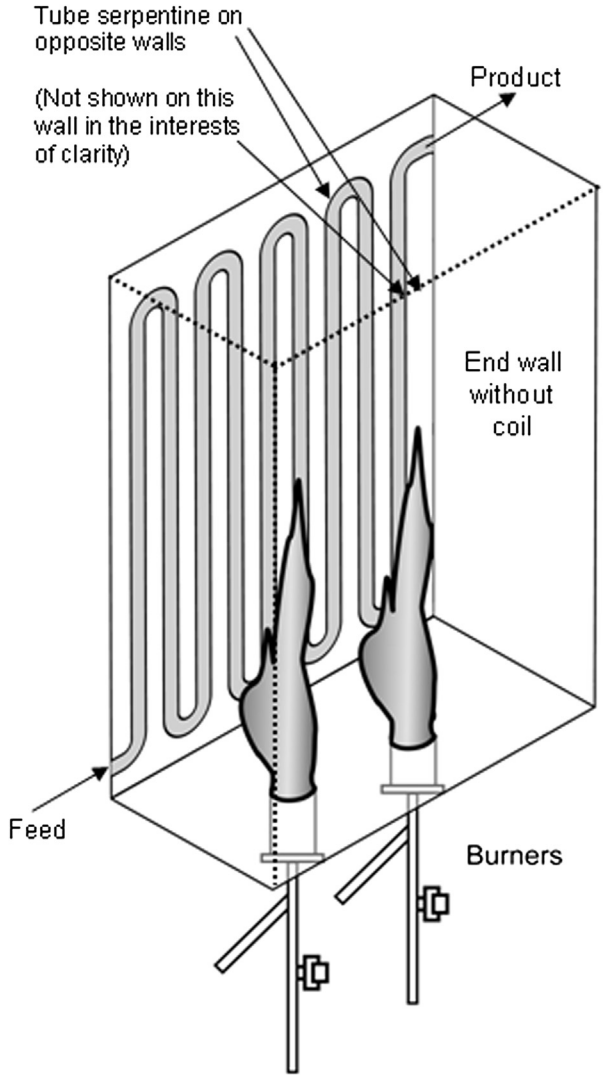


Figure 12.12 Schematic diagram of a typical rectangular tube-still heater

heating furnace. The results indicate that the height:length or height: diameter aspect ratios studied (~ 8:1 to 2:1) are not very significant with respect to thermal performance. Reference is again made to Figure 6.4.

The critical factor in the design of this type of furnace is to avoid locally high heat fluxes. This implies that the burner(s) need to be disposed inside the furnace to give a controlled combustion pattern. How to achieve this will be discussed later in this chapter, but it is

Table 12.6 Well-Stirred Furnace Analysis of Rectangular Oil Heating Furnace Designs

Oil velocity in pipe m/s	v	0.91	0.91	0.91
Pipe length in furnace ($v \cdot \tau \cdot 60$) m	l_t	245.7	245.7	245.7
Furnace height m	h	8	6	4
Number of tubes (Integer of l_t/h)	N	31	41	62
Tube spacing between centres m	p	0.1	0.1	0.1
Furnace length ($(N+1) \cdot p/2$	l	1.55	2.05	3.1
Furnace width m	w	2	2	2
Refractory area m^2	A_r	56.8	48.6	40.8
Openings area m^2	A_o	0	0	0
Furnace volume m^3	V	24.80	24.60	24.80
Well stirred furnace model results				
Fuel rate kg/s	m_f	0.0371	0.0370	0.0368
Mass of combustion gases ($m_f(1 + SAR \cdot (1 + XS/100))$) kg/s.	m	0.7129	0.7110	0.7071
Thermal input ($m_f \cdot C_v$) kW	H_f	1882	1877	1867
Dimensionless firing density	D'	0.12	0.12	0.13
Dimensionless efficiency	Q'	62.98	62.41	61.84
Heat losses kW		148.05	127.53	107.83
Thermal efficiency	η	66.3	66.7	67.0
Average furnace gas temperature °C	T_g	1053	1058	1064
Flue gas temperature °C		422	461	499
Average heat flux kW/m^2		29.97	29.59	29.17
Firing density kW/m^3		75.89	76.30	75.28

Table 12.7 Well-Stirred Furnace Analysis of Cylindrical Oil Heating Furnace Designs

Oil velocity in pipe m/s	v	0.91	0.91	0.91
Pipe length in furnace ($v \cdot \tau \cdot 60$) m	l_t	245.7	245.7	245.7
Furnace height m	h	8	6	4
Number of tubes (Integer of l_t/h)	N	31	41	62
Tube spacing between centres m	p	0.1	0.1	0.1
Furnace diameter ($(N \cdot p/\pi) + p$) m	d_f	1.09	1.41	2.07
Refractory area m^2	A_r	28.24	28.04	29.43
Openings area m^2	A_o	0	0	0
Furnace volume m^3	V	7.42	9.30	13.51
Well stirred furnace model results				
Fuel rate kg/s	m_f	0.0352	0.0352	0.0352
Mass of combustion gases ($m_f(1 + SAR \cdot (1 + XS/100))$) kg/s.	m	0.6428	0.6428	0.6428
Thermal input ($m_f \cdot C_v$) kW	H_f	1786	1786	1786
Dimensionless firing density	D'	0.13	0.13	0.13
Dimensionless efficiency	Q'	61.22	61.2	61.35
Heat losses kW		75.03	74.53	78.04
Thermal efficiency	η	67.9	67.9	67.8
Average furnace gas temperature °C	T_g	1068	1068	1066
Flue gas temperature °C		551	552	544
Average heat flux kW/m^2		27.61	27.61	27.66
Firing density kW/m^3		240.7	192.0	132.2

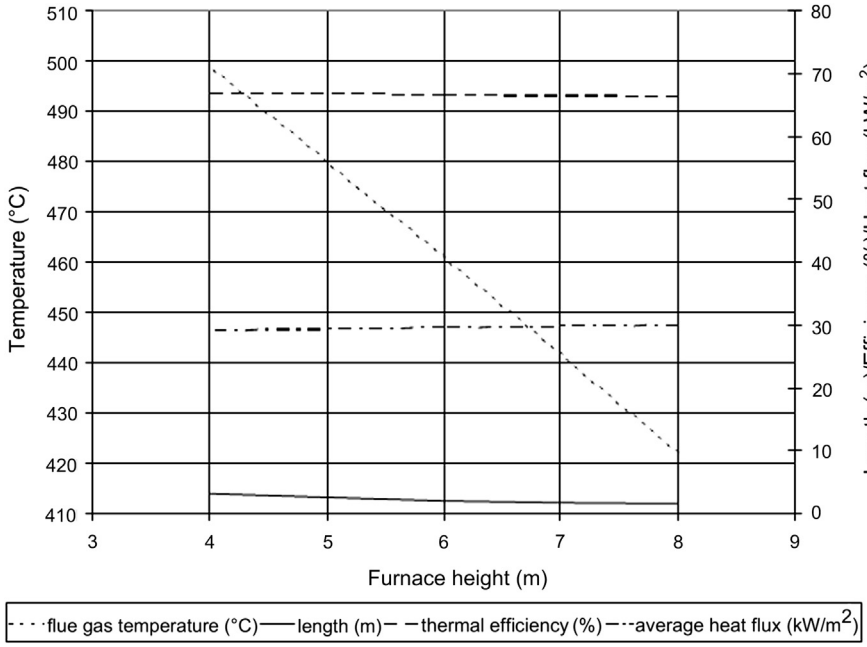


Figure 12.13 Effect of furnace height on principal parameters in the design of a rectangular oil heating furnace

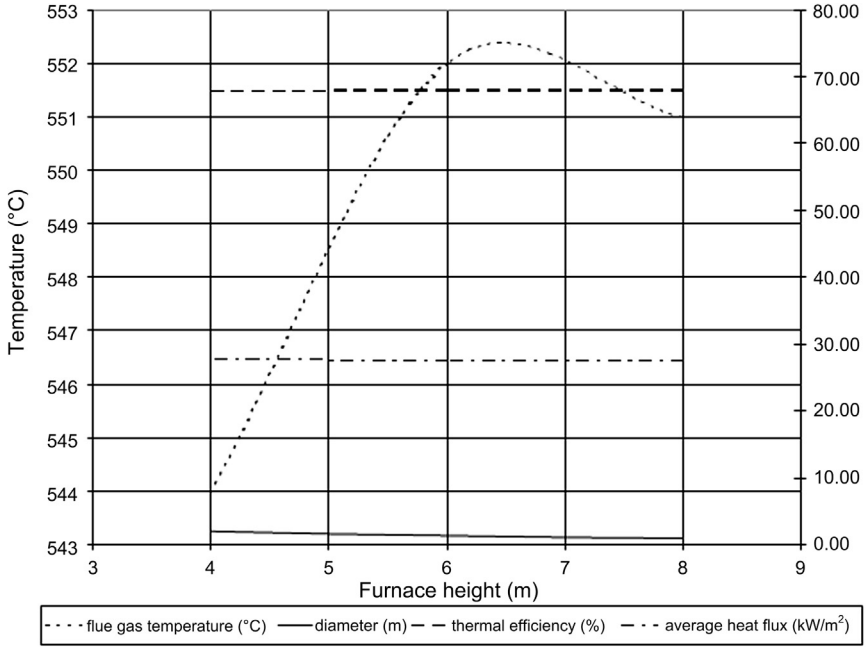


Figure 12.14 Effect of furnace height on principal parameters in the design of a cylindrical oil heating furnace

instructive to look at Figure 5.8 and the related text in section 5.2 to appreciate how the burner design and operation can be adjusted to meet these requirements.

Aggregate Processing Furnace

Since the aggregate material ranges from 25 mm to 200 mm in size, it is most suited to processing in a shaft kiln. The volume of material in the furnace can be calculated from the mass in the furnace, see Table 12.3, and the apparent density. Allowing for the voidage, the actual volume occupied by the material can be calculated, this being equal to the kiln volume. Thus for a given kiln diameter, the height can be calculated. Table 12.8 shows these calculations for a number of kiln diameters and presents the results of well-stirred furnace analyses for each design excluding any product cooling.

Figure 12.15 illustrates how the effect of the kiln diameter changes the furnace height, thermal efficiency, and flue gas exhaust temperatures. The calculations clearly indicate that the thermal efficiency increases with the kiln diameter, although with an exponentially diminishing advantage. There are other design considerations that would also lead to a larger diameter kiln. The civil and mechanical engineering requirements for a tall, slender structure are much more

Table 12.8 Well-Stirred Furnace Analysis of Aggregate Processing Shaft Furnace Designs

Shaft diameter m	d_f	1	2	3
Bed voidage	φ	0.35	0.35	0.35
Furnace height $((m_c/\rho \cdot (1-\varphi))/(\pi \cdot d_f^2/4)$ m	h	61.2	16.3	6.8
Refractory area $(\pi \cdot d_f \cdot h)$ m^2	A_r	192.1	96.1	84.0
Openings area m^2	A_o	0	0	0
Furnace volume m^3	V	48.04	48.04	48.04
Well stirred furnace model results				
Fuel rate kg/s	m_f	0.1667	0.1484	0.1448
Mass of combustion gases $(m_f(1 + SAR \cdot (1 + XS/100)))$ kg/s.	m	3.2033	2.8517	2.7825
Thermal input $(m_f \cdot C_v)$ kW	H_f	8457	7427	7346
Dimensionless firing density	D'	0.024	0.021	0.021
Dimensionless efficiency	Q'	61.06	66.73	66.70
Heat losses kW		440.91	196.28	130.80
Thermal efficiency	η	66.7	75.9	76.7
Average furnace gas temperature °C	T_g	1059	975	975
Flue gas temperature °C		532	450	471
Average heat flux kW/m^2		3.27	3.10	3.10
Firing density kW/m^3		176.05	154.61	152.92

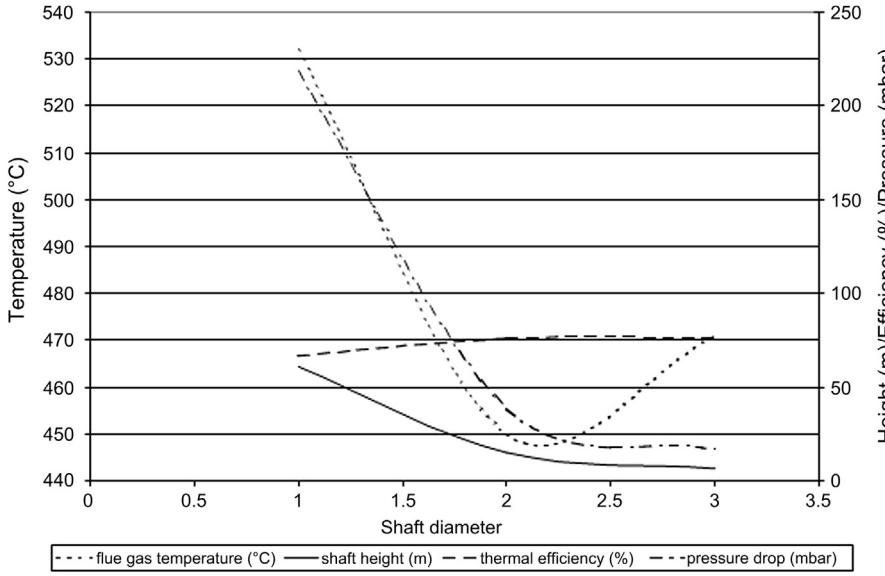


Figure 12.15 Effect of kiln diameter on principal parameters in the design of a shaft kiln

difficult and expensive. Operational consideration must also be given to the gas flow through the bed, since the pressure drop will determine the capital and running costs of any fans. Using a calculation method for fluid flow in packed beds, Spiers 1961, Table 12.9 shows the effect of kiln diameter on the bed pressure drop. This is also plotted in Figure 12.15.

In the previous two examples, heat recovery has not been considered, although there is a significant amount of recoverable energy available in the flue gases, and it could be readily used to preheat the combustion air as shown in chapter 9. In this type of furnace, it would be expedient to cool the product at the bottom of the furnace by extending the height to accommodate the additional residence time required. See Figure 12.16, which is a schematic of the oil fuel, side-fired vertical shaft lime kiln shown in Figure 1.5. Cooling can then be effected by the air required for combustion, thereby preheating it and improving the thermal efficiency. Table 12.10 summarises

Table 12.9 Analyses of the Effect of Kiln Diameter on Pressure Drop Through Packed Bed of Aggregate

Shaft diameter *m*	d_f	1	2	3
Bed depth m		61.2	16.3	6.8
Mean gas velocity in bed m/s		35.02	7.08	3.10
Pressure drop over bed mbar		218	39	17

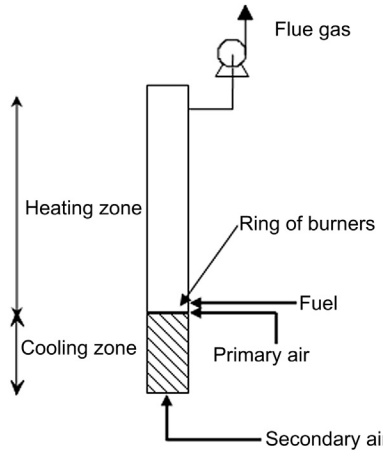


Figure 12.16 Schematic of shaft kiln with integral product cooling and air preheating

Table 12.10 Well-Stirred Furnace Analysis of Aggregate Processing Shaft Furnace Designs Including Integral Product Cooling by Combustion Air

Shaft diameter m	d_f	1	2	3
Bed voidage	φ	0.35	0.35	0.35
Mass of product in furnace including cooled material ($Q_c \cdot (\tau_{heat} + \tau_{cool})$ kg	m'_c	60000	60000	60000
Furnace height $((m'_c/\rho \cdot (1-\varphi))/(\pi \cdot d_f^2/4)$ m	h	87.0	21.7	7.1
Adiabatic flame temperature K	T_{af}	2215	2264	2282
Refractory area ($\pi \cdot d_f \cdot h$) m^2	A_r	273.3	136.6	91.1
Openings area m^2	A_o	0	0	0
Furnace volume m^3	V	68.32	68,32	68.32
Well stirred furnace model results				
Fuel rate kg/s	m_f	0.1007	0.0925	0.0898
Mass of combustion gases $(m_f(1 + SAR \cdot (1 + XS/100)))$ kg/s.	m	1.9351	1.7775	1.7256
Thermal input ($m_f \cdot C_v$) kW	H_f	5109	4693	4556
Thermal input from air preheat kW		1971	1989	1996
Dimensionless firing density	D'	0.0083	0.0073	0.00070
Dimensionless efficiency	Q'	75.76	76.99	77.41
Heat losses kW		544.94	272.34	181.28
Thermal efficiency	η	79.6	84.3	86
Average furnace gas temperature °C	T_g	960	959	958
Flue gas temperature °C		168	263	299
Average heat flux kW/m^2		2.30	2.22	2.18
Firing density kW/m^3		74.78	68.69	66.68

the re-calculated values to include a product cooling zone. It is important to appreciate the significance of this energy recovery measure. The thermal efficiency is improved by ~10%, but of more significance is the reduction in fuel consumption of ~40%. The value of the pre-heated air is not just in the replaced heat capacity of the fuel by hot air, but also from the increased adiabatic flame temperature, which enhances the heat transfer by increasing the temperature difference between the source and sink.

12.4 Burner Selection

The burner design and burner configuration must be selected to get the desired heat transfer profile. The combustion space and shape may be determined by physical, mechanical or structural factors, as illustrated in the previous examples, but that space must be able to accommodate efficient aerodynamic mixing and combustion of the fuel, and generate the desired heat flux profile for the product. All of the design calculations have so far assumed a well-stirred furnace, giving an even heat flux to all surfaces. It has been shown from the preceding chapters that the heat release, and hence heat flux generated from most industrial burner flames is not even. It is generally high in the region near to the burner port, where fuel and air are plentiful, and reduces as the flame develops, owing to the depleting fuel content, and by losing heat to its surroundings. The burner design can modify this profile, but it can never mimic a fully well-stirred reactor.

The actual heat flux profile for the process can be determined from the time-temperature enthalpy data, by dividing the rate of change of enthalpy by the heat transfer area/unit mass, a.

$$q = \frac{\delta h_c}{a\delta t} \tag{12.7}$$

Figures 12.17, 12.18 and 12.19 show the calculated heat flux profiles derived using equation (12.7) from the time-temperature-enthalpy data for each of the processes. For each profile, the time may be easily equated to a physical location of the product in the furnace. Thus for the slab furnace there is a requirement for the heat fluxes to be high at 5–10 minutes and 15–22 minutes into the heating cycle, which for a 0.9 m wide furnace would equate to 1.5 to 3 m and 4.5 to 6.8 m from the product charging door. This would indicate that the desired heat flux profile could be created by two rows of burners, located across the furnace width at ~3 m and ~7 m from the furnace feed end, firing back towards the feed end to give a counter-current flow. In the case of the oil heater, the tube heat fluxes are highest at the region where the oil enters the furnace, but low at the exit. The original calculations have assumed that the tubes are arranged as

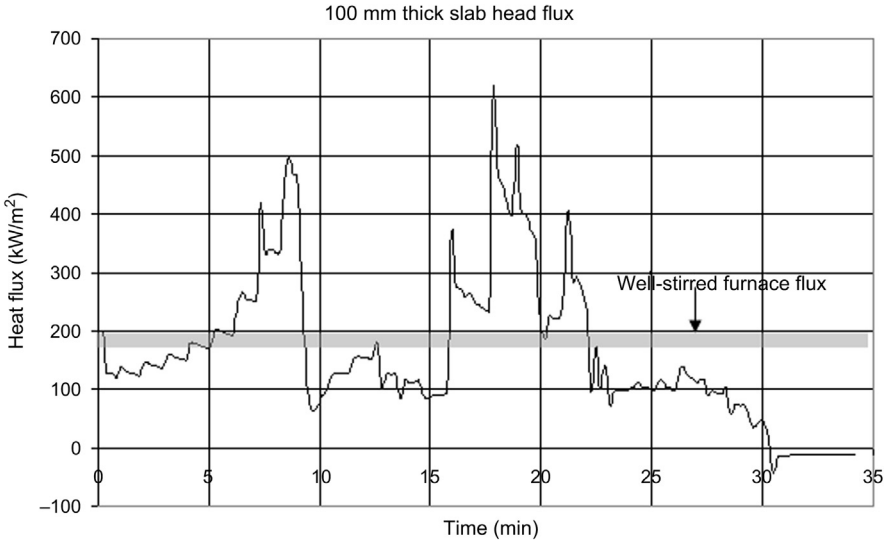


Figure 12.17 Surface heat flux profile for slab heating

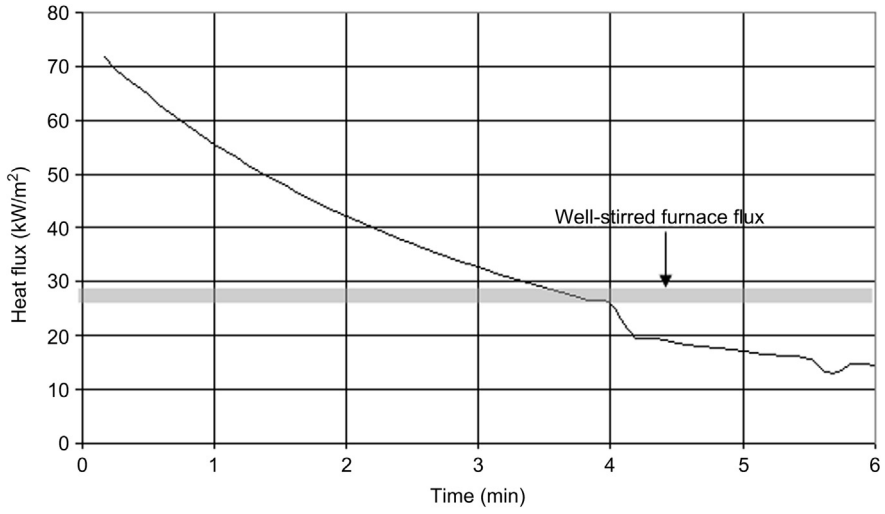


Figure 12.18 Surface heat flux to outside of tube for oil heating

a single vertical pass around the furnace walls, but if the burner(s) are to be located on the furnace floor, a horizontal tube arrangement may be more advantageous. In this arrangement the oil enters at the bottom of the furnace, and flows upward through successive horizontal passes to the top. The wall heat flux demands would then match the natural heat release pattern of the flames. A similar effect could be

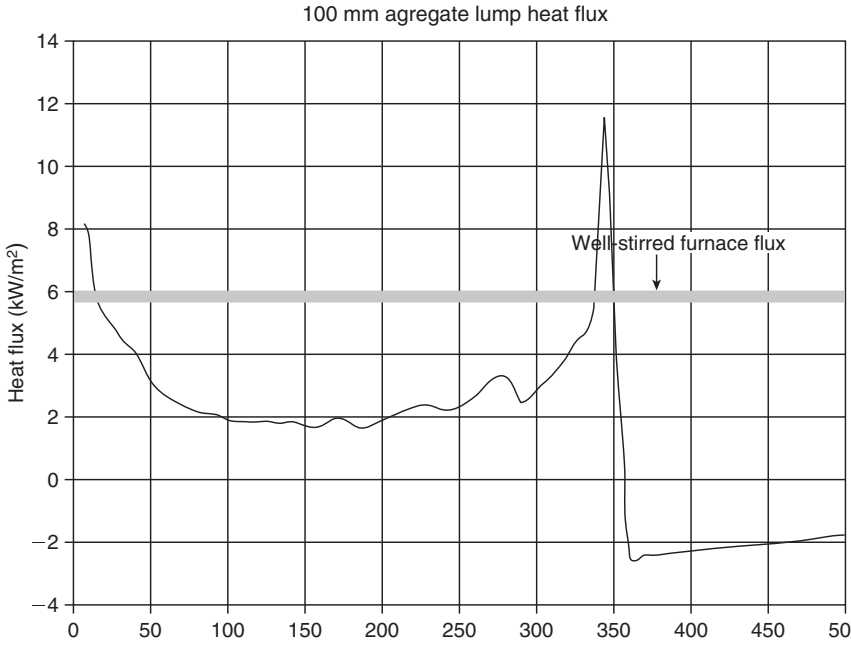


Figure 12.19 Surface heat flux to lump for aggregate processing

achieved by splitting the vertical tube arrangement into two or more sections. For the minerals processing kiln, there is a very 'peaky' heat flux requirement between 320 and 350 minutes. Thus for a 2 m diameter kiln with a product cooling section (see Table 12.10) this equates to a region ~6.5–7.5 m from the bottom of the shaft. This indicates that a ring of burners should be located just below this zone, at ~6 m from the bottom of the shaft.

Having determined the burner locations, the next step is to define the required burner performance. In the first two cases, the burners would be of a register or package type as described in chapter 5, where all the air required for combustion passes through the burner. Discussions with bu rner manufacturers, and reference to their technical literature, will identify suitable burner designs and give important mechanical information. By way of example, a medium velocity nozzle mixing gas burner, identified as suitable for the slab reheating furnace, has the specification supplied by a manufacturer as shown in Table 12.11 (Stordy 2006). To meet the thermal duty of the furnace, calculated as ~5.6 MW, will require 12 burners. From the data supplied, which states that the mounting flange has a diameter of 330 mm, it would only be possible to fit three burners in a row across the 0.9 m wide furnace. This implies that the design would involve rows firing above and below the slabs at both the previously

Table 12.11 Manufacturer's technical data on nozzle mixing gas burner for slab heating furnace (after NA-Stordy Combustion Ltd.)

Nominal thermal capacity	440	kW
Air pressure @ nominal capacity	33	mbar
Gas pressure @ nominal capacity	18	mbar
Exit velocity @ nominal capacity	100	m/s
Maximum thermal capacity	656	kW
Air pressure @ maximum capacity	73	mbar
Gas pressure @ maximum capacity	40	mbar
Exit velocity @ maximum capacity	150	m/s
Flame length @ nominal capacity	800	mm
Flame tube material 1400–1600 °C	refractory	
Turndown ratio	8:1	
Exit port diameter	145	mm
Refractory tube outside diameter	264	mm
Mounting flange diameter	330	mm

identified locations. If the 1.9 m wide furnace design is selected then the burners could be fitted as a single row either above or below the slabs if desired. The burners would be on a pitch of ~330 mm, equivalent to 2.27 exit port diameters. A general rule with respect to burner spacing is that the pitch is greater than 2 burner exit port diameters to avoid flame interference. Close pitching of burners changes the combustion aerodynamics, altering the flame shape, temperature etc. as shown by the experimental measurements (Apak 1972) in Figure 12.20.

The burner design for the shaft kiln would be different, since the majority of the combustion air is preheated and dispersed across the shaft. High velocity gas jets, injected horizontally, or with a small downward angle must be used to promote rapid mixing and combustion. The detailed design of these jets should be carried out using the modelling techniques described in chapter 6.

12.5 Detailed Analysis and Validation of the Furnace Design

The preceding section has shown how to develop a basic furnace design. At this stage the mass and energy balance should be rechecked and revised to account for any changes that have been introduced since the last version was completed. The next stage would be to engineer the basic mechanical structure of the furnace to meet the design criteria, including the preferred heat recovery systems.

Before starting on the detailed mechanical and structural design, a physical and/or mathematical model of the proposed design should be built to validate the basic design parameters, optimise the system aerodynamics, ensure that the burner design will meet the thermal and

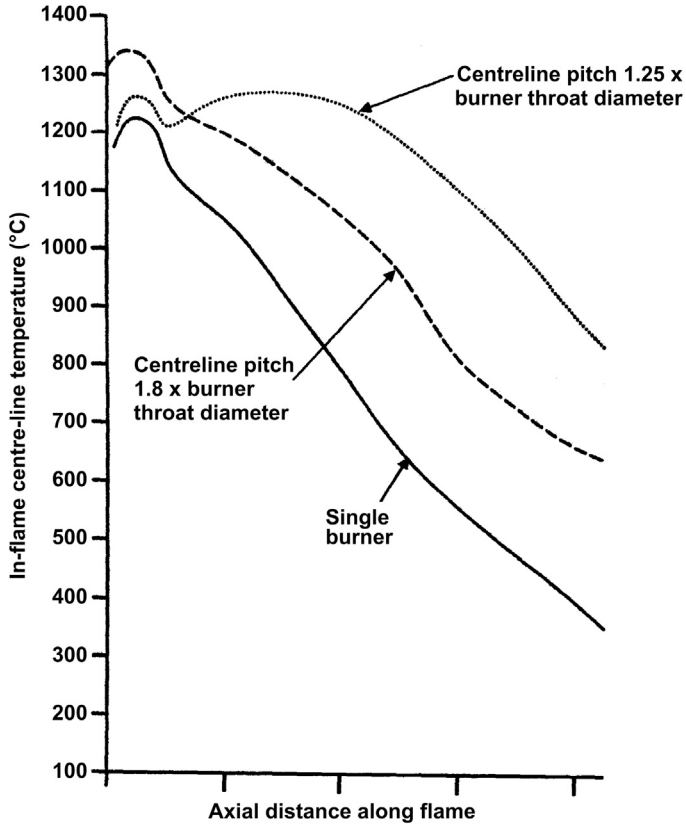


Figure 12.20 Effect of adjacent burners on measured flame temperature of the centre burner of a set of three (Apak 1972)

combustion efficiencies required and estimate the emissions performance. The modelling techniques available are fully described in chapter 6. Following completion of the modelling the mass and energy balance should once again be updated to reflect any changes that have resulted from the modelling.

Modelling may seem to be an expensive and unnecessary step but it is the last opportunity to make low cost changes to the design before the expensive detail design and manufacturing processes commence. Our experience has shown that this process always results in further refinement of the design that significantly enhances performance and, in some cases, uncovers major problems that can be corrected while still in the design stage. Almost all poor furnace performance can be attributed to omission of this vital stage in the design process. The cost of lost production and remedial engineering is several orders of magnitude greater than the cost of modelling, assuming that the

problem can be resolved. In the event that it cannot be resolved, the plant is condemned to continue operation at reduced output with poor product quality and high fuel consumption for its remaining life or, in extreme cases, is abandoned completely.

12.6 Furnace Instrumentation and Controls

Few, if any, modern industrial furnaces are manually controlled and all rely on some form of instrumentation and control system. This subject has already been discussed in detail in chapter 8 so this section will be limited to selection of appropriate instrumentation. The four basic functions of a control and instrumentation system are:

- To enable safe operation by including safety interlocks
- To control the process and provide warnings to the operator indicating that manual intervention is required
- To gather data to allow process analysis and assist further process improvement
- To demonstrate compliance with emissions regulations

The first and last requirements are generally clearly specified by legislation, codes and standards and process operating licences and are hence the minimum legal requirements. Furnace designs failing to comply with these requirements are outside the outer polygon in Figure 12.1.

More problematic for the designer is how to meet the process control and process analysis needs. The nature of furnace operation, especially the hostile environment for instrumentation and the long time constants of many furnace operations, together with the difficulty of directly measuring product quality in most instances, mean that the design and specification of furnace control systems and instrumentation is not easy. For control purposes and safe operation the operator ideally needs to know:

- Product (feed) temperature through the various heating and processing stages
- Product (feed) flowrate through the various heating and processing stages
- Furnace gas temperature in each zone
- Heat transfer to the product (feed) in the various heating and processing stages
- Fuel flow rate to each burner
- Combustion air flow rate to each burner
- Trends in temperature and product quality
- Inleakage airflow

Apart from fuel and air flow, most of these measurements cannot readily be achieved with currently available instrumentation and even accurate measurement of fuel flow is restricted to clean liquids and gases. In some furnaces measurement of product flowrate is readily achievable and in others virtually impossible, at least with any reasonable degree of accuracy. Product temperature is also difficult to measure with accuracy. The temperature of solid materials can be measured optically but this measurement is subject to significant error owing to surface emissivity issues and stray radiation. In principle, granular materials can also be measured optically but changing surface effects add to the emissivity and stray radiation errors. The temperature of liquids can be measured by submerged thermocouples but most process liquids aggressively attack thermocouple sheaths. In these circumstances the designer tends to fall back on what it is possible to measure, namely temperature with thermocouples and optical instruments, overall fuel and air flows, of fuel and air flows to zones rather than each burner. The operator has to interpret furnace operation from these secondary measurements that are available. Fortunately, given a consistent feed, most furnaces are relatively stable and can be operated effectively with relatively little information by an experienced operator.

The stable nature of many furnace systems means that a control system based on ensuring that the inputs of feed, fuel and air are stable would be very effective but this is rarely achieved in many instances owing to unstable upstream plant operation, especially where the furnace is closely integrated into the overall process. As discussed above, the furnace cannot correct off-specification feed and variable feed rates require significantly different thermal inputs to match the varying heat sink load to which the furnace cannot readily respond, owing to its long time constants. In our experience, engineers rarely make the connection between poor furnace performance and upstream process problems and, even when it is recognised, seem reluctant to takes the necessary steps to resolve the feed issues.

However, unstable operation is not simply a process issue but introduces real danger. All process explosions involving fuel occur either during start-up or during unstable operation. We have never heard of an explosion occurring during steady operation, except when cooling water has leaked into a hot liquid, such as molten metal or molten salt and caused a steam explosion. Unstable operation contributes to increased risk of explosion in two ways. Firstly by creating nuisance shutdowns caused by safety interlock trips, hence increasing the number of start-ups and the associated risks and secondly by off stoichiometric combustion or partial flame out caused by local quenching by excess feed, resulting from the control system's inability to respond to the upset.

While a skilled operator will usually successfully operate a furnace with restricted information and make decisions based on intuition and

past experience, conventional control systems do not possess such skills, so for many years furnace operation defied most attempts at automation. The only assistance provided to the operator was simple control loops covering individual variables such as fuel input, or zone temperature. In was not until the 1980s that the development of rule based and fuzzy logic systems which received inputs from a range of measurements and then took actions based on the combination of measurements that a significant degree of automatic control became possible. This was achieved by mimicking the actions of the better operators.

Finally it is important to emphasise that the furnace control system and the safety interlock system, usually known as the burner management system (BMS) must be totally independent systems, as discussed in chapter 8, to maintain the safety integrity of the BMS during control system malfunctions.

Nomenclature for Chapter 12

a = surface area/unit mass
A = area
b = thickness
Cp = specific heat at constant pressure
Cv = calorific value of fuel
d = diameter, constant of proportionality
D' = dimensionless firing density
h = heat to process unit mass
H = enthalpy
l = length
L' = dimensionless furnace heat loss
m = mass
t = time
T = temperature
q = heat flux
Q = mass flowrate
Q' = dimensionless furnace efficiency
SAR = stoichiometric air requirement of fuel
U = overall heat transfer coefficient
V = volume
XS = excess air

Greek Letters

δ = incremental step change
Δ = difference between two values
ε = emissivity

η = thermal efficiency
ρ = density
τ = time, dimensionless temperature ratio

Subscripts

af = adiabatic flame
c = charge or product
f = fuel
g = gas
L = liquid phase
o = ambient
m = melting or fusion
r = chemical reaction
R = radiation
s = sink
sd = solid

References

Apak, G. (1972). *Private communication*.
Martin, G. B. (1932). *Chemical engineering and thermodynamics applied to the cement rotary kiln*. London: Crosby Lockwood.
NA-Stordy Combustion Ltd.. FRG Series Gas Burners, Bulletin 1.1 November 2006. www.na-stordy.com.
Nelson, W. L. (1949). *Petroleum Refinery Engineering* (3rd ed.). McGraw-Hill, Table 111, p547.
Sinnott, R. K. (1999). *Coulson and Richardson's Chemical Engineering, Vol. 6, Chemical Engineering Design*. Oxford: Butterworth-Hinemann. p2.
Spiers, H., & M. (1961). *Technical data on fuels* (6th ed.). London: The British National Committee, World Power Conference.
Weber, R. (1998). *The spirit of Ijmuiden* (pp. 31–35). The Netherlands: International Flame Research Foundation, Ijmuiden, ISBN 90-801495-2-7.

Chapter 13

Economic Evaluation

Chapter contents

13.1	Cost Accounting	508
13.2	Distinction Between Capital and Revenue	509
13.3	Profit and Profitability	511
13.4	Financial Ratios	511
13.5	Project Costing	514
13.6	Investment Evaluation	517
13.7	Determining Financial Benefits	518
13.8	Post Project Analysis	536
References		536

In this chapter we will present some guidelines for the calculation of the economic benefits that may accrue from design process improvements or changes identified using the engineering tools described in previous chapters. Many technically viable proposals to improve equipment performance or efficiency fail at the financial hurdle, because the financial incentives are not sufficiently attractive, or consequential benefits (e.g. improved refractory life, reduced maintenance, higher availability) are not considered in the critical assessment. Unlike the other chapters of this book, the subject matter covered here may not be familiar to many practicing engineers, and hence we have assumed that the reader has no prior knowledge of accounting or economic practices.

The specific costs and benefits of any process improvement or change are influenced by innumerable variables, some of which may be predictable, e.g. capital cost of new equipment, internal accounting practices; some that are variable over the furnace life e.g. fuel price, cost of finance, labour, marginal profit on product; and some that are outside the control of the owner or operator, e.g. government taxation policy, environmental legislation.

13.1 Cost Accounting

A system of cost accounting is requisite in most commercial operations to demonstrate fiscal control, but these systems can also be used to operational advantage. The information required when developing a financial case should consider each item of equipment, all materials that are purchased, and a detailed analysis of the overhead costs (i.e. those costs that are not directly attributed to some operational function, such as heating, lighting, rent and rates, administration, etc.). A common method of expressing these costs is in terms of unit cost, i.e. cost/unit of product (e.g. $/tonne) under various categories.

Table 13.1 shows the two most common methodologies for breaking down the costs of a typical furnace process system. The cost by natural expenditure is more commonly used by the financial and management departments of most businesses, as it conforms to typical accounting presentation practice. It defrays abnormal expenditure, such as re-bricking or repairs of a furnace over an accounting period by making annual allowances.

The cost by process area based on daily, weekly or monthly data is of much greater value to the operations departments, since it allows for rapid scrutiny of cost trends and abnormalities, helping to identify those process operations that will bring maximum financial benefit from changes in operating practice and engineering improvements. In operations where different grades of material or products are

Table 13.1 Methodology of Categorising Detailed Cost Analysis

Cost By Process Area	*Cost By Natural Expenditure*
• Raw materials (extraction and/or bought-in)	• Operating salaries
• Raw materials storage and handling	• Operating and service labour (sub-contractors)
• On-site raw material preparation (comminution, pre-treatment)	• Supplies, rental and services
• On-site services (steam raising, power, water, compressed air, etc.)	• Consumables (refractories, grinding media, etc.
• Process operations (pre-heating, main furnace operations, cooling)	• Bought —in raw materials
• Final product preparation (comminution, annealing, tempering, etc.)	• Fuel
• Packing and distribution	• Power
• Manufacturing overhead	• Maintenance and repair
	• Parts and labour

made, often requiring different thermal treatment or residence times, it is important to identify these in the analysis.

Both methods of cost analysis are created from the same set of basic input data and are not mutually incompatible. Good practice should use both to provide all personnel with the best management tools.

Before we consider the process of financial assessment of an engineering proposal, it is important to understand some of the basic accounting principles by which it is likely to be judged.

13.2 Distinction Between Capital and Revenue

The income and expenditure incurred by any business is allocated to either a revenue or capital account. Revenue is the money employed in the day-to-day financial transactions of the business. The difference between the income and expenditure represents a profit or loss. Profits can be added to the capital, or withdrawn from the business as dividends or bonuses, whilst losses represent deductions from the capital.

Capital may be defined as the money used to produce income, and is therefor maintained intact. It is the assets (i.e. what is owned) less the liabilities (i.e. what is owed). The assets are further divided into fixed assets, which include the plant, machinery, land, etc. that are more or less permanently held for the primary production of the business, and liquid or current assets, which include money (used as working funds to finance the revenue flows), stock and investments.

In a complex business operation the distinction between the two kinds of transactions is in some cases rather ill-defined and may

involve differences of opinion, however it is important that a level of consistency is maintained from year to year to reflect the trends.

13.2.1 Fixed and Variable Costs

Fixed costs generally include permanent labour salaries, fixed power charges, lease/rental equipment costs, depreciation and amortisation charges, insurance and taxes (other than on profits/income). These costs are the baseline expenditure of being in business, irrespective of actually producing anything, and as the term implies are inflexible in the short to medium term.

Variable costs include fuel, power, services, sub-contract labour, purchased raw materials, spares and maintenance. All these costs are subject to the productivity of the operation and typically account for about two thirds of the manufacturing costs at full capacity. As the production rate is reduced, the fixed costs become a significantly more important component of the overall cost.

Direct costs or cost of goods (COG) are those costs associated directly with the production of goods, and would typically include raw materials, labour directly employed in production, fuel and power. This may embody both fixed and variable cost elements, depending on the nature of the business. Indirect costs make up the balance of the total costs and include management, maintenance and support staff, spares, services, lease/rental equipment costs, depreciation and amortisation charges, insurance and taxes. Indirect costs are often termed as the operating cost, or expenditure; and referred to by the acronym OPEX.

13.2.2 Capital Costs

Investment in equipment that is expected to have a lifetime of typically more than one financial year is usually considered on the balance sheet as a capital cost, and becomes part of the fixed assets. The investment of funds for this purpose is often referred to by the acronym CAPEX.

Financing the purchase of equipment may come from the capital reserve of liquid assets (i.e. use available cash resources), in which case the total capital of the business remains unchanged, whilst the balance of fixed to liquid assets is increased. Alternatively, additional external funds may be sourced through loans, debentures, share issues, etc. thereby increasing the liabilities. In both cases the 'cost' of employing the money for the purchase must be considered in any investment decision. The first question that is asked in a financial analysis of capital investment is "Will I get a better rate of return on my investment by spending it on capital equipment relative to the

interest the same money could earn by buying into an investment product (e.g. fixed rate government bonds)?". Making a sound commercial case for a project depends on the amount of profit that it will generate, and the rate at which it accrues, rather than on the viability of the engineering.

13.3 Profit and Profitability

The profit or earnings is the difference between income and expenditure. The gross profit is the difference between income and the direct costs. The net profit is the difference between income and the total costs (fixed and variable). Profit may also be expressed as EBIT, which is the earnings before the deduction of interest charges and taxes, thereby excluding those variable costs that are beyond the control of the business activity.

The financial assessment of profit depends on the viewpoint of the stakeholder. At the board level, profit is gauged by the return on assets, which is a ratio of the net profit to the total capital employed, and is a broad measure of the efficiency of the business. A shareholder is more concerned with the return on equity, which is a ratio of the net profit to the investors fixed capital (equity), since this will determine the dividends policy and allocation of reserves. Management considers profit as a measure of the efficiency of each function of the business and direct their attention to the control of unit costs, rather than any consideration of capital employed.

Profitability is a measure of the profit in relation to the sales income. The gross profit margin is the ratio of gross profit to sales income, whilst the net profit margin is the ratio of net profit to sales income. This is used as an indicator of how well a business is currently performing relative to competitors, or previous operating periods. The greater the profitability, the better are the margins on sales.

Gross income	-	income less direct costs
Operating income	-	income less sales, general and administration expenses
Net income	-	income less total costs

13.4 Financial Ratios

For those who are interested in a business, but who do not have any knowledge of its operation, their assessments are normally based on its market performance as defined by a number of critical ratios.

Table 13.2 Financial Performance Ratios

Name	*Ratio*	*Comments*
	Liquidity ratios	
Current ratio	$\frac{\text{current assets}}{\text{current liabilities}}$	A value of <1 indicates poor financial health
Quick **or acid test** ratio	$\frac{\text{current assets} - \text{inventory}}{\text{current liabilities}}$	A value of <1 indicates very poor financial health
Net working capital to sales ratio	$\frac{\text{current assets} - \text{current liabilities}}{\text{sales}}$	Measure of ability to convert assets into sales. A low value implies low risk
	Profitability ratios	
Gross profit margin	$\frac{\text{gross income}}{\text{sales}}$	Measure of efficiency of use of raw materials, labour, and fixed assets
Operating profit margin	$\frac{\text{operating income}}{\text{sales}}$	Measure of how well the business is managed
Net profit margin	$\frac{\text{net income}}{\text{sales}}$	Commonly termed the 'bottom line'
	Shareholder ratios	
Earnings per share	$\frac{\text{net income avaialble to shareholders}}{\text{number of shares outstanding}}$	Single most important ratio in determining share price.
Dividends per share	$\frac{\text{dividends paid to shareholder}}{\text{number of shares outstanding}}$	Growing value implies confidence in the growth of the business
Dividend payout ratio	$\frac{\text{dividends}}{\text{earnings}}$	Shows the company view of its dividends policy

Price earnings (P/E) ratio	$\frac{\text{market price per share}}{\text{earnings per share}}$	A high value implies an expectation of future earnings growth
	Return ratios	
Basic earnings power ratio	$\frac{\text{operating income}}{\text{total assets}}$	Indicates the ability of assets to generate income
Return on assets (ROA)	$\frac{\text{net income}}{\text{total assets}}$	Measure of how profitable the company is relative to its assets
Return on equity (ROE)	$\frac{\text{net income}}{\text{shareholders equity}}$	Indicator of how well company uses investor funds to generate growth
	Financial leverage	
Total debt to asset ratio	$\frac{\text{total debts}}{\text{total assets}}$	Measure of financial risk by determining how much of the assets are financed by debt
Long term debt to asset ratio	$\frac{\text{long term debts}}{\text{total assets}}$	Year on year measure of company's debt position
Total debt to equity ratio	$\frac{\text{total debts}}{\text{total shareholders equity}}$	Measure of debt used to finance growth. Generally higher for capital intensive industries
Equity multiplier	$\frac{\text{total assets}}{\text{shareholders equity}}$	A high value indicates high financial leverage (i.e. high debt)
Interest coverage ratio	$\frac{\text{earnings before interest and taxes(EBIT)}}{\text{interest}}$	Measure of debt burden. Less than 1.5 indicates difficulty in meeting debt payments, Less than 1 is a bad investment risk
Fixed charge coverage ratio	$\frac{\text{EBIT} + \text{lease payments}}{\text{interest} + \text{lease payments}}$	Critical measure of company's debt position

Some of these have already been defined in the preceding sections, but Table 13.2 presents a more comprehensive list of the most commonly quoted ratios. Whist it may appear that these financial ratios bear little relationship to furnace operations, we will see later in this chapter that it is not only the cost and benefit of implementing operational changes to a furnace, but also the means by which that cost is funded that may ultimately influence its viability.

13.5 Project Costing

An essential requirement for the development of the financial cost estimation of a project for both equipment suppliers and users is a comprehensive database of equipment, labour, installation and overhead costs. Such databases are built up from analysis of the experiences of past project work, and by maintaining an up to date catalogue of the specifications and costs of basic equipment parts. The extent to which this database is used depends on the required degree of accuracy. Commonly used phrases such as, 'just give me a ball park figure', 'I only want a budget cost', or 'I need a fully detailed breakdown' are commonly used when making financial assessments, often without understanding the implications. Table 13.3 gives some indication of the expectations of the accuracy for different costing exercises, and the related effort in manpower required to achieve that result (Gerrard 2000, Dysert 2003).

13.5.1 Order of Magnitude Costing

Order of magnitude estimates are usually determined by scaling from costs of existing similar furnaces using either internal or literature information. The first step in scaling is to apply a scaling factor, the most commonly applied of which is the six tenths power law (Williams 1947).

$$(\text{cost } 1/\text{cost } 2) = (\text{size } 1/\text{size } 2)^{R} \tag{13.1}$$

where R is typically 0.6.

Table 13.3 Levels of Cost Estimation

Level of Costing	*Purpose*	*Accuracy*	*Cost of Costing as a Percentage of Project Cost Figure*
Order of magnitude	Screening	±30 to ±50%	0–0.1%
Study	Feasibility	±20 to ±30%	0.1–0.2%
Preliminary	Budget authority	±10 to ±25%	0.4–0.8%
Definitive	Tender control	±5 to ±15%	1–3%
Detailed	Bid checking	±2 to ±5%	5–10%

The cost used is usually the total installed cost, i.e. turnkey cost. Depending on the source of the original cost, further adjustments may be required to allow for inflation.

It may also be possible to use information on major equipment items and tasks to build up an approximate installed cost. At this level of refinement annual maintenance costs of 10% of installed costs may be assumed.

13.5.2 Study Costing

A study cost estimate requires more detailed information than an order of magnitude assessment, generally including

- Process flow diagrams (PFDs)
- Sizing of all major equipment items
- Known plant location

It is important to determine a defined scope of work prior to building up a cost estimate sheet. The items to be considered in the cost build up are

- Cost estimates for all major items in the scope of work, This will include not only mechanical equipment, but also fans, motors and electrical panels
- Allowances for all other costs included in the scope of work
- Making provision for omissions, extras, etc.

The first step is to obtain cost estimates either from suppliers, equipment directories or in-house information for all the major plant items. It is preferable to get delivered prices, but where the location may be uncertain, or transportation difficult, most equipment suppliers will quote a factory gate, or FOB (free on board) price, which is the price leaving their factory gate, or 'on board' some form of transport (usually road or rail) at a designated point of delivery. Depending on the status of the design information, it may only be possible to obtain budget prices for very large pieces of equipment at this stage. If historical information is used, then the prices should be adjusted to make due allowances for inflation, and for any variations that might occur owing to local manufacturing or currency conversion costs. Similarly if smaller items of standard equipment are estimated by scaling from a cost database, a suitable scaling factor should be applied using equation 13.1. Table 13.4 gives some guidelines for R values (Peters, Timmerhaus and West 2002).

The second step is to 'convert' the bought-in costs to an 'as erected and installed' cost. The costs involved in erection and installation

Table 13.4 Typical Scaling Factors for Costs of Standard Equipment

Equipment	*Size Range*	*Scaling Factor*
Compressor (reciprocating)	15 to 700 m^3/h	0.69
Compressor (rotary)	150 to 1500 m^3/h	0.79
Centrifugal fan	1500 to 15000 m^3/h	0.44
Centrifugal fan	30000 to 100000 m^3/h	1.17
Heat exchanger	10to 40 m^2 surface area	0.60
Motor, induction, 440V explosion proof	5 to15 kW	0.69
Motor, induction, 440V explosion proof	15 to 150 kW	0.99
Pump, reciprocating with motor	10 to 500 lit/min	0.34
Pump, centrifugal with motor	$3x10^6$ to $3x10^7$ lit/min x kPa	0.33

include civil engineering (buildings and foundations), steelwork, piping, cabling, installation and commissioning labour, procurement, project engineering and management labour, temporary facilities, consumables, equipment hire, tools etc., and overhead costs (insurance, bonuses etc.). For a study costing Lang (or equipment) factors may be used to quickly make this calculation (Lang 1947, 1948). Lang's work investigated the ratio of total installed & erected cost to purchased equipment cost for major process plant, and determined that there was a relatively constant value for this ratio, depending on the types of material being processed. He proposed the following

- Solid processing plant 3.9
- Solid / fluid processing plant 4.1
- Fluid processing plant 4.8

This approach has been refined to individual items of equipment, and reference to recently published data is recommended to find current ratios (Dysert 2003). Table 13.5 shows a typical calculation using this approach applied to a heat exchanger.

Table 13.5 Determination of Lang Factor for a Heat Exchanger

Item	*Lang Factor*
Ex-works equipment cost	1
Installation labour	0.05
Foundations	0.11
Structural steelwork	0.11
Piping	1.18
Electrical parts	0.05
Instrumentation	0.24
Painting	0.01
Insulation	0.11
Total	2.86

The final step is to apply suitable 'safety' margins to the overall cost to make provision for unforeseen occurrences. This is usually termed as a contingency and experience is required to guide judgement on allowances. It is usually applied as a percentage of the total cost and is based on a judgment of the accuracy of the pricing information used to build up the total cost figure; a knowledge of the history of similar projects, the suppliers and/or the clients with respect to the likelihood of design and specification changes that might arise during the execution of the project; the timescale and its impact on the value of the costs (i.e. an escalation allowance).

The cost estimate should be independently reviewed at the end of each step by a representative cross section of people involved (viz. designers, plant operations, plant engineers, financial controllers, procurement department, management representatives) to hopefully ensure that the result is the best it can be.

13.6 Investment Evaluation

Investment decisions are based on an assessment of the benefits to the revenue stream of the operation over a period of time. There are two basic approaches to this assessment

- Non discounted methods
  - Pay-back
  - Return on investment
- Discounted methods
  - Net present value (NPV)
  - Internal rate of return (IRR)

Non discounted methods are quick to apply, simple to understand and are commonly used by many businesses as the yardstick for investment approval. They give a good measure of the risk, but ignore the future revenue profits beyond the payback or return period and the future value of the money invested.

Payback is calculated using the following formulae

$$P = \frac{C}{R} \qquad (\text{pre} - \text{tax}) \tag{13.2}$$

$$P = \frac{C}{R - t(R - D)} \qquad (\text{post} - \text{tax}) \tag{13.3}$$

where

P - Payback period
C - Capital cost of investment

R - Savings/unit time period (month/year etc.)
D - Allowable depreciation on capital over time period
t - Tax rate

Project approval is simply measured against a pre-determined criterion for a maximum payback period. This criterion can vary between six months and three years and depends entirely on company policy.

The net present value is determined from the project's net cash flow, so if we know that the cash flow return in the first time period (period 0) is R_0, in period 1 it is R_1 etc., then for n periods the NPV is calculated using the following formula

$$\mathrm{NPV} = \sum_{k=0}^{n} \frac{R_k}{(1+i)^k} \tag{13.4}$$

where

i - Discount rate

A project is approved if NPV ≥ 0. The time period chosen may typically be months or years, the value of n usually being based on the same criterion as for a payback calculation. The discount rate should be equal to the company's weighted average cost of capital plus an allowance for risk. The internal rate of return (IRR) is the discount rate at which the value of NPV=0, and is calculated by trial and error using equation (13.4).

In any business there is usually a limit to the capital and resources available for investment, so when considering a number of projects that may all meet the payback or NPV criteria a further measure for the 'capital efficiency' required to ensure the correct choices are made. The present worth profitability index (PWPI) or more simply the profitability index (PI) measures the NPV per unit of CAPEX, and is defined as

$$\mathrm{PWPI} = \frac{\mathrm{NPV}}{\text{Present value of project cost(CAPEX)}} \tag{13.5}$$

Projects with the highest PWPI values should be selected.

13.7 Determining Financial Benefits

It is often the case that there are a number of projects competing for financial investment from a limited budget on a furnace, and it is therefor important to prepare reasoned financial and engineering justifications for each, in order that the correct investment decisions are made. As a demonstration of how this might be executed, an example of a feasibility costing exercise for a steel reheating furnace will be

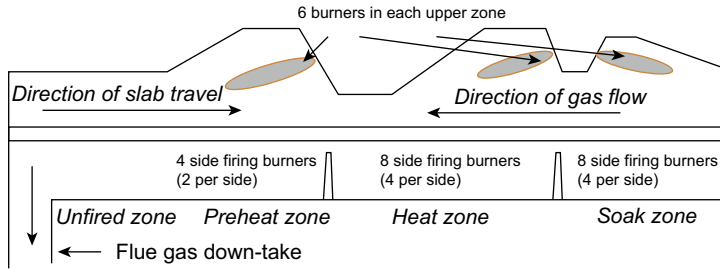


Figure 13.1 General arrangement of 3 zone slab reheating furnace

used. The furnace arrangement is shown in Figure 13.1, and may be recognised as that shown in Figure 1.19 in the introduction. The performance and financial figures used in the example, whilst being realistic and typical at the time of preparing this analysis are not intended to be taken by the reader as anything other than a vehicle to provide a framework to demonstrate the methodology.

The furnace is a conventional three zone reheating furnace, or six zones if top and bottom are considered separately, as is sometimes the case. There is a further unfired zone at the front (slab entry) end of the furnace where the slabs are initially heated by exiting flue gases. The furnace is side fired underneath the slabs and end fired over the top of the slabs. It currently heats 78 tonnes/h of slab steel from ambient temperature to 1250°C, using waste fuel oil (blended recycled oils) as the heating source. The burners are designed to operate with preheated air from a stack recuperator, but over the period of the last 5 year operating campaign the recuperators have become ineffective owing to excessive leaking between the air and flue gas channels, and have been taken out of service.

The unit is scheduled for a major refurbishment, relining with new refractory and refitting, and the opportunity therefor is available to make improvements during the shutdown. A number of suggestions have been advanced, and those most favoured are

1. Dispense with the current insulation backing for the re-bricked furnace as this will save refractory costs and installation time.
2. Convert the furnace to natural gas firing, since a new gas supply line is being run near to the plant and the cost of gas will be lower than that of fuel oil.
3. Option 2 together with a new calcium silicate refractory lining since this has significant advantages over the current refractory and will be suitable for the change of fuel. Calcium silicate is rapidly degraded by oil firing and therefor is not an option for the current furnace arrangement.

4. Reinstate the stack recuperators, either by repair or renewal.
5. Option 4 together with conversion of the burners to fire blast furnace gas, which is available as a by-product gas from the iron production units and is essentially free.
6. Install new self–recuperative burners as replacements for the existing burners. This should give a similar performance to the stack recuperators, but may be a cheaper and easier to maintain option.
7. Convert the burners to operate with oxygen enriched air. Oxygen enrichment enhances the heat transfer rates, and should reduce the fuel consumption per unit of product.

As the first stage in the evaluation process, a simulation of the furnace has been developed using the Hottel well stirred furnace model, WSF, (see section 6.2.1 equation (6.28)), treating each of the seven zones as individual furnaces. The flows and enthalpies of flue gases passing from each zone into the adjacent zone are considered as an additional thermal input, thus the values of H_f and m are adjusted accordingly. The heat transfer rates predicted from the WSF model were linked to a transient conduction slab heating model, based on the numerical method described in section 4.1. The sink temperature was thus determined, the value revised in the WSF model and an iteration procedure used to converge both models to a balanced solution. The model was first validated against a range of current operating data to provide a level of confidence to all parties concerned in the evaluation process. A summary of the modelling inputs and results are shown in Table 13.6.

It can be seen in the tabulated data that the residual heat in the flue gases contribute to the total enthalpy of the adjacent zone, thus the flue gas heat from zone 7 is added into the total heat in zone 5, and the flue gas heat from this zone then contributes to zone 3. The flue gas heat from zones 2 and 3 provides the thermal input to zone 1. This modelling approach is a hybrid version of the long furnace model, see section 6.2.2. The iterated modelling results produce an overall heat balance with an error of 1.34%, and agree closely with the plant operating data, indicating an overall thermal efficiency of 38.76%, and a specific energy consumption of 2.17 GJ/tonne steel slab.

The second stage is to use the model to analyse the seven proposed options, primarily to determine the changes in fuel consumption for the same production rate. Tables 13.7 to 13.13 are the summaries of these model studies. In each case a constant heat transfer rate of 18.213MW to the steel has been used as the set point, and the quantity of fuel adjusted to meet this duty. A number of engineering design assumptions have been made, depending on the case being studied, and these are summarised as

- The emissivity of the flame for each case is calculated from the fuel carbon:hydrogen ratio as described in section 4.3.2.
- For case 1 the 50mm of insulation backing material with a thermal conductivity of 0.09 W/m°C is replaced with standard refractory with the thermal conductivity of 0.94 W/m°C.
- For case 3 the refractory and insulation is replaced by 350mm of hot face silicate material with the thermal conductivity of 0.12 W/m°C.
- For case 4 the cross-flow stack recuperator is assumed to have a thermal efficiency of 58%
- For case 5 the cross-flow stack recuperator is assumed to have a thermal efficiency of 38% owing to the lower potential mean temperature difference and higher mass flow loading than for case 4
- For case 6 the self-recuperative burners are assumed to have a thermal efficiency of 38%, this figure being based on published literature
- For case 7 the combustion air is enriched with oxygen to 30% by volume

Table 13.6 Summary of WSF Modelling of Reheating Furnace – Oil Fired Base Case

Zone No	*1*	*2*	*3*	*4*	*5*	*6*	*7*
H_f MW	26.74	17.55	17.09	9.41	10.08	4.70	4.70
T_{af} °C	1201	1541	1505	1639	1744	1998	1998
D′	5.81	3.27	3.52	0.62	0.56	0.12	0.34
Q′	0.186	0.209	0.278	0.315	0.389	0.426	0.429
τ	0.285	0.481	0.491	0.666	0.631	0.649	0.649
Heat loss MW	1.84	1.47	1.12	0.92	0.89	0.60	0.56
Heat flux kW/m^2	122	234	304	82	108	46	133
Mean gas temperature °C	1084	1257	1431	1188	1258	1273	1388
Steel surface temperature °C	133	570	498	1059	956	1292	1210

Overall heat balance			
Heat In	MW	Heat out	MW
Fuel	46.989	Steel product	18.213
Preheated air	0.034	Flue gases	17.202
		Structure losses	7.410
		Cooling water	3.568
		Unaccounted	0.630
Total	47.023	Total	47.023

Key
Zone 1 - unfired zone (top and bottom)
Zone 2 - lower preheat zone
Zone 3 - upper preheat zone
Zone 4 - lower heat zone
Zone 5 - upper heat zone
Zone 6 - lower soak zone
Zone 7 - upper soak zone

Table 13.7 Summary of Modelling for Case 1- Re-Brick with No Insulation

Zone No	*1*	*2*	*3*	*4*	*5*	*6*	*7*
H_f MW	27.30	17.95	17.49	9.62	10.30	4.80	4.80
T_{af} °C	1209	1541	1506	1640	1742	1998	1998
D′	5.95	3.34	3.59	0.64	0.57	0.12	0.34
Q′	0.188	0.210	0.277	0.315	0.388	0.425	0.429
τ	0.285	0.481	0.491	0.666	0.632	0.649	0.649
Heat loss MW	2.10	1.62	1.24	1.00	0.97	0.63	0.80
Heat flux kW/m^2	116	240	310	84	110	47	136
Mean gas temperature °C	1078	1255	1431	1188	1250	1274	1389
Steel surface temperature °C	135	577	505	1066	963	1293	1212

Overall heat balance

Heat In	MW	Heat out	MW
Fuel	48.041	Steel product	18.213
Preheated air	0.035	Flue gases	17.503
		Structure losses	8.158
		Cooling water	3.568
		Unaccounted	0.632
Total	48.076	Total	48.076

Table 13.8 Summary of Modelling for Case 2 - Conversion to Natural Gas

Zone No	*1*	*2*	*3*	*4*	*5*	*6*	*7*
H_f MW	26.31	17.25	16.87	9.23	9.90	4.61	4.61
T_{af} °C	1239	1574	1544	1671	1778	2038	2038
D′	5.15	3.26	3.52	0.69	0.62	0.15	0.38
Q′	0.198	0.210	0.277	0.313	0.390	0.429	0.435
τ	0.280	0.473	0.481	0.655	0.621	0.637	0.637
Heat loss MW	1.83	1.46	1.12	0.91	0.86	0.59	0.56
Heat flux kW/m^2	117	231	298	80	105	46	132
Mean gas temperature °C	1095	1283	1463	1215	1296	1295	1421
Steel surface temperature °C	132	568	496	1058	951	1314	1227

Overall heat balance

Heat In	MW	Heat out	MW
Fuel	46.163	Steel product	18.213
Preheated air	0.033	Flue gases	16.572
		Structure losses	7.346
		Cooling water	3.568
		Unaccounted	0.497
Total	46.196	Total	46.196

Table 13.9 Summary of Modelling for Case 3 – Conversion to Natural Gas with New Calcium Silicate Lining

Zone No	*1*	*2*	*3*	*4*	*5*	*6*	*7*
H_f MW	25.72	16.83	16.45	9.00	9.67	4.50	4.50
T_{af} °C	1241	1574	1543	1670	1780	2038	2038
D′	5.01	3.18	3.44	0.68	0.60	0.14	0.37
Q′	0.196	0.209	0.278	0.313	0.391	0.430	0.435
τ	0.279	0.473	0.481	0.655	0.620	0.637	0.637
Heat loss MW	1.56	1.31	1.00	0.83	0.80	0.55	0.51
Heat flux kW/m^2	113	223	291	78	103	44	129
Mean gas temperature °C	1101	1285	1463	1214	1296	1294	1420
Steel surface temperature °C	130	560	490	1050	943	1312	1225

Overall heat balance

Heat In	MW	Heat out	MW
Fuel	45.036	Steel product	18.214
Preheated air	0.032	Flue gases	16.240
		Structure losses	6.555
		Cooling water	3.568
		Unaccounted	0.491
Total	45.068	Total	45.068

Table 13.10 Summary of Modelling for Case 4 – Reinstate Stack Recuperators

Zone No	*1*	*2*	*3*	*4*	*5*	*6*	*7*
H_f MW	19.20	13.57	13.05	7.36	8.09	3.91	3.91
T_{af} °C	1274	1696	1637	1816	1980	1998	1998
D′	3.47	1.79	2.00	0.34	0.28	0.06	0.15
Q′	0.246	0.277	0.354	0.398	0.486	0.533	0.534
τ	0.273	0.443	0.457	0.609	0.565	0.569	0.569
Heat loss MW	1.64	1.26	0.94	0.75	0.73	0.47	0.45
Heat flux kW/m^2	106	236	292	80	106	47	135
Mean gas temperature °C	1101	1258	1428	1193	1263	1281	1401
Steel surface temperature °C	113	517	457	1015	922	1289	1204

Overall heat balance

Heat In	MW	Heat out	MW
Fuel	31.845	Steel product	18.215
Preheated air	5.700	Flue gases	9.516
		Structure losses	6.227
		Cooling water	3.568
		Unaccounted	0.010
Total	37.546	Total	37.546

Table 13.11 Summary of Modelling for Case 5 – Conversion to Blast Furnace Gas with Stack Recuperators

Zone No	*1*	*2*	*3*	*4*	*5*	*6*	*7*
H_f MW	90.56	50.42	50.01	26.27	26.40	11.10	11.10
T_{af} °C	1193	1273	1263	1312	1317	1346	1346
D′	24.73	22.17	23.27	5.52	5.74	1.83	4.54
Q′	0.068	0.065	0.088	0.102	0.131	0.103	0.125
τ	0.288	0.565	0.568	0.803	0.800	0.910	0.910
Heat loss MW	2.47	2.05	2.20	1.47	1.38	1.11	0.91
Heat flux kW/m^2	140	217	292	77	99	28	97
Mean gas temperature °C	1222	1197	1440	1191	1284	1221	1324
Steel surface temperature °C	241	786	713	1181	1074	1394	1233

Overall heat balance

Heat In	MW	Heat out	MW
Fuel	80.000	Steel product	18.212
Preheated air	23.879	Flue gases	70.591
		Structure losses	11.020
		Cooling water	3.568
		Unaccounted	0.488
Total	103.879	Total	103.879

Table 13.12 Summary of Modelling for Case 6 – Install Self-Recuperative Burners

Zone No	*1*	*2*	*3*	*4*	*5*	*6*	*7*
H_f MW	1.71	9.59	8.34	5.88	6.16	3.17	3.15
T_{af} °C	25	2682	2378	2758	2891	2256	2247
D′	—	0.23	0.32	0.05	0.05	0.05	0.15
Q′	—	0.556	0.615	0.666	0.722	0.523	0.531
τ	—	0.295	0.329	0.420	0.402	0.582	0.585
Heat loss MW	0.67	0.88	0.61	0.51	0.49	0.41	0.42
Heat flux kW/m^2	—	316	308	101	115	38	109
Mean gas temperature °C	537	1449	1469	1245	1281	1263	1364
Steel surface temperature °C	39	344	341	916	895	1267	1210

Overall heat balance

Heat In	MW	Heat out	MW
Fuel	26.734	Steel product	18.216
Preheated air	4.034	Flue gases	4.721
		Structure losses	3.928
		Cooling water	3.568
		Unaccounted	0.335
Total	30.768	Total	30.768

Table 13.13 Summary of Modelling for Case 7 – Oxygen Enrichment

Zone No	*1*	*2*	*3*	*4*	*5*	*6*	*7*
H_f MW	18.06	12.94	12.38	7.00	7.75	3.80	3.80
T_{af} °C	1254	1724	1657	1848	2023	2405	2405
D'	3.26	1.57	1.76	0.29	0.23	0.05	0.13
Q'	0.252	0.293	0.372	0.417	0.506	0.561	0.562
τ	0.276	0.437	0.452	0.600	0.554	0.550	0.550
Heat loss MW	1.57	1.21	0.89	0.71	0.70	0.44	0.43
Heat flux kW/m^2	102	237	290	79	105	47	136
Mean gas temperature °C	1037	1285	1417	1186	1252	1279	1398
Steel surface temperature °C	109	504	447	992	903	1273	1188

Overall heat balance

Heat In	MW	Heat out	MW
Fuel	37.587	Steel product	18.213
Preheated air	0.021	Flue gases	10.140
		Structure losses	5.959
		Cooling water	3.568
		Unaccounted	−0.272
Total	37.608	Total	37.608

The modelling results indicate that in cases 2,3,4,6 and 7 there will be a reduction in the specific fuel consumption. Cases 1 and 5 indicate that the specific fuel consumption will increase, in case 1 owing to the increase in furnace structure heat losses and in case 5 owing to the very low calorific value of the gas lowering the adiabatic flame temperature. The analysis indicted that it would not be possible to operate the furnace with blast furnace gas unless air preheating is also incorporated to boost the flame temperatures to above the exit steel temperature of 1250°C.

The third stage is to use the engineering study analyses to extract the data required for the economic evaluation, see Table 13.14, and gather the financial operating data, see Table 13.15. Information is also required to build up study costing sheets for the seven proposals, as well as a base case costing for a 'like for like' refurbishment for comparison.

13.7.1 Base Case Costing

The primary cost for the base case refurbishment of the furnace is to replace all the refractory. Other maintenance items that are to be carried out during the shutdown are already scheduled into the maintenance budget and are therefor omitted from the project cost. The cost consists of the bought in cost of refractory, insulation and their

installation. Current refractory and insulation prices are readily obtained from suppliers, and past experience of refurbishments gives accurate information on the installation time and labour required, hence a current daily rate can be obtained from a local installer.

Table 13.14 Summary of Process Modelling Data Required for Economic Study

Case No	*Base*	*1*	*2*	*3*	*4*	*5*	*6*	*7*
Total thermal input MW	47.02	48.08	46.02	45.07	37.55	103.88	30.77	37.61
Specific fuel consumption GJ/tonne steel	2.17	2.22	2.13	2.08	1.47	3.69	1.23	1.73
Thermal efficiency %	38.76	37.91	39.45	40.44	57.19	22.76	68.13	48.45
Fuel flow rate kg/s	1.10	1.13	0.93	0.90	0.75	32.06	0.63	0.88
Air flow rate kg/s	16.55	16.92	15.63	15.25	11.21	21.47	9.41	9.35
Oxygen flow rate kg/s	—	—	—	—	—	—	—	0.57
Flue gas flow rate kg/s	17.65	18.04	16.56	16.15	11.96	53.43	10.04	11.07
Flue gas temperature ex-furnace °C	945	941	920	924	912	1272	937	893
Flue gas temperature ex-recuperator °C	—	—	—	—	488	913	362	—
Preheated air temperature °C	—	—	—	—	496	1033	369	—
Recuperator thermal input MW					6.33	28.30		
Average flame emissivity	0.40	0.40	0.23	0.23	0.40	0.16	0.46	0.47
Average adiabatic flame temperature °C	1738	1738	1774	1774	1960	1309	2535	2011
Flue gas CO_2 mass %	19.86	19.86	19.60	19.69	19.86	45.00	19.86	25.71
Tonne C/tonne steel	0.044	0.045	0.041	0.040	0.030	0.303	0.025	0.036

Table 13.15 Summary of Process Operating Cost Data Required for Economic Study

Item	*Cost/Value*	*Units*
Waste fuel oil	0.28	$/kg
Natural gas	0.15	$/kg
Blast furnace gas	0.001	$/kg
Oxygen	0.08	$/kg
Electricity	0.05	$/kWh
Carbon tax	0.043	$/kg of carbon
Selling price of hot rolled carbon steel	0.7	$/kg
Net profitability of carbon steel sales	4	%
Base case combustion air fan power	100	kW
Base case induced draft fan power	350	kW
Base case other power	30	kW
Average campaign life	5	Years
Unit availability	90	%

Table 13.16 Base Case Costing Sheet

Item	*Unit Cost*	*Density*	*Quantity*	*Cost*
Basic refractory	\$300/tonne	2650 kg/m^3	274.33 m^3 @300mm thickness	*\$218094*
Insulation	\$170/tonne	800 kg/m^3	45.72 m^3 @50mm thickness	*\$6218*
Refractory installation	\$2800/day		14 days	*\$39200*
Insulation installation	\$2800/day		4 days	*\$11200*
Sub-total				***\$274712***
Contingency	7%			*\$19230*
Total installed cost				**\$293942**

13.7.2 Case 1 Costing – Re-Brick with No Insulation

In this case the insulation refractory is to be omitted, and the cost is readily derived from the information in 13.5.1.

The savings derived from this relative to the base case are \$18637, together with 4 additional days of production gained on the installation time.

13.7.3 Case 2 Costing – Conversion to Natural Gas

Conversion to natural gas firing will involve the provision of a high pressure gas main spur onto the site, and replacing all the current burners with dual fuel firing capability, since the gas supply price quoted is based on an interruptible supply. The ex-works budget price of suitable dual fuel burners, controls and gas valve trains can be obtained from a number of competing burner suppliers within a reasonable time frame (less than 1 month), and therefor current prices can be used. Suitable Lang factors are then used to obtain an installed cost. The cost installing of the spur has been quoted by the gas supply

Table 13.17 Re-Brick with No Insulation Costing Sheet

Item	*Unit Cost*	*Density*	*Quantity*	*Cost*
Basic refractory	\$300/tonne	2650 kg/m^3	274.33 m^3 @300mm thickness	*\$218094*
Refractory installation	\$2800/day		14 days	*\$39200*
Sub-total				***\$257294***
Contingency	7%			*\$18011*
Total installed cost				**\$275305**

Table 13.18 Conversion to Natural Gas Costing Sheet

Item	*Unit Cost*	*Quantity*	*Ex-works Cost*	*Lang Factor*	*Installed Cost*
Dual fuel refit for burners	$15000	38	$570000	2.75	*$1567500*
New flame detectors	$1000	72 (IR+UV)	$72000	1.40	*$106400*
Gas valve trains	$2100	38	$79800	2.29	*$182742*
New gas main installation	$300/m	3000 m			*$900000*
Design and engineering costs (overhead costs)	30% of ex works equipment cost				*$556992*
Sub total					***$3313635***
Contingency	5%				***$165682***
Refractory costs as for base case					***$293942***
Total installed cost					**$3773259**
Refractory installation		18 days			
Burner commissioning		4 days			
Total shut-down time		22 days			

company as $300/m, and the site is 3 kilometres from the nearest connection point to the main.

13.7.4 Case 3 Costing – Conversion to Natural Gas with New Calcium Silicate Lining

This option is similar to case 2 costing, but with a revised refractory installation

Table 13.19 Conversion to Natural Gas with New Lining Costing Sheet

Item	*Unit Cost*	*Density*	*Quantity*	*Cost*
Sub-total as for case 2				***$3313635***
Contingency	5%			***$165682***
Calcium silicate	$1250/tonne	900 kg/m^3	228.61 m^3 @250mm thickness	*$257186*
Refractory installation	$2800/day		14 days	*$39200*
Sub-total				*$296286*
Contingency	7%			*$20747*
Total refractory cost				***$317133***
Total installed cost				**$3796450**
Refractory installation			14 days	
Burner commissioning			4 days	
Total shut-down time			18 days	

Table 13.20 Reinstate Stack Recuperators Costing Sheet

Item	*Unit Cost*	*Scale Up Ratio*	*Scaling Factor*	*Ex-works Cost*	*Lang Factor*	*Installed Cost*
3 MW recuperator unit	$1050000					
6.33 MW recuperator unit		6.33/3=2.11	0.6	$1643891	2.96	*$4865916*
Design and engineering costs (overhead costs)	30% of ex works equipment cost					*$493167*
Sub total						***$5359083***
Contingency	5%					*$267954*
Total for recuperator						***$5627037***
Total refractory cost						***$293942***
Total installed cost						**$5920979**
Refractory installation			18 days			
Additional recuperator installation			8 days			
Re-commissioning			4 days			
Total shut-down time			30 days			

13.7.5 Case 4 Costing – Reinstate Stack Recuperators

The largest cost item for this case is the stack recuperators. These are custom designed for the furnace and cost information is therefor very limited unless they have been replaced on previous occasions. This is not the case and inspection of the equipment indicates that they are beyond economic repair, and replacement is the preferred option. A price is available for a smaller 3MW heat input unit that has been recently installed on another furnace, and this is used to scale up (reference Table 13.4 for heat exchanger value) in the costing sheet.

13.7.6 Case 5 Costing – Conversion to Blast Furnace Gas with Stack Recuperators

This is a major project since the modifications required for this case include larger stack recuperators, new forced draft and induced draft fans for the larger gas volumes, and new burners and gas pipework.

The new fans are costed from known prices for spare fans for the existing unit, scaled up in size using the fan laws (fan power α volumetric flow rate) and then scaled for cost using scaling factors taken from Table 13.4. The low CV of blast furnace gas, which reduces

Table 13.21 Conversion to Blast Furnace Gas with Stack Recuperators Costing Sheet

Item	*Unit Cost*	*Scale Up Ratio*	*Scaling Factor*	*Ex-Works Cost*	*Lang Factor*	*Installed Cost*
3 MW recuperator unit	$1050000					
28.3 MW recuperator unit		28.3/3=9.43	0.6	$4036553	2.96	*$11948196*
Current air fan	$75000	100kW				
New air fan		21.47/16.55=1.29	1.17	$101150	1.25	*$126437*
Current ID fan	$90000	350kW				
New ID fan		53.43/17.65=3.03	1.17	$328924	1.25	*$411155*
Dual fuel refit for burners	$20640	38		$784320	2.75	*$2156880*
New flame detectors	$1000	72		$72000	1.40	*$106400*
Gas valve trains	$6100	38		$231800	2.29	*$530882*
Design and engineering costs (overhead costs)	30% of ex works equipment cost			*Sub-total= $5666264*		*$496167*
Sub total						***$16979769***
Contingency	5%					*$848998*
Total for new equipment						***$17828758***
Total refractory cost						***$293942***
Total installed cost						**$18122700**
Refractory installation			18 days			
Additional equipment installation			30 days			
Re-commissioning			6 days			
Total shut-down time			54 days			

the thermal efficiency, requires the burners to have a larger thermal rating, and the low energy density of the gas increases the valves, pipework etc. to a significantly larger diameter than for natural gas, hence the increased unit costs compared to cases 2 and 3.

13.7.7 Case 6 Costing – Installation of Self-Recuperative Burners

The best budget price for an oil fired recuperative burner has been obtained from comparison of recent manufacturers quotations. The contingency has been increased to 15% to reflect an uncertainty at this stage in the possible need use a higher grade of refractory owing to the increased flame temperatures of the burners.

13.7.8 Case 7 Costing – Oxygen Enrichment

The equipment changes required are relatively small in nature, involving the modification of the burners to fit oxygen lances, associated small bore pipework and control valves etc. for the oxygen. However, the engineering analysis, and experience of oxygen enriched firing systems indicates that the furnace environment will be significantly hotter and it is therefor expected that an upgrade of the refractories will be necessary.

Table 13.22 Install Self-Recuperative Burners Costing Sheet

Item	*Unit Cost*	*Quantity*	*Ex-Works Cost*	*Lang Factor*	*Installed Cost*
Oil fired recuperative burners	$25000	38	$950000	2.75	*$2612500*
Flue gas ductwork	$100/m fabrication	300 m	$30000	2.3	*$69000*
Design and engineering costs (overhead costs)	30% of ex works equipment cost				*$294000*
Sub total					***$2975500***
Contingency	15%				***$446325***
Refractory costs as for base case					***$293942***
Total installed cost					**$3715767**
Refractory installation		18 days			
Burner commissioning		7 days			
Total shut-down time		25 days			

Table 13.23 Oxygen Enrichment Costing Sheet

Item	*Unit Cost*	*Quantity*	*Ex-Works Cost*	*Lang Factor*	*Installed Cost*
Burner oxygen lances	$15000	38	$57000	2.75	*$156750*
Oxygen valve trains	$800	38	$30400	2.29	*$69616*
Controls	$500	38	$19000	1.4	*$26600*
Design and engineering costs (overhead cost)	30% of ex works equipment cost		Sub-total= $106400		*$31920*
Sub total					***$284886***
Contingency	5%				***$14244***
Item	Unit cost	Density	Quantity		
Magnesite refractory	$850/tonne	2900 kg/m^3	274.33 m^3 @250mm thickness		*$676229*
Insulation	$170/tonne	800 kg/m^3	45.72 m^3 @50mm thickness		*$6218*
Refractory installation	$2800/day		15 days		*$42000*
Sub-total					*$735647*
Contingency	2%				*$14713*
Total refractory cost					***$750360***
Total installed cost					**$1049490**
Refractory installation			15 days		
Burner commissioning			3 days		
Total shut-down time			18 days		

13.7.9 Cost-Benefit Analysis

The benefits that accrue from all of these changes are manifest as changes to the variable operating costs, through a reduction in fuel used and/or fuel price, electricity used, and carbon taxes. We now have sufficient information to evaluate the cost benefits for each on the projects, and make comparisons. Table 13.24 shows the changes to the variable operating costs for the furnace based on the energy used as fuel, electricity (changes in fan power requirements with air and flue gas volumes) and carbon tax. The values are derived from the information in Tables 13.14 and 13.15. A special mention is made of case 5. The conversion of the furnace to blast furnace gas has already been shown to be the most capital intensive project, involving extensive re-engineering, but its consideration is merited by the financial benefit realised through the minimal cost of the fuel as a by-product waste gas from other parts of the process, and the fact that it incurs no carbon tax by virtue of the same reason.

It is also of interest to note that, even though the variable costs for the reheating process are relatively small with respect to the total production cost of $672/tonne steel, all of the cases considered have a measurable influence on the profit margin.

Table 13.24 Variable Cost Analysis for Case Options

Case Number	*Base*	*1*	*2*	*3*	*4*	*5*	*6*	*7*
Fuel cost/tonne steel	$14.23	$14.55	$6.42	$6.26	$9.65	$1.48	$8.10	$11.38
Oxygen cost/tonne steel	—	—	—	—	—	—	—	$2.12
Electricity cost/tonne steel	$0.31	$0.31	$0.28	$0.27	$0.28	$1.30	$0.22	$0.19
Carbon tax/tonne steel	$1.90	$1.94	$1.76	$1.71	$1.29	$0	$1.08	$1.54
Variable cost/tonne steel	$16.44	$16.90	$8.44	$8.23	$11.22	$2.78	$9.40	$15.23
Marginal profit	4.00%	3.95%	5.14%	5.17%	4.75%	5.85%	5.01%	4.17%

The final stage of the analysis is to consider the investment potential. The operating cost data, together with the cost for the individual projects are summarised in Table 13.25, together with the calculated project criteria based on the following methods as defined in section 13.6.

- Simple payback
- Simple payback allowing for the loss/gain of production during the shutdown
- Net present value based on a three year period at a discount rate of 4%
- PWIP value
- IRR

The variable costs used in the analysis are derived by subtracting the base case values to derive the cost/benefit data. Thus for example the simple payback for case 3 would be

$$\mathrm{P} = \frac{3796450}{842881 - 422759} = 9.04$$

The loss or gain in production profit is treated as an addition to the CAPEX when calculating the payback period.

In order to calculate the NPV, the project costs must be defrayed over a time period at the start of the work. Estimates of the project timescales have therefor been made, and it has been assumed that the costs are equally divided over the last half of this period. Thus for case 2, month 0 in the NPV calculation is 9 weeks before the furnace is commissioned.

The financial treatment of the data for case 1 requires a different approach, in that this is a proposal for cost saving, with an additional benefit of reducing the shut down time. The savings in costs for the refractory insulation are $18637, whilst the monthly variable costs have increased by $18803 owing to the higher heat losses. The benefits in refractory costs are therefor negated within one month, but if we also consider the additional marginal profit of $209800 gained by 4 days of extra productivity then the financial advantage is maintained

Table 13.25 Analysis of Investment Potential for Projects

Case Number	*Base*	*1*	*2*	*3*	*4*	*5*	*6*	*7*
Variable cost/month	$842881	$861684	$433287	$422759	$574755	$142406	$482011	$781255
CAPEX	$293842	$275305	$3773259	$3796450	$5920979	$18122700	$3715767	$1049490
Simple payback time months	—	(1)	9.21	9.04	22.08	25.87	10.30	19.03
Additional days for shut-down	0	−4	4	0	12	36	7	3
Lost/gain net profit on production	0	$209800	−$209780	0	$629426	−$1888052	−£367199	−$157347
Payback including lost production	0	(12)	9.72	9.04	24.03	28.57	11.31	19.58
Project lead time months	2	2	18	18	8	12	6	4
NPV for 36 months @4%	—	−$356436	$6571692	$6813420	$2161374	$1686716	$7493062	$925508
PWPI		—	1.742	1.795	0.365	0.093	2.017	0.882
IRR		—	88.7%	90.7%	27.0%	10.3%	106.8%	55.2%

Table 13.26 Relationship Between Capital Cost and Project Payback

Case	*Investment Cost*	*Months to NVP Break-Even*
No insulation	$275305	14
Natural gas conversion	$3773259	18
Natural gas conversion + ceramic lining	$3796450	18
Reinstate recuperators	$5920979	27
Blast furnace gas conversion	$18122700	33
Recuperative burner refit	$3715767	13
Oxygen enrichment	$1049490	19

for 12 (payback) to 14 (NPV) months depending on the method of evaluation used.

The financial analysis indicates that from Table 13.24, case 5 yields the best return increasing the marginal profit from 4% to 5.85%, whereas Table 13.25 indicates that case 6 has the best PWIP value, making the best use of the invested capital. Both tables show that conversion to natural gas firing is a close second choice. The 36 month criterion chosen for the NVP return on investment in the example is quite long, but detailed analysis of the NVP calculations clearly show a relationship between the project cost and the period required to reach a break-even NVP, see Table 13.26.

The project analysis presented here is an example of how to develop a costing methodology, the numbers used only being representative of data at the time of its preparation. The results are not intended to be definitive, but only to show how to arrive at a reasoned set of information against which decisions can be made as to what projects should be favourably considered. This analytical approach can be readily imported into a spread-sheet, thereby making it very easy to explore the sensitivity of the whole process to changes in variables, such as fuel price, selling price of steel etc., which will also help to define the risks.

The foregoing has demonstrated the level of detail required to perform a comprehensive study analysis, and prepare cases for the engineering and financial benefits and risks for each option from which investment decisions can be made. Having chosen one or more options, the next stage would be to progress the engineering study using more detailed design tools, as discussed in chapters 6 and 12, and to concurrently refine the cost estimations as suggested in Table 13.3.

13.8 Post Project Analysis

It is important not only to monitor and control project costs during the period of its activity, but to also benchmark its outcome against the predictions and expectations. It is a common result of the implementation of any 'improvement' that the furnace will show immediate benefits. As much as 5% of any initially observed improvement may be attributable to a 'new baby' effect, whereby operating and maintenance staff will subconsciously take more interest and care than before because of the obvious 'company investment' shown. Within a relatively short period, this interest will wane and it is at this time that the true engineering benefits may be accurately monitored.

Most projects that result in a fuel saving will also have a potential for increasing the production capacity of the furnace. For example in the reheating furnace analysis above, if the furnace were fired at the same base case fuel oil input rate, but with self-recuperative burners, the production capacity would increase by $\sim$50% to 120 tonne/h steel and the thermal efficiency to $>$70%. We have already seen in section 9 that furnaces are most efficient at their maximum production rate, since the relative contribution of the thermal losses are minimised. If there is a market demand for the additional product, then throughput will increase, but if the market is limited, operating practices or schedules may need to be revised to take the best advantage of the increased efficiency gain (e.g. move from a 4 week to 3 week working cycle). It becomes more difficult to make a true assessment of the benefits in this case, and engineering judgement needs to be exercised.

References

Dysert, L. R. (June 2003). Sharpen your cost estimating skills. *Cost Engineering, 45*(6).

Gerrard, A. M. (2000). *Guide to capital cost estimating* (4th ed.). Rugby, UK: IChemE. ISBN 0 85295 399 2.

Lang, H. J. (Oct 1947). Cost Relationships in Preliminary Cost Estimation. *Chem. Eng., 54*(10).

Lang, H. J. (June 1948). Simplified Approach to Preliminary Cost Estimates. *Chem. Eng., 55*(6).

Peters, M., Timmerhaus, K., & West, R. (2002). *Plant Design and Economics for Chemical Engineers*. McGraw-Hill. ISBN 978–0072392661.

Williams, R., Jr. (December 1947). Six-Tenths Factor Aids in Approximating Costs. *Chem. Eng., 54*(12).

Chapter 14

Selected Examples of Real Furnace Applications

Chapter contents

14.1 Design of a New Burner for a Lime Sludge Kiln 538
14.2 Optimising Flash Furnace Design 547
14.3 Contribution to the Design of a New Reforming Process for Fuel Cell Applications 556
14.4 Resolving Tube Internal Coking and Premature Tube Failure in a Refinery Heater 571
14.5 Unsuccessful Attempts to Resolve Severe Problems with a Preheater Cement Kiln 580
14.6 Investigation and Elimination of Coal Firing System Problems 595
14.7 Concluding Remarks on Implementation 605
References 605

In this chapter we describe how we applied the techniques to real situations. Every application is different, and over the years, we worked on more than 250 individual processes. The applications outlined here have been chosen from those applications to illustrate the wide-ranging processes that these techniques can be applied to.

Examples are drawn from the successful implementation of a difficult waste fuel to fire a lime recovery kiln in the paper industry, development of a new methodology for the design of Alcoa flash furnaces, a major contribution to the development of new reformer technology for hydrogen production and solving premature tube failure problems in a refinery heater. In a few cases, the fuel supply system itself was so poorly designed that it severely limited process output and increased fuel consumption; one such example is described, namely the refurbishment and upgrade of a poorly designed and constructed coal grinding system. The work was undertaken to debottleneck and increase production in a coal fired cement kiln. In addition there is a short description of a coal firing system that failed to work but that failure was fortuitous since the system was so badly flawed, it was positively dangerous.

Generally, the techniques covered in this book could be used to solve difficult problems in many types of industry and types of furnace. However, in rare examples, the problem was relatively easy to diagnose but no simple economic solution existed because the original design was fundamentally flawed; one example of this type is also included.

14.1 Design of a New Burner for a Lime Sludge Kiln

Lime sludge kilns are an integral part of the liquor recovery process used in the pulp and paper industry. The kiln is frequently the highest user of fossil fuel within the paper mill, so its overall efficiency can have a dramatic effect on process costs. The fuel of choice is natural gas because it is both convenient and relatively low capital cost. Back up is usually provided by heavy fuel oil to accommodate times when natural gas is unavailable.

In the mid 1980s a small paper mill in Everett, Washington State, USA was offered a very low cost supply of petroleum coke, which if it could be burned successfully, would result in a significant reduction in operating costs. However, petroleum coke is a low volatile fuel and difficult to burn in a limekiln, as the mill engineers discovered when they commissioned the coke delivery system and injected the new fuel into the existing burner. Their target was to replace 80–85% of the current natural gas consumption with coke but only 40–50% substitution of the natural gas was achieved, which meant that the anticipated savings were not realized.

In early 1986, we were set the challenge to design, fabricate and commission a new burner to provide 85% of the thermal input from petroleum coke.

14.1.1 The Lime Regeneration Process

Lime is used to regenerate sodium hydroxide from sodium carbonate. Firstly, the lime is slaked to form calcium hydroxide.

$$CaO + H_2O > Ca(OH)_2 \quad (1)$$

The calcium hydroxide is then reacted with the sodium carbonate to form sodium hydroxide and calcium carbonate.

$$Na_2CO_3 + Ca(OH)_2 > 2NaOH + CaCO_3 \quad (2)$$

The calcium carbonate is then sent to the kiln where is it calcined to reform lime.

$$CaCO_3 <> CaO + CO_2 \quad (3)$$

The system is therefore a closed circuit with lime constantly regenerated. There are many impurities that accumulate in the calcium carbonate mud, particularly sulphur and residual sodium compounds, which cause various operational problems but that is beyond the scope of this example. The calcination reaction is highly endothermic requiring the addition of 1619 kJ/kg of lime.

The process is undertaken in a long rotary kiln, using wet slurry feed because the calcium carbonate is in an aqueous suspension, known as lime sludge or mud, Figure 14.1. The feed is introduced at the cool end and moves counter currently towards the flame. Firstly, the feed is dried and chains are used in this section to improve heat transfer, being alternatively heated in the gas stream and cooled when lying in the slurry, followed by preheating to calcination temperature when the endothermic reaction commences. Typical temperature profiles are shown in Figure 14.2. The main energy consuming processes are calcination and drying with 1619 kJ/kg of lime required for the endothermic calcination reaction and 2257 kJ/kg of water evaporated for the drying. By comparison, preheating only requires 660 kJ/kg of feed for heating from 100°C to 900°C.

In an open system such as a rotary kiln, the kinetic rate of reaction will increase with temperature until the partial pressure of CO_2 in contact with the solid reaches one atmosphere, which occurs at approximately 900°C. The rate of calcination is largely dependent on the rate that the heat can be supplied from the flame to meet the heat demand of 1619 kJ per kg of lime. The calcination reaction is the largest heat load because, although the latent heat of evaporation is higher on a specific basis, water makes up only 20–30% of the feed.

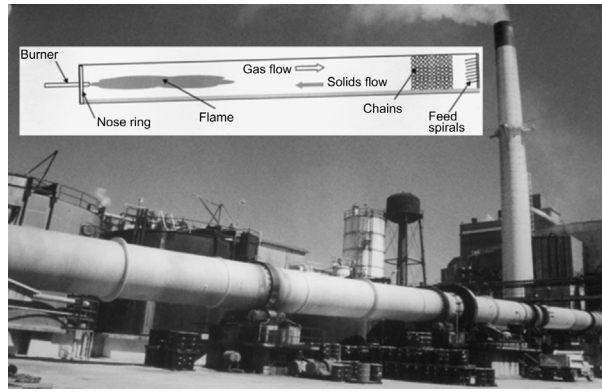


Figure 14.1 The Everett lime sludge kiln with a schematic of the internal fittings

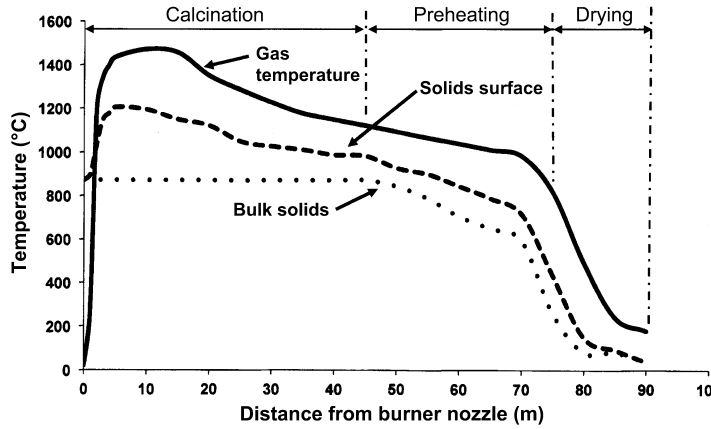


Figure 14.2 Typical temperature profiles in a lime sludge kiln

The Everett kiln did not use a product cooler to recover heat because the lime dropped out of the kiln directly into the slaker where reaction 1 occurs. Fuel economy is therefore dependent on ensuring the lowest possible kiln exit flue gas temperate, which in turn, is dependent of achieving a high rate of heat transfer in the calcining zone. If the heat transfer in the calcining zone is inadequate, then the heat remaining on the combustion gases is higher than can be absorbed in preheating and drying, resulting in an excessively high kiln exit gas temperature, thus wasting a significant proportion of the input energy.

14.1.2 Design Objectives for the Multi-Fuel Burner

The design process commenced with consideration of the basic characteristics of petroleum coke as a fuel and the heat requirements of the process.

The petroleum coke was a residue collected from the dust emission suppression system of a dockside coke export facility. As a consequence it had an unusual size distribution being bi-modal with a proportion of fine material less than 100 micron but with the majority of the coke in the 300–400 micron range. This makes it quite different from a normal pulverized coal/coke, which follows the Rosin-Rammler distribution, as shown in Figure 5.6. It had also been calcined so was ultra-low in volatiles (<8%) and could be considered as particulate carbon.

The very low volatile content, together with the coarse particle size, implies a long burnout time. It will also be slow to ignite owing to the low proportion of volatiles and their tar like nature. Using the rule of thumb quoted in section 5.1.3, the coarser particles could take in the order of 2–3 seconds or more to burn. Hence, this fuel posed a significant challenge with respect to designing a burner to achieve near complete burnout, given that the typical residence time of a particle in a flame is approximately ½ second.

The long burnout time was clearly demonstrated by the failure of the fuel to burn effectively when injected into the primary air of the existing burner. This burner's primary air velocity was approximately 50 m/s. Assuming the coke was conveyed at, or close to, this velocity as would be expected, then the residence time in the flame was less than ½ second. The residence time could be improved by reducing the primary air velocity but this would reduce its momentum and result in a severe deterioration of fuel-air mixing. Hence, this action would not improve the coke combustion and would result in the heat release moving towards the back of the kiln reducing heat transfer to the lime further decreasing kiln production capacity.

The basic burner functional requirements for coke combustion can therefore be deduced as:

- Excellent mixing between the fuel and combustion air
- Long residence time for the coke particles in the flame
- High temperature zone close to the burner nozzle to promote early ignition

To achieve these objectives required significant departure from traditional lime kiln burner design. Each of these objectives is considered in turn below:

Fuel/Air Mixing

As discussed in chapter 2, fuel air mixing is dependent on primary air momentum, which requires a relatively high velocity, in the order of

50–80 m/s for a small rotary kiln. While, in principle, similar momentum can be achieved by a lower velocity and higher primary air mass flow, this results in an excessive cooling effect in the root of the flame, which would have a detrimental effect on the coke ignition.

Coke Particle Residence Time

To maximize the residence time in the flame the coke must be injected at a relatively low velocity. It must also be distributed evenly in the flame to achieve good mixing with the combustion air. To achieve this requirement it is necessary to inject the coke separately from the primary air.

High Temperature Zone Close to the Burner Nozzle

Early ignition of the coke particles is essential to maximize the time available for burning. High rates of heat transfer to the lime bed close to the burner nozzle are required to maximize the lime production rate and fuel efficiency. Given the low volatile content of the coke and its relatively coarse particle size, support fuel in the form of natural gas will be required to compensate for the missing volatile component. It is also desirable to minimize the quantity of primary air to reduce the cooling effect in the flame establishment zone.

14.1.3 Design Methodology

Modelling

The first step was to design and build a transparent plastic model of the kiln calcining zone and the kiln hood and use acid/alkali modelling, as described in Chapter 6, to check the kiln aerodynamics and to determine the primary air quantity and velocity required to achieve the optimum flame shape and length. This was found to coincide with a Craya-Curtet parameter of 2.2.

The results from the acid/alkali modelling were translated to determine the full size primary airflow rate and velocity, maintaining the Craya-Curtet similarity parameter at 2.2 for the full size burner. These conditions were then used to predict the heat transfer to the kiln wall and lime bed using the one-dimensional zone model, also described in Chapter 6.

Provided the predicted heat transfer is satisfactory then the mechanical design proceeds, otherwise further primary air variations were tried using the one-dimensional zone model until a satisfactory

heat transfer profile is obtained. The new primary air conditions are then checked in the acid/alkali model to ensure that the flame shape and length remain satisfactory.

While the combination of modelling techniques used to design the burner is time consuming and therefore relatively expensive, an optimum burner design is achieved from the start. The alternative design method based on the heat release rate alone is unlikely to provide the optimum heat transfer, so will result in extended trial and error during commissioning and higher long term costs.

Mechanical Design

This consists of four critical elements:

1. Gas nozzle – designed as described in Chapter 5, section 5.3.4
2. Coke transport and injection system - designed to achieve low velocity (5–10 m/s) fully distributed injection into the flame zone
3. Primary air nozzle – designed to achieve to primary airflow rate and velocity determined from the modelling described above
4. The oil sprayer – a standard Y-jet type steam atomizer was used

Gas Nozzle

The client's requirements were that the kiln should be capable of full production using 100% natural gas firing or using a mixture of gas and coke with a capability of firing at least 85% coke with 15% gas as support fuel, all on a thermal input basis.

The gas nozzle, Figure 14.3 was therefore designed for 110% of the required duty (full load +10% margin) and a turndown ratio of 15:1.

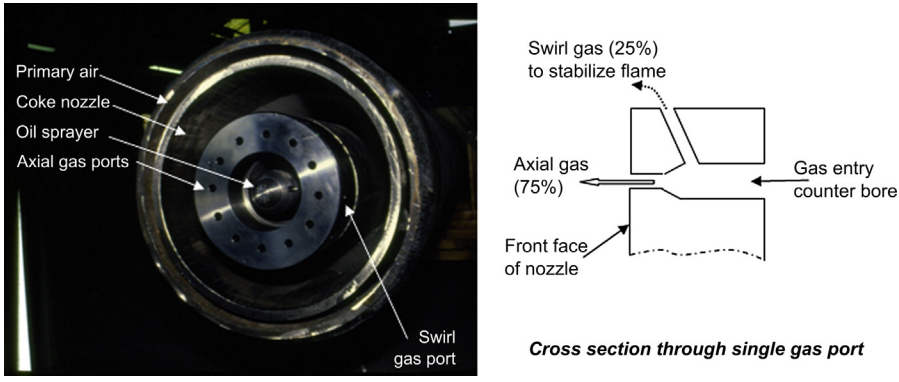


Figure 14.3 The multi-fuel burner nozzle with a cross section of a gas port

A stable flame was mandatory over the entire operating range. To achieve a stable flame the nozzle used 2 sets of gas ports, 16 holes on the front of the nozzle providing axial jets accounting for 75% of the gas flow while the remaining 25% of the gas flow is injected through 16 swirl radial ports. The gas issuing from the swirl radial ports causes a recirculation zone of burning gas on the face of the nozzle, thus ensuring flame stability.

Individual ports are preferred over annular injection nozzles because the individual gas jets entrain air and the gaps between the jets facilitate gas/air mixing.

The nozzle was machined from a forged billet of A304L stainless steel. This material has 18% chromium and 8% nickel and has more than adequate heat resistance for this application since the gas flowing through the nozzle cools it, keeping temperatures relatively low (<800 °C), except during oil firing. During oil firing the gas nozzle is cooled by an auxiliary airflow in the annulus between the oil sprayer and the inner tube of the gas gun.

The suffix L indicates that the carbon content of the steel is less than 0.03%. This is important to prevent inter-granular corrosion resulting from chromium depletion at the grain boundaries caused by chromium reacting with carbon to form chromium carbide, which can occur in the temperature range that the nozzle experiences.

Coke Transport and Injection System

The coke was fed to the burner using the existing dense phase conveying system that transported the coke at 20 m/s. Hence, to achieve the target 5–10 m/s injection velocity, the coke particle velocity had to be reduced.

To reduce the coke injection velocity a diffuser is used, Figure 14.4. This consists of a divergent cone with a very narrow angle, less than 15° included. This narrow angle is required to prevent flow breakaway and ensure that the conveying air velocity is uniformly reduced and, with it, the coke velocity. To minimize the effect of roping (See Chapter 7, section 7.3.10 pulverized coal conveying) on the coke distribution, a tangential coke stream inlet was used, distributing the coke in the transport annulus. This had the benefit of further reducing the forward velocity component of the coke at the nozzle exit, owing to the radial velocity component. However, this radial component must be modest otherwise there is the risk of coke impingement on the kiln walls.

The external tube of the gas gun was externally lined with a silicon carbide sleeve at the coke inlet to minimize wear since petroleum coke is very abrasive. This had been demonstrated with the old burner when the coke wore a hole in the gas pipe after a few months operation. Any breach of the gas pipe is a major safety hazard but,

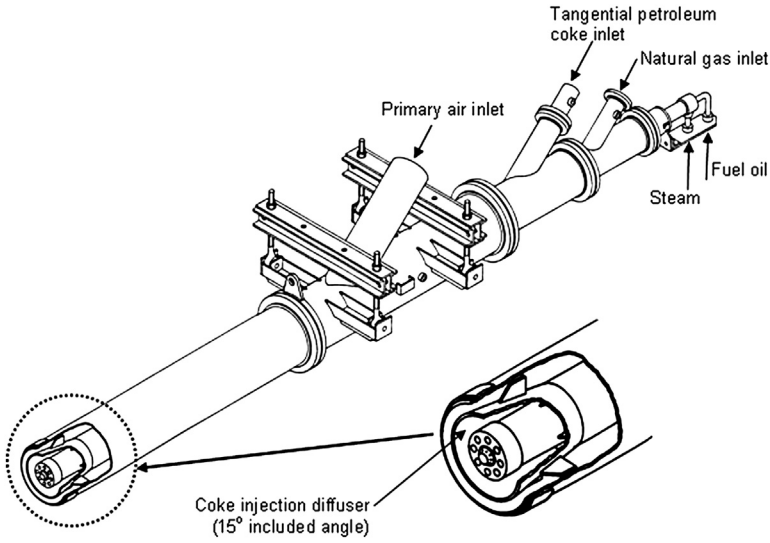


Figure 14.4 Isometric sketch of the multi-fuel burner

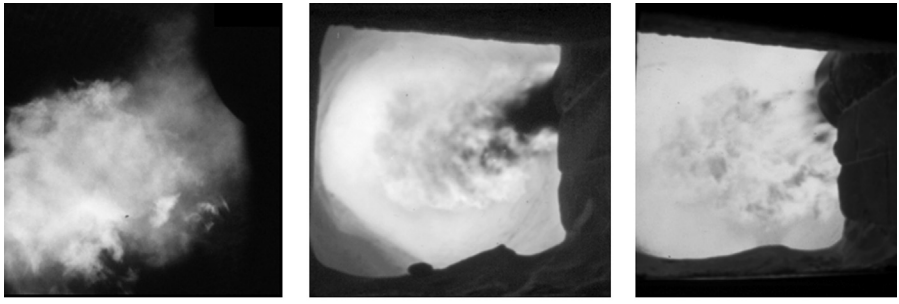


Figure 14.5 Everett kiln flames for all fuels

fortunately in this instance, there were no adverse effects beyond the need to shut the kiln down to repair the burner.

Primary Air Nozzle

The primary air channel surrounded the coke channel and the final nozzle was sized to give the required primary air velocity of 75 m/s at the design flow rate. The outer tube was standard 14-inch pipe with 3/8 inch wall. The material was again A304L with the hot end

reinforced with an outer band of Inconel to minimize the risk of distortion. In the current design, the required primary velocity could be obtained by optimizing the angle and length of the coke diffuser since this could be achieved without compromising the coke velocity or distribution. Where this is not the case the outer tube must be coned down to produce a reduced primary air nozzle diameter to accelerate primary air to the required velocity.

14.1.4 Commissioning

The burner was fabricated in Ontario, west of Los Angeles and transported to site by road and installed by the client under our supervision. Peter M was on site for the commissioning, which was expected to be relatively difficult, particularly the change over from 100% gas to 85% coke firing. In practice it was remarkably easy and was accomplished in less than a week. Firstly, the kiln was warmed up using gas firing. Feed commenced and the kiln was brought to full production. It was allowed to stabilize overnight and coke firing commenced early the next morning.

The coke delivery system had limited turn down so coke firing commenced at 25% gas replacement. The kiln was allowed to stabilize for 2–3 hours before another 10% of the gas was replaced by coke. At the end of the day the kiln was firing 60% coke so had already exceeded the capability of the previous burner.

Overnight the kiln became far too hot and, as a result, I was called from my bed in the early hours. It appeared to me that the kiln was being over-fired. The operators agreed and decided to reduce the coke input. However, I suggested that before they did that perhaps we should try reducing the gas by 5%. They agreed and the kiln stabilized within an hour.

That led to the realization that we had overlooked one important factor in the design, which had been based on the gross calorific value of both fuels, as was the normal specification basis for this industry. However, with the very low hydrogen content of petroleum coke, its gross and net calorific values are virtually the same. This meant that, as gas was substituted by coke, the net heat input to the kiln was increasing. This, together with the increased radiation emissivity from the high carbon fuel (see Figures 3.3 & 3.4), severely overheated the calcining zone of the kiln.

With the kiln once again stabilized, we were ready to further increase coke firing and reduce gas. I decided to reduce gas flow by 15% and increase coke firing by 10%, so we were now at 75% coke firing on a gross CV basis. The kiln continued to run steadily and by the end of the day 90% substitution of natural gas by coke (gross basis) had been achieved. I slept well that night!

The next day everyone wanted to push the capabilities of the burner, so gas was further reduced and coke increased to achieve 95% substitution. The kiln continued to run steadily, so early afternoon we decided to try coke firing alone. For the first hour or so the kiln appeared to run stably but after that the calcining zone started to cool owing to the delayed ignition of the coke. Replacement of 5% of the coke with natural gas quickly stabilized the kiln.

It was agreed by the mill staff that all their objectives had been achieved. The burner operated trouble free until the mill closed in 1992. Its small size, the need for expensive upgrades to meet improved environmental standards together with increased wood chip costs, sealed its fate.

14.2 Optimising Flash Furnace Design

Flash furnaces, as shown in Figure 1.16, are used for processing a number of finely divided minerals. Although Geoffrey Martin developed the concept of the flash furnace in the 1920s, with his floatation kiln (Martin, 1932), the process was not applied for another thirty years. The first commercially successful flash furnace was designed and built by Alcoa in the 1960s with units operational in Suriname in 1965 and Kwinana, Australia in 1966 (Williams & Schmidt 2012). Since that time the technique has been adopted by a wide range of industries including, cement, copper, lime, nickel, etc.

For several decades, design was based on empirical rules but in the mid 1980s Alcoa considered that a better understanding of the fundamentals of calciner operation could lead to improved output with current plants and was essential to the design of the larger units planned for the future. As a result, Alcoa called for expressions of interest in gaining a better understanding of calciner operation. We submitted a proposal on behalf of our company, Fuel & Combustion Technology Limited (FCT). This proposal consisted of a site investigation to determine a number of current process operating conditions, together with a unit-by-unit mass and energy balance followed by physical and mathematic modelling of the furnace process.

In the alumina industry flash furnaces are used for removing the water of crystallisation from aluminium tri-hydroxide:

$$2Al(OH)_3 \rightarrow Al_2O_3 + 3H_2O$$

This reaction is strongly endothermic and requires temperatures up to 650°C to drive the dehydration reaction to completion but temperatures as high as 1050°C are required to achieve the required alumina crystal phase properties, so the reaction consumes large amounts of energy. The product quality is sensitive to the residence time at that temperature. Prior to the introduction of the flash furnace by Alcoa,

rotary kilns were used for calcination but the flash furnace provided a significant reduction in energy consumption owing to the reduced external surface area, thicker refractory, improved upstream and downstream heat recovery systems and improved reliability.

14.2.1 Site Investigation

FCT was provided with some basic operating data and a process flow diagram of the calciner system, Figure 14.6.

The feed of aluminium tri-hydroxide, known as alumina tri-hydrate or simply hydrate for convenience, is fed to the vacuum filter table as an aqueous suspension. The dewatered feed with 5–10% residual free moisture is fed to the riser duct and gas conveyed to the preheating cyclones and hence to the fluid bed drier (the name being somewhat misleading as no drying actually occurs in this vessel). The fluid bed drier is simply a surge vessel to help smooth out the transfer of solids to the downstream vessels. The hydrate is then subjected to counter-current preheating by the combustion products until it enters the main furnace where it is heated to calcination temperature using either natural gas or heavy fuel oil. The air supplied to the furnace has been preheated, firstly by counter current flow with the cooling product then to 1000–1050°C by direct firing in the air preheat furnace. After preheating the incoming combustion air by counter current flow the product is further cooled in the fluid bed

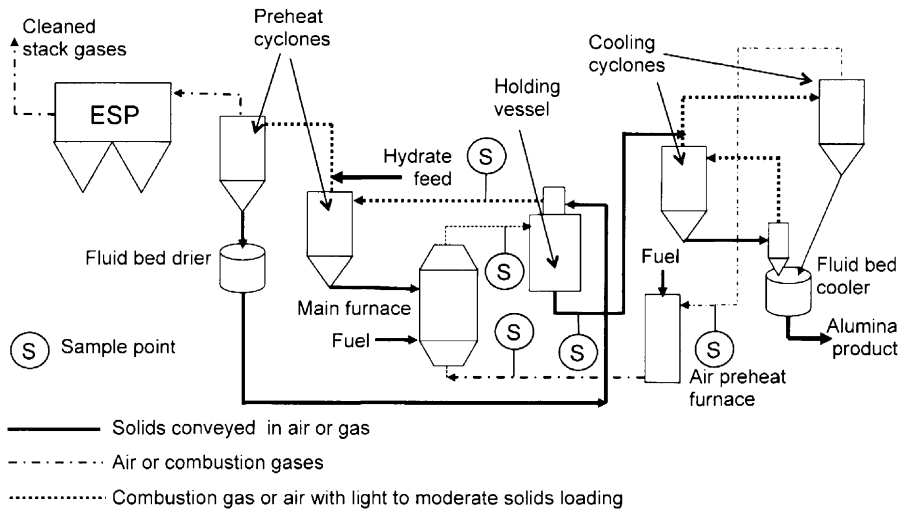


Figure 14.6 Simplified process flow diagram of the Alcoa calciner system showing the sampling points (After Williams & Schmidt 2012)

cooler. Forced draft blowers supply the combustion air through the base of the fluid bed cooler fluidising the product to enhance heat exchange through water-cooled tube bundles.

The flash furnace operates under quasi-isothermal conditions with the heat added from the fuel approximately equal to the heat absorbed by the dehydration reaction, resulting in a minimal temperature rise. From the flash furnace, the de-hydrated alumina is gas conveyed to the holding vessel where the alumina is held at temperature to achieve the required product quality.

The pressure loss through the fluid bed cooler and the various cyclones is significant so the entire system is under positive pressure. Most of the ducts carry hydrate, calcined alumina or a mixture of both in a hot air or hot combustion gas stream.

From the diagram and the above brief description of the process it can be seen that a process investigation and unit-by-unit mass and energy balance is not a trivial exercise. For example, it is necessary to know the temperature of the air or gas stream in each of the major ducts, the mass of solids conveyed in that stream together with the composition of the solid material in the stream. To obtain this information it was required to sample the stream under hot (up to 1050°C), pressurised conditions (up to 25 kPag). Unless this was planned and executed carefully, serious safety issues could arise.

Methodology Adopted

Firstly the authors designed and manufactured the water-cooled sampling probe shown in Figure 8.9. The sample tube was mounted within the water jacket and could be rotated throughout 360°. Gas was drawn through the probe by a suction pump or naturally driven by the pressure in the furnace system. The outlet connection, marked "to analyser" in Figure 8.9 was connected to a standard BUCRA/Airflow Developments Ltd. dust sampling cyclone (Hawksley et al, 1997). This cyclone was part of a comprehensive set of equipment designed for measuring dust emissions to atmosphere from furnace stacks. Since much higher dust loadings were expected in the current application the cyclone was equipped with a larger collection pot than used for air dust emission monitoring. A double valve lock system using gate valves was designed to allow the probe to be inserted into the pressurised duct and removed from it without the escape of hot gas and dust, Figure 14.7. Five of these valve and seal assemblies were manufactured and installed by Alcoa at the points marked "S" in Figure 14.6 during a maintenance shut down.

In normal operation, both valves were tightly closed. Prior to taking the sample the probe was hoisted by a block and tackle and suspended over the sample point. Valve 1 was opened and the probe inserted. A seal was provided by ceramic fibre rope. Once the probe

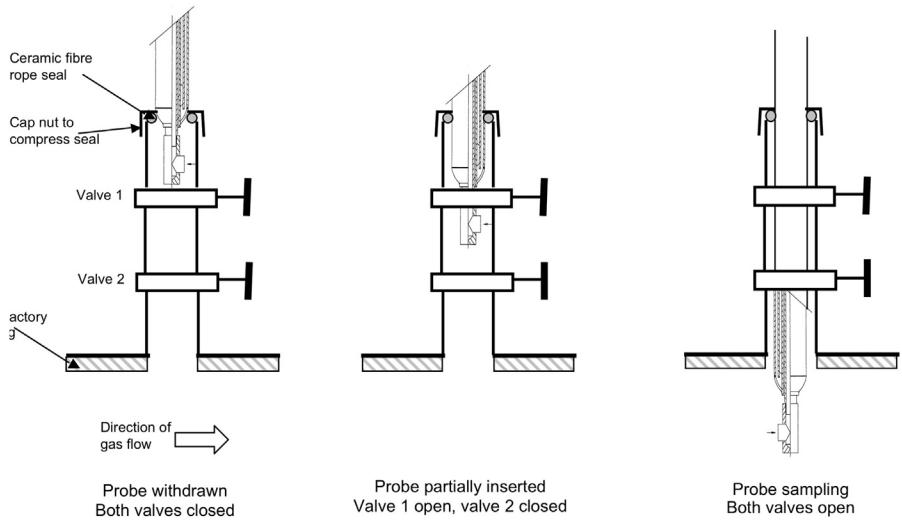


Figure 14.7 The double valve lock and seal system allowing safe probe insertion and withdrawal

was in position, a safety chain was attached to prevent accidental withdrawal beyond the seal when retracting the probe (not shown in Figure 14.7). Valve 2 was then opened and the probe inserted into the duct. During insertion and later at the end of the sample period during withdrawal, the nozzle was facing away from the gas flow.

Sampling Procedure

All the standards for dust sampling specify isokinetic sampling. For isokinetic sampling, the velocity of the sample drawn into the probe must be the same as the free velocity in the duct. However, in the current case that was not possible owing to a number of reasons, including:

- The velocity profile in the duct was unknown despite the fact that the approximate average velocity could be calculated
- The local velocity could not be measured by a standard pitot-tube owing to dust blocking the dynamic and static pressure tapping ports

However, the probe used was equipped with both dynamic and static pressure measuring facilities and a shielded thermocouple to measure the local gas temperature so an approximate gas velocity could be obtained.

Despite the inability to achieve true isokinetic sampling, it was considered that worthwhile results could be achieved by sampling as close as practical to isokinetic conditions. The procedure adopted was as follows:

1. The probe was inserted into the duct as described above and advanced to the first sampling point with the nozzle pointing away from the gas flow.
2. The nozzle was turned through 180° to face the gas stream and the static and dynamic pressures measured, together with the gas temperature.
3. The approximate gas velocity was calculated using the conventional pitot-tube formula.
4. The sample extraction system was started and the flow adjusted to as close to isokinetic sampling as possible. In ducts where the gas was combustion products a sample was taken and analysed to determine the gas composition.
5. The nozzle was then turned 180° to face flow downstream and the sample flow was shut-off using a quick acting valve. The dust collected was weighed to determine an appropriate sampling time, then discarded.
6. To collect a sample, the nozzle was turned 180° to face the gas flow, the timer started and the quick acting valve opened simultaneously.
7. During sampling the flow was manually adjusted to maintain the target sample flow rate.
8. At the end of the sample time the nozzle was then turned 180° to face flow downstream and simultaneously the sample flow was shut-off using the quick acting valve and the timer stopped.
9. The sample collected was weighed and the total volumetric gas flow integrated over the sample time.
10. The dust loading was then calculated in terms of mass/m^3 and converted to kg of dust per kg of gas.
11. The process was repeated at each sample point, with 6–8 sample positions across the duct at each sample point.
12. Finally a steady traverse of the duct was made to collect a composite sample.

All the dust samples collected were tested in the laboratory to determine the mass of water in the sample. Where calcination or partial calcination had occurred, the alumina phases present were also determined.

In all, the testing took a full week so the unit had to be run at quasi steady state for the entire time. From the data obtained it was possible to prepare a mass and energy balance around pre-heat furnace, main furnace and holding vessel. The results showed a previously

unsuspected dust recycle and the principle region of the calcination reaction. The results were used to both improve the Aspen process model used by Alcoa and as an input into FCTs physical modelling and mathematical modelling of the process described below.

14.2.2 Physical Modelling

Water-bead modelling and acid-alkali modelling were undertaken to investigate the flow patterns and the fuel/air mixing in both the preheat and main furnaces. The latter was of particular interest because fluctuating CO levels were detected in the presence of reasonably high levels of excess air (~20–25%) during otherwise steady operating conditions.

Sample photographs of the operating acid/alkali model are shown in Figure 14.8. The dark area is pink in the original and caused by phenolphthalein pH indicator demonstrating that this area is alkaline, representing unburnt fuel, see chapter 6, section 1.

The modelling showed that the inlet to the preheat furnace induced a strong swirling motion to the flow with a strong vortex core throughout the unit but, more importantly, revealed an unstable fuel/air mixing regime in the main furnace. In normal circumstances the combustion reaction was largely completed in the lower half of the furnace, Figure 14.8 left. The onset of unstable conditions was indicated by a "tail" of unmixed, and therefore unburnt gas, in the vortex core, Figure 14.8 centre. Relatively frequently, with no

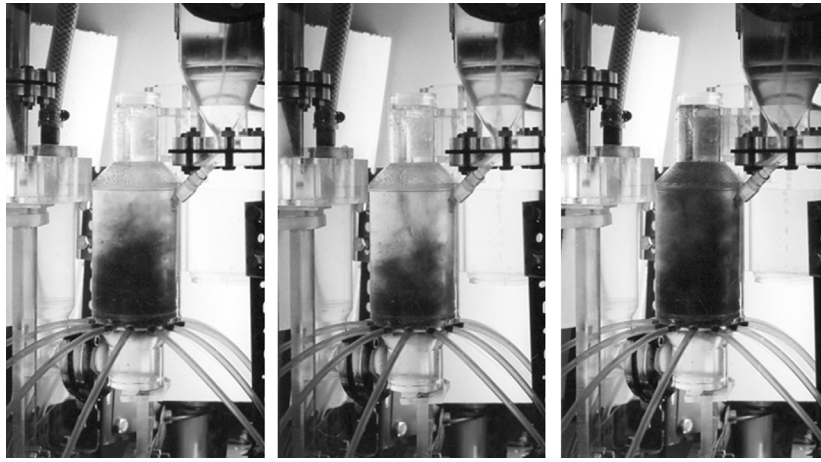


Figure 14.8 Acid Alkali Model of main furnace combustion showing normal operation on the left and intermittent unstable conditions in the centre and to the right

detectable change in flows the fuel/air mixing would completely fill the furnace and spill over into the downstream duct when the reaction was quenched owing to the lower temperature environment, Figure 14.8 right. It was this condition that was producing the CO that was intermittently detected.

Various solutions were tested on the model, starting with varying the number of gas injectors and changing their position because this is the cheapest potential solution on the real plant. These changes were trial and error but cheap to implement in a model. Fortunately, a solution was found by reducing the number of injectors to four and moving them to the parallel inlet below the cone. Existing calciners were successfully modified. The smaller number of burners in the lower position was utilised in new designs.

14.2.3 Mathematical Modelling

Since the furnace is effectively a well-stirred system, the heat transfer was modelled using Hottel's model described in section 6.2.1. This showed that the furnace was adequately sized and may be amenable to increased output, provided that this could be accommodated by the rest of the system, particularly the need for increased airflow to burn the additional fuel required to provide the additional heat needed to drive the endothermic reaction.

Computation fluid dynamics (CFD) was used to investigate the distribution and residence time of the differing sized particles in the furnace. At that time, CFD modelling was in its infancy as a commercial application and severely limited by the available computing power. This required the grid to be built up laboriously and this was an extremely time consuming process. Despite these limitations it was possible to produce a 3-dimensional grid, Figure 14.9. For the actual investigations both 3-dimensional and "slice" grids were used.

Colour printers were generally not available at that time (1988–1990). Those available were extremely expensive and the software not readily adapted to print the CFD results. Therefore the results were recorded by photographing the computer screen, Figure 14.10. The techniques available also limited quality of the resulting interpretive diagrams. However, we considered that the original diagrams should be reproduced, rather than be redrawn to show what could be achieved with limited techniques.

In Figure 14.10, the left hand photograph shows the gas velocity profile in a cross section of the furnace while the right hand shows the predicted particle trajectories of the 104-micron particles. From photographs like these it was possible to build up a detailed picture of the air and particle velocity profiles Figure 14.11, and the concentrations within the furnace, Figure 14.12.

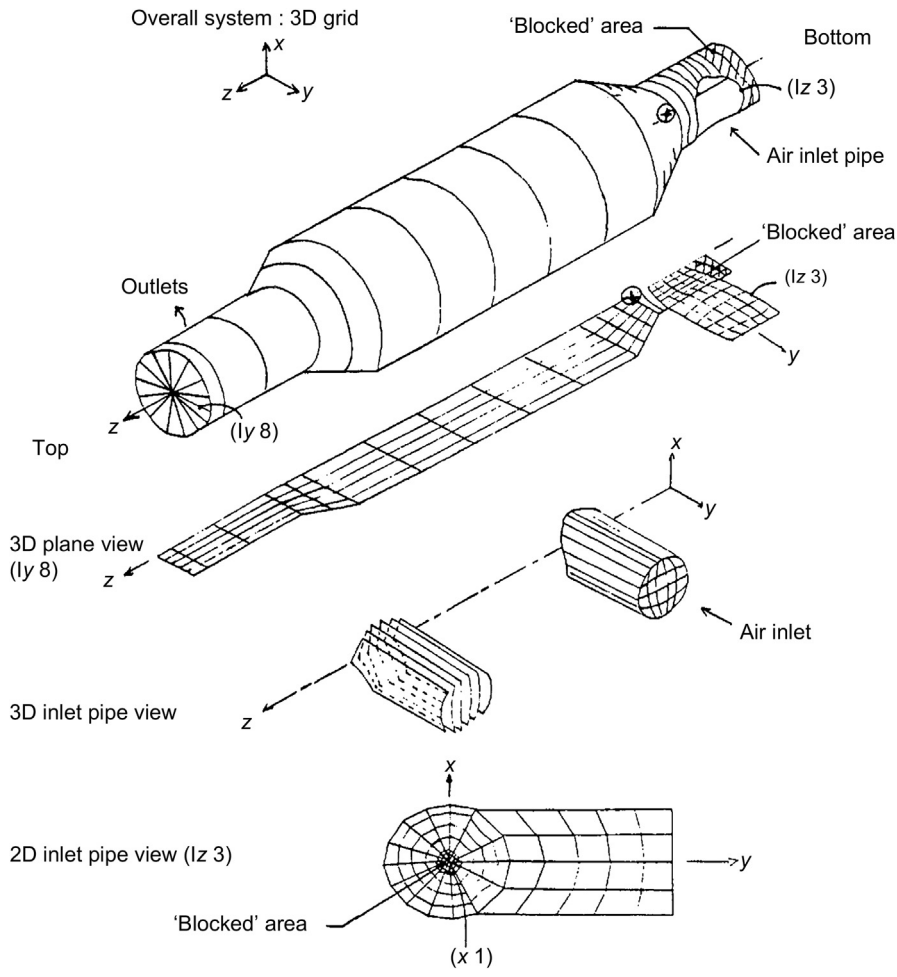


Figure 14.9 The 3-dimensional grid used for the CFD modelling (Bertrand, 1991)

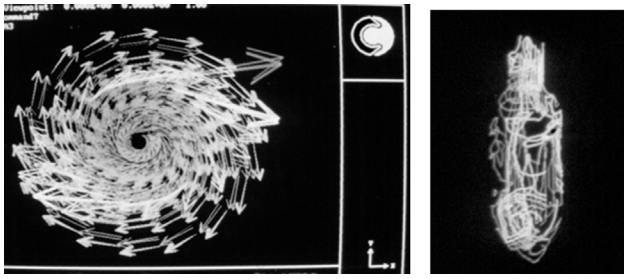


Figure 14.10 Photograph of the computer screen showing two CFD Modelling results

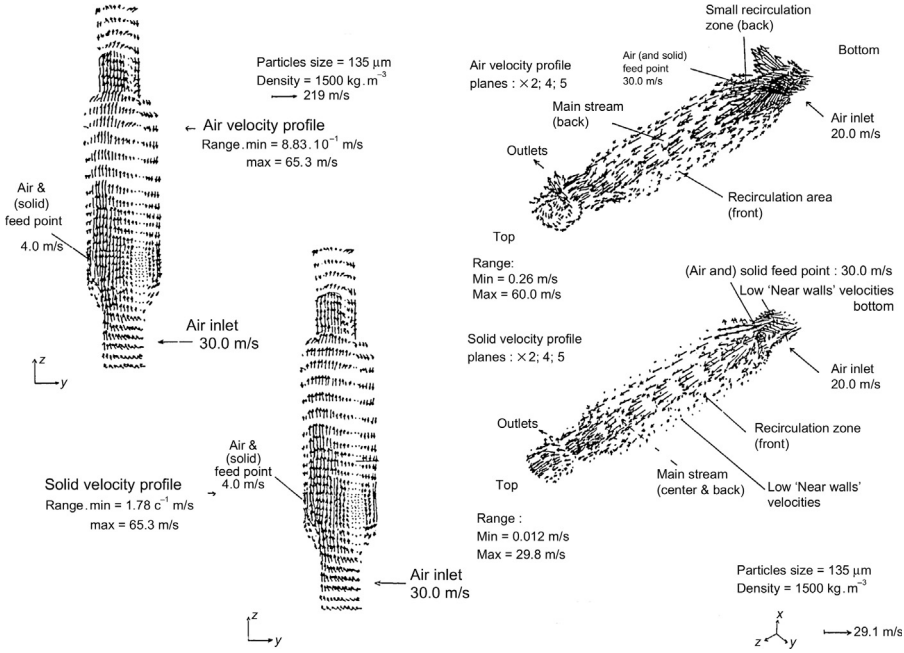


Figure 14.11 Example of the air and particle velocity profiles in the flash furnace showing a slice model (left) and 3-D model (right) (Bertrand, 1991)

The main interest from a process viewpoint was the residence time of the individual particle size fractions because this affected the product characteristics. From the large number of velocity and concentration results obtained, it was possible to estimate with a reasonable degree of accuracy the average residence time of each particle size band. This was validated against the product characteristics, which suggested that the residence time was too long for some sizes and too short for others.

Further CFD modelling was undertaken to optimise the feed position and the injection velocity. It was found that a lower feed injection velocity was desirable. This was implemented of a full size unit with considerable success and as a result, existing units were retrofitted and the new feed design was incorporated into new units. A more recent presentation of the CFD work, using a later version of the original software code can be read in the IFRF on-line Journal (Jenkins & Bertrand, 2001).

Shortly after this initial work was completed, Alcoa established their own in-house CFD modelling capability. Over the years, they have developed their capability in this field to a very high level of excellence. Many of the limitations described in this example have been relaxed with the latest versions of CFD software, which now

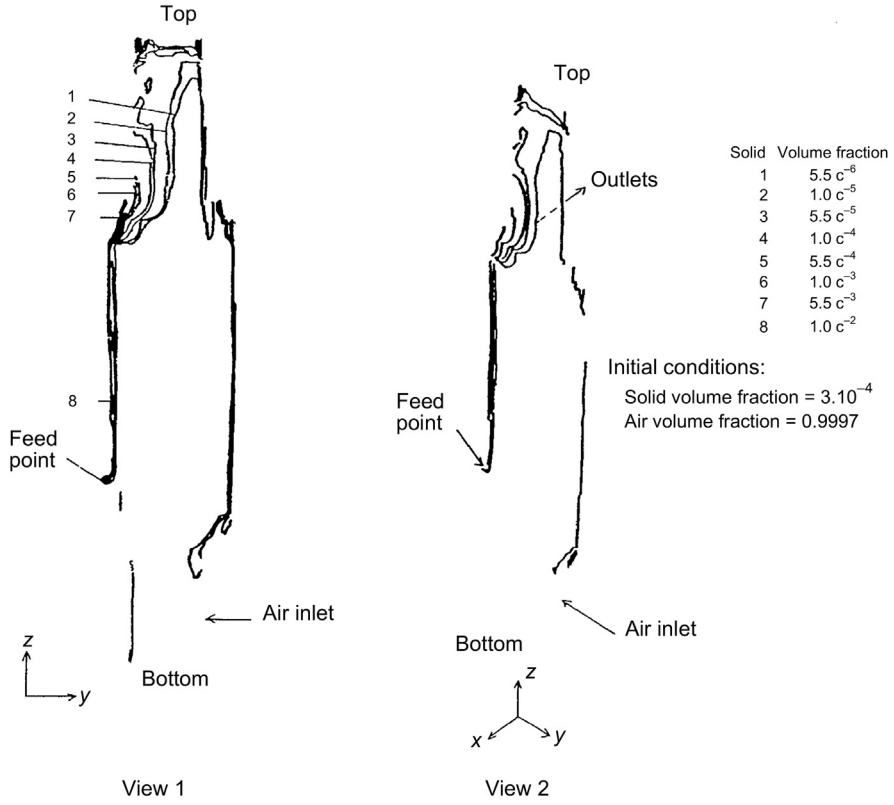


Figure 14.12 Example of the particle concentration profiles in the flash furnace (Bertrand, 1991)

allow for effective modelling of two-phase flows. This has enabled Alcoa to gain significant advances in their understanding of the furnace dynamics. As a result, they have been able to diagnose failure mechanisms, where these occur, and to develop effective solutions.

14.3 Contribution to the Design of a New Reforming Process for Fuel Cell Applications

The techniques described in this book are especially amenable to the design of new processes from conceptual stage through to detail design. While we rarely designed a new process alone, we worked with several well-known process engineering companies and process operators where our input was very important, or even critical, to the success of the project. A particularly good example of this type of work was our cooperation with Haldor Topose A/S to design a new reforming process.

Steam reforming is used widely to produce hydrogen using, natural gas, naphtha or kerosene together with steam. The principle reaction for natural gas feed is shown below:

$$CH_4 + H_2O \leftrightharpoons 3H_2 + CO$$

This reaction takes place at high temperature and pressure over a nickel based catalyst bed and is strongly endothermic. For naphtha or kerosene the reactions are different but the products similar. Most of the CO is then converted to CO_2 and more hydrogen via that water gas shift reaction. This reaction is slightly exothermic and takes place at lower temperature.

$$CO + H_2O \leftrightharpoons H_2 + CO_2$$

In the conventional steam reforming process, the catalyst is housed in tubes that are fired externally on both sides by a large number of burners, Figure 14.13. Reformers are available from a number of suppliers and the burners may be arranged for down firing, up firing or side firing. In all cases a large number of burners are used and achieving equal fuel and air distribution between burners is a serious challenge, see section 5.6.3. In addition, owing to the height of the furnace there is significant internal natural draft resulting from the low density of the high temperature combustion products.

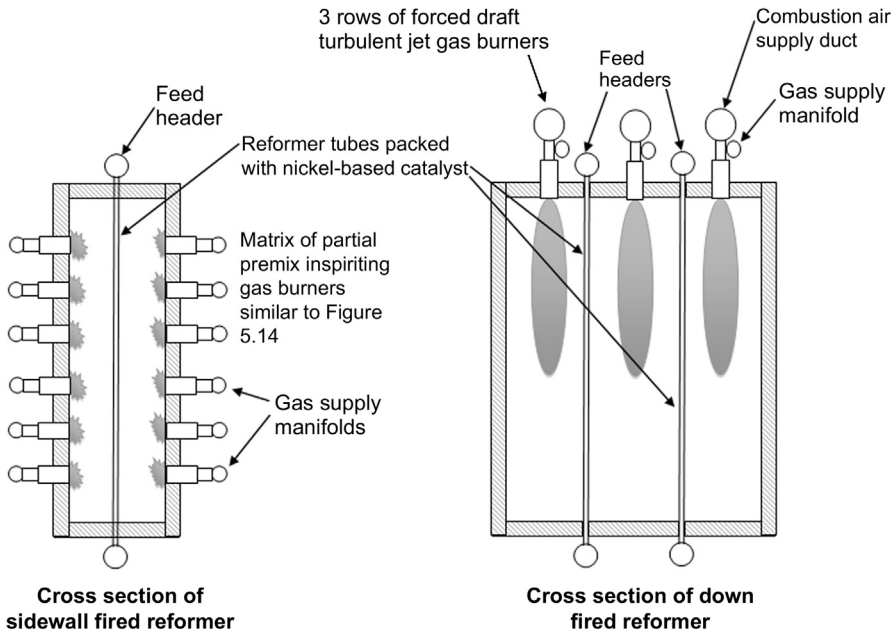


Figure 14.13 Schematic of typical tubular steam reforming plant

Table 14.1 Typical Dewatered Catalytic Steam Reformer Gas Properties

Component Gas	*Volume%*
Hydrogen	70–74
Water vapour	1–10
Carbon monoxide	0.1–14.2
Carbon dioxide	7.7–24.9
Methane	0.4–5.3
Nitrogen	0–0.5

With temperatures in the order of 1000°C and pressures up to 40 bar, the duty is severe and great attention must be paid to the mechanical design of the tubes and their support systems to minimise the risk of failure. The gases leave the combustion chamber at high temperature and to maximise thermal efficiency a convective heat recovery system and a waste heat boiler are often used.

As indicated above the reactions are reversible so do not go to completion. The exact composition of the gaseous product depends on the reformer feedstock, which is typically natural gas or naphtha but occasionally kerosene. The typical range of reformer gas compositions are given in Table 14.1.

Tubular reformers are suitable for large-scale steady production and do not respond well to frequent load changes or to regular start up and shut down, owing to the limitations of their mechanical design and the need to manage differential thermal expansion.

14.3.1 Reformers for Fuel Cells

In the 1980s there was significant interest in the potential for fuel cells to produce electrical power based on their high efficiency and apparent simplicity. As a result, a range of test and demonstration plants were proposed and several were constructed using phosphoric acid fuel cells, Figure 14.14.

The phosphoric acid fuel cell (PAFC) requires a source of hydrogen and since electricity must be manufactured and supplied on demand the supply of hydrogen must also be available in varying flow rates to suit the fuel cell's requirements. These fuel cells are tolerant of CO_2 but poisoned by CO, so conditions must be chosen to drive the reversible water gas shift reaction to the right. For this a catalyst is also utilised. Further CO removal may also be used, if required. The feed to the PAFC is therefore a mixture of hydrogen and carbon dioxide unless the latter is removed.

Owing to its design and construction the conventional tubular steam reformer was not suitable for either the varying load required

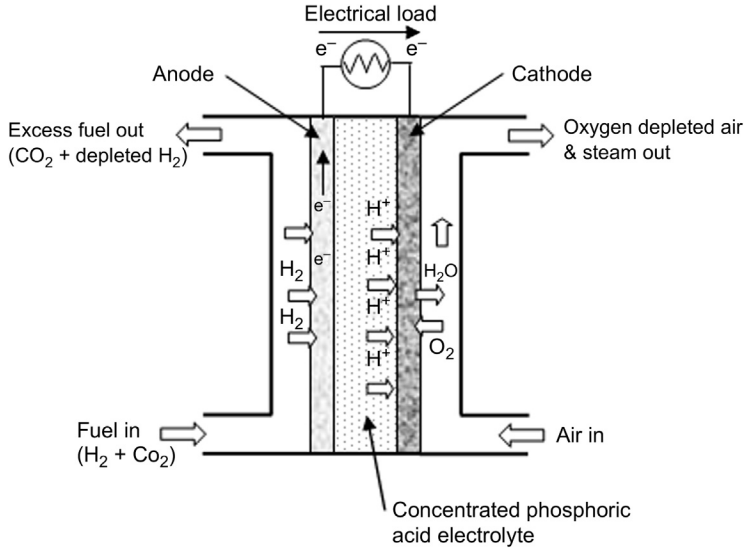


Figure 14.14 Schematic of a phosphoric acid fuel cell

or the smaller scale of operation of the proposed fuel cells (200kW to 5 MW). To meet this requirement Haldor Topsoe designed their revolutionary convective heat exchange reformer, Figure 14.15.

The tubes were eliminated and the catalyst was arranged in two annular beds. The process gas (steam and methane) flowed counter currently to the combustion products providing the potential for very high heat recovery and hence high efficiency. However, the new design required a completely different approach to burner design from the conventional tubular reformer, since radiant heat transfer was no longer required. The high thermal efficiency resulting from the counter-current flow eliminated the need for a waste heat boiler.

During normal operation the burner would be firing with the off-gas from the fuel cell, a depleted hydrogen stream with carbon dioxide from the anode. Oxidant would be an oxygen depleted air stream with water vapour from the cathode. Since the fuel cell operated under pressure, the combustion was also to be undertaken at a pressure of up to 1000 kPa (145 pisg).

Anode off-gas was not available during start-up so the reformer feed, normally natural gas but occasionally kerosene, was used as the start-up fuel. Once the reformer was operating, but before the fuel cell was generating, the burner was required to burn the H_2/CO_2 reformer product. These three quite different fuels required a fundamental assessment of the burner duties to meet the client's needs.

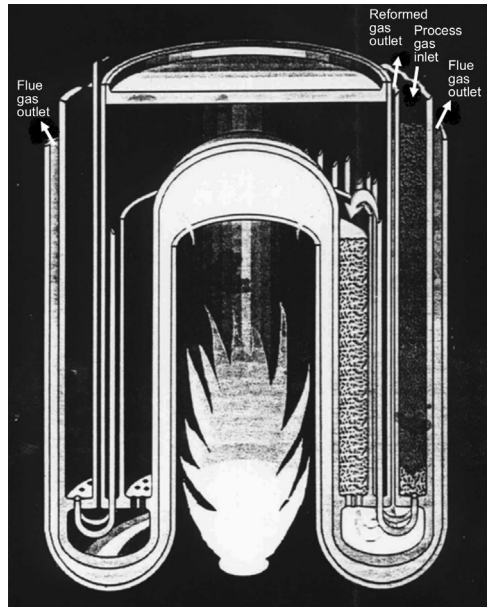


Figure 14.15 The Haldor Topsoe convective heat exchange reformer (Reproduced with kind permission of Haldor Topsoe A/S.)

14.3.2 Burner Design

As noted above, the specification required a burner to perform over a range of duties, not previously encountered for any application that we were aware of. It was therefore not possible to extrapolate from an existing design to produce a burner for this application. Therefore the design had to be developed from basic principles. Careful consideration of the flame characteristics was undertaken and the following requirements derived:

- The flame must be long compared with the diameter because the length:diameter ratio of the combustion space was much greater than indicated in Figure 14.15 being in the order of 350 mm internal diameter and approximately 5 m long;
- Since radiant heat transfer is not required, and is actually undesirable, a very flat heat flux profile with a low peak was required;
- The burner must be able to perform equally well on three quite different fuels;
- The combustion must take place under ambient conditions and at pressure. In both cases, NOx and all residual unburnt species needed to be minimized to meet stringent environmental requirements.

These requirements were a significant challenge for Barrie and myself. Long flames with flat heat flux profiles require slow rates of mixing, yet minimizing residual unburnt species required complete mixing, see Chapter 2 section 2.4. Furthermore, very little data is available for combustion reaction kinetics at high pressure, reducing our confidence in the mathematical modelling of the combustion process.

We chose a simple jet entrainment system to provide fuel air mixing, Figures 2.8 and 2.9. The heat input with the rich natural gas start-up fuel was similar to the heat input when generating, using lean anode off-gas. The Wobbe number for the natural gas fuel was in the order of 48 MJ/m^3 while that for the anode off gas was less than 20 MJ/m^3. Owing to these very different characteristics between the start up fuel and the running fuel two independent fuel inlets were required because the lean gas nozzle had to have between 2 and 3 times the flow area to achieve a similar heat input.

The burner design was very simple and consisted of a series of concentric tubes arranged around a conventional, forced draft nozzle-mixing pilot burner that was installed on the axis of the burner, Figure 14.16.

The burner was strongly constructed to API pressure piping codes owing to the high operational pressure. The air and gas supply pipes for the pilot can be seen entering the centre of the flange at the back of the burner. The pilot was ignited with conventional spark ignition.

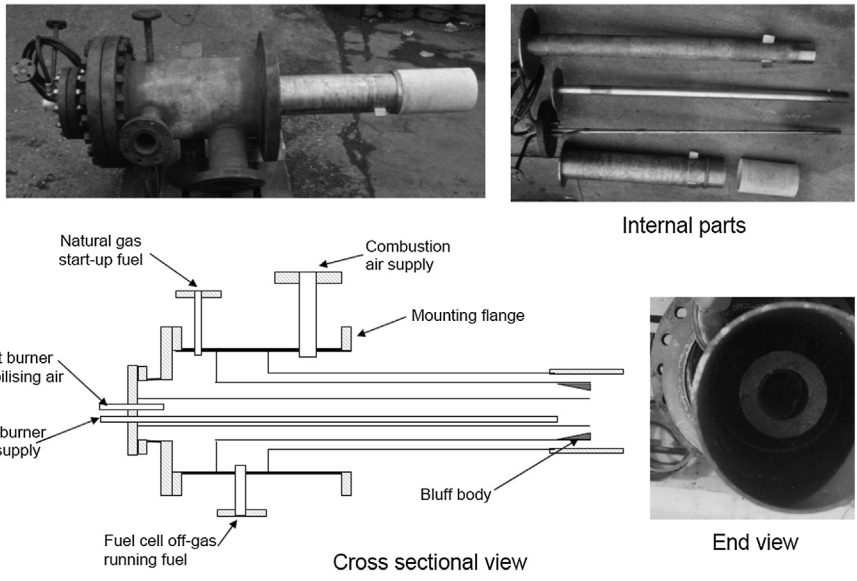


Figure 14.16 Multi-fuel burner for convective heat exchange reformer

The natural gas start-up fuel was supplied through an annular nozzle surrounding the pilot. A bluff body was fitted to the end of the natural gas supply tube to allow the nozzle area to be set to provide an appropriate natural gas jet velocity.

The lean fuel cell off-gas was supplied through an annular channel surrounding the start up fuel nozzle. The internal diameter of this channel was sized to provide an appropriate lean gas jet velocity.

The original design featured a silicon carbide refractory nozzle surrounding the pilot flame stabilisation zone and separating the fuel supply from the combustion air supply but this nozzle proved to be vulnerable to thermal shock, so was later replaced by an Inconel sleeve. Finally, the combustion air was supplied via the outer annulus.

14.3.3 Physical and Mathematical Modelling

Since we had chosen a simple jet entrainment burner for this application the momentum ratios controlled the fuel/air mixing rates. Therefore the critical combustion process design parameter was the velocity of the combustion air together with the velocity of each of the fuel jets. The combustion air velocity was set by the reformer design, specifically the internal diameter of the furnace tube and the operating temperature and pressure and therefore beyond our control.

Modelling was utilised to determine the momentum and hence velocity of each of the fuel jets needed to achieve suitable mixing rates over the wide range of operating conditions. Both physical and mathematical modelling techniques were used and the methodology adopted is described in detail below.

Preliminary Mathematical Modelling

As previously mentioned, to achieve the long flame with the flat heat flux profile required a low fuel jet momentum. Initially the long furnace mathematical model was used to estimate the jet momentum required to achieve this slow mixing under the principle operating conditions of natural gas start up, reformer product (H_2/CO_2) and fuel cell off-gas. This required several runs of the model; each run took all night owing to the limited computing power of the "state of the art" Apple IIe computers in use in 1985.

Although, where appropriate, the long furnace model input data represented the operating conditions at pressure, the lack of kinetic data for reactions at pressure meant that the results were approximate with unknown errors. However, in the opinion of the authors, the work was still worthwhile because it was anticipated that errors introduced by the high pressure would be second order effects and therefore could be neglected at this preliminary stage.

From the mathematical modelling, approximate injection velocities were determined for the natural gas start up fuel and the lean anode off-gas used for normal running. The combustion air injection velocity was set by the diameter of the combustion chamber tube in the reformer, although the option existed to increase combustion injection velocity by inserting a restriction in the burner air outlet, if required.

Physical Modelling

The nozzle sizes determined by the mathematical modelling were for the full size burner. The small-scale physical model was designed based on the full-size injection velocities and nozzle areas. The model set-up was designed to use a standard Perspex acrylic plastic tube, see Figure 14.17. The two gas nozzles were then sized using the Craya-Curtet similarity parameter to maintain dynamic similarity between the full size burner and the scale model, ensuring that the model mixing is representative of the full size burner system. The Craya-Curtet parameter was used in preference to the any other similarity parameters because it is more suitable for closely confined systems.

The flows of acid and alkali were chosen as described in Chapter 6, section 6.1.6. Firstly, the volumetric flow of acid (combustion air) was decided based on a Reynolds Number to maintain turbulent flow. Next the volume flow of each alkali stream (fuel) was decided based

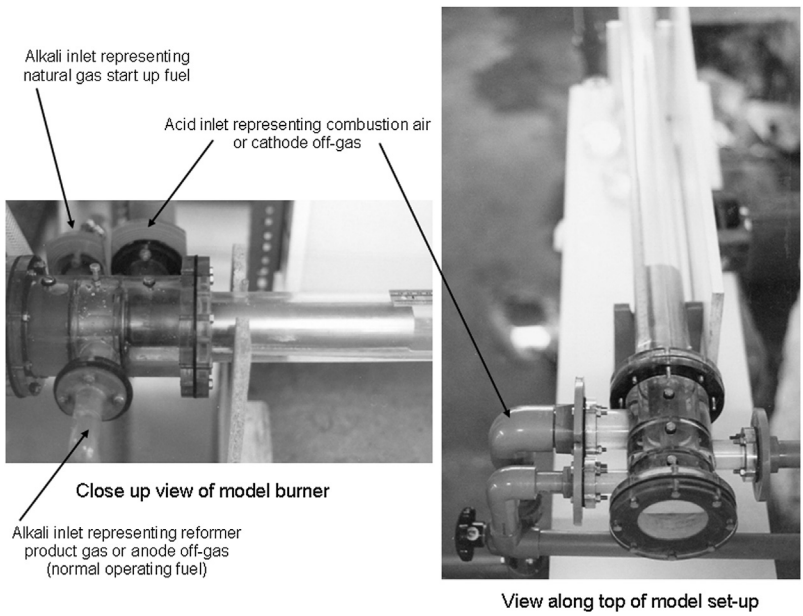


Figure 14.17 The acid alkali model set up

on a similar volumetric ratio as for the full size under the relevant pressure. Finally, the concentrations of the acid and alkali were chosen to maintain stoichiometric similarity. This is described in more detail in the following paragraph.

The complexity of the fuel cell operation required a large number of model runs to ensure that each operating condition was assessed. Typically, combustion air is represented by dilute hydrochloric acid with a concentration of 0.1N. To maintain a similar stoichiometric ratio, natural gas is represented by dilute caustic soda with a concentration in the range of 0.8–1N. For example, to represent a gas with a stoichiometric air requirement of 9.4 Nm^3 of air per 1 Nm^3 of gas an alkali concentration of 0.94N would be used. For pure hydrogen with a stoichiometric air requirement of 2.38 Nm^3 of air per 1 Nm^3 of hydrogen a concentration caustic soda concentration of 0.238N with 0.1N acid. Both the acid and alkali concentrations had to be adjusted to represent the range of conditions that the full size burner were expected to operate over, see Table 14.2.

For each of the above fuels the model was run to simulate the entire operating range from maximum fuel rate to minimum turndown with a range of flows to simulate different excess oxygen levels. Each condition was photographed and recorded. Two typical photographs are shown in Figure 14.18. The dark area is pink in the original and caused by phenolphthalein pH indicator demonstrating that this area is alkaline, representing unburnt fuel, see chapter 6, section 6.1.

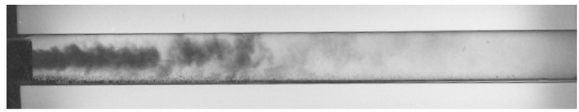
For each model run the length of the simulated flame was measured and recorded. This length then had to be corrected for the density because the heat release in the flame causes an expansion of the gas, lowering its density and reducing the primary jet's entrainment rate, thus lengthening the flame. The correction applied is described in Chapter 6, section 6.1.8. The temperature used to calculate the density, was determined as part of the initial mathematical modelling described earlier. Finally, the predicted flame length was plotted against the excess air for each of the anticipated operating conditions, Figure 14.19.

The flame length was optimised by trial and error. A simulated flame longer than desired indicated that the mixing was too slow. To improve the mixing the velocity of the alkali jet (representing the fuel) needed to be increased, so a new nozzle with reduced flow area was fitted to the model, thus increasing the entrainment capability. Too short a flame required a reduced mixing rate and hence a larger nozzle with reduced jet velocity and entrainment capability. This process was continued until both the normal running condition, burning anode off-gas and the start up with natural gas had been optimised.

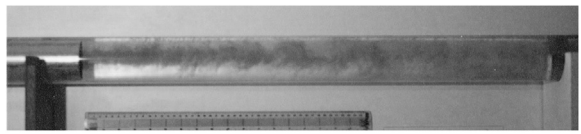
The flame length produced when firing reformer gas could not be optimised because it was fired through the same nozzle as the anode off-gas. In any case, optimisation would serve little purpose given

Table 14.2 Acid and Alkali Concentrations used to Represent the Different Fuels

Reformer Operation	*Fuel*		*Oxidant*	*Oxidant/Fuel Requirement*	*Model Fluid Concentrations*	
	Source	**Composition**		**(vol/vol)**	**Alkali (fuel)**	**Acid (oxidant)**
Start-up	Natural gas	CH_4 – 96% C_xH_y – 4%	Air	9.6	0.96N	0.1N
Reformer operating, fuel cell shut down	Reformer gas	H_2 – 72% CH_4 – 2.4% CO_2 – 21.6% H_2O – 4%	Air	1.94	0.194N	0.1N
Fuel cell generating electricity	Anode off-gas	H_2 – 34% CH_4 – 5.7% CO_2 – 50.9% H_2O – 9.4%	Cathode off-gas (10.4% O_2)	2.73	0.135N	0.049N



Typical simulated flame based on start up conditions



Typical simulated flame based on running conditions with depleted hydrogen fuel cell anode off-gas fuel and oxygen depleted air from cathode

Figure 14.18 Typical flames simulated using acid alkali modelling

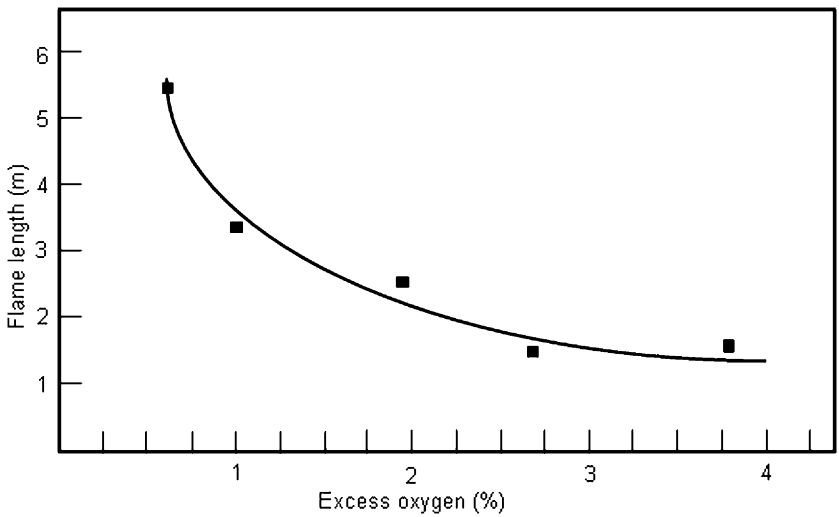


Figure 14.19 Typical plot of flame length versus excess oxygen predicted by acid alkali modelling

that the changeover time was relatively short. The modelling of the operation with this fuel was therefore limited to ensuring that the flame length and heat release rates were acceptable, that is they would not cause any operational difficulties or damage to the reformer.

Heat Flux Modelling

Following optimisation of the combustion conditions using acid alkali modelling, the long furnace model was used again, this time to predict the heat transfer to the furnace walls. These results were used as input to Haldor Topsoe's own reactor side annular reformer model to

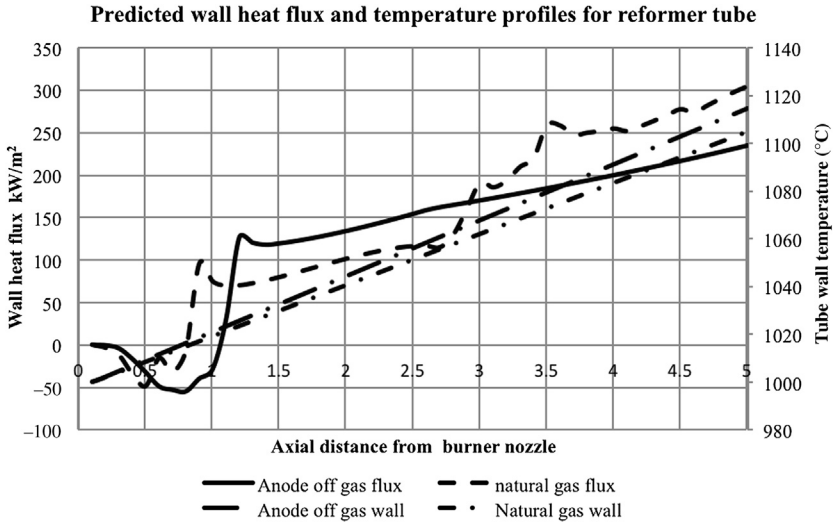


Figure 14.20 Predicted heat flux profile for normal operation with anode off-gas

confirm that the burner performance would match the enthalpy requirements of the reforming process. A typical plot of the predicted heat flux profile is shown in Figure 14.20.

14.3.4 Full Size Testing

The mechanical drawings for the burner shown in Figure 14.16, especially the gas nozzle details, were finalised based on the results from the modelling described above. Following completion of the detail design, the burner was manufactured to API Standards in Galveston, Texas by a company experienced in fabrication for the local refinery industry.

To reduce the risk of the burner not performing in the prototype reformer, the burner was subjected to full scale testing on Haldor Topsoe's test facility in Houston. The testing confirmed the predicted flame characteristics on all proposed fuels and operating conditions but revealed two mechanical problems; the silicon carbide refractory nozzle failed by cracking early in the testing program and leakage occurred between the hydrogen fuel chamber and the combustion air chamber. While both these failures introduced reliability issues, the latter was particularly worrying since it allowed the uncontrolled mixing of hydrogen and combustion air and thus introduced potential safety issues. Fortunately the problem was discovered before any incident occurred and the burner was returned to the fabricator to rectify the seal-weld between the air and fuel chambers.

Silicon carbide had also been chosen for the furnace tube for the reformer that surrounded the flame. This tube also failed within the early testing period. Although silicon carbide had been chosen after careful consideration of its properties and extensive discussions with the manufacturer, it was clearly unsuitable for the proposed application. The cause of the failure was considered to be differential thermal expansion with the inner side of the tube heating more rapidly than the outside, creating excessive tensile stress in the outer skin, often known as thermal shock, Figure 14.21. Since silicon carbide can be made in thinner sections and had a higher thermal conductivity than most other refractories, it was unlikely that any other ceramic material would be more successful.

Fortunately, with the maximum flame temperatures predicted by modelling in the range of 1100–1200°C, it was considered than a high nickel alloy such as Inconel 601 would be suitable for this duty. Both the burner sleeve and the furnace tube were manufactured in Inconel 601 and these new parts proved totally satisfactory.

Over the years, a number of burners were supplied to Haldor Topsoe for heat exchange reformers to provide hydrogen for fuel cells, including one small burner that was especially challenging. This burner was required to start-up on kerosene before changing over to hydrogen as the intermediate fuel and then to anode off-gas once the fuel cell was generating. This had to be undertaken automatically because the plant was intended to operate with remote supervision.

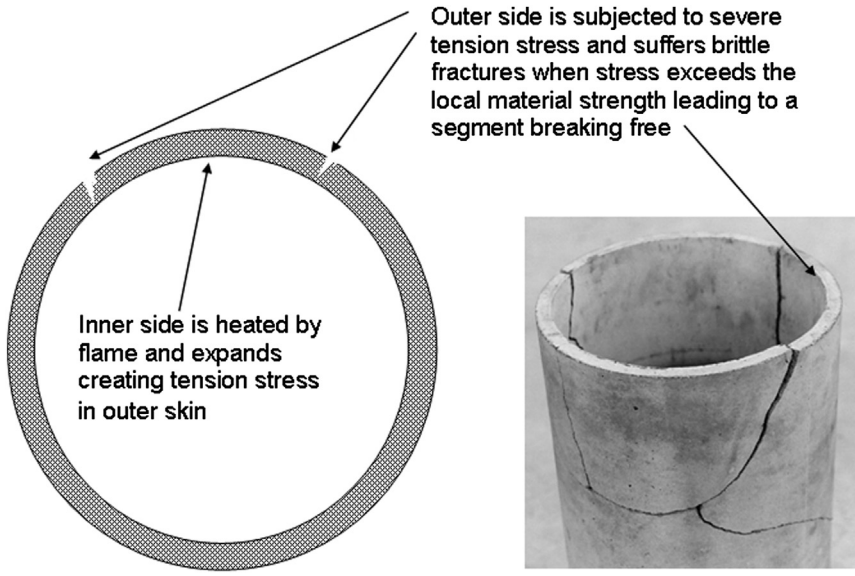


Figure 14.21 Likely failure mechanism of silicon carbide burner nozzle

An additional design challenge was the need for the burner and all the operating mechanisms to be accommodated within a low headroom.

To light the start-up flame a high-energy (HE) igniter was used which is capable of lighting an oil flame without the need for a gas pilot burner thus dispensing with that complication. However, the HE igniter must be removed from the flame following successful ignition. This necessitated a retraction mechanism using a pneumatic cylinder, which, owing to the limited headroom, had to be mounted horizontally and transmit its motion to the igniter via a slotted quadrant that can be seen in Figure 14.22.

It was decided to undertake a full-scale test at our High Wycombe premises because it was particularly challenging to achieve suitable flame characteristic and heat transfer patterns for this application owing to the large difference in emissivity between kerosene and hydrogen. Furthermore, the results from previous testing could not be used to validate the modelling. To undertake this test temporary test facility was constructed in the yard. An overview of the system is shown in Figure 14.22.

The burner had a central kerosene sprayer using pressure atomisation and was surrounded by an annular gas gun, which fired both the anode off-gas fuel and the intermediate hydrogen. Primary and secondary air was split within the windbox and the former swirled to provide flame stabilisation, particularly for the start up flame. A flame detection system was also installed on the burner.

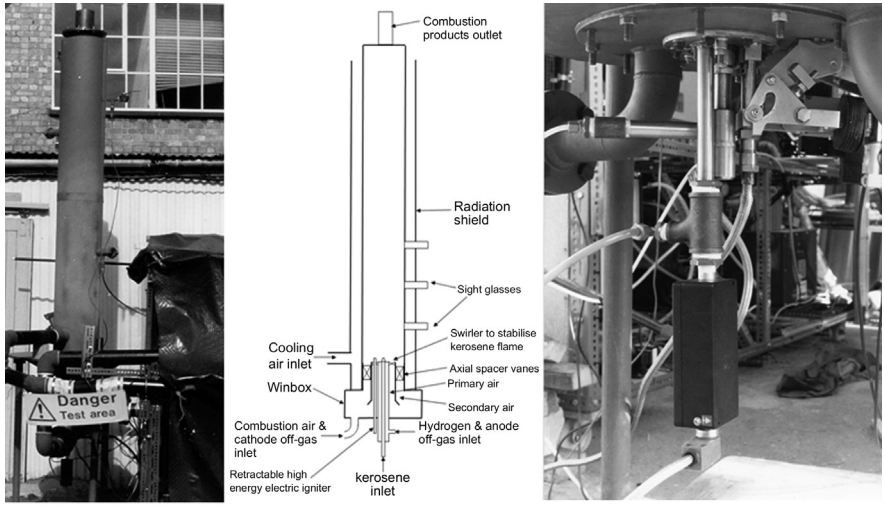


Figure 14.22 The temporary test facility for the tri-fuel burner

Kerosene was supplied from a small tank via a high-pressure pump. Hydrogen was supplied from manifolded packs of cylinders. To represent the anode off-gas, hydrogen was mixed with carbon dioxide via a mixing station. The CO_2 was stored as liquid under pressure in an insulated cylinder and evaporated by an electrically power vaporizer. All flows were measured to ensure representative gas was supplied to the burner.

Cathode off-gas was simulated by adding additional nitrogen to normal air in a mixing station then adding steam generated by an electrode steam boiler. Again all flows were measured to ensure representative oxygen deficient and humidified air was supplied to the burner.

The testing proved the both the mechanical and process aspects of the design. Following analysis of the results and a witness test for the client, the test work was documented, the rig was disassembled and the burner packed and shipped to the customer.

14.3.5 Concluding Remarks

While superficially, fuel cells offer the possibility of power generation with no moving parts, this advantage only applies to the fuel cell itself and not the complete system. In the case of the PAFC, when combined with its hydrogen supply reformer, the overall system becomes complex with several reactor vessels in addition to the reformer, many heat exchangers an air compressor and a turbo-expander, Figure 14.23.

Given that such a complex system only offers a very small gain in efficiency compared with a modern high temperature combined cycle

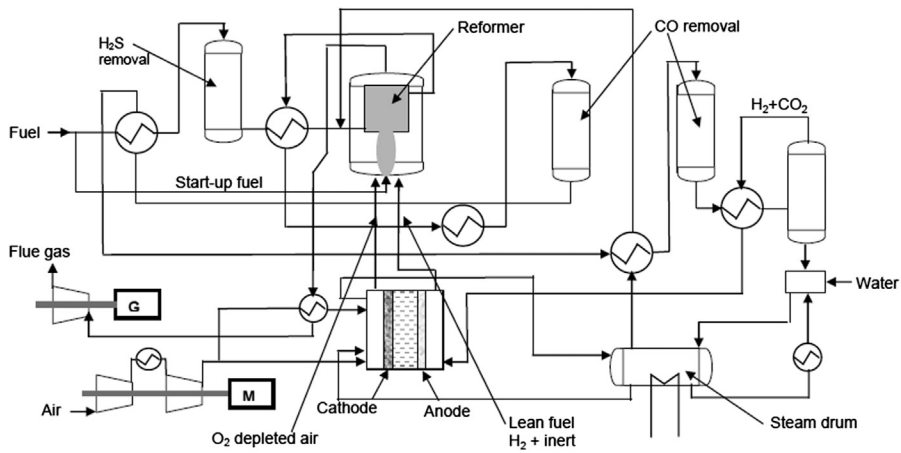


Figure 14.23 Simplified process flow diagram for a typical fuel cell stationary PAFC system (Note some heat exchangers and recycle lines omitted for clarity)

power generation system, the authors consider that it is unlikely that fuel cells will make a significant contribution to stationary base load power generation in the near future. Furthermore, combined cycle systems are inherently simple and are well established in the market, being commercially available at relatively low cost in a wide range of sizes from a few MW to several hundred MW.

Haldor Topsoe have continued to offer their heat exchange reformer for hydrogen production but current models use an external combustion chamber which relieves the burner designers of some of the constraints that we faced but requires a larger plot size.

14.4 Resolving Tube Internal Coking and Premature Tube Failure in a Refinery Heater

Direct-fired heaters are used in the refining and refinery industries for heating many hydrocarbon liquids from naphtha to heavy residual oils, see Figures 1.24 and 1.25. Normally these heaters are very reliable but occasionally problems arise with premature tube failure, which incurs an economic cost, but more seriously, presents a serious safety hazard owing to the risk of the leaking hydrocarbon fluid igniting. Some aspects of this example have been provided in earlier chapters but the following is a detailed description of the problem, its diagnosis and how it was resolved.

In mid 1986 we were asked to attend a meeting at an oil refinery in northeast England to discuss tube failure in a cabin heater. The unit was installed on a delayed coker and its duty was to heat residual oil from the vacuum distillation unit to approximately 480°C under pressure prior to feeding to the coke drum where most of the volatiles were driven off. The heater was very long, relative to its width and had a single 100 mm ID coil on each longitudinal sidewall. A sketch of the heater is shown in Figure 14.24.

The residual oil inlet was at the base of the coil with the heated oil leaving at the top, to minimise the risk of vapour locking, should evaporation occur. The pressure and temperature at the inlet and outlet of the coil were both monitored and relayed to the control room operator. The end walls were refractory lined and a single line of 18 forced draft burners firing upwards were mounted in the refractory lined hearth. The fuel was refinery gas, which is recovered from various units in the refinery and hence has variable fuel composition. It also has a low emissivity owing to its high hydrogen content. The combustion air was preheated to approximately 200°C.

At the meeting, the refinery engineers raised a number of operational issues, which they considered were caused by flame impingement. These included, high rates of coke formation within the tubes,

restricted production and most worryingly, high tube metal skin temperatures that occasionally resulted in localised bulging.

The coke formation was detected by excessive pressure loss across the coil. This requiring regular shutting down of the unit to steam out the coke while the tube bulging required a longer shutdown for tube replacement. During steaming the coke was removed via the following reactions:

$$C + H_2O \leftrightharpoons CO + H_2$$
$$C + 2H_2O \leftrightharpoons CO_2 + 2H_2$$
$$C + CO_2 \leftrightharpoons 2CO$$

The heater was equipped with four sight-ports, which gave a good view of the inside of the furnace. Although visual inspection of flames does not always reveal very much, in this case it was easy to see that the flames, particularly those close to the end viewing ports, were very short and wide, the length being approximately one third of the furnace height. If their heat flux pattern was typical for a gas flame, this implied a very high heat flux to the tubes at the end of the flame, as shown previously in Figure 3.4. Given that this was also the area in which the coking occurred, there was clearly a strong possibility that the operational problems were caused by the flame characteristics.

We suggested that heat transfer modelling be utilised to investigate the current operation and to determine a suitable solution. The refinery engineers accepted that suggestion and the rest of the day was

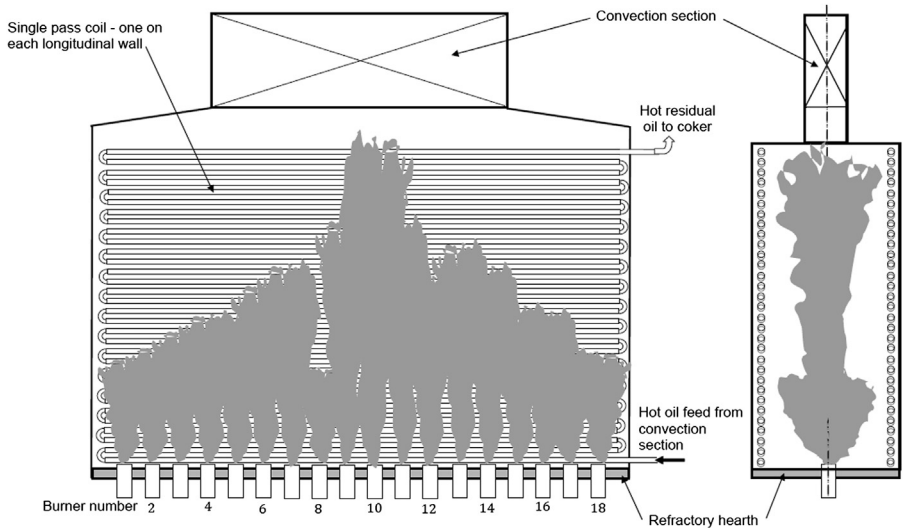


Figure 14.24 Residual oil cabin heater supplying delayed coker plant (Note: windbox omitted for clarity)

spent collecting operational data, such as gas calorific value and flowrate, combustion airflow and temperature, together with excess oxygen and CO at the top of the furnace. The latter was particularly revealing because the excess oxygen level fluctuated between 4 and 5%, indicating that the furnace was operating with high to very high levels of excess air but was also accompanied by high CO readings in the range of 0.5–1%. At these levels of excess air the CO would be expected to fluctuate between 20–100 ppm at the most. High CO with high excess air suggests very poor fuel/air mixing, or, in a multiburner furnace, poor combustion air distribution, the latter leading to at least one of the burners operating with insufficient combustion air.

During the initial visual inspection of the flames, most attention was paid to the burners close to the inspection ports near each end of the furnace because these were the easiest to see. Following the gas analysis, a further inspection of the flames was undertaken and it was noticed that the flames in the middle of the furnace were longer and more luminous than the flames close to the viewing ports but with an extremely short flame close to the windbox air inlet adjacent to burner number 8. This suggested that the middle burners, except number 8, were operating with less air than the end burners. We therefore concluded that combustion air distribution was contributing to the problem.

Following the data collection and the second inspection of the flames, we suggested that the scope of work be expanded to include physical modelling of the air ducting. The refinery engineers agreed with this extension of the work and we provided a costed proposal within a few days and were promptly given the order to proceed.

14.4.1 Diagnostic Modelling

The first step was to use modelling to either confirm or refute our suspicions and to determine the full extent of the combustion problem. To do this both physical and mathematical modelling were utilised.

Firstly, an acrylic plastic scale model of the windbox and combustion air ducting was designed and manufactured. Since the combustion air ducting has a major influence on the air distribution this was modelled in its entirety from the fan inlet to the windbox. Manufacture and erection of a complex model such as this takes several weeks, so in the meantime mathematical modelling of the heat transfer was undertaken using the data collected during the site visit.

Mathematical Modelling

Full mathematical modelling of an 18-burner furnace is complex and well beyond the computing capability of the Apple IIe computers in

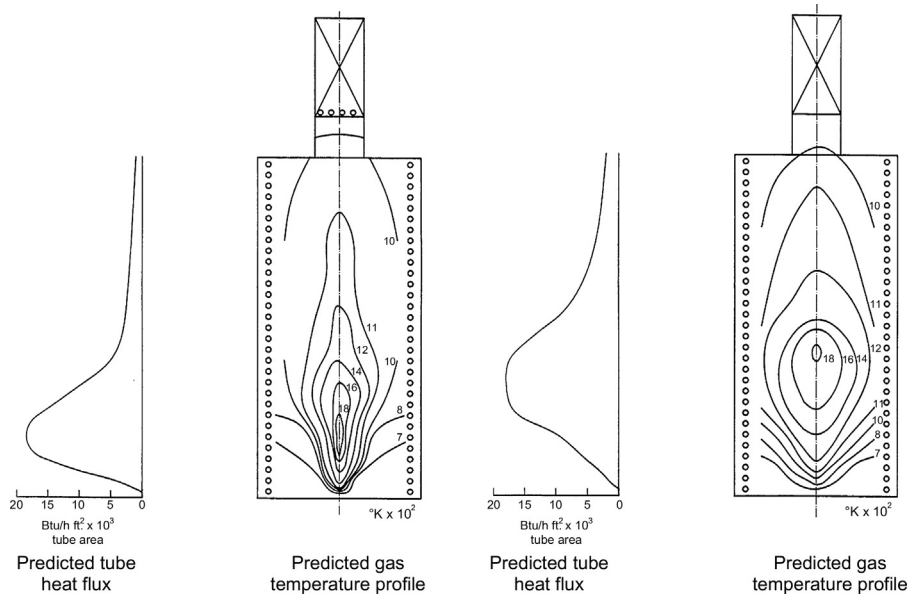


Figure 14.25 Predicted heat flux profiles for current operation (left) and for proposed low excess air operation (right)

use at the time. So a "slice model" of the heater through the cross section of one-flame was developed based on the long furnace model described in Chapter 6, section 6.2.2.

This model was run with the high levels of excess air measured during the site visit and successfully simulated the short flames and revealed that the peak heat flux was at approximately one third of the furnace height and nearly 3 times the average heat flux, thus confirming the thoughts of the refinery engineers, Figure 14.25 left.

Further runs of the mathematical model, with lower levels of excess air, and hence longer flames, resulted in slower mixing and slower combustion, therefore extending the heat release over a longer distance. This reduced the peak heat flux by 12%, moved it further up the furnace and spread it over more tubes, Figure 14.25 right.

At the same time the average heat flux was increased from 7,000 Btu/h.ft^2 (22.1 kW/m^2) to 10,000 Btu/h.ft^2 (31.6 kW/m^2). The overall increase in heat transfer resulted from eliminating the cooling effect of the high excess air that was currently required. See Figure 5.13 for the effect of excess air on flame temperature. However, operation at low excess air was not achievable with the current air distribution or burner design, so the air distribution needed to be resolved using physical modelling to produce a workable solution to the problem.

Physical Modelling

Once assembly and erection of the clear acrylic plastic scale model of the windbox and combustion air ducting in our laboratory was complete, it was operated on air with the lid removed so that the flow through each burner could be measured using a miniature pilot tube and an electronic micro-manometer, Figure 14.26.

This was a time consuming business since each burner had to be traversed and the velocity readings summed across the burner flow area and converted to flow. This was done for each burner in turn and the total flow through all the burners summed and compared with the inlet flow, which was measured by a calibrated rotameter. This was required to check for errors. This model test revealed an appalling air distribution, Figure 14.27.

The problem largely arose because the heater had been built as a natural draft unit for another role and had been converted to forced draft within a very restricted plot. As a consequence, the combustion air ducting followed a convoluted route and entered the windbox adjacent to burner No. 8, rather than in the middle adjacent to burners 9 and 10. Furthermore the windbox was very narrow with extra depth to provide acceptable air velocities. However, the unintended result was that, apart from burner 8, the air by-passed the centre burners and was preferentially supplied to the burners at either end of the firebox, resulting in flame shapes something like those shown in Figure 14.24. The model test results were therefore consistent with the observed flames.

The lid was then fitted to the model and the return flow piped up so that the model could be run on water. The water was dosed with

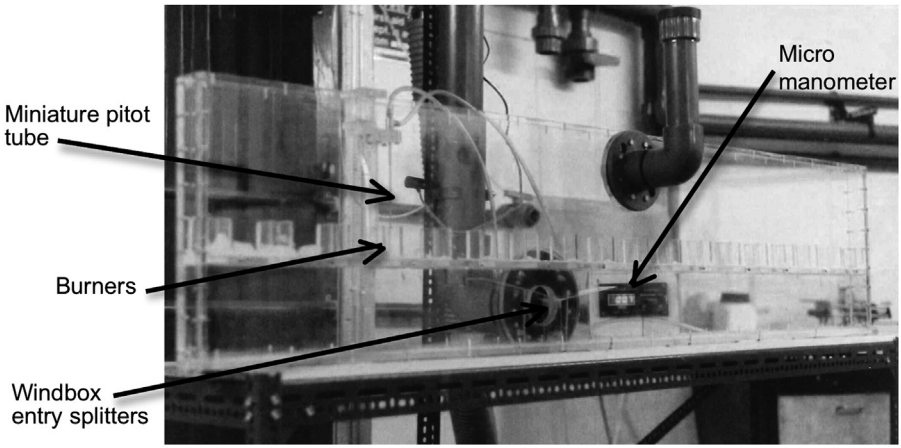


Figure 14.26 The physical model set up for airflow measurement following the installation of windbox entry splitters (photo provided courtesy of KFS)

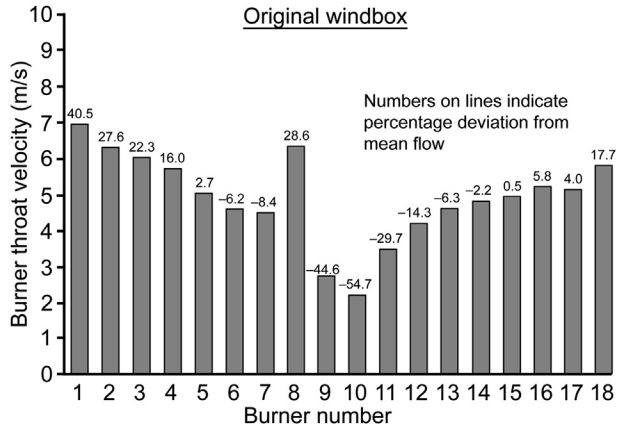


Figure 14.27 Existing air distribution determined using physical modelling

unexpanded polystyrene beads that are a similar density to water and follow the water streamlines, thus allowing visual observation and photographing of the flow patterns. This was done to determine the features in the air ducting and windbox that caused the poor distribution.

14.4.2 Correcting the Poor Air Distribution

Once the existing flow patterns are known, then turning and straightening vanes are installed in the air ducting to correct areas of poor flow and provide a uniform air velocity at the windbox inlet. Once the flow distribution in the air ducting is satisfactory then the major regions of poor flow within the windbox are tackled, again by installing thin acrylic baffles and turning vanes, as appropriate. Once this initial poor flow in the windbox had been corrected so that it appeared visually satisfactory, then the secondary regions of poor flow were tackled. Finally the regions of minor maldistribution were tackled. The process was iterative and took several attempts over 3–4 weeks of continuous work to achieve a satisfactory flow pattern.

The model was then drained and run on air and the flows through the burners once again measured as described previously. Although greatly improved, the flow distribution was still not sufficiently similar through each burner for the low excess air operation required to produce the heat flux pattern shown in Figure 14.25 right, so further minor adjustments were made to the baffles and the flows remeasured. Several more iterations were made until the airflow through each burner was acceptable, Figure 14.28.

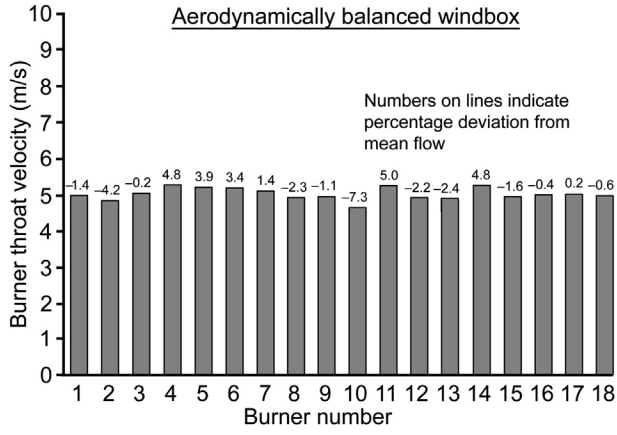


Figure 14.28 The improved air distribution achieved by physical modelling

The improved flows were much more even, but with ±5% as a normal target, this combustion air distribution would still be considered poor for low excess air operation. However, with the lowest flow being 7.3% below the average and the highest flow 5% above the average, the air distribution was greatly improved, especially given the starting variation of +40.5%/−54.7% from the mean. Although not ideal, this improved air distribution was expected to be satisfactory for the current purposes. Furthermore, it was anticipated that further investment in modelling time was not likely to yield a significant improvement in flow distribution, especially given the complexity of the baffles needed to achieve this improvement.

Detailed fabrication drawings of each baffle and turning vane were prepared for manufacture together with a dimensioned installation drawing with details of the fixing mechanisms and temporary jigs required. Detailed installation instructions were also prepared, the latter being particularly important owing to the need for accurate placement and the confined working conditions within the windbox.

In addition to modelling the windbox, a larger scale model of an individual burner was manufactured and tested in the same way as the windbox. This was undertaken because it was suspected that the right angle air entry and adjustable damper would have a detrimental effect on the air distribution in the burner throat. In the event, it was found that there was far more air on the inlet side of the burner than on the far side with over 70% of the combustion air in a quadrant vertically above the air inlet. Further modelling demonstrated that the airflow could be greatly improved by locking the hand damper fully open and installing bluff bodies as shown in Figure 14.30. These serve to create a wake in each of their paths, thus reducing areas of high velocity that caused the maldistribution of the air.

14.4.3 Burner Modifications

The design of modifications to the burners was undertaken while the modelling was progressing. The existing burners were equipped with swirl gas nozzles, Figure 14.29. These nozzles produced a self-stabilised flame with an included angle at the root of 90°, hence the short flames with the intense heat release that were observed with the end burners.

The manufacturer had provided the hand damper to balance the airflows between individual burners. From the existing operation of the heater it is clear that this was not achievable. Indeed in the authors' experience, such dampers are virtually useless because when the damper on one burner is adjusted, it affects the airflow to all the remaining burners. While, with significant perseverance, it may be possible to balance 3 or 4 burners this way, no one has the stamina to tackle a furnace with 18 burners. The time required to balance the flows between many burners would be months and cost of that time would be prohibitive and even then, the target is unlikely to be achieved. Furthermore, as mentioned previously, when partially closed the hand damper has a detrimental effect on the combustion air distribution within the burner, owing to the manner in which it biases the flow in the inlet duct.

To achieve the heat release pattern shown in Figure 14.25 right, required slow fuel/air mixing to produce long flames that were

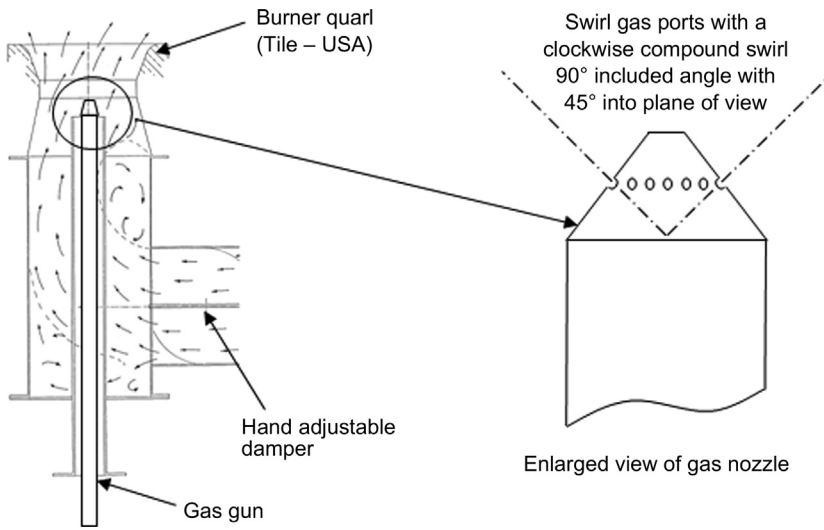


Figure 14.29 Schematic of the existing swirl burners (diagram of airflow pattern provided courtesy of KFS)

approximately 60% of the furnace height. For this a new gas nozzle with a significant proportion of forward facing gas was required, similar to that used in rotary kilns. While the flame might have remained stable, given the high hydrogen content of refinery gas, we considered that a swirler was advisable to ensure flame stability under all conditions. In addition, two bluff bodies were found to be required by the physical modelling described previously, to correct the air distribution within the burner. The overall arrangement is shown in Figure 14.30.

As for the windbox, detailed fabrication drawings were prepared for the manufacture of the burner modification kits, together with a dimensioned installation drawing, temporary jigs and detailed installation instructions.

Finally, all the parts were manufactured and installed under our engineer's supervision during a special shutdown. Once complete the heater was re-commissioned. The coking was reduced to a normal level owing to the elimination of the excessive peak heat fluxes. Surveys of the tube surface temperatures, using a hand held remote infrared thermometer, showed even temperatures with no hot spots. In addition, the furnace operators found that they could now operate steadily with a flue gas oxygen value of 1–2%. The predicted improvement in the overall heat transfer of 31.6 kW/m^2 compared with the previous 22.1 kW/m^2 meant that more of the firebox heat was transferred to the oil and, as a result, the heater provided 5–10% more output than its previous best, eliminating a process bottleneck.

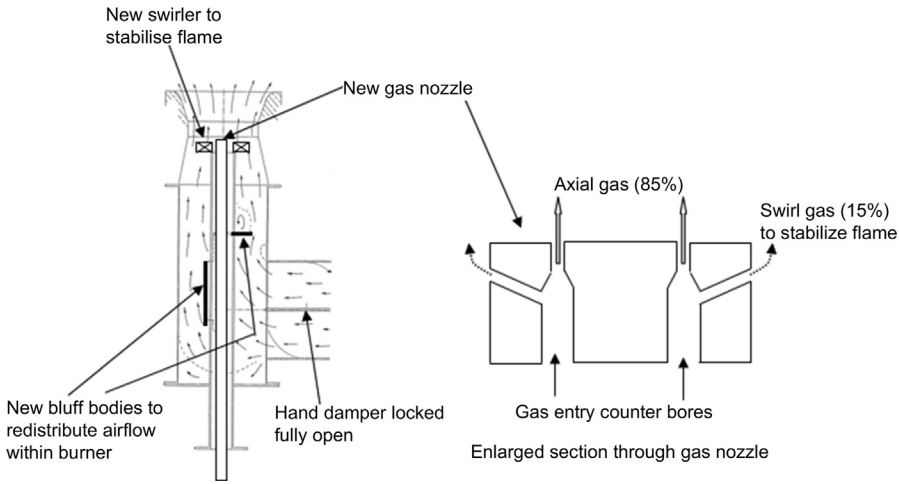


Figure 14.30 Schematic of the modified burners (diagram of airflow pattern provided courtesy of KFS)

14.5 Unsuccessful Attempts to Resolve Severe Problems with a Preheater Cement Kiln

Not all problems we tackled had straightforward solutions and while the problem could invariably be identified, it could not always be resolved. While this was a rare occurrence, we experienced a couple of these examples; both were relatively large cement kilns designed and built in the 1970s. The following example describes the background to one of these examples, the diagnosis of the problem and the reasons that a practical solution was not available.

During the late 1960s and early 1970s the world cement industry was experiencing a considerable increase in demand for its product and many new kilns were ordered and built. These kilns were much larger than their predecessors and usually oil fired because that was the lowest cost fuel at the time. Where natural gas was available, this was used because, in general, it was even cheaper than oil.

October 1973 also saw a major increase in the cost of oil and other fuels as a result of restrictions of the supply of crude oil by many Middle Eastern countries. As a consequence the installation of wet process kilns virtually stopped overnight. Indeed at least one proposed wet kiln was not erected as originally intended and the project was delayed with the kiln being modified for the semi-wet process. Many of the kilns designed for oil and gas firing were converted to burn coal. Often this conversion was rushed and shoddily done owing to the economic urgency of converting to coal firing and the lack of current experience of coal handling and firing within the industry's suppliers.

In early 1987 we were asked to visit a cement plant in the Pacific North West of North America. The plant was a large dry process, gas fired preheater kiln rated at 3200 tonnes/day of clinker. It had been converted to burn pulverised coal and oil in addition to gas and was fitted with a tri-fuel burner.

The plant management experienced a number of operation problems with the kiln, including unstable operation, reduced output compared with its rated capacity, and the kiln never achieved more than 2,500 to 2,600 tonne/day. Excessive build-ups near the kiln inlet and in the lower cyclones and ducts of the preheater tower contributed to this production shortfall. Before describing the diagnosis of the problem, a brief description of the cement manufacturing process is provided for readers not familiar with the industry.

14.5.1 Cement Manufacture by the Dry Process

Portland cement is a calcium alumina silicate compound and is manufactured from limestone and clay (or shale) with minor amounts of

Table 14.3 Typical Cement Kiln Raw Mix Feed (Alsop 2001)

Mineral	*Contribution to Product*	*Proportion in Mix*
Limestone	CaO	85%
Clay or shale	SiO_2, Al_2O_3 & Fe_2O_3	13%
Additives	SiO_2, Al_2O_3 or Fe_2O_3	<1% each

iron oxide, silica sand and alumina as additives where required to balance the mineral composition. A typical raw mix is shown in Table 14.3.

For high cement strength and good durability these components must be precisely proportioned, ideally to a tolerance of less than ±0.1%, so raw material preparation is a critical part of the process, but often not done well. A simplified process flow diagram is shown in Figure 14.31. Firstly, the raw materials are pre-blended in two stockpiles to provide a consistent feed of limestone and shale. Measured quantities of each raw material is drawn from the stockpile and fed to the raw mill where they are ground and dried together to produce a fine power, known as raw meal which is collected in the electrostatic precipitator (ESP). If additives are required they are added to the raw materials at the mill inlet and inter-ground with the raw materials. Consistency of kiln feed is critically important for stable operation so in most cases, the raw meal is further mixed in large blending silos to provide a consistent blend.

Kiln feed is drawn from the blending silos at a measured rate and fed to the top of the preheater tower and, as it progresses down the tower, it is preheated counter-currently by the upward flowing kiln

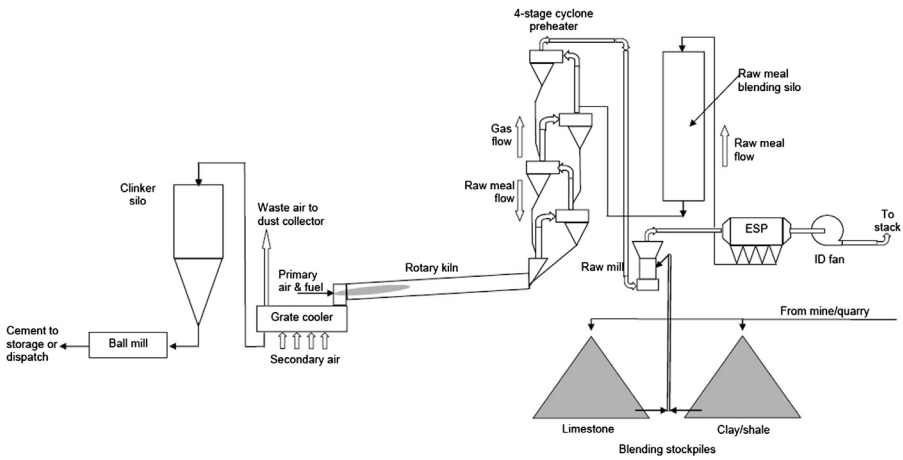


Figure 14.31 Simplified process flow diagram for dry process cement manufacture

exit gases. In the lower cyclones, some calcination may occur if the feed temperatures are sufficiently high. Calcination is the major heat consuming process and occurs at the back of the kiln. Following calcination, the minerals combine and sinter to form cement clinker. This is a crystalline product bound together with a small proportion of glass phase. The clinkering reaction is slightly exothermic so does not consume heat but needs a sufficiently high temperature to trigger the reaction; the clinker is then cooled by preheating the secondary air in the cooler at the kiln discharge. Finally, the clinker is ground with a small quantity of gypsum to produce the familiar grey powder that is Portland cement. The gypsum acts to delay setting and make the concrete and mortar mixes more workable. These days other additives are also used but this was not the case in the late 1980s.

Important Considerations in Kiln Operation

Cement strength and the rate at which the strength develops are the principle performance criteria of interest to the large-scale user. To achieve high early strength small crystals with sharp well-defined boundaries are required. These are achieved by rapid heating of the calcined material to sintering temperature followed by a rapid quench once sintering has occurred. To achieve the rapid heating requires a flame with a high heat flux close to the burner nozzle. If the heat release is further along the kiln then the sintering reaction takes place too early and too far from the cooler inlet. As a consequence, the clinker remains very hot for too long and the crystals grow and the boundaries become more diffuse, both of which have a detrimental effect on strength development. Where this occurs the clinker has to be ground finer, in some cases much finer, to meet the required specification. This has a significant cost both in terms of energy and reduced cement mill output.

A review of Figure 3.4 will show that natural gas has the worst heat flux profile to meet the above requirements, with high volatile coal providing the ideal early heat transfer owing to the rapid release of volatiles in the flame together with the high emissivity owing to the particulate carbon. Heavy fuel oil (No 6 oil) is somewhere in between. A survey of the cement kilns of a large multi-national producer undertaken by Moles and Jenkins in 1976 showed that this was borne out by the users' experience with oil fired kilns producing approximately 5% more output than gas fired kilns with pulverised coal fired kilns producing 5–8% more output than oil fired kilns.

It should be noted that there are additional factors at play than just the heat transfer. For example, the higher the hydrogen content of the fuel, the greater the volume of combustion products, and this in itself will restrict output for oil and gas firing, where the induced draft fan capacity is limited. For coal firing, the ash, which contains all the

cementious elements, becomes part of the product, adding further to the production. When using coal, the chemistry of the raw mix is adjusted to compensate for both the ash composition and quantity.

14.5.2 Diagnosis of the Problem

As mentioned previously, the plant was a large dry process gas fired preheater kiln rated at 3200 tonnes/day of clinker. It was equipped with a four-stage cyclone preheater as in Figure 14.31 but with satellite coolers instead of a grate cooler. It was one of a number of kilns with this configuration built during the early 1970s. Satellite coolers had been in use for many years, first appearing during the early part of the 20th Century but most operational experience was with wet process kilns up to approximately 1000 tonne/day capacity, so these new kilns pushed the boundary in many ways, which are summarised in the Table 14.4.

It can been seen that the much higher mass flow rate of clinker, combined with the much higher air temperatures, placed a much more onerous duty on the satellite coolers used on the large dry process kilns compared with the previous generation of wet kilns. Additionally, only the secondary air was available for cooling the clinker, unlike the grate cooler in Figure 14.31, where there is no limit to the cooling air that can be used because the additional air can be sent to waste. This was not a problem for satellite coolers installed on wet kilns with the relatively high air/clinker ratio but became a serious problem with dry process kilns owing to the lower airflow, associated with the lower specific fuel consumption. This resulted in poor clinker cooling and excessive crystal growth in the clinker. Therefore to maximise the cooler airflow, the primary air was minimised so that a greater proportion of the combustion air was supplied as secondary air. This in turn, gave a low primary jet momentum and a higher secondary air momentum than for the wet process, creating very poor fuel/air mixing.

Furthermore, these large dry process kilns rotated at higher speeds than the previous wet kilns, typically up to 4 RPM compared with

Table 14.4 Comparison Between Existing Wet Kilns and the New Large Dry Process Kilns

Parameter	*Wet Process*	*Dry Process Preheater*
Clinker production rate	Max 1000–1500 t/day	Max 4000 t/day
Clinker flow/cooler (10 off)	4.2–6.3 tonne/h	16.7 tonne/h
Secondary air/clinker ratio	1.5:1 to 2:1	Approx. 1:1
Secondary air temperature	Typically 400–500°C	Typically 900–1000°C

approximately 1 RPM for the older kilns. This higher rotational speed, together with the larger kiln diameter, resulted in a much higher peripheral speed and much greater mechanical stresses on the cooler elbows and the cooler retaining collars. In addition, the fatigue cycle for kiln shell in the region of the coolers was 10 times kiln RPM, not kiln RPM, so a kiln rotating at 4 RPM experiences 57,600 fatigue cycles per day. As a result, serious fatigue related failures showed up quickly, sometimes in a few years and occasionally in a much shorter timeframe.

In addition to the mechanical problems, which were an availability and maintenance issue, these large dry process satellite cooler kilns suffered from serious process problems as a result of poor combustion caused by the airflow characteristics. To allow for thermal expansion and to ensure that as little clinker as possible spilled back into the kiln when the cooler was on top, the coolers were offset relative to the opening in the kiln shell, Figure 14.32. This offset opening had the effect of imparting a swirl on the secondary air as shown in the Figure.

As mentioned previously, this kiln suffered from a number of operational problems, including unstable operation, poor clinker quality, high levels of CO at the top of the preheater tower, indicating incomplete combustion, reduced output compared with its rated capacity and excessive build-up of deposits in the back of the kiln and the lower regions of the preheater tower requiring shut downs to allow their removal. An economic cost was associated with each of these symptoms providing motivation to find a solution. By the time we became

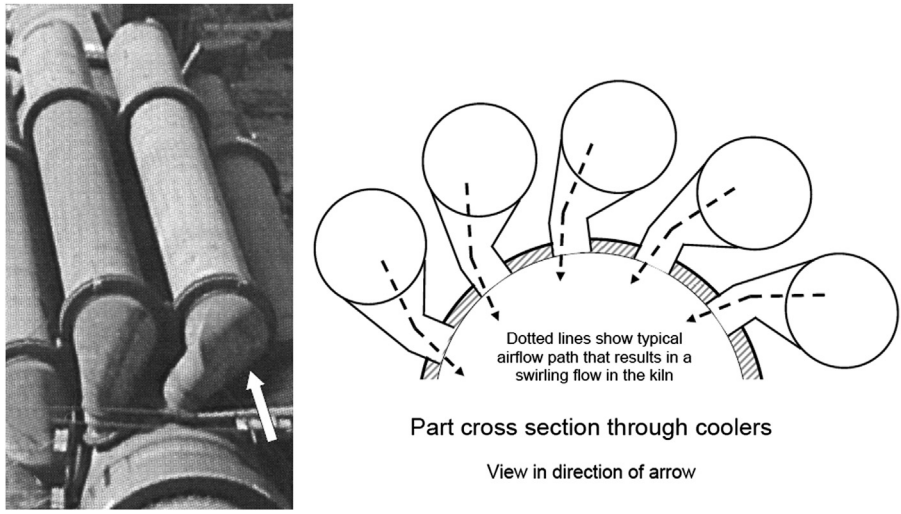


Figure 14.32 View of the cooler offset elbows showing the resulting airflow pattern

involved the problems had been evident for nearly a decade and the plant management were no nearer to finding a solution. At the time of our investigation gas was the normal fuel owing to its availability and low cost so our work was limited to gas firing.

To diagnose the problem we first visited the site to collect operational data. To model any process the input data needs to be correct. In the context of combustion modelling the flowing input data is crucial:

- Primary air mass flow and velocity
- Fuel calorific value, mass flow and velocity
- Secondary air mass flow and velocity
- Clinker temperature in the burning zone

In an industrial context, none of these, apart from fuel flow, are usually measured by plant instrumentation, so they have to be measured by temporarily installed instrumentation during a site survey as described in Chapter 9 section 9.2.1, or derived by calculation from plant instrumentation. In some instances the required information is calculated from data collected from a combination of plant and temporarily installed instrumentation. The kiln internal diameter is also required but this is normally available from the refractory installation drawing, provided that there is not an excessive thickness of coating near the burner.

In the current context, determination of the clinker burning zone temperature and secondary air mass flow and velocity were especially difficult owing to lack of access caused by the satellite coolers. Normally, the clinker temperature is measured optically at the cooler inlet using the infrared principal, shown in Figure 8.4 but in this case the distance of the cooler inlet from the viewport, together with the dust carried by the secondary air, made that very difficult and subject to error. Equally, it was not possible to measure the secondary air temperature using a temporarily installed suction pyrometer (Figures 8.2 & 9.4) because the distance of the cooler clinker inlets from the access door was much greater than the longest suction pyrometer available. Needless to say, with the induced draft satellite cooler system the secondary airflow cannot be measured.

The primary air was measured using a pitot tube and manometer in accordance with the standard procedure for this technique. Fortunately, the primary air ducting had a sufficiently long length of straight duct to allow this. The velocity could then be calculated from the volumetric flow rate and the nozzle discharge area. The temperature of the clinker discharged from the cooler was measured by collecting a sample in a bucket and inserting a thermocouple, Table 14.5 shows the data collected.

Table 14.5 Operational Data Collected from Temporary and Plant Instrumentation

Fuel flow rate (scm/hr)	12600
Fuel supply pressure (kPa)	190
Calorific value (MJ/scm)	35.17
Primary Air Rate - swirled (scm/hr)	6227
Production Rate (tonne/day)	2688
Clinker Temperature - ex coolers (°C)	120—200
Preheater oxygen concentration (dry%)	1—5
Preheater CO concentration (dry%)	0.1—0.3

Determining Secondary Airflow

Secondary air cannot be measured so had to be estimated from the flue gas oxygen concentration. Firstly, the excess air had to be determined as accurately as the system allowed. The only measurement available was the flue gas analyser at the top of the preheater tower. This provided oxygen and CO concentrations only. With cement and lime manufacture the oxygen concentration in the flue gas is lower for the same excess air than for normal combustion systems owing to the dilution effect of the CO_2 emitted from the process. Calculation of excess air is therefore more complex than described in Chapter 8, section 8.2.3 since the additional volume of the CO_2 must be allowed for. The CO is normally low (<1%) and is ignored. The procedure for calculating the secondary airflow is described below:

1. The stoichiometric airflow is calculated from the fuel flow and the fuel's stoichiometric air requirement;
2. The stoichiometric flue gas volume flow rate and analysis was determined for the fuel only case as described in Chapter 2;
3. The mass of CO_2 in the flue gas is calculated from the measurement of raw meal fed to the preheater tower using the following method based on atomic mass;

$$CaCO_3 > CaO + CO_2$$
$$100 > 56 + 44$$

   Thus 1 tonne of limestone yields 440kg of CO_2. However, a typical raw meal contains 85% limestone, so a tonne of raw meal yields 440 x 0.85 = 374 kg of CO_2. Hence the mass flow rate of CO_2 in kg/s from the charge was calculated from the raw meal feedrate;
4. The volume flow of CO_2 was calculated at the flue gas temperature (approx. 400°C) using the ideal gas laws;
5. The volume of CO_2 from the charge was added to the volume of CO_2 for the fuel only case determined in step 1 to give the overall stoichiometric flue gas composition for the kiln process;

6. The overall real flue gas composition was now calculated from the stoichiometric flue gas composition calculated in step 5, the measured oxygen concentration and the nitrogen associated with the excess oxygen;
7. The volume flow rate of oxygen was now calculated from its concentration in the known kiln flue gas composition to yield the volume flow rate of excess air. However, the preheater tower and kiln are under suction, so the excess air calculated from the measured oxygen at the top of the tower includes in-leakage air;
8. The in-leakage air was then estimated and subtracted from the volume of air calculated in step 6 to give the total air supplied to the flame;
9. Finally the primary airflow rate is subtracted from the total airflow to provide the secondary airflow.

With the exception of steps 6, 7 & 8, which must be undertaken in actual volumes at temperature, the above calculation may be undertaken in either mass (e.g. kg/s) or consistent units of volume (Nm^3/s).

It can be seen that estimating the secondary airflow is tedious and subject to inaccuracy owing to the difficulty of estimating the in-leakage air, raw meal weigh feeder instrument errors and calibration errors for the gas analyser.

Next the secondary air temperature was estimated using the following procedure:

1. The temperature of the clinker discharged from the cooler was measured as described previously;
2. The ambient air temperature was measured;
3. The cooler outer shell temperatures were measured and the radiant heat loss from the shell was calculated based on an estimated skin emissivity;
4. The convective heat loss from the cooler shells was calculated based on an estimated natural convection heat transfer coefficient;
5. The values calculated in steps 4 & 5 were summed to provide an overall heat loss;
6. The clinker mass flow as calculated from the raw meal feed rate allowing for the loss of 374kg of CO_2 per tonne of feed;
7. The secondary air temperature was then calculated by a heat balance as follows:

$$\Delta T_{air} \times m_{air}\, cp_{air} = (T_{c\ in} - T_{c\ out}) \times m_c \times cp_c - Q_{loss}$$

Where:

ΔT_{air} = temperature rise of the secondary air
m_{air} = mass flow rate of secondary air

cp_{air} = specific heat capacity of air (mass basis)
$T_{c\ in}$ = temperature of clinker into cooler (assumed to be 1390°C)
$T_{c\ out}$ = temperature of clinker discharged from cooler (measured)
cp_c = specific heat capacity of clinker
mc = mass flow rate of clinker
Q_{loss} = heat loss from cooler shell

Again this calculation is subject to inaccuracy, owing to the need to assume the clinker inlet temperature and difficulty of calculating the cooler shell heat loss accurately.

Using the secondary air temperature, the actual volume flow rate of secondary air at temperature is calculated using the ideal gas laws and then the velocity using the kiln internal diameter to give the cross sectional area.

Once the input data was available, acid alkali modelling was used to investigate the fuel air mixing and resulting flame profile, while mathematical modelling was used to examine the heat transfer from the flame to the charge.

Physical Modelling

The model was constructed using a standard size clear acrylic plastic tube to represent the kiln and the model scale chosen to suit the tube, subject to the constraint that the model was not too small. The satellite coolers were manufactured from grey ABS pressure piping because it was readily available and it was not necessary to view the cooler internals during operation. The cooler inlets to the kiln were faithfully offset as for the full size, see Figure 14.33.

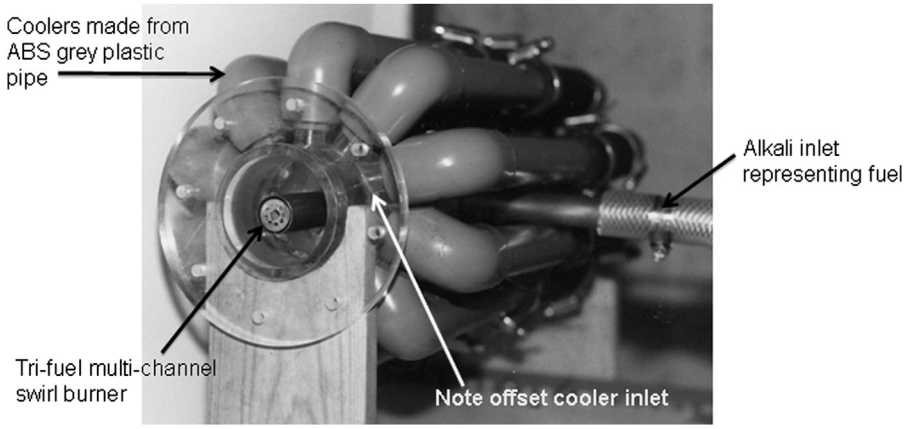


Figure 14.33 Model of coolers and burner shown with kiln tube removed

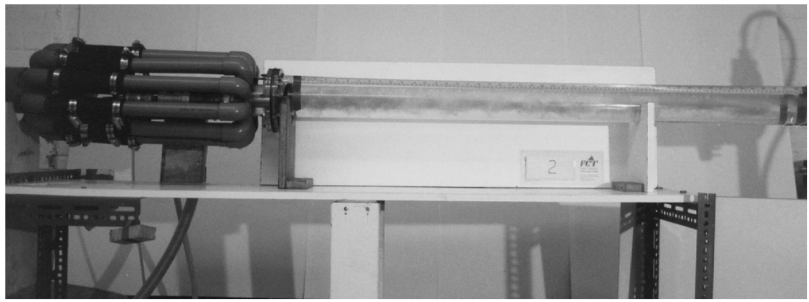


Figure 14.34 Model of existing firing conditions, note the dark region of unmixed alkali in the vortex core

Copper tube was used to make the low momentum multi-channel burner with the nozzle machined from solid copper, again shown in Figure 14.33. It was scaled from full size using the Craya-Curtet Parameter since this is the most appropriate scaling parameter for closely confined jets.

The physical modelling revealed a very long flame, running the whole length of the kiln and confined to the vortex core, Figure 14.34. The dark colour is unmixed alkali representing unburnt fuel. We had not seen this before with previous kiln models but in the full size kiln, the secondary air swirl could be seen in the full size kiln by looking in alongside the burner and observing the trajectory of the fine clinker dust returning to the kiln entrained in the secondary airflow. As a result, we were confident that the model was faithfully representing the full size plant.

It is also consistent with the very low momentum of the burner jet, the primary air representing only 5% of the stoichiometric combustion air. While the velocity of the gas jet contributes to the momentum and was modelled accordingly, that contribution is insufficient to entrain the secondary air into the jet and suppress the secondary air vortex. Furthermore, the kiln's poor operational symptoms were consistent with long flames that have poor heat flux profiles.

Mathematical Modelling

Following the physical modelling, the heat transfer was investigated using the long furnace model described in Chapter 6, section 6.2.2. This revealed an extremely poor heat flux profile, Figure 14.35.

The initial peak heat flux at 5–6 metres into the kiln is the result of the gas initially igniting and burning in the primary air. However, owing to the poor entrainment capacity of the low momentum jet, the oxygen in the primary air is soon consumed so the reaction stops.



Figure 14.35 Predicted heat flux profile for exiting gas-firing conditions

Heat release ceases and heat is transferred from the hot clinker product (>1300°C) to the cooler gas jet (~300 to 500°C).

At about 8–10 metres into the kiln, the gas has entrained sufficient secondary air to raise the oxygen concentration enough for the reaction to recommence at a low rate and gradually heat the primary jet until it is hotter than the clinker product and transfer of heat to the product recommences at about 15–16 m from the burner nozzle. The maximum heat release occurs in the 35 to 50 metre zone, which is too far from the coolers, for stable kiln operation or to produce good quality clinker. The peak heat flux is also too flat to produce small crystals, while the cooling zone (starting ~15 m from the cooler inlets) is too long to maintain sharp boundaries between crystals.

Summary of the Problem

From the modelling work described it was concluded that the operational problems with the kiln were primarily caused by poor heat transfer from the flame to the charge. This resulted in a very long cooling zone within the kiln with the burning zone towards the rear of the kiln, reducing the kiln's effective length, and hence production capacity. The poor product quality was caused by the slow rates of heating and cooling of the calcined raw meal and resulting clinker respectively.

The slow rates of heating and cooling were the result of the poor heat transfer profile which was caused by slow and incomplete fuel/air mixing, combined with the low emissivity of the natural gas fuel owing to its low C:H ratio. The former can be alleviated by improving

the fuel/air mixing, but it requires a fuel change to improve the emissivity.

The build-up in the rear of the kiln and preheater ducts and cyclones is largely related to minor components in the raw materials, especially volatile alkali and sulphur compounds. These evaporate in the burning zone and recondense in cooler parts of the system, such as the rear of the kiln and the preheater tower cyclones. Combustion influences these cycles because reducing conditions, specifically the presence of CO and lack of oxygen, tend to increase the rate of volatilisation in the hot zones, providing more material to condense in the cooler zones, hence exacerbating build-up problems.

14.5.3 Attempted Resolution of the Problem

It was clear that any solution would involve increasing the jet momentum of the burner, either by increasing the quantity of primary air or its velocity, indeed perhaps both would need to be increased. Various conditions were modelled using both mathematical and acid/alkali methods. However, it was not possible to find an effective and practical solution for the reasons explained in the following paragraphs.

As mentioned previously, increasing the primary airflow results in a decrease in secondary airflow and hence less effective cooling of the clinker. The reduced mass flow of secondary air, relative to the clinker flow, results in an increased secondary air temperature, hence maintaining the high secondary air velocity, even with the reduced mass flow. If the primary air quantity is increased to that necessary to cause recirculation and shorten the flame effectively and improve the heat transfer profile, the clinker discharged from the coolers would be too hot to be ground in the cement mill.

Since primary jet momentum is the product of the mass flow and the velocity, jet momentum can also be increased by using a higher primary air velocity. To achieve recirculation with the current gas flow and primary airflow would require supersonic velocities for both jets. Higher swirled primary jet momentum was modelled using acid alkali modelling and the result is shown in Figure 14.36. The combination of high momentum swirled primary air and the high momentum swirl on the secondary air defected the flame to the kiln wall and rotated with the secondary air swirl. Unfortunately, the colour photograph did not convert well to black and white, so some of the combustion zone cannot be seen, but deflection is relatively clear.

This deflected flame was not suitable for full size replication since it would have resulted in rapid refractory damage, a problem that did indeed occur some years later when the kiln was equipped with a

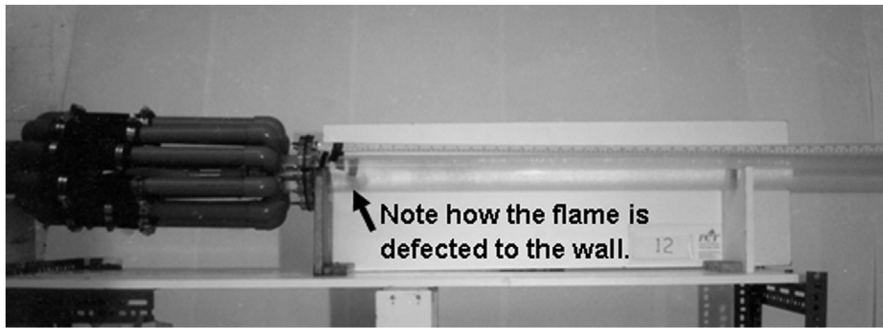


Figure 14.36 Acid alkali model simulation for high momentum swirled primary air

new swirl burner supplied by a well known company. That burner caused rapid refractory failure, especially when coal firing.

To eliminate the deflected flame would also require converting the swirled primary air to axial air. However, if the high momentum, low primary air jet (with or without swirl) had provided a solution on the model, its full size implementation was hardly practical owing to the excessive blower power required to achieve the required velocity. The pressure needed was even higher than for the current gas jet, being in the order of 200kPa. The electric motor to power the blower would be rated at approximately 1.5 MW. This would have required a major upgrade to the electrical power supply for that part of the site, costing tens of millions of dollars and was beyond the capital then available.

The options were discussed with the plant engineers and it was decided to increase the momentum as much as practical with the current fan and available electrical power. Mathematical modelling of the proposed primary airflow and velocity showed a modest improvement in the heat flux profile, Figure 14.37. Although the overall profile looks similar, the flame no longer runs out of oxygen once that in the primary air is consumed, so the large negative heat transfer 6 to 15 m zone is eliminated and the overall heat transfer is increased. For example, at 20 m from the nozzle the heat flux is now nearly 100 kW/m^2 compared with only 35 kW/m^2 for the existing burner. Moving the heat transfer towards the burner nozzle also reduced the length of the cooling zone prior to the cooler inlets, so increasing the rate of cooling. Overall, this was considered sufficiently encouraging to organise a full-scale trial.

The performance of the kiln with the modified burner was extremely disappointing. Whilst combustion was satisfactory, in that carbon monoxide did not form until the burner operated at less than 1% oxygen, the kiln production did not increase. Furthermore, the kiln was reluctant to 'pick up' from cold and considerable deposits occurred continuously on the feed inlet chute at the back of the kiln.

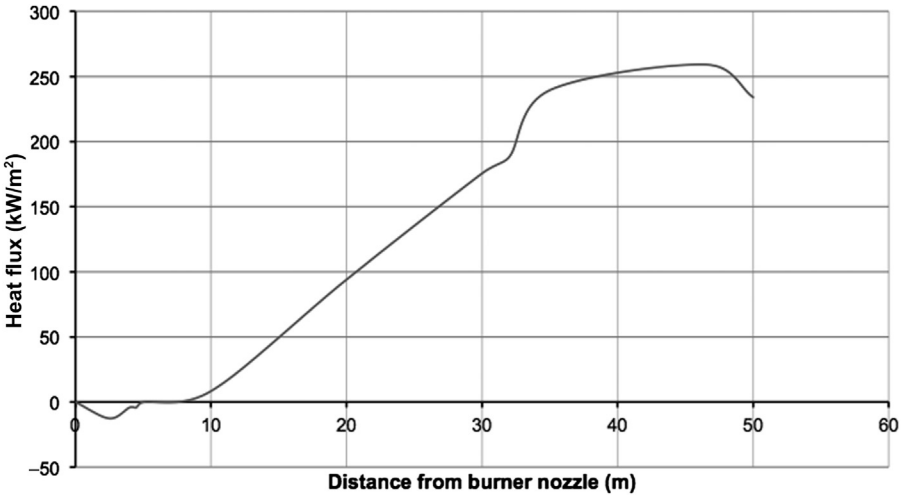


Figure 14.37 Predicted heat flux profile for the proposed gas-firing conditions

Moving the heat transfer forward in the kiln had moved the deposit from the lower cyclone into the chute. Had the build-up moved into the kiln it would have been less of a problem but the feed chute is just about the worst place for build-up since it already has a small cross sectional area compared with the kiln, lower cyclone or riser duct, so any obstruction is a greater problem, rapidly restricting gas flow and requiring an urgent kiln stop for cleaning.

Following cleaning and a restart the blockage quickly recurred and, since kiln availability is critical to economic success, it was considered prudent to return to the previous firing conditions.

14.5.4 Concluding Remarks

Many other attempts were made to improve the operation of the kiln, both by us and by other organisations but all led to disappointing results. The aerodynamics of the secondary air appeared to control the whole combustion and heat transfer process, with burner momentum having apparently relatively little influence.

We concluded that the kiln cross sectional area was too small for the firing rate required to achieve full output. This problem seems to have arisen as a consequence of the scale-up parameters used by the kiln designers. At this time is was widely considered that the capacity of a kiln was related linearly to its volume, so kilns were scaled by volume at a constant volume/tonne production, keeping an approximate length to diameter ratio, Figure 14.38. A comparison of the resulting operating parameters is shown in Table 14.5.

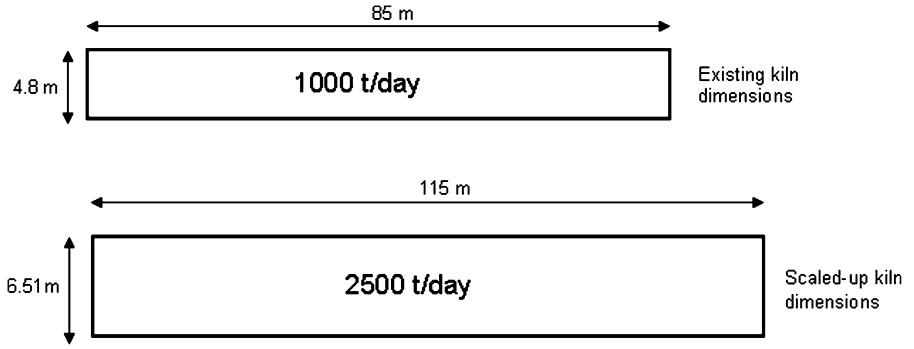


Figure 14.38 Comparison of existing and scaled up cement kiln dimensions

Table 14.6 Comparison of Existing and Scaled Up Cement Kiln Operating Parameters

	Existing kiln 1000 tonne/day	*New kiln 2500 tonne/day*
Volume	1538 m^3	3845 m^3
Cross sectional area	18.1 m^2	33.3 m^2
Secondary air velocity	5 m/s	6.8 m/s

In the example above, the scaled up kiln was designed for two and a half times the production of the existing kilns but the cross section flow area of larger kiln is only just double that for the smaller kiln. Since the specific fuel consumption was similar, the larger kiln required 2.5 times the airflow, leading to an increase in secondary air velocity to nearly 7 m/s from a previously acceptable (from a fuel/air mixing viewpoint) value of 5 m/s. The above example is an over simplification of the real scenario because it does not allow for the space taken by the refractory lining or any increase in secondary air temperature for the larger kiln. Furthermore, a diameter of 6.5 m was close to, or above the limit, that could be accommodated inside the kiln tyres or riding rings so, some kilns were built smaller for even higher production capacities, implying much higher secondary air velocities.

A major modification was undertaken later to improve the kiln operation by conversion to a precalciner using the air-through system. In this system approximately 40% of the fuel is burnt in a separate flash furnace between the lower cyclone and the kiln feed chute. The calcining reaction to drive off most of the CO_2 is undertaken in this furnace. This enables less fuel to be burnt in the kiln and for the kiln burner to operate at higher excess air. During the conversion, the satellite coolers, which were life expired, were cut off and replaced

with a very large grate cooler. This modification involved significant capital investment but again the results proved disappointing.

As a satellite cooler kiln, it had been virtually impossible to fire, as a consequence of high secondary air velocities. It was particularly unfortunate that the air-through system was chosen for the precalciner upgrade because the combustion air requirement of the precalciner furnace required even more air to pass through the kiln; further increasing the secondary air velocities. But a compensating factor was that the grate cooler and large kiln hood improved the secondary air distribution and eliminated the swirl.

A much better choice for the upgrade would have been an air-separate precalciner system. In this case the additional air for the precalciner is taken separately from the grate cooler via a tertiary air duct to the precalciner furnace, thus reducing the secondary airflow and velocity into the kiln.

We concluded the kilns with very high secondary air velocities are very difficult to fire successfully, even when equipped with grate coolers. Modelling identified the reasons for the poor performance of the kiln and the poor performance of the modified burner has in no way invalidated the modelling technique since it was a compromise that was considered "worth a try" rather than an true solution because that was impractical owing to the fan power requirements. The difficulties with these large preheater satellite cooler kilns were such that, as far as the authors are aware, none survive in their original format.

The development and implementation of precalciner technology, using a separate tertiary air duct, has largely eliminated these problems because the thermal duty of the main kiln is greatly reduced and it is fed with a much smaller quantity of secondary air, the remainder bypassing the kiln via the duct to the precalciner furnace.

14.6 Investigation and Elimination of Coal Firing System Problems

Coal firing systems were discussed in some detail in Chapter 7 but, despite the basic format of the technology having around for over 100 years, in our experience many coal firing systems designs are fundamentally flawed and some are positively dangerous. As explained in section 7.3.5 coal dust is explosible and that is a topic large enough for a book on its own. The subject is effectively covered by Eckhoff (1991), Bartknecht (1981), NFPA 8503, NFPA 68, the IChemE guidelines and HSE (2003).

It is the responsibility of everyone involved with the design, construction and operation of coal firing systems to be familiar with the

technology and the safety issues, including being familiar with these codes and to understand those parts that apply to the system that they are responsible for. Before we discuss the main subject of this section we will describe a scenario where a coal firing system had been designed and constructed without an understanding of these fundamental requirements.

14.6.1 A flawed and Dangerous Coal Firing System

In 2001 we were asked to advise on the failure of a coal firing system for the direct reduction of iron ore to metallic iron using a submerged lance system. In this system, high volatile pulverised coal was to be fed to a lance submerged in a bed of iron ore and burnt substoichiometrically with oxygen enriched air. A schematic of the furnace is shown in Figure 14.39.

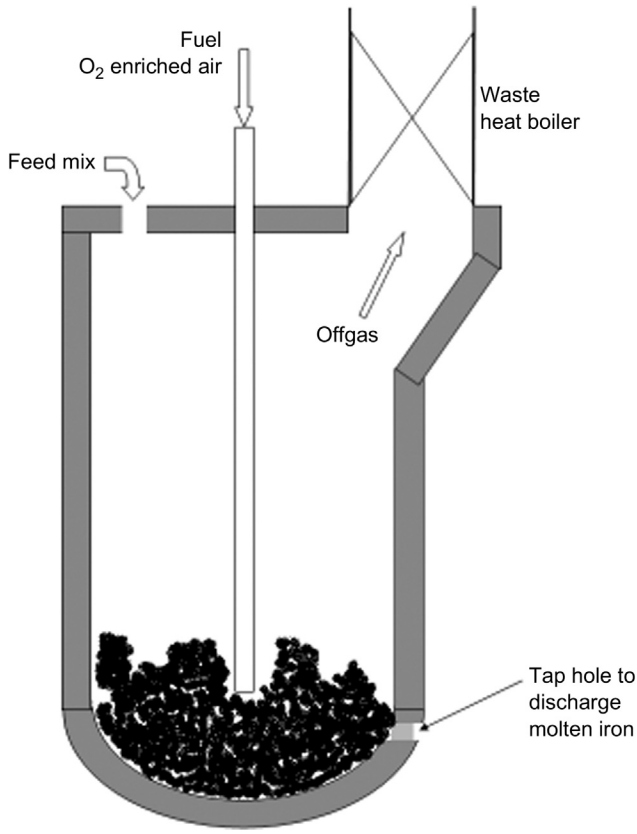


Figure 14.39 Schematic of the submerged combustion direct reduction smelter

This type of smelter was developed in Australia by CSIRO and has been used successfully for lead and copper production and is marketed commercially by Xstrata as ISAsmelt. The sub-stoichiometric combustion provides heat and CO to reduce the iron ore directly to metallic iron. The reactions in the bath are violent and a very deep vessel is required. There was nothing wrong with the smelter concept but, on the plant in question, it proved impossible to feed the coal to the lance because the coal could not be effectively dried and ground by the coal firing system that was installed. As a result the process needlessly failed.

A major engineering contractor (not Xstrata) designed the coal firing system and a simplified process flow diagram is shown in Figure 14.40. The centrepiece of the system was a direct fired rotary drier but this proved ineffective as it failed to dry the coal sufficiently for it to be ground effectively.

Raw high volatile, semi-bituminous coal with 15–20% moisture was stored in a small coalbunker. The coal was small, typically under 20–25 mm, and very friable so contained a significant quantity of fines. It was drawn from the bunker by a belt feeder and fed at the rate of approximately 1.4 kg/s (dry basis) to a gas fired counter current rotary drier. The airflow rate through the drier was approximately 5 kg/s. It was intended that coal would progress through the drier and be discharged dried to 9% moisture at the burner end and then conveyed to a small hammer mill where it would be ground to sub 200 micron and stored in a fine coal silo before feeding to the furnace. The system was intended to dry and grind in the order of 6 tonnes of raw coal per hour.

The designer was surprised that coal fed to the rotary drier was being discharged as a sticky cake, wetter than the feed. Normally, coal is flash dried in a coal mill using hot air typically in a ratio of 1.8–4 kg air/kg raw coal. Where flue gas is used for drying, the

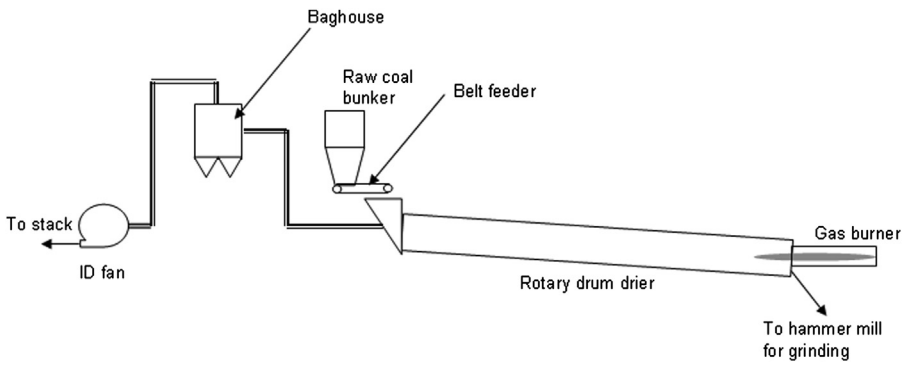


Figure 14.40 Simplified process flow diagram of rotary drum coal drying system

mass flow is on the higher end of the range and condensation of water onto the coal is the limiting parameter.

The combustion products of natural gas typically contain around 15% water vapour. In a rotary drier the proportion of vapour in the gas stream would be lower than 15% owing to the dilution air but it would still be substantial. In addition, the gas stream will contain all the moisture driven off from the coal in the hotter zones of the drier. There is therefore a large mass of water available to condense on the feed coal, which is at ambient temperature (20–40°C).

The failure to dry the coal was caused by water vapour from both the combustion and from the coal in the hot zone being absorbed by the raw coal at the dryer inlet. Effectively, some of the moisture from the combustion of the natural gas was added to the moisture already in the coal.

Condensation in the bag house suggested that the exit flue gas was below dew point, in which case moisture pick-up by the incoming coal was inevitable. Condensation in the bags also restricts the airflow through the fabric and through the whole drier system further reducing the drier airflow, hence exacerbating the dying problem.

It was clear when visiting the site and inspecting the system that the designers had not reviewed any of the publicly available information on coal firing systems and knew nothing about the explosion risks or the codes of practice intended to help engineers manage those risks effectively.

Earlier laboratory testing of this coal had revealed an ignition temperature of 380°C for a dust cloud and 260°C for a layer, ACIRL (1987). Obviously, rotary dryers tumble the coal through the hot gas steam and hence with a friable and dusty material such as sub-bituminous coal, the drier creates a dust cloud. Tumbling dried coal dust through the natural gas flame would have inevitably ignited it and a dangerous and destructive dust explosion would have resulted. It was indeed fortunate that the drier failed to dry the coal.

A dust explosion is not a trivial event and over the years hundreds of people have been killed and seriously injured by dust explosions in a wide range of industries from coal mining to food processing. For example, coal, wheat, sugar, some metals, wood and pharmaceutical dusts are all explosible. These risks have been known since the late 1700s when a dust explosion was recorded in a bakery in Milan. The resulting explosions can be extremely destructive. Figure 14.41 shows a dust explosion in a coal mill.

Ironically, the small hammer mills intended for grinding the coal could also have dried it had they been air-swept with hot air as intended by their manufacturer, so the rotary drier was redundant. Had the designer taken the trouble to understand the basics of coal

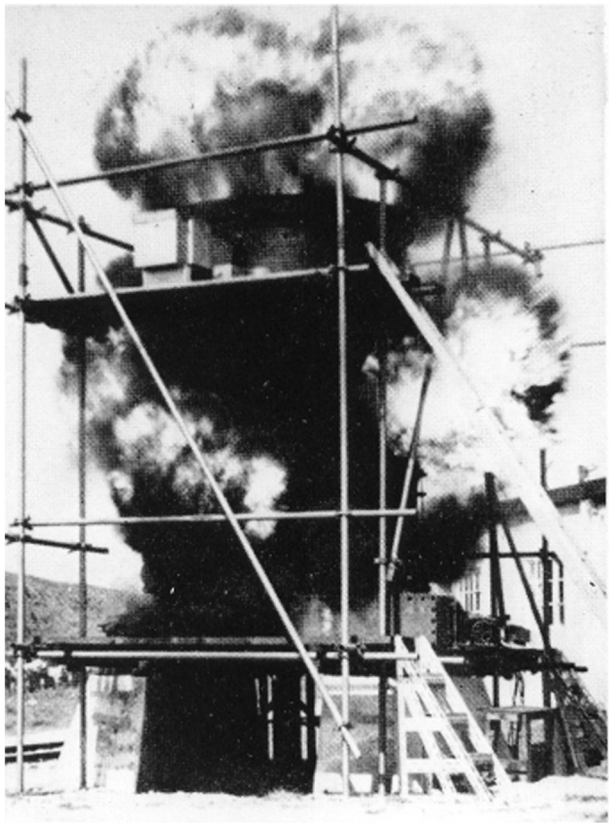


Figure 14.41 A coal dust explosion in a grinding mill – test undertaken at the HSE Buxton Research Laboratory (Used with permission of HSE)

grinding and firing, the resulting system would not only have worked but it would have been safe and substantially cheaper!

While, the above is a particularly poor example of engineering design with a complete lack of attention to the basic principles or the relevant safety issues, it is unfortunately only one example of many such problems that have occurred, and continue to occur in industry, see Kletz, 1988, 1991 & 2003.

14.6.2 Reducing Fuel Consumption and Increasing Output by an Upgrade of a Poorly Performing Coal Firing System

In 1992 we were invited to visit a cement plant in the Caribbean region that operated one wet process kiln with a nominal output of 750 tonne/day and a dry process kiln of 1300 tonnes/day; both kilns

burnt a mixture of coal and petroleum coke. The plant management had concerns over the operation of the kilns, particularly with regard to the very high levels of primary air necessitated by the firing system then installed.

The two kilns were equipped with semi-direct firing systems, nominally separate but linked together so that either firing system could fire either kiln. Roller mills were used similar to that shown in Figure 7.9a and, owing to the high airflow required by these particular mills, they were equipped with a mill air recycle system (shown dotted in Figure 14.42) to allow a higher mill airflow than the primary air flow. This mill air recycle, together with the linking between the firing systems, resulted in a system that was very complex as can be seen from the process flow diagram, Figure 14.42. Despite the relatively poor reproduction of the drawing the complexity of the system is clear.

As noted in Figure 7.12, recirculating coal mill air introduces a significant fire and explosion hazard and use of this system had been discontinued on this plant owing to repeated mill fires, so the primary airflow was equal to the coal mill airflow.

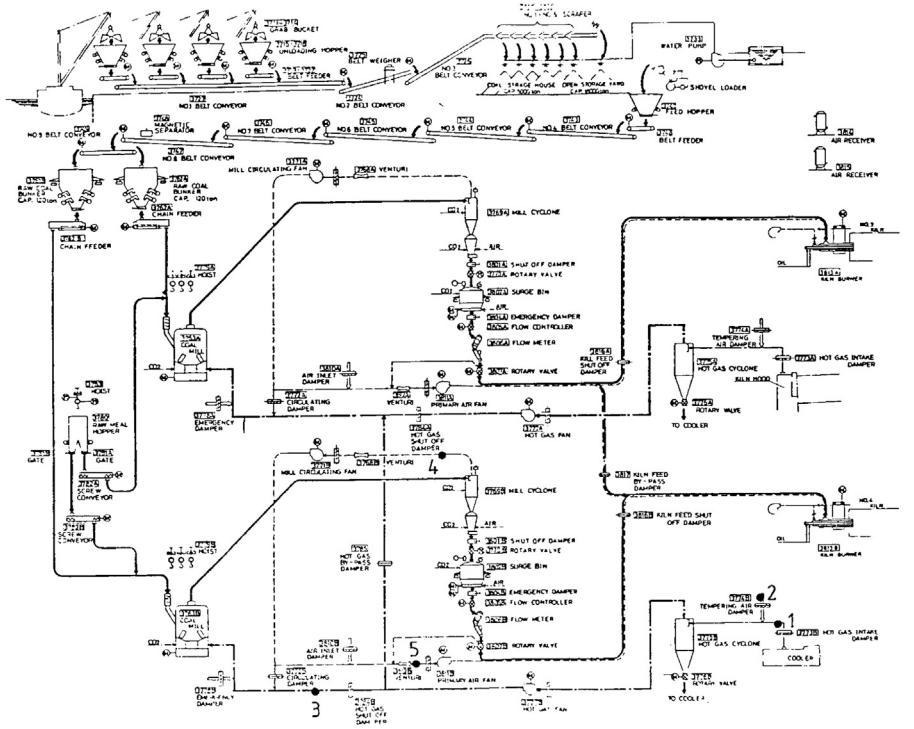
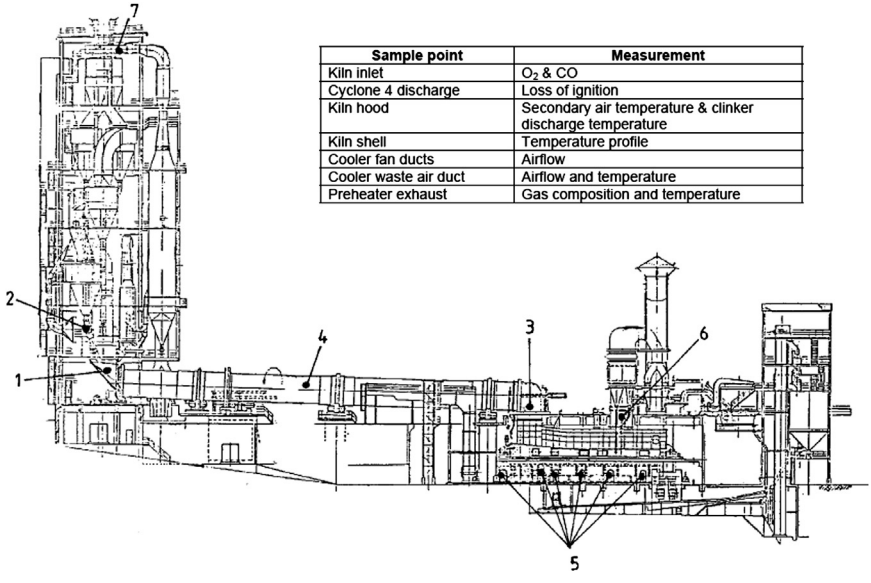


Figure 14.42 The original coal firing system installed on the plant

As was often the case, the first step was to undertake a site survey to determine current operating conditions. While both kilns were upgraded this description will concentrate on the dry process kiln since this is more relevant to the current and future environment. As described previously, measurements were taken using portable instrumentation in addition to readings taken from the plant instrumentation. Figure 14.43 shows the location of the sample points for portable instruments. Having a grate cooler, access was much better than for the satellite cooler kiln described previously.

The data collected from both the plant instrumentation and the sample point measurements, together with similar measurements taken around the coal firing system, were used to construct an overall heat balance of the kiln system, Figure 14.44. To achieve the degree of accuracy to that shown requires great care in undertaking all the various measurements.

The mass and energy balance shows a production rate of 14.73 kg/s of clinker for a fuel input of 55.86 MW. This is equivalent to a specific energy consumption of 3792 kJ/kg (906 kcal/kg) of clinker, which is high compared with the industry norm 3350–3355 kJ/kg. The main cause of this higher heat consumption was poor heat recovery from the clinker with only 8 MW being recovered in the secondary air compared with 21.43 MW in the clinker entering the cooler, giving a cooler efficiency of only 43% compared with an industry



Sample point	Measurement
Kiln inlet	O_2 & CO
Cyclone 4 discharge	Loss of ignition
Kiln hood	Secondary air temperature & clinker discharge temperature
Kiln shell	Temperature profile
Cooler fan ducts	Airflow
Cooler waste air duct	Airflow and temperature
Preheater exhaust	Gas composition and temperature

Figure 14.43 Location of sample points used to measure operational data with portable instrumentation

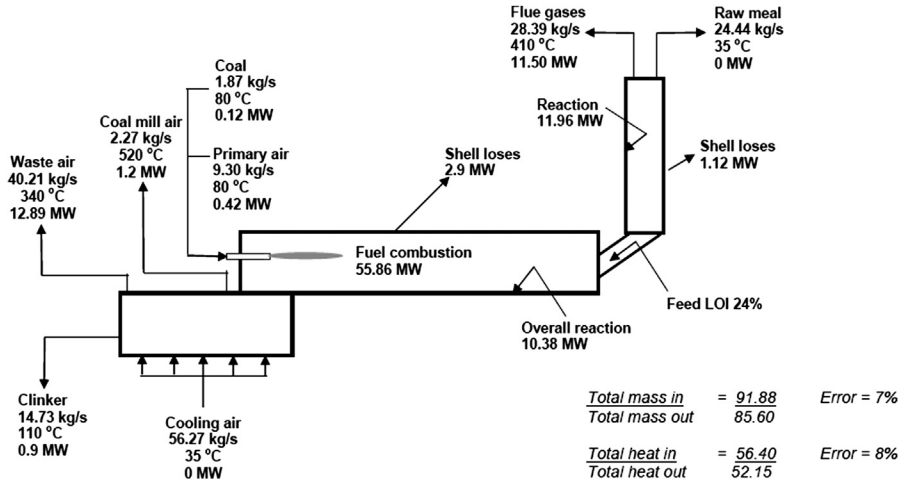


Figure 14.44 The overall mass and energy balance for the preheater kiln

expectation of at least 75%. The main energy loss was to the waste air, which contained 12.89 MW of heat, Figure 14.45.

The principle cause of the low cooler efficiency was the high primary airflow, which was 55% of the fuel's stoichiometric air requirement, compared with a more normal 15–25%. The consequence of the high primary airflow is low secondary airflow and poor heat recovery from the clinker, the remaining heat being lost in the waste air and in hot clinker discharged from the cooler.

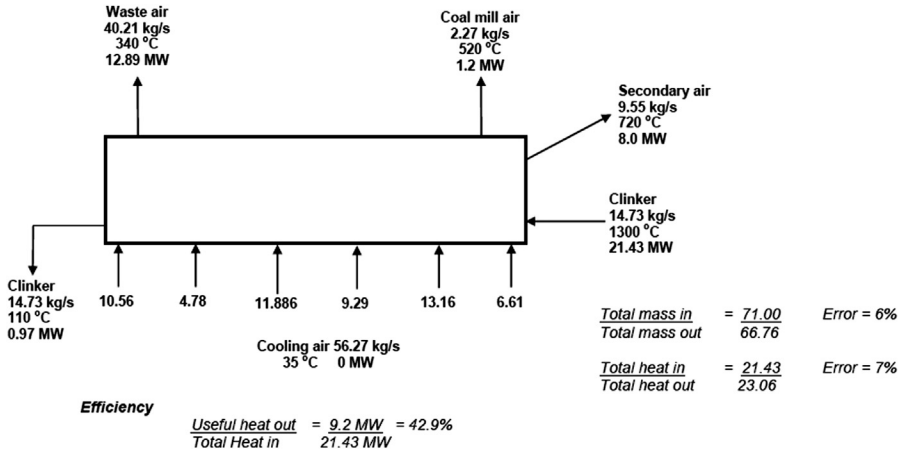


Figure 14.45 Cooler mass and energy balance

The next step was to undertake an engineering study to investigate ways of reducing the primary airflow and the costs and benefits associated with the various options. In addition to the various engineering options, this study included both acid alkali modelling and mathematical modelling to optimise the future firing conditions.

It was concluded that the most effective option was to separate the two firing systems and convert both to fully indirect firing at a capital cost of approximately US$750,000 each. It was expected that this would save at least 210 kJ/kg of clinker or 6%, equivalent to 430 kg of fuel per hour. It was also anticipated that a significantly larger proportion of the cheaper petcoke fuel could be burnt, increasing the proportion from 20% coke to at least 50% coke.

Implementation

Plant management accepted our recommendations and the system that was implemented on the plant is shown in Figure 14.46. This system reused the majority of the existing equipment, the new equipment consisting of a new bag filter to separate the ground coal from the mill conveying air, a new primary air fan, the existing one being reused for the bag filter, and new ducting.

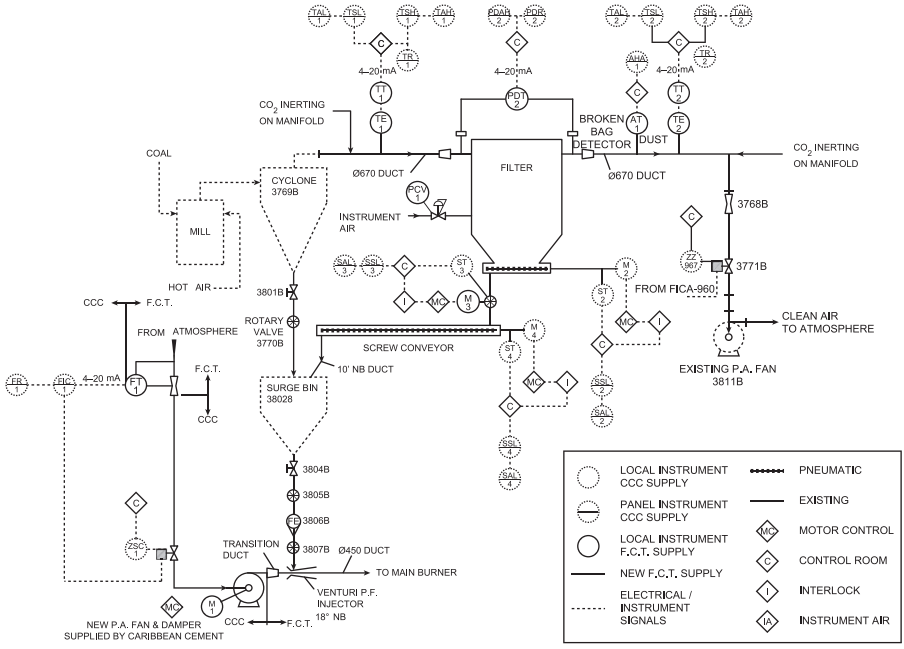


Figure 14.46 Process and instrument diagram of revised coal grinding and firing system

It can be seen from the process and instrument diagram that extensive new instrumentation was provided to allow better control of the firing system, and hence the kiln, together with a significant improvement in fire detection and fire fighting provisions.

Benefits Achieved

It is critical that the results of any process change or upgrade are monitored to assess whether the expected befits have been achieved. Figure 14.47 is a plot of the performance prior to the upgrade as provided by the plant management compared with the performance after the upgrade also provided by the plant. All data has been measured on the same basis.

It can be seen that prior to the upgrade the kiln output was in the order of 53 tonne/hour at a specific energy consumption of 940 kcal/kg (3936 kJ/kg). After the upgrade the specific fuel consumption was clearly reduced to approximately 830 kcal/kg, a saving of 110 kcal/kg or 12%, double that estimated during the study. However, since the kiln production was limited by the combustion process this energy saving was accompanied by an increase in production of nearly 2 tonnes/hour of clinker or just under 16,000 tonnes in a typical year of 330 operating days. The savings achieved and the extra production

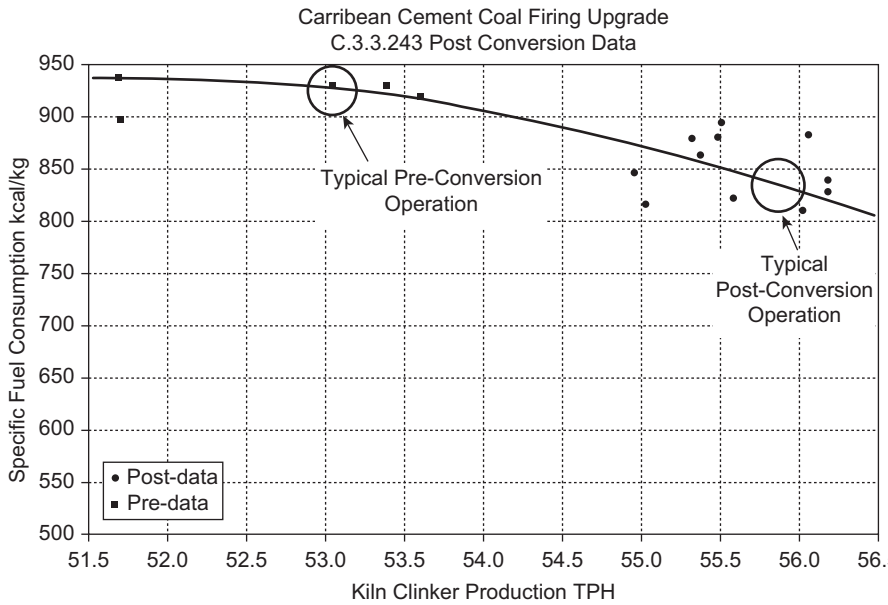


Figure 14.47 Performance of the preheater kiln prior to and following the upgrade

was therefore much greater than predicted and resulted in a payback time of a few months.

14.7 Concluding Remarks on Implementation

The examples discussed in this chapter are a small but representative sample of the work undertaken by our engineers and us over a period of some 20 years. The examples cover a range of industries and each example has been chosen to demonstrate a different practical aspect of the application of the techniques.

Each example illustrates the need for careful collection of the relevant operating data, together with careful analysis of the data and methodical application of process modelling to diagnose a problem and to devise a solution to that problem. Where a new process is being developed a clear understanding of the process requirements must be defined before a solution can be engineered. Once the process solution has been developed it must be practically implemented and this requires close attention to the mechanical and electrical engineering aspects of the design, together with a well thought out control and instrumentation package, with particular attention paid to the safety aspects of the design.

Failure to apply a methodical approach to the process and detail design of the system design is likely to result in process failure, such as in the satellite cooler cement kiln example, or both process failure and danger to operators as in the rotary coal drier described.

Fuels, fuel systems, fuel storage, combustion processes and furnaces are inherently dangerous. Great care needs to be taken when designing, constructing and working with these systems. Only engineers, technicians, operators and maintenance staff with the appropriate, skills, knowledge and training should work in this field.

References

Alsop, P. A. (Ed.). (2001). *The cement plant operations handbook* (3rd ed.) (pp. 4). Dorking, UK: Tradeship Publications.

Bartknecht, W. (1981). *Explosions, course, prevention, protection, Springer-Verlag*. Berlin & New York.

Bertand, C. (1991). *The use of mathematical modelling in the optimization of flash calciner design*. London: International Kiln Association Conference on Operations and the Environment.

Coal Hazard Assessment Test Program, Report no 06/2792/2, Australian Coal Australian Coal Industry Research Laboratories, 1987

Eckhoff, Rolf, K. (1991). *Dust explosions in the process industries*. Oxford: Butterworth-Heinemann.

Gorog, J. P. (Dec 2002). *Lime Sludge Kin Operation, 1*. Seattle: Presentation at the University of Washington. http://faculty.washington.edu/malte/seminar/Au04/LimeKilnOperations.pdf.

Hawksley, P. G. W., Baszioch, S., & Blackett, J. H. (1997). *Measurement of Solids in Flue Gases* (2nd ed.). London: The Institute of Energy.

HSE. (2003). *Safe handling of combustible dusts: Precautions against explosions, 103*. UK Health and Safety Executive publication HSG, 2Ed.

IChemE Guide to dust explosion and protection:
Part 1 Venting
Part 2 Ignition prevention, containment, inerting, suppression and isolation
Part 3 Venting of weak vessels and the effects of vent ducts

Jenkins, B, Bertrand. C., Improvements in the design and operation of alumina flash calciners, IFRF Online Combustion Journal, Article Number 200110, November 2001, ISSN 1562–479X. http://www.journal.ifrf.net

Kletz, T. A. (1988). *What went wrong, Case histories of process plant disasters* (2nd ed.). Gulf Publishing Company.

Kletz, T. A. (1991). *An Engineer's View of Human Error* (3rd Ed.) IChemE.

Kletz, T. A. (2003). *Still going wrong, Case histories of process plant disasters and how they could have been avoided*. Butterworth-Heinemann.

Martin, G. (1932). *Chemical engineering and thermodynamics applied to the cement rotary kiln*. London: Crosby Lockwood.

Moles F. D., Jenkins B. G., Optimal heat transfer from rotary kiln flames, Blue Circle Works Manager's Conference. Oct. 1976, see also Jenkins B. G., Modernisation and Technology Upgradation in Cement, Chapter 17, page 353, Progress in Cement and Concrete Vol. 5 ed. Ghosh S. B. & Kumar K., Akademia Books International, India, 1999.

NFPA 68 "Guide to venting of deflagrations", 2002NFPA 68 "Guide to venting of deflagrations", 2002 Edition, National Fire Protection Association, Quincy, MA, USA (Due for revision in 2006)

NFPA 8503: Standard for pulverized fuel systems, 1997 ed., National Fire Protection Association, Quincy, MA, USA

VDI 3673 Blatt 1, Pressure venting of dust explosions, 2002-11 Ed., VDI Verein Deutscher Ingenieure, Düsseldorf, Germany

Williams, F., & Schmidt, H. W. (2012). Flash and CFB Calciners, History and Difficulties of Development of Two Calcination Technologies. *Light Metals*, 135–140.

Chapter 15

Future Trends and Concluding Remarks

Chapter contents

15.1 Trends in New Materials 608
15.2 Trends in Furnace Emissions and Fuels for Furnaces 609
15.3 Prospects for Alternative Electrical Energy as a Power Source 619
15.4 Trends in Furnace Controls 620
15.5 New Applications for Furnaces 621
15.6 Concluding Remarks 621
References 622

> "In a fast-moving, progress-conscious world, the consumer expects to be dizzied by progress. If he could completely understand advertising jargon he would be badly disappointed. The half-intelligibility which we expect, or even hope, to find in the latest product language personally reassures each of us that progress is being made: that the pace exceeds our ability to follow."
> **Daniel J Boorstin, The Image, 1961.**

The above quotation, made over 50 years ago, epitomises humanity's inherent quest for improving on what has already been done. The blind faith of the human race demands a certainty that we will never achieve perfection. The demand for innovation increases globally year upon year, but it is likewise the case that the result of errors and failures create globally felt consequences. The widely held belief that there are rapid changes in technology today is largely illusionary. It took some forty years before computers came into general use, the first being constructed in 1943 and the Apple II becoming available in the early 1980s. In the early part of the 19th Century there was a similar timeframe for the role out of railways. The first practical steam locomotive on rails was demonstration by Trevithick in 1804 and by 1844 there was in the order of 21,000 route miles of railway in Britain, most of it double track; a similar timescale for the wide scale availability of computers. In the same way that computing speed has increased so did train speeds with 100 mph being achieved by 1904.

The contents of this book are a distillation of the millennia of experiences of mankind since he first controlled fire. The ancient industries of charcoal and lime burning, brickmaking and metal-craft are the foundations of our industrial society. The progression of the basic industries on which our modern society relies has all involved furnaces, and hence their designs have matured beyond the stage where innovative step changes are likely. Modern furnaces have extensively explored and exploited the laws of mathematics and physics over the last two hundred years to arrive at the designs we see today. Engineers have developed and optimised designs that will accommodate all the options shown in Figure 1.3, so future significant developments will lie principally in the application of new materials of construction, different fuel or energy sources and environmentally driven restrictions rather than any engineering sea-change.

15.1 Trends in New Materials

There have been significant recent advances in the development of new refractory, ceramic, insulation and high temperature metallic materials and in the product quality of existing refractories, much of which has been a spin-off from the development of jet engines, rockets and

space exploration. Whilst the applications in rocketry, where refractories have a 'short and exciting' life, are far removed for those of a furnace, which expects durability and longevity, the governmentally funded investment in materials research has expanded our understanding far beyond what might have been the case had the refractories industry relied only on their normal R&D expenditure. As a furnace designer or operator, one is much more likely to find suitable high temperature materials, both metallic and ceramic, to meet the demands of a particular process, albeit at a cost premium compared to basic steels and firebricks. Universal business models, irrespective of the product, require companies to maximise productivity, be 'lean' and competitive. For a furnace operator this translates into no spare capacity, maximum availability, minimum maintenance and maximum thermal efficiency. The decision to use the new generation of materials is primarily economic, balancing the advantages of higher productivity, extended furnace life and lower specific energy consumption against the additional capital investment costs.

15.2 Trends in Furnace Emissions and Fuels for Furnaces

As we have seen in chapter 4, all gases with a dipole moment are selective absorbers and emitters of radiation. Common gases that fall in this category include all gaseous hydrocarbons (methane, ethane, etc.), water vapour and carbon dioxide. The concentration of these gases in the atmosphere is linked to climate changes. This is evident from the carboniferous era, where high CO_2 and humidity changed the world into a giant greenhouse that eventually laid down a large proportion of the fossil fuels that we use today. Notwithstanding any scientific debate on the relative contributions of natural and man-made CO_2 in the atmosphere, there is an almost unstoppable politico-social will to limit man made CO_2. Although substantial scientific research and political negotiation has been undertaken over the last 30 years, a widely agreed solution to anthropogenic climate change has yet to be agreed.

It is unknown exactly what level of CO_2 in the atmosphere can be sustained without causing 'dangerous' or 'extremely dangerous' climate change, although a maximum of 450 vppm CO_2 is quoted (Anderson and Bows, 2011), which by some forecasters could be realised in the next 30 years if the current rate of emissions remain unchanged. Therefore, it is unsurprising that a number of schemes have been proposed to counteract climate change through direct manipulation of the Earth's climate system, referred to as 'geoengineering'. (The Royal Society, 2009). Long term sustainability will only be realised by mitigation methods such as decarbonisation of energy supply, lower carbon intensive consumption and land use

management to preserve terrestrial carbon pools, but the significant technical and financial challenges, and international political will required to bring about such a change suggests this could take a whole century to be fully implemented. Until then, some developed and developing technologies are being implemented to mitigate some of the more harmful effects of climate change. These are beginning to and will continue to have a major influence on the design of industrial process plant to meet increasingly more onerous emissions limits. CO_2 emissions can be reduced in a process by:

- Improving the energy efficiency
- Replacing fossil fuels with alternative fuels (e.g. biofuels, or wastes)
- Increasing the quantity of recycled product (e.g. paper, scrap steel, glass)
- Using or developing a more energy efficient process method
- Replacing high carbon fuels with low carbon fuels (e.g. coal to natural gas)
- Removal of CO_2 from the exhaust gases

The first four options in the list would be economically advantageous to the process, and therefore attractive to the producer. The last two options would entail additional costs for no production benefits while removal of CO_2 from the exhaust gases also reduces the overall process efficiency. No producer would willingly implement these steps unless forced or incentivized to do so. We have already touched on all of these options in the preceding chapters, but will here expand on the last option, since this is our expectation of the most likely direction for industrial CO_2 mitigation in the near future.

15.2.1 Carbon Capture and Storage

The approach to CO_2 capture can be divided into three distinct categories:

- Post-combustion - capture of CO_2 from process flue gases
- Pre-combustion - conversion of fossil based fuels to H_2 and CO, or CO_2 prior to combustion
- Oxy-combustion - burning fuel in pure oxygen rather than with air, to produce concentrated CO_2 with recycled flue gases used to control the combustion temperature

Figure 15.1 shows how the process heat or power for a furnace operation fits into each of these combustion systems. The post combustion route potentially has the smallest impact on any current

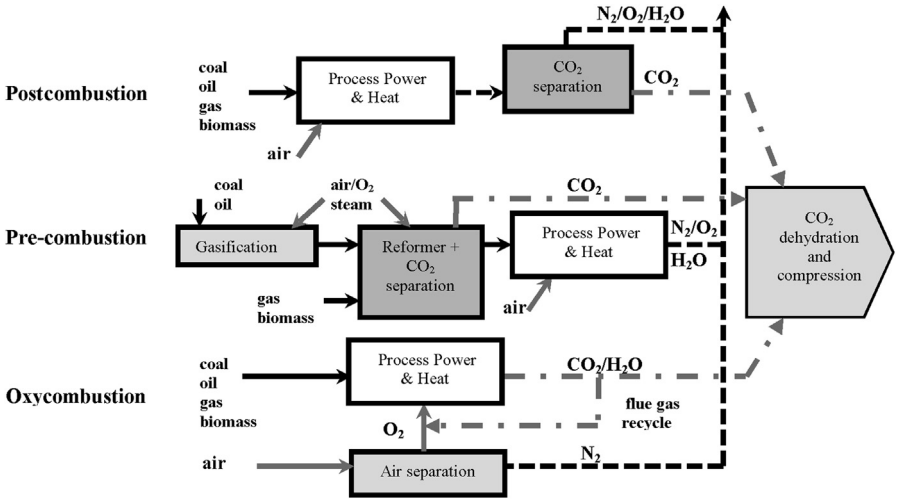


Figure 15.1 CO_2 capture processes. After Metz et al. (IPPC 2005)

process design, since the existing furnaces etc. require no modification. Technologies for the separation of CO_2 from the flue gases include:

- Absorption with an alkaline oxide (CaO or MgO)
  - Once through capture
  - Chemical looping
- Absorption into aqueous and organic solvents
- Cryogenic separation

Although the CO_2 is removed from the system at opposite ends of the process in pre- and post-combustion the equipment used for separating the CO_2 is similar. Although the oxy-combustion route provides a concentrated form of CO_2, the hydrogen becomes water and, for pipeline transportation to a sequestration site the CO_2 must be compressed to a dense phase state and be totally anhydrous to minimise pipeline corrosion, so the water must be separated. This is not a trivial requirement because failure of a pipeline containing supercritical CO_2 would be extremely dangerous owing to the Joule-Thompson effect causing rapid cooling of the steel to sub-zero temperatures. Under these conditions carbon steel suffers severe embrittlement and splits several kilometres long can result. Similar failures have occurred in natural gas pipelines with catastrophic results (Connolly & Cusco 2007).

Absorption is the most commonly proposed and researched option for removal of CO_2 from exhaust gases, and Table 15.1 summarizes the strengths and weaknesses identified for the scrubbing and looping

Table 15.1 Absorption Options for CO_2 Capture

Technology	*Description*	*Strengths*	*Challenges*
Solvent scrubbing with chemical absorption	Absorption of CO_2 from flue gases using aqueous amine solvents, dimethyl ethers of polyethylene glycol or chilled ammonia	• Established technology and widely used in industry (ex ammonia) • Can be employed with conventional plants	• Toxicity concerns • Sensitivity to degradation • High power or steam requirements • Complex flowsheet
Solvent scrubbing – physical absorption	Uses cold methanol solvent to physically absorb CO_2	• Established technology widely employed • Available as the Rectisol® process	• Methanol needs to be cooled to between −30°C & −60°C • High refrigeration costs • Complex flowsheet
Calcium looping	High-temperature CO_2 scrubbing using calcium based sorbent	• Smaller energy penalty than amine scrubbing • Cheap, widely available and non-toxic limestone reagent	• Rapid loss of activity of sorbent after multiple cycles

methods. Solvents that exploit both physical and chemical absorption are available from a number of suppliers. Most of these processes absorb all acid gases, including H_2S, SO_2 and SO_3. Some of the processes can be designed to selectively absorb one gas and reject others but this is beyond the scope of this book. For further information, see Higman and van der Burgt, 2008, pp328–338. It should be noted that contamination of the recovered CO_2 with sulphur gases could present problems in the subsequent compression and transportation processes.

Pre-combustion options involve pre-treatment of the fuel to reduce or remove carbon. The clean fuel is then burnt in the existing furnaces etc. as a replacement for the original fuel. This may result in some equipment modifications and operational changes. Technologies that can be applied are:

- Gasification of solid and liquid fuels (including biomass)
  - Steam reforming
  - Fuel cell
- Liquefaction of solid fuels
- Hydrogenation of liquid and gaseous fuels

Gasification and liquefaction technologies have been utilised since the introduction of town gas to London in 1812 by the London Gas, Light and Coke Company (Higman & van der Burgt 2008) and their further development in Germany during the 1930s, the breakthrough being the commercialisation of cryogenic oxygen separation by Carl von Linde in the 1920's which allowed development of the Lurgi pressurised oxygen-blown gasifier patented in 1927 and was first applied commercially in 1931 (Higman & van der Burgt 2008). The other major breakthrough was the synthesis process developed by Drs Franz Fischer and Hans Tropsch in 1925 to produce synthetic crude oil (Stynberg & Dry 2004). South Africa has been a world leader in converting coal to oil and gas for over 50 years using Lurgi gasifiers and the Fischer-Tropsch process. The technologies used are proven, mature, and are in a research category that involves 'tweaking' to get a better outcome, rather than requirements for any fundamental breakthroughs. Hydrogenation is also a mature technology, practiced in almost every oil refinery in the world.

All these fuel conversion technologies, such as coal to liquid fuels or coal and water to hydrogen are less efficient than direct use of the original fuel, so they do not in themselves reduce emissions. For example, using the US Department of Energy computer model "GREET" - Greenhouse Gases, Regulated Emissions, and Energy Use in Transportation (Argonne, 2009) which was developed to calculate the "well to wheel" CO_2 emissions predicts that the CO_2 emissions that would be created by gasification of South Australian lignite and the subsequent

production of "clean diesel" using the Fischer-Tropsch process will be 50–100% greater than those for diesel produced by conventional refining of crude oil. In reality, the carbon in any fossil fuel always ends up as CO_2 no matter what route is chosen.

Oxy-fuel combustion systems are already applied in many industrial furnaces, particularly those used for metal and glass melting, and to boost production from furnaces with limited drafting capacity. In these applications the aim is to increase the flame temperature and thereby enhance heat transfer rates within a given furnace space. On-site generation of oxygen from air can be carried out by one of two primary methods

- Pressure swing adsorption (PSA)
- Cryogenic air separation (ASU)

Two factors affect the selection of the best option.

- Required consumption rate of oxygen
- Purity

The furnace temperatures and gas flow volumes are controlled by recycling cooler flue gases, which are primarily CO_2 and water vapour, to mimic the temperatures and flows normally passing through the system under conventional fuel firing conditions. A particular bonus for this route to carbon capture is the virtual elimination of thermal NO_x formation, owing to the absence of nitrogen in the furnace, although the in-leakage of false air must be carefully controlled for this to be achieved. However, it should be noted that the specific heat capacity of the CO_2/H_2O furnace gases will be higher, and the emissive radiation properties will change, which will impact on both the radiative and convective heat transfer distribution.

The potential value in these alternative conversion routes is that the CO_2 is in concentrated form and CO_2 capture techniques are readily available for application to a centralised large-scale plant. The final stage after CO_2 has been captured from the exhaust gases is its safe disposal. Whilst the cost of Carbon Capture and Storage (CCS) systems is mostly comprised of capture costs, (McKinsey and Company 2008), the costs of compression, transportation and storage of the waste gas are likely to be significant and should be considered carefully.

The variation in the cost of post-capture processes can be considerable. The values in Table 15.2 are for a very large scale project. The comparative cost of transportation by pipeline, in particular, decreases significantly as the mass flow rate increases. In most cases, CO_2 must be transported from the site where it is generated and

Table 15.2 Variation of CO_2 Control Cost Predictions for a Large Scale Project

CCS stage	*$min*	*$max*
Compression [per tonne]	8.131	8.131
Transport [per km per tonne]	0.019	0.019
Sequestration [per tonne]	0.200	30.200
Monitor [per tonne]	0.040	0.06

captured to another site where it may be stored. The options for transportation are:

- Transport by pipeline
- Transport by tanker ship

The factors that govern the optimum method of transport are the volume of CO_2, distance between sink and source, and type of terrain between them.

Figure 15.2 illustrates how these factors can influence the decision of optimal transportation method. There are other, less easily quantifiable factors that must also be considered. Constructing a new pipeline involves negotiating many legal barriers, and if the proposed route passes close to areas with a high population density then the legal complexity is increased. CO_2 can be transported in solid, liquid or gaseous states. The state depends on the temperature and pressure regimes within which transport occurs. The high costs of the refrigeration and compression necessary to achieve and maintain the solid state make it economically unfavourable. The difference in volume

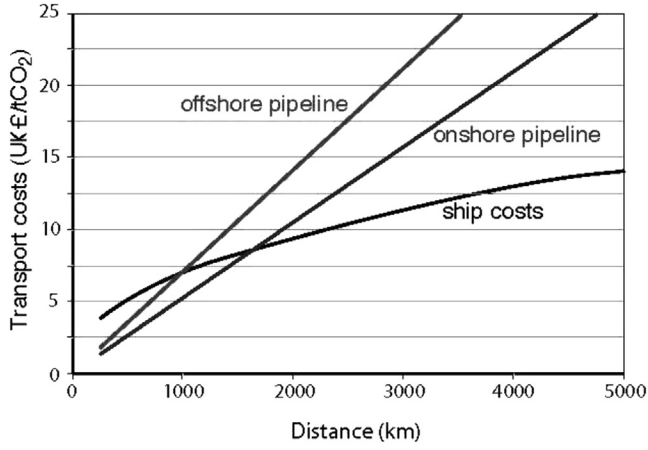


Figure 15.2 Costs for Transportation of CO_2 (IPCC 2005)

between the density of the solid and liquid states is far less than that between the liquid and gaseous states. The liquid state requires pressurisation and refrigeration but the savings possible due to the decreased volume make it favourable for transportation by ship. Gaseous carbon dioxide has a very low density at atmospheric pressure, so in order to transport it cost-effectively it is usually compressed though it need not be refrigerated.

For pipeline transport it is important that the stream of CO_2 is relatively pure, in order to prevent corrosion. The following specification has been used for a CO_2 pipeline in the Canyon Reef Enhanced Oil Recovery project in Texas, and the IPCC (Metz et al., 2005) suggest that future CO_2 pipelines would follow similar specifications.

- 95% Carbon Dioxide
- no free water, not more than 0.489 m^{-3} in the vapour phase
- not containing more than 1500 ppm, by weight, of hydrogen sulphide.
- not more than 1450 wppm of sulphur.
- not more than five mole percent (5%) of hydrocarbons
- not containing more than 10ppm of oxygen by weight
- not more than 4×10^{-5} L m^{-3} of glycol and at no time shall glycol be present in a liquid state

When carbon dioxide is compressed from atmospheric pressure to 10 MPa, the volume is reduced by a factor of one hundred. CO_2 is not refrigerated for pipeline transportation, and there is no need to reach the supercritical state. Natural gas pipelines routinely operate with pressures between 10 and 80 MPa, and so higher pressure conditions can be used if they are required. Initial pressurisation is often high to allow for a gradual pressure drop along the pipeline, and as an alternative to using booster stations.

CO_2 pipelines are a mature technology. Commercial carbon dioxide pipelines have existed for over thirty years, often in Enhanced Oil Recovery (EOR) projects. Table 15.3 shows several existing long distance pipelines.

The volumes of these projects are in the same range of 1 to 10 Mt/year. Existing technology allows pipelines to be constructed across almost any terrain and in almost any environment. Underwater pipelines can be laid in depths as great as 2200 m, though they are more expensive than land pipelines they may still be cheaper than ship for high capacity short distance transportation. The proximity of the sources to potential storage sites, and the relative simplicity of the terrain between them make pipelines the preferred method with which to transport CO_2.

Transport of CO_2 from capture to storage facilities by ship may be cost effective over large distances. Transportation by ship may be

Table 15.3 Existing Carbon Dioxide Pipelines (IPCC 2005, DNV 2010)

Pipeline	*Location*	*Operator*	*Capacity* ($MtCO_2yr^{-1}$)	*Length (km)*	*Year completed*	*Origin of* CO_2
Cortez	USA	Kinder Morgan	19.3	808	1984	McElmo Dome
Sheep Mountain	USA	BP Amoco	9.5	660	–	Sheep Mountain
Bravo	USA	BP Amoco	7.3	350	1984	Bravo Dome
Canyon Reef Carners	USA	Kinder Morgan	5.2	225	1972	Gasification plants
Val Verde	USA	Petrosource	2.5	130	1998	Val Verde gas plants
Bati Raman	Turkey	Turkish Petroleum	1.1	80	1983	Dodan field
Weyburn	USA/ Canada	North Dakota	5	328	2000	Gasification plant
Snøhvit	Barents Sea	Statoil	0.7	153	2008	Hammersfest
Total			50.6	2744		

important in the future if CO_2 is traded internationally; a situation can be envisioned whereby countries without sufficient storage facilities or expertise pay to export CO_2.

Storage options for sequestered CO_2 can be broken down into three main categories: geological storage, ocean storage or industrial use. Geological storage has the greatest potential to accept large volumes of CO_2 with a good level of retention. Ocean storage is not as mature a technology and is environmentally controversial. Current commercial use of CO_2 is unlikely to be able to cope with the output of a large-scale CCS system.

Geological storage covers: storage in depleted oil or gas fields; storage in coal beds and storage in saline aquifers. These alternatives are illustrated in Figure 15.3.

- **Storage in depleted oil or gas fields.** CO_2 has been successfully injected into depleted oil and gas fields at a number of demonstration projects. Four industrial scale project (>1Mt/year) are currently active: Sleipner and Snøhvit, in the North Sea; Weyburn, in Canada; and In Salah in Algeria. Some fields also inject CO_2 in order to enhance recovery. Enhanced Oil Recovery (EOR) is potentially a way for CCS projects to become viable at low carbon prices, because pure CO_2 is a valuable commercial product for EOR operations. Over $30MtCO_2y^{-1}$ is used for EOR in Texas, US (IPCC (Metz et al., 2005), p31).

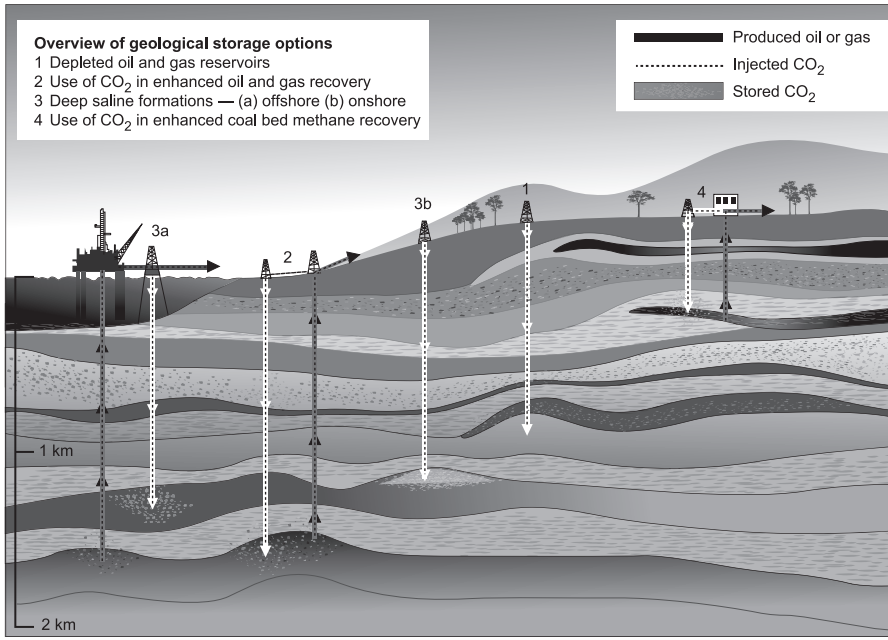


Figure 15.3 Geological Storage Options IPCC (Metz et al., 2005)

- **Storage in coal beds.** Injecting CO_2 into un-minable coal beds can result in natural gas production. Methane (CH_4) adsorbs to the surface of coal, but is preferentially replaced by CO_2. As with EOR, this approach can generate revenue from the operation by the sale of CO_2 as a commercial product. However, this storage process is still in the demonstration phase (IPCC (Metz et al., 2005), p30).
- **Storage in saline formations.** Saline formations are deposits of water held in porous rock. Injected CO_2 is initially dissolved but at higher pressures and quantities it displaces the in-situ fluid. The saline formation is encased by a non-porous formation, which forms an impermeable barrier to the CO_2, thus preventing it from escaping to the surface.

Several mechanisms have been proposed for ocean storage of CO_2. If the CO_2 is injected at a depth of greater than 1,000 m then slow deep sea diffusion could isolate it from the atmosphere for centuries. If the CO_2 is injected at greater depths, below 3 km, then it becomes denser than water and forms a falling plume, descending to the seabed. This approach would increase the duration of isolation, but would also create localised 'lakes' of CO_2, which would require constant monitoring. The various ocean storage options are shown in Figure 15.4. This method has the potential to absorb high quantities

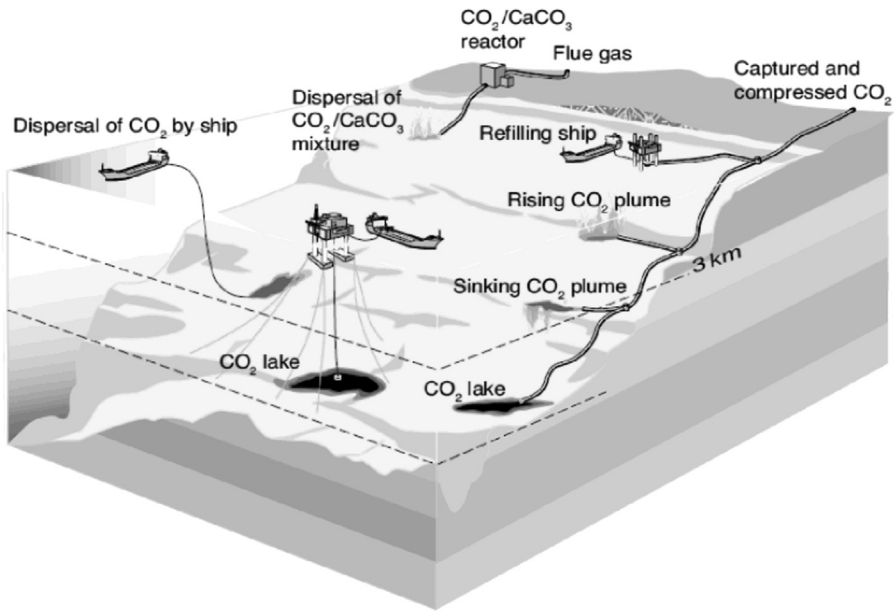


Figure 15.4 Ocean Storage Options for CO_2 (IPCC 2005)

of CO_2 and would cost considerably less than geological storage. However, the legal status of ocean storage is currently uncertain, and studies have shown a negative public reception to these types of ocean storage (IPCC (Metz et al., 2005), p.39).

15.3 Prospects for Alternative Electrical Energy as a Power Source

Some work has been undertaken with a view to assessing the potential for solar energy powered furnaces. For example, the Paul Scherrer Institute in Switzerland has investigated the potential to use solar energy for cement manufacture (Imhof, 1991,1997, 2000) but it is not clear that this work is continuing. Work at the University of Adelaide investigated the potential for use of solar energy to make lime (Craig, 2010). It was demonstrated that limestone could be calcined to produce commercial quality quicklime using solar radiant heat alone. The concept of a practical furnace with heat recovery from the evolved CO_2 was also developed. However, the intermittent nature of solar radiation together with the extremely high capital cost of the solar collector field meant that the lime produced this way would cost several orders of magnitude more than by conventional means and would be simply unaffordable.

Much emphasis is placed on clean energy from electricity, which may be derived from natural sources (hydro-electric, solar, wind and wave) or by conversion of fuels (conventional or alternative). We have been beneficiating fossil fuels since the construction of the first power station to generate electricity in the 19th century, and ironically, power generation is now identified as the primary cause of anthropogenic CO_2 emissions. A typical current generation, water tube power station is ~38–44% thermally efficient, depending on the location. This limit on efficiency is a consequence of the steam cycle. Next generation boilers (super-critical) will improve this to ~50%. A combined cycle gas turbine (CCGT) system can achieve 50–60% efficiency, but uses a precious commodity (natural gas) or an already treated syngas. Latest fuel cell technologies can achieve ~65–70% efficiency. It is therefore clear that unless the electrical power is derived from a non-fuel source there is a carbon penalty of between 30% and 60% between the 'clean' electrical power and the 'dirty' fossil fuel power.

With the exception of hydroelectric power, which relies totally on geographical location for its availability, the technologies of the other potential non-fossil fuel options are not sufficiently advanced to be applied to demands of most energy intensive industrial processes. Indeed it is almost certain that these sources of electricity will primarily remain applicable to domestic, public (i.e. office buildings, shops, hospitals, street lighting, etc.), light industrial and perhaps transport demands.

15.4 Trends in Furnace Controls

Advances in telemetry and the power of computers to process and handle data are already impacting on the operation of many furnaces. The ability to almost instantly process operating data and the development of many more on-line analytical instruments makes the task of operating furnaces easier, providing that the information is presented to the operator in a clear, concise format. Unfortunately it is often the case that the control room screen information is less than perfect, ranging from those designs that present every measurement on very crowded and confused spread-sheets, to a Spartan set of numbers that give a general management overview of the operation, but are of little use to the operator. There is a potential for the 'smart' technologies that IT systems are developing at breakneck speed to obscure the basic information demands and over-analyse data beyond its true value. Such systems have great potential to confuse operators, especially in a process emergency, where "data overload" can render the operator impotent and cause a serious accident, such as an explosion.

15.5 New Applications for Furnaces

Although further evolution of furnace design is likely to be incremental, there is a strong probability of completely new applications that will require new types of furnace or major adaptions of existing designs. Emerging needs, currently evident, include the production of a range of nano-materials, recycling and separation of the various metals from discarded electronic equipment, processing of potential new minerals, etc.

The techniques described in this book should enable the straightforward design of a furnace for a new process, provided that the requirements of the application are well understood. This understanding of the process requirements is fundamental, without it the design of a new furnace becomes a trial and error affair, at best. A wide range of engineering simulation programs are available to assist the development of processes today but their use requires considerable intellectual input to achieve realistic predictions. Provided this input is forthcoming, as they were for the heat exchange reformer described in section 14.3 of the previous chapter, then the design of a new process is relatively straightforward using the techniques described in this book.

If a suitable furnace design cannot be developed for the process, then the process requirements will need to be re-examined to ensure that the conditions are realistic. Using the available physical and mathematical modelling techniques, all this can be undertaken using modelling, avoiding the risk of failure involving expensive prototypes. However, once the design has been derived, it advisable to build a pilot plant to test the concept before building the full size plant. This will identify any operational problems that may not be adequately detected during the steady state modelling stage.

15.6 Concluding Remarks

As mentioned previously, predicting the future is extremely difficult or practically impossible, especially it seems with regard to the cost of energy. Unforeseen, individual events can have a huge impact, particularly on the supply of fossil fuel.

For example, during the 1960s natural gas was only generally available in North America and Algeria with the Methane Pioneer transporting the first cargo of liquefied natural gas from Louisiana to Canvey Island in the UK in 1959 (Noble 2009).

At that time in Europe, cheap oil was rapidly replacing expensive coal as the fuel of choice. Both industrial furnaces and coal fired power stations were converted to burn heavy (No6) fuel oil and new large oil-fired power stations were being constructed such as at Fawley and Pembroke in the UK, each of 2000 MWe, Torrens Island in South

Australia and Malmo and Vasteras, both in Sweden. Yet even before the final units were commissioned, closure of the Suez Canal in 1967 heralded the end of cheap oil. However, at the same time, and less than 10 years since the Methane Pioneer set sail with it's first cargo of LNG, Australia, The Netherlands and the UK had their own indigenous supplies of natural gas. Where available, natural gas became the fuel of choice.

The best economic and engineering brains in the early 1960s saw oil as the fuel of the future and invested large sums in capital plant as consequence. However, even before all the plant was commissioned, the economic scenario had changed resulting in the plant being uneconomic or redundant. These events have not been described in order to criticise the economists and engineers who made those decisions but to illustrate the difficulty of making any predictions in this field. Those who opted for fuel flexibility were the clear winners.

By contrast, environmental trends are generally easier to predict, because of the long lag time between initial discussion and implementation. Typically, concern is raised amongst the scientific community regarding the need to reduce emissions of a particular pollutant. This concern is then debated in the community, legislation follows and finally implementation, the whole process taking one or two decades. The development of new processes usually occupies a similar gestation time frame, so those needs can also be foreseen.

Furnace design manufacture and supply is a competitive business and it is important that engineers and managers in the field stay up to date with current requirements. Those who also spend time researching process developments, look to the future and maintain process flexibility will have an added competitive advantage.

References

Anderson, K., & Bows, A. (2011). Beyond 'dangerous' climate change: emission scenarios for a new world. Philosophical Transactions of the Royal Society A: Mathematical. *Physical and Engineering Sciences, 369*, 20–44.

Argonne, (2009). *GREET (Greenhouse Gases, Regulated Emissions, and Energy Use in Transportation*. Available free at http://greet.es.anl.gov/ (accessed 15 Feb 2013).

Boorstin, D. J. (1961). *The Image. A guide to Pseudo-events in America* (1st ed.), eISBN 978-0-307-81916-1

Connolly, S., & Cusco, L., 2007, Hazard for high pressure carbon dioxide releases during carbon dioxide sequestration processes, Loss Prevention 2007, 12th International symposium on loss prevention and safety promotion in the process industries, Edinburgh.

Craig, R. A. (2010). *The use of concentrated solar energy to thermally decompose limestone*. PhD Thesis. University of Adelaide.

DNV (Det Norske Veritas). (2010). *Design and operation of CO_2 pipelines*. Recommended Practice DNV-RP-J202.

Higman, C., & van der Burgt, M. (2008). *Gasification* (2nd ed) (pp. 2–4). Oxford: Elsevier.

Imhof, A. (1991). The cyclone reactor – An atmospheric open solar reactor. *Solar Energy Materials, 24*(1–4), 733–741.

Imhof, A. (1996). Decomposition of limestone in a solar reactor. *Renewable Energy Materials, 10*(2–3), 239–246.

Imhof, A. (2000). Solar cement plants – an interesting challenge for business and Science. *ZKG International, 53*(8), 239–246.

McKinsey and Company, (2008). *Carbon Capture and Storage: Assessing the Economics*. New York, NY: McKinsey Report.

Metz, B., et al. (Ed), IPCC, 2005, Special Report on Carbon Dioxide Capture and Storage, Geneva, Switzerland.

Noble, P.G., LNG Shipping 1959–2009, Society of Naval Architects and Marine Engineers, Texas meeting, Feb 2009, available at http://higherlogicdownload.s3.amazonaws.com/SNAME/1dcdb863-8881-4263-af8d-530101f64412/UploadedFiles/c3352777fcaa4c4daa8f125c0a7c03e9.pdf. Accessed 16/2/2013.

Steynberg, A., & Dry, M. E. (Eds.). (2004). *Fischer-Tropsch Technology* (pp. 17–30). Amsterdam: Elsevier.

The Royal Society, (2009). *Geoengineering the climate: Science, governance and uncertainty*.

Index

Note: Page numbers followed by "f" denote figures; "t" tables; and "b" boxes.

A

Abraham Darby, 2, 13, 14f, 416
Absorptivity, *see* Radiation
Acid mist, 387t
Acid rain, 378–379
Acoustic coupling, *see* Noise, combustion, driven oscillations
Activation energy, 20, 38–39, 380, 442, 467
Aeration of fine coal bins, 276
Aerodynamics, 59–61, 182–193, 236–237, 500–502
AGA, *see* Australian Gas Association (AGA)
AIChE, *see* American Institution of Chemical Engineers (AIChE)
Air. *See also* Combustion, air supply
  combustion, 140, 143
  cooling, 431
  damper, effect on flow, 191
  distribution, 20, 62–63, 189–193, 192f, 576–577
  duct design, 188–191
  excess, 12, 27, 34–36, 47, 51, 61–62, 158, 188, 216, 226, 268, 299–301, 315, 346, 405–406, 474
  flow patterns, multi-burner burner systems, 62–63, 188
  flow patterns, single burner systems, 185–188
  in-leakage, 157, 184, 200–201, 259, 301, 306, 315, 359
  lock, 255–256
  plenum and windbox design, 191–193
  primary, 50–56, 155, 162–164, 177, 181–182, 265–269, 279–280. *See also* Primary air, momentum; velocity
  purge, *see* Furnace, air purge
  register, 158, 192f
  secondary, 49–51, 59–61, 155, 163–164, 181–182, 194–196, 214, 405, 569, 585–589, 591, 593–595. *See also* Secondary air velocity
Alcoa calciner, 548f
American Institution of Chemical Engineers (AIChE), 327
Anchors, *see* Refractory, anchors
And gate, *see* Fault tree analysis
Anode, 16, 128–129
  off gas, 559, 561, 565t
Anti-friction lining, *see* Coal, bunker
Anti-node, 200
Arch roof, 429, 429f. *See also* Furnace, roof construction
  effect on gas velocities, 430
Arrhenius equation, 38–39, 40f
ASA, 246
Asbestos, 420, 440
Assets
  fixed, 509–510
  liquid or current, 509–511
Ash, *see* Coal, ash; Fuel, ash; Particulates, emissions
Asphaltene, 77
ASTM, 263
Atmospheric dispersion models, *see* Modelling
Atomisation, 144–145
Atomiser, 173–180, 250
Atomiser, pressure jet
  duplex, 176
  flow number, 175
  spill return, 174f, 175–176
  swirl spray, 174f, 175–176
  tip shut-off, 252
Atomiser, rotary cup, 249
Atomiser, twin fluid
  calibration curves, 179
  high pressure air or steam, 177
  low pressure air, 178f
  medium pressure air, 178f

Atomising temperature, 250
Australian Gas Association (AGA), 287
Australian Standards, 319

B

Babcock E-Mill, *see* Coal, mill, vertical spindle
Bag filter, 267, 321, 603
Balanced draft, *see* Combustion, air supply
Ball mills, *see* Coal, mill, ball type
BATNEEC, *see* Best available techniques not entailing excessive cost (BATNEEC)
Beehive kilns, 7–8, 416, 429
Belt feeder, *see* Coal, feeder raw coal
Belt weigher, 298–299
Besta feeder, *see* Coal, feeder raw coal
Best available techniques not entailing excessive cost (BATNEEC), 398
Bitumen (as fuel), 252
Bituminous coal, *see* Coal
Blast furnace, *see* Furnace, blast
Bleed valve, *see* Valve, vent
Blister copper, *see* Copper, blister
Bluff body, *see* Flame, stabilisation by
BMS, *see* Burner management system (BMS)
Boundary layer, 53, 99–100, 103–107, 211–212
Brick. *See also* Refractory, brick
Brick making, 7–8
British Gas Midland Research Station, 458
Bronze age, 2
BSI, 246, 322, 436–437
BTU deception, 476
Bubble principle, of emissions permitting, 398
Buckstay, *see* Furnace, roof construction
Burgess-Wheeler Law, 73–74
Burner
  Bunsen, 140
  coal, pulverised, 180–182
  design basics, 149–155, 542–546, 560–562
  effect of spacing on flame characteristics, 50, 200
  function, 541
  functional requirements, 541
  gas precessing jet, 403–404
  gas premixed
    low NO_x, 159
    nozzle mix, 156–157, 500–501, 501t
    nozzles, 160, 160f, 166
    radiant wall, 158
    safety issues with, 159–162
    size limitation, 162
    tunnel, 156f
    venturi mix, 156
  gas turbulent jet diffusion, 155
  modifications, 578–579
  multi-fuel, 541–542, 543f, 545f, 561f, 569f
  oil, 170–180
  oil, rate turndown, 173
  petroleum coke, 538, 541, 544–545
  pipe failure, 428–429
  quarls, 423–424, 435–436, 438
  reducing atmosphere, *see* Furnace, reducing atmosphere
  self-recuperative, 458, 531
  self regenerative, 458
  testing, 567–570
Burner management system (BMS), 252, 290, 321–333
  danger of tampering with timers, 317–319
  safety requirements, 322–324, 327–330

C

Cabin heater, refinery, 299
Calcining, 3–4, 9–10, 18, 149, 196, 462, 467–468
Calorific value (CV), 68, 70–72, 77–78, 142–143, 268, 298
Calorific value net, definition of, 222b, 293
CAPEX, *see* Costs, capital
Capital account, 509
Capital cost, *see* Furnace, capital cost
Carbide precipitation, 428. *See also* Intergranular corrosion; Weld decay
Carbon dioxide
  absorption/scrubbing, 611–613
  cryogenic separation, 610–611
  chemical looping, 610–611
  emissions, 29, 458, 609–610, 613–614, 620
  formation, 33
  oxy-fuel combustion, 614

radiation, 117–118
sequestration, 408–409
Carbon monoxide
emissions, 86, 276, 401, 402f
formation of, 34, 250–251, 379–380
in-flame concentration contours, 143–144
as fuel, 68
measurement, 312, 346
Castable refractory, *see* Refractory, castable
Cathode off gas, 565t, 570
Cement
bond, *see* Refractory, castable
clinker, 11
high alumina, 235, 236f, 420
kiln cooler mass and energy balance, 602f
kiln mass and energy balance, 601–602
kiln operational problems-attempted resolution, 591–593
kiln operational problems–diagnosis, 583–591
Portland, 8, 467
Cenosphere, 45–46, 144, 394–395
Center for Chemical Process Safety, *see* American Institution of Chemical Engineers (AIChE)
Ceramic fibre. *See also* Kiln; Refractory, fibre, lining
CERAM Research, 447
CFD, *see* Modelling
Chalcopyrite, 13
Char, *see* Combustion, char
Charcoal, 2, 13
Chemical reaction, *see* Reaction
Claudius Peters EM mill, *see* Coal, mill, vertical spindle
Climate change, 609–610
Close circuit cooling, *see* Furnace, cooling systems
Coal
ash, 399
bunker, 254–256
burner, *see* Burner, coal
conveying roping, 281
conveying velocity, 280–281
deposits in furnaces, hazards of, 317–320
de-watering curves, 256
drying, 256, 269–273
feeder pulverised, 269–273
feeder raw coal, 254–256
fineness, 263–264
firing system-dangerous, 596–599
firing system direct, 265–269
firing system fans, 273–274
firing system indirect, 265–266
firing system-poorly performing, 599–604
firing system-upgrade, 599–604
froth flotation, 399
grinding, 256, 258–259, 259f, 260f, 265–269, 538, 603f
mill
ball type, 258–259
grinding capacity, 256, 263–265
heat balance, 271f
high speed, 258t, 261–262
inlet temperature, 269, 272f
outlet temperature, 269–271
vertical spindle, 260–261
moisture, 256
moisture inherent, 256, 272f
pulverised, 253–283. *See also* Coal, feeder pulverised
feeding, 277–279
storage, 274–276
raw coal reception, storage and handling, 254
residue on sieve, 263
washed, 399
Coalbrookdale, 2
Coke, 2, 13
Coke, petroleum, 182, 258–259
Cold plugs, *see* Oil, cold plugs
Combustion
air supply, balanced draft, 184
air supply, forced draft, 184
air supply, induced draft, 184
air supply, natural draft, 183
char, 43–46, 74f, 144, 265, 346, 383–384, 394–395
chemistry, 32–33, 108, 238–239, 378–379, 409–411
heterogeneous, 144–149
intensity, 149–150, 155–156, 193–194
noise, *see* Noise, combustion
pulsation, *see* Noise, combustion, driven oscillations
roar, *see* Noise, combustion
of sprays, 171–172
system scaling, 193–196
volatiles, 45–46

Combustion control, *see* Furnace control, air/fuel ratio control
Commissioning, 546–547
Computational fluid dynamics, *see* Modelling
Conceptual design, *see* Furnace design, conceptual
Conduction
  steady state, 91–92
  transient, 92–99
Consequential losses, 185–186, 327
Constant combustion intensity scaling, *see* Combustion, system scaling
Constant residence time scaling, *see* Combustion, system scaling
Constant velocity scaling, *see* Combustion, system scaling
Consumables, 509t, 515–516
Contingency, 517
Convection
  convective heat transfer coefficient, 99–107, 217, 220–221, 294, 341
  forced, 90, 103–104, 128–129, 218–219, 294, 371–374, 446, 467, 486–487
  natural, 90, 93, 103, 128–129, 230, 341, 416–417, 469–470
Converter, *see* Copper, converter
Cooler, clinker, 11
Cooling systems, *see* Furnace, cooling systems
Cooling water
  quality, 431
  temperatures, 306–307
  treatment, 432–433
Copper
  blister, 13–16
  converter Pierce-Smith, 13, 15f
  matte, 13
  refining, 16
  smelting, 13–16
Corrective action, *see* Sub-stoichiometric, operation (unintentional)
Costs
  fixed, 510
  variable, 510
  capital, 510–511
Cost accounting, 508–509
Cost effective design, *see* Furnace design, cost effective
Cost scaling factor, 514
Counter current heat transfer, *see* Heat exchanger; Heat recovery
Cracked oil, *see* Oil, high asphaltene
Craya-Curtet parameter, *see* Similarity parameter
Critical pressure, 198–199
Critical time for ignition, 319–320
Crossed strings, 122–123
Current density, 129–130
CV, *see* Calorific value (CV)
Cyclone, 11, 407–408

D

Danger-side failure, *see* Programmable logic controller (PLC), failure modes
Darby's blast furnace, *see* Abraham Darby
DCS, *see* Distributed control system (DCS)
Dead legs, in oil pipework, 77, 252
Dense phase conveying, *see* Coal, pulverized; conveying
Design, *see* Furnace design
Design validation, *see* Furnace design, validation of
Devolatilisation, 43–45, 404
Dewpoint, 267, 308
Diesel oil, *see* Oil, distillate
Differential thermal expansion, *see* Thermal expansion, differential in furnaces
Dimensional analysis, 100–101
Dimensionless groups, 93, 100–101, 104–107
  Biot modulus, 98–99, 368
  Buckingham's theorem, 101
  Grashof number, 102
  Lewis number, 108–109
  Nusselt number, 102–103
  Prandtl number, 102–103, 109
  Reynolds number, 57–58, 102, 104b, 131–133, 161b, 211–212, 216, 238, 563–564
  Stanton number, 103
  swirl number, 57–59, 154–155
DIN standards, 246, 443
Dioxins, 388–391
Direct firing, *see* Coal, firing system direct
Discretization, 232

Distributed control system (DCS), 290–291, 330
Drag chain feeder, *see* Coal, feeder raw coal
Drop, *see* Droplet
Droplet
  oil, 144–149, 175–176, 238, 386–387
  size, 146–149, 179–180
  size prediction, 179–180
Drying and curing of refractory, *see* Refractory, drying and curing
Dust, *see* Particulates

E

EBIT, *see* Profit/profitability
Efficiency
  combustion, 33, 155–156, 185, 302, 346, 359, 403–404
  conversion, 313, 359–361
  electrical, 129–130
  thermal, 13–16, 29–30, 47, 61, 217, 218f, 338, 340, 359–360, 399, 482, 487–488, 491–492, 495–498, 508–509, 529–531, 536, 559
Electricity generation
  super-critical boiler, 620
  CCGT, 620
  fuel cell, 613
  hydro-electric, 620
Electrical heating
  arc, 126, 128–129, 440
  dielectric, 130–131
  induction, 126, 129–130
  infra-red, 131
  resistance, 126–128
Electrical resistivity, 126–128
Electrostatic precipitator, 317, 321, 324, 407–408, 581
Electrostatic sparks, 321
Emergency shut down, 325
Emissions taxation, 458
Emissions, particulate, *see* Particulates, emissions
Emissivity, *see* Radiation
Emissivity data, 134t–137t
Endothermic, *see* Reaction
Energy balance, 124, 152, 219, 229–230, 343–360, 468, 501–502, 547, 549, 551–552, 601–602, 602f
Energy triangle, 360–361
Entrainment, 48–50, 48f, 50f, 51f, 153–154, 156, 163–164, 172f, 198–199, 211, 227, 561, 564
Environmental Protection Agency (EPA), 327
Equilibrium constant, 38–39, 43, 63–64, 381–382
Equipment factor, *see* Lang factor
Equity, 511
Excess air, *see* Air, excess
Exchange area
  direct, 123–124, 228
  total, 124–125, 219–221
Exchange factor, *see* Exchange area, total
Exergy, 364–365
Expansion joints, 420
Explosion
  effect zone, 326
  occurrence, 320–321
  pressure, 319
  risk, 16–17, 25, 157, 252, 255–256, 258–259, 269, 285, 316–317
  vent, 248–249, 276
Explosive factor, *see* Explosion, effect zone; Safety

F

Fail-safe requirements, *see* Burner management system (BMS), safety requirements
False, trips, 324
False air, *see* Air, in-leakage
Fan noise, *see* Noise, fan
Fatigue failure, 423, 427–428
Fault tree analysis, 327–329, 328f
FGR, *see* Flue gas recirculation (FGR)
Filter
  gas, 248, 300–301
  oil, 249–250
Financial leverage, *see* Financial ratios
Financial ratios, 511–514
Fine coal
  conveying, *see* Coal, conveying
  feeding, *see* Coal, pulverized, feeding
  storage, *see* Coal, pulverized, storage
Fire detection, 276
Fire fighting, 276
Fire risk, 258–259, 267, 269, 273–274
Fire safe, *see* Valve, fire safe

Fire triangle, 316, 316f
Flame
  confinement, 153
  detector, 322–323, 331
  diffusion, 140–141, 393
  luminous, 141, 165, 475
  non-luminous, 141, 155–157
  premixed, 142f, 155, 161b, 402f
  quenching, 160–162, 321, 390–391
  soot formation, 81, 228, 392–394
  speed, 142–143, 160, 401
  stabilisation, definition of, 152
  stabilisation by bluff body, 142, 154, 171–172, 191, 281–282, 562
  stabilisation by re-radiation, 152–153, 181–182
  stabilisation by swirler, 153
  stability, 47–48, 50, 52t, 153, 155, 262, 543–544, 578–579
  temperature effect of excess air on, 157–158. *See also* Burner
Flammability limits
  calculation for gas mixtures, 72–73
  definition, 72–75
  effect of pressure, 73–75
  effect of temperature, 73–75
  in premix burners, 141–143, 158–162, 166, 170
  values at room temperature, 73t
Flammable mixtures, sources of, 316
Flare pulsation, *see* Combustion, pulsation
Flash smelter, 16, 16f, 18
Flat roof, *see* Furnace, roof construction
Flexible hose, *see* Hose
Flow control valve, *see* Valve, flow control
Flow number (FN), *see* Atomiser, pressure jet, flow number
Flow sheet, 343–344, 464–465
Flue gas recirculation (FGR), 158, 400–403
Flue gas sampling and analysis, 302–313
  extractive systems
    cold gas systems, 308
    dilution systems, 308–309
    hot wet gas systems, 308–309
  in-situ analysers
    CO_2 analysers, 312
    CO analysers, 312
    cross duct analysers, 312–313
    dust monitors, 309–310
    folded beam analysers, 312
    optical absorption spectroscopy, 312–313
    oxygen analysers, 310–311
    SO_2 analysers, 312
Flux density, 228–229
Fog, 378
Forced draft, *see* Combustion, air supply
Formwork and moulds, for castable refractory, 423–425
Fouling index, 396, 398. *See also* Slagging
Free radical, 37, 387t
Fuel
  air mixing, *see* Mixing, air and fuel
  ash, 68, 76t, 77–79, 78t, 84, 181, 253, 261–262, 268, 346, 394–396, 399, 473–475
  ash effect on furnace and product, 473
  availability, 68
  beneficiation, 620
  biomass, 69, 78–79
  blast furnace gas, 71, 524t, 529–531
  butane, 69, 71
  carbon/hydrogen ratio, effect on emissivity, 81, 82f
  carbon monoxide, 83
  charcoal, 78–79
  choice, 68, 84, 472–476
  coal bituminous, 78–79
  coke, 77
  costs, 84–85, 192–193, 458, 472–473
  distillate oil, 472–473
  economy, 416, 540
  effect on heat transfer, 75, 79–82
  ethanol, 68
  explosion risk, *see* Safety
  flame radiation from, 75, 117
  gasification, 399–400, 613
  handling systems, 245–288
  hydrogenation, 613
  hydrogen, 68
  lean gas, 70–71
  lignite, 77, 78t
  liquifaction, 399–400, 613
  methanol, 68
  natural gas, 69
  non-hydrocarbon, 68
  propane, 69, 71
  proximate analysis, 346
  residual oil, 75

rich gas, 70–71
security of supply, 84–85
sulphur, 69, 86, 474
ultimate analysis, 34b, 346
used lubricating oil, 77
wastes, 79–80
wood, 77
Fuel cells, 558–559, 570–571
Furans, 388–391
Furnace. *See also* Kiln
air purge (safety), 317
annealing, 23–24, 23f
anode, 16, 17f
atmosphere, 16–17, 17f, 25
billet, 20–21. *See also* Furnace, slab
blast, 13, 83, 465–466
capital cost, 28
classification, 5
continuous, 21
cooling systems, 431–433
efficiency, *see* Efficiency
flash, 18–20, 19f, 547–556
flexibility of operation, 83
fluid bed, 18–20
incinerators, 24–25
ingot reheating, 542
modelling, *see* Modelling
multiple hearth, 25
noise, *see* Noise
performance, effect of feed inconsistency, 471
performance chart, 340–343
pusher, 431
reducing atmosphere, 16–17, 25, 157
refinery and petrochemical, 26–27
resource recovery, 24–25
reverbatory, 13, 15f, 18
roof construction, 429–431
slab, 498–500. *See also* Furnace, billet
smelting, 13–16, 18
steel reheating, 22–23
steelwork, 427–429
structural loadings, 427
structure, construction methods, 417–433
structure, performance requirements, 416–417, 445
suspension, *see* Furnace, flash
walking beam, 22–23
zones, 22–23
Furnace control
air/fuel ratio control, 314–315
controlled inputs, 291
control strategy, 291–292
excess air, 299–301
flow, air, 291, 299–301
flow, gaseous fuels, 291, 297–298
heat input, 298–299
Furnace design
burner selection, 498–501
charging, 489–491
conceptual, 462–481
constraints, 460
cost effective, 459, 462
dimensions, effect on efficiency, 489, 491–492
duty, establishment of, 464–465
life, 68
new processes, 469–470
open ended nature, 462
process functions, 464–466
process knowledge, reliability of, 468–470
selection of instrumentation and controls, 503–505
size, determining factors, 481–482
sizing, 481–498
using the well stirred model, 487–488, 491, 495
worked examples, 482–483
validation of, 501–503
Furnace instrumentation. *See also* Flue gas sampling and analysis
flow, liquid fuels, 297–298
flow, solid fuels, 298–299
fuzzy logic, 292
pressure switch, 323
pressure transmitter, 329
process control, 290
product temperature, 291–292
rule based, 292
signal transmitters, 323
temperature, 292–296
temperature, by radiation, 292–293, 295
temperature, by ultrasonic device, 292–293, 296
temperature, resistance thermometer, 292–293
temperature, suction pyrometer, 294
temperature, thermocouple, 292–293

Furnace instrumentation (*Continued*)
temperature, venturi pneumatic pyrometer, 294–295, 295f
Furnace safety, 315–321
Furnace start-up, 317–320
Furnace start-up, hazards with oil firing, 317–320
Fuzzy logic, *see* Furnace instrumentation, fuzzy logic

G

Gas, as fuel, *see* Fuel
Gas burner, *see* Burner, gas
Gas leaks, safety issues, 316
Gas manufactured, 69–71
Gas nozzle
drilling pattern, 168–169, 423
port sizing, 166–168, 543–544
supersonic flow, 167–168, 591
Gas plasma, 128–129
Gas valve train, *see* Valve, train, gas
Gas velocity, *see* Velocity, gas
Geoengineering, 609–610
Glass tank, 11–12
Global warming, 458
Greenhouse gas, 3, 29
Grinding capacity, *see* Coal, mill, grinding capacity
Gunning, *see* Refractory, gunning
Gyrotherm burner, *see* Burner, gas precessing jet

H

Haldor Topsoe, 549–550, 558–559, 566–569, 571
Hardgrove Index, 263
Hardwired shut down, 290
Hastelloy, *see* Proprietary high nickel alloys
Health and Safety Executive (HSE), 325
Heat balance, *see* Energy balance
Heat exchanger
design, 251–252
recuperative, 366–368
regenerative, 437, 480
Heat flux, 90, 101t, 113, 149–152, 150f, 157, 210, 231, 232f, 485–486, 486t, 489, 491–495, 498–500, 500f, 566–567
effect of burner design, 498–501
effect of furnace arrangement, 500–501
profiles, importance of, 465
Heat recovery, 476–481
air preheating, 11, 226, 371, 372t, 487–488, 497f
from cooling water, 480–481
economic considerations, 481
estimating the potential for, 477–478
from hot flue gas, 478–480
from hot product, 477–478
recuperators, 12, 22–23, 478, 529. *See also* Burner, self recuperative; Heat exchanger, design
from shell losses, 480–481
by steam generation, 11, 226, 371, 372t, 480, 487–488, 497f
Heating value, *see* Calorific value (CV)
Heavy metal, catalyst, 386–387, 389–390
Heavy metal, emissions, 286
Herreschoff roaster, *see* Furnace, multiple hearth
Higher heating value, *see* Calorific value (CV)
High grade heat, 362–363, 477
High speed mills, *see* Coal, mill, high speed
High temperature alloys, 442–445
High temperature and refractory metals, 440–445
High temperature process, definition, 3
Hose, 196, 199–200
Hot gas sampling
probe, 549
procedure, 550–552
Hot spots, 21–22, 27
HSE, *see* Health and Safety Executive (HSE)
Hydrogen, 16–17, 68
economy, 476
flames, heat transfer from, 476
sulphide, 387

I

IChemE Guidelines, *see* Institution of Chemical Engineers (IChemE) Guidelines
IGE, *see* Institution of Gas Engineers (IGE)
Igniter, 170–171, 317
Ignition sources, 316–317, 321
elimination of, 321

Incoloy, *see* Proprietary high nickel alloys
Inconel, *see* Proprietary high nickel alloys
Indirect firing, *see* Coal, firing system indirect
Induced draft, *see* Combustion, air supply
Inert gas, 72, 276
Inherent moisture, *see* Coal, moisture inherent
Injection velocity, of pulverised coal, 182
Institution of Chemical Engineers (IChemE) Guidelines, 265, 276, 327, 595
Institution of Gas Engineers (IGE), 322
Insulating layer, 151, 419
Intergranular corrosion, 444. *See also* Weld decay; Carbide precipitation
Internal rate of return (IRR), 517–518
Iron bridge, 2, 2f
IR radiation, 331–332
Irreversible expansion, *see* Refractory, irreversible expansion
Isothermal, 19–20

J

Jet
  confined, 49–51, 50f, 163–164, 214, 589
  entrainment, 48–50, 153–154, 164–165, 167, 227, 561–562
  free, 48–50, 48f, 51f
  laminar, 57–58, 104, 161b, 170, 393
  momentum, 59, 164–165, 181–182, 211, 265, 562, 589–591
  noise, *see* Noise, jet
  plasma, 128
  turbulent, 51–52, 143–144, 153, 155, 162–165, 198–199, 213

K

Kerosene, *see* Fuel, distillate oil
Kiln. *See also* Furnace
  cement, 11f, 61, 62f, 144, 230f, 231f, 266f, 299–300, 463f
  downdraft, 7–8
  lime, 9f, 10f, 284, 475
  mineral sand, 25f
  mixed feed, 9–10, 9f
  pottery, 3–4, 7–8
  preheater, 13–16
  rotary, 10–11, 19–20, 59, 60f
  rotary, evolution of, 462
  shaft, 9, 235, 236f
  twin shaft, 9–10
  vertical, 9
Kirchhoff's law, 116–117, 121

L

Laboratory and pilot plant data, 464–465, 482, 491
Lagging, 91–92, 252. *See also* Refractory, insulating
Lang factor, 516t
Latterite ore, 25
Leak testing, 71, 248–249
Lean phase conveying, *see* Coal, conveying
Le Chatelier's rule, 72–73
Level indicators for fine coal bin, 276
Liabilities, 509–511
Ligaments (oil), *see* Atomisation
Lime, 8–11, 9f
  kiln temperature profiles, 540f
  regeneration process, 539–540
  sludge kilns, 538–547
Liquefied natural gas (LNG), 69, 621
Liquidity, *see* Financial ratios
Live loading, *see* Furnace, structural loadings
Load recuperation, 22–23, 458
Log mean temperature difference, 366
Long furnace model, *see* Modelling
Lower heating value, *see* Calorific value, net, definition of
Low grade heat, 362–363, 477, 480–481
Low NO_x combustion
  flameless oxidation, FLOX, 403–404
  flue gas recirculation, FGR, 158, 400–403
  high efficiency HEC, 403–404
  reburn, 405–406
  staging, 404, 406–407
Low temperature process, definition, 3
LPG, *see* Fuel, propane; butane

M

Mass balance, 34b, 343–344, 352t, 357t, 359
  by key component, 348t

Mass flow feeders, *see* Coal, feeder pulverised
Mass flow in bunkers and bins, 254–256
Matte, *see* Copper, matte
Maximum flammable concentration, *see* Flammability limits
Maximum permissible oxygen concentration to prevent ignition, 72
Mean beam length, 125–126
Mechanical agitation of fine coal, 274–276
Metallic furnace components, effect of intermittent service on life, 444
Metallic furnace components, service duty, 440–441
Meter, flow, 253
Minimum flammable concentration, *see* Flammability limits
Mixing
  air and fuel, 33, 47–51, 52t, 57, 140, 142–143, 154, 160–162, 264, 279–280, 315, 319, 360, 379–380, 400–407, 541–542, 561, 578–579, 583, 588, 590, 594
  diffusion, 47, 140–141, 143–144, 155, 162–165, 210
  length, Prandtl, *see* Turbulence
  premix, 41–43, 47, 50, 140–149, 155–162, 198, 201
Mixture. *See also* Excess air
  fuel/air, 142–143
  stoichiometric, 141–142
Model grids
  body-fitted, 234
  structured, 234
  unstructured, 234
  zone, 234
Modelling, 164, 209–244
  acid/alkali, 212–213, 542–543, 552, 591
  air, 59, 190, 211–212, 575–576
  atmospheric dispersion, 409–411
  combustion chemistry, 45–46, 386
  computational fluid dynamics (CFD), 58–59, 104, 217, 232–238, 239t, 386, 409–411, 553, 554f, 555–556
  convergence, 237–238
  diagnostic, 573–576
  flow similarity, 213, 216
  geometric similarity, 213
  heat flux, 566–567, 582, 592
  long furnace, 152, 226–228, 562, 566–567, 573–574, 589
  mathematical, 217–238, 553–556, 573–574, 589–590
  partial, 210
  physical, 185–186, 190, 192–193, 211–217, 211f, 431, 552–553, 575–576, 577f, 588–589
  scaling, 144, 193–196
  two phase flow, 238
  validation of, 470
  water, 59, 211–212, 211f, 575–576
  well-stirred furnace, 152, 217, 231, 371, 487–488, 488t, 490t, 491, 493t, 495, 495t, 497t, 498, 520, 553
  zone
    three dimensional, 228–231
    two dimensional, 228–231
Momentum
  flux, 48–49, 164
  jet, *see* Jet, momentum
  ratio, 50, 164, 168, 195
Monolithic lining, 417–419, 418f, 421–427
Mortar, 420
Mouldable refractory, *see* Refractory, mouldable and rammable
Moulds, *see* Formwork and moulds, for castable refractory
Multiple discharge bins, *see* Coal, pulverized, storage

N

Natural draft, *see* Combustion, air supply
Needle reinforcing (for refractory), *see* Refractory, needle reinforcing
NEPA, 246, 253, 265, 322
Net present value (NPV), 517–518
Nimonic, *see* Proprietary high nickel alloys
Nitrogen oxides (NO_x). *See also* Low NO_x combustion
  effect of furnace size on emissions, 491
  emissions, 6t, 12
  formation, 380–386
  fuel, 380, 382–384
  measurement, 302, 308, 312
  prompt, 384–385
  selective catalytic reduction (SCR), 407

selective non-catalytic reduction (SNCR), 407
thermal, 302, 381–382, 401–402, 409–411
Node, 200, 203
Noise
attenuation, 200–201
combustion, 201–204
driven oscillations, 201–204
fan, 199
flow through pipe and valve, 199–200
gas, 248
jet, 198–199
measurement, 198
nozzle, 198–199
occupational exposure, 198
reverberation, 200
North American Combustion Handbook, 246–248
NO_x, *see* Nitrogen oxides (NO_x)

O

Oil. *See also* Fuel
burner, *see* Burner, oil
cold and viscous, 317
cold plugs in pipes, hazards of, 252–253
cracked, 249
deposits in furnaces, hazards of, 316
desulphurisation, 399
distillate, 472–473
film, *see* Atomisation
filter, *see* Filter, oil
heating, 249–250
high asphaltene, 251–252
leaks, safety issues, 316, 567
pumping, 249–252
quality, 251–252
reformed, 249
residual, 151
ring main, 249–250
storage, 249–252
velocity, *see* Velocity, oil
viscosity, 75, 175, 179, 249
Open circuit cooling, *see* Furnace, cooling systems
Operator, 292
OPEX, *see* Costs, fixed; variable
Or gate, *see* Fault tree analysis
Outokumpu process, 13–16
Oxidation of metals, 442
Oxygen enrichment, 531

P

Packed bed, gas flow pressure loss, 495–496
PAH, *see* Polycyclic aromatic hydrocarbons (PAH)
Particle
burning time, 149
drag, 238
size, 146–149
swelling, 43–45
Particulates
bag filter, 317, 390–391, 407–408
electrostatic precipitator, 317, 321, 407–408
emissions, 286, 310, 378, 391–398
measurement, 295–296, 296f, 298, 302, 344–346, 359
Passivation of metals, 442
Pay back, 517–518
PCB, *see* Polychlorinated biphenyls (PCB)
Penetration depth, 129–130
Petroleum coke, *see* Coke, petroleum
PFD, *see* Probability of failure on demand (PFD)
Pfister feeder, 278–279
P &ID, *see* Process and Instrument diagram (P&ID)
Pierce-Smith converter, *see* Copper, converter
Pilot plant, role in risk reduction for new processes, 470
Pilot plant data, *see* Laboratory and pilot plant data
Pinch point, 364–365
Pipework standards, 249–250
Plastic, refractory, *see* Refractory, plastic
PLC, *see* Programmable logic controller (PLC)
Plenum, *see* Air, plenum and windbox design
Poiseuille's equation, 161b
Polychlorinated biphenyls (PCB), 388–391
Polycyclic aromatic hydrocarbons (PAH), 388, 392, 398–399
Power factor, 130

Preheating, 4, 9, 11, 13–16, 22–23, 226, 340, 371, 372t, 467, 478, 548–549, 581–582
Premixed burner, *see* Burner, gas premixed
Present worth profitability index (PWPI), 518
Pressure control valve, *see* Valve, pressure control
Pressure switches, *see* Furnace instrumentation, pressure switch
Primary air. *See also* Air, primary
  momentum, 162–163, 181–182
  velocity, 182, 194
Probability of failure on demand (PFD), 325–326. *See also* Burner management system; safety requirements
Process and Instrument diagram (P&ID), 246, 252, 275f
Process control, 69
Process design, *see* Furnace design
Process envelope, 343–344
Process excursion, 324
Product quality, 291
Product temperature, 291–292
Product transport, 427–428
Profit/profitability, 511
Profit margin, 511
Programmable logic controller (PLC), 290, 324–326
  failure modes, 290, 324–326
  safety requirements, 324–326
Project costing, 514–517
Proprietary high nickel alloys, 445
Public consultation, 79–80
Pulverisation of coal, 144–145
Pulverised coal burner, *see* Burner, coal, pulverised
Pulverised coal storage, feeding, and firing systems, *see* Coal, firing systems
Pumping and heating unit, oil, 250
Purge
  air, *see* Furnace start-up
  oil, 246

Q

Quarls, *see* Burner, quarls

R

Rabble arm, 25
Radiation
  absorption coefficient, 115, 119
  absorptivity, 116–120
  black body, 113–115
  dust, particulates, 118–119, 227
  emissivity, 114, 116–120, 125–126, 218–219, 226, 228, 399, 546, 582, 590
  equivalent grey surface, 124–125
  gas body, 115, 125–126
  grey body, 114–115
  opacity, 118–119
  reflectivity, 121–122
  rough surface, 113, 116t
  selective absorption/emission, 115
  smooth surface, 113
  soot, 118–119, 227
  transmissivity, 131–133
  view factor, 112–113, 120–125
  weighted grey gases, 118, 228
  white body, 113t
Rammable refractory, *see* Refractory, mouldable and rammable
Rate determining step, 4
Rat-hole flow, 254, 274
Raw coal feeder, *see* Coal, feeder raw coal
Reactedness, 41
Reaction
  chain, 32, 37, 39
  char surface coefficient, 46–47
  diffusion coefficient, 46
  furnace feed and product, 470–471
  kinetics, 37–47, 155–156, 210, 386–387
  rate, 38–43, 43f, 45, 63–64, 144, 157, 379–382, 401, 407, 409–411
Recirculation
  external, 50–51, 154
  internal, 50–51, 154–155, 171–172
Recuperator, *see* Heat recovery
Redler feeder, *see* Coal, feeder raw coal
Reducing conditions, effect on metallic components, 444
Redundancy (in BMS systems), 290
Refinery flare pulsation, *see* Noise, combustion, driven oscillations
Refinery heater-tube failure, 571–579

Reformed oil, *see* Oil, high asphaltene
Refractory
  alumina, aluminous, 437–438
  anchors, 423
  brick
    heating rate, 420–421
    laying methods, 419
    lining, 419–422
    special profile, 421
  carbon, 440
  castable, 422–423
    cement bond, 426
    ceramic bond, 426
    low cement, 422
  ceramic fibre, 417–419, 435–440
    lining, 417–419
    rope, 420
  chromite, 438–439
  cold crushing strength, 436–437, 439
  concrete, *see* Refractory, castable
  density, 436–437, 449t, 450t, 451t, 452t, 453t, 454t
  dolomite, 439
  drying and curing, 425–427
  failure, 420–421, 426–427
  gunning, 425–427, 430–431
  hearth, 23–24
  insulating, 440, 454t
  irreversible expansion, 420
  life, 84
  magnesite, 438–439, 451t, 452t
  mouldable and rammable, 427
  moulds, *see* Formwork and moulds, for castable refractory
  needle reinforcing, 426
  permanent dimensional change on heating, 452t
  plastic, 422. *See also* Refractory, mouldable and rammable
  porosity, 436–437
  refractoriness, 436–437
  refractoriness under load, 436–437
  silica, siliceous, 437
  specific gravity, true and apparent, 436–437
  specific heat, 436–437
  thermal conductivity, 436–437
  thermal expansion, 436–437
  thermal shock resistance, 436–437
  zircon, zirconia, 439
Regenerator, checker brickwork, 12. *See also* Heat recovery
Relay logic, 322–323, 323f
Reliability, 468–470
Re-radiation, 459
Resistance thermometer, *see* Furnace instrumentation, temperature
Resonant frequency, *see* Noise, combustion, driven oscillations
Return on investment (ROI), 517, 535
Revenue account, 509
Reverbatory furnace, *see* Furnace, reverbatory
Reverberation, *see* Noise, reverberation
Reynolds number, 104b, 211–212
Risk factors in furnace operation, 315–317
Roaster, *see* Furnace, fluid bed, multiple hearth
Roping, *see* Coal, conveying roping
Rosin Rammler distribution, 147–148, 148f
Rotary cup atomiser, *see* Atomiser, rotary cup
Rotary kiln, *see* Kiln, rotary
Rotary valve, *see* Fine coal, feeding
Rule based control, *see* Furnace instrumentation, fuzzy logic

S

Safety, 7, 85–86, 315–321
  check, pre-start, 248, 317–320
  shut-off system, 248–249
  shut-off valve, *see* Valve, fire safe, oil; safety shut off, gas
Safety integrity level (SIL), *see* Burner management system (BMS), safety requirements
Sardon Saxifrage mill, *see* Coal, mill, high speed
Sauter mean diameter, 146–147
Scale formation from cooling water, 432–433
Scaling, *see* Combustion, system scaling
SCRS, *see* Simple chemically reacting system (SCRS)
Sea water, for cooling, 438
Secondary air velocity, 148–149, 194. *See also* Air, secondary

Self-recuperative burners, *see* Burners, self-recuperative
Semi-direct firing, 266–267
Semi-indirect firing, 266–267
Service temperature, of metallic components, 444
Shock wave, *see* Noise, nozzle
Siemens furnace, *see* Glass tank
Signal transmitters, *see* Furnace instrumentation, signal transmitters
Similarity parameter
  Becker throttle factor, 54t, 214–215
  Craya Curtet, 53, 54t, 54b, 164, 214, 563, 589
  Curtet number, 54t, 215
  Thring Newby, 54t, 214
Simple chemically reacting system (SCRS), 32, 37, 227–228
Site investigation, 547–552
Six tenths power law, 514
Sizing of aggregate processing furnace, *see* Furnace design, sizing, worked examples
Sizing of oil heating furnace, *see* Furnace design, sizing, worked examples
Sizing of slab re-heating furnace, *see* Furnace design, sizing, worked examples
Slagging, 84. *See also* Fouling index
Smelting, 13–16
Smog, 378–379
Solid waste fuel. *See also* Fuel, wastes; wood
  handling, 284–286
  size distribution, 285–286
Sonic velocity, *see* Noise, nozzle
Soot emissions, 295–296, 388, 392–394. *See also* Radiation, soot
Sound transmission, 197–198. *See also* Noise, attenuation
SO_x, *see* Sulphur oxides (SO_x)
Spalling
  of passive oxide layer, 428, 444
  of refractory, 84, 420–421
Spontaneous combustion, 85–86, 254, 276
Spontaneous ignition, *see* Spontaneous combustion
Spray
  angle, 171–173, 176
  combustion of, 170–171, 171f
  hollow cone, 171–172, 172f
  solid cone, 171–172
Stack, suction produced by, 183
Stainless steel. *See also* High temperature alloys
  advisory service, 447
  classification, 443t
Standing waves, *see* Noise, reverberation
Steam
  boilers, 4, 324
  engines, 2–3
Steam reforming
  gas composition, 558
  heat exchange, 558–559
  tubular, 557f, 558
Stoichiometric air requirement, 34–36, 49b, 50, 216, 403f, 504, 563–564
Sub-stoichiometric, 314–315, 320–321, 360
  operation (unintentional), corrective action, 320–321
Sulphur, *see* Fuel, sulphur
Sulphur oxides (SO_x)
  dry scrubbing, 408
  emissions, 18, 34b, 300–301, 308, 378, 401
  measurement, 312
  wet scrubbing, 300
Swirl, 19–20, 47–48, 57–59, 153–155, 175–176, 181, 191–192, 237–238, 400–401
Swirler, *see* Flame, stabilisation by swirler
Swirl number, *see* Dimensionless groups

T

Table feeder, *see* Coal, feeder raw coal
Telemetry, 620
Temperature measurement, *see* Furnace instrumentation, temperature
Thermal conductivity, 92, 100, 101t, 436–437. *See also* Refractory
Thermal expansion, differential in furnaces, 425
Thermal fluid, 249–250, 299–300
Thermocouple, *see* Furnace instrumentation, temperature
Tip shut-off atomiser, *see* Atomiser, pressure jet, tip shut-off
TNT, *see* Explosion, effect zone

Toxic equivalence factor (TEQ), 389
Trace heating, 252
Tramp material, 261
Tube mills, *see* Coal, mill, ball type
Tube still, *see* Refinery heater
Turbulence, 41–43, 57–59, 212–213, 232–233, 233t, 237–238, 400–401, 466–467
  equivalent viscosity models, 58–59, 233t
  k-e model, 58, 233t
  Prandtl mixing length, 58, 233t
  Reynolds stress models, 58–59, 233t
Turbulent mixing, 58–59, 143
TUV, 246, 322, 329

U

Ultrasonic flow measurement, *see* Furnace instrumentation, flow
Ultrasonic temperature measurement, *see* Furnace instrumentation, temperature
UV detector tubes, *see* Flame, detector
UV radiation, 331–332

V

Valve
  fire safe, oil, 252
  flow control, 246, 253
  pressure control, 250–251
  safety shut off, gas, 248–249
  train, gas, 246–249
  vent, 248
VDI 3673, 276
Velocity
  air, *see* Primary air, velocity; Secondary air velocity
  gas in pipework, 246–248
  oil in pipework, 250
Vent valve, *see* Valve, vent
Vertical spindle mills, *see* Coal, mill, vertical spindle
View factor, *see* Radiation
Viscosity of oil, *see* Oil, viscosity
VOC, *see* Volatile organic compounds (VOC)
Volatile organic compounds (VOC), 408–409
  emissions of, 379, 387–388
Volatiles in coal, 582. *See also* Combustion
Volumetric feeders, *see* Coal, feeder pulverised

W

Wake, 171–172
Warming up, *see* Refractory, drying and curing
Waste fuel
  environmental benefits, 286
  handling, 283–286
  health hazards, 286
  liquid fuel handling, 284
  solvents, use as fuel, 79–80
Water cooling, 431–432
Water vapour, 267–268
  measurement, 301, 312, 345–346
  radiation, 117
Waves, *see* Atomisation; Noise, reverberation
Weld decay, 423, 444. *See also* Carbide precipitation; Intergranular corrosion
Well-stirred furnace model, *see* Modelling, well-stirred furnace
Wigg's equation, 179–180
Windbox, *see* Air, plenum and windbox design
Wobbe Index, 70–71, 142–143, 298

Y

Y-jet, *see* Atomiser, twin fluid, high pressure air or stream

Z

Zone method, 228–231
Zone modelling. *See also* Model grids; Modelling